

SYNTHESIS AND MOLECULAR PHARMACOLOGY OF THE DIAZONAMIDES

APPROVED BY SUPERVISORY COMMITTEE

Patrick Harran, Ph.D.

Micahel Roth, Ph.D.

Jef De Brabander, Ph.D.

Steven McKnight, Ph.D.

David Corey, Ph.D.

DEDICATION

To my parents and family. They have made all things possible for me.

SYNTHESIS AND MOLECULAR PHARMACOLOGY OF THE DIAZONAMIDES

by

ANTHONY WILLIAM GEORGE BURGETT

DISSERTATION

Presented to the Faculty of the Graduate School of Biomedical Sciences

The University of Texas Southwestern Medical Center at Dallas

In Partial Fulfillment of the Requirements

For the Degree of

DOCTOR OF PHILOSOPHY

The University of Texas Southwestern Medical Center at Dallas

Dallas, Texas

December, 2006

Copyright

by

Anthony William George Burgett, 2006

All Rights Reserved

SYNTHESIS AND MOLECULAR PHARMACOLOGY OF THE DIAZONAMIDES

Publication No. _____

Anthony William George Burgett, Ph. D.

The University of Texas Southwestern Medical Center at Dallas, 2006

Supervising Professor: Patrick Harran, Ph.D.

Michael Roth, Ph. D.

Diazonamide A is structurally novel, marine-derived natural product potentially capable of inhibiting the growth of the cultured human cancer cell lines *in vitro*. Following the re-assignment of diazonamide structure in 2001, we began a program to understand the compound's cellular mode of action. I determined that the diazonamides are potent anti-mitotic agents that induce the formation of mono-aster mitotic spindles. The synthesis of numerous analogs established structure activity relationships which guided the preparation of biotinylated, fluorescent, and radiolabeled forms of the natural product. These analogs were used in a variety of experiments to demonstrate diazonamide A effects mitotic spindle assembly in novel manner distinct from conventional tubulin interacting agents. This finding suggests diazonamide A will prove a valuable probe of new cell biology and a unique chemotherapeutic drug lead.

The second major focus of my work involved the total synthesis of diazonamide A. The central feature of our approach employed a hypervalent iodine species to oxidatively install the central diazonamide diarylaminal. This net two electron oxidative internal crosslink between tyrosine and tryptophan accesses the diazonamide core from a simple peptide-derived substrate. Building on the discovery, fully synthetic diazonamide A was prepared in a total of 19 operations from 5 segments of comparable complexity. This successful synthesis allows for a truly scalable and practical synthesis of diazonamide structures for further pre-clinical evaluation as new anti-cancer drugs.

TABLE OF CONTENTS

CHAPTER ONE.....	2
The Diazonamide Natural Products: Introduction and Background	2
1.1 The Diazonamide Natural Products: Isolation and Characterization.....	2
1.1.1 Marine Derived Natural Products	2
1.1.2 Isolation and Characterization of the Diazonamide Natural Products ..	4
1.2 Diazonamide A as a Synthetic Target	10
1.2.1 Introduction.....	10
1.2.2 Overview of Diazonamide A as a Target for Total Synthesis.....	11
1.2.3 Synthetic Research Towards the Original Diazonamide A Structure (4)	
13	
1.2.3.1 The Moody Group Diazonamide A Research.....	13
1.2.3.2 Konopelski Group Diazonamide A Research	15
1.2.3.3 Pattenden Group Diazonamide A Research	17
1.2.3.4 Liebscher Group Diazonamide A Research.....	18
1.2.3.5 Jamison Diazonamide A Research.....	19
1.2.3.6 Wipf Group Diazonamide A Research.....	21
1.2.3.7 Vedejs Group Diazonamide A Research	25
1.2.3.8 Magnus Group Diazonamide A Research	28
1.2.3.9 Wood Group Diazonamide A Research.....	32
1.2.3.10 Nicolaou Group Diazonamide A Research	33

1.2.3.11	Harran's Total Synthesis of the Original Diazonamide A and B Structures (2001).....	41
1.3	Structure Revision of the Diazonamides.....	50
1.4	Synthetic Research Towards the Revised Diazonamide A Structure (9)	56
1.4.1	Fu Group Diazonamide A Research.....	56
1.4.2	The Feldman Group Diazonamide A Research	57
1.4.3	The Vedejs Group's Approach to the Revised Diazonamide A Structure.....	59
1.4.4	Nicolaou's First Total Synthesis the Revised Diazonamide A Structure	61
1.4.5	Nicolaou's Second Total Synthesis the Revised Diazonamide A Structure.....	65
1.5	Diazonamide Biosynthesis.....	66
1.6	Diazonamide Biological Activity	67
1.6.1	Introduction.....	67
1.6.2	Initial Diazonamide Cytotoxicity Data.....	67
1.6.3	Initial Research into Diazonamide A's Biological Activity	68
1.7	Conclusions.....	69
1.7.1	Synthetic Studies	69
	CHAPTER TWO Characterization of Diazonamide Biological Activity.....	72
2.1	Introduction	72

2.1.1	Cytotoxic Natural Products and the Search for New Cancer	
	Chemotherapeutic Agents	72
2.1.2	Microtubules and Tubulin	73
2.1.3	Tubulin Binding Compounds	74
2.2	Material and Methods	77
2.2.1	Chemicals and Reagents	77
2.2.2	Buffers and Solution	78
2.2.3	Cell Lines and Tissue Culture	78
2.2.4	Determination of Cytotoxicity of Compounds in Tissue Culture	79
2.2.4.1	Direct Cell Counting (Method 1)	79
2.2.4.2	96-Well Colorimetric Assay (Method 2).....	80
2.2.4.3	96-Well Luminescent Assay (Method 3).....	80
2.2.5	Indirect Immunofluorescence of Cells.....	81
2.2.6	Thymidine Mitotic Block and Tubulin Imaging Procedure in BS-C-1 Green Monkey Cells.....	82
2.2.7	FACScan Analysis Cells	83
2.2.8	Isolation of MAP Enriched Tubulin from Bovine Brain	83
2.2.9	<i>In Vitro</i> Tubulin Polymerization Assay	85
2.2.10	Characterization Data for Diazonamide-Based Reagents	85
2.3	Results	93
2.3.1	Cellular Activity of Compounds Related to the Structure Originally Proposed for Diazonamide A.....	93

2.3.1.1	Molecules Lacking the C16-C18 Biaryl Linkage	93
2.3.2	Cellular Activity as a Confirmatory Guide to the Revised Diazonamide Structures	97
2.3.3	Further Biochemical Evaluations of (-)Diazonamide A and (-)Syndistatin (271)	101
2.3.4	Effect of Diazonamide A and Syndistatin (271) on <i>In Vitro</i> Tubulin Polymerization	104
2.3.5	Effects of Diazonamide A and Syndistatin (271) on Mitotic Spindle Formation	108
2.3.6	Further Examination of the Interaction of Diazonamide A and Syndistatin with Microtubules (Comments on Studies by the Hamel Group)	111
2.4	Discussions	112
2.4.1	Diazonamide A and Syndistatin SAR.....	112
2.4.2	Characterization of the Diazonamide A and Syndistatin Biological Activity	114
2.5	Conclusions.....	117
2.6	Appendix.....	117
CHAPTER THREE Synthesis and Application of Syndistatin Probe Analogs		132
3.1	Introduction	132
3.1.1	Background Literature	133
3.2	Synthesis and Evaluation of Syndistatin Probe Analogs.....	134
3.2.1	Design for Derivatization	135

3.2.2	Probe Analog Synthesis	136
3.3	Evaluation of the Syndistatin Probe Analogs	139
3.4	Utilization of Syndistatin Probe Analogs	139
3.4.1	Experiments with the Syndistatin Radiochemical Analog 298	139
3.4.2	Experiments with the Syndistatin Fluorescent Analog 297	145
3.4.3	Syndistatin Affinity Chromatography Experiments.....	147
3.4.3.1	Utilization of Biotinylated Analog 296	148
3.5	Discussion.....	150
3.6	Conclusions.....	152
3.7	Experimental Section.....	152
3.7.1	Determination of Cytotoxicity of Compounds in Tissue Culture	152
3.7.2	<i>In Vitro</i> Tubulin Polymerization Assay	152
3.7.3	Nonspecific Binding of Radiolabeled Analog 298	152
3.7.4	TLC and Autoradiography of Radiolabeled Analog 298.....	153
3.7.5	Determination of Binding of Radiolabeled Analog 298 to Tubulin and Microtubules Using Gel Exclusion Chromatography	153
3.7.6	Imaging of Fluorescent Analog 297	154
3.7.7	Affinity Chromatography with Syndistatin Reagents.....	154
3.7.7.1	Affinity Chromatography with Biotinylated Syndistatin Reagents 296 and 301 in MAP(+) Tubulin	154
3.7.8	Synthesis Experimental Section	155
3.8	Chapter 3 Appendix	168

CHAPTER FOUR Total Synthesis of Diazonamide A	188
4.1 Introduction	188
4.2 Retrosynthesis	189
4.3 Total Synthesis of Diazonamide A.....	192
4.3.1 Synthesis of Peptide Derived Oxidation Substrate	192
4.3.2 Formation of the Diazonamide C10 Macrocycle Via a Hypervalent Iodine Oxidation Reaction.....	194
4.3.2.1 Possible Hypervalent Iodine Oxidation Mechanisms	196
4.3.3 Synthesis and Photochemistry of Bis-Oxazole 346.....	198
4.3.4 Successful Photochemical Formation of the Diazonamide Core	201
4.3.5 Diazonamide Chlorination and Endgame	202
4.4 Discussion	204
4.5 Conclusions.....	206
4.6 Experimental Section.....	206
4.6.1 General Methods	206
4.6.2 Compound Data.....	208
4.7 Chapter 4 Appendix	246
CHAPTER FIVE Synthesis and Evaluation of Diazonamide A Analogs	316
5.1 Introduction	316
5.2 Synthesis and Evaluation of Simplified Diazonamide Analogs	317
5.3 Synthesis of Extended Side Chain Diazonamide A Analogs.....	319
5.4 Synthesis of Diazonamide A Probe Analogs	320

5.5	Synthesis of Proline Containing Diazonamide Core	323
5.6	Discussion	325
5.7	Conclusions.....	326
5.8	Experimental Section.....	327
5.8.1	General Notes	327
5.8.2	Compound Data.....	327
5.9	Chapter 5 Appendix	349
	References	409

PRIOR PUBLICATIONS

Anthony W.G. Burgett, Qingyi Li., Qi Wei, Patrick G. Harran. "A Concise and Flexible Total Synthesis of Diazonamide A." *Angewandte Chemie. Int. Ed* **2003**, 42,4961-4966.

Jing Li, Anthony W.G. Burgett, Lothar Esser, Carlos Amezcua, Patrick G. Harran. "Total Synthesis of Nominal Diazonamides- Part 2. On the True Structure and Origin of Natural Isolates." *Angewandte Chemie Int. Ed.* **2001**, 40(24) 4770-4773.

Jing Li, Xin Chen, Anthony W.G. Burgett, Patrick G. Harran. "Synthetic seco Forms of (-)-Diazonamide A." *Angewandte Chemie Int. Ed.* **2001**, 40(14) 2682-2685.

LIST OF FIGURES

FIGURE 1-1: ASCIDIAN-DERIVED NATURAL PRODUCTS	3
FIGURE 1-2: NMR ASSIGNMENT AND X-RAY STRUCTURE.....	8
FIGURE 1-3: DIAZONAMIDE A-D AS ASSIGNED BY FENNICAL.....	9
FIGURE 1-4: DIAZONAMIDE A STRUCTURES.....	13
FIGURE 1-5: REVISED STRUCTURE FOR DIAZONAMIDE A AND B.....	54
FIGURE 2-1 SAR STUDIES OF NON-CYCLIZED DIAZONAMIDE A ANALOGS..	94
FIGURE 2-2 FACSCAN ANALYSIS SHOWS NON-CYCLIZED ANALOGS ARE NOT ANTI-MITOTIC AGENTS:.....	95
FIGURE 2-3: OVCAR-3 CELLS TREATED WITH FLUORESCENT ANALOG 265:	97
FIGURE 2-4 DIAZONAMIDE SIDE CHAIN ANALOGS	98
FIGURE 2-5: EXAMPLE OF GROWTH INHIBITION DATA: CYTOTOXICITY OF DIAZONAMIDE ANALOGS IN OVCAR-3 CELLS:	99
FIGURE 2-6 OTHER SYNDISTATIN ANALOGS AND CYTOXICITY VALUES ...	100
FIGURE 2-7 SYNDISTATIN (271) AND DIAZONAMIDE A ARE POTENT ANTI- MITOTICS:	102
FIGURE 2-8 DIAZONAMIDE A AND SYNDISTATIN (271) INDUCE CELLULAR MICROTUBULE DEPOLYMERIZATION AT HIGH CONCENTRATIONS:.....	103
FIGURE 2-9 DIAZONAMIDE A PREVENTS THE POLYMERIZATION OF IN VITRO MAP(+)-TUBULIN:	105

FIGURE 2-10 EFFECT OF DIAZONAMIDE A ON <i>IN VITRO</i> TUBULIN POLYMERIZATION:.....	106
FIGURE 2-11 EFFECT OF COMPOUNDS ON PREFORMED MICROTUBULES..	109
FIGURE 2-12 EFFECT OF COMPOUNDS ON PREFORMED MICROTUBULES	110
FIGURE 2-13 EFFECT OF COMPOUNDS ON MITOTIC SPIDLE FORMATION ON SYNCHRONIZED BS-C-1 CELLS AT 9.5 HR.....	112
FIGURE 3-1 SYNDISTATIN C37 ACETYL ANALOG	136
FIGURE 3-2: SYNDISTATIN SIDE CHAIN ANALOGS.....	137
FIGURE 3-3: EFFECT OF PROBE ANALOGS ON <i>IN VITRO</i> TUBULIN POLYMERIZATION.....	141
FIGURE 3-4: CHARACTERIZATION OF RADIOLABELED ANALOG 298	144
FIGURE 3-5: DETERMINATION OF BINDING OF 298 TO TUBULIN/MICROTUBULES WITH GEL FILTRATION.....	145
FIGURE 3-6: IMAGING OF FLUORESCENT ANALOG 297 IN BS-C-1 CELLS..	146
FIGURE 3-7 AFFINITY CHROMATOGRAPHY WITH SYNDISTATIN REAGENTS 296 AND 303 IN MAP(+) TUBULIN IS UNSUCCESSFUL:.....	150

LIST OF SCHEMES

SCHEME 1-1: MOODY'S DIAZONAMIDE RETROSYNTHESIS AND APPROACH	16
SCHEME 1-2: KONOPELSKI'S DIAZONAMIDE SYNTHETIC PROGRESS	17
SCHEME 1-3: PATTENDEN'S SYNTHESIS OF C-D-E-F MODEL FRAGMENT ...	18
SCHEME 1-4: LIEBSCHER'S DIAZONAMIDE SYNTHETIC PROGRESS	19
SCHEME 1-5: JAMISON'S DIAZONAMIDE RETROSYNTHESIS AND APPROACH	22
SCHEME 1-6: WIPF'S DIAZONAMIDE RETROSYNTHESIS AND APPROACH...	24
SCHEME 1-7: VEDEJS' DIAZONAMIDE A RETROSYNTHESIS AND SYNTHESIS OF BENZOFURANONE FRAGMENT	26
SCHEME 1-8: VEDEJS' SYNTHESIS OF DIPHENYLACETAL DIAZONAMIDE FRAGMENT	27
SCHEME 1-9: MAGNUS' DIAZONAMIDE RETROSYNTHESIS AND SYNTHESIS OF BISOXAZOLE INDOLE FRAGMENT	29
SCHEME 1-10: MAGNUS'S ADVANCED DIAZONAMIDE SYNTHESIS	31
SCHEME 1-11: WOOD'S DIAZONAMIDE RETROSYNTHESIS AND PROGRESS	32
SCHEME 1-12: NICOLAOU'S DIAZONAMIDE A RETROSYNTHESIS	34
SCHEME 1-13: NICOLAOU'S INITIAL PROGRESS	36
SCHEME 1-14: NICOLAOU'S SYNTHESIS OF THE ABCDE MACROCYCLE	38

SCHEME 1-15: NICOLAOU'S LATE STAGE SYNTHESIS	39
SCHEME 1-16: HARRAN'S RETROSYNTHESIS.....	42
SCHEME 1-17 HARRAN'S SYNTHESIS OF THE TRIARYLETHYLENE CORE ...	44
SCHEME 1-18: DIHYDROXYLATION OF THE TRIARYLETHYLENE CORE.....	45
SCHEME 1-19: HARRAN'S SYNTHESIS OF A NONCYCLIZED DIAZONAMIDE COMPOUND	47
SCHEME 1-20: DIAZONAMIDE A TOTAL SYNTHESIS ENDGAME (HARRAN) ...	49
SCHEME 1-21: FU'S DIAZONAMIDE METHODOLOGY	56
SCHEME 1-22 FELDMAN'S RETROSYNTHESIS AND PROGRESS.....	58
SCHEME 1-23 VEDEJS' SYNTHESIS OF THE ABCDE MACROCYCLE (REVISED STRUCTURE).....	60
SCHEME 1-24: RETROSYNTHESIS OF NICOLAOU'S FIRST TOTAL SYNTHESIS OF DIAZONAMIDE A	62
SCHEME 1-25: NICOLAOU'S FIRST TOTAL SYNTHESIS OF DIAZONAMIDE A	64
SCHEME 1-26: NICOLAOU'S SECOND TOTAL SYNTHESIS OF DIAZONAMIDE A	66
SCHEME 3-1: SYNTHESIS OF EXTENDED SIDE CHAIN ANALOG	138
SCHEME 3-2: SYNTHESIS OF BIOTINYLATED AND FLUORESCENT ANALOGS	140
SCHEME 3-3: SYNTHESIS OF TRITIATED SYNDISTATIN ANALOG	139
SCHEME 3-4: SYNTHESIS OF NONCYCLIZED BIOTINYLATED ANALOG	149

SCHEME 4-1: BIOSYNTHETIC ORGINS OF THE REVISED DIAZONAMIDE STRUCTURE.....	188
SCHEME 4-2: DIAZONAMIDE A RETROSYNTHESIS (PART 1).....	190
SCHEME 4-3: DIAZONAMIDE A RETROSYNTHESIS (PART 2).....	191
SCHEME 4-4: SYNTHESIS OF TRIPEPTIDE OXIDATION SUBSTRATE	193
SCHEME 4-5: HYPERVALENT IODINE OXIDATION - ENTRY INTO THE DIAZONAMIDE SERIES	195
SCHEME 4-6: PHENOLIC OXIDATION MECHANISM.....	197
SCHEME 4-7: INDOLE OXIDATION MECHANISM.....	198
SCHEME 4-8: SYNTHESIS OF PHOTOCHEMISTRY SUBSTRATE	200
SCHEME 5-1: SYNTHESIS OF CBZ-PROTECTED DIAZONAMIDE CORE	317
SCHEME 5-2: SYNTHESIS OF DIAZONAMIDE A ANALOGS	318
SCHEME 5-3: SYNTHESIS OF EXTENDED SIDE CHAIN DIAZONAMIDE A ANALOGS.....	320
SCHEME 5-4: SYNTHESIS OF DIAZONAMIDE PROBE ANALOGS	321
SCHEME 5-5: SYNTHESIS OF NONCYCLIZED PROBE ANALOGS.....	322
SCHEME 5-6: SYNTHESIS OF PHENOL ANALOGS	323
SCHEME 5-7: SYNTHESIS OF PROLINE ANALOG DIAZONAMIDE CORE	324

CHAPTER ONE

The Diazonamide Natural Products: Introduction and Background

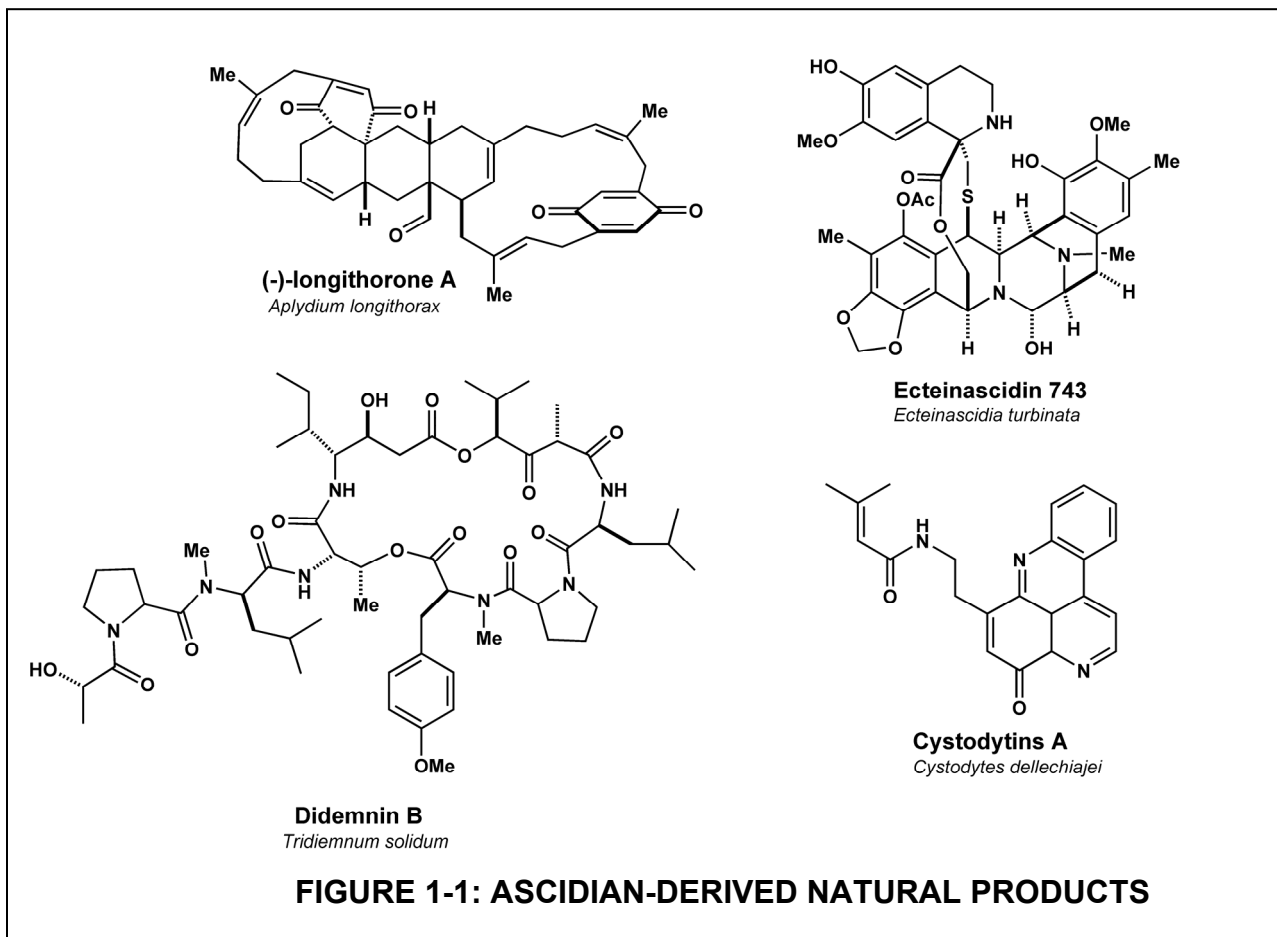
1.1 The Diazonamide Natural Products: Isolation and Characterization

1.1.1 Marine Derived Natural Products

The diverse ocean biome is a rich source for natural products, and marine invertebrate species have provided innumerable bioactive, structurally-complex molecules.^{1, 2} Marine-derived natural products have become a focal point in the search for new anti-cancer compounds, with several marine natural products in development as possible cancer chemotherapeutics.^{2 3} Perhaps the most recent class of marine invertebrate to become a focus for natural products isolation is the subphylum Urochordata. Urochordata is the most evolutionarily advanced subphylum of marine invertebrates. This subphylum belongs to the Chordata phylum, which contains all vertebrate species. This subphylum includes the ascidians, also known as tunicates. These organisms are typically benthic sessile filter-feeding organisms, and unlike phenotypically similar, less-complex marine invertebrates, Urochordata species produce motile larvae which possess many features of vertebrate life.⁴ Therefore, the Urochordata organisms are believed to resemble intermediate species that developed during the evolution of invertebrate into vertebrate life.⁴

In addition to the evolutionary advancement of the subphylum, the Urochordata have been an especially rich source for marine natural products.⁵ In contrast to the other marine invertebrate phylum extensively explored for natural products, Urochordata species

produce a disproportionately large number of nitrogen and peptidyl natural products.⁵ In the last two decades, ascidian derived natural products have gained a preeminent role as targets



of total synthesis and pharmaceutical leads. For example, many of the natural products under development as anti-cancer agents were isolated from Urochordata species including didemnin B and ecteniascinidin 743 (**Figure 1-1**).

The true origins of the ascidian secondary metabolites has not been extensively explored,⁵ and it is not known whether the natural products are produced by commensal microorganisms. It is also unclear why the ascidians produce such a large number of amino acid-derived natural products. Further, the role of the cytotoxic natural products in the

ascidian organism is also unknown, but speculation and inconclusive experimental data⁶ suggest the toxic compounds may serve as anti-feedant agents for the motile larvae.

1.1.2 Isolation and Characterization of the Diazonamide Natural Products

In 1991, the Fenical group at the Scripps Institution of Oceanography disclosed the discovery and structural assignment of a new ascidian-derived class of natural products termed the diazonamides. The diazonamides were isolated from the Urochordata species *Diazonia angulata* (originally the isolation organism was incorrectly identified as *Diazonia chinesis*^{6, 7}) in 15-25 m deep caves off Siquijor Island, Philippines.^{6, 7} The translucent colonies were gathered, lyophilized, and then extracted with methanol, acetone, dichloromethane, and finally 85:15 methanol/water to isolate secondary metabolites.^{6, 7} The combined organic extractions were partitioned and fractionated over a gel filtration column using methanol elution.^{6, 7} The partially-fractionated components were further purified using a combination of chromatographic techniques to yield four separated diazonamide compounds: diazonamide A, B, C, and D.^{6, 7} 256.2 g of dried organism yielded 54 mg of diazonamide A, 132 mg of diazonamide B, 35 mg of diazonamide C, and 35 mg of diazonamide D.

The structural assignment of the diazonamides was made using a combination of mass spectrometry, NMR, and X-ray crystallography techniques. The available references^{6, 7} detailing the isolation and characterization of the diazonamide class of natural products lack the clarity and specificity to understand the exact chronological process used to assign the diazonamide structures. The initial ¹H and ¹³C NMR data indicated that the four major metabolites possessed a common molecular architecture.⁶ The structural characterization of

the least-polar compound, termed diazonamide A, apparently was begun with HRFAB mass spectrometry. The isotopic pattern of molecular masses detected indicated multiple halogen atoms were present in the molecule. Use of energy dispersive spectrometry established chlorine as the only heavy atom present in the metabolite. A combination of ^{13}C NMR, DEPT, and XHCORR NMR experiments revealed diazonamide possessed forty carbon atoms, nineteen of which are not bound to hydrogen. Twenty-nine protons were identified as being bonded to the carbon atoms.⁶ Eleven of these protons had chemical resonances in the aromatic region and ten of the protonated carbon had aliphatic resonances.⁶ In addition, four deuterium oxide exchangeable protons were identified, and, based on the chemical shifts and ^1H - ^1H coupling constants, two of these exchangeable protons were identified as amide protons.⁶

Further analysis of the ^{13}C and ^1H NMR resonances and ^1H - ^1H coupling signals indicated two valine residues were present in the structure.⁶ This presumptively conclusive identification was corroborated by an intense band in the infrared absorption spectra at 1680 cm^{-1} , and the identification of two carbonyl amide carbons were shown to be coupled to the signature valine side chains.⁶ The α -proton chemical shifts of the two valine residues differed considerably (3.88 ppm and 4.85 ppm), and based on the chemical shift of the α -carbon and its attached proton, one valine was assigned as possessing a free amine base.⁶ Significantly, the α -proton of the free amine valine was determined to be coupled to only one deuterium exchangeable proton.⁶ This result, termed “unexpected,”⁶ is not consistent with a free-amine valine assignment, but no further explanation is offered.⁶ Based on characteristic proton couplings, the spectroscopic data also suggested the presence of a tyrosine residue.⁶

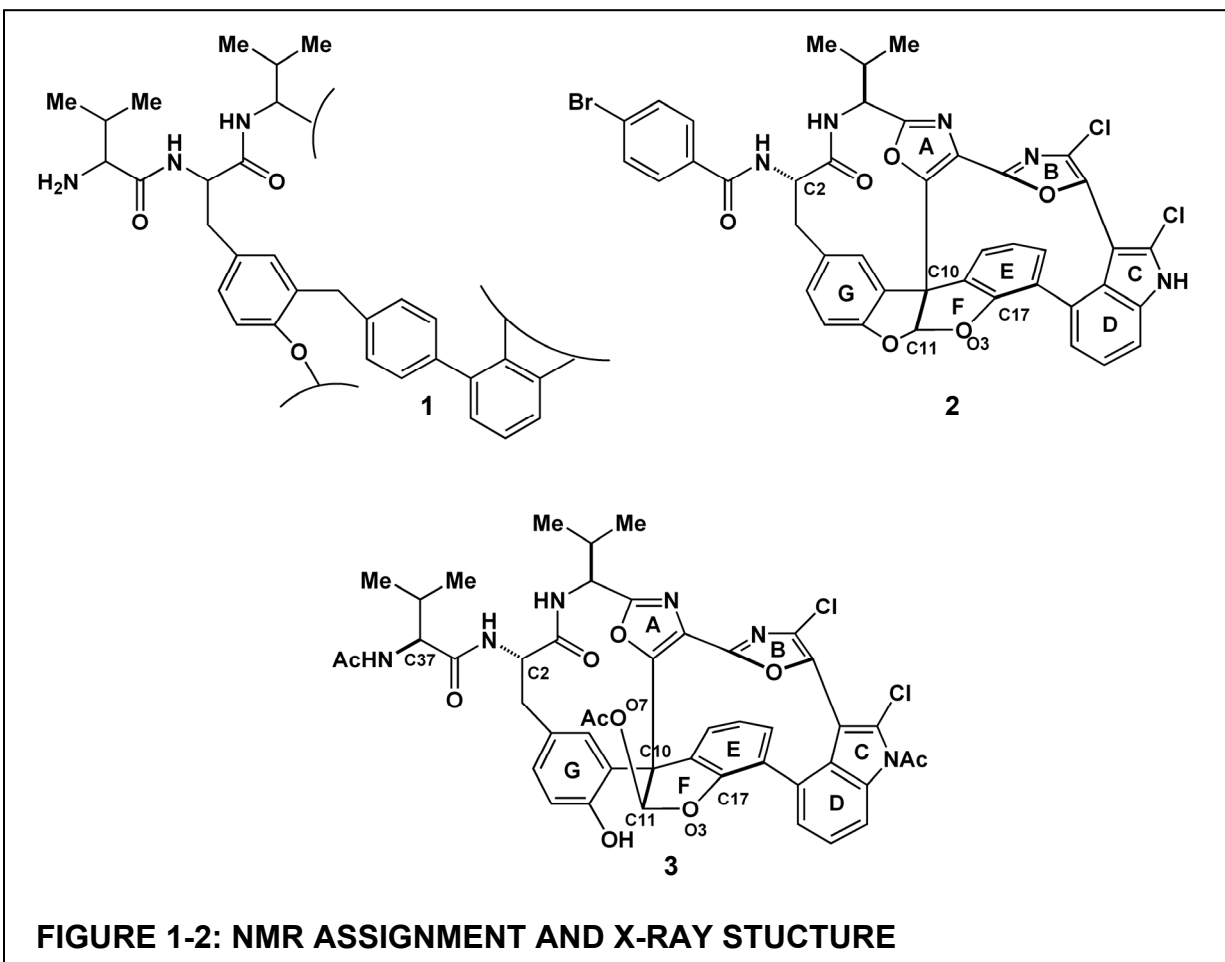
Based on distinctive NMR chemical shifts and coupling constants, the remaining deuterium exchangeable proton was identified as a hydroxyl hemiacetal proton.⁶ In the ¹H NMR spectrum, this proton was coupled to a doublet with a resonance $\delta = 6.36$ ($J = 4.2$), and the XHCORR experiment showed this exchangeable proton was coupled to a one-bond removed carbon atom ($\delta = 106.1$). A ¹J_{C-H} coupling constant of 174 Hz for the proton coupled to the carbon resonating at $\delta = 106.1$ was presented as “confirmation,” based on precedent, that the structure of diazonamide A possessed a hemiacetal functional group.⁶

Guided by the initial identification of the constituent three amino acid residues and the hemiacetal unit, a proposed molecular formula of C₄₀H₃₅N₆O₆Cl₂ (requires 765.1999 amu) was generated, and it matched very well the observed HRFABMS of 765.1998 (Δ 0.3 ppm) for diazonamide A. With a presumptive molecular formula and several subunits of diazonamide identified, long range proton-carbon coupling (COLOC) experiments were performed to designate a molecular framework. The COLOC experiments established a basic connectivity between the known subunits (**Figure 1-2, 1**). The tyrosine residue was shown to be bonded to both the valine components through amide bonds.⁶ The COLOC experiments indicated one aromatic carbon of the tyrosine phenol was directly bonded to a quaternary carbon center.⁶ This quaternary center was also determined to be bonded to another aromatic ring system that possessed a 1,2,3 substitution pattern. This 1,2,3, substituted ring system was also directly bonded to the hemiacetal carbon.⁶ However, the NMR methods were unsuccessful in assigning a large portion of the structure.

The diazonamide natural products were subjected to several chemical transformations in order to aid in the structure elucidation. Acid hydrolysis of diazonamide A did not

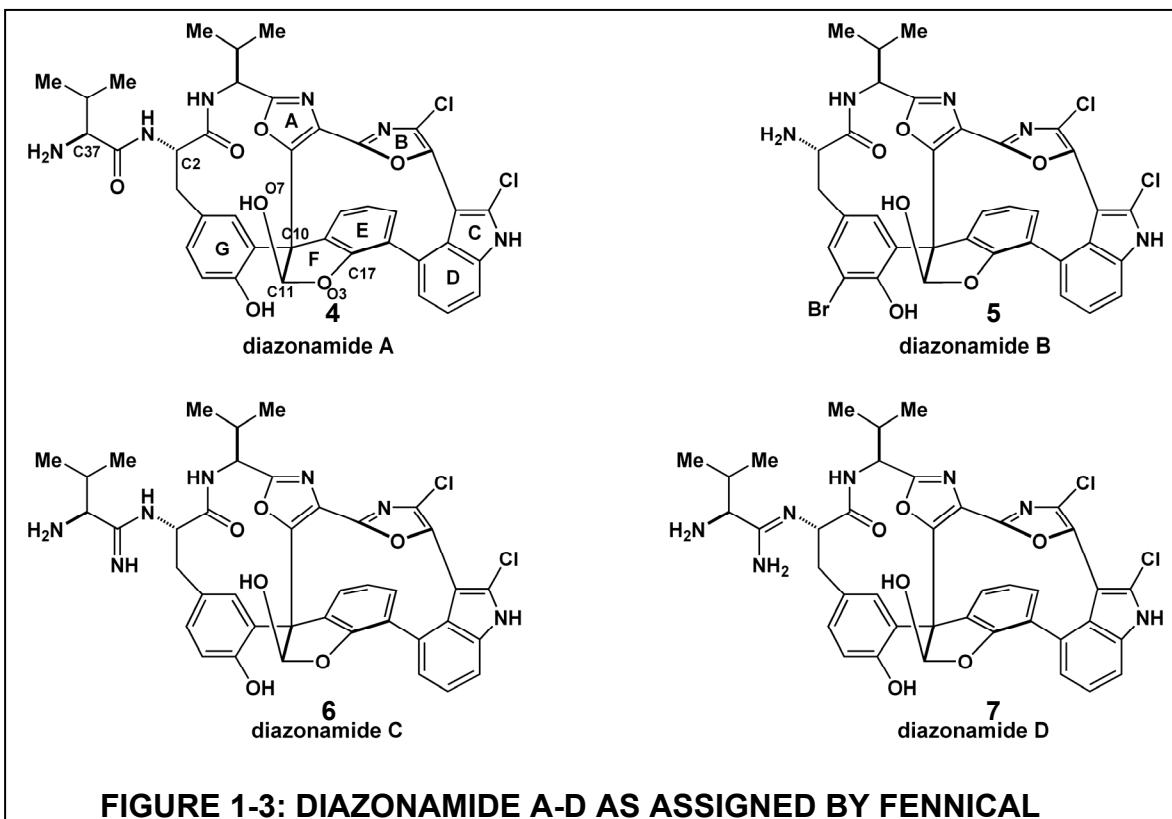
generate any useful structural insights, and also, significantly, failed to produce free amino acids upon peptide bond hydrolysis. Methylation and sodium borohydride reduction of the diazonamide structures were not productive. Acetylation of diazonamide A did produce a useful derivative. Three methyl singlets in the ^1H NMR spectrum and the HRFABMS confirmed an triacetylated derivative, but unexpectedly, the acetylated compound only possessed two new IR absorptions at 1760 cm^{-1} and 1725 cm^{-1} . Although the absorption at 1760 cm^{-1} was identified as being characteristic of an phenolic acetate ⁶, the authors concluded that both the hemiacetal alcohol and the valine free amine were acetylated. This assignment was based on signals assigned to these functional groups changing in the ^1H NMR spectrum upon acetylation. The third acetate methyl resonance could not be assigned to any functional group although the authors apparently assigned it to the IR absorption band at 1725 cm^{-1} .⁶ The apparent discrepancy between the number of IR absorption bands for the triacetylated derivative is not discussed.⁶ The authors also fail to comment on the assignment of the hemiacetal acetate to an IR band that is characteristic of an aromatic acetate.⁶

While unsuccessful in identifying diazonamide A's structure, the described experiments were able to establish a conserved molecular framework for the four isolated products. The NMR analysis indicated diazonamide B differed from diazonamide A in two respects. The structure possessed only one isopropyl unit, and the aromatic ring of the tyrosyl residue contained an additional substituent. Also, energy dispersive spectrometry of diazonamide B detected the presence of bromine in addition to chlorine. X-ray crystallography was subsequently employed to elucidate the diazonamide structure. X-ray



quality crystals of diazonamides A and B and their acetylated derivatives could not be attained,⁶ but a *p*-bromobenzamide derivative of diazonamide produced cubic crystals suitable for X-ray diffraction.⁶ The structure of these crystals was solved by the Clardy group at Cornell University yielding the molecular architecture of the diazonamide class of natural products (**Figure 1-2, 2**).^{6, 7}

The partial structural assignment developed through the NMR methods (1) was largely consistent with solved crystal structure with the exception of the absence of the hemiacetal functional group. Based on the NMR assignment, the hemiacetal hydroxyl was shown to be coupled to C11. To accommodate this previous assignment, the authors determined that the hemiacetal was converted into the cyclic acetal during the synthesis of the *p*-bromobenzamide derivative. This was consistent with the assignment of the atoms in the Clardy X-ray structure. The fact the crystal structure was of the cyclic acetal compound (2) barred a complete assignment of the hemiacetal functionality. The C11 stereochemistry could not be assigned from the X-ray data, nor could it be determined whether C11 was bound



to the E-ring or the G-ring phenol. The assignment of the hemiacetal as forming a five-membered ring with the E-ring phenol was based on long range J_{C-H} correlations.⁶ A presumptive assignment of the C11 stereochemistry was made based on calculated geometric preferences.⁶

The X-Ray structure of the diazonamide B derivative facilitated completing the structural assignment of the other diazonamides (**Figure 1-3**). Diazonamide A, C, and D possessed different appended side chains on the conserved diazonamide polycycle structure. Diazonamide A (**4**) was determined to possess a valine side chain of unknown absolute configuration. Diazonamide C (**6**) was assigned as having an amidine side chain based primarily on the HRFABMS data.⁶ The assignment of diazonamide D (**7**) was facilitated by its slow conversion into diazonamide C upon storage, and the diazonamide D side chain was assigned as a tautomeric form of the diazonamide C amidine side chain.⁶

1.2 Diazonamide A as a Synthetic Target

1.2.1 Introduction

Structurally complex natural products have always provided molecular targets for total synthesis. Natural product total synthesis is a critical venue for advancing synthetic organic chemistry research. The pursuit of a complex structure requires the correct utilization of synthetic reactions in a designed pathway, and beyond creating a route to the desired product, this undertaking expands the general knowledge of chemical reactivity and synthetic chemistry. Novel and intricate structures are particularly important total synthesis targets because such molecules test the existing repertoire of synthetic solutions. Often, the synthesis

of a complex natural product requires the development of new reactions and methodologies to surmount the limitations of the existing methods. Natural product total synthesis inspires, and often requires, innovative solutions to new synthetic challenges, and thus, advances the knowledge and capabilities of synthetic organic chemistry.

After its disclosure in 1991, diazamide A motivated several research groups to undertake its total synthesis, and this pursuit continues to inspire research efforts.⁸ The unprecedented structure of diazamide A presented several formidable synthetic challenges in an unique molecular context, and a myriad of approaches and methodologies have been developed and applied by researchers engaged in its total synthesis. In addition to fueling new developments in synthetic organic chemistry, the importance of developing a diazamide A total synthesis was augmented by the compound's potent and unexplored biological activity. The inability to harvest significant quantities of the compound from its natural source mandated total synthesis as the only real supply of diazamide A. Therefore, the study of diazamide A's molecular pharmacology and biological activity is completely dependent on the development of a successful total synthesis of the molecule.

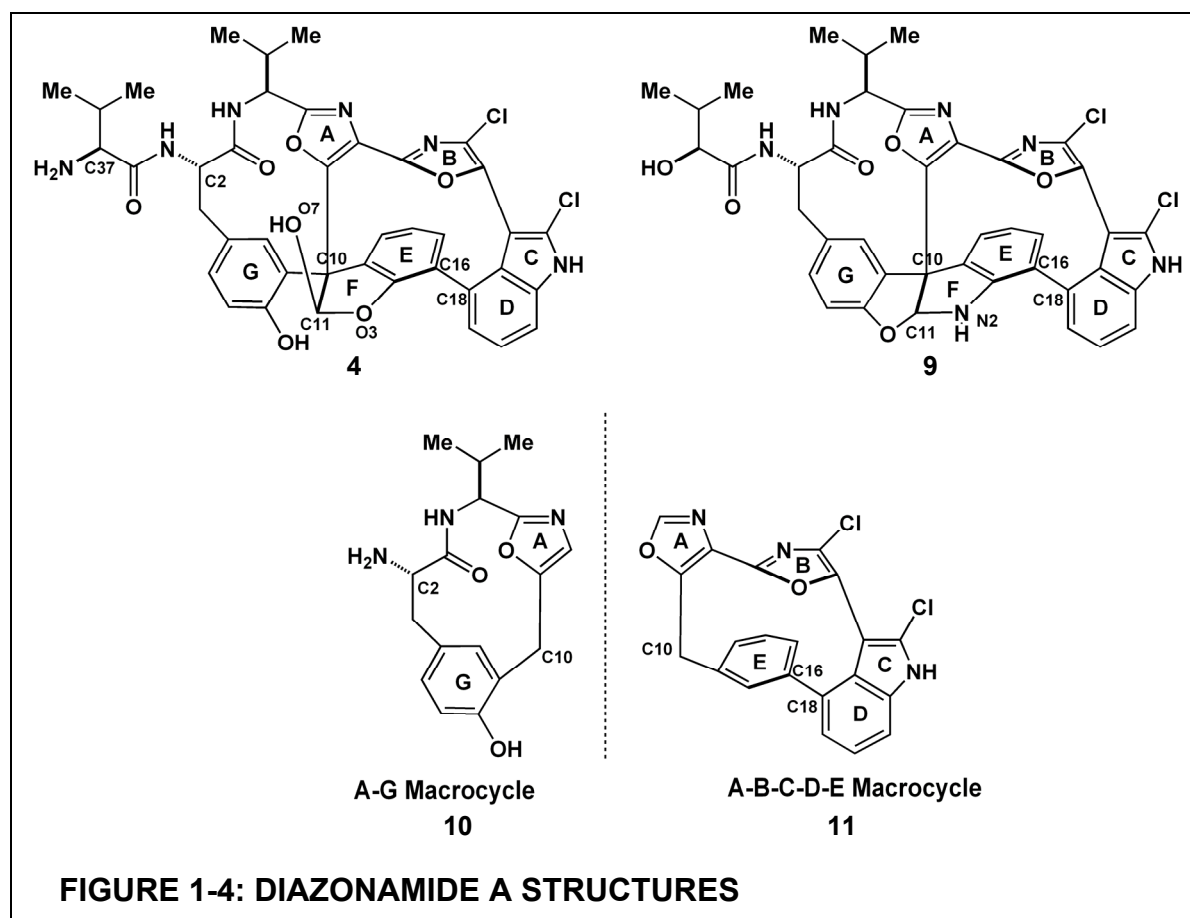
1.2.2 Overview of Diazamide A as a Target for Total Synthesis

Due to the incorrect original structural assignment, the research conducted into the total synthesis of diazamide A has in fact targeted to two different molecules. Although the originally assigned structure (**Figure 1-4, 4**) and the revised structure (**9**) of diazamide A share a large amount of structural identity, the unexpected revision impacted all of the diazamide synthetic efforts. The revelation of the structural corrections in 2001 completely

negated several synthetic designs, but several other ongoing approaches could be applied to the revised diazonamide A target. Therefore, this discussion of the diazonamide A synthetic research will be divided into efforts undertaken before and after the 2001 structure revision.

The diazonamide A structures (**4** and **9**) consist of a macrocyclic core and an appended side chain. The cores for both diazonamide A structures (**4** and **9**) share two identical macrocycles fused at the A ring oxazole and the C10 quaternary center. The twelve membered macrocycle **10** consists of an incorporated tyrosine residue and a oxazolyl valine component bridged through the C10 center. The right hand macrocycle (**11**), also a twelve atom ring, consists of the ABCDE aromatic rings connected through aryl linkages with the exception of the C10 center bridging the A and E rings. Unlike the duplicate fused macrocycles, the original (**4**) and the revised diazonamide A (**9**) structures possess dissimilar functionality bridging the E and G aromatic rings. Incorporating the C11 hemiacetal moiety is an especially challenging aspect in designing a synthetic route to **4**.

Perhaps the most daunting synthetic challenge for either diazonamide structure is the construction of the C10 center. In addition to the inherent synthetic challenges of quaternary carbon centers, the diazonamide C10 center fuses two twelve-membered macrocycles in addition to the C11 functionality. The sterically congested, bridging C10 center is the crux of the diazonamide A problem. In addition, the synthesis of the disparate macrocycles (**10**, **11**) considered independently, are also daunting synthetic challenges. For example, closing the twelve membered lactam ring at the C1 position to form the A-G macrocycle (**10**) is a formidable synthetic problem, especially in the context of a nearly completed diazonamide A structure that possesses an intact macrocycle **11**. A major challenge in constructing the



ABCDE macrocycle (**11**) is the issue of atropisomerism across the biaryl bonds. Diazonamide A exists as one atropisomer, but the correct axial chirality must be established during the course of a designed total synthesis.

1.2.3 Synthetic Research Towards the Original Diazonamide A Structure (**4**)

1.2.3.1 The Moody Group Diazonamide A Research

In 1994, the Moody group published the first account of research towards the total synthesis of diazonamide A.⁹ A synopsis of the Moody group's approach to diazonamide A, as elaborated in subsequent papers,¹⁰⁻¹⁵ is detailed in **Scheme 1-1**. In the Moody

retrosynthetic analysis^{9, 10, 14, 15}, **4** is deconstructed to a protected valine urethane derivative (**12**), a 4-bromotryptamine congener (**14**), and the diazo benzofuranone compound **13**. The Moody group envisioned using a dirhodium (II) catalyzed decomposition of α -diazo- β -ketoester **13** to generate a rhodium carbenoid species capable of inserting in the N-H bond of urethane **12**. Dehydration would then generate the A-ring oxazole and subsequent lactamization, via peptide coupling, will produce the A-G ring macrocycle. The two step dirhodium (II) N-H insertion reaction/cyclodehydration methodology could also be employed to form the B-ring oxazole.¹⁵ Structure **13** would arise from tyrosine benzofuranone **15**.¹⁰ Coupling of **14** and **15** would, upon oxazole formation, introduce the B-C-D rings into the structure. The diazamide core would then be completed upon formation of the C16-C18 biaryl bond through transition metal mediated cross coupling.

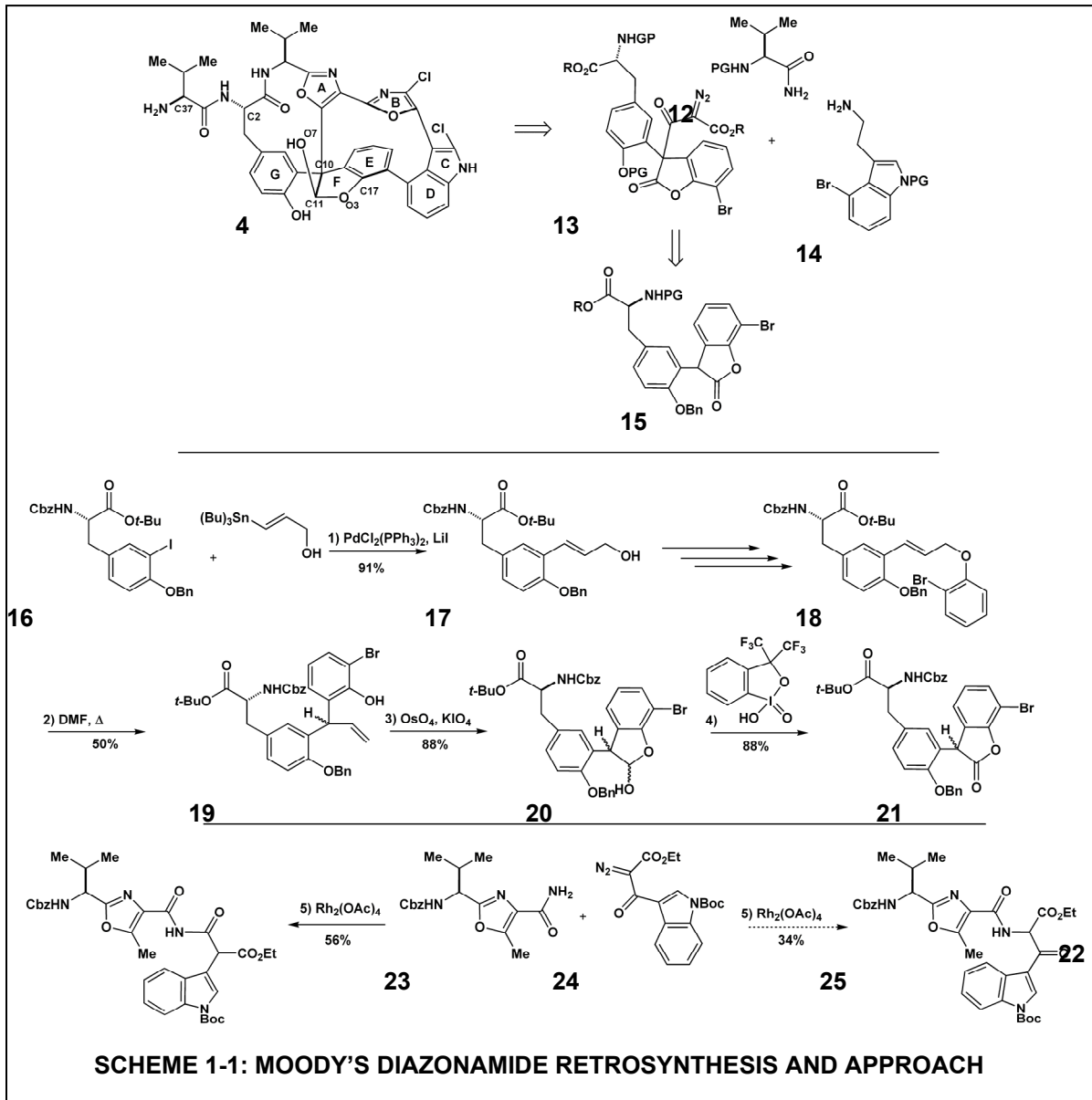
The Moody group accessed the tyrosine benzofuranone fragment **15** through elaborating a protected 3-iodotyrosine derivative via Stille coupling. Subsequent steps formed **18**, which underwent Claisen rearrangement upon heating to produce olefin **19** as a mixture of diastereomers.¹¹ Olefin oxidative cleavage with osmium tetroxide/potassium periodate produced lactol **20**, which upon hypervalent iodine oxidation with Greico's iodine afforded the benzofuranone **21**.¹¹ The conversion of **21** into a diazo compound (**13**) was envisioned as being performed through ethyl diazoacetate addition to a C10 aldehyde, presumably using the diethylzinc protocol developed previously by the Moody and coworkers. Similar to the Vedjes approach¹⁶ (vide infra), the Moody group proposed to introduce the requisite C10 aldehyde using the Black acylation reaction,¹⁰ but the synthesis of the C10 aldehyde congener of **21** has not been reported.

Moody and coworkers initially chose to explore the dirhodium(II) catalyzed intermolecular N-H carbenoid insertion reaction in the context of A-B-C-D ring diazonamide fragment (**25**). In 2000, the Moody group reported this dirhodium(II) reaction with oxazole urethane (**23**) and diazo compound **24** was a successful reaction yielding the desired ketoamide product (**25**) in 56% yield.¹³ Ketoamide **25** was then reported to form the B-ring oxazole using Wipf's Robinson-Gabriel cyclodehydration conditions (I₂, PPh₃, Et₃N).¹³ However, this claim was withdrawn in 2005 after the Moody group reassigned the product of the dirhodium (II) reaction as imide **22**.¹⁷ Imide **22** is a product of a dirhodium catalyzed Wolff rearrangement of the α -diazo- β -ketoester **24** generating an incipient ketene, which is then trapped by oxazole urethane **23**. In a later publication, the dirhodium(II) catalyzed intermolecular N-H carbenoid insertion reaction was successfully executed with a structure related to **24**, albeit in poor yields (< 30%).¹⁵ Like several other research groups, Moody and coworkers have also explored using a Suzuki reaction to form the C16-C18 biaryl bond in a simplified diazonamide model system.^{12, 15}

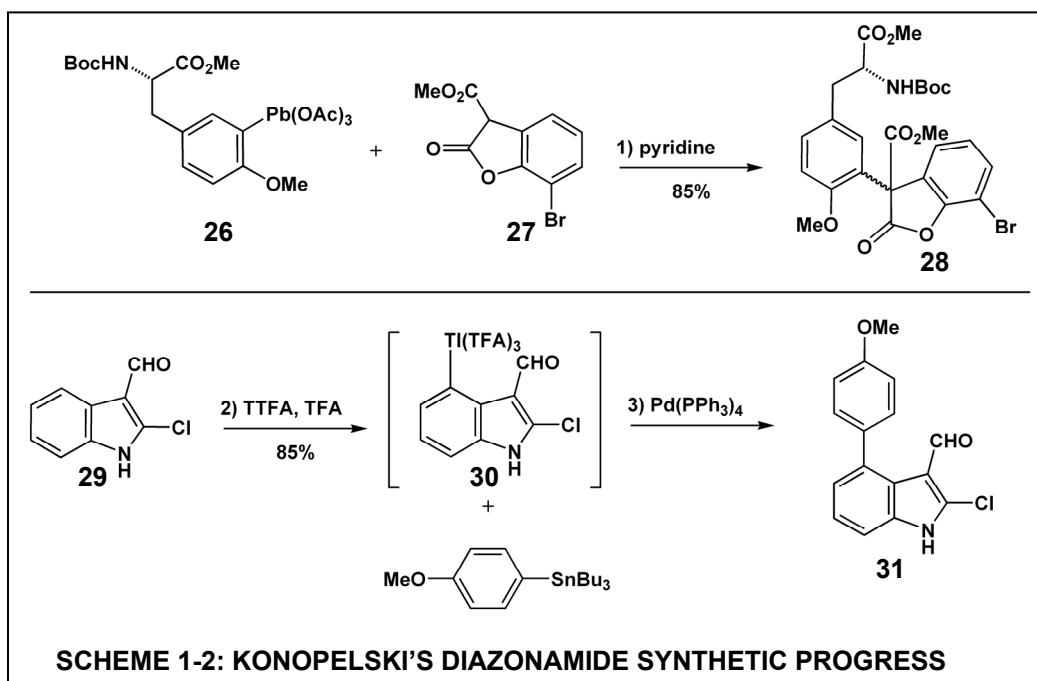
Based on the recent Moody group publications, their intent is to apply the approaches outlined here to the revised diazonamide A structure, including the use of the dirhodium(II) catalyzed decomposition of α -diazo- β -ketoester methodology.^{14, 15} Although simplified diazonamide A fragments have been accessed, there are currently no reports detailing the use of the developed Moody methodologies in undertaking a total synthesis of diazonamide A.

1.2.3.2 Konopleski Group Diazonamide A Research

The Konopleski group published the second account of synthetic efforts in the diazonamide arena in 1996.¹⁸ These initial efforts focused on employing metal catalyzed aryl



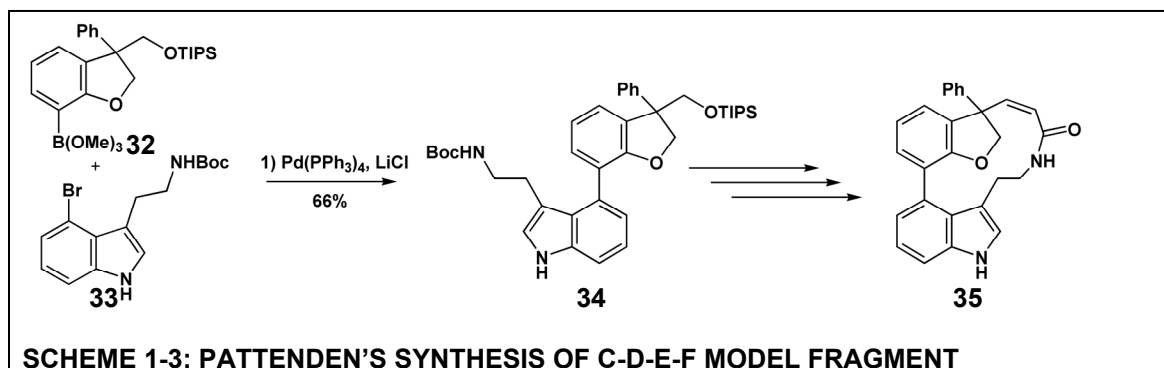
coupling reactions to construct segregated fragments of the diazonamide structure (**Scheme 1-2**).¹⁸ The Konopleski group accessed the G-F-E diazonamide fragment **28** using a lead triacetate tyrosine derivative (**26**) and the 7-bromobenzofuranone compound **27**. Aryl lead triacetate **26** was indirectly prepared from 3-iodotyrosine. First, palladium catalyzed tin-



halogen exchange produced the arylstannane tyrosine compound, which was then plumblyated with catalytic mercury.¹⁸ Similarly, the Konopelski group also sought to use the established thallation chemistry of the 4-indolyl position (**29**, **30**) to achieve a biaryl coupling with simple aryl tin compounds (**31**). This method would be used to form the C16-C18 biaryl bond in diazonamide A.

1.2.3.3 Pattenden Group Diazonamide A Research

The Pattenden and coworkers have focused their diazonamide synthetic efforts on the ABCDE macrocycle, and like several other groups, they explored transition metal catalyzed sp^2 - sp^2 coupling reactions to construct the biaryl bonds in this heteroaromatic system (**Scheme 1-3**).¹⁹ The Pattenden group sought to employ a Stille reaction with 3-stannyl substituted indoles and 3-bromooxazole to synthesize the B-C-D fragment. They accessed

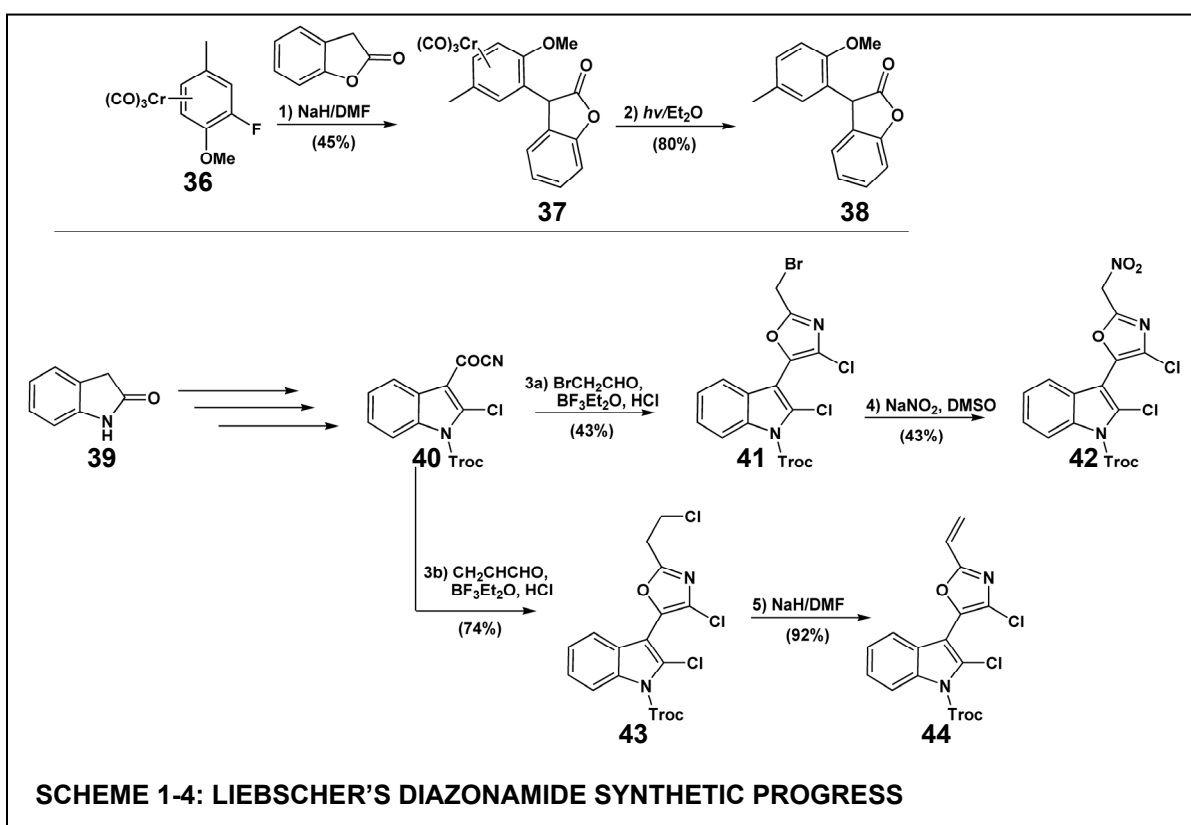


boronate benzofuran **32** in a short sequence of steps, including a Heck reaction, from a dihalogenated phenol derivative.¹⁹ After attempts to form the C16-C18 bond through use of a Ulman reaction failed, a Suzuki reaction successfully produced the desired biaryl bond between **32** and the Boc-protected 4-bromotryptamine (**33**) to form **34**.¹⁹ Standard methodology was then used to complete lactam **35**. No further elaboration of **35** was reported, nor has this developed chemistry been applied to structures more relevant to the total synthesis of diazonamide A.

1.2.3.4 Liebscher Group Diazonamide A Research

Liebscher and co-workers²⁰ developed an electrophilic arylation methodology for the formation of benzofuran-2-ones that could be applied to diazonamide C10 problem (**Scheme 1-4**).²⁰ This method uses tricarbonylchromium complexation to siphon off aryl election density and thereby activate the aromatic system for nucleophilic substitution.²⁰ In addition, the aryl tricarbonylchromium species poses a plane of asymmetry, allowing for possible diastereomeric induction.²⁰ Nucleophilic displacement of aryl fluoride **36** with the generated 2-benzofuranone enolate gave **37** in a modest 45% yield and a 85:15 diastereomeric ratio of products.²⁰ UV decomplexation of the light-sensitive tricarbonylchromium species **37** produced the racemic 3-arylbenzofuran-2-one **38**.

The Liebscher group also explored methodology to synthesize the chlorooxazole-indole fragment of diazonamide A (**Scheme 1-4**).²¹ This approach accesses both alkylnitro and aryl olefin B-C-D fragments (**42**, **44**) from oxindole (**39**) through a common Troc-protected chloroindole **40**.²¹ The B-ring oxazole of both **41** and **43** were formed using the Davis modification of the Fisher oxazole synthesis. Compounds **42** and **44** were prepared to allow for flexible incorporation of the B-C-D fragment into the diazonamide structure.



1.2.3.5 Jamison Diazonamide A Research

As part of his doctoral dissertation at Harvard University, Timothy Jamison pursued the total synthesis of diazonamide A.²² The Jamison retrosynthesis (**Scheme 1-5**) starts by removing both the valine side chain and the C-ring chlorines and by masking the reactive

C11 hemiacetal group as the benzofuranone (**45**). The chlorooxazole B-ring would be introduced via oxidative cyclization and decarboxylative chlorination of **45**. The C and D-ring components would be introduced from 4-bromotryptophan (**48**) through peptide coupling and sp^2 - sp^2 cross-coupling with the intact A-G macrocycle (**47**). The critical step in the Jamison retrosynthesis is the conversion of benzofuran **49** into benzofuranone **47** via a benzofuran–epoxidation rearrangement. In this designed operation, the A-ring oxazole would migrate, contracting the macrocycle, to form the quaternary C10 center. The thirteen membered lactam in **49** would be accessed from structure **50** through introduction of valine and oxidation of the oxazoline. Compound **50** would be synthesized through the introduction of the oxazoline A-ring precursor to structure **51**, which would arise from a cross coupling reaction of iodobenzofuran **53** and a protected form of 3-iodo-tyrosine (**52**).

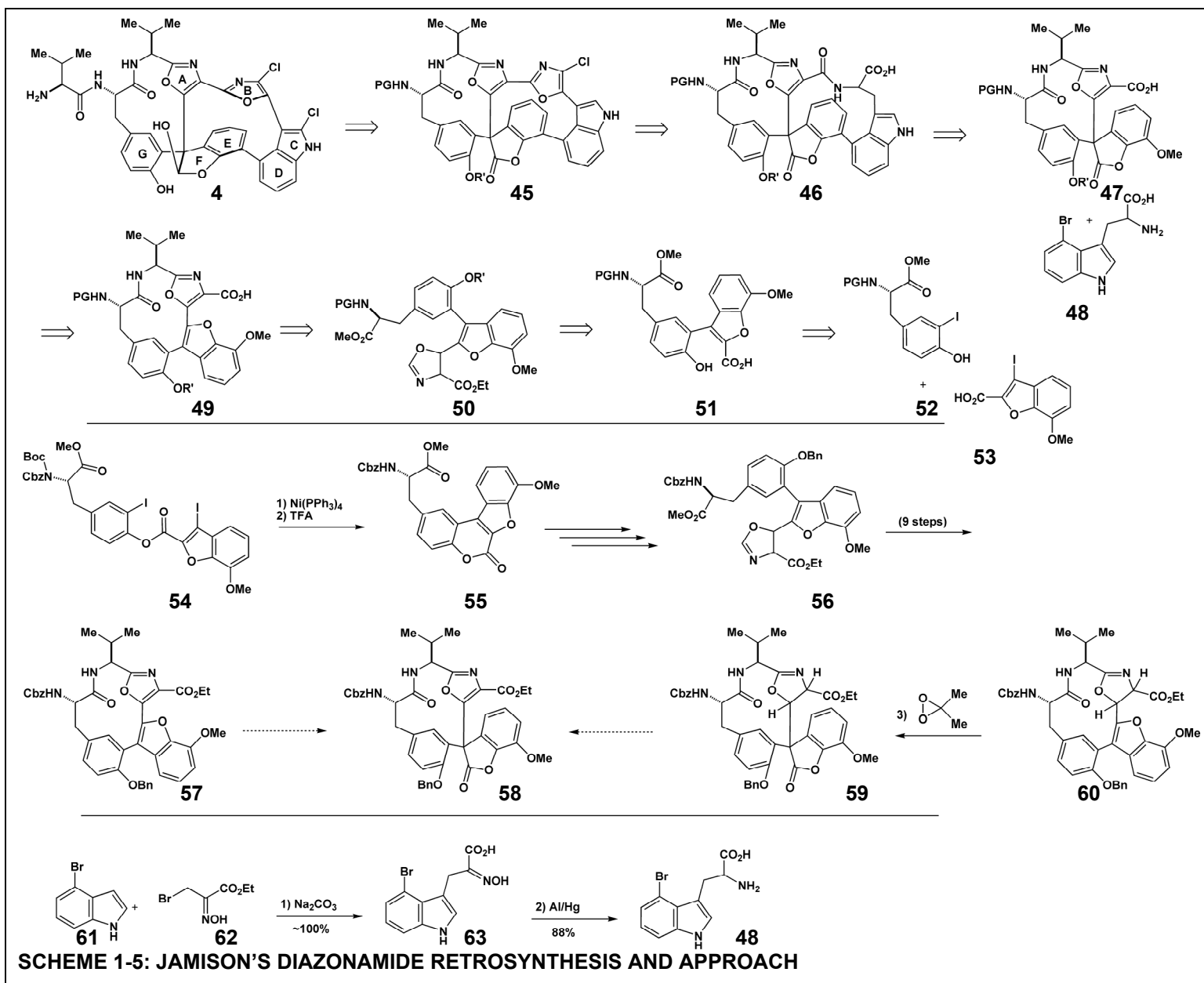
Due to an inability to cross-couple the tyrosine and benzofuran components intermolecularly, Jamison instead utilized a nickel (0) catalyzed, intramolecular Semmelhack reaction on diiodine **54** to form the desired aryl carbon-carbon bond (**55**). Straightforward elaboration produced oxazoline **56**, and after nine steps, including oxidation, protecting group manipulation, valine introduction, and macrolactamization, the benzofuran-epoxidation substrate (**57**) was prepared.²² However, all attempts to induce the migration/ring contraction epoxidation reaction with **57** failed, either through decomposition or through the formation of undesired byproducts.²² However, the benzofuran-epoxidation migration reaction was successful on simplified oxazoline structures. Based on this precedent, the desired C10 containing macrocycle (**59**) was produced via the epoxidation of oxazoline **60** with 3,3-dimethyldioxirane, although the configuration of the C10 center could not be

unambiguously assigned.²² However, oxazoline **59** could not be oxidized into oxazole **58**, with all attempts resulting in either decomposition or no reaction. Jamison performed no further research in preparing the diazonamide A core, but he did make significant progress in synthesizing the C-D ring component which would arise from 4-bromo-tryptophan. Jamison employed a [4+2] cycloaddition reaction developed by Rapoport with 4-bromoindole (**61**) and bromopyruvate oxime ethyl ester (**62**) to form oxime **63**. Aluminum/amalgam reduction generated 4-bromo-tryptophan (**48**).²²

1.2.3.6 Wipf Group Diazonamide A Research

In the Wipf group's retrosynthesis of diazonamide A (**Scheme 1-6**), the critical intermediate synthetic target is structure **64**, which contains both the B-C-D-E macrocycle and the tyrosine component.^{23, 24} The Wipf design seeks to utilize a Chan rearrangement²⁴ of amide **65**, which would be formed upon the elaboration and cyclization of benzofuran **66**. Structure **66** would arise from simpler aromatic components through the use of transition metal cross coupling reactions. In the Wipf design, both the C16-C18 bond connecting the E and D rings and the C10 center would be made through sp^2 - sp^2 coupling reactions, and the use of a chiral ligand with the transition metal catalyst would possibly allow for a stereoselective formation of the C10 center.²³

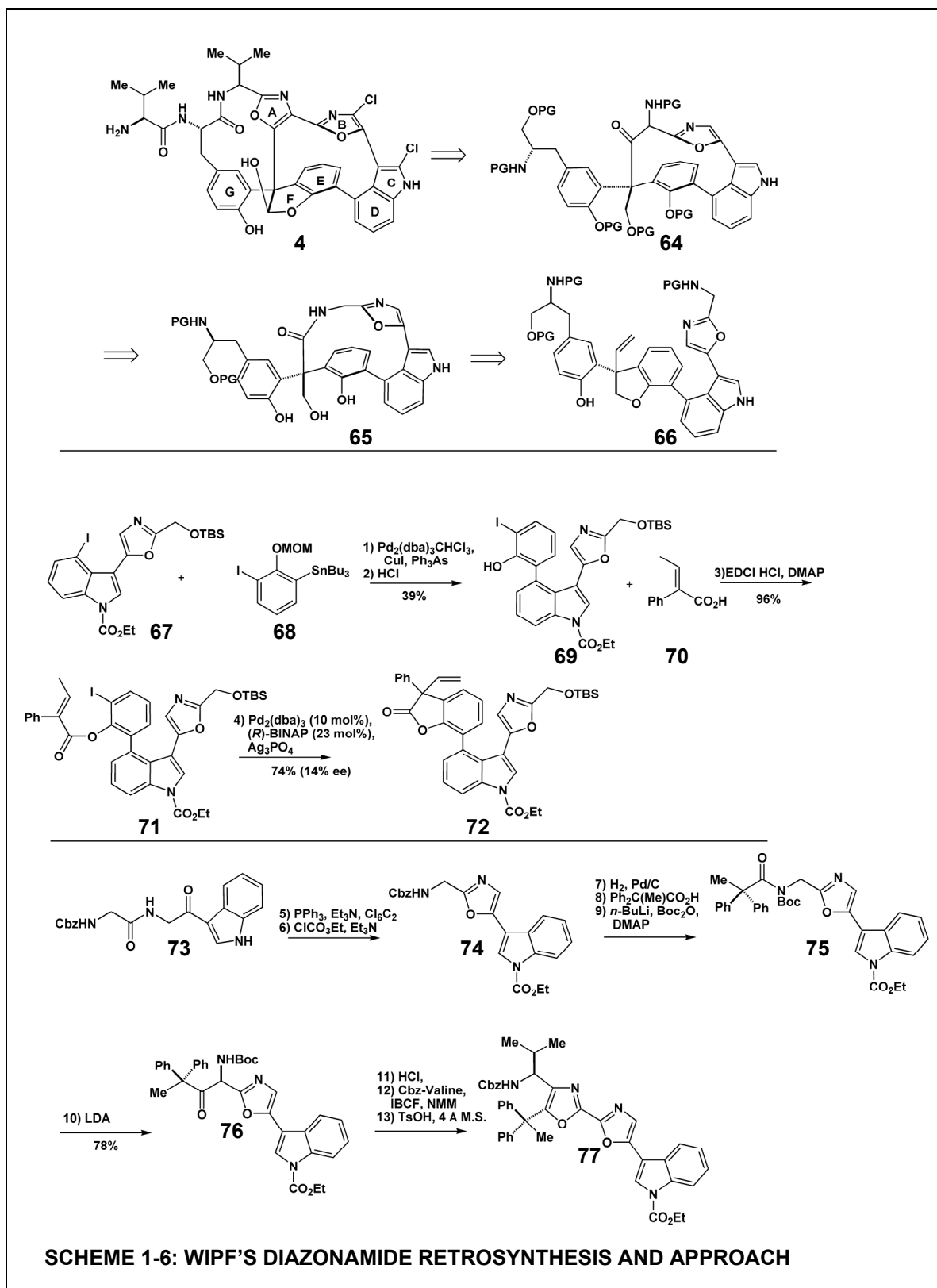
In Wipf's initial diazonamide publication with Yokokawa, diazonamide fragment **72** was accessed in a short sequence of reactions which included two cross coupling reactions.²³ This route to **72** started with preparation of the oxazolyndole compound **67** from tryptamine



through a brief synthesis that used regioselective thallation (similar to Konopelski's work¹⁸), followed by iodine transmetallation and standard oxidation/cyclodehydration methodology to form the oxazole ring.²³ **67** was cross coupled to iodophenol **68** via a Stille reaction, and following deprotection of the phenol (**69**), an EDC reaction with acrylic acid **70** yielded coupled product **71**. An intramolecular Heck reaction with the chiral (*R*)-BINAP ligand formed the C10 center in a good yield (74%) but with poor asymmetric induction (14% ee).¹⁸ Several other chiral ligands were screened but produced even less satisfactory results. Although **72** is a simplified model structure, it is easy to imagine its application to the diazonamide synthesis, especially if a tyrosine derivative is used in place of arylstannate **68**.

In addition to the chemistry described, the critical transformation in the Wipf approach was the development of the Chan rearrangement to convert the amide **65** into the oxazole precursor **64**. Wipf and Methot explored this reaction by synthesizing the oxazolyndole fragment **75** from the extended, oxidized tryptamine compound **73** in five operations.²⁴ **75** is a model system for the diazonamide framework with the diphenyl propanamide moiety serving as a C10 surrogate. Upon treatment with LDA, the tertiary amide **75** underwent the desired Chan rearrangement in 78% yield (**76**).²⁴ Removal of the Boc group, peptide coupling with Cbz-valine, and acid induced cyclodehydration produced the valine-A-B-C-D ring fragment **77** of diazonamide A.²⁴

Although the Wipf group has demonstrated the capability of their route to access the advanced diazonamide fragments **72** and **77**, there have been no published reports seeking to incorporate these fragments into a total synthesis of diazonamide A. It remains to be shown



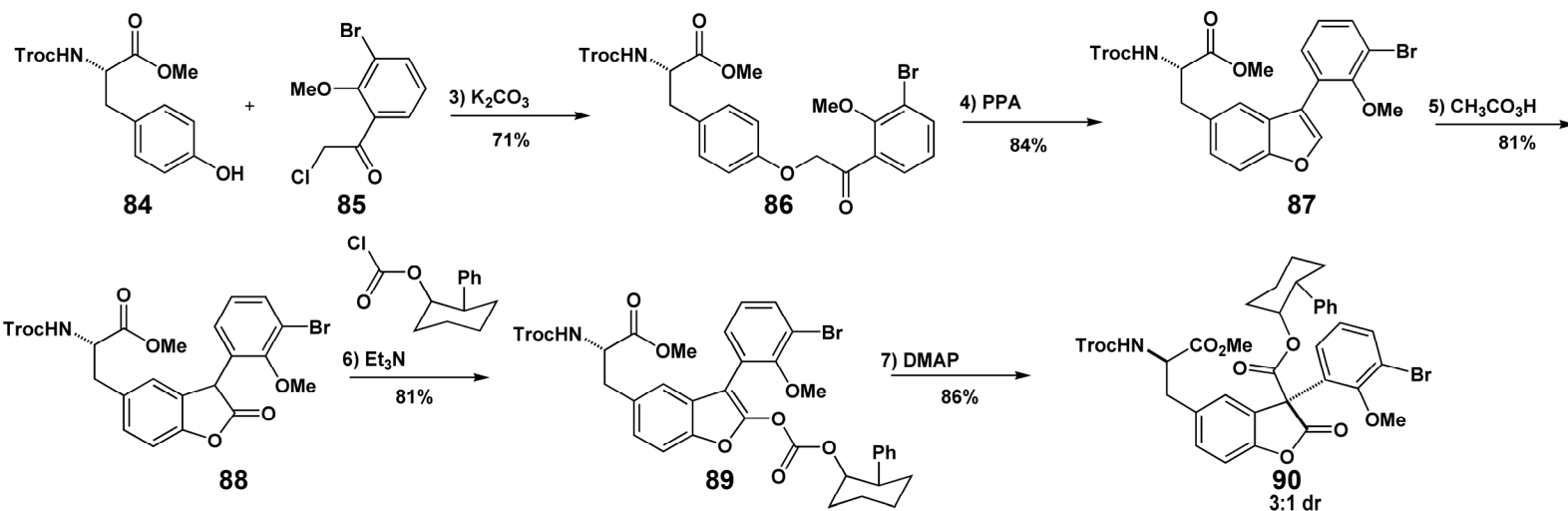
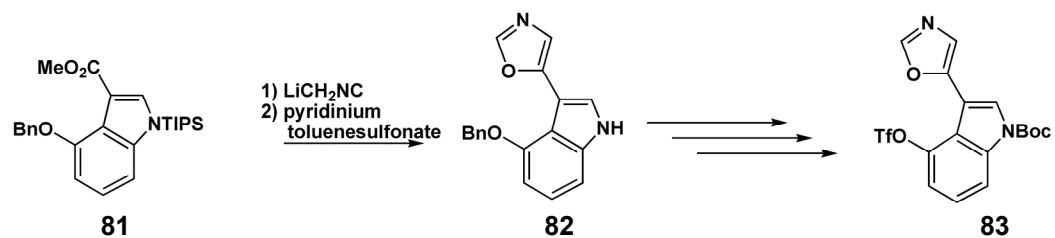
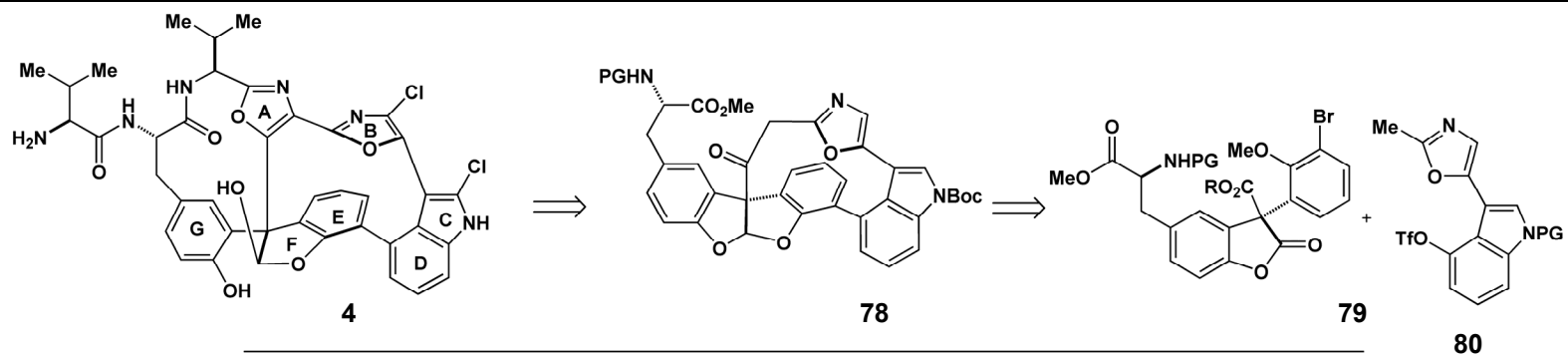
SCHEME 1-6: WIPF'S DIAZONAMIDE RETROSYNTHESIS AND APPROACH

whether the methodologies developed by Wipf may be used in union to access the diazonamide A skeleton.

1.2.3.7 Vedejs Group Diazonamide A Research

The Vedejs group's retrosynthetic analysis of diazonamide A (**Scheme 1-7**) centers on the simplification **4** into acetal **78**, which possesses a complete B-C-D-E ring macrocycle.^{16, 25-27} In their design, **78** would arise from cross coupling aryltriflate **80** with a restructured diphenylacetal form of arylbromide **79** to create the C16-C18 bond. Dieckmann cyclization would then complete the formation of the macrocycle **78**.²⁶ Vedejs and Barda were able to access the TIPS protected methyl indole-3-carboxylate compound **81** in a short route from 4-benzyloxyindole.²⁵ Utilization of the Schöllkopf reaction with lithiated propionitrile followed by treatment with pyridinium toluenesulfonate generated the oxazolyl indole **82**, which was then converted into the aryl triflate **83**.²⁵ Conversion of **83** into methyloxazole triflate, similar to **80**, was performed using *n*-BuLi deprotonation followed by alkylation with methyl triflate.²⁶

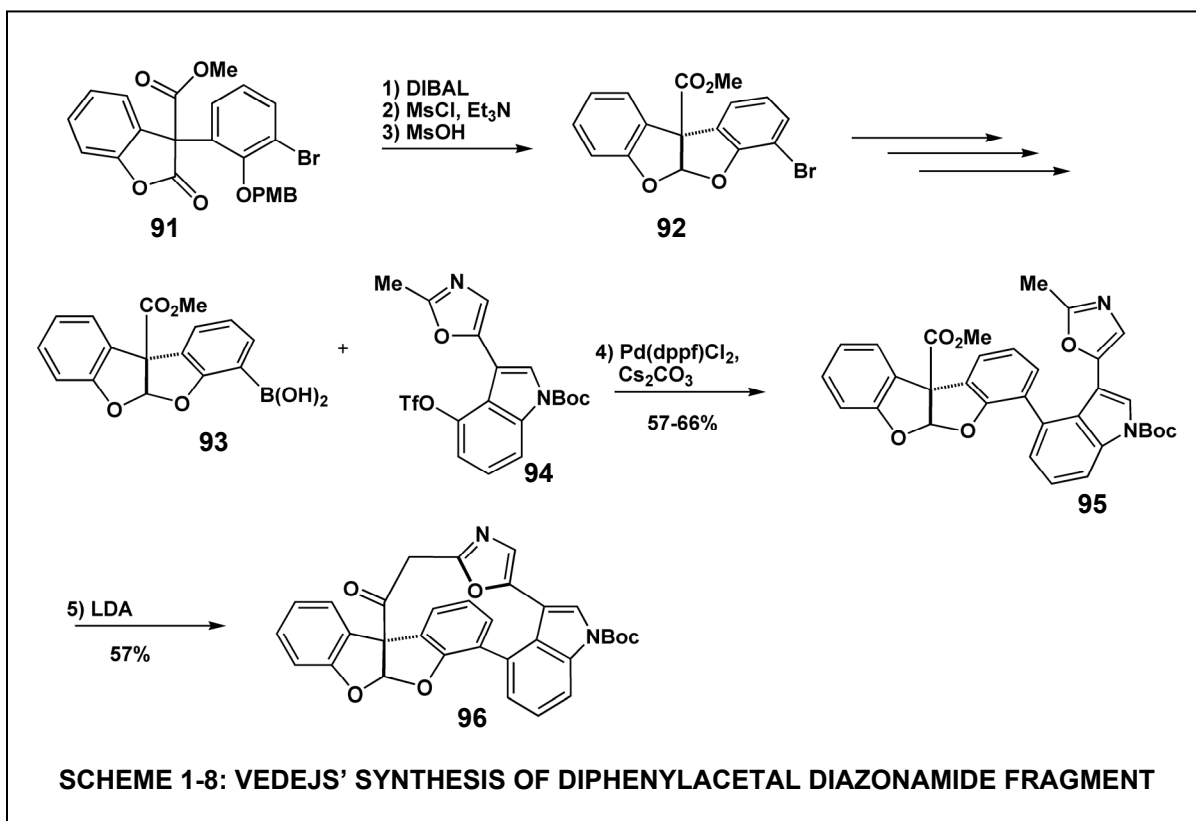
The Vedejs approach to the benzofuranone tyrosine fragment began with formation of benzofuran **87** from acid induced aromatization of **86** with polyphosphoric acid. **86** was produced through a simple nucleophilic displacement reaction of protected tyrosine **84** and α -chloro arylketone **85**.¹⁶ Benzofuran **87** was efficiently converted into benzofuranone upon treatment with peracetic acid.¹⁶ Enol carbonate **89** was formed by enolization followed by treatment with the chiral chloroformate reagent. The introduction of a chiral directing group was designed to control the diastereomeric outcome of the Black acylation reaction, which



SCHEME 1-7: VEDEJS' DIAZONAMIDE A RETROSYNTHESIS AND SYNTHESIS OF BENZOFURANONE FRAGMENT

occurred readily with DMAP catalysis to form the desired compound **90** in a high yield (86% combined for both diastereomers) and a 3:1 ratio of diastereomeric products.¹⁶ The assignment of the major diastereomeric product **90** as possessing the correct diazonamide C10 configuration was made using X-ray crystallography of the minor diastereomer.¹⁶

With the methodology developed to form the B-C-D ring fragment (**83**) and the tyrosine benzofuranone structure **90**, Vedejs and Zajac focused on the synthesis of the intact B-C-D-E macrocycle in a model system (**Scheme 1-8**).²⁶ Starting from a simplified benzofuran **91**, diphenylacetal **92** was prepared and converted into the arylboronate **93**.²⁶ Suzuki coupling of **93** and **94** produced the cross coupled product **95** in a respectable yield. Deprotonation with LDA induced the desired Dieckmann cyclization reaction to occur in a 57% yield.²⁶ X-ray crystallography and NOE experiments demonstrated that only the desired

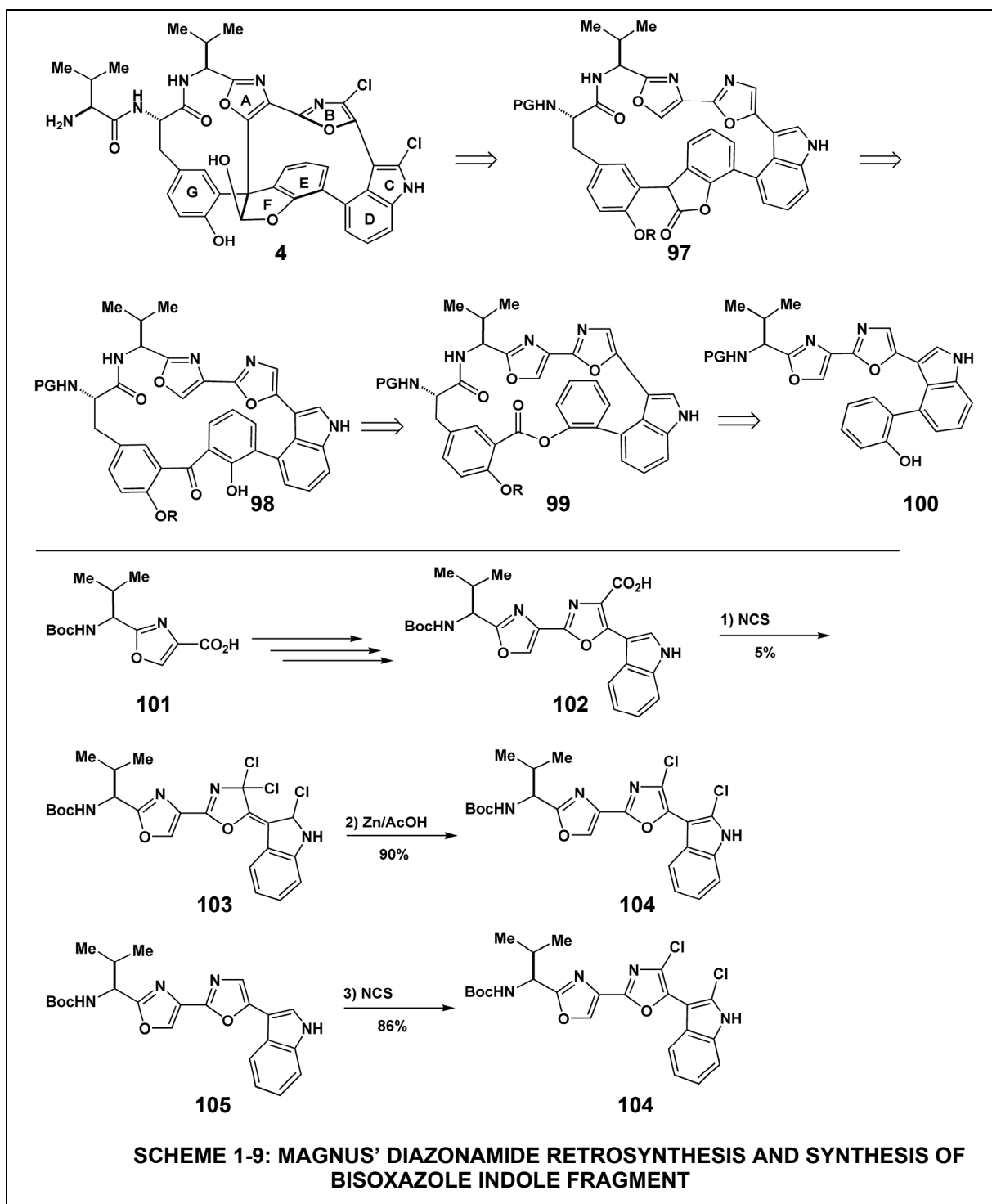


oxazole atropisomer was formed.²⁶ Although no other reports from the Vedejs group detailing the application of these described methodologies to the original diazonamide structure, the basic Vedejs retrosynthesis and design have been employed to undertake the total synthesis of the revised diazonamide A structure (vide infra Section 2.4.3).²⁷

1.2.3.8 Magnus Group Diazonamide A Research

The Magnus group's retrosynthetic approach to diazonamide A commences with the removal of the valine side chain and the peripheral chlorines, followed by elimination of the central C10 A-ring oxazole bond to yield the 23-membered polyheterocycle benzofuran **97**.²⁸⁻³¹ This approach³¹, shared by the Feldman group³², (vide infra, Section 1.4), is distinct in that it does not pursue either of the fused diazonamide macrocycles (**Figure 1-4, 10, 11**) as intermediate synthetic targets. Benzofuran **97** would arise from ketone **98**, which is to be accessed through a photo-Fries rearrangement of ester **99**. Excision of the tyrosine residue yields the valine-ABCDE fragment **100**. **100** is further disassembled into a valine bisoxazole-indole ABCD fragment and the E ring phenol.

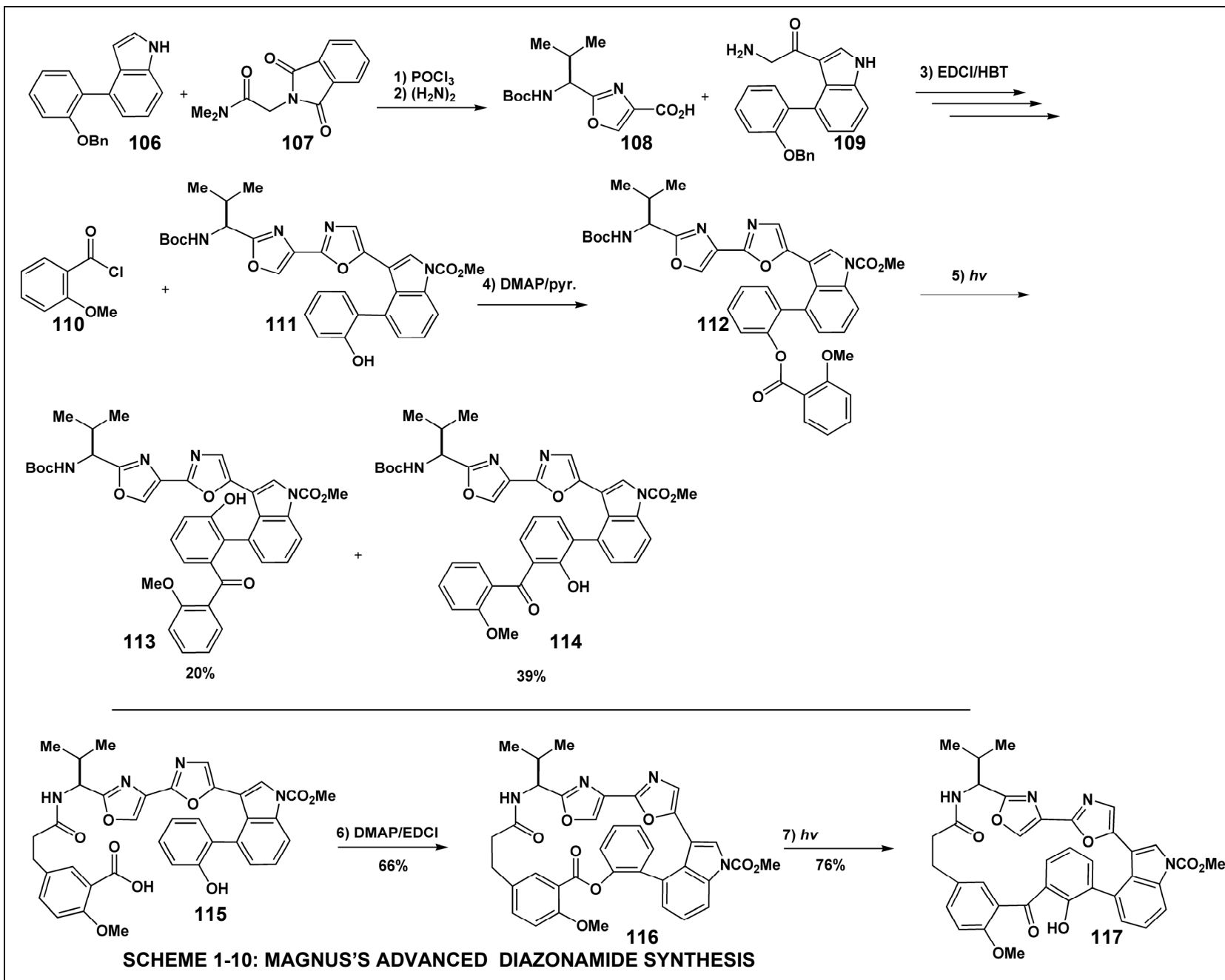
The ABCD bisoxazole indole fragment was accessed via a concise route starting from valine oxazole **101**.²⁸ Valine oxazole **101** was treated with triethylamine and isobutyl chloroformate followed by methyl tryptophan.²⁸ DDQ induced oxidation/cyclodehydration yielded bisoxazole **102**. The Magnus group performed a possible biogenetic decarboxylative chlorination with NCS but only obtained a 5% yield of decarboxylated trichloro compound **103**, which could be converted into the desired diazonamide dichloro ABCD fragment (**104**)



upon treatment with zinc in acetic acid.²⁸ A more efficient chlorination with NCS was performed on the bisoxazole tryptamine compound **105** to produce **104**.²⁸

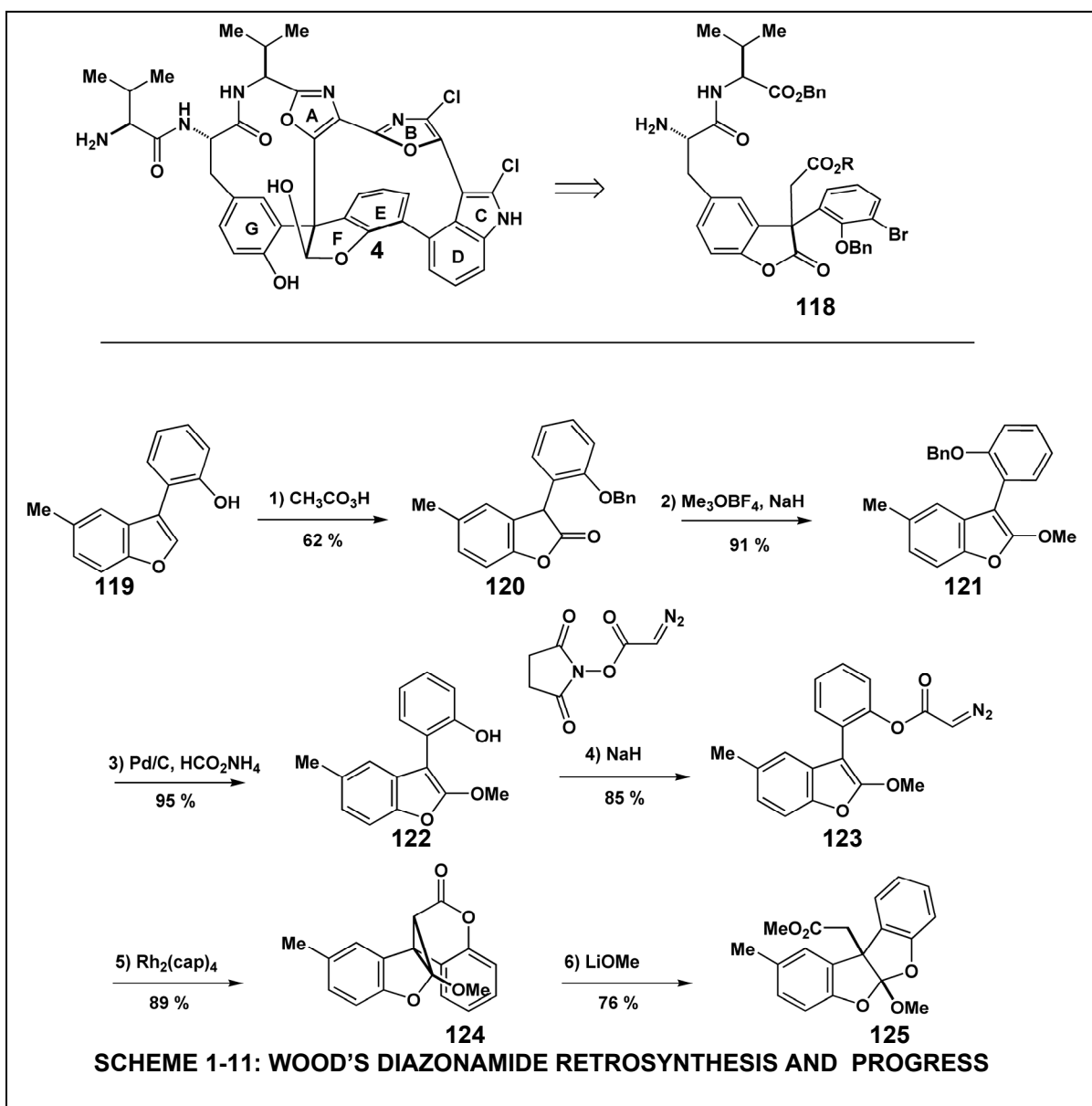
Magnus and coworkers were then able to construct the A-B-C-D-E fragment **111** through use of Vilsmeier methodology.²⁹ The *N,N*-dimethylamide phthalimido compound **107** was reacted with indole **106**, and following hydrazinolysis, oxotryptamine compound **109** was produced. This C-D-E ring fragment (**109**) was coupled with the valine oxazole compound **108** using EDC, and following protecting group manipulation and cyclodehydration, compound **111** was produced.²⁹ The Magnus group then coupled **111** and benzoyl chloride **110** with DMAP to achieve **112** as a model substrate for the photo-Fries rearrangement.³⁰ Photolysis of **112** gave two rearrangement products, an undesired regioisomer **113** and the desired ketone **114**.³⁰

The Magnus group then applied this approach and the photo-Fries reaction to the diazonamide relevant structure **115**.³⁰ DMAP/EDC treatment produced the intramolecular coupled product **116**.³⁰ Photolysis of **116** under highly dilute conditions produced the desired compound **117** in 76% yield as a 2:1 mixture of room temperature atropisomers.³⁰ Despite having accessed the macrocycle (**117**), there were no subsequent reports detailing the successful formation of the C10-A-ring oxazole bond. The Magnus group did report model studies with simple benzofuran compounds³¹, but they likely had abandoned this approach upon learning of the revised diazonamide structure in 2001.



1.2.3.9 Wood Group Diazonamide A Research

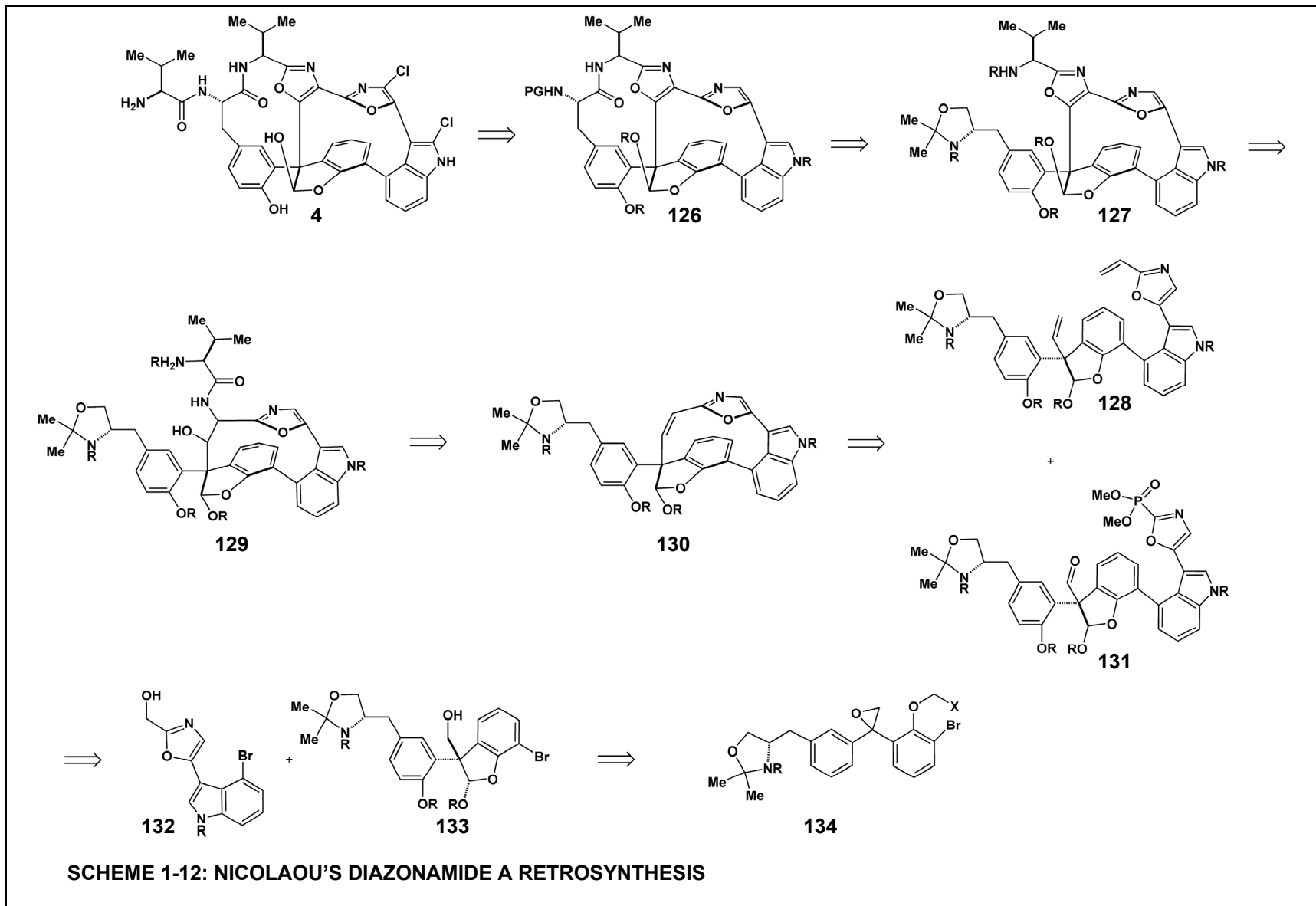
The Wood group's efforts dealing with the total synthesis of diazonamide A focused on methods to access the C10-centered G-F-E diazonamide fragment.^{33, 34} In the Wood group's retrosynthetic design, the ABCDE polycycle is removed to give benzofuranone **118**



as an intermediate synthetic target (**Scheme 1-11**).^{33, 34} The Wood group developed an innovative cyclopropanation/ring-opening approach to form the C10 center.^{34,35} Benzofuran **119** was converted into α -diazo ester **123** through a short sequence of reactions (**120-122**).³⁴ Dirhodium(II) decomposition of the diazo compound efficiently formed the desired cyclopropane ring (**124**) in 89%.³⁴ Treatment of cyclopropane **124** with lithium methoxide yielded cyclic structure **125** containing the C10 quaternary center.³⁴ A major advantage of the cyclopropanation/ring opening strategy is the capability of induce asymmetry in the formation of the C10 center through use of a chiral dirhodium catalyst.³⁴ Use of Doyle's catalyst was able to form cyclopropane **124** in 45 ee%. Following Harran's structural correction in 2001, the Wood group applied the cyclopropanation strategy to a simple model system relevant to the revised structure, revised structure.³³

1.2.3.10 Nicolaou Group Diazonamide A Research

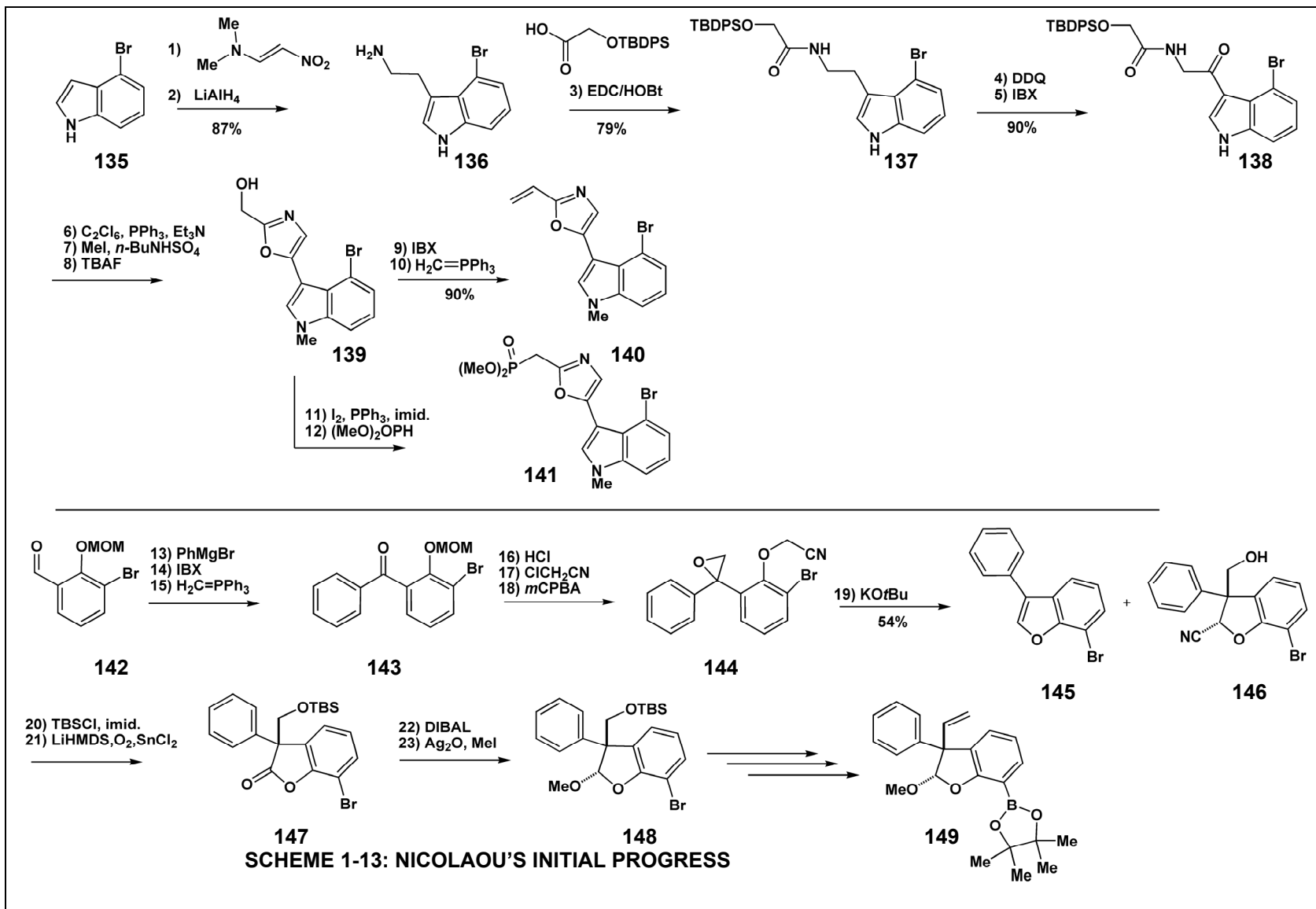
In 2000, the Nicolaou group began publishing accounts detailing their research towards the total synthesis of diazonamide A.³⁶⁻⁴⁰ The Nicolaou retrosynthetic approach (**Scheme 1-12**) began with simplifying **4** into protected hemiacetal **126**, followed by breaching the A-G macrocycle at the amide bond to give **127**.³⁶⁻³⁹ Opening the A-ring oxazole (**129**) followed by the removal of valine and the amino alcohol functionality would give olefin **130**. In the initial design, macrocycle **130** would arise either from olefin metathesis of **128** or through Horner-Wadsworth-Edmonds olefination of **131**.³⁶⁻³⁹ Structures **128** and **131** are deconstructed into oxazolyl indole **132** and benzodihydrofuran **133**, and these fragments would be joined through use of biaryl cross coupling.³⁶⁻³⁹



Benzodihydrofuran **133** would be accessed through a rearrangement of epoxide **134**.³⁶⁻³⁹

The Nicolaou group commenced their work in the diazamide A arena by exploring methodologies that would allow for closing macrocycle **130** through intramolecular olefination.^{36, 39} Using established chemistry, the Nicolaou group was able to elaborate 4-bromoindole (**135**) into oxazolyl indole **139** in eight operations.^{36, 39} **139** was a critical intermediate capable of being converted into terminal olefin **140** through oxidation to the aldehyde followed by a Wittig reaction.^{36, 39} **139** was also converted into phosphonate **141** through iodination of the hydroxyl, followed by S_N2 displacement of the primary iodine with deprotonated dimethylphospite.³⁶ By using this flexible route, diazamide B-C-D fragments capable of olefin metathesis or undergoing a HWE reaction were achieved.³⁶

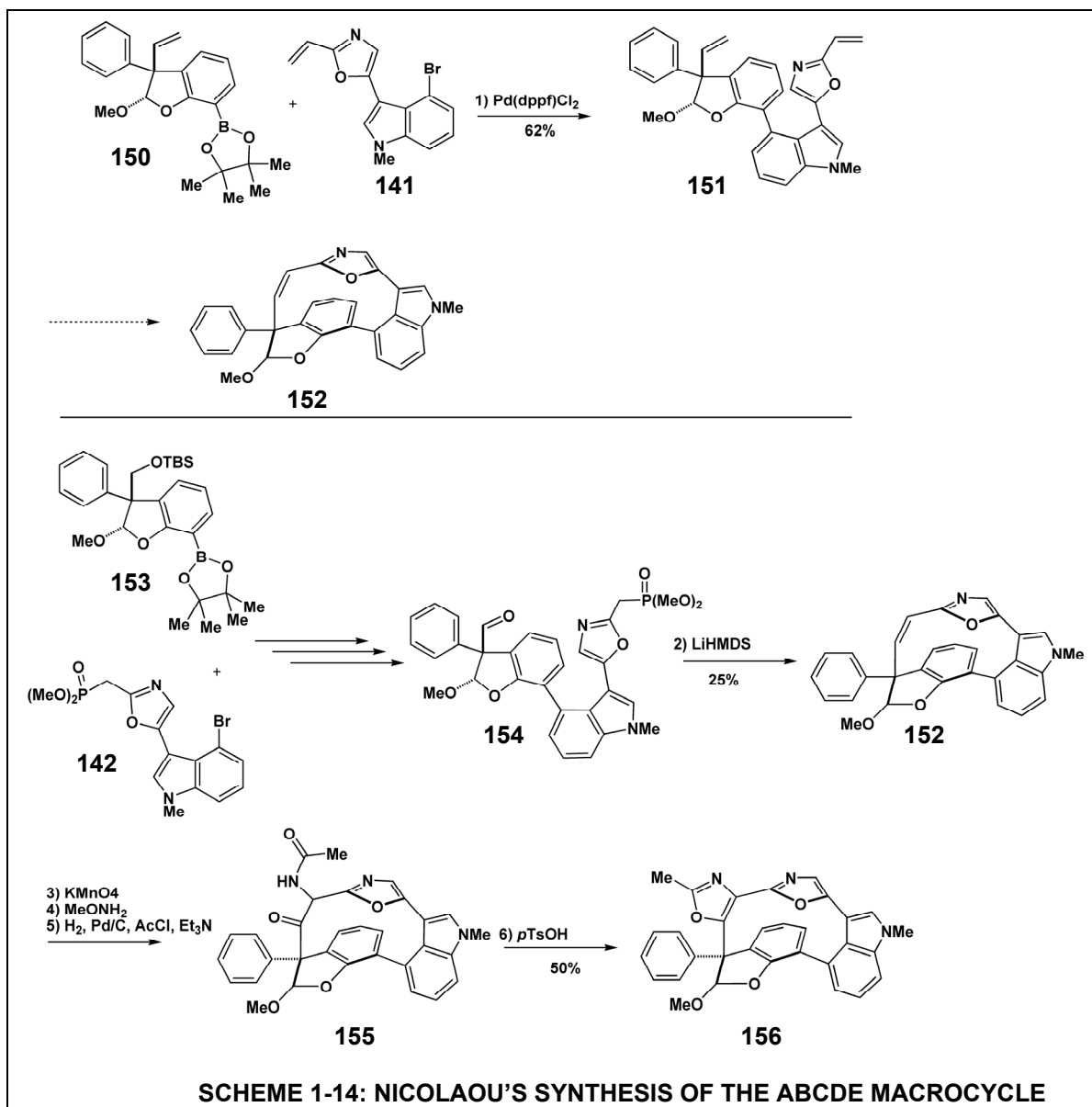
Nicolaou and coworkers accessed the benzodihydrofuran component starting from aldehyde **142**.³⁶ Introduction of phenyl Grignard followed by IBX oxidation and Wittig olefination produced methylene **143**.³⁶ Protecting group substitution was then followed by epoxidation with *m*CPBA to produce epoxide **144**.³⁶ After screening several bases and substrates,³⁹ treatment of **144** with potassium *tert*-butoxide produced the desired benzofuran compound **146** in a 54% yield, in addition to a small amount of byproduct benzofuran **154**.³⁶ Deprotonation of the cyano methylene group leads to a selective 5-*exo*-tet opening of the epoxide ring to produce the desired *trans* racemic product **146**.^{36, 39} Stereoselective



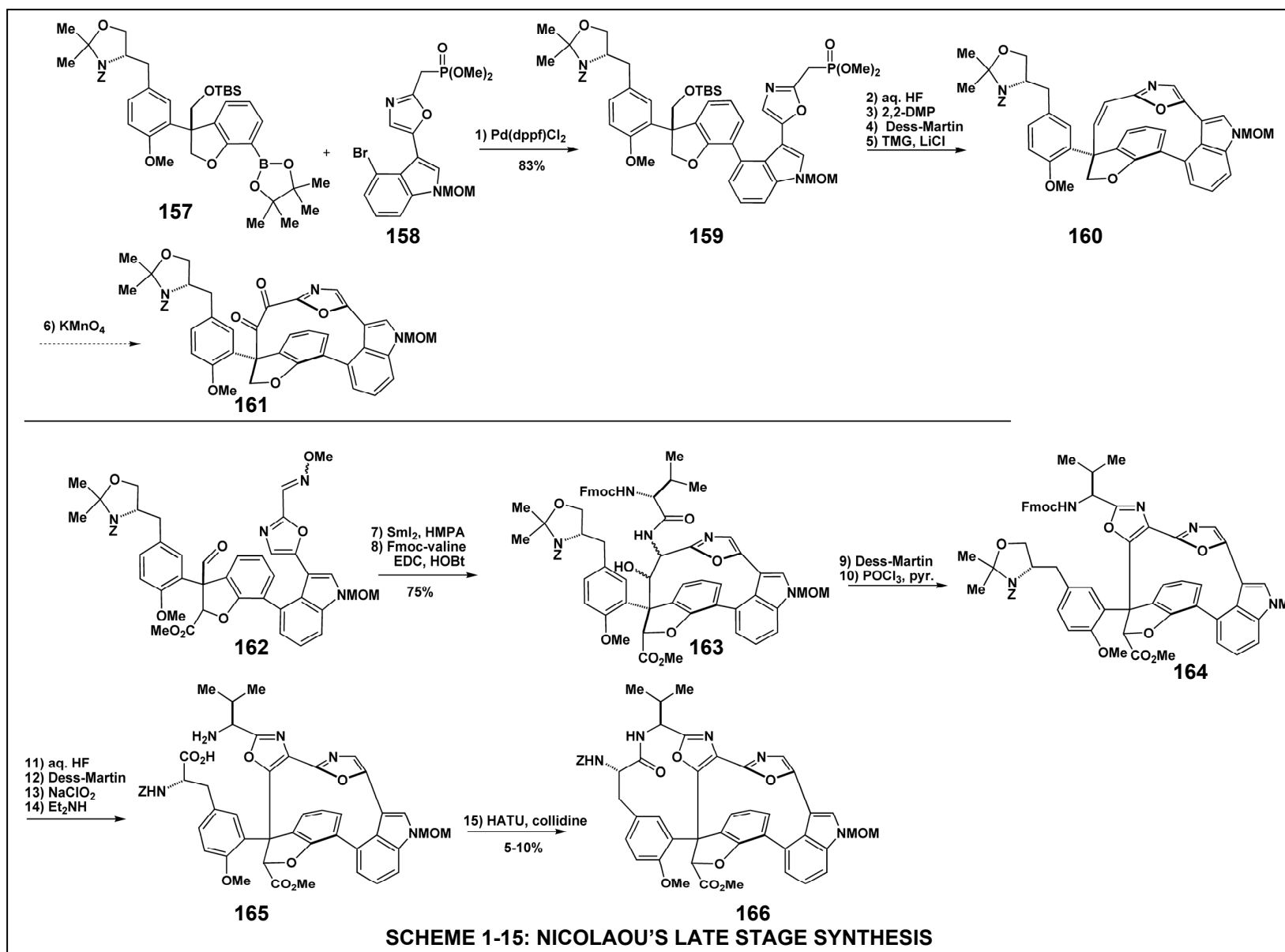
epoxidation might allow for the developed of a enantioselective route in forming the C10 quaternary center in **146**.³⁶ Silyl protection of **146** followed by oxidation yielded benzofuranone **147**.³⁶ After reduction and methylation (**148**), several subsequent conventional steps produced olefin boronate **149**.^{36, 39} Palladium mediated Suzuki cross-coupling between components **150** and **141** produced the bridging C16-C18 biaryl bond in **151**.(Scheme 1-14)^{36, 39} However, macrocycle **152** could not be formed through a olefin metathesis reaction.^{36, 39} This failure was conjecturally attributed to the severe steric hindrance of **151**.^{36, 39}

The Nicolaou group was able to access **152**, albeit in a low yield, through use of the alternative HWE reaction with phosphonate **154**. The HWE was performed at 0 °C since **154** underwent a fragmentation reaction producing the unwanted benzofuran compound (similar to **145**) at higher temperature.^{36, 39} However, at 0 °C, **154** exists as a 1:1 mixture of two non-converting atropisomers, which limits the maximum yield of the olefination reaction to 50%.^{36, 39} Compound **152** was produced as only one atropisomer, and unexpectedly, material with the opposite stereochemistry (**154**) at the C11 position failed to participate in the olefination reaction.^{36, 39} **152** was elaborated to introduce the A-ring oxazole through oxidation to the diketone, methyl oxime formation, and a combined oxime reduction/amine acetylation reaction to give oxazole precursor **155**.³⁷ Cyclodehydration with p-toluenesulfonic acid in refluxing benzene gave the completed ABCDE macrocycle **156**.³⁷

With **156** achieved, the Nicolaou group sought to apply their developed model system methodologies to the total synthesis of diazonamide A (Scheme 1-15).³⁹ Tyrosine-containing compound **157** was readily prepared³⁹ and Suzuki coupled with phosphonate **158**.³⁹ **158** was



converted into the HWE substrate, and the desired olefin compound (**160**) was successfully achieved in a substantially improved yield (55-60%) over the model system.³⁹ However, macrocycle **160** proved completely resistant to olefin oxidation, making introduction of the A-ring oxazole impossible.³⁹



In response to this impasse, the Nicolaou group developed a samarium (II) iodide induced hetero pinacol reaction to form the BCDE macrocycle.^{37, 38} This reaction was first found to be successful on a model system similar to **154**.^{37, 38} The hetero pinacol substrate was accessed by incorporating a hydroxyl oxazolyl indole fragment (similar to **139**) into the established synthetic route.³⁸ Oxidation of the hydroxyl group to the aldehyde followed by treatment with hydroxylamine produced the oxime functionality.³⁸ In applying this reaction to structures relevant to the total synthesis of diazonamide A, the Nicolaou group modified the oxidation state at the C11 position from methoxy into the methyl ester (**162**).³⁸ By introducing the ester group, the undesired benzofuran-forming fragmentation reaction was made inoperable.³⁸ This more stable substrate allowed for the utilization of higher reaction temperatures in exploring the hetero pinacol reaction.³⁸

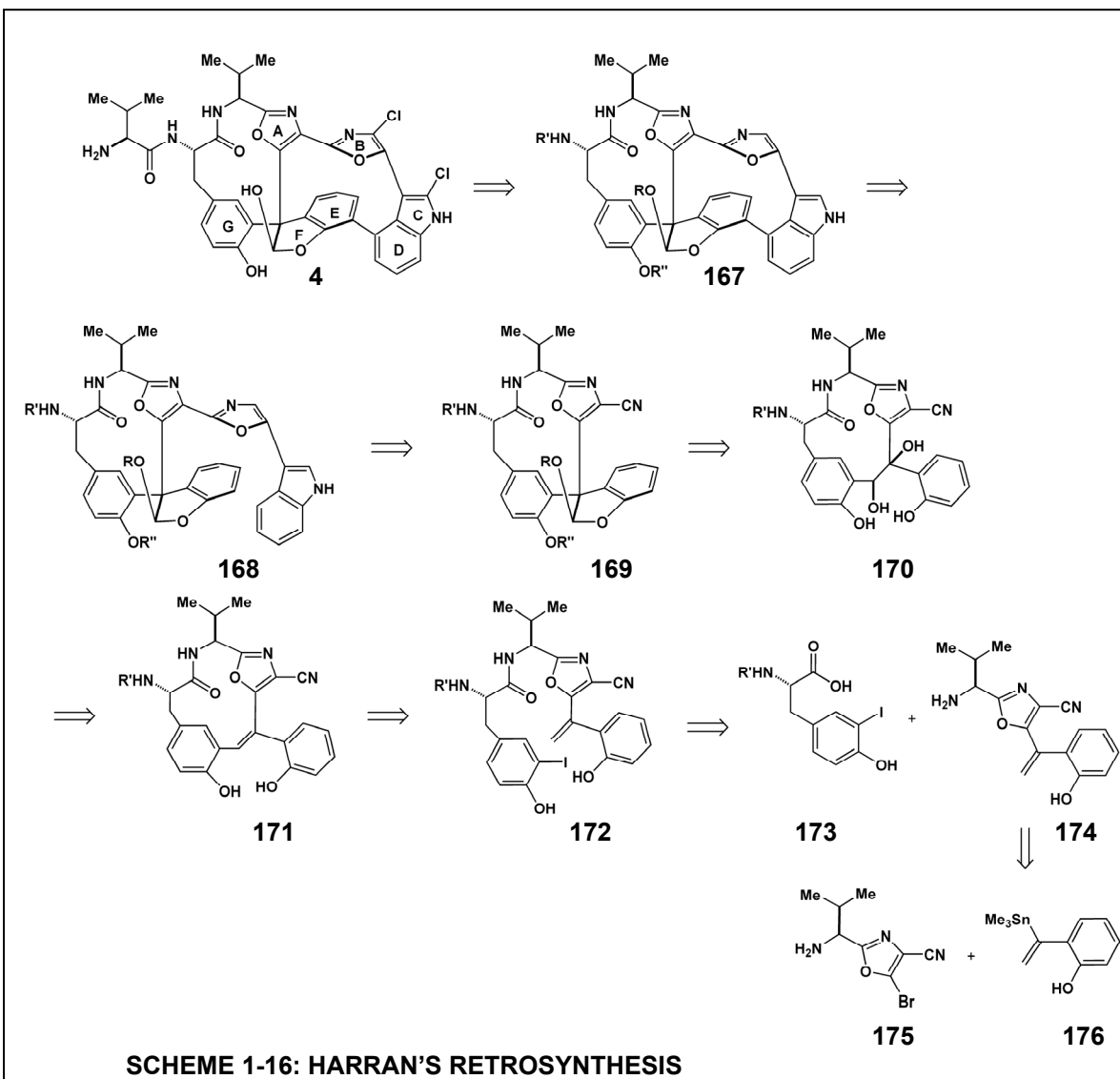
Subjecting oxime aldehyde **162** to samarium (II) iodide in the presence of HMPA at 25 °C, followed by acylation of the produced amine with Fmoc-valine, yielded the desired macrocycle **163** in modest yields (40-45%).³⁸ Formation of the A-ring oxazole via oxidation/cyclodehydration was successful (**164**).³⁸ Lactamization substrate **165** was prepared from **164** through protecting group removal and oxidation of the alcohol to the carboxylic acid.³⁸ HATU coupling produce the desired diazonamide core **166**, albeit in very poor yields (5-10%).³⁸ The conversion of **166** into diazonamide A would only require deprotection, halogenation, C11 reduction, and introduction of the valine side chain to complete the total synthesis.³⁸ However these final steps were never carried out by the Nicolaou group due to the Harran group's completion of the total synthesis of **4** and publishing the revised structure.

Much of the chemistry developed in this route however, was applied to a subsequent total synthesis of the revised diazonamide A structure (*vide infra*, Section 1.2.4).^{41, 42}

1.2.3.11 Harran's Total Synthesis of the Original Diazonamide A and B Structures (2001)

The Harran approach to the synthesis of diazonamide A⁴³⁻⁴⁶ focused on two major challenges. The stereoselective construction of the C10 quaternary center in the context of the completed A-E-F-G ring structure of the molecule and the formation of the C16-C18 biaryl bond as the final skeletal construction. By synthesizing an intact A-G macrocycle (**Figure 1-4, 10**) before the introduction of the C16-C18 bond, atropisomerism in the ABCDE polyheterocycle (**11**) could be avoided. The Harran retrosynthesis (**Scheme 1-16**) begins with the masking of the labile C11 hemiacetal and the removal of the valine side chain and peripheral chlorines (**167**). The critical formation of the C16-C18 biaryl bond would arise from the acyclic variant (**168**) requiring the adoption of the desired atropisomer for the bond to form. The B,C, and D-rings would be made through oxazole formation of the peptide coupled tryptamine, or a related congener, with the diazonamide core (**169**). The stereoselective formation of the triarylacetaldehyde diazonamide core (**169**) is the critical construction within this approach, and it was envisioned as being accessed through a ring-contracting pinacol rearrangement of the precursor diol (**170**) to afford the C10 quaternary center.⁴³ The pinacol ring contraction allows transference of the defined stereochemistry, with inversion, in forming the C10 center. Formation of the 13-membered macrocycle **171** was envisioned as proceeding through a metal catalyzed cross-coupling reaction involving a

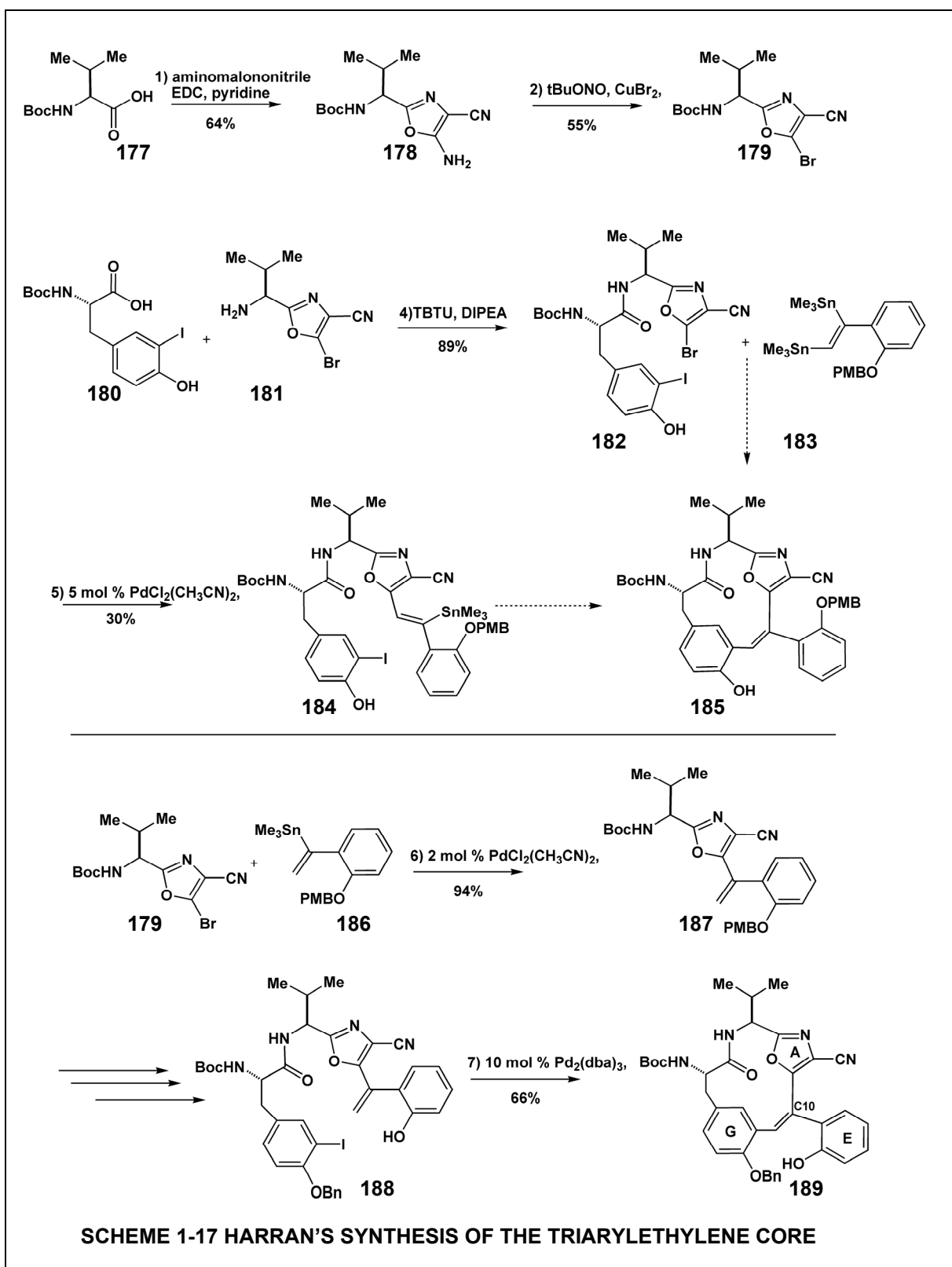
modified tyrosine residue (**173**), a halogenated valine oxazole derived A-ring precursor (**175**), and a styrene derived E-ring fragment (**176**).



This synthesis commences with formation of the A ring fragment through EDC peptide coupling of BOC-protected valine (**Scheme 1-17**, **177**) and aminomalononitrile to afford aminooxazole **178**.⁴³ Sandmeyer bromination then produced the desired aryl cross-coupling component (**179**).⁴³ The initial efforts sought to form the macrocycle through a

tandem, or stepwise, Stille reaction(s) with the peptide coupled A-G fragment (**182**) and a stannylated styrene derivative (**183**). Although the single cross-coupled Stille product (**184**) could be isolated, subsequent endocyclization was not attained.⁴³ However, this unsuccessful effort revealed that selective protodestannylation of the bis-stannylated compound **183** occurred upon treatment with oxalic acid-infused silica gel. This discovery allowed for a successful sequential cross coupling reaction to be employed.⁴³

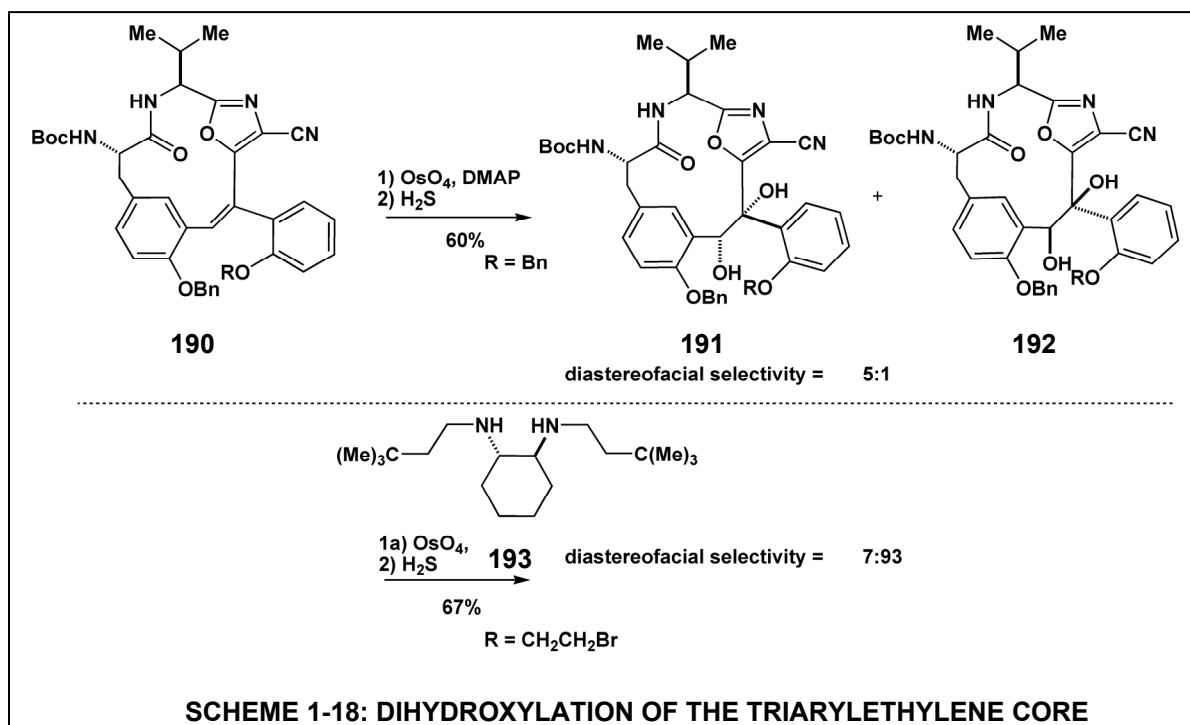
First, the bromooxazole A fragment (**179**) was coupled to the protected mono-stannane **186** via a Stille reaction. In subsequent publications, a zirconium mediated Negishi cross coupling reaction using α -chlorostyrene was developed to replace the Stille reaction, eliminating the need for stannate formation.⁴⁶ Removal of both the carbamate and benzoate protecting groups produced the aminophenol compound **187**, that was peptide coupled with *N*-BOC-protected 3-iodotyrosine to form **188**.⁴³ The desired ethylene compound (**189**) was then formed via a palladium catalyzed Heck reaction.⁴³ The initial Heck conditions of 10% [Pd₂(dba)₃] with an equivalent of silver phosphate⁴³ were later improved upon introduction of the 2-(di-*tert*-butylphosphanyl)biphenyl ligand to the reaction.⁴⁴ This ligand likely produces a more robust catalyst increasing catalytic turnover.⁴⁴ Interestingly and unexpectedly, the removal of the phenol protecting group was critical for the successful Heck reaction, suggesting that pre-organization of the palladium catalyst with the free phenol is required for



SCHEME 1-17 HARRAN'S SYNTHESIS OF THE TRIARYLETHYLENE CORE

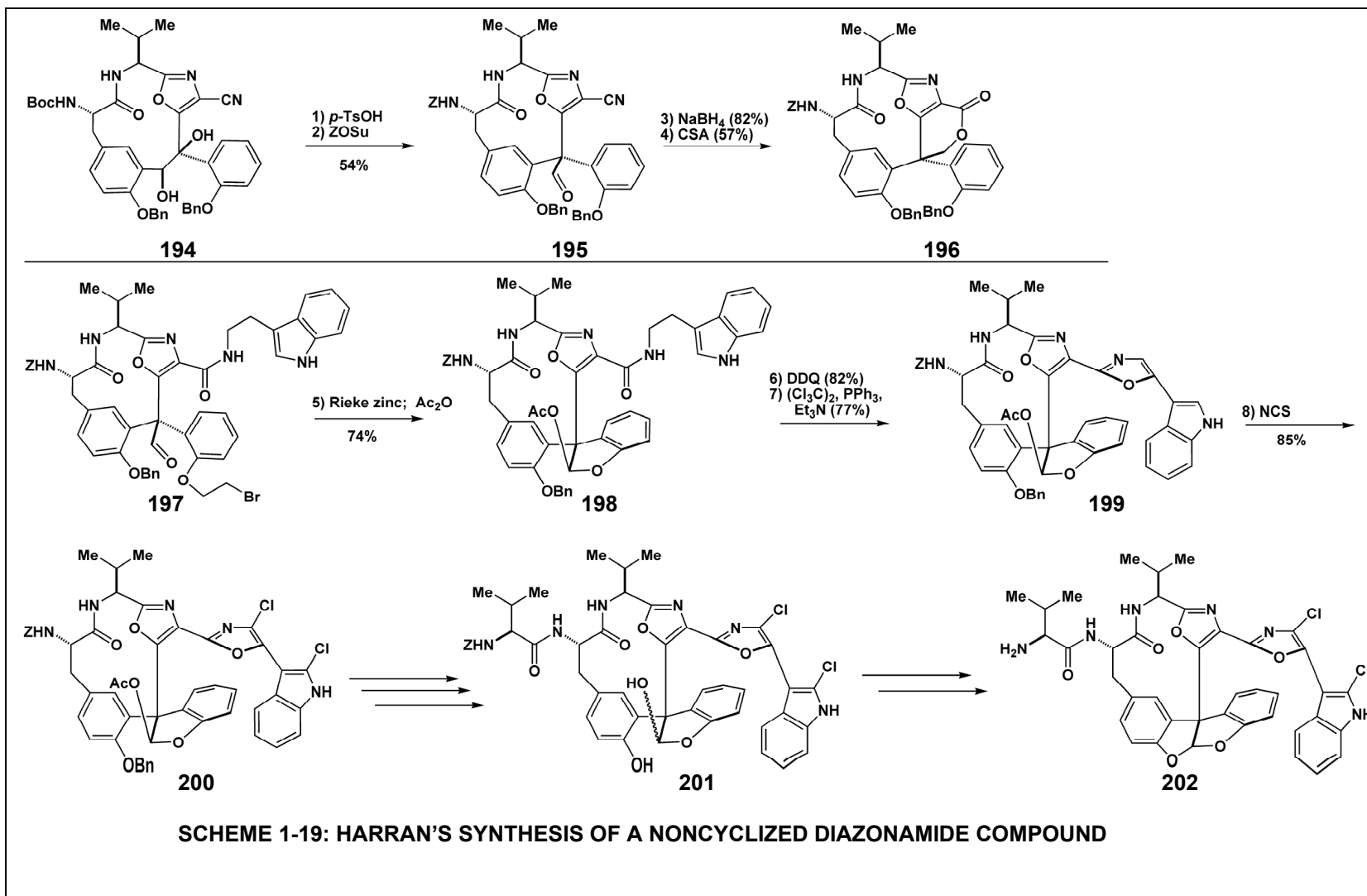
cross-coupling to occur. The triarylethylene compound achieved (**189**) possess the diazonamide A-G ring macrocyclic (**10**) framework.

Dihydroxylation of **189** was realized through stoichiometric osmylation followed by treatment with hydrogen sulfide to decompose intermediate osmium glycolates (**Scheme 1-18**).⁴⁴ Efforts to predict the facial bias of the triarylethylene compound to osmylation were inconclusive,⁴⁴ but the undesired α -glycol was produced in a 5:1 d.s. ratio (**191:192**).⁴⁴ This result was later improved to a 93:7 diastereofacial selectivity for the desired syn β -glycol (**192**) using the complexed osmium reagent **193** to achieve a mismatched stereochemical induction.⁴⁶ The facially selective dihydroxylation is the only stereochemical inducing reaction in the Harran total synthesis. Critically, the desired pinacol rearrangement does



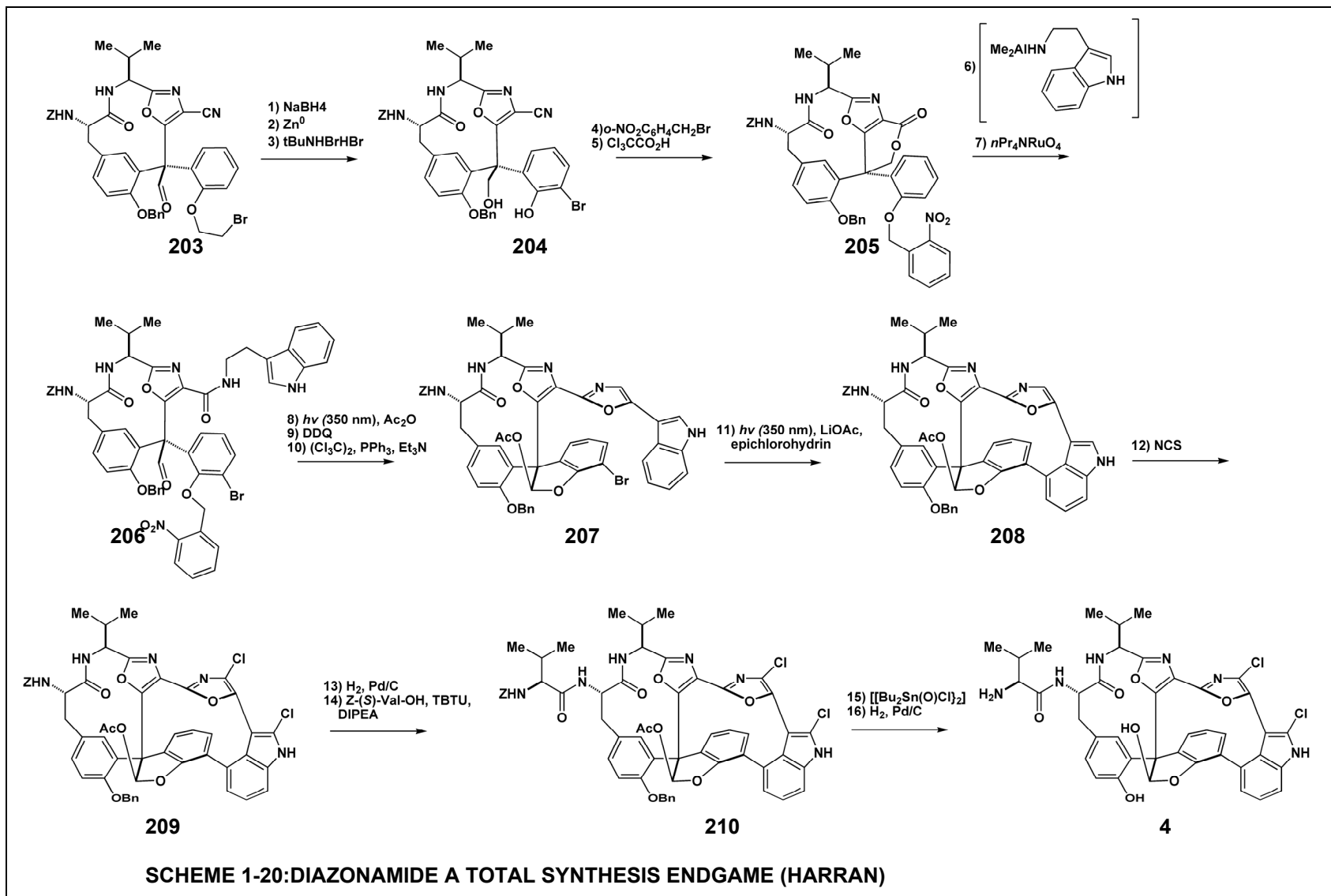
occur under forcing conditions with complete transference of C10 stereochemistry, with inversion, to the product (**Scheme 1-19, 195**).⁴⁴ This event is likely mediated by a bridging phenonium ion, and stereochemical fidelity is maintained in both syn glycol epimeric series.⁴⁴

With the diazamide core successfully accessed, the major challenge remaining was the formation of the C16-C18 biaryl bond. Several methods to achieve this linkage were attempted including internal oxidative phenolic coupling of a serotonin derived B-C-D ring fragment⁴⁴ and Michael addition to an indoloquinone.⁴⁵ Although unsuccessful, these attempts developed the methodologies and ideas that ultimately allowed for the attainment of the C16-C18 bond formation. Following Cbz protection of the C2 amine, the diazamide core (**195**) was elaborated through sodium borohydride reduction of the C11 aldehyde.⁴⁴ At this point in the Harran group's synthetic efforts, several divergent routes were employed to produce the various substrates to attempt C16-C18 bond formation.⁴⁴⁻⁴⁶ A common feature of all the routes explored is the utilization of the C10 carbinol as an internal nucleophile to convert the heteroaryl nitrile into an ester equivalent.⁴⁴⁻⁴⁶ Hydrolysis of the aryl nitrile could only be achieved through formation of valerolactone **196**.⁴⁴ The introduction of tryptamine, and various tryptamine congeners, through peptide bond formation was uncomplicated (**197**).⁴⁴⁻⁴⁶ The Harran group also used different methods to mask the reactive C10 functionality, but the most important approach was formation of the acetylated hemiacetal (**198**).^{45, 46} Four electron oxidation produced the β -ketoamide, and subsequent dehydration yielded the B ring oxazole; the final



diazonamide aryl substituent (**199**). This substrate (**199**) allowed for the development of methodologies useful in the diazonamide endgame. Using the procedure published by the Magnus group,²⁸ the non-cyclized substrate **199** readily underwent controlled, sequential aryl chlorination with *N*-chlorosuccinimide (**200**).⁴⁵ Deprotection of both remaining protecting groups through hydrogenolysis was tolerated by the halogenated substrate, and acylation of the produced free amine with *N*-Cbz protected valine introduced the diazonamide side chain.⁴⁵ The difficult deacetylation of the C11 hemiacetal was achieved through transesterification with methanol catalyzed by a Otera stannoxane.⁴⁵ The resultant hemiacetal **201** was unstable to handling, but the cyclic acetal congener was readily accessible upon treatment of the deacetylated compound with acidic resin. Removal of the side chain Cbz group produced a non-cyclized, dehydrated form of diazonamide A (**202**), and the late stage methodologies developed were now available for use by the Harran group upon successful formation of the C16-C18 bond.⁴⁵

UV irradiation of the highly-fluorescent, brominated E-ring substrate (**207**) finally achieved the synthesis of the C16-C18 biaryl bond (**Scheme 1-20**). This substrate (**207**) was synthesized through *ortho*-bromination of the free-phenol form of **203** give **204**. The free phenol was converted into the photolabile *o*-nitrobenzyl ether, and the aryl nitrile was hydrolyzed to form the valerolactone (**205**).⁴⁶ Reaction of the activated valerolactone with dimethylaluminum-activated tryptamine directly produces the appended product, and perruthenate oxidation of the C10 carbinol produced **206**.⁴⁶ Photochemical unmasking of the phenolic nucleophile in the presence of acetic anhydride produced the acetylated hemiacetal, and a two step oxidation-cyclodehydration procedure produced the photochemical substrate



(207). The mechanism proposed for this Witkop-type transformation invokes initial photoinduced electron transfer from the C-D indole to the E-ring bromophenol to form a radical anion that undergoes mesolytic elimination of bromide.⁴⁶ Subsequent collapse of the radical pair to form the biaryl linkage, followed by prototrophy to regenerate indole aromaticity would generate the observed product.⁴⁶ Anecdotal support, including the beneficial role of lithium cations, supports this proposed mechanism.⁴⁶ The Nicolaou group also managed to create the C16-C18 bond in a similar substrate through a radical cyclization reaction^{47, 48} (vide infra, Section 2.4.4), and this successful result bolsters the proposed mechanism for the Witkop photocyclization.

With the diazamide polycyclic structure accomplished (208), the aforementioned methods (Scheme 1-19) allowed for the subsequent chlorination, side chain acylation, hemiacetal deacetylation, and final deprotection to yield putative diazamide A (4). This stereoselective synthesis converges five readily accessible components, two of which are commercial product, through 24 total steps to produce the first successful route to the structure proposed for diazamide A.

1.3 Structure Revision of the Diazonamides

In 2001, the Harran group at UT-Southwestern Medical Center at Dallas was the first group to complete the total synthesis of diazamide A.⁴⁶ However, the synthetic diazamide A produced differed in several key respects from the isolated natural product. First, the synthetic product exhibited unexpected instability, including under conditions used in the isolation of the natural product. Direct comparison of the NMR spectra of the final product showed undeniable differences from the reported Fenical group data. Further, the

final synthetic product possessed a dramatically different R_f on thin-layer chromatography as compared to a sample of the natural product. These results presented two inescapable possibilities: the Harran group had made structural misassignments and were mistaken in their assertion of having synthesized diazamide A. Or, alternatively, the Harran group had exactly constructed the structure assigned to diazamide A, but that structure was not the true form of the molecule. The Harran group had obtained extensive validation of their synthetic products, including X-ray analysis of a late stage intermediate, and confidence in their structural assignments led them to reexamine the original diazamide data.⁴⁹

As previously discussed, the structural assignment of the diazamide natural products was based primarily on NMR and mass spectral data interpreted in combination with a X-ray crystal structure of a dehydrated, *p*-bromobenzamide derivative of diazamide B (**2**). Unlike the rest of the diazamide natural products, diazamide B (**5**) did not possess an appended side chain, and the assignment of the diazamide A side chain was based on the interpretation of the NMR data. As the only part of the diazamide structure lacking supporting crystal data in its designation, the Harran group initially believed that the side chain was the most likely the part of the structure misassigned.⁴⁹ This idea was corroborated by the Harran group's observation of diketopiperazine formation during DBU deprotection of a Fmoc protected valine side chain.⁴⁶ Upon reevaluating the diazamide isolation data, the Harran group uncovered multiple possible discrepancies with the structural assignment of the diazamide A side chain. First, acid digest of diazamide A failed to produce valine as would be expected.^{6, 49} Also, the chemical shift of the C37 carbon in the ¹³C NMR is not consistent with the chemical shift of the analogous carbon in valine.^{6, 49}

Most importantly however, was the Harran group's reinterpretation of the chemical shifts of the N7 amine protons. The diazamide A side chain resonances were easily identifiable as those not present in the diazamide B spectrum. The isolation data ^1H NMR executed in DMSO identifies the N7 chemical shift as a pronounced doublet at δ 5.46 integrating to one proton, which is not the expected splitting pattern. Further, upon formation of the N7 acetamide during acetylation (**Figure 1-2, 3**), the C37 proton resonance appears as a doublet, which is also not consistent with the expected splitting pattern.^{6, 49} These factors clearly suggested to the Harran group that the diazamide A side chain did not contain an amine, but that the data was consistent with the side chain possessing a C37 hydroxyl with unknown stereochemistry.⁴⁹ However, assigning the diazamide side chain as a α -hydroxy isovaleric conjugate required a further correction in the diazamide A structure to compensate for the change in molecular mass: namely, another proton must be present on the structure to account for the observed HRFABMS mass. This fact led the Harran group to reevaluate the overall structural assignment, and they discovered a discrepancy between the predicted and the observed masses for diazamide B.⁴⁹ The Harran group recognized that the predicted mass for presumptive diazamide B molecular formula of $\text{C}_{35}\text{H}_{26}\text{N}_6\text{O}_5\text{Cl}_2\text{Br}$ $[[\text{M}^+\text{H}]-\text{H}_2\text{O}]$ was incorrectly calculated as being 743.0590 amu. This is the exact calculated mass value for $\text{C}_{35}\text{H}_{24}\text{N}_6\text{O}_4\text{Cl}_2\text{Br}$, which is an incorrect molecular formula for $\text{C}_{35}\text{H}_{26}\text{N}_6\text{O}_5\text{Cl}_2\text{Br}$ $[[\text{M}^+\text{H}]-\text{H}_2\text{O}]$. The correct calculated mass for $\text{C}_{35}\text{H}_{26}\text{N}_6\text{O}_5\text{Cl}_2\text{Br}$ $[[\text{M}^+\text{H}]-\text{H}_2\text{O}]$ is 744.0416 amu, and this value is almost 1 Da greater than the HRFABMS mass for diazamide B. This finding by the Harran group indicated that the assigned

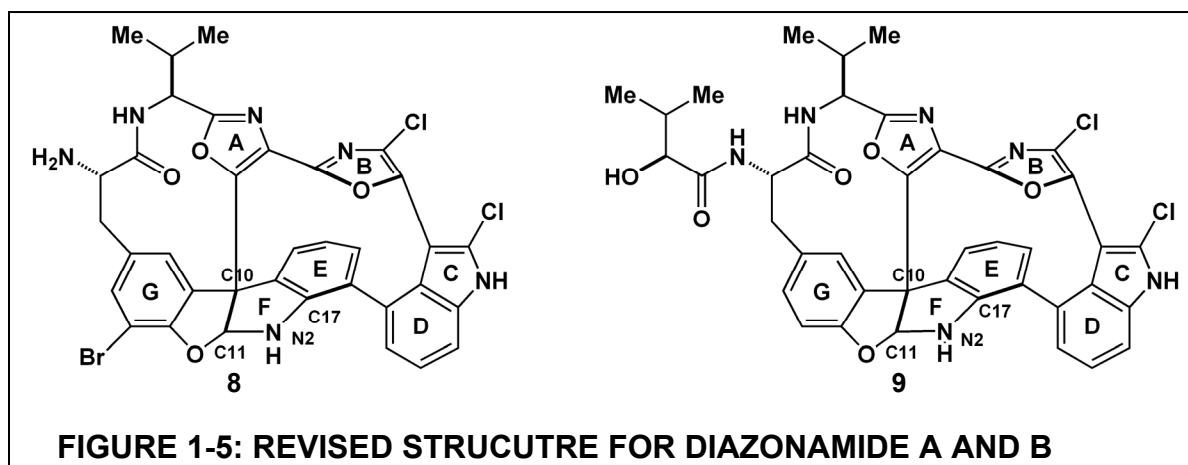
diazonamide B structure actually possessed an extra proton: the additional Da that was required for the side chain reassignment.

The Harran group also recognized that the HRFABMS mass of diazonamide B was more consistent with the molecular formula $C_{35}H_{25}N_6O_4Cl_2Br$ ($\Delta = 2.4$ ppm), suggesting a protonated nitrogen had been mistaken for an oxygen atom in the X-ray structure of the dehydrated diazonamide B *p*-bromobenzamide derivative.⁴⁹ The Harran group reexamined the crystallographic data focusing on the assignment of the oxygen atoms in the X-ray, and they were able to identify the assignment of O3 as being suspect based on its aberrantly long carbon-oxygen bond lengths and its atypical thermal motion.⁴⁹ In fact, the C17-O3 bond significantly exceeds the range of bond length in a comparison of all related structures.⁴⁹

These factors led the Harran group to conclude that the O3 oxygen was the location in the diazonamide structures of the misassigned protonated nitrogen (**Figure 1-4**). The Harran group provided experimental evidence supporting this reassignment by performing a 2D $^1H/^{15}N$ -HSQC NMR on a small sample of natural diazonamide A.⁴⁹ This experiment clearly shows that four nitrogen-proton bonds are present in diazonamide A, supporting the proposed Harran molecular formula.⁴⁹ Critically, the singlet at $\delta = 7.16$ ppm assigned as the O7H hemiacetal proton signal was shown to be a nitrogen-bonded proton.⁴⁹ This result provided direct evidence refuting the existence of a C11 hemiacetal in the diazonamide natural products. Further, the $^1H/^{15}N$ -HSQC experiment demonstrated that the NMR singlet at $\delta = 5.46$ ppm originally assigned as the N7 side chain amine protons was not in fact a nitrogen bonded proton.⁴⁹ This finding validated the reassignment of the diazonamide A side chain as a α -hydroxy isovaleric conjugate. Further support of the Harran group's diazonamide

reassignment was provided through the experimental evaluation of the biological activity of various diazonamide analogs (*vide infra*, Chapter 2). The final validation of this reassignment was provided via total synthesis of the revised diazonamide A structure by the Nicolaou group in 2002⁴⁷ and by the Harran group in 2003 (*vide infra*).⁵⁰

There is an established history for total synthesis leading to structural revisions of natural products.⁵¹ However, the misassignment of the diazonamide natural products is especially notable due to the fact an X-ray structure used to identify the diazonamide structure was shown to be incorrect. In examining the structural assignment of the diazonamide natural products made by the Fenical group, the identification of the C11 hemiacetal was apparently based solely on a ¹H NMR vicinal coupling constant between the C11 proton and an exchangeable proton.^{6, 49} This initial assertion then biased interpretation of the remaining data. For example, the final analysis of the HRFABMS required a $[[M^+ + H] - H_2O]$ *m/z* molecular formula to be invoked for all of the diazonamide natural products due to



the dehydration of the labile hemiacetal alcohol group. The only exception to this HRMS interpretation was for the *p*-bromobenzamide derivative (**2**), which was known from the crystal structure to be lacking a hemiacetal moiety. The authors also chose to assign the molecular formula of the triacetylated derivative (**3**) of diazonamide based on the same $[[M^+H]-H_2O]$ m/z ionization pattern while also assigning the O7 alcohol of the hemiacetal as being acetylated (HRFABMS observed 891.2312 amu, requires $C_{46}H_{42}N_6O_{10}Cl_2$ $[[M^+H]-H_2O]$).⁶ However, to attain the observed mass the acetylated hemiacetal would have to undergo dehydration without losing an acetate group, and the author do not propose a mechanism through which this dehydration would occur.

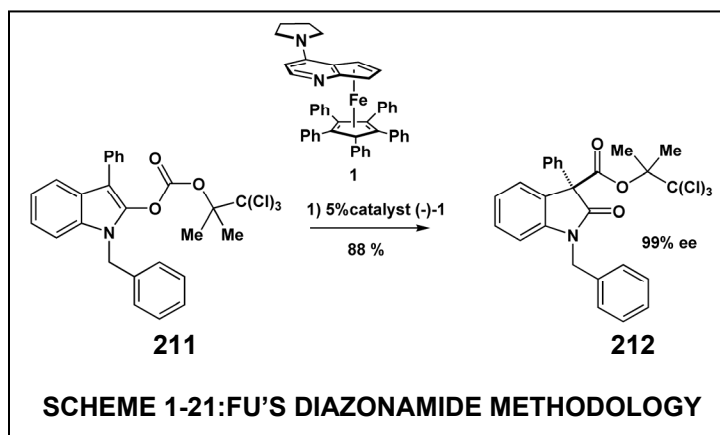
The interpretation of the X-ray structure was also guided by this initial hemiacetal assignment, and it was reasonable to suggest that the C11 hemiacetal would be converted into a diphenylacetal during the formation of the *p*-bromobenzamide derivative. Significantly however, the NMR data provided for the *p*-bromobenzamide derivative was only reported in methanol, not DMSO. The characteristic O7 hemiacetal proton would not be expected to be observed in methanol, and it seems reasonable to assume the loss of the hemiacetal was only discovered upon solving the X-ray structure. If the 1H NMR of the *p*-bromobenzamide diazonamide B derivative (**2**) had been performed in DMSO, the misidentified O7 proton and its vicinal coupling to the C11 proton would have still been observed, and this would have clearly indicated that the diphenylacetal was not present in the crystal structure. However, the failure to correctly interpret the X-ray crystal data was the most egregious error in the structural assignment of the diazonamide natural products. In retrospect, it seems remarkable that the postulated existence of the C11 hemiacetal, based solely on a single NMR coupling,

biased the interpretation of the X-ray data to the point of incorrectly identifying the molecular framework of the diazonamides.

1.4 Synthetic Research Towards the Revised Diazonamide A Structure (9)

Obviously, the identification of a new diazonamide A target impacted the research into its total synthesis. Several groups were able to adapt their strategies to target the revised structure, but for others, Harran's revelation required a complete recasting of their synthetic approach.

1.4.1 Fu Group Diazonamide A Research

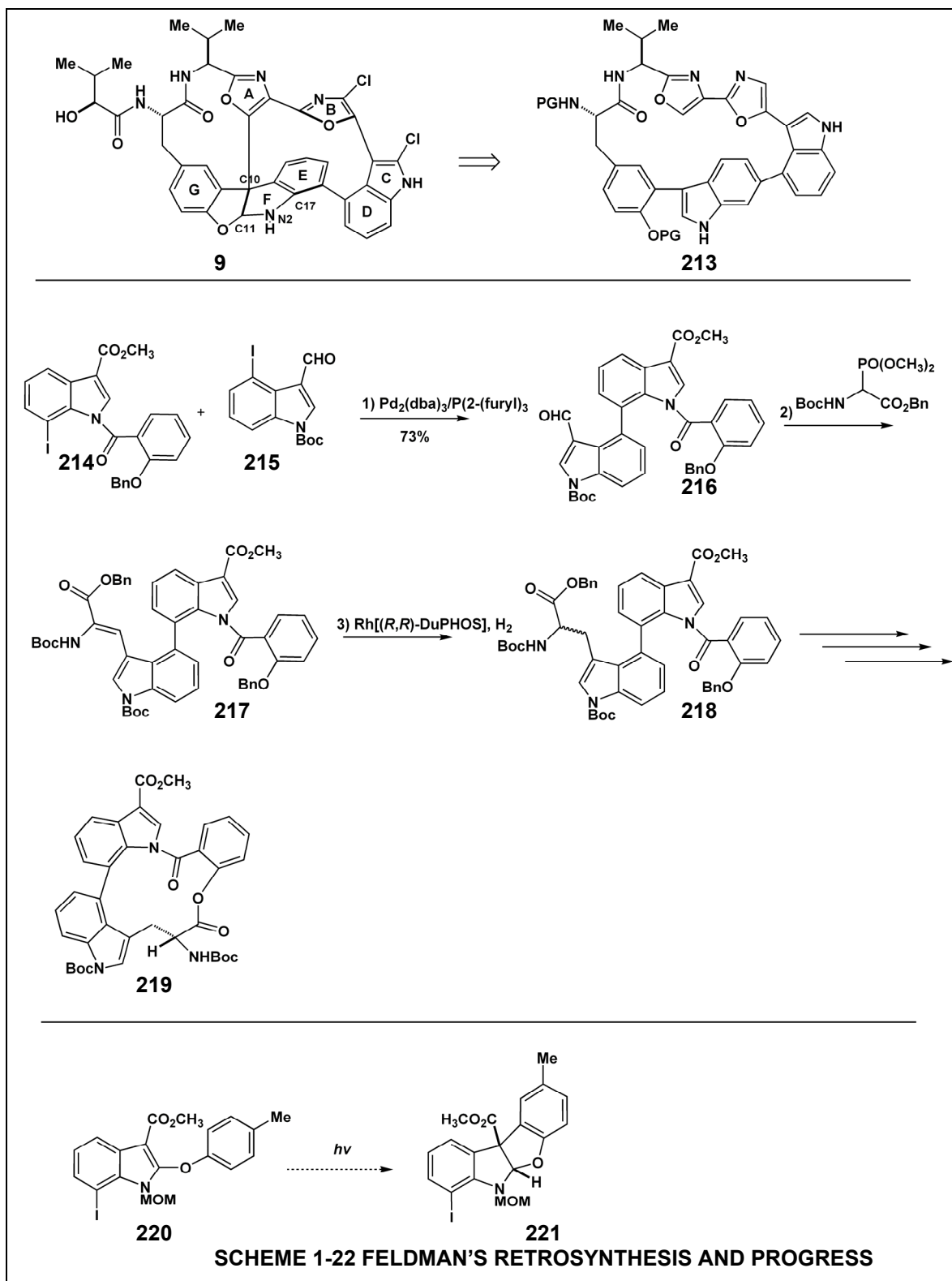


Hills and Fu utilized a chiral version of 4-(pyrrolidino)pyridine (PPy) catalyst to induce an asymmetric rearrangement of *O*-acylated oxindole enolates.⁵² In the context of the simple oxindole model system explored (Scheme 1-21, **211**), this method allows for the enantioselective formation of the diazonamide A C10 quaternary center (**212**) with high yields.⁵² This reaction is a variation of the Black acylation reaction, which both Moody¹⁵ and Vedejs¹⁶ sought to employ in their pursuit of the original diazonamide A structure. This

reaction was found to proceed with higher enantioselectivity with larger carbonate groups, with optimal results being attained with the trichloro-tert-butyl group. In addition, the ee of the reaction is unchanged over time, indicating the C-acylation of the enolate is irreversible. There have been no further publications from the Fu group concerning the total synthesis of diazepam A.

1.4.2 The Feldman Group Diazepam A Research

The Feldman group envisioned forming the diazepam C10 center via a transannular oxidative cyclization reaction, both in the original (**4**) and the revised diazepam structure (**9**).³² This approach is similar to that of the Magnus group³¹ (Section 2.3.8). This design entails developing a method to construct the heteroaromatic diazepam polycycle **213** (Scheme 1-22).³² The Feldman group also planned on setting the C16-C18 axial chirality via asymmetric hydrogenation.³² To explore the designed synthesis, the Feldman group employed a simplified bis-indole model system **216**, which was accessed through a Negishi coupling of the elaborated indole subunits **214** and **215**.³² A Horner-Wadsworth-Emmons reaction with the protected amino acid phosphonate produced the predominately (*Z*) olefin product (10:1 *Z/E*) in compound **217**.³² Asymmetric rhodium hydrogenation using the (*R,R*)-DuPHOS ligand produced a 1.5:1 mixture of interconverting diastereomers (**218**). Following deprotection of the carboxylic acid, the desired lactone **219** was formed with in a 3:1 ratio of enantiomers. This result suggested that only one of the equilibrating diastereomers underwent the lactonization.³² More recent, unsuccessful work



from the Feldman group sought to form the diazonamide aminal core (**221**) via a photochemical cyclization from 2-aryl indolyl ethers (**220**).⁵³

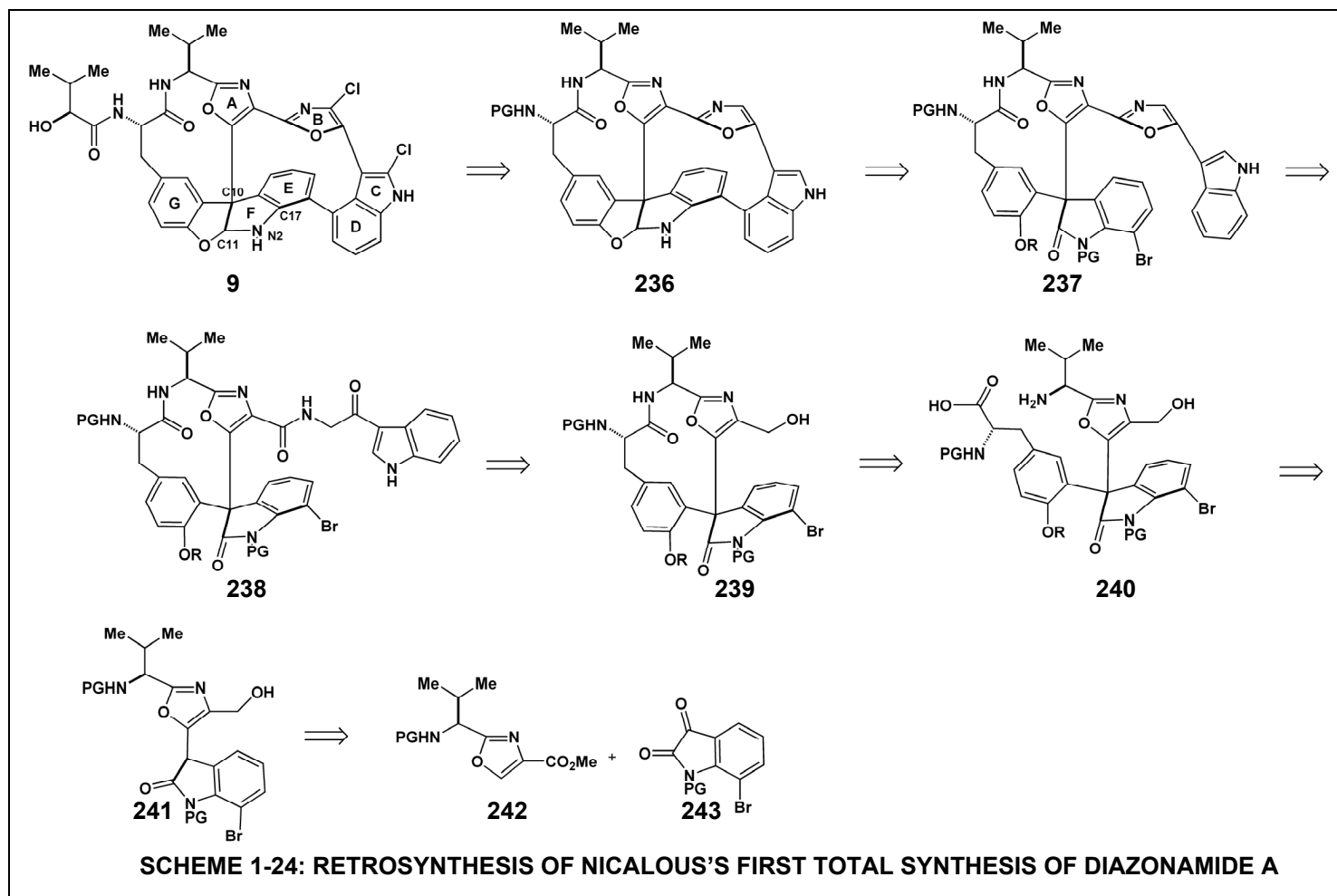
1.4.3 The Vedejs Group's Approach to the Revised Diazonamide A Structure

The Vedejs group amended their approach to the original diazonamide A structure (**Scheme 1-7**) to undertake the revised structure of diazonamide A (**Scheme 1-23**).²⁷ Therefore, their retrosynthesis is largely the same, and their intermediate target is the construction of the BCDE macrocyclic aminal **223** through use of Dieckmann reaction instead of the macrocyclic acetal **222**.²⁷ Zajac and Vedejs converted 7-bromoisatin (**224**) into elaborated indoline **226** through use of conventional transformations.²⁷ **226** was treated with methanesulfonic anhydride and triethylamine to produce the cyclized aminal G-F-E ring system.²⁷ After four steps, the aminal G-F-E ring fragment was converted into stannane **227**.²⁷ A Stille cross coupling reaction between stannane **227** and palladium complexed oxazolyl indole **230** produced the C16-C18 biaryl bond in compound **228** as two interconverting atropisomers ($t_{1/2}$ of interconversion at 0°C = 3.5 min).²⁷ Using the prior precedent for the Dieckmann macrocyclization reaction²⁶, **228** was treated with LDA at 0°C. A complex mixture of compounds was produced, but the major compound was identified as by-product indole **229**.²⁷ **229** likely arises from deprotonation of the aminal nitrogen, followed by carboxyl transfer to achieve indole aromaticity.²⁷ A solution to this unwanted side reaction was to install a protecting group on the aminal nitrogen.²⁷ However, the presence of the MOM protecting group produced a 2:1 ratio of unwanted (**232**) to desired (**231**) atropisomers that were stable to interconversion up to 60 °C, at which compound

decomposition began to occur. Due to the poor rate of atropisomer interconversion and the instability of compound **231/232** at elevated temperatures, the Dieckmann cyclization was performed at temperatures below the limit of atropisomer interconversion, meaning that only 33% of the desired atropisomer would be available to cyclize.²⁷ Therefore, the Dieckmann reaction product **233** was successfully achieved by treating the mixture of **231/232** with LDA at -78°C but only in a 29% yield.²⁷ The 92% of the remaining starting material was recoverable and could be reequilibrated and resubjected to the cyclization reaction.²⁷ Zajac and Vedejs were able to convert **233** into the ABCDE macrocycle **235** through installation of the A-ring oxazole.²⁷ There have been no publications from the Vedejs group seeking to apply this synthetic design to the full diazonamide A structure.²⁷

1.4.4 Nicolaou's First Total Synthesis the Revised Diazonamide A Structure

The Nicolaou group has completed two total syntheses of the revised diazonamide A structure.^{41, 42, 47, 48} The first completed total synthesis began after the announcement of the revised structure in 2001 and was achieved through a new synthetic approach.^{47, 48} The second total synthesis was accomplished by adapting the route used in the Nicolaou group's pursuit of the original diazonamide structure (**4**, Section 2.2.10).^{41, 42} The retrosynthetic design for the first total synthesis is shown in **Scheme 1-24**. This approach converts the diazonamide A core **236** into acyclic compound **237** through breaking the C16-C18 biaryl bond and the C11-oxygen bond to produce the oxindole.^{47, 48} The C-D ring fragments would arise from coupling a tryptamine congener to the A-G macrocycle **239**.^{47, 48} Opening the lactam in macrocycle **239** would give **240**, and **240** is comprised of a tyrosine derivative and the oxindole component **241**.^{47, 48} **241**

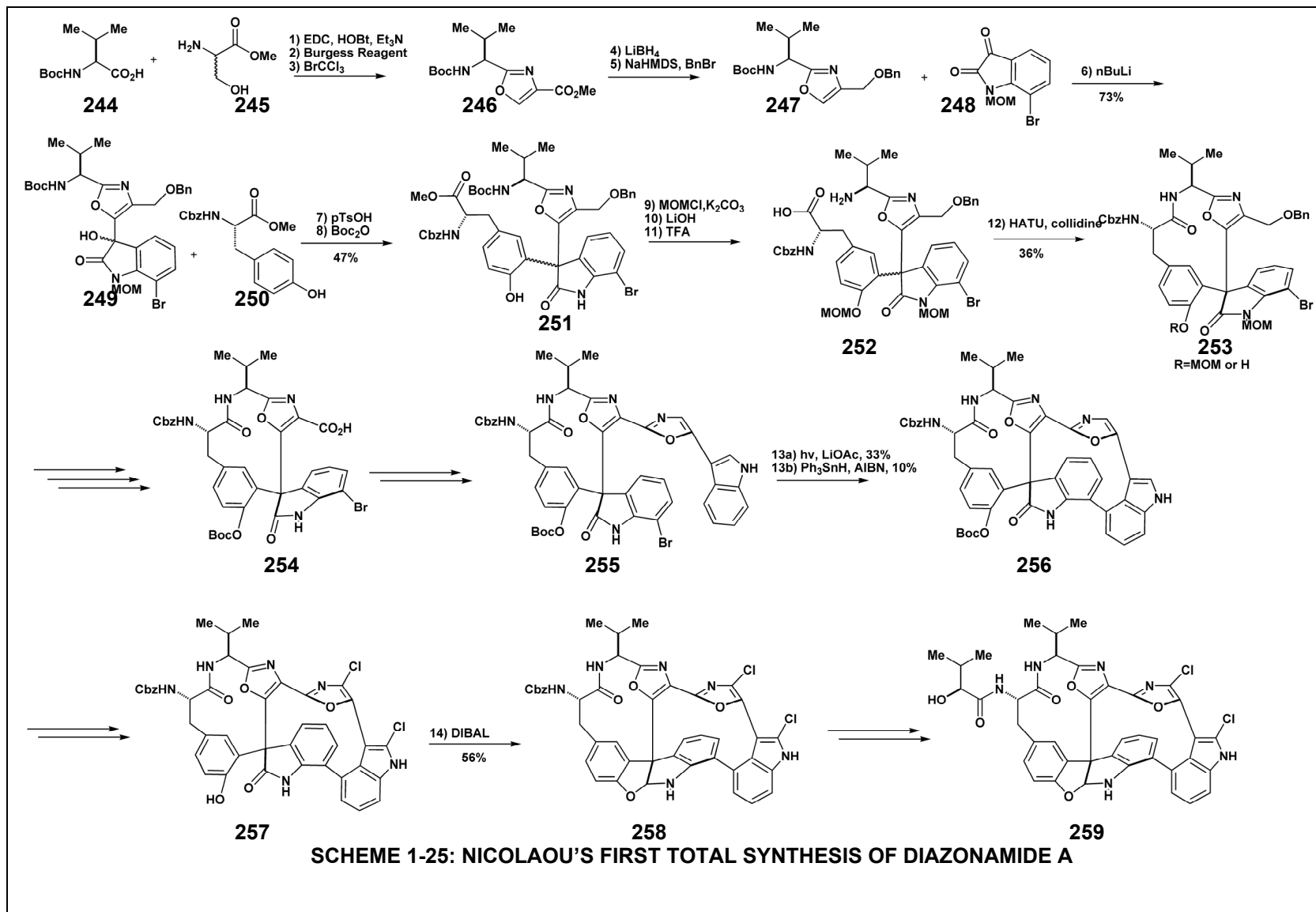


may be deconstructed into valine oxazole **242** and *N*-protected 7-bromoisatin **243**.^{47, 48}

This total synthesis (**Scheme 1-25**) begins with formation of valine oxazole **246** through cyclodehydration of the peptide coupled Boc valine **244** and serine methyl ester. Following reduction of the methyl ester and protection of the produced alcohol, **247** was deprotonation with *n*-butyl lithium and acylated with isatin **248** to give oxindole compound **249**. The diazonamide C10-containing compound **251** is formed as a mixture of diastereomers through refluxing **249** and tyrosine **250** with *p*-TsOH, followed by Boc reprotection of the free amine.^{47, 48} The mixture of diastereomers was carried forward through protecting group manipulation to form substrate **252**.^{47, 48} Lactamization with HATU successfully formed the desired A-G macrocycle **253**.^{47, 48} Importantly, only the desired diastereomer underwent lactamization; the unwanted diastereomer underwent a dimerization reaction.^{47, 48}

The MOM-phenolic protecting group in macrocycle **253** was replaced with a Boc group, and the oxazolyl alcohol was deprotected and oxidized to acid **254** with IBX and sodium chlorite.^{47, 48} The B-C-D rings were then introduced through coupling of tryptamine and cyclodehydration to form the B-ring oxazole.^{47, 48} The Nicolaou group developed a radical cyclization reaction to form the C16-C18 biaryl bond in **256**, but the desired cyclized product was only produced in 10% yield.^{47, 48} Therefore, the Nicolaou group applied Harran's Witkop photocyclization (Section 2.3.11) used to form the C16-C18 bond in the original diazonamide A structure to produce **256** in 33% yield.^{47, 48}

Using the *N*-chlorosuccinimide method established by Magnus²⁸ and used by Harran⁴⁵, oxindole compound **256** was chlorinated and then Boc protected to form **257**. DIBAL reduction of the oxindole produced the cyclic aminal compound **258**, and then upon introduction of the α -



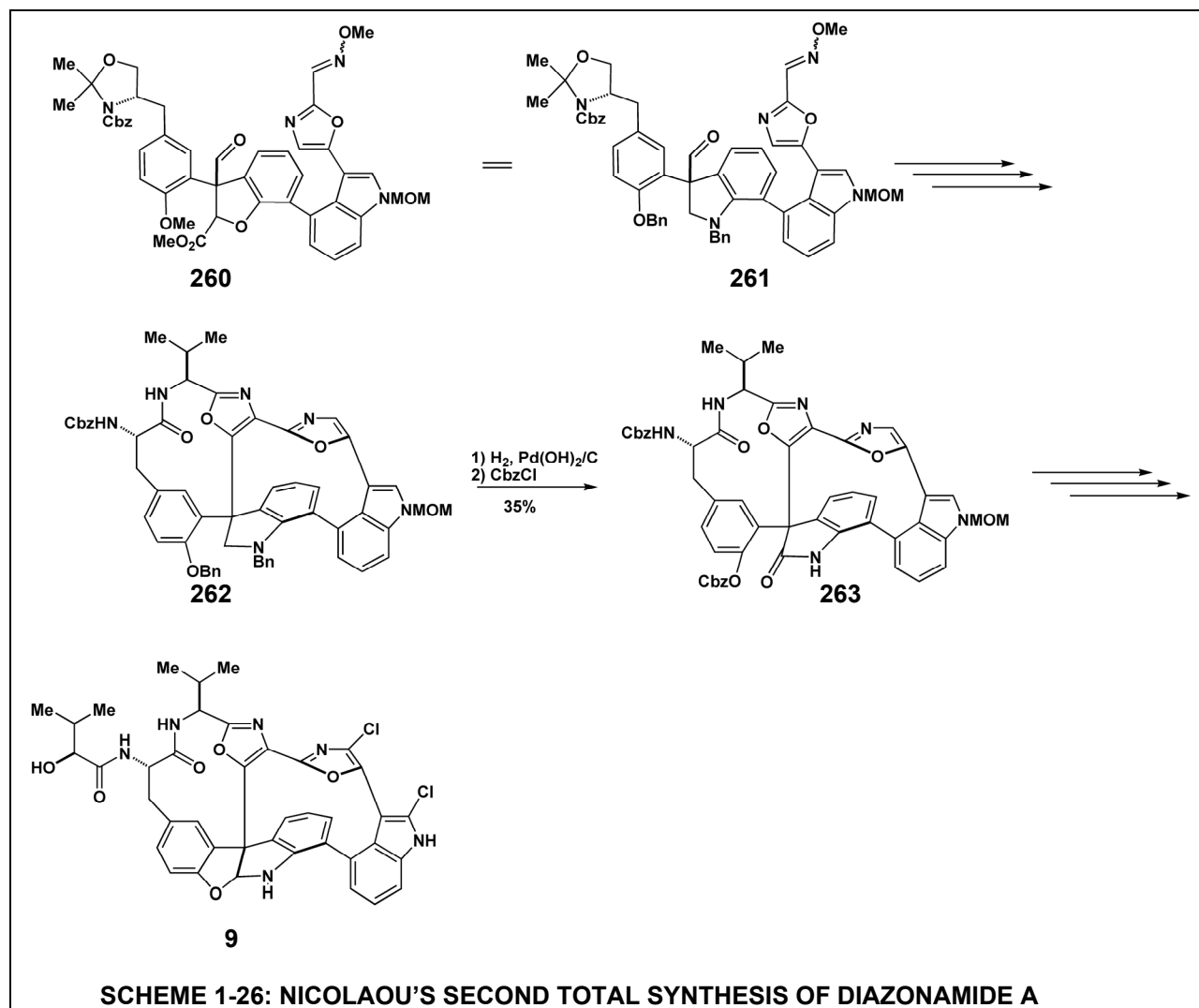
hydroxy isovaleric acid (HIV) side chain, the total synthesis of diazonamide A was complete. The diazonamide core was acylated with both side chain epimers, and based on comparison with the Fenical isolation data, the side chain was assigned as having the (*S*) configuration. The longest linear sequence of this total synthesis is twenty-one steps.

1.4.5 Nicolaou's Second Total Synthesis the Revised Diazonamide A Structure

In 2003, the Nicolaou group published their second total synthesis of diazonamide A.^{41, 42} The design of this total synthesis (**Scheme 1-26**) is related to the Nicolaou group's previous efforts in synthesizing the original diazonamide A structure. (Section 2.3.10). Hetero pinacol substrate **261** was prepared using very similar methodology described for the synthesis of benzodihydrofuran **260**.^{41, 42} The oxime aldehyde hetero pinacol reaction, installation of the A-ring oxazole, and macrolactamization was achieved using methods previously described (**Scheme 1-15**).^{38,41, 42} With both of the diazonamide macrocycles achieved, the Nicolaou group had only to introduce the final C11 ring to complete the diazonamide A core, and this would require oxidizing the C11 to the oxindole, similar to **257**.^{41, 42}

Fortuitously, however, the C11 oxidation unexpectedly occurred during hydrogenolytic deprotection of the phenolic benzyl group using Perlman's catalyst.^{41, 42} A mechanism has been proposed for this unexpected oxidation reaction⁴², and the result is that, following Cbz protection of the phenol, oxindole **263** was then transformed into diazonamide A using the methods already described (**Scheme 1-27**).⁴² The longest linear sequence of this total synthesis is thirty-one steps.

^{41, 42}



1.5 Diazonamide Biosynthesis

As noted by Fenical *et al*⁷, the diazonamide natural products as originally assigned cannot be assigned were of ambiguous biosynthetic origin. These structures would have to arise from non-ribosomal peptide synthesis combined with the incorporation of an unidentified component to generate the C10-C17 portion of the molecule (**Figure 1-3, 4**). There is no ambiguity, however, in the biosynthetic origins of the revised diazonamide A structure. As presented by Harran⁴⁹, the diazonamide core is composed of four oxidatively cross-linked, proteinogenic amino acids with an appended (*S*)- α -hydroxy isovaleramide side chain.

1.6 Diazonamide Biological Activity

1.6.1 Introduction

In order to identify new compounds with anti-cancer activity, the Developmental Therapeutics Program (DTP) at the National Cancer Institute implemented the Human Tumor Cell Screen in 1990.⁵⁴ This assay evaluates the activity of compounds against 60 cultured human cancer cells lines.⁵⁴ The screen tests multiple concentrations of compounds against the cell lines, and analysis of the data provides three concentration values that characterize a compound's cytotoxic activity: the inhibitory concentration 50% (IC₅₀), the total growth inhibition concentration (TGI), and the lethal concentration 50% value (LC₅₀).⁵⁵ By establishing these values against a common tumor cell line panel, the Human Tumor Cell Screen provides a standardized protocol for evaluating potential new anti-cancer compounds. The DTP Human Tumor Cell Screen has generated cytotoxic profiles for thousands of compounds, and through examining a compound's activity in the 60-cell line screen, it is possible to identify small molecules that likely possess common mechanisms of action. The COMPARE statistical analysis matches new compounds with similar activity profiles in the screen.⁵⁶ The degree of relatedness in the COMPARE analysis is represented through a Pearson correlation coefficient (PCC).⁵⁶

1.6.2 Initial Diazonamide Cytotoxicity Data

Fenical et al reported diazonamide A to be a potent cytotoxin that inhibited the proliferation of HCT-116 human colon carcinoma cells and B-16 murine melanoma cells with IC₅₀ values of less than 15 ng/mL.^{6, 7} Diazonamide B was also reported to be a cytotoxic

agent but less potent than diazonamide A. The specifics of diazonamide B's biological activity, including its potency, are not disclosed,⁶ and there is no mention of diazonamide C or D being evaluated for cytotoxicity.⁶

Based upon these initial results, diazonamide A was submitted by the Fenical group for evaluation in the DTP Human Tumor Cell Screen, and the compound was found to possess a mean IC₅₀ value of 11 nM, a TGI value of 65 nM, and a LC₅₀ value of 95 nM.⁵⁷ The COMPARE analysis of the diazonamide A cytotoxic profile identified a weak correlation with several known anti-mitotic agents.^{57, 58} Diazonamide A has the strongest correlation with anti-mitotic tubulin-binding natural products, including vinblastine and paclitaxel, but the PCC values from the COMPARE analysis were not of a sufficiently high level to be conclusively correlative with a known cellular mode of action.⁵⁷

1.6.3 Initial Research into Diazonamide A's Biological Activity

The Fenical group also pursued a preliminary exploration into diazonamide A's biological activity. An account of this research is provided in the doctoral dissertation of Helene Vervoot.⁵⁸ The COMPARE data prompted the Fenical group to determine whether diazonamide A inhibited cell division. FACScan analysis of 2008 human ovarian carcinoma cells treated with 40 nM of diazonamide A showed an approximate doubling of the tetraploid cell population after 24 hours of exposure to compound. Diazonamide A possessed an IC₅₀ of 10.0 nM against this cell line, which was comparable to the values for paclitaxel (IC₅₀ of 9.6 nM) and vinblastine (2.5 nM).⁵⁸ The FACScan experiment used only the sole 40 nM diazonamide A concentration, and it is significant that this concentration of the natural product - four times the IC₅₀ level - was not sufficient to block mitosis.⁵⁸ The treatment with

40 nM paclitaxel and 10 nM vinblastine – concentrations also four times the respective IC_{50} levels – produced a much more substantial affect on cell cycle progression. As observed microscopically, treatment of 2008 human ovarian carcinoma cells with 40 nM of diazonamide A increased the number of rounded cells. In this evaluation, all rounded cells were scored as being mitotic.⁵⁸ The Vervoot data supports a conclusion that, in the 2008 human ovarian carcinoma cells, 40 nM of diazonamide impeded the progress of mitosis, but not to the extent of a equipotent concentration of paclitaxel or vinblastine.⁵⁸ Immunofluorescent visualization of microtubules in 2008 human ovarian carcinoma cells treated with diazonamide A was also performed.⁵⁸ Diazonamide A was shown to cause microtubules to disappear at 100 nM and 1 μ M.⁵⁸ The effect of diazonamide A resembled the effect of vinblastine on microtubules.⁵⁸

1.7 Conclusions

1.7.1 Synthetic Studies

The goal of total synthesis is not only to achieve a route to the molecular target, but also to develop new, generally applicable methodologies. The pursuit of the total synthesis of diazonamide A by various groups led to a variety of different methods being employed and several new reactions being discovered. A subset of diazonamide synthetic reports detail the utilization of a specific reaction methodology to access designated structures related to components of a molecular target. The described contributions of Liebscher, Pattenden, and

Fu are examples of researchers undertaking a portion of a total synthesis to showcase a particular reaction.

Of the retrosyntheses designed to complete total synthesis of the molecule, there were three major strategies. These approaches center on the sequence in which the A-G and the ABCDE macrocycles were to be formed. The retrosynthetic approach for Jamison, Harran's total synthesis of the original diazonamide A structure, and Nicolaou's first total synthesis of the revised diazonamide A structure all focused on forming the A-G macrocycle (**10**) first. As recognized by Harran, establishing the A-G macrocycle before elaborating the ABCDE macrocycle (**11**) alleviates atropisomerism formation. Several groups sought to form the ABCDE macrocycle first in their diazonamide retrosynthetic approaches. This approach, as proposed by the Wipf,^{23, 24} Vedejs,^{16, 25-27} and the Nicolaou groups,^{36, 37, 41, 42} did not factor in possible atropisomerism in designing their total synthesis. Atropisomerism did prove a major obstacle in forming the ABCDE macrocycle for both the Nicolaou^{36, 39} and the Vedejs groups²⁷. The third basic retrosynthetic design is that of Feldman³² and Magnus²⁸⁻³¹, and to a lesser extent Moody.¹⁰⁻¹⁵ With this approach, both the A-G and ABCDE macrocycles would be formed simultaneously through introduction of the A-ring oxazole/C-10 bond. The groups undertaking this strategy have not yet reported any successful outcome for this approach.

As described, the formation of the C10 center and the C16-C18 biaryl bond are the two most difficult synthetic challenges in the diazonamide A structure. Several different methods were employed to produce the C10 quaternary center, both in model systems and in the context of the diazonamide structure, but it is surprising how few asymmetric syntheses of the C10 center were achieved. In the research aimed at the original structure, both

Vedejs¹⁶ and Wood³⁴ were able to induce modest enantioselectivity in model systems. Nicolaou's approach to the original structure proposed using asymmetric epoxidation in order to produce a chiral C10 center, although a successful implementation of this idea was not reported. Fu and coworkers accomplished the enantioselective formation of the C10 center in a very simplified diazamide model system.⁵² The Harran group was the only group to establish the proper C10 configuration through a stereoselective synthesis in the context of the diazamide A structure.⁴⁴

Similarly, the Harran group also developed a novel method for the formation of the C16-C18 biaryl bond.⁴⁶ Most efforts focused on forming this biaryl linkage used sp^2 - sp^2 cross coupling methodologies. The Harran group's Witkop-like photocyclization is the only other viable alternative to cross-coupling thus far developed for diazamide synthesis. Nicolaou and coworkers developed a radical cyclization reaction to form the C16-C18 bond, but due to poor yields, they adopted a similar photochemical approach to solve the problem.

47, 48

CHAPTER TWO

Characterization of Diazonamide Biological Activity

2.1 Introduction

This chapter details research into diazonamide biological activity. Initial efforts employed late stage intermediates from on-going synthetic efforts within the Harran group. When the total synthesis of the originally assigned structure was complete, focus shifted to evaluating and characterizing the biological activity of diazonamide A and a closely related analog we named syndistatin. These studies also established a set of diazonamide structure activity relations (SAR), which further supported the structural reassignment for diazonamide A.

2.1.1 Cytotoxic Natural Products and the Search for New Cancer Chemotherapeutic Agents

Cytotoxic, or cell-killing, agents capable of directly destroying tumor cells constitute a vital treatment for cancer.⁵⁹ With very few exceptions, cytotoxic chemotherapeutic agents have severe side effects, and often the extent of the chemotherapy treatment is limited by the patient's tolerance to the toxicity. In fact, nitrogen mustard compounds initially developed and used as chemical warfare agents were the first cancer chemotherapeutic agents shown to be clinically effective.⁶⁰ In the 50 years since this discovery, research into cancer biology has progressed from a basic, etiological understanding to a sophisticated molecular view of the underpinnings of the disease. During this period of time, the efficacy and undesired side effects of chemotherapeutic agents have been improved.⁶¹ However, despite improvements

in drug development and biomedical research, most anti-cancer agents remain essentially ameliorated poisons capable of extending patients' lives without permanently resolving the cancer. The deficiencies of current chemotherapeutic compounds fuel the pursuit of new cancer-selective agents functioning through novel modes of action.⁶¹

2.1.2 Microtubules and Tubulin

Most anti-mitotic natural products exert their activity on the cell cycle by affecting microtubules.^{62 63} Microtubules are protein cytoskeletal elements found in all eukaryotic cells. Microtubules serve as universal components of the cellular scaffolding essential for numerous cellular processes, including vesicle transport and mitosis. Microtubules consist of associated protofilaments which spontaneously bundle through lateral interactions to form microtubules.⁶⁴ Each protofilament is formed through the polymerization of tubulin heterodimers composed of α and β tubulin. α and β tubulin are closely related proteins sharing approximately 50% amino acid sequence identity.⁶⁵ The $\alpha\beta$ tubulin heterodimers polymerize into microfilaments in a GTP dependent process.⁶⁶ Both α and β tubulin bind GTP, but only β tubulin is a GTPase, hydrolyzing GTP to GDP to drive forward microtubule polymerization.⁶⁴ The orientation required for heterodimers to polymerize gives microtubules a polarity with designated plus and minus ends.⁶⁴ In cells, microtubules form at mitotic organizing centers (MTOC), and after initial nucleation at the MTOC, microtubule elongation proceeds in a GTP dependent process toward the plus end of the microtubule. The plus and minus ends differ greatly in their dynamics of polymerization, with the plus end undergoing a dramatically higher rate of change.⁶⁵

Microtubules are highly dynamic structures constantly undergoing modification, and the inconstant nature of microtubules permits cells to rapidly restructure their cytoskeleton.⁶⁶ ⁶⁷ The dynamics of tubulin polymerization has been extensively studied both in cells and in *in vitro* experiments.⁶⁷ Microtubules are formed outside of cells from purified or partially-purified tubulin protein in the presence of GTP and Mg²⁺.⁶⁶ Cellular microtubules are constantly alternating between elongation or shortening in a stochastic, non-equilibrium process known as dynamic instability⁶⁶, and dynamic instability is not observed with microtubules formed under the *in vitro* conditions. Dynamic instability is driven by the hydrolysis of GTP, which only occurs at the microtubule ends during polymerization. Although dynamic instability has been shown to occur at both polar ends, the plus end undergoes a much higher rate of change. Since the microtubule plus end is in a constant state of flux, minute changes in the kinetics of dynamic instability dramatically affects microtubule elongation and depolymerization. Recently, several microtubule associated proteins (MAPs) have been identified that alter the dynamic instability of microtubules.⁶⁸⁻⁷⁰ MAPs modulate the kinetics of polymerization allowing the cell to rapidly restructure its microtubule network.

2.1.3 Tubulin Binding Compounds

Several small molecules have been determined to interact with tubulin and microtubules, and through this small molecule/protein interface, tubulin-binding compounds dramatically affect cellular function. Tubulin-binding drugs are capable of arresting cellular mitosis at low nanomolar concentrations.⁷¹ Depending on the site of interaction, tubulin-

binding compounds are capable of both stabilizing cellular microtubules or inducing their depolymerization. Tubulin is the most abundant cellular protein, and the capability of tubulin-binding drugs administered at very low concentrations to alter microtubule polymerization is due to the dynamic instability of microtubules.⁷¹ That is a critical aspect of the tubulin/small molecule interface; a small molecule only needs to effect the equilibrium of microtubule polymerization to dramatically affect cellular microtubules.⁷¹

Through their effects on microtubule polymerization, tubulin-binding drugs prevent the formation of normal mitotic spindles and block mitosis. The cell, sensing a malformed mitotic spindle, arrests cell division at metaphase through activation of the spindle assembly checkpoint.^{72, 73} By arresting the rampant cell division characteristic of cancer cells, several anti-mitotic agents currently serve as important chemotherapeutic agents.⁶³ In addition, some new anti-mitotic agents are being evaluated as anti-cancer anti-vascular agents, capable of blocking the requisite blood supply to tumors.⁶³ The most common method to demonstrate that a compound binds to tubulin is through competition experiments with known radiolabeled or fluorescently labeled tubulin ligands. This approach identifies new compounds that bind to the known ligand binding sites on tubulin. A more extensive exploration of the compound/tubulin interaction is then typically undertaken using standard biochemical methods, but it is essential to initially know whether compound binding is linked to tubulin self association.⁷⁴

Tubulin-binding compounds may be divided into two class based on the effect tubulin polymerization has on ligand binding.⁷⁴ One class of ligands, particularly those of the colchicine class, interact with tubulin regardless of its state of self-association, and therefore,

binding is independent of tubulin polymerization.⁷⁴ This allows for the use of equilibrium binding methods such as equilibrium dialysis and Hummel-Dreyer Column Gel Permeation.⁷⁴ For the other major class of ligands, binding is linked to tubulin polymerization. This quality, possessed by the *Vinca* class of compounds, mandates that the state of tubulin self-association has a critical effect on ligand binding.^{74,67} Many of these tubulin-binding compounds also have a demonstrated higher affinity for tubulin at the termini of the microtubules than unassociated tubulin.⁶³

Tubulin possesses three major small molecule binding sites, termed the *Vinca*, taxol, and colchicine binding sites after the initial ligands discovered.⁶³ Compounds of this class induce the depolymerization of microtubules, both *in vivo* and *in vitro*. *Vinca* alkaloids isolated from nature, such as vinblastine and vincristine, have been in clinical use for over four decades. More recently, semisynthetic derivatives of these natural products such as vinorelbine and vinflunine have come into use.⁶³ The *Vinca*-derived compounds are primarily used in the treatment of haematological cancer.⁶³ Several natural products have been shown to interact at the *Vinca* domain of tubulin, including spongistatin⁷⁵, rhizoxin⁷⁶, cryptophycin 52⁶³, the halichondrins⁶³, the dolastatins⁶³, the hemiasterlins⁶³, and maytansine⁷⁶. The other major class of compounds inducing microtubule depolymerization is the colchicines class of agents. It was actually through use of a radiolabeled analog of colchicine that the protein tubulin was discovered.⁷⁷ Natural products targeting the colchicine-binding site include podophyllotoxin⁷⁸, curacin A⁷⁹, and nocodazole. Excessive patient toxicity has, to date, barred any member of this class of compounds for use in cancer treatment⁸⁰, although colchicine is still used as a treatment for gout.⁶³

Taxol was first isolated from the bark of the Pacific yew tree *Taxus brevifolia* in the late 1960's.⁶³ Its cytotoxic properties were identified soon after its isolation, but several years elapsed before its mechanism of action was understood.^{81, 82} Taxol was the first compound discovered that blocked mitosis through the stabilization of microtubules.^{81, 82} Many other natural products have since been determined to bind at or near the taxol site on tubulin, including the marine-derived compounds discodermolide⁶³, the epothilones⁶³, eleutherobin⁸³, and the sarcodictyins⁸³. In addition, the natural products peloruside A and laulimalide also stabilize microtubules⁸⁴, but these compounds do not bind tubulin at the taxol-binding site.⁸⁵ Unlike the *Vinca* and colchicine compounds, taxol does not bind tightly to free unassociated tubulin, instead binding with great avidity to the tubulin heterodimers present in microtubules.⁶³ Taxol showed great promise in initial clinical trials, but it could not come into general use until a new source of compound was developed. Currently, paclitaxel, the commercial name for taxol, is produced via semi-synthesis starting from a related product isolated from *Taxus* tree needles.⁸⁶ Paclitaxel is approved for the treatment of breast and ovarian cancer, non-small-cell lung carcinoma, and Kaposi's sarcoma.⁶³ The complex taxane structure has inspired a great deal of research in the synthetic chemistry community⁸⁷, and new taxol analogs are currently under clinical evaluation.⁶³

2.2 Material and Methods

2.2.1 Chemicals and Reagents

The following chemicals were purchased from Sigma-Aldrich: thymidine, vinblastine, paclitaxel, colchicine, propidium iodide, guanosine triphosphate, Hoescht 33433

dye, and RNase. CellTiter Glo® and CellTiter 96® Aqueous cell viability reagents were purchased from Promega and used as indicated. Antibodies: anti- α -tubulin antibody (mouse anti-human), fluorescently labeled Alexa Fluor 488 conjugated goat anti-mouse antibody were purchased from Molecular Probes.

Natural diazonamide A was first provided by the Fenical group and later synthesized on-site. The diazonamide derivatives utilized were synthesized by members of the Harran group at UT-Southwestern Medical Center at Dallas using our published procedures.^{45, 46} Dr. Jing Li, currently at Millennium Pharmaceuticals, Boston, MA, provided the majority of the diazonamide-based reagents.

2.2.2 Buffers and Solution

PEM tubulin polymerization buffer: 80 mM PIPES, 0.5 mM MgCl₂, 1 mM EGTA, pH 6.9.

Vindelov's propidium iodide solution: 50 μ g/mL propidium iodide, 0.01 M Tris base, 10 mM NaCl, 0.1% IPEGAL, 0.01 mg RNase.

2.2.3 Cell Lines and Tissue Culture

Cell lines were purchased from the American Type Culture Collection (ATCC) and cultured following the ATCC protocols for each cell line.

HCT-116- (ATCC# CCL-247) colonrectal carcinoma from human male.

OVCAR-3- (ATCC# HTB-161) ovarian adenocarcinoma from sixty-year old Caucasian female human.

SK-MEL-5- (ATCC# HTB-70) malignant skin axillary node melanoma from twenty-four year old Caucasian female human.

BS-C-1- (ATCC# CCL-26) kidney epithelial cell line from African green monkey (*Ceropithecus aethiops*)

2.2.4 Determination of Cytotoxicity of Compounds in Tissue Culture

The determination of cytotoxic activity of compounds against multiple transformed cancer cell lines grown *in vitro* was performed using three different methods. The experiments were performed either by the author or by Maria Kosfiszner, a member of the Roth lab.

2.2.4.1 Direct Cell Counting (Method 1)

30,000 HCT-116 cells, counted using a Coulter Counter, were aliquoted per well of a Costar 12-well plate. 1.5 mL of media was added and the plate was incubated for 8 hours. Ethanol stock solutions containing compound were then added to triplicate wells to produce various concentrations. Vehicle (ethanol) and an untreated control were included in triplicate wells. The plates were incubated for 48 hours, during which the wells were microscopically examined multiple times. At 48 hours, the media was removed, washed with sterile PBS buffer, and incubated with 0.5 mL of 0.25% trypsin for 10 minutes at 37 °C. 1.0 mL of media was then added to each well to inactivate the trypsin. A small amount of cells dosed with the highest concentration of compounds were removed, stained with trypan blue, and microscopically examined to verify the cells were alive. Then 100 µL of culture from each well was diluted in 10 mL of PBS buffer and counted in Coulter Cell Counter with an aperture setting of 15 µm. The population of each well was determined, and triplicate values were averaged and plotted to give growth inhibitory values for the compounds tested.

2.2.4.2 96-Well Colorimetric Assay (Method 2)

0.1 mL of a 2×10^4 cell/mL HCT-116 culture was dispensed into 96-well tissue culture plate(s) using a multi-channel pipettor. A time-zero plate containing three wells of culture and three wells of media was made. Following overnight incubation, compound was diluted from stock solutions into 0.1 mL of media and added to triplicate wells in the experimental plate. Vehicle control and non-treated control wells were also included. Then, 20 μ l of the CellTiter 96® Aqueous reagent was added to each well of the time-zero control plate. The plate was placed in the 37 °C CO₂ incubator for 1 hour. The absorbance of each well was then determined using a 96-well plate reader. The experimental plates were incubated for 48 hours, and then treated identically to the time-zero plate. The experimental absorbance values were averaged, plotted, and the cytotoxicity of each compound was determined relative to vehicle control values.

2.2.4.3 96-Well Luminescent Assay (Method 3)

0.1 mL of a 4×10^4 cells/mL OVCAR-3 culture was dispensed into opaque 96-well tissue culture plates using a Titertek Multidrop 96-well plate dispenser. The plates were incubated overnight, and the time-zero control plate was then placed at room temperature for 30 min. CellTiter Glo (Promega) reagent was thawed, mixed, and allowed to equilibrate at room temperature (~10 min). 100 μ l of CellTiter Glo was added per sample well, and the plate was placed on an orbital shaker for 5 min. The 96-well plate was then kept at room

temperature for 10 min. Luminescence was determined using a Torcon AML-34 96-well luminometer. 0.1 mL of serial dilutions of the test compounds in culture media were added to triplicate wells in the experimental plate(s). A triplicate set of wells containing a vehicle (dimethyl sulfoxide (DMSO) and/or ethanol) control and an untreated control (media only) were included. The experimental 96 well plate was incubated for 48 hours. At 48 hours, 0.1 mL of media was removed from each well, and the plate was treated and analyzed as described for the time-zero plate. The experimental values were averaged, plotted, and the cytotoxicity of each compound was determined relative to vehicle control values (see **Figure 2-5** for an example of this data).

2.2.5 Indirect Immunofluorescence of Cells

Cells were grown on 2 cm glass cover slips in tissue culture wells. Media containing compound was added at various concentrations and incubated for either 12 or 24 hrs. Hoescht 33343 nuclear dye was added directly to the media (1.5 $\mu\text{g}/\text{mL}$) and incubated at 37 $^{\circ}\text{C}$ for 30 min. Coverslips were then washed three times with 1X PBS and fixed for 10 min. at -20 $^{\circ}\text{C}$ with pre-cooled (-20 $^{\circ}\text{C}$) 100% methanol. Coverslips were washed three times with a 1X PBS/ 1% BSA solution and treated directly with a 1/2000 dilution of anti- α -tubulin antibody (mouse anti-human). Coverslips were washed three times with 1X PBS/1% BSA and treated with a 1/500 dilution of fluorescent labeled (Alexa Fluor 488) conjugated goat anti-mouse antibody. Coverslips were washed three times with 1X PBS/1% BSA and mounted on microscope slides using mounting media (Aqua Poly Mount). Images were

obtained with Zeiss Axiovert 100M digital light microscope and Bio Rad 60-WL-DZ model confocal microscope.

2.2.6 Thymidine Mitotic Block and Tubulin Imaging Procedure in BS-C-1 Green Monkey Cells

BS-C-1 cells were grown on 2 cm glass cover slips in tissue culture wells for 24 hours prior to use. Culture media containing 2 mM thymidine was then added to the wells and incubated for 17-20 hrs. The thymidine-containing media was removed, the cells were briefly washed twice with pre-warmed culture media, and then media containing 100 nM of the test compounds (syndistatin (**265**), vinblastine, taxol, colchicine, and natural diazamide A) were added to the wells. A 0.01 % DMSO vehicle control was included. Plates were incubated for 9.5 hours, then the coverslips were washed three times, very briefly, with 1X PBS and fixed for 10 min. at -20 °C with -20 °C 100% methanol. Extreme caution was used in handling the cover slips to prevent detachment of the rounded mitotic cells. The coverslips were then washed three times with a 1X PBS/1% BSA solution and treated directly with a 1/2000 dilution of anti- α -tubulin antibody (mouse anti-human). Coverslips were washed three times with 1 XPBS/1% BSA, and then treated with a 1/500 dilution of a fluorescently labeled (Alexa Fluor 488) conjugated goat anti-mouse antibody. Coverslips were washed three times with 1X PBS/1% BSA and mounted on microscope slides using mounting media (Aqua Poly Mount). Images were obtained using a Bio Rad 60-WL-DZ model confocal microscope.

2.2.7 FACSscan Analysis Cells

OVCAR-3 cells were grown to ~60% confluency in six-well tissue culture plates. Media containing 0.003% DMSO (vehicle control), 30 nM paclitaxel, 30 nM vinblastine, 30 nM syndistatin, and 30 nM natural diazonamide A were added to cells and incubated for 4 hr, 8 hr, 12 hr, and 16 hr. At these time points, cells were harvested with a 0.25% trypsin/1mM EDTA solution, and transferred to 1.5 mL Eppendorf tubes. Cells were pelleted and washed three times with 1X PBS. Cells were then fixed in -20 °C 100% ethanol and stored at 4 °C. Cells were pelleted from 100% ethanol, washed once with 1X PBS, and treated with Vindelov's propidium iodide solution and 1 mg/mL RNase for 30 min at 37 °C. FACSscan analysis was performed with propidium iodide detection using a Beckman-Dickinson FACSscan instrument . Data was analyzed with Cell Quest software.

2.2.8 Isolation of MAP Enriched Tubulin from Bovine Brain

The procedure used was adapted from the Mitchison group's (Harvard Medical School) tubulin isolation protocol.⁸⁸ Four bovine brains were obtained from freshly slaughtered animals (Dallas City Packing) and stored on ice. Approximately 35 minutes later, the brains were homogenized at 4 °C with 2 L of PBS in a Waring Blender on the high speed setting (3X at 15 sec of blending). The homogenate was centrifuged for 90 minutes at 10,000 rpm at 4 °C using a JA-10 rotor in a Beckmann J2-21M centrifuge. The approximate 2 L of supernatant was decanted into two 2 L flasks, and solid GTP, ATP, and MgCl₂ were added to give a final concentration of 0.1 mM GTP, 1.5 mM ATP, and 0.5 mM MgCl₂. 500 mL of 37 °C glycerol was added to each flask of supernatant, and the flasks were then placed

in a 37 °C water bath. Once the supernatant temperature reached 32°C, the flasks were kept in the 37 °C water baths from 60 minutes. The solution was then dispensed into polycarbonate ultracentrifugation tubes, placed in a prewarmed 37 °C Ti45 rotor, and centrifuged at 37 °C at 19,000 rpm for 150 minutes in a Beckmann L8-70M ultracentrifuge. The supernatant was decanted, and the desired transparent gelatinous pellets were re-suspended in the minimal amount of PBS required. At 4 °C, the suspended pellets were homogenized manually thirty times with a 40 mL dounce and pestel. The light yellow homogenized solution was placed on ice for 30 minutes and then manually homogenized thirty more times. The protein concentration was determined to be 14.4 mg/mL using the Bradford assay. The homogenized supernatant was then centrifuged at 35,000 rpm in the L8-70M ultracentrifuge at 4 °C for 30 minutes. Approximately 140 mL of supernatant was decanted, and solid GTP and MgCl₂ were added to give a final concentration of 0.5 mM GTP and 4.0 mM MgCl₂. 70 mL of 37 °C glycerol was added to the supernatant, and the solution was warmed in a water bath with an internal temperature of between 32-37 °C for 60 minutes. The supernatant was then centrifuged again at 35,000 rpm at 35 °C for 60 minutes. The protein pellet was re-suspended in PBS and homogenized as before. The yellow solution was then placed on ice for 30 minutes, and the protein concentration was determined to be 17.0 mg/mL. The supernatant was then centrifuged at 40,000 rpm at 4 °C for 30 minutes. The supernatant was decanted, the protein concentration was determined to be 13 mg/mL. The supernatant was then aliquoted and frozen in liquid nitrogen. The MAP-enriched tubulin aliquots were then stored at -80 °C.

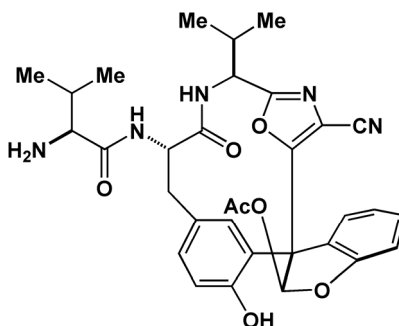
2.2.9 *In Vitro* Tubulin Polymerization Assay

MAP-enriched tubulin was briefly thawed in a 37 °C water bath, and then centrifuged at 14,000 rpm at 4 °C to pellet insoluble protein. The MAP tubulin was then placed on ice until use. The PEM buffer was degassed by stirring under house vacuum immediately before use. 1.2 mL of the 13 mg/mL MAP tubulin was diluted with 4.5 mL PEM buffer to give a final protein concentration of 2.3 mg/mL. 0.75 mL of glycerol and 0.262 mL of a 100 mM MgCl₂ solution (to give a final MgCl₂ of 4 mM) were added. The MAP tubulin solution was kept on ice. A transparent flat-bottomed 96 well plate (Costar #3595) was also placed on ice. The compounds being tested were diluted in PEM buffer, and 15 µL of the compound/PEM solution was placed in triplicate wells in the 96 well plate. A DMSO vehicle control was also diluted in PEM and plated in triplicate wells. 12 µL of a 500 mM GTP solution was added to 6 mL of the MAP-tubulin solution. The solution was gently mixed, and immediately 135 µL of the GTP/MAP-tubulin solution was added per well in the 96 well plate. 135 µL of the MAP tubulin solution without GTP was also added to the 96 well plate. The plate was placed in a SpectroFluor 96 Well Absorbance Plate Reader prewarmed to 37 °C, and the absorbance reading were taken at 340 nm every 30 seconds. The data was generated using xFluor software V3.21 and then analyzed and plotted using Microsoft Excel.

2.2.10 Characterization Data for Diazonamide-Based Reagents

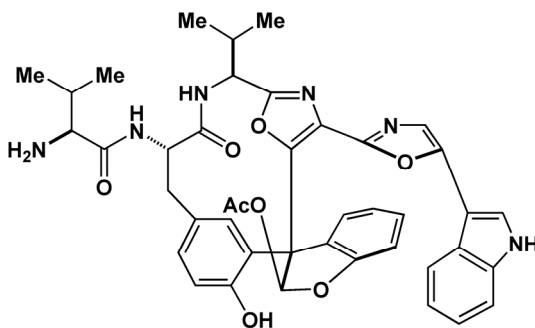
The diazonamide derivatives and congeners described were synthesized in the Harran laboratory.^{45, 46} Analogs **264**, **275**, and **276** were synthesized by myself. The remaining molecules were prepared by Dr. Jing Li.

Truncated Acetyl Hemiacetal 264



See attached appendix, Compound **264** ^1H NMR Spectra

seco Des-chloro Acetyl Hemiacetal 265

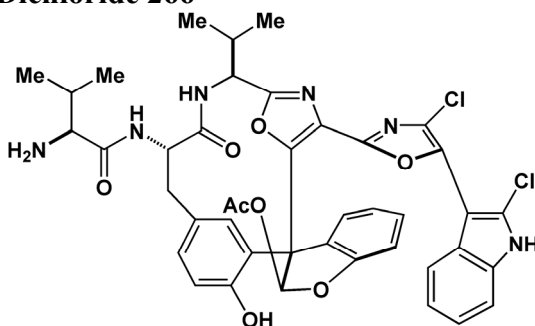


265: $R_f = 0.14$ (10% MeOH / CH_2Cl_2). $[\alpha]_D^{25} = -268.8^\circ$ ($c = 0.16$, MeOH). UV/Vis: $64 \mu\text{M}$ in MeOH: $\epsilon = 1790 \text{ Lmol}^{-1}$ at 324 nm. ^1H NMR (400 MHz, CD_3OD): δ 0.94-1.01 (m, 9H), 1.12 (d, $J = 6.4\text{Hz}$, 3H), 1.93 (s, 3H), 1.98 (m, 1H), 2.11 (m, 1H), 2.62 (dd, $J = 2.4, 13.2\text{Hz}$, 1H), 3.17 (m, 2H), 4.45 (dd, $J = 2.4, 12.0\text{Hz}$, 1H), 4.55 (d, $J = 10.0\text{Hz}$, 1H), 6.24 (d, $J = 2.4\text{Hz}$, 1H), 6.48 (t, $J = 7.6\text{Hz}$, 1H), 6.67-6.79 (m, 4H), 7.02 (dd, $J = 2.0, 8.0\text{Hz}$, 1H), 7.13-

7.23 (m, 3H), 7.32 (s, 1H), 7.43 (d, $J = 7.6\text{Hz}$, 1H), 7.72 (d, $J = 8.0\text{Hz}$, 1H), 7.95 (s, 1H).

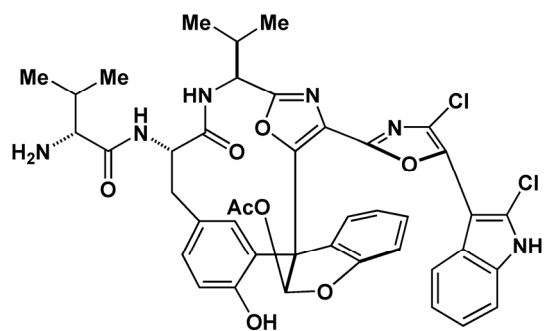
HRMS (FAB) calcd for $\text{C}_{42}\text{H}_{42}\text{N}_6\text{O}_8$ (M^+): 759.3142, found: 759.3153.

***seco* Acetyl Hemiacetal Dichloride 266**



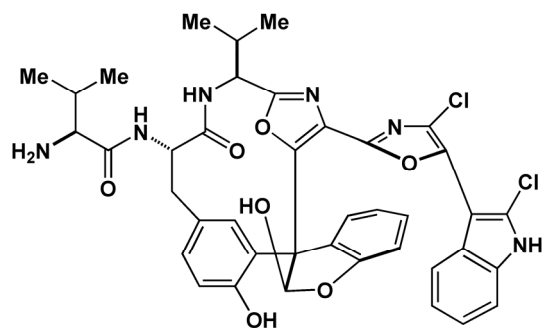
266: $R_f = 0.21$ (10% MeOH / CH_2Cl_2). $[\alpha]_D^{25} = -246.9^\circ$ ($c = 0.34$, MeOH). IR (film) 3250, 2961, 1759, 1728, 1650, 1609, 1512, 1265, 1217, 1054, 998, 956, 900, 745 cm^{-1} . ^1H NMR (400 MHz, CD_3OD): δ 0.93-1.02 (m, 9H), 1.12 (d, $J = 6.4$ Hz, 3H), 1.95 (s, 3H), 1.96 (m, 1H), 2.10 (m, 1H), 2.60 (dd, $J = 2.8, 13.2$ Hz, 1H), 3.18 (m, 2H), 4.45 (dd, $J = 2.8, 12.0$ Hz, 1H), 4.54 (d, $J = 9.6$ Hz, 1H), 6.24 (d, $J = 2.0$ Hz, 1H), 6.34 (d, $J = 8.4$ Hz, 1H), 6.53 (td, $J = 0.8, 7.6$ Hz, 1H), 6.62 (td, $J = 1.2, 7.6$ Hz, 1H), 6.70 (m, 2H), 7.01 (dd, $J = 2.0, 8.4$ Hz, 1H), 7.15 (td, $J = 0.8, 7.6$ Hz, 1H), 7.25 (td, $J = 0.8, 7.6$ Hz, 1H), 7.39 (d, $J = 8.0$ Hz, 1H), 7.45 (d, $J = 8.0$ Hz, 1H), 7.90 (s, 1H). ^{13}C NMR (75 MHz, CD_3OD): δ 17.9, 19.7(2C), 20.2, 20.9, 31.1, 38.6, 56.2, 58.0, 61.1, 65.3, 67.0, 99.4, 102.5, 110.8, 112.0, 117.7, 120.4, 121.8, 122.2, 123.9, 124.6, 125.4, 127.2, 127.5, 128.3, 129.2, 129.9, 130.4, 130.9, 132.2, 132.4, 133.6, 136.2, 142.3, 154.1, 154.7, 159.7, 165.6, 169.3, 170.4, 174.8. HRMS (FAB) calcd for $\text{C}_{42}\text{H}_{40}\text{Cl}_2\text{N}_6\text{O}_8$ (M^+): 827.2363, found: 827.2346.

***epi*-C37 *seco* Acetyl Hemiacetal Dichloride 267**



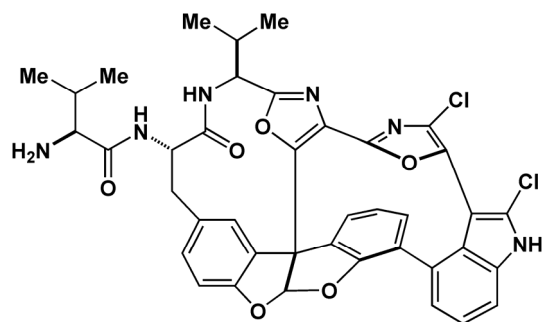
See attached appendix: Compound **267** ^1H NMR Spectra

***seco* Original Diazonamide A Structure 268**



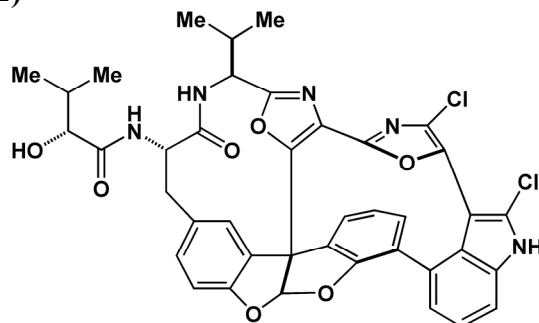
See attached appendix: Compound **268** ^1H NMR Spectra

C37-Amine Acetal 269



CD₃OD): δ 7.51 (d, $J = 2.0$ Hz, 1H), 7.47 (dd, $J = 1.2, 8.8$ Hz, 1H), 7.36 (t, $J = 7.6$ Hz, 1H), 7.27 (dd, $J = 2.0, 8.0$ Hz, 1H), 7.20 (dd, $J = 1.2, 7.6$ Hz, 2H), 7.07 (dd, $J = 1.2, 7.6$ Hz, 1H), 6.93 (t, $J = 7.6$ Hz, 1H), 6.88 (d, $J = 8.8$ Hz, 1H), 6.84 (s, 1H), 4.98 (d, $J = 6.0$ Hz, 1H), 4.61 (dd, $J = 3.2, 11.6$ Hz, 1H), 3.89 (d, $J = 4.0$ Hz, 1H), 3.47 (t, $J = 8.4$ Hz, 1H), 2.81 (dd, $J = 3.2, 12.8$ Hz, 1H), 2.34-2.26 (m, 1H), 2.14-2.06 (m, 1H), 1.10 (d, $J = 6.8$ Hz, 3H), 1.03 (d, $J = 6.8$ Hz, 3H), 0.96 (d, $J = 6.8$ Hz, 3H), 0.92 (d, $J = 6.8$ Hz, 3H). ¹³C NMR (75 mHz, CD₃OD): δ 175.8, 175.2, 163.2, 159.8, 159.3, 154.9, 153.7, 141.8, 136.7, 132.4, 131.8, 131.3, 131.2, 130.7, 130.4, 129.5, 128.7, 127.9, 127.6, 127.0, 125.2, 124.2, 124.1 (2C), 122.7, 119.7, 112.5, 111.8, 98.1, 77.0, 62.2, 57.3, 56.5, 39.0, 33.4, 31.6, 19.7, 19.6, 18.7, 16.6. ES-MS: calcd. for C₄₀H₃₃Cl₂N₅O₇ [M+H]⁺: 766.18, found: 766.30; calcd. for C₄₀H₃₃Cl₂N₅O₇ [M-H]⁻: 764.16, found: 764.31. HRMS (FAB) calcd for C₄₀H₃₃Cl₂N₅O₇ (M+Li): 772.1917, found: 772.1962.

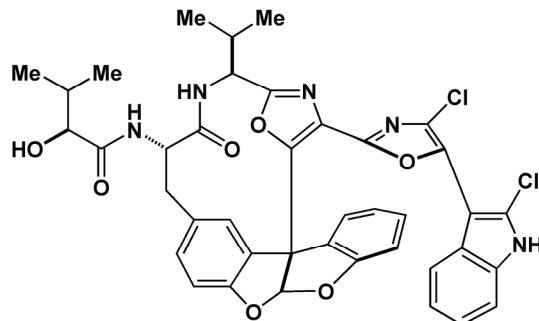
***epi*-C37 Syndistatin (272)**



272: ¹H NMR (400MHz, CD₃OD): δ 7.52 (d, $J = 1.8$ Hz, 1H), 7.47 (dd, $J = 1.2, 8.5$ Hz, 1H), 7.38 – 7.34 (m, 1H), 7.26 (dd, $J = 1.8, 7.9$ Hz, 1H), 7.21 – 7.19 (m, 2H), 7.08 (dd, $J = 1.2, 7.9$ Hz, 1H), 6.96 – 6.87 (m, 2H), 6.84 (s, 1H), 4.98 (d, $J = 6.0$ Hz, 1H), 4.60 (dd, $J = 3.2, 11.6$

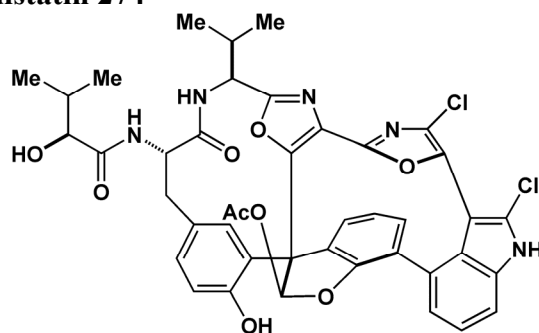
Hz, 1H), 3.92 (d, $J = 3.6$ Hz, 1H), 3.50 (app t, $J = 12.2$, 1H), 2.83 – 2.79 (dd, $J = 3.6$, 12.8 Hz, 1H), 2.35 – 2.25 (m, 1H), 2.16 – 2.06 (m, 1H), 1.11 (d, $J = 6.8$ Hz, 3H), 1.01 (d, $J = 6.8$ Hz, 3H), 0.95 (d, $J = 6.8$ Hz, 3H), 0.84 (d, $J = 6.8$ Hz, 3H).

seco Syndistatin 273



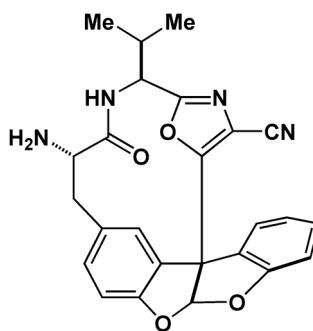
273: ^1H NMR (400 MHz, CD_3OD): δ 7.40 – 7.37 (m, 1H), 7.27 – 7.22 (m, 2H), 7.19 – 7.05 (m, 4H), 6.93 (d, $J = 8.2$ Hz, 1H), 6.81 (td, $J = 1.5$, 7.6 Hz, 1H), 6.72 (td, $J = 0.92$, 7.6 Hz, 1H), 6.40 (d, $J = 7.6$ Hz, 1H), 5.49 (s, 1H), 4.72 (d, $J = 7.3$ Hz, 1H), 4.52 (dd, $J = 4.0$, 11.9 Hz, 1H), 3.88 (d, $J = 4.0$ Hz, 1H), 3.19 – 3.13 (m, 1H), 2.86 – 2.82 (m, 1H), 2.51 – 2.47 (m, 1H), 2.27 – 2.08 (m, 1H), 1.04 – 1.00 (m, 9H), 0.90 (d, $J = 6.8$ Hz, 3H).

Acetyl Hemiactal Syndistatin 274



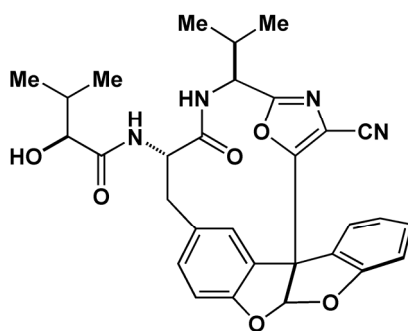
274: ^1H NMR (400 MHz, CD_3OD): δ 8.77 (s, 1H), 7.43 (d, $J = 8.5$ Hz, 1H), 7.33 (dd, $J = 8.5$, 8.5 Hz, 1H), 7.15 (d, $J = 7.3$ Hz, 1H), 7.13 (dd, $J = 2.4$, 8.5 Hz, 1H), 6.85 – 6.75 (m, 4H), 6.51 (d, $J = 2.4$ Hz, 1H), 4.57 (dd, $J = 3.0$, 12.2 Hz, 1H), 4.49 (d, $J = 9.1$ Hz, 1H), 3.88 (d, $J = 3.6$ Hz, 1H), 3.18 (app t, $J = 12.2$ Hz, 1H), 2.67 (dd, $J = 3.0$, 13.4 Hz, 1H), 2.16 – 2.01 (m, 2H), 1.85 (s, 3H), 1.08 (d, $J = 6.8$ Hz, 3H), 1.03 (d, $J = 6.8$ Hz, 3H), 0.95 (d, $J = 6.8$ Hz, 3H), 0.91 (d, $J = 6.8$ Hz, 3H).

Acetal Core 275



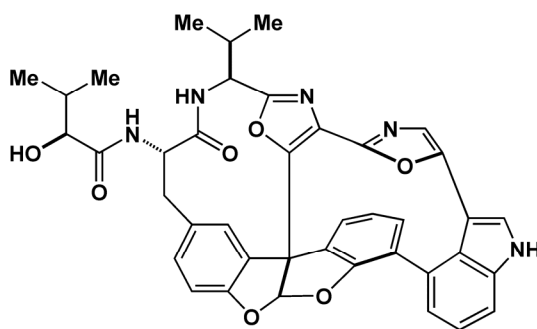
275: ^1H NMR (400 MHz, CDCl_3): δ 7.47 (dd, $J = 1.1$, 7.7 Hz, 1H), 7.38 – 7.33 (m, 1H), 7.13 – 7.03 (m, 3H), 6.94 (d, $J = 1.8$ Hz, 1H), 6.88 (s, 1H), 6.87 (d, $J = 8.4$ Hz, 1H), 5.52 (d, $J = 7.7$ Hz, 1H), 4.80 (t, $J = 7.3$ Hz, 1H), 3.08 (d, $J = 6.2$ Hz, 1H), 2.82 – 2.70 (m, 1H), 2.12 – 2.01 (m, 1H), 1.03 (d, $J = 6.8$ Hz, 3H), 0.99 (d, $J = 6.8$ Hz, 3H).

Truncated Acetal 276



276: ^1H NMR (400 MHz, CD_3OD): δ 7.58 (dd, $J = 1.2, 7.3$ Hz, 1H), 7.41- 7.37 (m 1H), 7.27 (dd, $J = 1.8, 8.5$ Hz, 1H), 7.15 – 7.11 (m, 1H), 7.07 (d, $J = 7.9$ Hz, 1H), 6.99 (s, 1H), 6.96 – 6.90 (m, 2H), 4.51 (d, $J = 8.5$ Hz, 1H), 4.45 (dd, $J = 3.6, 11.5$ Hz, 1H), 3.87 (d, $J = 4.3$ Hz, 1H), 3.10 (*app t*, $J = 12.2$ Hz, 1H), 2.83 (dd, $J = 3.6, 12.8$ Hz, 1H), 2.15 – 1.96 (m, 2H), 1.01 (d, $J = 6.8$ Hz, 6H), 0.97 (d, $J = 6.8$ Hz, 3H), 0.90 (d, $J = 6.8$ Hz, 3H).

Des-Chloro Syndistatin 277

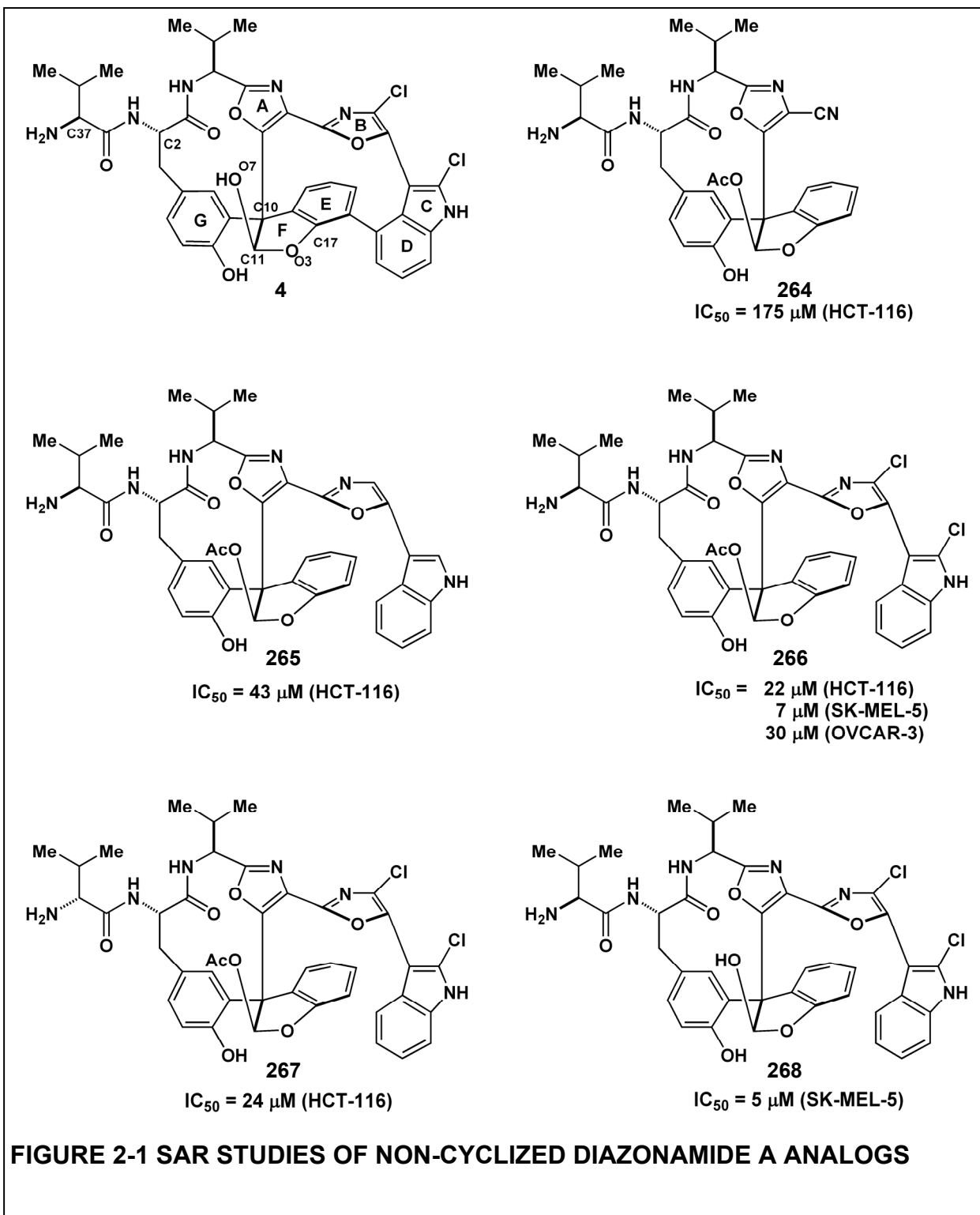


See attached appendix: Compound **277** ^1H NMR Spectra

2.3 Results

2.3.1 Cellular Activity of Compounds Related to the Structure Originally Proposed for Diazonamide A

2.3.1.1 Molecules Lacking the C16-C18 Biaryl Linkage



Prior to completing the total synthesis of the original diazonamide A structure (**4**), the Harran group accessed several advanced diazonamide intermediates. The biological activity of these compounds was evaluated in an attempt to establish preliminary SAR in the diazonamide series and perhaps to identify simplified, more-accessible biologically-active diazonamide analogs. As described earlier (Section 1.2.3.11), the Harran group was able to synthesize the intact diazonamide A structure lacking the C16-C18 biaryl bond.⁴⁵ This

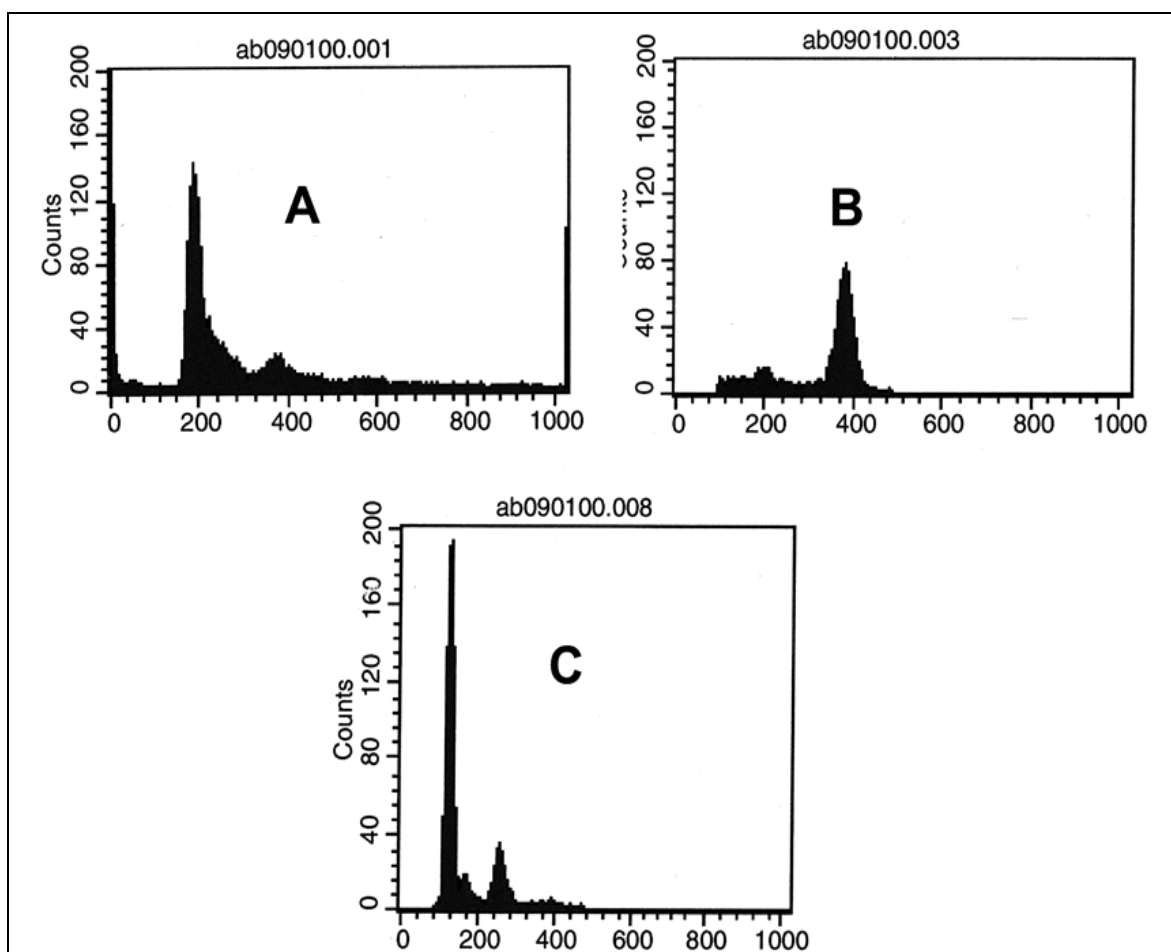


FIGURE 2-2 FACSCAN ANALYSIS SHOWS NON-CYCLIZED ANALOGS ARE NOT ANTI-MITOTIC AGENTS: After 16 h incubation with compound, OVCAR-3 were fixed with ethanol and treated for 30 min with Vindelov's propidium iodide solution and 1 mg/mL RNase at 37 °C: A) Vehicle Control (DMSO 0.01%) B) 40 nM paclitaxel C) 30 μ M 266

allowed access to several late-stage analogs (**Figure 2-1**), including an acetylated, non-cyclized form of the original diazonamide A structure (**266**). All of these diazonamide congeners exhibited greatly reduced cytotoxicity relative to the natural product. For example, compound **266** was determined to possess an IC₅₀ value against the HCT-116 cell line of 22 μM. The NCI DTP IC₅₀ value for diazonamide A against this cell line is 4 nM.⁵⁷

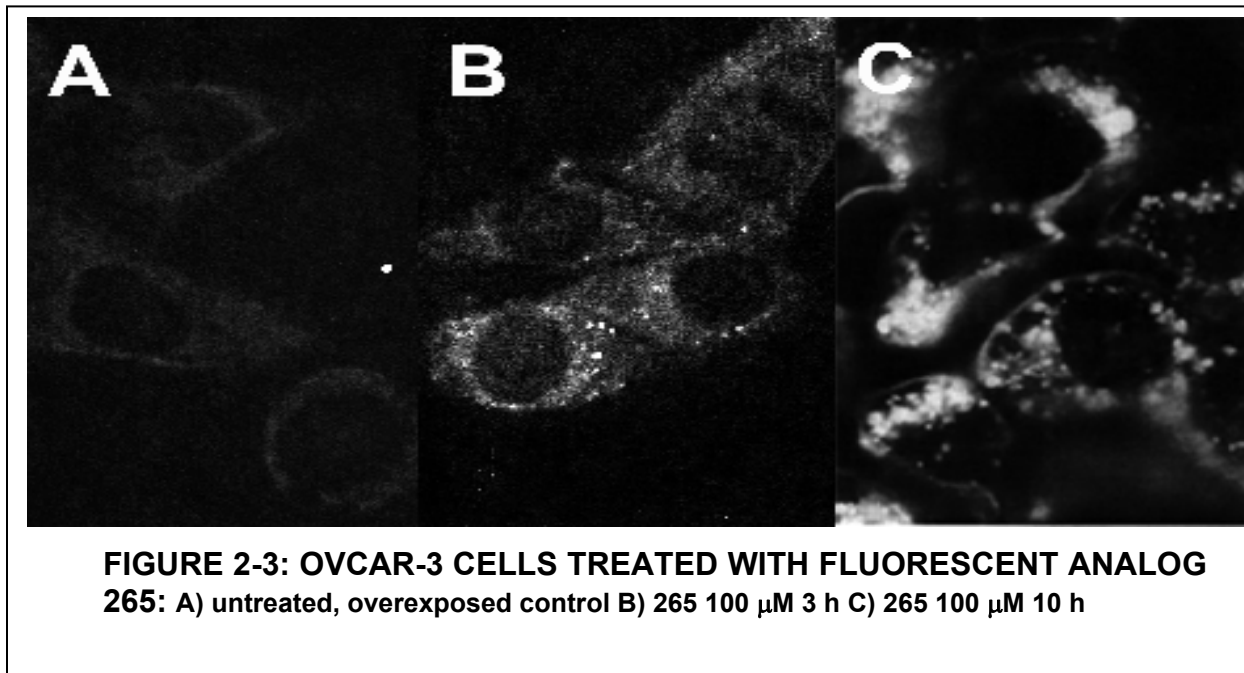
Despite its lack of potency compared to the parent structure, the effect of compound **266** on cell division was evaluated using FACScan analysis (**Figure 2-2**). Exposure of HCT-116 cells for 48 hrs to 30 μM **266** did not induce a shift of the cell population to the tetraploid state, whereas 40 nM of the anti-mitotic control compound paclitaxel causes the expected accumulation of the 4N population. The lack of potency and absence of anti-mitotic activity indicated that **266** induces cytotoxicity through a means distinct from diazonamide A. Obviously, this precluded meaningful conclusions about diazonamide A SAR. For example, compound **267** contains the (*D*)-valine conjugated side chain, but is virtually equipotent as **266**. Therefore, in this series of compounds the stereochemistry of the C37 side chain is immaterial for activity. At the time these experiments were performed, prior to the structural revision, the data interpretation was that diazonamide A potency would only be realized with formation of the final C16-C18 biaryl bond.

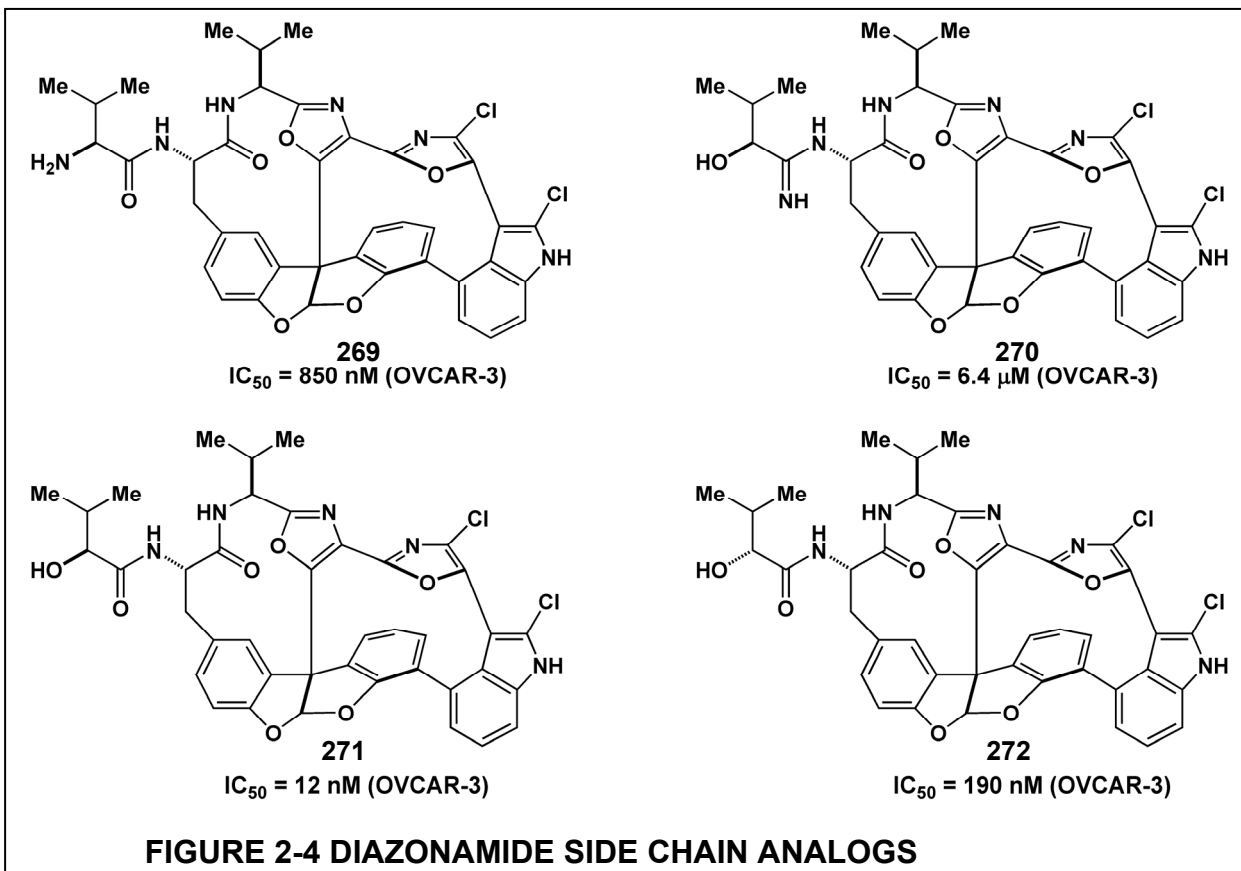
Non-chlorinated analog **265** is a brightly fluorescent compound with a strong emission at the 424 nm wavelength.⁴⁵ Fluorescence imaging of compound **265** directly in cells was performed. OVCAR-3 cells treated with 100 μM of **265** clearly showed concentration of the compound into brightly fluorescent areas on the cells over time (**Figure 2-2**). Based solely on the fluorescent imaging however, it cannot be determined whether

compound **265** is being concentrated inside of the cell, or if the fluorescent areas are located on the cell surface. There is no indication of the compound binding to any cellular structure such as the nucleus or microtubule network.

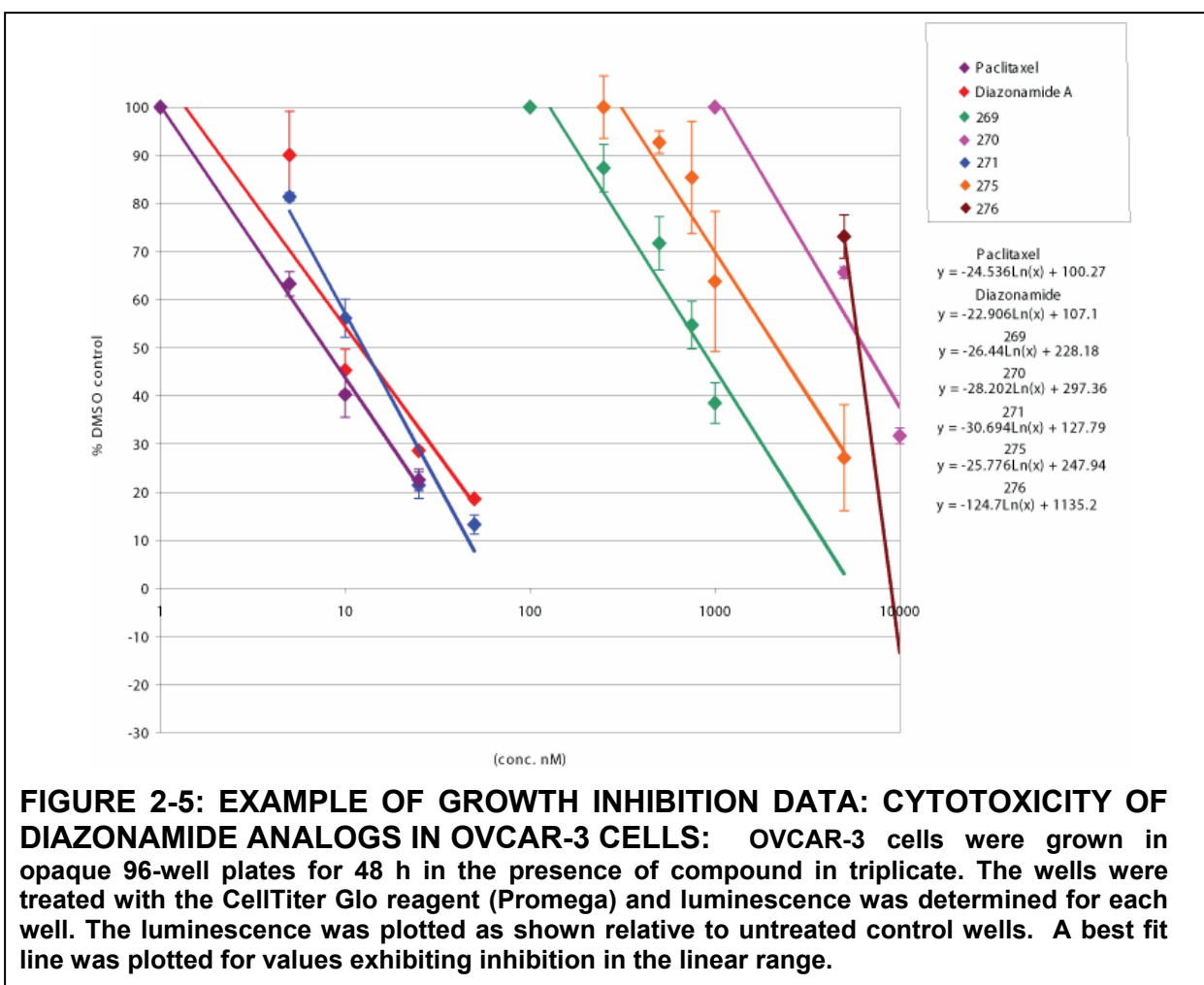
2.3.2 Cellular Activity as a Confirmatory Guide to the Revised Diazonamide Structures

The Harran's group revision of the diazonamide A structure was partially guided by evaluating the cellular activity of various analogs synthesized. The Fenical group provided a small amount of natural diazonamide A to confirm the total synthesis was complete, and this material was used in the following biological experiments. As described previously (Chapter 1.4), the Harran group initially focused on the diazonamide side chain as the location of the structural misassignment, and several analogs with different side chains were synthesized and screened for biological activity. Due to its inherent instability, the C11



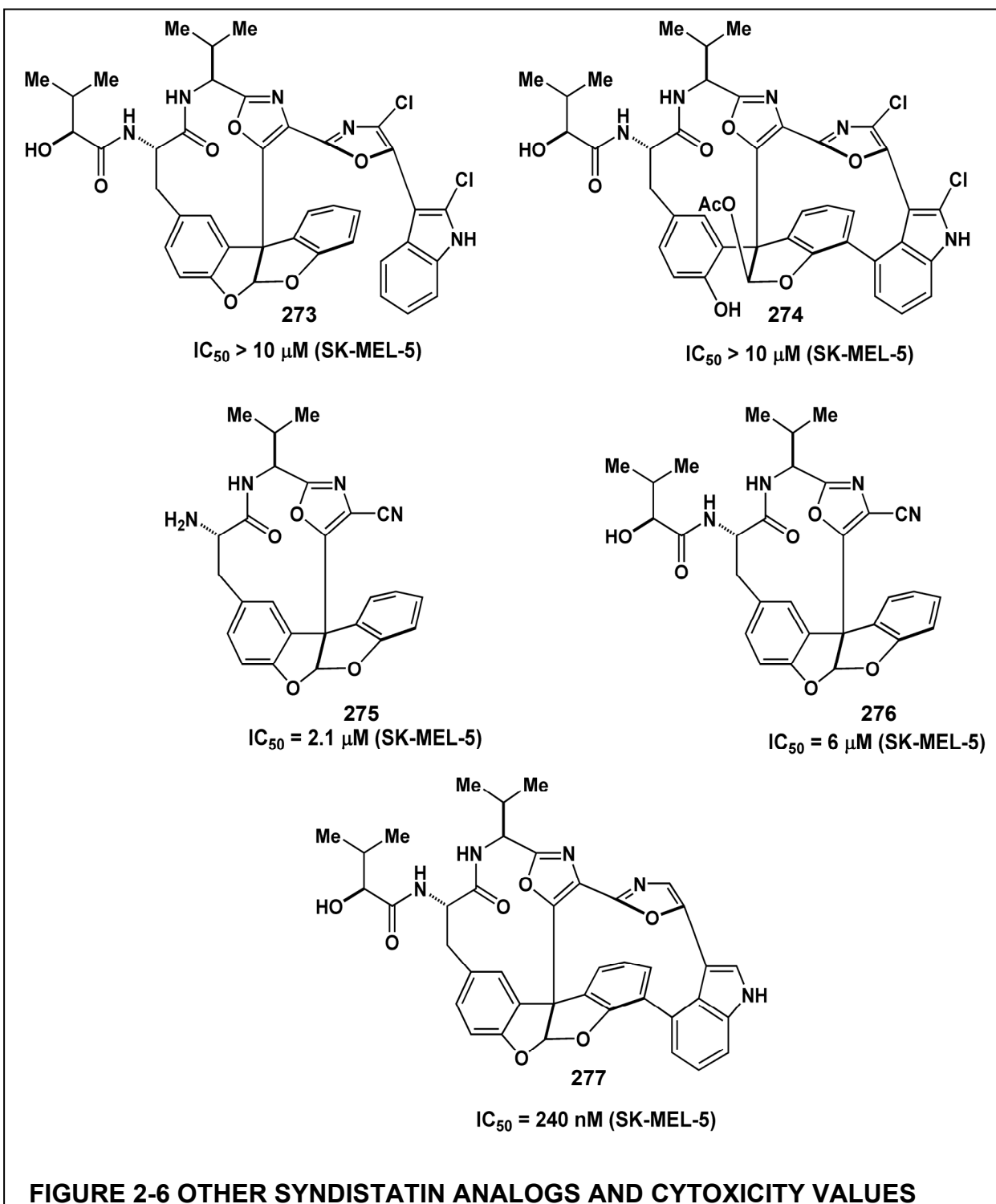


hemiacetal was converted to a diaryl acetal in this series (**Figure 2-4, 2-6**). A reexamination of the original isolation data indicated an α -hydroxy isovaleric acid conjugate could have been mistaken for a valine residue. This assertion was validated by the cytotoxicity of compound **271**, which approximated the potency of the sample of natural diazonamide A (**Figure 2-4, 2-5**). Analog **270**, which possess the valine side chain as originally assigned, was significantly less active with an IC_{50} of 850 nM. Another possible candidate for the reassignment of the side chain was amidine-containing compound **269**. However, this substance was dramatically less (IC_{50} of 6.4 μ M). Furthermore, both α -hydroxy isovaleric



acid epimers were screened, and the C37 stereochemistry was tentatively assigned as (*S*) based on relative potency (**Figure 2-4, 272**). Compound **271**, termed syndistatin, differs from diazonamide A at a single position, oxygen for nitrogen in the core of the structure.

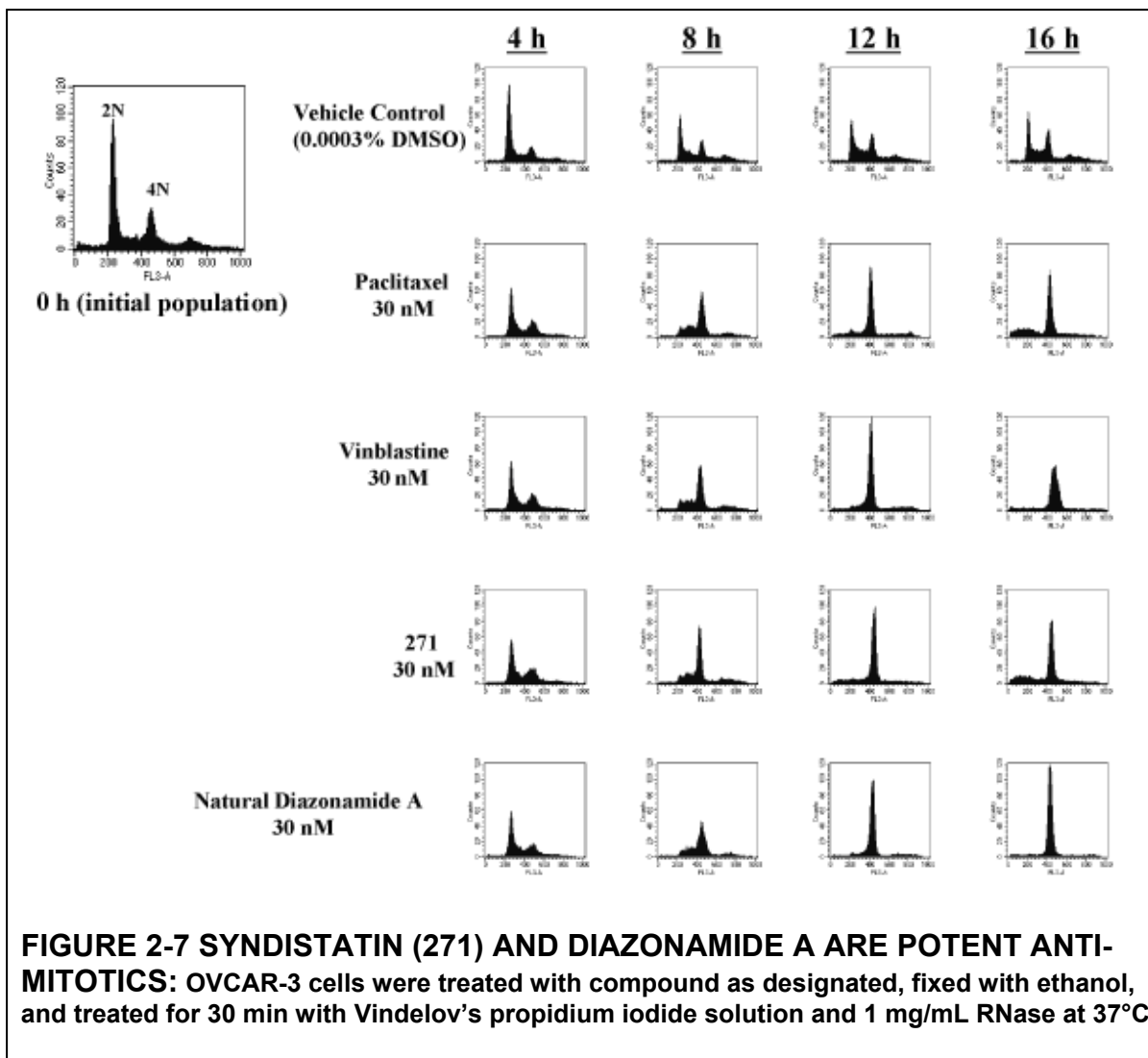
Beyond permutations of the side chain, SAR was explored through the synthesis of compounds varying the diazonamide core (**Figure 2-6**). Preparing C11 diaryl acetals proved a good choice, since the C11 acetylated hemiacetal analog **274** did not exhibit significant cytotoxicity. Compound **273**, which lacks the C16-C18 bond, also does not possess discernable anti-proliferative activity. Further, diazonamide ‘half’-structures **275** and **276** are



several hundred fold less active than diazonamide A and syndistatin (**271**). Des-chloro analog **277** is approximately 20-fold less active than syndistatin (**271**).

2.3.3 Further Biochemical Evaluations of (-)Diazonamide A and (-)Syndistatin (271)

In addition to quantifying the potency of diazonamide-related compounds, their effect on cell-cycle arrest were also characterized. These experiments aimed to determine whether syndistatin was mechanistically related to diazonamide A. FACscan analysis clearly showed both syndistatin (**271**) and diazonamide A blocked the progression through mitosis when dosed at 30 nM concentrations in OVCAR-3 cell culture; an effect indistinguishable from standard anti-mitotic compounds paclitaxel and vinblastine (**Figure 2-7**). The effect of diazonamide compounds was then explored in cell culture using fluorescent antibodies specific for tubulin (**Figure 2-8**). The diazonamide compounds clearly showed a depolymerizing effect on the cellular microtubules, similar to the observed vinblastine and colchicine controls. The depolymerizing effect was concentration and time dependent. 1 μ M of either diazonamide A or syndistatin completely depolymerized microtubules in BS-C-1 cells after 24 hrs. However, dosing BS-C-1 cells with 100 nM for 24 hr showed no overt effect on cytosolic microtubules (result not shown).



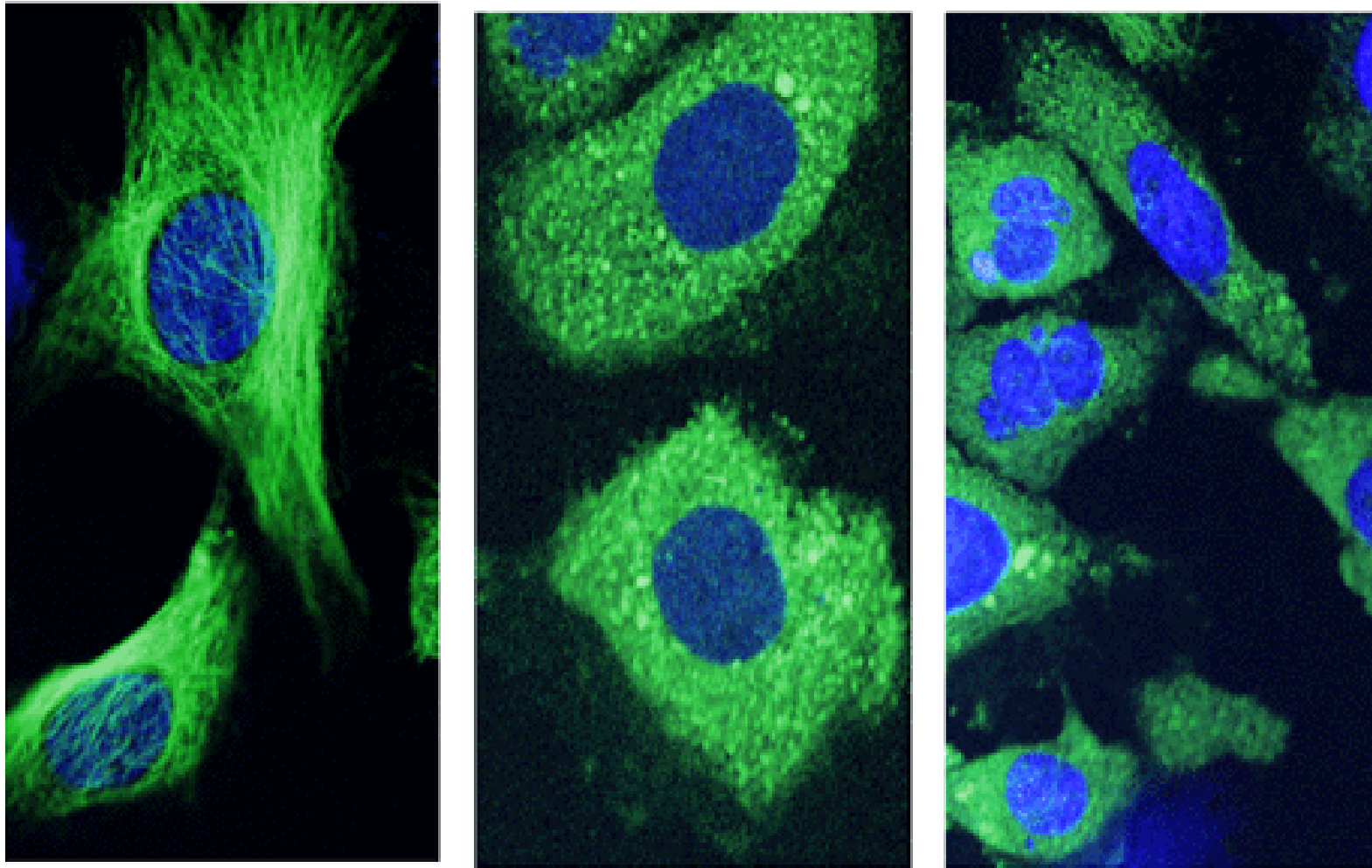


FIGURE 2-8 DIAZONAMIDE A AND SYNDISTATIN (271) INDUCE CELLULAR MICROTUBULE DEPOLYMERIZATION AT HIGH CONCENTRATIONS:

BS-C-1 cells on glass cover slips were treated with compound for 24 h. Then Hoescht nuclear stain was added to the media for 30 min. The cells were then fixed in -20°C methanol and microtubules were visualized with tubulin specific antibodies. A) 0.01% DMSO B) 271 $1\ \mu\text{M}$ C) syndistatin $1\ \mu\text{M}$

2.3.4 Effect of Diazonamide A and Syndistatin (271) on *In Vitro* Tubulin Polymerization

The microtubule depolymerizing activity of syndistatin and diazonamide A were then studied in the *in vitro* tubulin polymerization assay. Using MAP-enriched tubulin purified from bovine brain, both diazonamide A (**Figure 2-9, 2-10**) and syndistatin (**Table 2-1**) prevented the polymerization of tubulin into microtubules in a concentration dependent fashion. The known tubulin-binding compounds paclitaxel and nocodazole were included as polymerization control compounds (**Table 2-1**). IC₅₀ values for the effects of syndistatin and diazonamide A on both the maximum level of tubulin polymerization and the rate of tubulin polymerization were determined. These values were observed through examination of the polymerization data, establishing the maximum value of polymerization for each concentration of compound (**Figure 2-10**). The rate of polymerization was determined through the analysis of the effect of compound concentration on the rate of tubulin polymerization during the linear rate of polymerization (**Figure 2-10**). Plotting the values for each concentration allowed for the establishment of the IC₅₀ values (**Table 2-1**).

Both diazonamide A and syndistatin were highly active in preventing both maximal tubulin polymerization and the rate of tubulin polymerization. The compounds are considerably more active than the known tubulin depolymerizing agent nocodazole. Syndistatin (**271**) proved to be even more active than diazonamide A in this assay (**Table 2-1**), although the compound is slightly less cytotoxic in cell culture. Syndistatin analogs **270**, **272**, and **276** were also evaluated in the tubulin polymerization assay. Amidine-containing

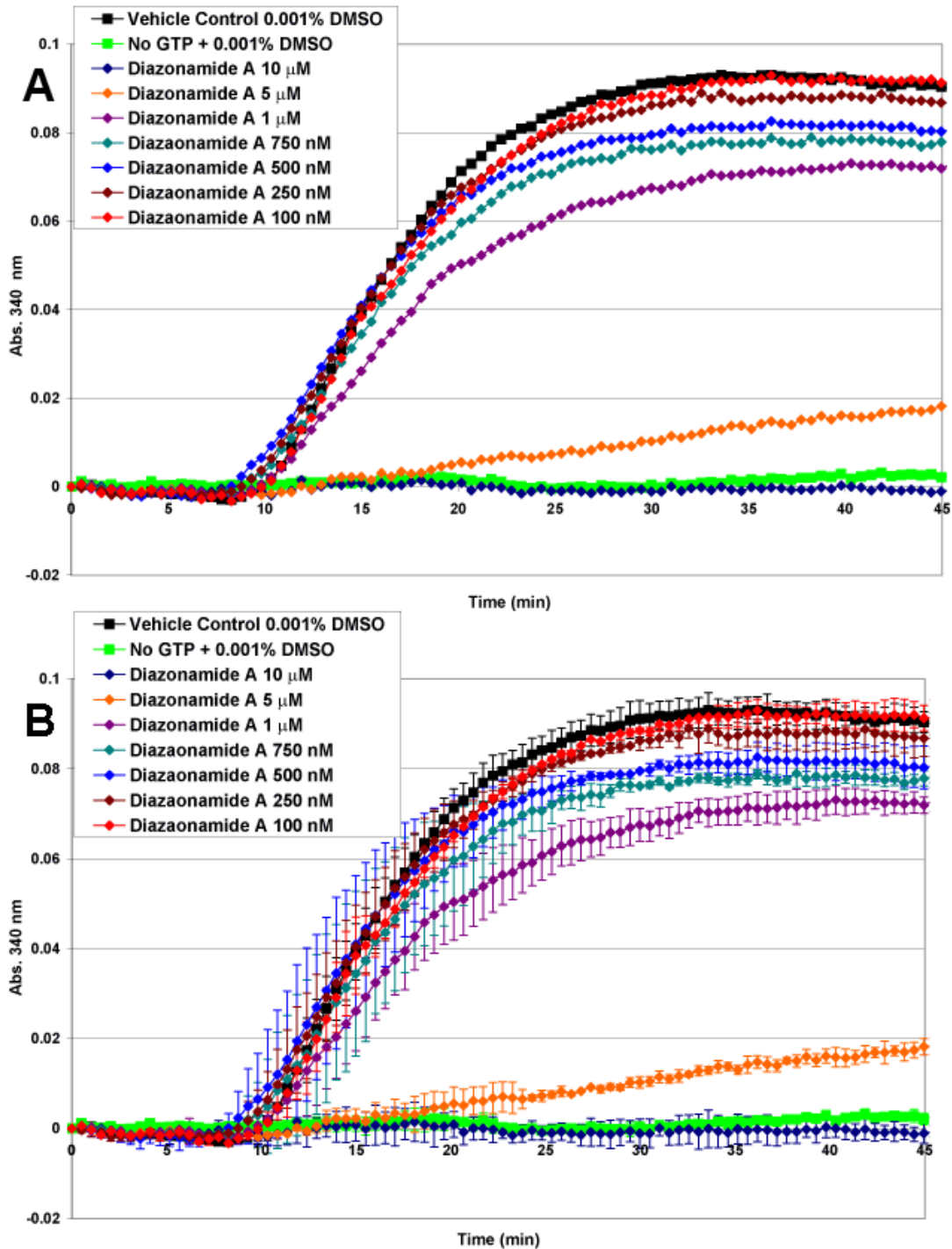
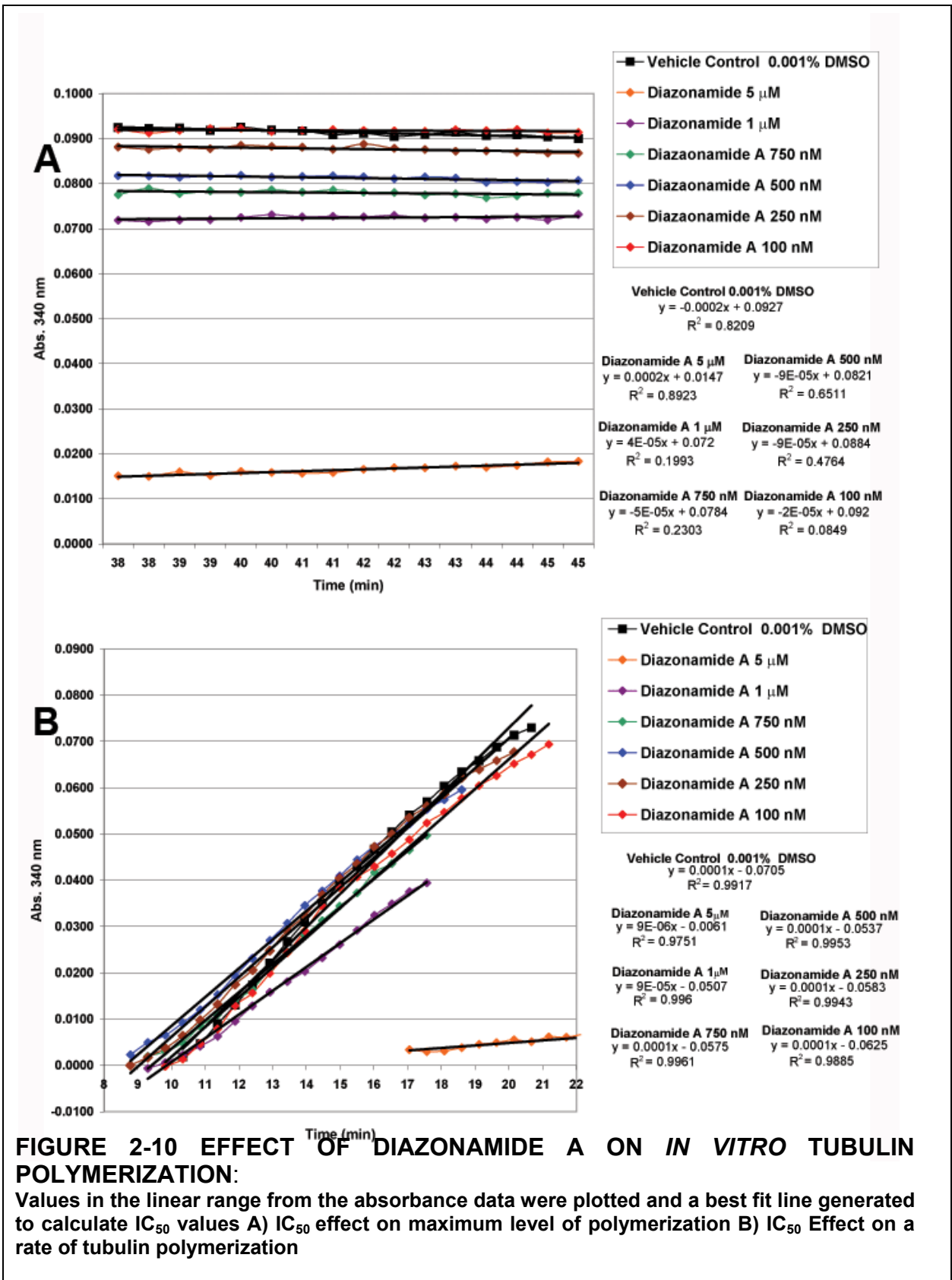


FIGURE 2-9 DIAZONAMIDE A PREVENTS THE POLYMERIZATION OF IN VITRO MAP(+)-TUBULIN:

Bovine MAP(+) in PEM buffer with GTP was incubated with compound in a transparent 96-well plate of diazonamide A. Absorbance at 340 nm was measured every 30 sec and plotted. A) Averaged triplicate values B) Averaged triplicate values with error bars



<u>Compound</u>	<u>IC₅₀ Max Level (μM)</u>	<u>IC₅₀ Rate of Poly. (μM)</u>
Nocodazole	4.8	6.8
Diazonamide A	2.2	2.2
270	6.7	18.0
271	1.2	1.2
272	1.6	1.6
276	No activity	No activity

TABLE 2-1 IC₅₀ VALUES FOR TUBULIN POLYMERIZATION:

analog **270** is five times less active at inhibiting the rate of tubulin polymerization and over fifteen times less capable of preventing maximal tubulin polymerization (**Table 2-1**). **270** is the only compound screened that had significantly different IC₅₀ values for the rate of polymerization and the maximal level of polymerization. Compound **272** is nearly as active as syndistatin in this assay, despite being over fifteen times less cytotoxic (**Table 2-1**). Half-structure **276** failed to have any inhibitory effect on polymerization, even at a concentration of 50 μM. In combination with its micromolar cytotoxicity, the inactivity in the tubulin polymerization assay supports the assertion that analog **276**, and probably the related analogs, exert their biological activity through a path separate from that of diazonamide A.

The effect of the diazonamide compounds on pre-formed *in vitro* microtubules was also determined. In this experiment, tubulin was allowed to reach a maximal level of polymerization before compound was added to the sample wells. The known tubulin depolymerizing compounds nocodazole and vinblastine were included as controls (**Figure 2-**

11). Both vinblastine and nocodazole induced the depolymerization of microtubules preformed from MAP-enriched tubulin in a concentration dependent manner (**Figure 2-11**). The diazonamide compounds, however, failed to induce the depolymerization of preformed microtubules in this experiment at any concentration (**Figure 2-12**).

2.3.5 Effects of Diazonamide A and Syndistatin (271) on Mitotic Spindle Formation

While examining interphase microtubules in diazonamide treated cells (Section 2.3.2, **Figure 2-8**), a pronounced effect on mitotic spindles was observed. To examine this phenomenon more closely, BS-C-1 cells were synchronized in S-phase using a thymidine block. Upon washing out the thymidine, cells were allowed to proceed into mitosis in the presence of compound. At the point in time where the highest percentage of the population entered mitosis, cells were fixed and their microtubules visualized using fluorescent antibodies. Diazonamide A and syndistatin (**265**) both caused the formation of aberrant, mono-polar mitotic spindles after 9.5 hours of treatment with 100 nM of compound (**Figure 2-13**).

This effect on mitotic spindles was present in a majority of mitotic cells, and not observed with the known microtubule depolymerizing agents vinblastine and nocodazole (data not shown). In contrast, 100 nM of nocodazole or 100 nM of vinblastine caused a poorly organized mitotic spindle in which the microtubules are clearly degraded. The microtubules radiating from the diazonamide-induced mono-aster spindles are well formed,

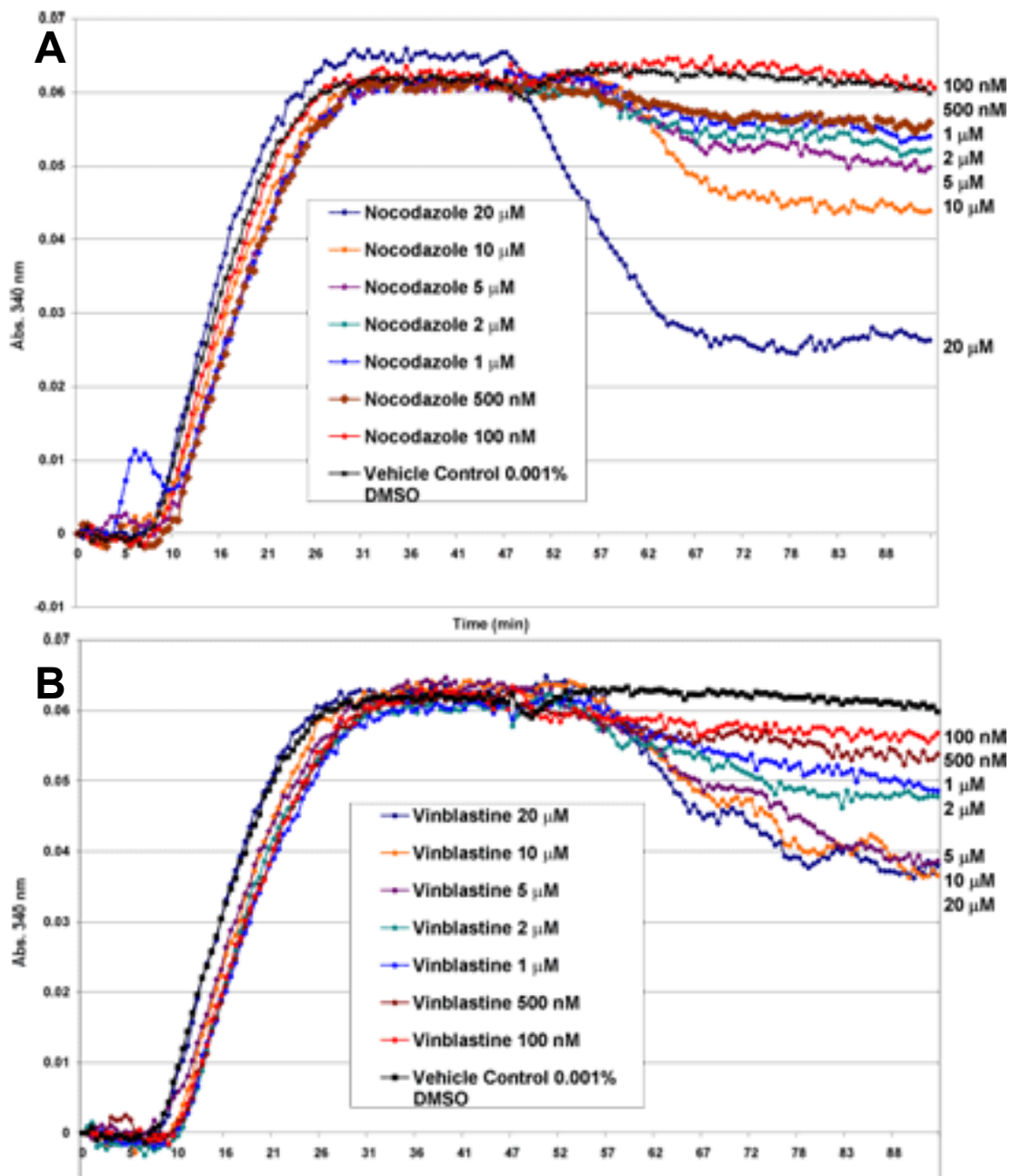


FIGURE 2-11 EFFECT OF COMPOUNDS ON PREFORMED MICROTUBULES
 MAP(+) Tubulin was allowed to polymerize at 37 °C for 45 min then treated with compound.
 A) Nocodazole B) Vinblastine

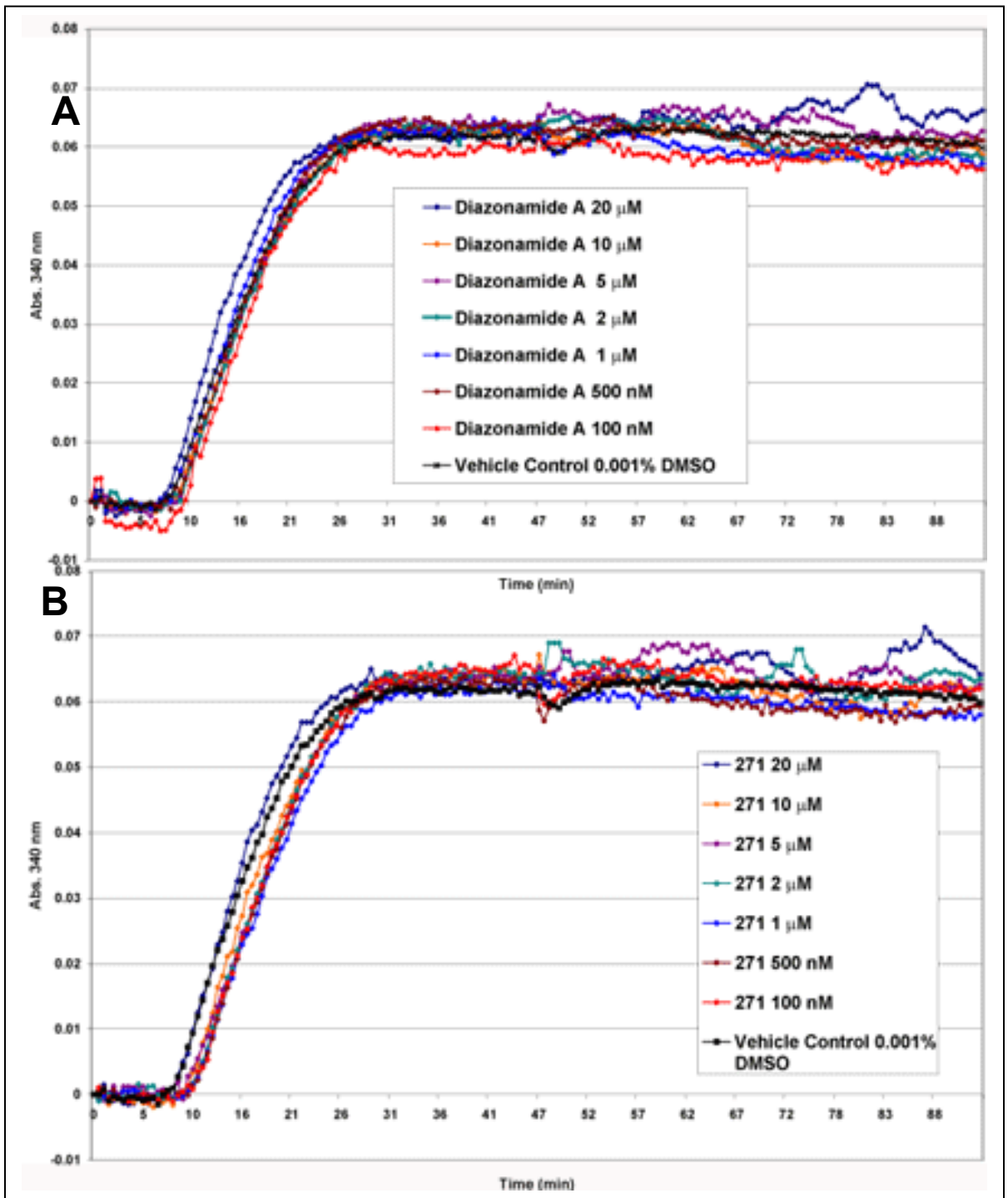
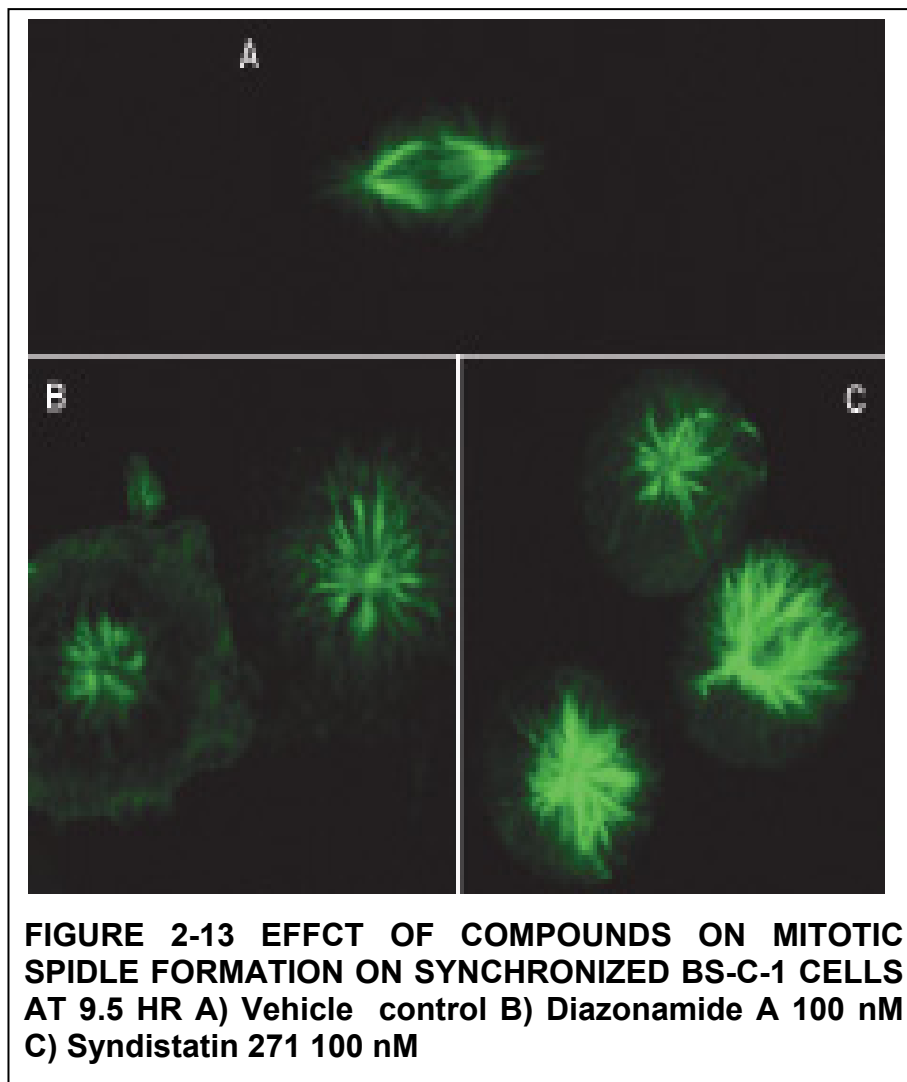


FIGURE 2-12 EFFECT OF COMPOUNDS ON PREFORMED MICROTUBULES
 MAP(+) Tubulin was allowed to polymerize at 37 °C for 45 min then treated with compound.
 A) Diazonamide A B) Syndistatin 271

and it is significant to note, that under these dosing conditions, the diazonamide compounds have no observed effect on interphase microtubules.

2.3.6 Further Examination of the Interaction of Diazonamide A and Syndistatin with Microtubules (Comments on Studies by the Hamel Group)

In addition to the results described above, the Hamel group at the NCI reported their own results concerning the interaction of diazonamide A and syndistatin with tubulin and microtubules.⁸⁹ Hamel *et. al.* confirmed the potent inhibitory activity of the diazonamide compounds on MAP(+) tubulin polymerization.⁸⁹ Further, they determined that diazonamide compounds were active in preventing the polymerization of purified, MAP-free tubulin in solutions containing high concentrations of glutamate.⁸⁹ This result would imply that diazonamide compounds bind directly to tubulin and not to a microtubule-associated protein. GTP hydrolysis is required for microtubule assembly, and diazonamide compounds were also found to potently inhibit tubulin-induced GTP hydrolysis under the MAP-free high-glutamate polymerization conditions.⁸⁹ Hamel and co-workers also observed that diazonamide A and syndistatin did not inhibit the binding of [³H] vinblastine, [³H] colchicine, [³H] dolastatin 10, or [¹⁴C] GTP.⁸⁹ The diazonamide compounds were also shown to be incapable of inducing the formation of stable tubulin aggregates.⁸⁹



2.4 Discussions

2.4.1 Diazonamide A and Syndistatin SAR

The SAR studies described served three purposes: 1) confirmation of the diazonamide total synthesis by demonstrating the requisite biological activity 2) identifying the structural components necessary and/or important for diazonamide-like biological activity 3) establishing a approach to produce simplified, more-synthetically-accessible analogs. The

limitations of the experimental systems used in the evaluating SAR should be noted. The capability of a compound to inhibit the proliferation of cells in tissue culture depends upon numerous variables that can be independent of an analog's affinity for a particular cellular target. These mitigating factors include cellular uptake, solubility, and stability. clearance. Typically, among a series of closely related structures, these factors are similar enough to be inconsequential, but this is difficult to verify. This caveat to the SAR results should be noted. To a lesser extent, this is also true of the tubulin polymerization assay.

The described results provided the first insights into diazonamide A's SAR, and these findings helped confirm the diazonamide structural reassignment.⁴⁹ Prior to the completion of the total synthesis of diazonamide A, acyclic compound **266** and related compounds were studied. As discussed in Chapter 2.3.11, the Harran group was initially unable to form the C16-C18 biaryl bond, but during this time, they did develop methodologies to complete all other parts of the diazonamide structure.⁴⁵ These SAR studies clearly showed that the acyclic structures (**Figure 2-1, 266**), although weakly cytotoxicity, did not exhibit the biological activity characteristic of diazonamide A. Compound **266** is several hundred times less active than diazonamide A and was shown by FACScan analysis (**Figure 2-3**) to be devoid of anti-mitotic activity. Compound **266** differs from syndistatin (**271**) in that it possess a C11 hemiacetal, a valine derived side chain, and lacks the C16-C18 biaryl bond. Each of these structural motifs were individually shown to be essential for diazonamide-like biological activity. Compound **273**, that differs only from syndistatin in the lack of the C16-C18 bond, was shown to have no inhibitory properties at concentrations up to 10 μ M. Introduction of a C11 acetylated hemiacetal (**274**) to syndistatin similarly defuses its

potency. In fact, none of the modifications to the diazonamide core were tolerated from a SAR viewpoint. The half-structures tested were devoid of nanomolar growth inhibitory activity, and unlike the syndistatin analogs (**270**, **271**, **272**) and diazonamide A, compound **276** had no activity in the tubulin polymerization assay (**Table 2-1**). This lack of activity is independent of its weak cytotoxic profile; amidine analog **270** has a very similar anti-proliferative activity in cells, but was still capable of inhibiting the *in vitro* formation of microtubules.

The efforts to identify simplified forms of diazonamide A that retained its biological activity were unsuccessful. Several compounds related to more accessible synthetic intermediates were screened and found to be impotent relative to the parent structure (**Figure 2-6**). The ability to probe less complex structures was, of course, dictated by the synthetic route employed by the Harran group (**Section 1.2.3.11**). Therefore, there were no half-structures with intact right-hand portions of the molecule produced, and also, the last skeletal construction in the bicyclic framework is the C16-C18 bond. The importance of this biaryl linkage is evident from the SAR data, but no other single skeletal bond has been evaluated. The probed SAR indicates very little modification of structure is tolerated.

2.4.2 Characterization of the Diazonamide A and Syndistatin Biological Activity

The research into characterizing the biological activity of diazonamide A sought to accomplish two goals. First, it was imperative to determine whether syndistatin possessed biological activity identical to diazonamide A. Due to the misassigned original structure, the

Harran group could not immediately access the natural product. With only trace amount of natural diazonamide A extant, further exploration into the diazonamide class of compounds would be possible with syndistatin, but only if syndistatin were shown to be viable surrogate. The second major goal was to fully characterize the biological activity of diazonamide A, and expanding on preliminary indications, determine whether diazonamide was an anti-mitotic. This included determining whether the diazonamides shared a mode of action with known anti-mitotic compounds.

Our results confirmed that syndistatin is a true proxy of diazonamide A in cells. The two diazonamide compounds possess nearly equipotent IC₅₀ values, and in all cellular experiments, both compounds elicited identical effects at identical concentrations. The one discrepancy was a relative lack of potency for diazonamide A in the tubulin polymerization assay relative to syndistatin (**Table 2-1**). Diazonamide A is still active in this assay compared to other compounds, and this discrepancy seems immaterial.

The diazonamide compounds were shown to be potently anti-mitotic, as demonstrated by FACScan in OVCAR-3 cells (**Figure 2-7**). Based on the fact that virtually all known small molecule anti-mitotics interact with tubulin, the diazonamide compounds were screened for effects on microtubules, both in cells and *in vitro*. These compounds, at concentrations many times their IC₅₀ values, induce the dissolution of cellular microtubules, similar to vinblastine or colchicine (**Figure 2-8**). Following literature precedent, this activity was then studied in the *in vitro* tubulin polymerization assay. This assay is commonly used as a proxy for studying microtubule polymerization, even though it quite poorly replicates the *in vivo* conditions under which microtubules form and depolymerize.

The diazonamide compounds were active in preventing the assembly of MAP-enriched tubulin into microtubules (**Figure 2-10, Table 2-1**). This outcome is once again similar to the known activity of tubulin depolymerizing agents, such as vinblastine and colchicine classes. The same experiment performed by the Hamel group yielded the same result for diazonamide A and syndistatin. Hamel et al. also chronicled the apparent inhibitory activity of the diazonamides in preventing the polymerization of MAP-free tubulin. Unlike nocodazole and vinblastine however, the diazonamide compounds did not induce the depolymerization of preformed microtubules *in vitro* (**Figure 3-17, 3-18**). This result indicated the diazonamide compound operated through a mechanism of action separate from the two major classes of tubulin depolymerizing agents. This distinction was validated by the competition experiments conducted by the Hamel group, in which neither syndistatin or diazonamide A competed for tubulin binding with radiolabeled vinblastine or colchicines. Taken together, these results indicate the diazonamide compounds induce the depolymerization of microtubules through interacting with tubulin in a new and novel manner. This is precisely what Hamel *et. al.* concludes in their account.

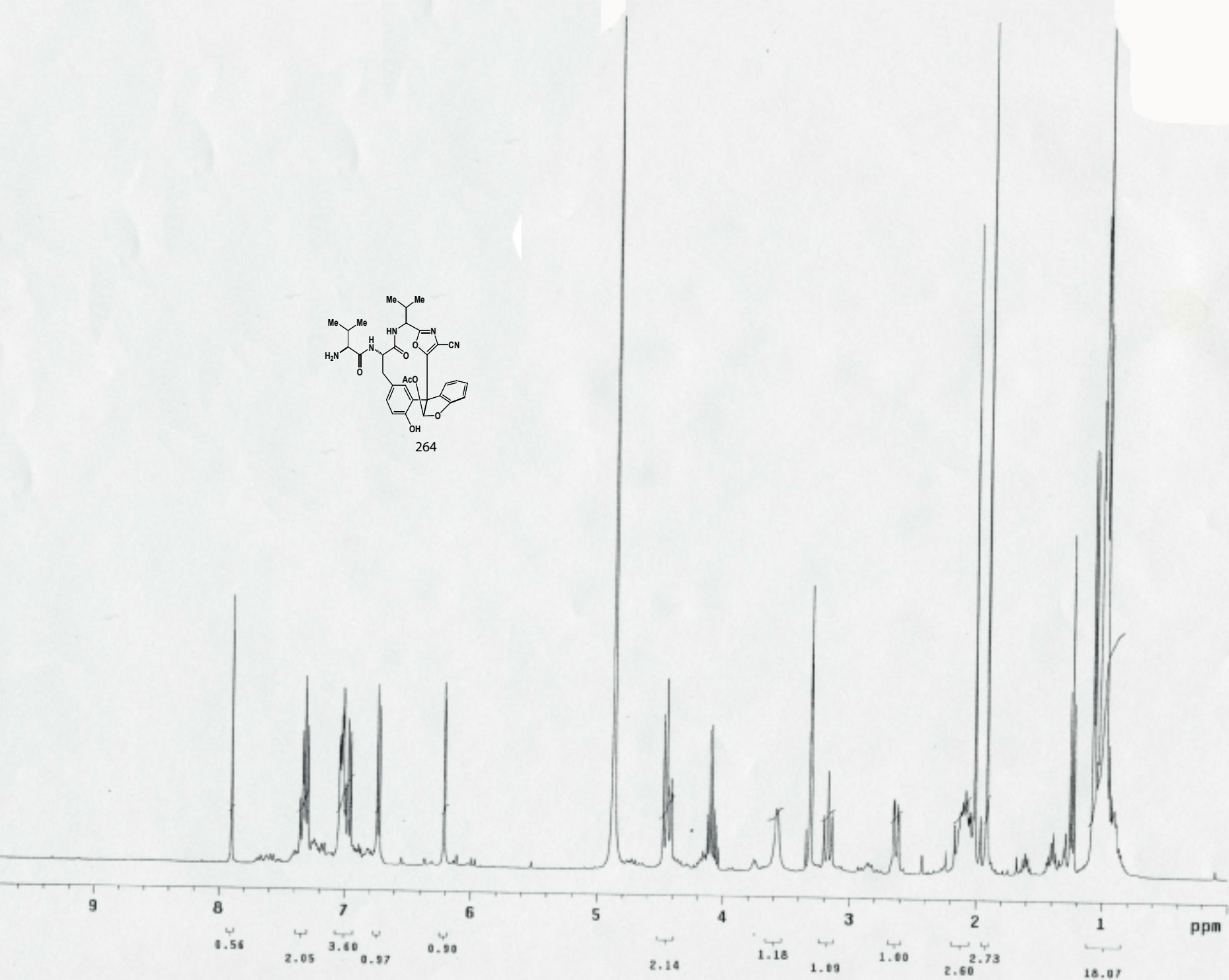
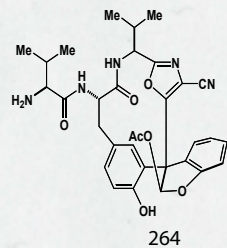
However, the most compelling and important results produced in these experiments were the effects of diazonamide compounds on the mitotic spindle. At 100 nM, both diazonamides induced formation of mono-polar mitotic spindles, and this intriguing result was not observed with the control compounds. The formation of such mono-polar spindles clearly indicates that diazonamide compounds possess a mechanism of action other simple tubulin depolymerization. The depolymerization of microtubules in cells and *in vitro* with concentrations of compound far above 100 nM is a real result too. The data supports two

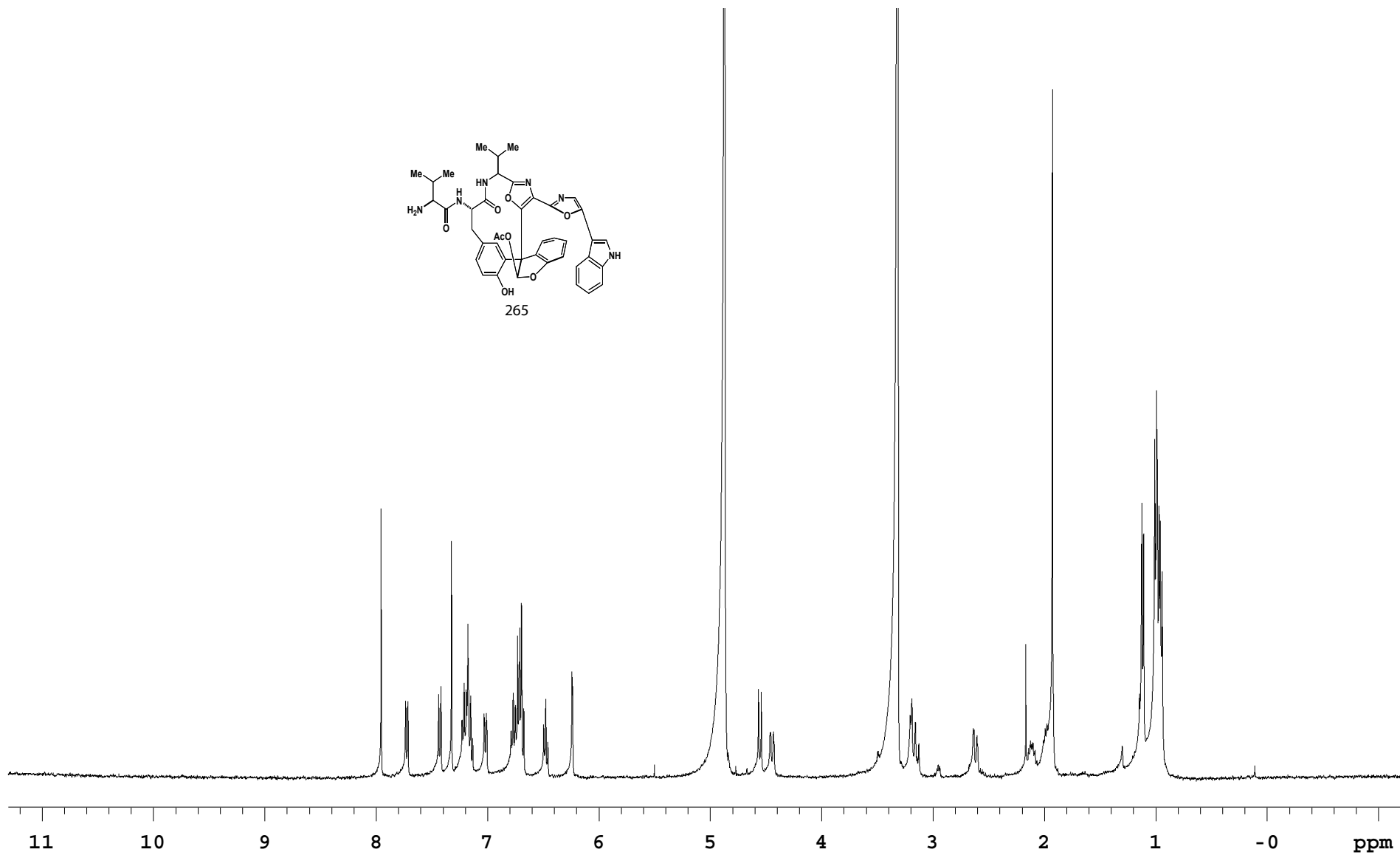
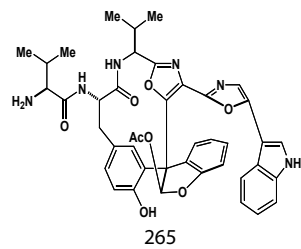
interpretations of the microtubule depolymerizing activity: 1) tubulin, or microtubules, is a secondary or lower affinity target of diazonamide A or 2) the depolymerizing effect is a downstream effect of diazonamide interacting with its true, high affinity target.

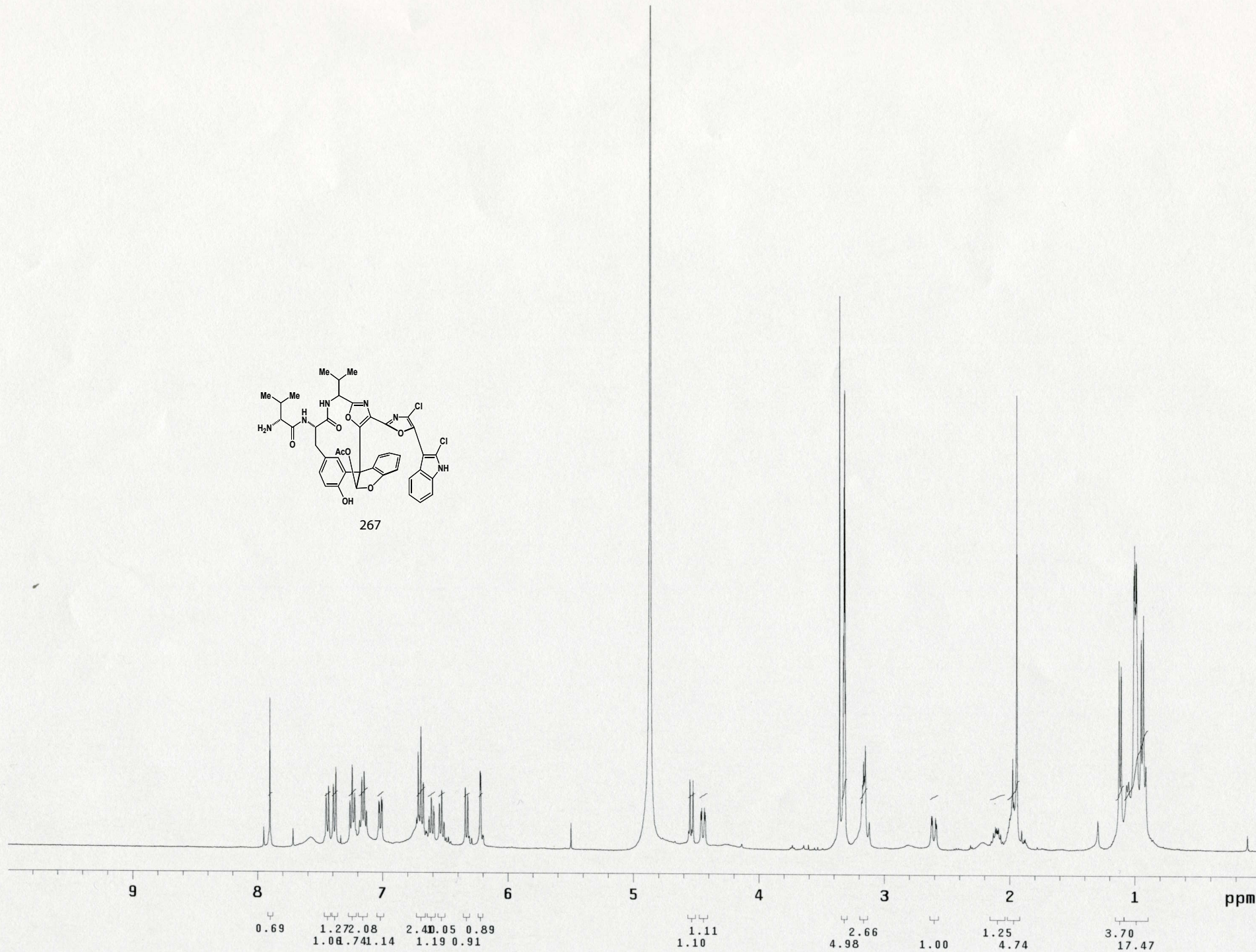
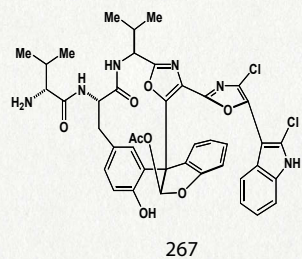
2.5 Conclusions

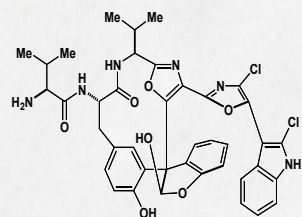
A fairly extensive exploration of the diazonamide A SAR indicates that little modification is tolerated and that the C37 functionality and stereochemistry is important to activity. Diazonamide A and syndistatin are equipotent compounds exhibiting identical biological activity. These diazonamide compounds are highly active anti-mitotic compounds possessing microtubule depolymerizing activity in cells and *in vitro*, but the diazonamides clearly do not share a common mode of action with the vinblastine or colchicine class of tubulin binding agents. Finally, the diazonamide compounds uniquely induce the formation of mono-polar mitotic spindles, suggesting this class of compound operates through an unprecedented and undiscovered mechanism.

2.6 Appendix

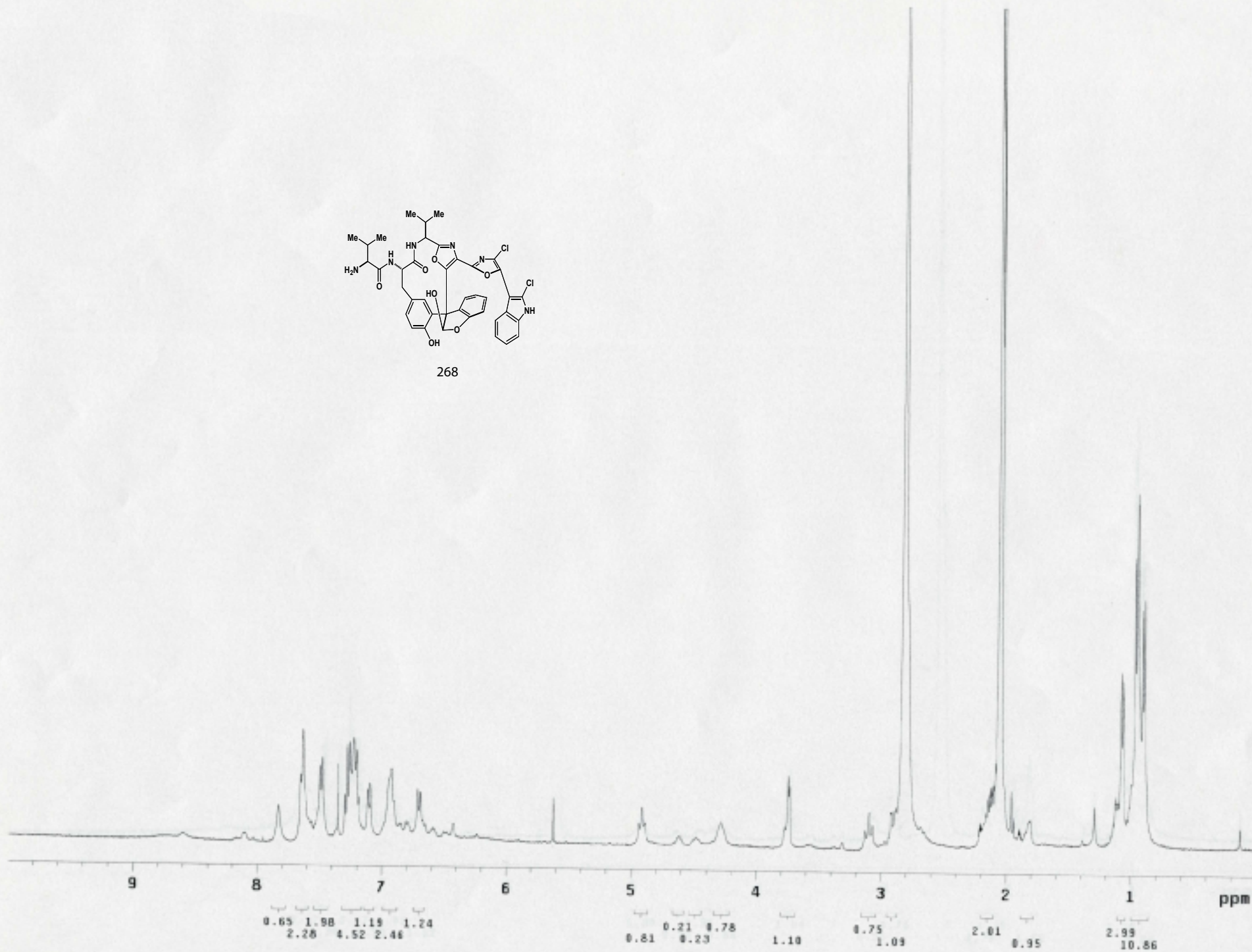


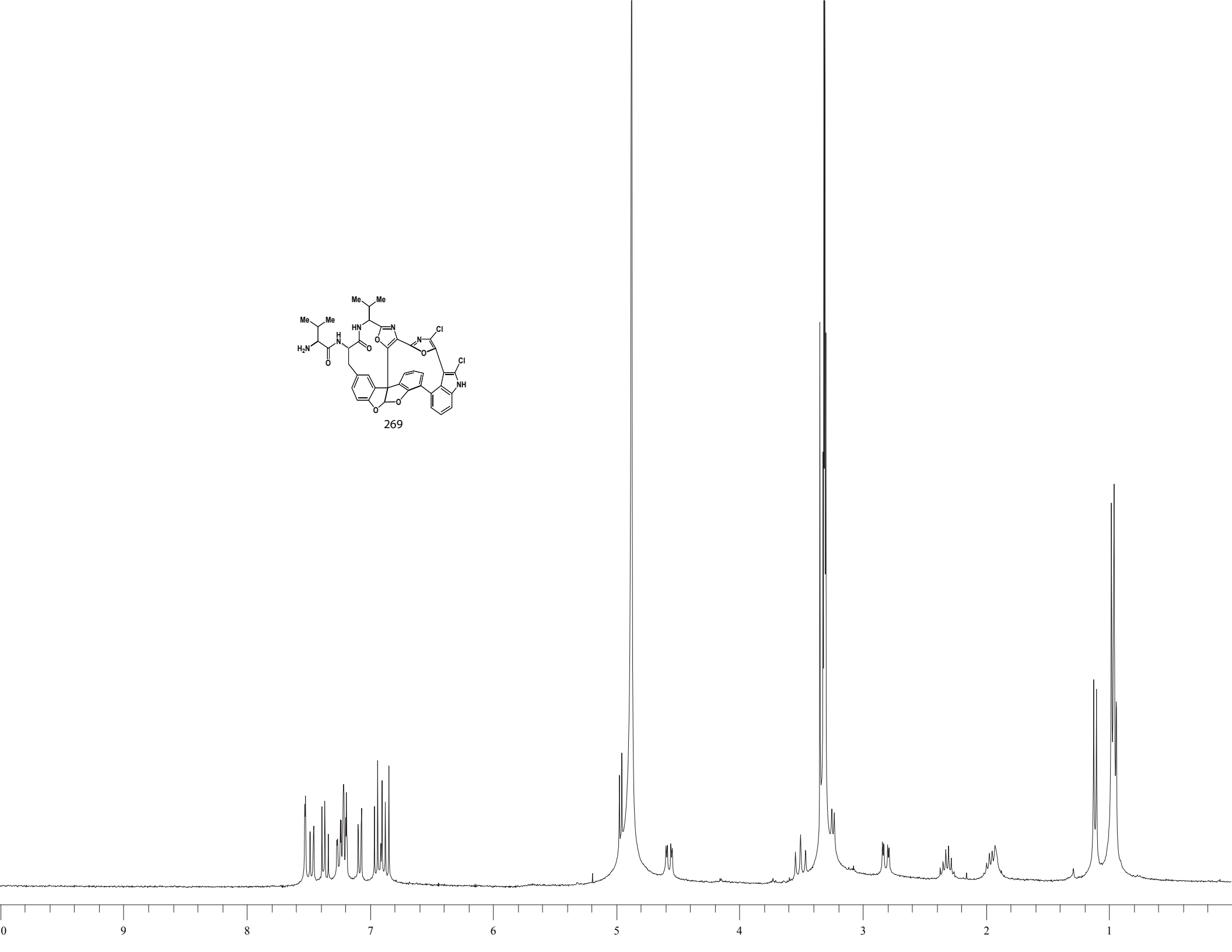
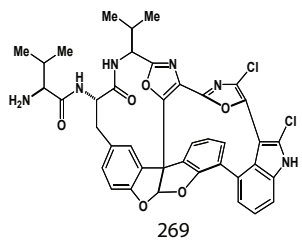


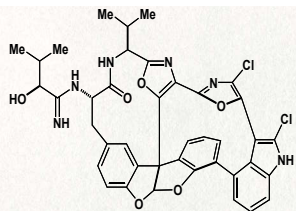




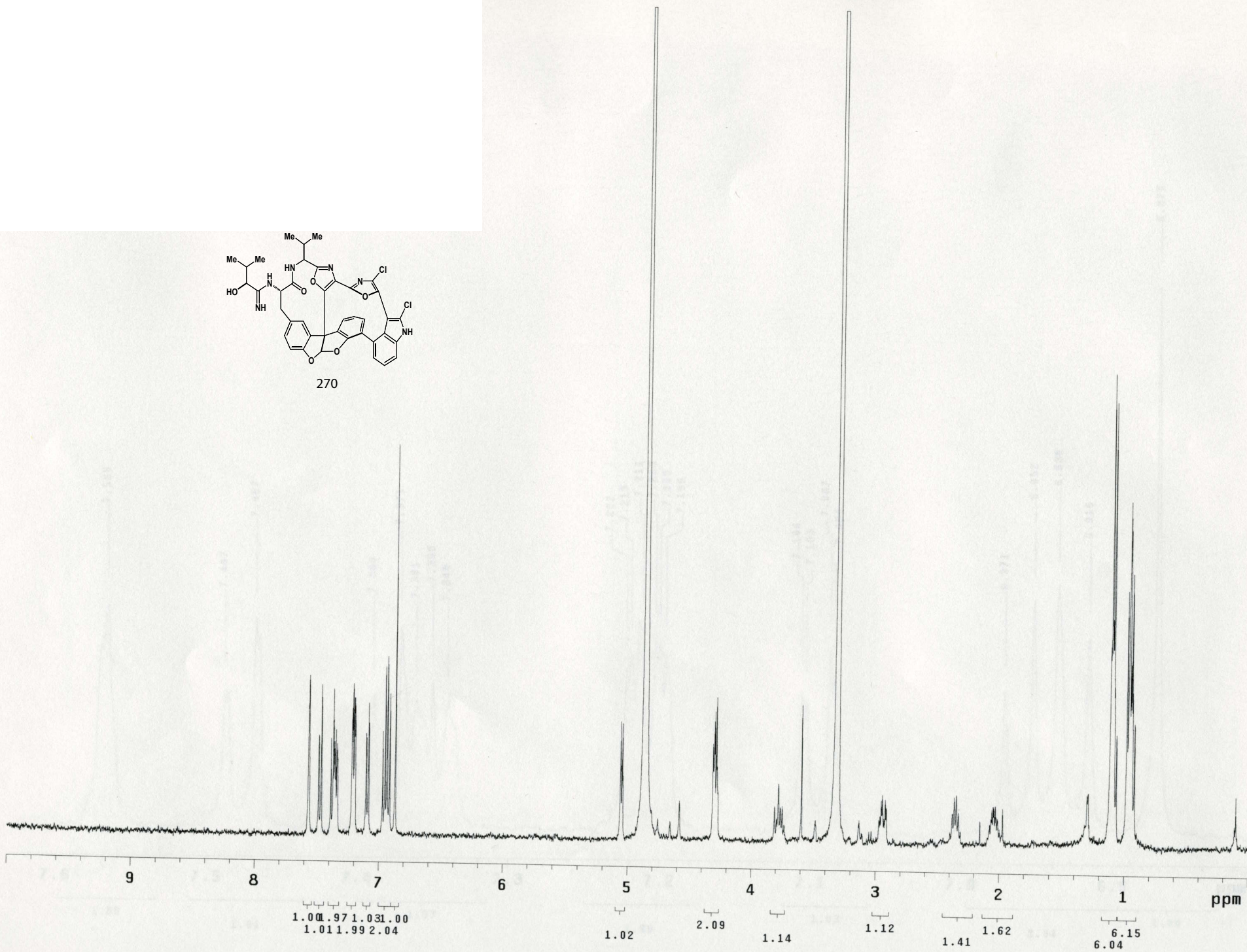
268







270



1H SENSITIVITY
0.1% ETHYLBENZENE

UTSW INOVA 400

Sensitivity

November 19, 1997

Abe Revilla

exp5 s2pu1

SAMPLE

date Oct 30 200

solvent cd3o

file ex

ACQUISITION

sfrq 399.771

tn H1

at 2.003

np 28032

sw 5080.0

fb 3000

bs 8

ss 2

pw 9.4

pw 9.4

tpwr 54

d1 2.000

tof 0

nt 200

ct 40

alock n

gain 26

FLAGS

il n

in n

dp y

hs nn

math 32768

1

werr

2 wexp

wbs

wnt

DISPLAY

sp -0.1

wp 3997.4

vs 156

sc 0

wc 250

hzm 15.99

ls 5036.24

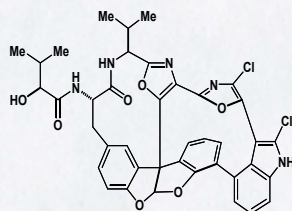
rfl 1808.0

rpf 1323.2

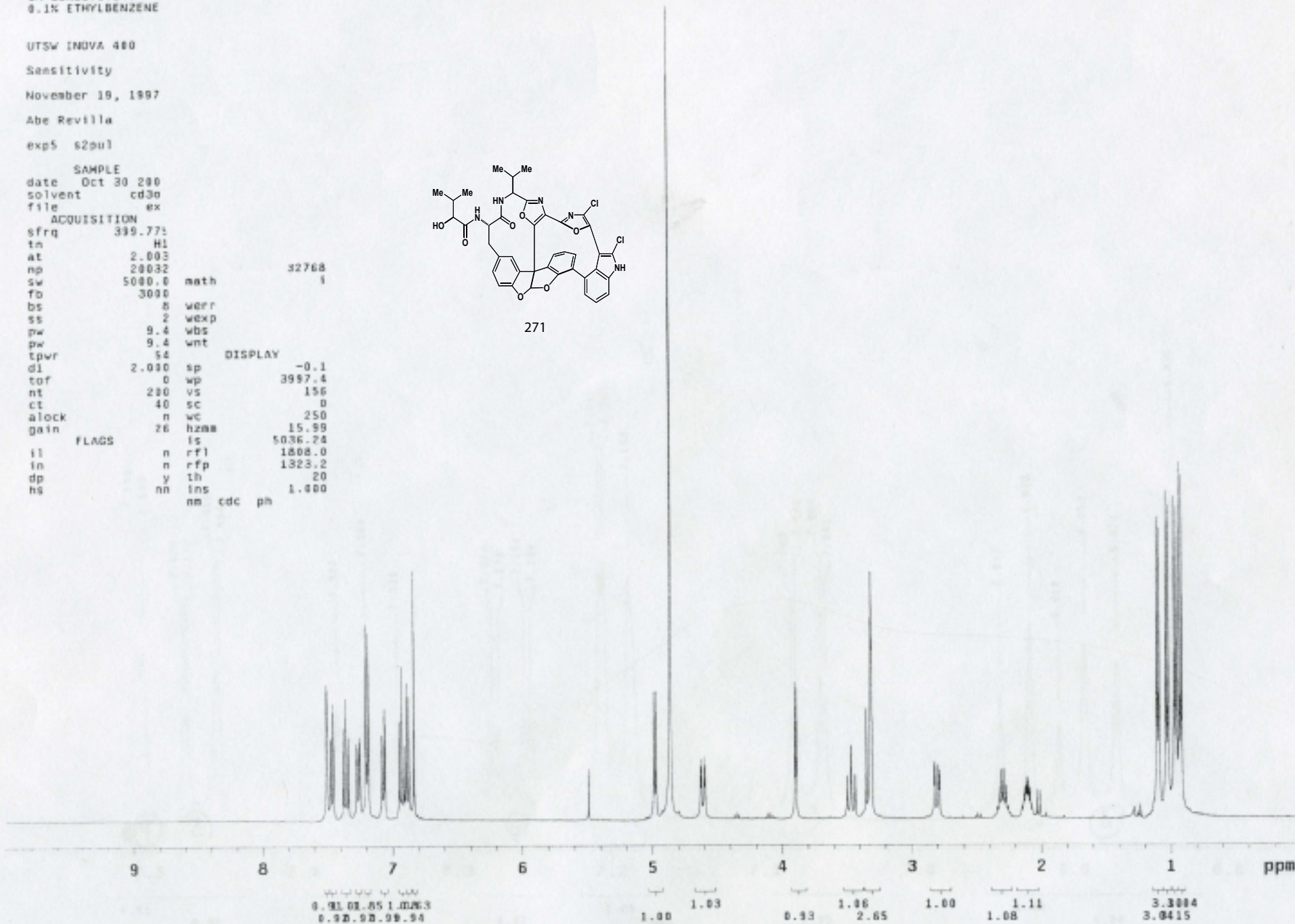
th 20

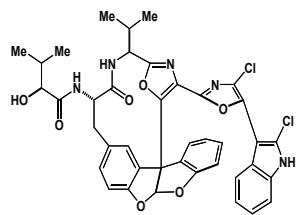
ins 1.400

nm cdc ph

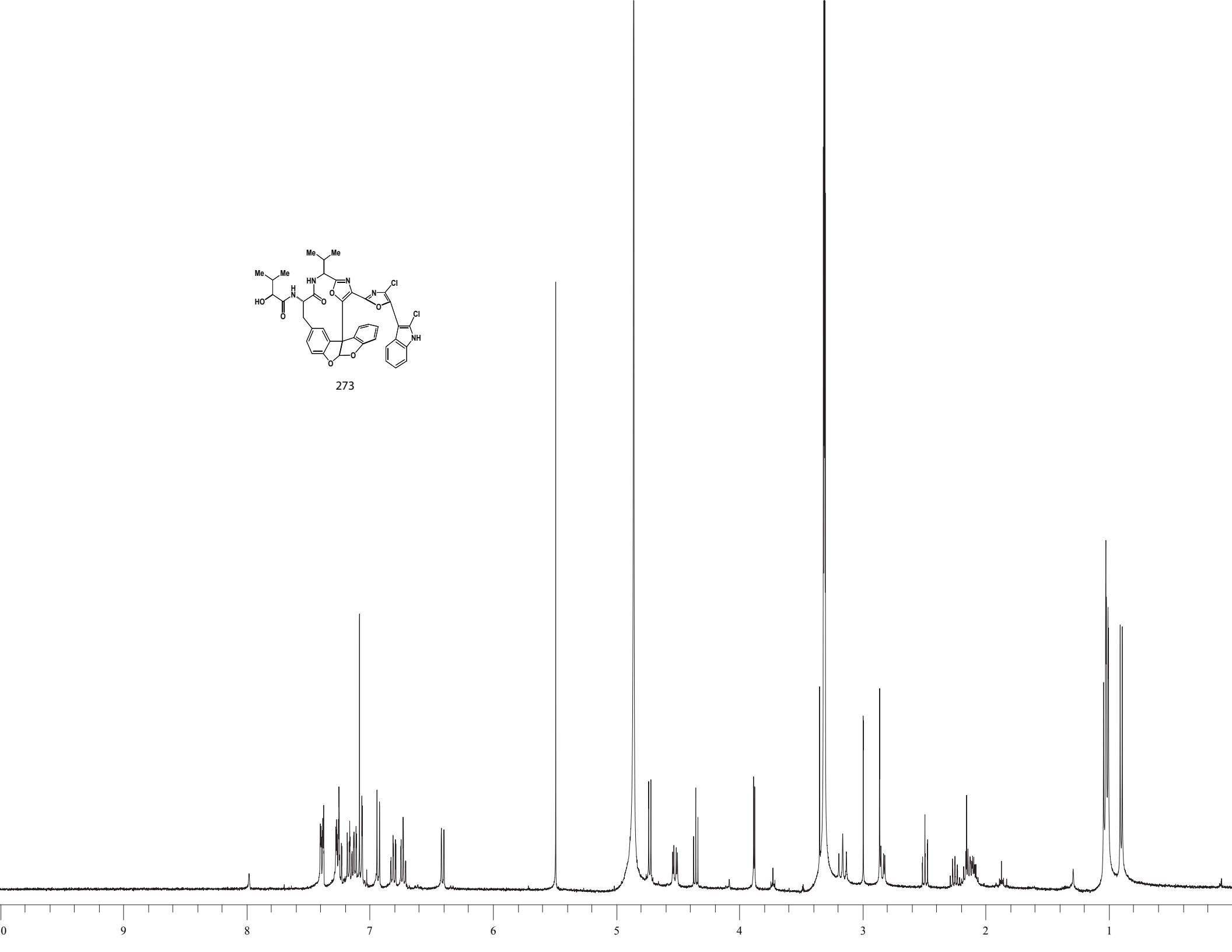


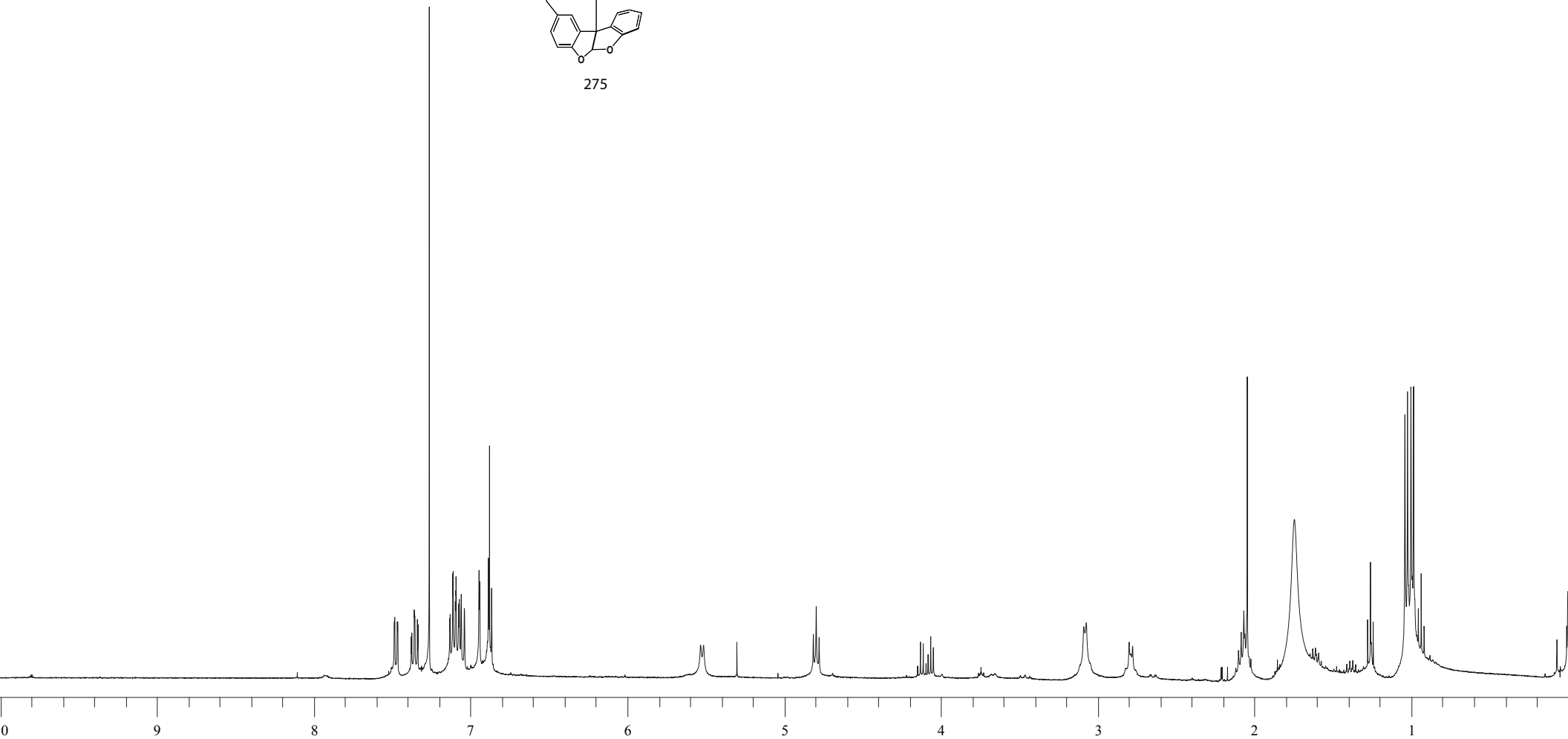
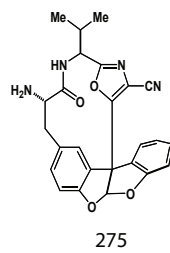
271

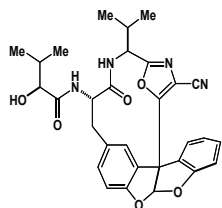




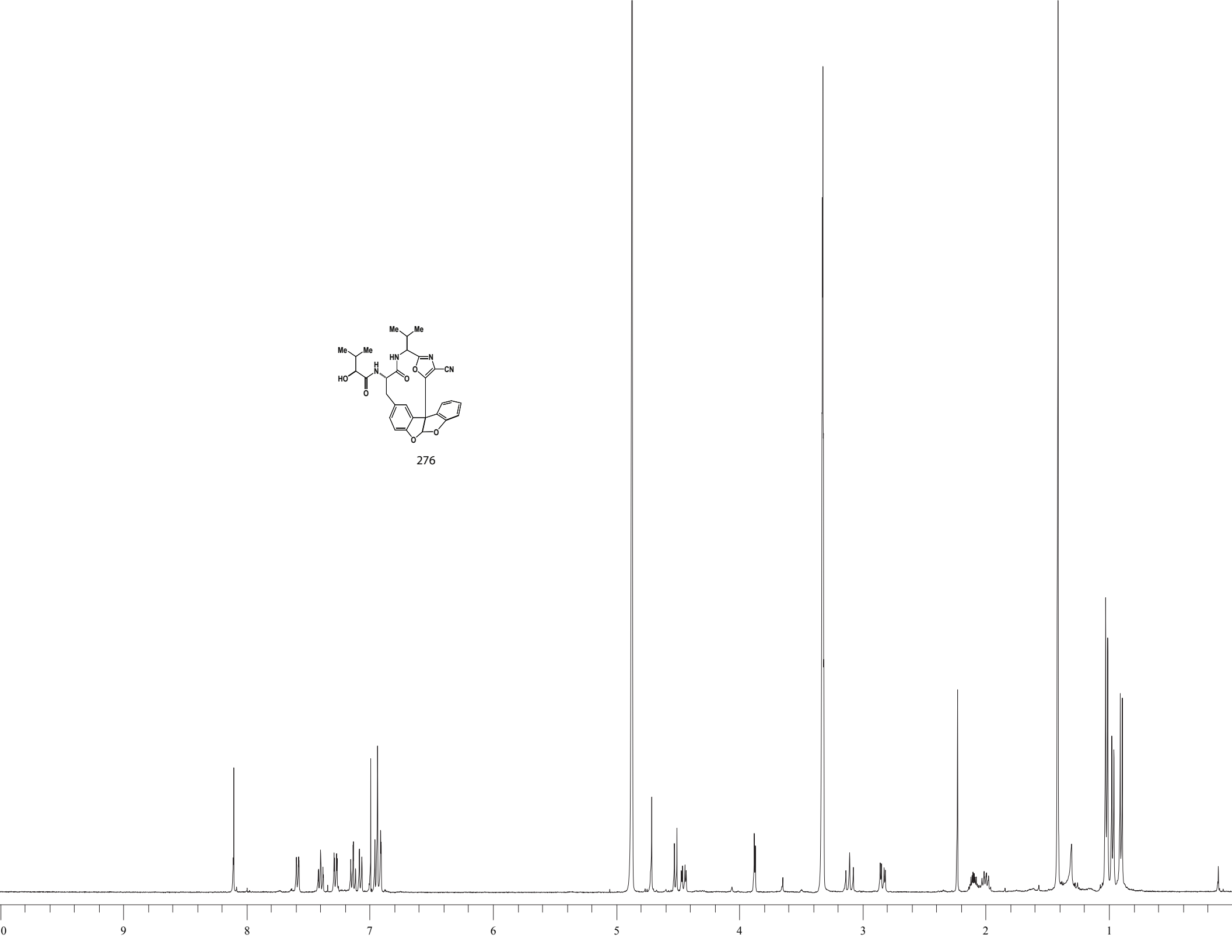
273

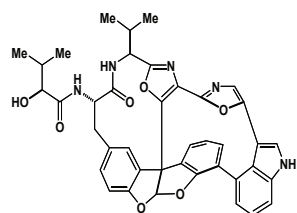




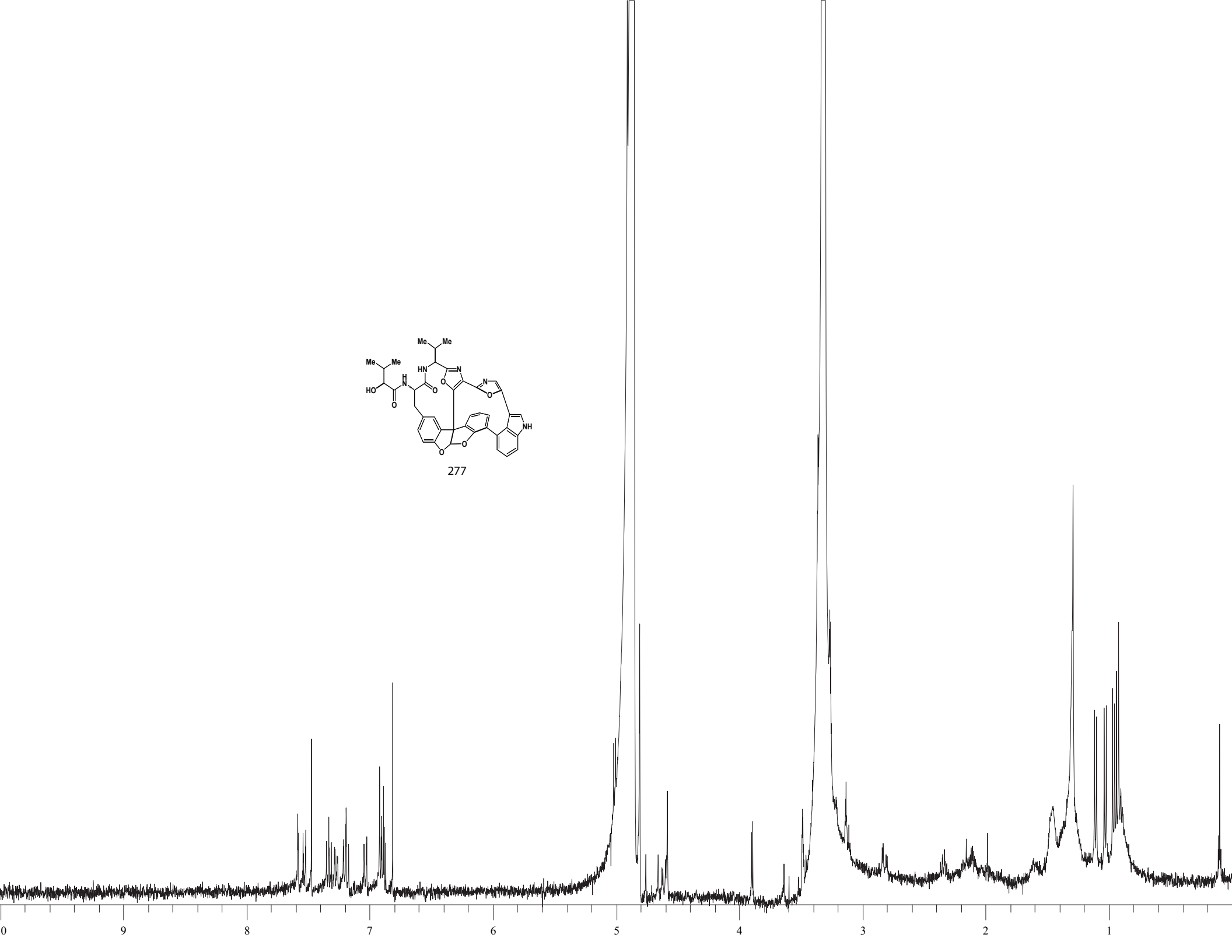


276





277



CHAPTER THREE

Synthesis and Application of Syndistatin Probe Analogs

3.1 Introduction

Complex, bioactive natural products have played an important role in probing cellular biology and the underlying biochemistry of human disease. It was through investigations into the mechanism of action of natural products that the protein tubulin was discovered,⁷⁷ ER to Golgi vesicle trafficking was better understood,⁹⁰ and the TOR signaling pathway was uncovered.⁹¹ Novel natural products exhibiting unique biological activities hold the promise of affecting biochemical processes in undiscovered ways. In addition, new classes of biologically active natural products have long been critical in the development of pharmaceutical drugs,⁹² especially antimicrobial and cancer chemotherapeutic agents. Research into the molecular pharmacology of complex, bioactive natural products will likely continue to drive new understandings in cellular biology and the development of new pharmaceuticals.

The most direct method available for demonstrating the cellular target of a novel, biologically active compound is through identification of a compound/target complex purified from cellular lysate. This approach conclusively demonstrates the interaction *in vivo* in an unbiased manner and allows for the detection of multiple high affinity targets. This method requires the synthesis of probe analogs (e.g. biotinylated, radiolabeled, etc.) which retain the potency and binding affinity of the parent compounds. In this respect, accessing a structure synthetically allows more flexibility and versatility in designing analogs for use as biochemical probes. In the absence of extensive, or definitive, SAR data the approach to probe analog synthesis should incorporate maximal flexibility. An adaptable method would allow for modification of structure at multiple positions and the incorporation of several useful

functionalities including a radiolabel, biotin, etc. The ultimate aim is to access a full suite of probe analogs, retaining the full potency and specificity of the parent structure. With such a collection of compounds, the molecular pharmacology of a molecule could be completely investigated and its cellular target and mechanism of action identified.

3.1.1 Background Literature

The identification of the cellular target of biologically active natural products is typically a complex undertaking. The most important criterion in uncovering the mode of action of a compound is the nature of the interaction between the small molecule and its protein target. Ligands that covalently modify their protein partner simplify the identification of their cellular targets. The relative abundance of the target protein is a critical factor in its purification and subsequent identification, and cellular targets that are abundant and steadily present in the cell are easier to identify. For example, the discovery of the protein tubulin as the target of colchicine was immediately evident upon running a protein gel with radiolabeled analog of the molecule.⁷⁷ In this case, representing one extreme, colchicine binds with high affinity to one target, which happened to be one of the most abundant proteins in the cell. In the other extreme, a small molecule might interact reversibly with a scarce, or transiently expressed, protein. There is also the complicating possibility of the compound binding to multiple cellular targets with differing affinities.

Identifying the association of a small molecule with a rare transcript against the backdrop of undifferentiated cellular lysate is a formidable challenge. Several methods have been developed to explore the molecular pharmacology of small molecules, including biochemical and genetic approaches. A review of the expansive relevant literature is beyond the scope of this introduction, but most of the prior precedents detailing the successful identification of a natural

product's cellular target follow a general pattern. Typically, the small molecule of interest was shown to interfere with a specific pathway or cellular activity. In the case of brefeldin, this fungi-derived natural product was identified as interfering with an early step in the protein secretory pathway.⁹⁰ Trapoxin was first shown to be an inhibitor of histone deacetylase activity.⁹³ Didemnin was preliminarily identified as an inhibitor of protein translation.⁹⁴ For all three of these molecules, the initial inhibitory activity was used to focus the search for the cellular target to the affected biochemical system. For example, since trapoxin was shown to be a histone deacetylase inhibitor, fractionated nuclear lysate was assayed for histone deacetylase activity.⁹³ This was done in conjunction with assaying the fractionated lysate for specific binding with a tritiated form of trapoxin. This detection was possible because trapoxin covalently modifies its target.⁹³ Upon identifying a lysate fraction enriched for the unknown trapoxin-binding protein, the Schreiber group then used a trapoxin affinity matrix to isolate the cellular target.⁹³ Identification of the protein target for didemnin^{95,96} was achieved in a related manner.

Diazonamide A and syndistatin were shown to be potent anti-mitotic agents that induce abnormal mitotic spindle formation (**Chapter 2.5**). These compounds also have an effect on cellular microtubule at high concentrations, but it is not known if this is an effect of directly interacting with tubulin or a downstream effect of the compounds interacting with another target(s). The preliminary characterization of the diazonamide biological activity failed to designate a discrete biochemical pathway as being affected. Mitosis and mitotic spindle formation are the products of numerous cellular processes interacting. Therefore, in searching for the diazonamide cellular target there is not a starting point as was the case for brefeldin, trapoxin, or didemnin.

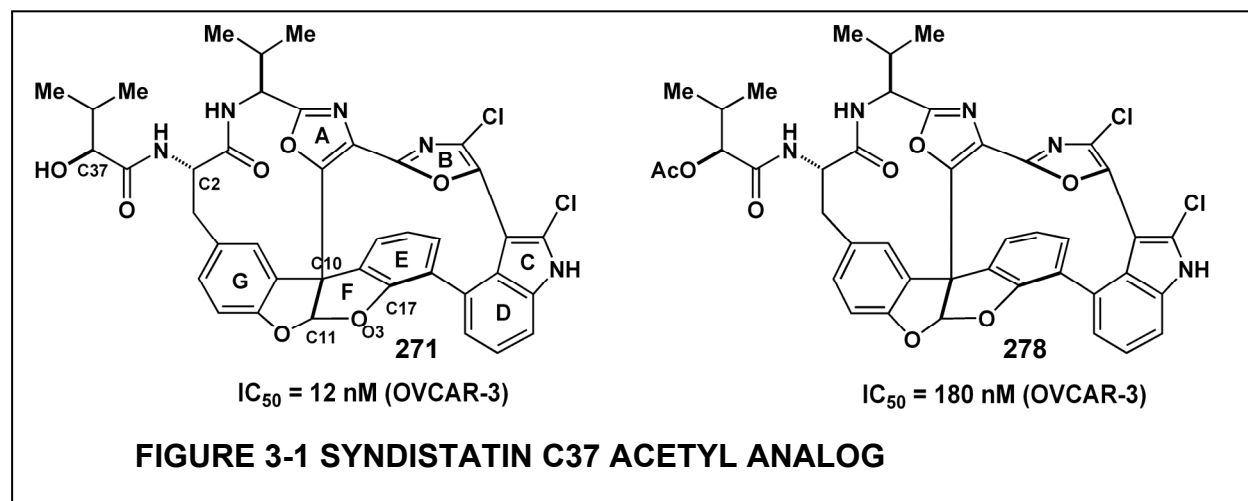
3.2 Synthesis and Evaluation of Syndistatin Probe Analogs

3.2.1 Design for Derivatization

Accessing syndistatin (**271**) through total synthesis provided for flexible derivatization of the compound. While the highly oxidized core of the compound is largely devoid of functionality suitable for chemical modification. The only clear exception is the C-ring indole nitrogen (**Figure 3-1**). From a practical standpoint, the ideal position for modification is at the α -hydroxy isovaleryl (HIV) conjugated side chain. This motif is appended to the syndistatin core at the end of the synthesis, making it the most readily variable segment. The C37 hydroxyl group was an obvious candidate for derivatization. Acetylation of C37 (**278**) significantly abrogated the biological activity (**Figure 3-1**), eliminating this site for modification. This result, combined with the SAR data discussed previously, indicated that the side chain C37 hydroxyl is vital for cytotoxic potency. However, the importance of the rest of the side chain functionality had not been determined.

To further evaluate SAR of the side chain, a minimally modified side chain was sought. Of the synthetic precedents that detail an enantiospecific synthesis of α -hydroxy carboxylic acids related to HIV, the Evans group's enantioselective catalytic copper(II) catalyzed carbonyl-ene reaction was an excellent solution to this synthetic problem.⁹⁷ This reaction uses C2-symmetric bis(oxazolanyl) copper(II) complex **279** as a Lewis acid catalyst for the carbonyl-ene reaction with simple glyoxylates and pyruvate esters (**Figure 3-2**).⁹⁷ Included in the published accounts was the reaction of *cis*-2-butene (**280**) with ethyl glyoxolate (**281**). This reaction was performed followed by HPLC purification and saponification of the diastereomeric mixture to yield compounds **282** and **283**.⁹⁷ Appending the α -hydroxy acids **282** and **283** on to the syndistatin core produced isomeric side chain analogs **284** and **285**, which are one-carbon-extended,

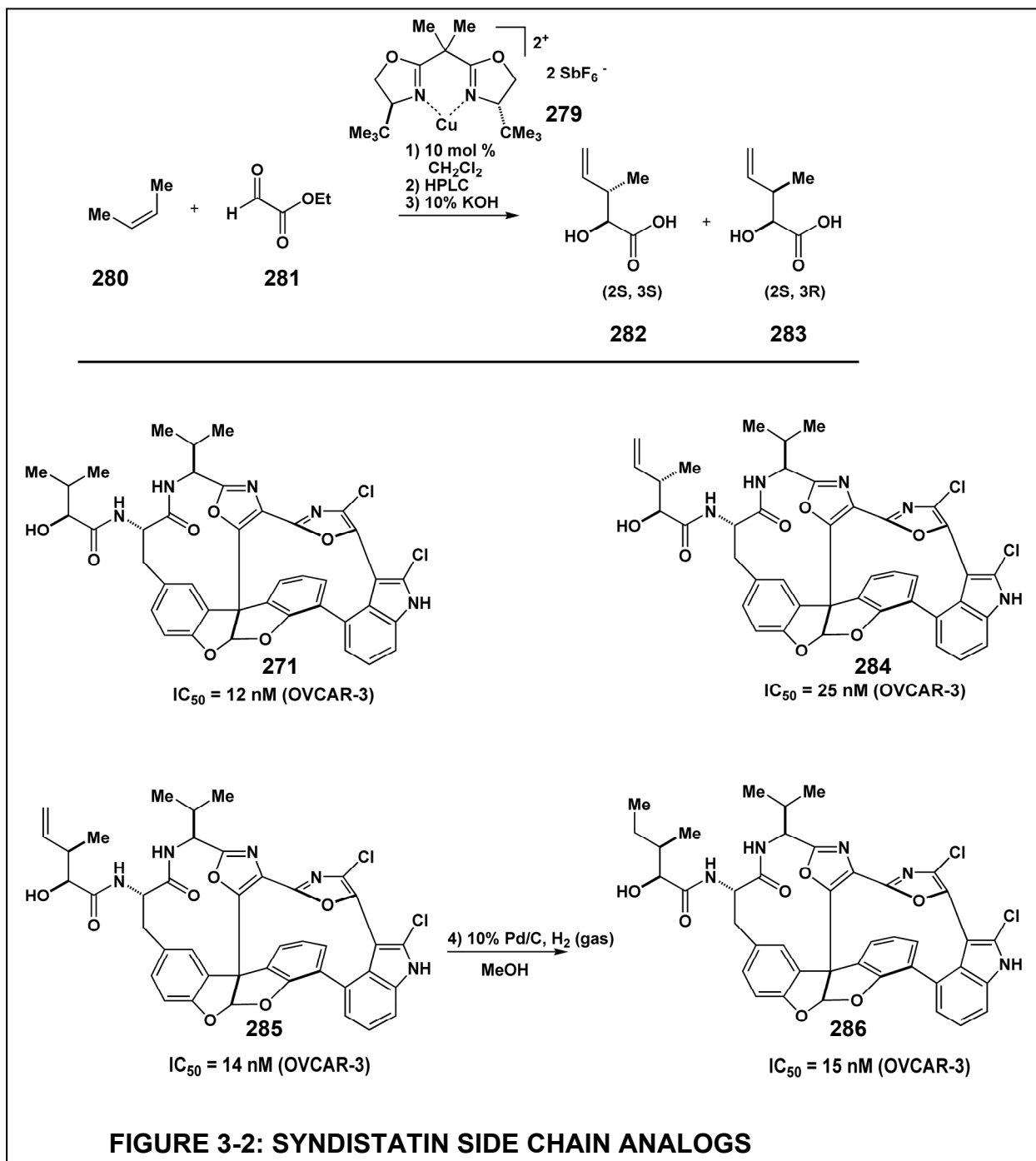
unsaturated analogs of syndistatin. In the context of the side chain, this represents one of smallest perturbations possible with the only detractor being the introduction of a new stereocenter.



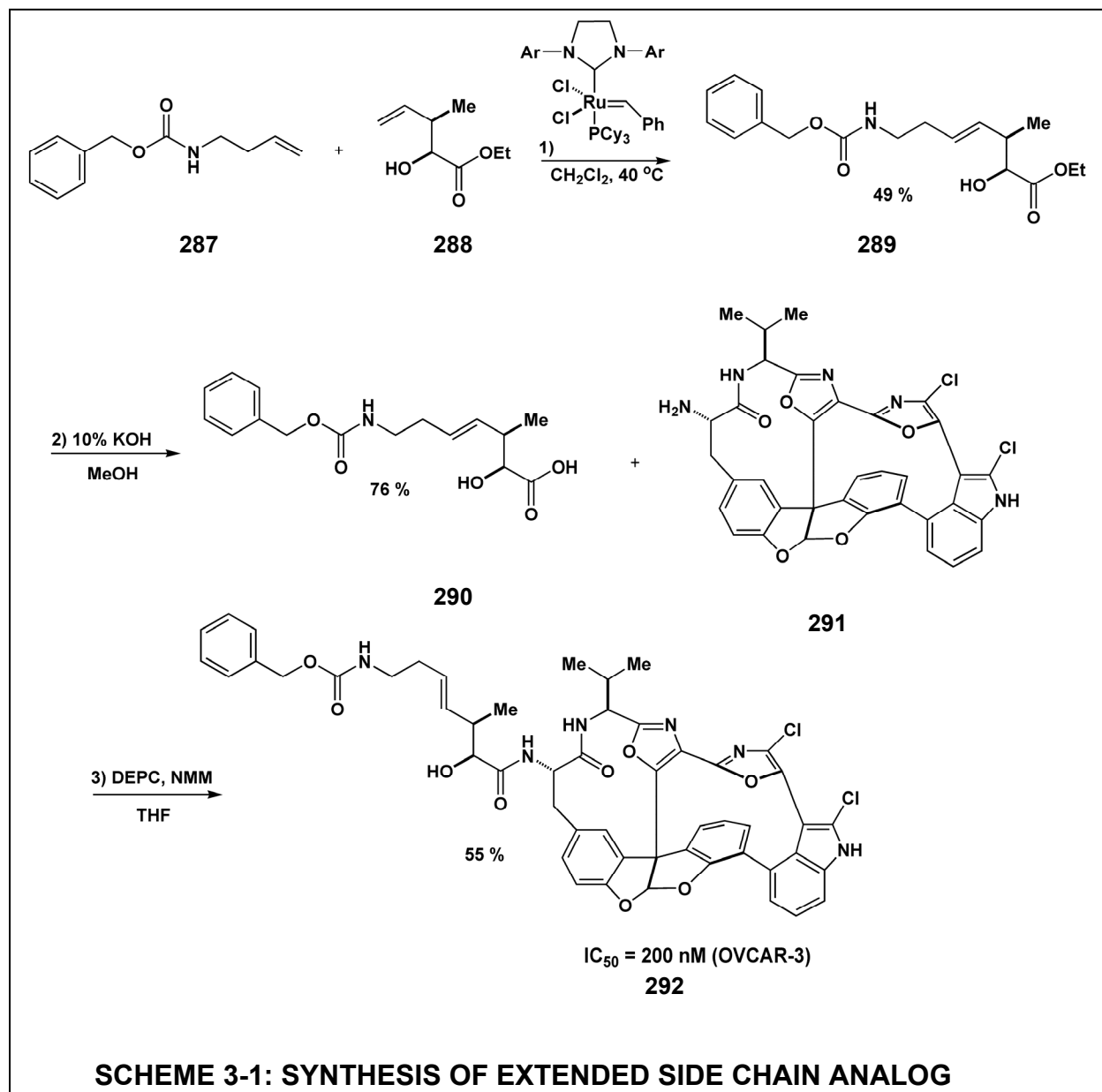
Analogs **284** and **285** were determined to possess cytotoxicity comparable to syndistatin, but only diastereomer **285** was equipotent to the parent structure. Heterogeneous hydrogenation of the terminal olefin in **285** produced **286**. This saturated analog retained full potency. Utilization of the Evans chemistry to derivatize the side chain is ideal, not only because it is accomplished in one step with very high enantiospecific formation of the C37 stereochemistry, but also due to the introduction of a versatile synthetic handle in the form of a terminal olefin.

3.2.2 Probe Analog Synthesis

Homoallylic alcohol **288** undergoes a ruthenium catalyzed cross metathesis reaction with butenyl amine **287** to produce adduct **289** in 49% yield (**Scheme 3-1**). This product was saponified with potassium hydroxide and appended onto the syndistatin core (**291**) via the corresponding acyl cyanide (DEPC, NMM). The cytotoxicity of resultant product **292** was



evaluated in OVCAR-3 cells and its IC_{50} value was determined to be 200 nM. Hydrogenolytic removal of the benzyl carbamate protecting group in **292** (Scheme 3-2) produced amine **293**. Derivatization was then a facile process coupling the amine with *N*-hydroxysuccinimide (NHS) activated esters (**294**, **295**). The activated biotin (Fluka) was an obvious choice for a probe analog. Biotin's strong affinity for the protein avidin has made it



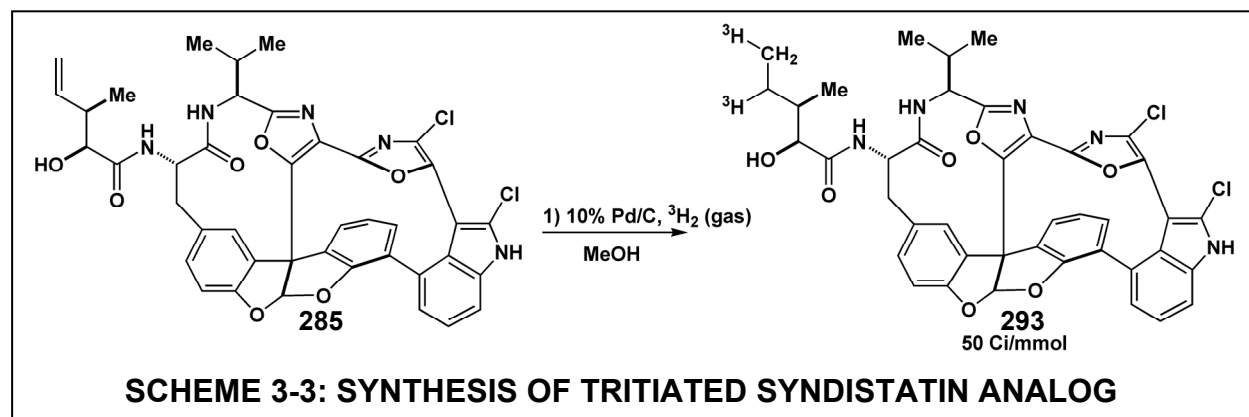
useful in various experimental biochemical methods, including affinity chromatography. The synthesis of biotinylated product **296** was a straight forward process. **295** is a NHS-activated form of the green fluorophore xanthoglow. The synthesis of this intensely fluorescent dipyrinone was detailed by Brower and Lightner⁹⁸, and it was converted into the NHS-activated ester in one step from the corresponding free acid. Xanthoglow's excellent fluorescent properties and small molecular weight made it an ideal choice for use in the synthesis of fluorescent syndistatin analog **297**.

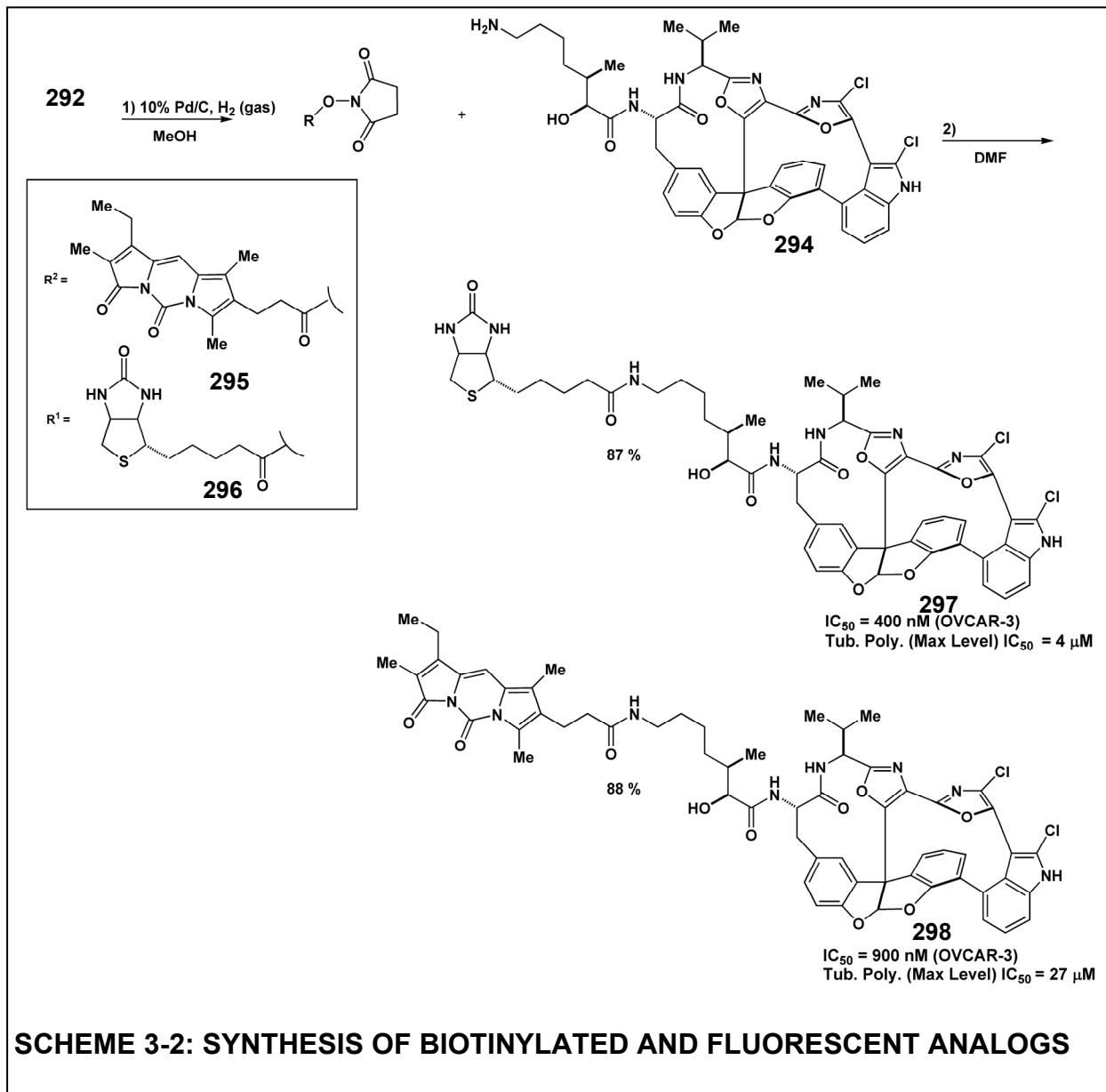
3.3 Evaluation of the Syndistatin Probe Analogs

The biotinylated (**296**) and fluorescent (**297**) analogs were both assayed for cytotoxicity and for activity in the tubulin polymerization assay. The compounds had significantly reduced potency in both assays (**Scheme 3-2, Figure 3-3**), and in both assays the biotinylated analog was much more active than the fluorescent analog.

3.4 Utilization of Syndistatin Probe Analogs

3.4.1 Experiments with the Syndistatin Radiochemical Analog **298**





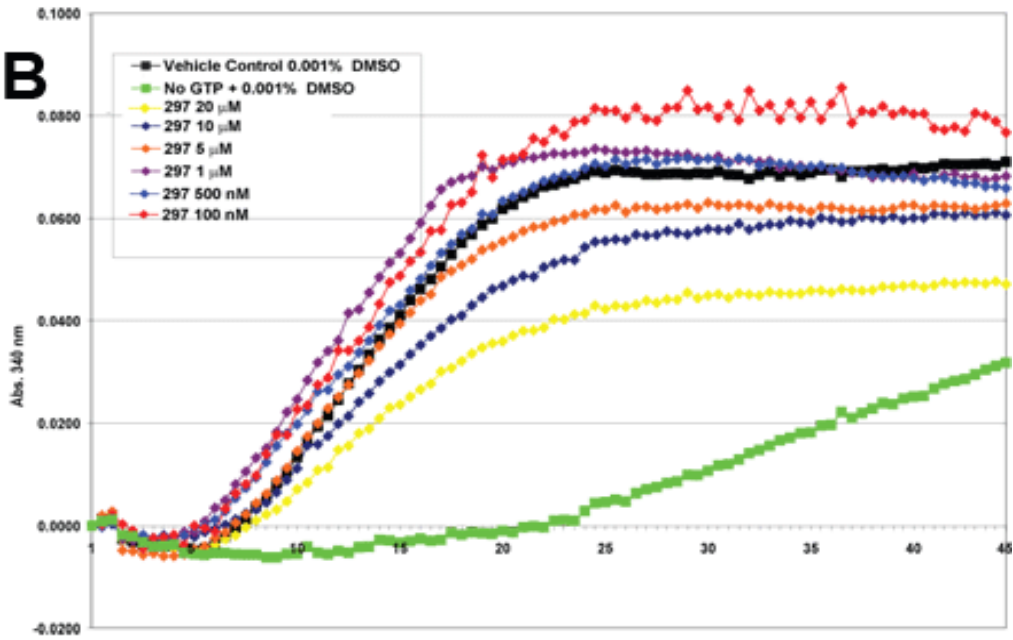
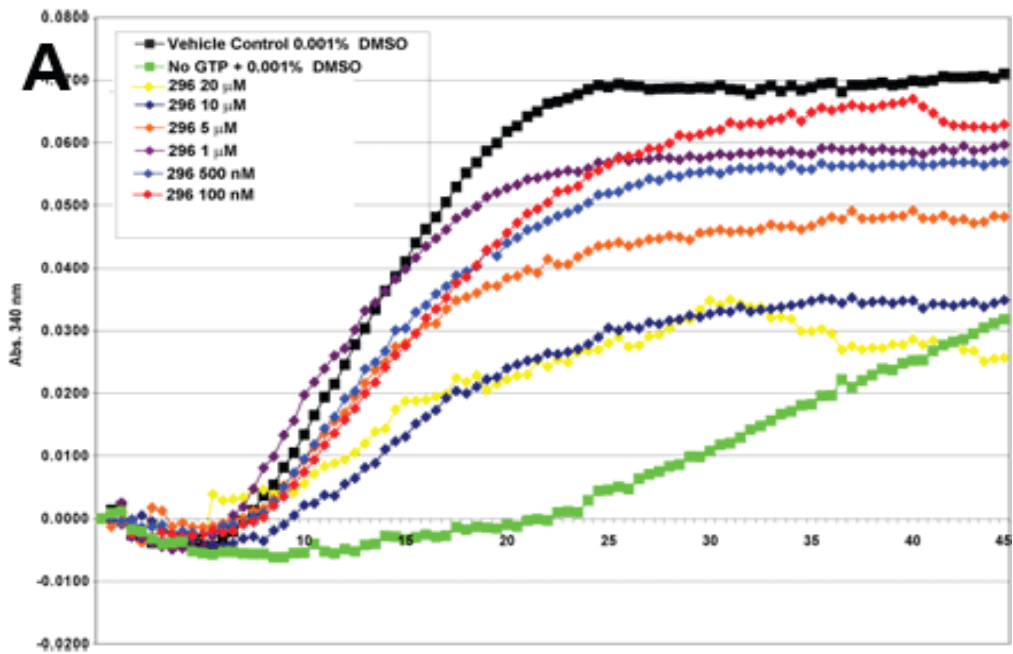


FIGURE 3-3: EFFECT OF PROBE ANALOGS ON IN VITRO TUBULIN POLYMERIZATION A) Biotinylated analog 276 B) Fluorescent analog 277

The determination that the saturated extended side chain (**Figure 3-2, 286**) was equipotent to syndistatin clearly indicated a route to the synthesis of a radiolabeled syndistatin analog. Performing the palladium mediated reduction in the presence of tritium gas (performed by the American Radiolabeled Chemicals Inc.) yielded the tritiated analog **298** with a specific activity of 50 Ci/mmol (**Scheme 3-3**). **298** is an ideal analog, possessing a very high specific activity with very minor structural permutations from the parent compound. Based on the cytotoxicity data, **298** should be a perfect, detectable mimic for syndistatin. This compound could have many uses, including investigating the cellular uptake of the compound and exploring its hydrophobicity and other intrinsic properties. The radiolabeled analog could also be an important tool in uncovering the cellular target. Perhaps the most important use of the radiolabeled analog is to demonstrate conclusive binding of the syndistatin compounds to isolated possible cellular targets. This is a direct and superior method in validating possible candidate proteins.

To ensure that the compound was free from other radioactive contaminants, compound **298** was spotted on to a silica gel TLC plate and developed (60% ethyl acetate/hexane). The plate was then sprayed with a tritium enhancer spray and placed with film to allow for autoradiography. Development of the film shows only one major spot with approximately the correct Rf (**Figure 3-4A**). With confidence in the purity and validity of **298** established, the initial experiments performed with this analog were designed to determine the relative hydrophobicity of the syndistatin compounds. A very simple experiment was executed in which **298** was dissolved in PBS buffer in an Eppendorf tube. After the designated amount of time, the tubes were mixed, some of the compound solution was aliquoted, and the amount of compound

was detected using scintillation counting. The results clearly showed a dramatic loss of counts over time (**Figure 3-4B**). Presumably this means the compound is partitioning out of the aqueous media onto the sides of the tubes. To understand if other kinds of tubes were better in this regard, two kinds of polypropylene (PP) tubes, a polystyrene (PS), and glass tubes were all examined. In all cases, there was a loss in counts upon incubation. The glass tube recorded the smallest loss of counts. The results do not represent the behavior of the syndistatin compounds in the DMSO stock solutions or complex buffers, such as cell media. .

Initial efforts focused on detecting specific binding of radiochemical **298** to tubulin or microtubules. Due to the nature of tubulin, it is possible that syndistatin could interact with free tubulin, tubulin in the process of polymerizing, or to fully-formed microtubules. Detection of compound binding was determined using gel filtration columns. Binding was assayed for in the absence of GTP to probe for binding to unassociated tubulin. Detection of binding was also attempted in the presence of GTP under polymerization condition to probe for binding to tubulin in the process of polymerization. Finally, tubulin was also fully polymerized before incubation with **298** to detect binding to microtubules. To ascertain whether binding was specific, a huge



A

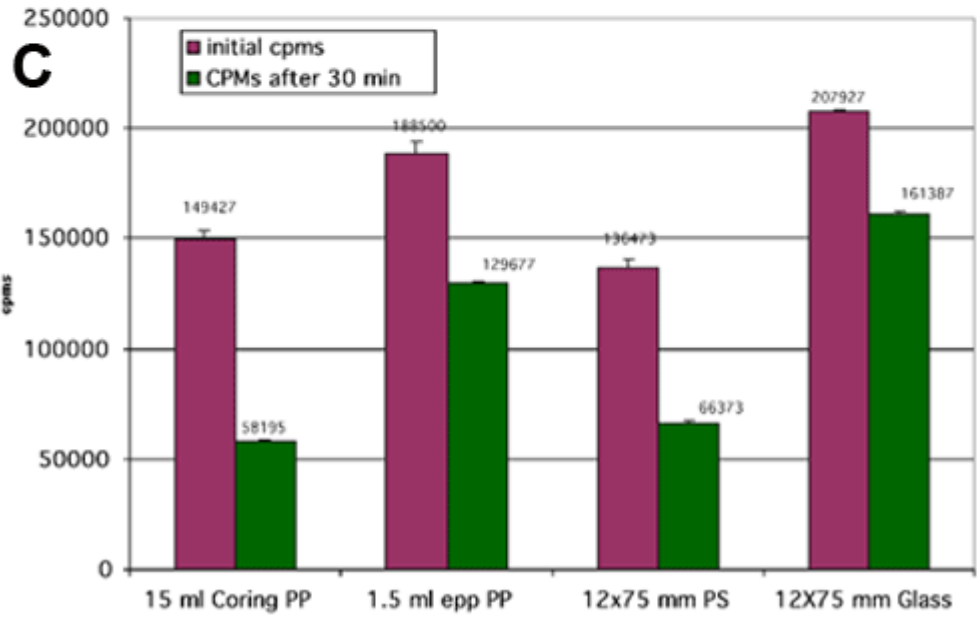
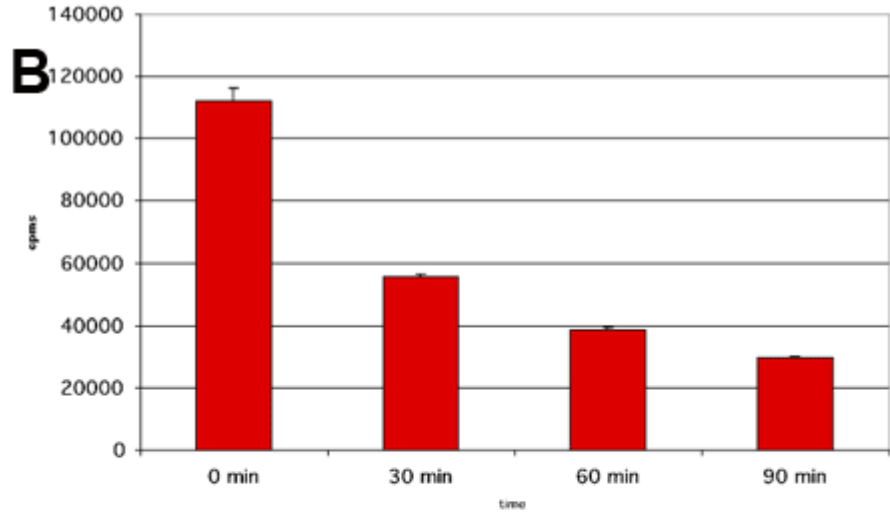
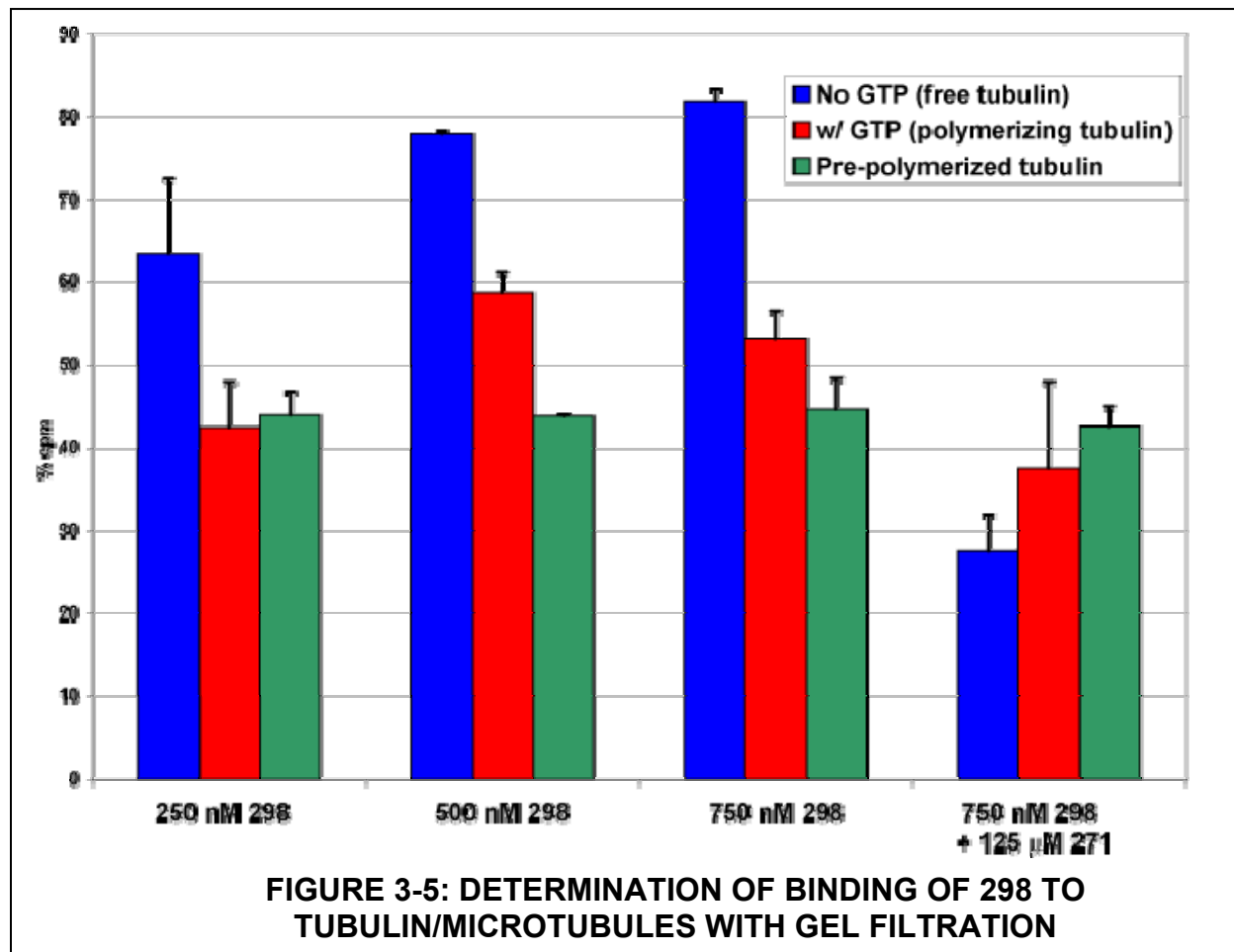


FIGURE 3-4: CHARACTERIZATION OF RADIOLABELED ANALOG 298 A) autoradiography TLC 298 B) nonspecific absorption of 298 over time in 1.5 mL Epp. tubes C) absorption in different tubes

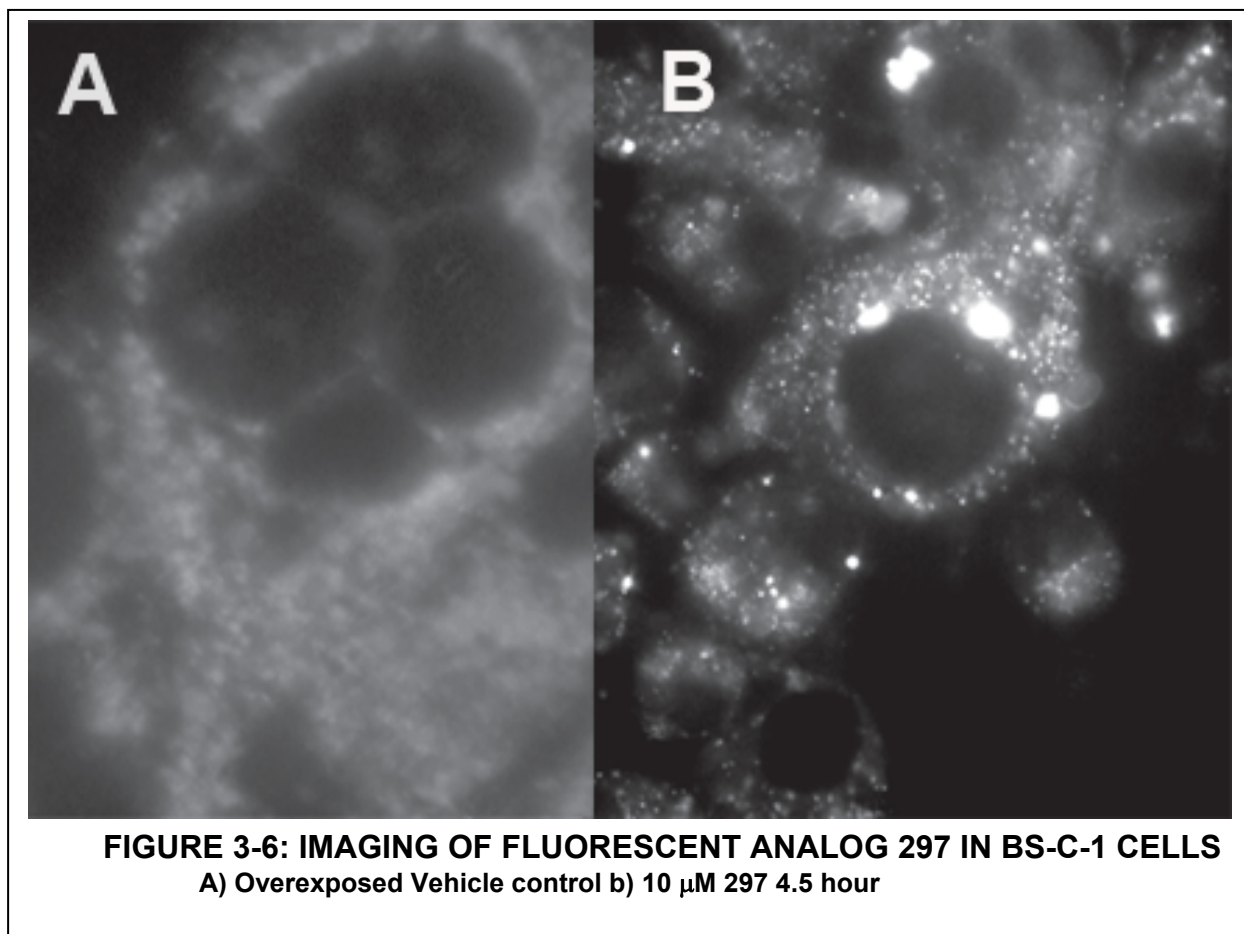


excess of syndistatin (**271**) was included in the experiment. The concentration of the tubulin was determined to be approximately 100 nM. Over a thousand fold excess of **271** failed to block the binding, suggesting that the assay did not detect specific binding of analog **298** to tubulin or microtubules. However, there was not a radioactive tubulin binding analog available, and without a positive control compound, these experiments are not conclusive.

3.4.2 Experiments with the Syndistatin Fluorescent Analog **297**

Fluorescent analog **297** also had several potential uses, mainly as a reagent for visualization in cells. However, compound **297** was significantly less active both in the

cytotoxicity assay ($IC_{50} = 900 \text{ nM}$) and the tubulin polymerization assay ($IC_{50} = 27 \text{ }\mu\text{M}$). The loss of potency raised serious questions of the compound's (**297**) ability to mimic syndistatin. The compound is still active, but it could have lost significant affinity for the cellular target, and this would void the utility of the fluorescent probe analog. Compound **297** was directly visualized in BS-C-1 cells (**Figure 3-6**). As compared to the overexposed control cells, there was no clear accumulation of fluorescence in the cells over a range of concentrations and time of incubations. The only fluorescence evident in cell culture from compound **297** was the formation of fluorescent globules as concentrations greater than $1 \text{ }\mu\text{M}$. These concentrated areas appear to form due to the poor solubility of **297** in cell media. These brightly fluorescent areas apparently did adhere to the exterior cells, but there is no indication of this compound being sequestered



inside of the cell. The pattern is very similar to that seen with the open syndistatin compound **265** (**Figure 3-3**). The impotent activity of **297** in the cell proliferation and tubulin polymerization assays, in combination with the cell imaging results, suggest that this probe analog is probably a poor mimic of syndistatin, and no further utilization of this compound was attempted.

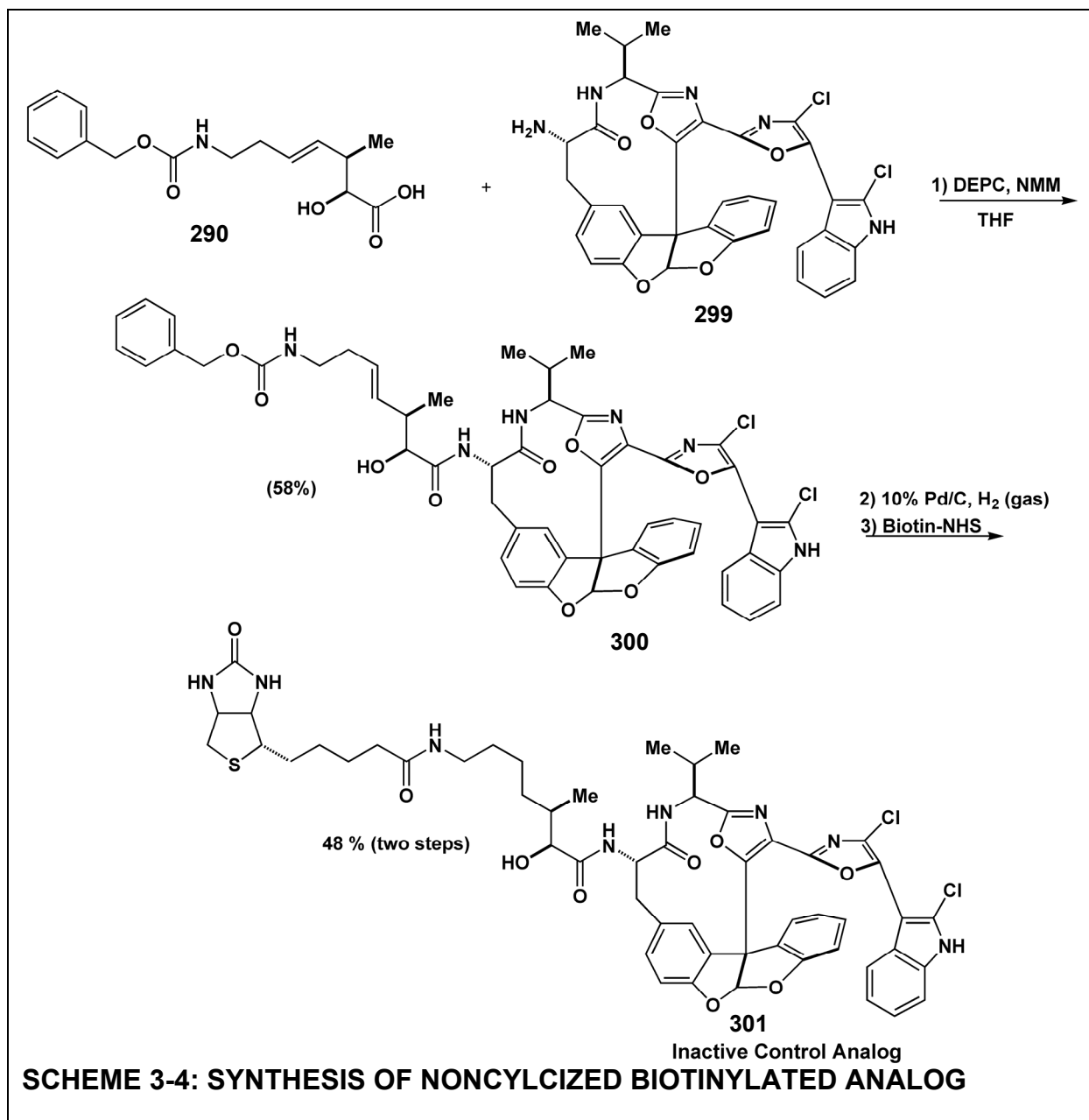
3.4.3 Syndistatin Affinity Chromatography Experiments

The most promising approach to identifying the diazonamide cellular target was through syndistatin affinity chromatography. Affinity chromatography could be performed with either a biotinylated syndistatin analog (**296**) or a syndistatin affinity matrix (**Figure 3-8**). This powerful method allows for the isolation of target proteins from a complex, unpurified cellular lysate. As detailed, this approach has been used successfully to identify the target of several biologically active small molecules (**Section 3.1**). However, in the literature precedent, affinity chromatography was performed in conjugation with another method capable of detecting the presence of the cellular target in the lysate. The other method, usually a biochemical assay, was used to partially enrich the cellular target prior to its successful purification with affinity chromatography. For diazonamide there was no basis for preliminary protein purification other than the results of the tubulin polymerization assay. Therefore, MAP-enriched tubulin was first explored as a source lysate for target identification. In designing the pull-down experiments, calculations were employed to approximate the amount of syndistatin reagent and protein lysate required. For example, successful visualization of a protein band with silver staining would require approximately 7-10 ng. Using different approximate values for the binding affinity and the abundance of individual proteins in the lysate, it was possible to calculate how much reagent and lysate might be required to isolate 10 ng of target protein.

3.4.3.1 Utilization of Biotinylated Analog **296**

Syndistatin affinity chromatography was first attempted from MAP(+) tubulin (see Section **3.7.7** for procedure). This initial foray used avidin-coated agarose beads to perform the pull-down experiments, and it used beads without compound as a negative control (result not shown). Based on these preliminary results, it was clear a better negative control would need to be employed. Several candidate bands were evident in the **296** pull-down lane, but it was evident a better negative control had to be introduced. The syndistatin-coated beads pulled down a larger number of proteins in greater amount than the empty beads. This likely is due to the effect of coating the avidin agarose beads with a relatively hydrophobic compound, such as **296**.

To identify possible target proteins, an inactive biotinylated analog needed to be used to control for the non-specific binding of proteins. The SAR determination suggested that a biotinylated analog derived from non-cyclized compound **273** (**Figure 3-6**) would be an ideal negative control analog. Inactive non-cyclized biotinylated analog **301** was synthesized using the developed methodologies (**Scheme 3-4**). Syndistatin affinity chromatography with **296** and **301** in MAP-enriched tubulin revealed no clear candidate bands were being enriched (**Figure 3-7**). Tubulin was also not selectively enriched with active syndistatin analog **296** relative to the negative control compound. This results is in accord with the gel filtration binding experiments performed with radiolabel analog **298** (**Figure 3-5**) that failed to detect any binding to tubulin.



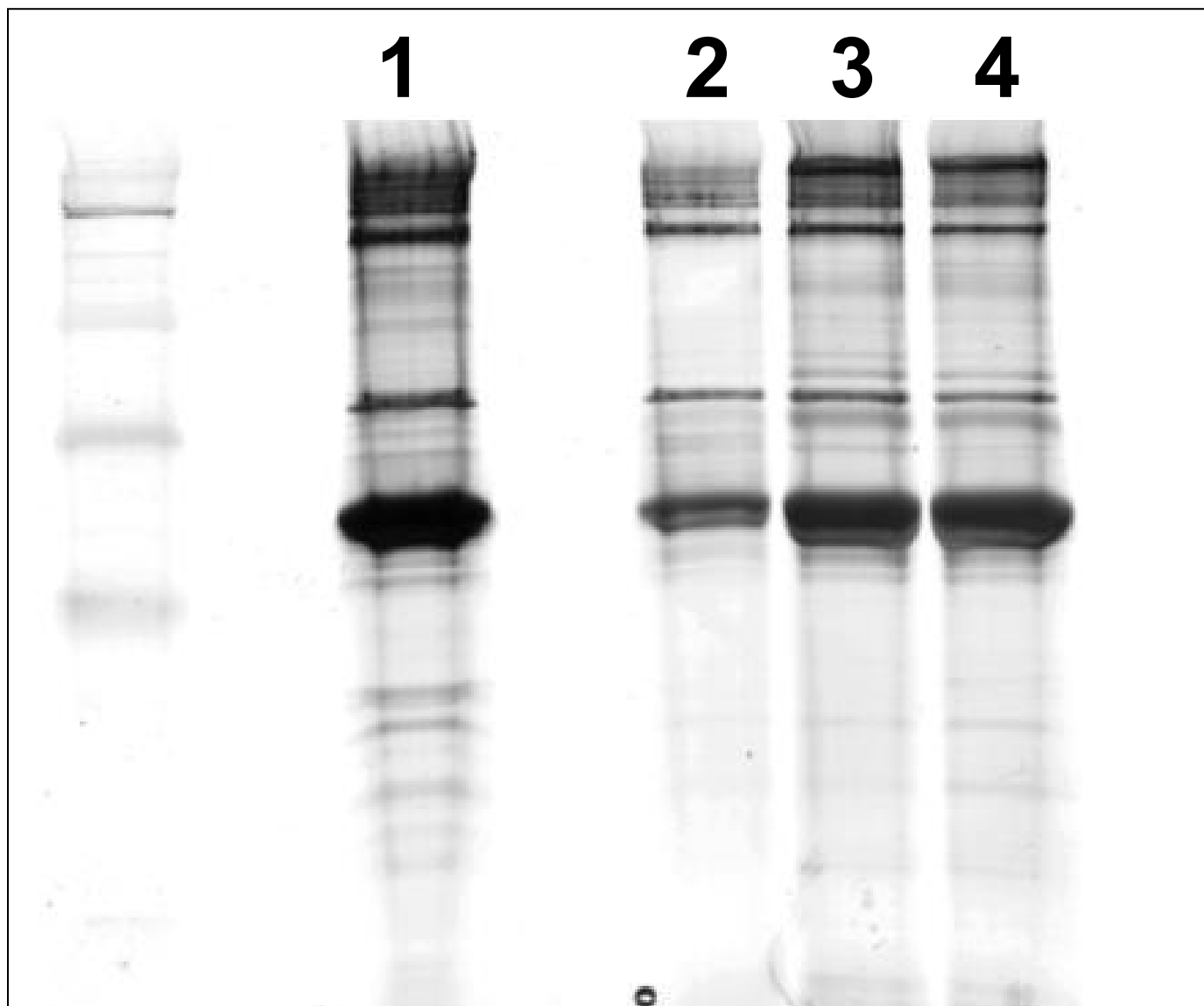


FIGURE 3-7 AFFINITY CHROMATOGRAPHY WITH SYNDISTATIN REAGENTS 296 AND 303 IN MAP(+) TUBULIN IS UNSUCCESSFUL: 1) MAP(+) Tubulin lysate Lane 2) no compound (-) control 3) pull-down with syndistatin biotinylated compound 296 4) pull-down with inactive biotinylated analog 301

3.5 Discussion

The synthesis of the full suite of syndistatin probe analogs was successful. Implementation of the extended, unsaturated side chain introduced a versatile synthetic handle

that allowed for the construction of several biologically active probe analogs. Several important findings were made with the probe analogs. First, the results detailing the nonspecific loss of radiochemical analog **298** in plastic tubes have clear and important implications for experiments in which syndistatin-related compounds are diluted in buffer. The tubulin polymerization is an example of such an experiment. It is very likely that in these experiments the concentration of compound required for an observed effect is significantly inflated. In the presence of complex media containing mixtures of proteins it is likely such losses of compound are minimized, but this was not shown experimentally.

The utilization of these analogs was unsuccessful in identifying the diazonamide cellular target. The failure to detect specific binding of the radiolabeled analog **298** to tubulin or microtubules and the inability of the biotinylated analog **296** to pull-down tubulin support idea that tubulin is not the cellular target for diazonamide A. However, the lack of success of the biotinylated and fluorescent analog experiment could be the result of these analogs poorly interacting with the high affinity cellular target. With only cytotoxicity data, and to a lesser extent tubulin polymerization data, to validate these compounds it is impossible to conclude whether they are competent syndistatin probe analogs. To some extent, this illustrates the major limitation of this research endeavor; it is only possible to determine the critical experimental conditions and reagents after the target has been successfully identified. This is especially true for the affinity chromatography experiments. Without a separate biochemical assay to guide the experimental design, many variables had to be arbitrarily decided on, including the lysate, buffer, wash conditions, incubation times, etc. Any of these variables could be critical in successfully purifying the target from the lysate, and this is assuming the biotinylated analog or the syndistatin affinity matrix posses a high affinity for the cellular target. It is possible that the

biotinylated analog is incapable of binding both the avidin matrix and the cellular target simultaneously. Once again, there was no way to ascertain the necessary linker length between syndistatin and biotin. Without a clear validation of the probe analogs and independent establishment of the experimental conditions used in the affinity purification, the successful identification of the diazonamide cellular target was only possible through random serendipity and screening many cellular lysate and experimental conditions.

3.6 Conclusions

Based on the SAR determinations, biologically active radiolabeled, biotinylated, and fluorescent syndistatin analogs were successfully synthesized. The radiolabeled analog showed the non-specific loss of compound dissolved in buffer, presumably due to compound's poor aqueous solubility. The efforts to identify the diazonamide A cellular target with the syndistatin probe analogs were unsuccessful. The radiolabeled and biotinylated analogs failed to specifically bind to tubulin or microtubules. This result supports the assertion that the diazonamide compounds induce their anti-mitotic activity through the interaction with a novel cellular target.

3.7 Experimental Section

3.7.1 Determination of Cytotoxicity of Compounds in Tissue Culture

See Section 3.2.4.3 for procedure.

3.7.2 *In Vitro* Tubulin Polymerization Assay

See Section 3.2.9 for procedure.

3.7.3 Nonspecific Binding of Radiolabeled Analog 298

Compound 298 in a DMSO stock solution was diluted in PBS buffer in the tubes and mixed. An aliquot was immediately removed as a time zero value. At the designated times, aliquots were removed. The amount of radioactivity was then determined in each aliquot using a Beckmann Scintillation Counter.

3.7.4 TLC and Autoradiography of Radiolabeled Analog 298

298 was spotted on a Whatman Diamond LK6DF Silica Gel (250 μ M thick) TLC plate. The plate was chromatographed with 60% ethyl acetate/hexane. After removal of solvent through air drying, the plate was sprayed with En³hance Autoradiography Development Spray (NEN). The plate was allowed to air dry for 20 minutes and then rotated and re-sprayed. The drying and spraying was repeated once more, and then the plate was allowed to dry overnight. The plate was loaded into an X-ray film cassette with Konica Medicinal Development Film in the darkroom, and the film was allowed to develop for 4 hours at - 80 °C. The film was then developed using a standard developer.

3.7.5 Determination of Binding of Radiolabeled Analog 298 to Tubulin and Microtubules Using Gel Exclusion Chromatography

MAP-enriched tubulin was briefly thawed in a 37 °C water bath and then centrifuged at 14,000 rpm at 4 °C for 15 minutes to pellet insoluble protein. The MAP (+) tubulin was then placed on ice until use. A DMSO stock solution of compound **298** was diluted in PEM buffer with or without GTP. Some tubes included a large excess of syndistatin (**271**). MAP-enriched tubulin was added to the tubes to a final concentration of 5.0 mg/mL. The tubes were incubated at 37 °C for 1 hour. To assay for binding to microtubules in the process of polymerizing, tubulin with GTP was incubated at 37 °C for 1 hour prior to introduction of analog **298**. After incubation, the

samples were loaded onto Micro Bio-Spin columns (Bio-Rad) and centrifuged for 4 minutes at 1000 x (g). The amount of tritium in the column flow through was determined in the column flow through using a Beckmann Scintillation Counter.

3.7.6 Imaging of Fluorescent Analog 297

BS-C-1 cells were grown on glass cover slips in 4-well tissue culture plates overnight. Compound **297** was added to wells, as well as DMSO vehicle control. The cover slips were incubated for the designated times with compound, and then the media was carefully removed, the coverslips were gently washed with PBS, and the cells were then visualized using a Zeiss Axial Digital Light Microscope with the fluorescent green filter set.

3.7.7 Affinity Chromatography with Syndistatin Reagents

Affinity Chromatography Buffer (ACB) (Crew et al. PNAS **93**: 4316): 10 mM $K_2HPO_4 \cdot 3H_2O$, 10 mM EDTA, 5 mM EGTA, 10 mM $MgCl_2 \cdot 6H_2O$, 2 mM Na_3VO_4 , 2mM Dithiothreitol, 5 mM NaF, 10 μ g/mL pepstatin, 10 μ g/mL leupeptin, 1mM PMSF, 150 mM NaCl.

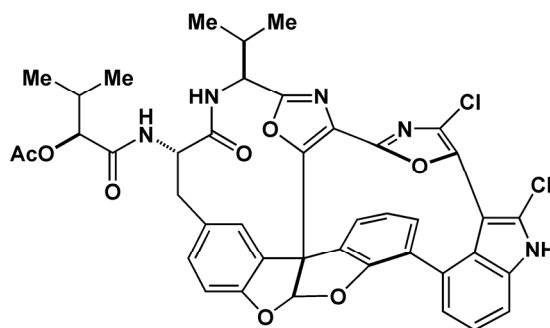
3.7.7.1 Affinity Chromatography with Biotinylated Syndistatin Reagents 296 and 301 in MAP(+) Tubulin

300 μ L of a 2-4 mg/mL avidin-coated agarose solution was placed in a 10 mL plastic fritted column and washed with 10 mL ACB, followed by 5 mL of ACB + 0.1% Triton X-100. 300 μ L of ACB was used to re-suspend the matrix, and 100 μ L of matrix was placed in 1.5 mL Epp. tubes. The tubes were briefly vortexed, and 4 μ L of either 1) DMSO (vehicle control), 2) 10 mM of a **296** DMSO stock solution (40 nmol), or 3) 10 mM of a **301** DMSO stock solution (40 nmol) were added to each tube. The tubes were shaken overnight at 4 °C. Then, the agarose

solution was diluted in ACB, transferred to the columns, and washed with 10 mL ACB followed by 10 mL ACB + 0.1 Triton X-100. 1.0 mL of a 10.9 mg/mL MAP-enriched tubulin was briefly thawed in a 37 °C water bath, and then centrifuged at 14,000 rpm at 4 °C for 15 minutes to pellet insoluble protein. The MAP-enriched protein was diluted with 0.5 mL of ACB, and 500 μ L of the ~5.5 mg/mL MAP(+) tubulin was added to the matrix in each column. ~1/3 of the buffer was allowed to flow through the column, at which point the column were capped and incubated at for 2 hours. Then, the buffer was allowed to flow through, and the matrix was washed with 5 mL ACB and then 3 mL of ACB + 0.1% Triton X-100. The buffer was removed, and then 50 μ L of SDS sample buffer was added to the matrix and incubated for 30 minutes. The sample buffer was collected, boiled for 3 minutes, and loaded and on a Protean pre-cast 4-15% gradient polyacrylamide gel (BioRad). Electrophoresis was done at 200 V, and the gel was then stained with the Silver Stain Plus Kit (Biorad).

3.7.8 Synthesis Experimental Section

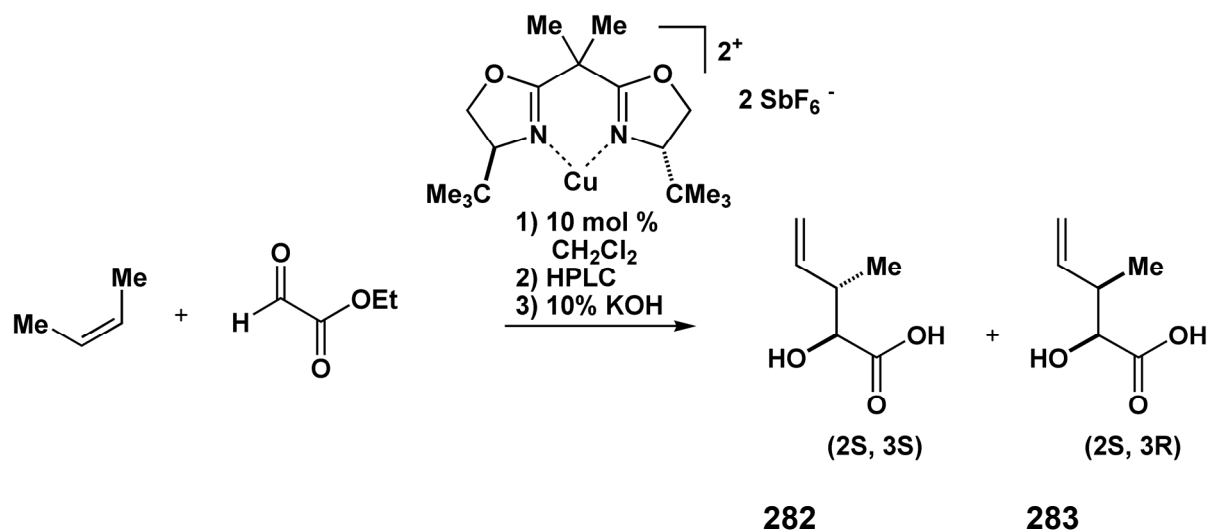
C37 Acetylated Syndistatin 278



278: ^1H NMR (400MHz, CD_3CN): δ 10.40 (s, 1H), 7.55 – 7.50 (m, 2H), 7.42 – 7.37 (m, 1H), 7.26 – 7.19 (m, 3H), 7.08 (dd, J = 1.2, 7.9 Hz, 1H), 7.02 (d, J = 7.9 Hz, 1H), 6.93 – 6.89 (m, 2H), 6.83 (d, J = 9.1 Hz, 1H), 6.82 (s, 1H), 4.96 (dd, J = 5.5, 8.5 Hz, 1H), 4.74 (d, J = 5.5Hz, 1H),

4.44 – 4.38 (m, 1H), 3.41 (*app* t, $J = 12.2$ Hz, 1H), 2.77 (dd, $J = 3.0$ Hz, 12.8 Hz, 1H), 2.32 – 2.22 (m, 1H), 2.10 (s, 3H), 1.02 (d, $J = 6.8$ Hz, 3H), 0.96 (d, $J = 6.8$ Hz, 6H), 0.88 (d, $J = 6.8$ Hz, 3H). MS: calculated for $C_{42}H_{35}Cl_2N_5O_8 [M+H]^+$: 806.19, found: 806.10 g/mol.

Compounds 282 and 283

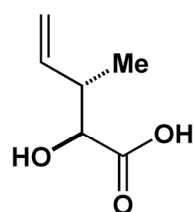


The procedure was performed with slight modification from the original Evans procedure (*JACS* (2000) 122: 7936-7943). (*S,S*)-2,2'-Isopropylidene-bis(4-*tert*-butyl-2-oxazoline) (0.986 g, 3.30 mmol) was charged to a dry reaction flask under a nitrogen atmosphere. Anhydrous copper (II) chloride (0.445 g, 3.31 mmol) was weighed under a nitrogen atmosphere and added to the ligand. 13.5 mL of dry CH_2Cl_2 was added via syringe and the reaction was stirred at ambient temperature under nitrogen, covered in foil, for five hours. The bright green solution was transferred via cannula through a glass syringe fitted with a 0.45 μm filter to a dry reaction flask. The solvent was removed to yield the product as a bright green powder (1.47 g, 88%).

Under nitrogen, solid AgSbF_6 (2.0 g, 5.82 mmol) was added to the $\text{Cu}(t\text{-Bu-Box})\text{Cl}_2 \cdot \text{CH}_2\text{Cl}_2$ product (1.47 g, 2.86 mmol). 57 mL of dry CH_2Cl_2 was added via syringe, and the reaction was stirred for 5 h in the absence of light. The solution turned a dark green color

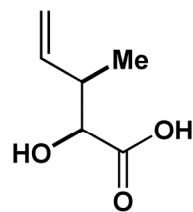
with white precipitate present. Under a nitrogen atmosphere, the reaction was filtered through a pad of oven dried Celite into a dry reaction flask. Freshly distilled ethyl glyoxalate (3.5 mL, 26.1 mmol) was added to the catalyst via syringe followed by dry CH₂Cl₂ (26 mL). An oven dried condenser was attached and used to condense *cis*-butene into the reaction (> 300 drops) at –78 °C. The reaction was allowed to warm to ambient temperature and stirred for 48 h protected from light. Solvent was removed from the blue-green reaction *in vacuo*, and the product was purified via column chromatography (20% ether/hexane). The desired product was obtained as a clear oil (1.2 g) as a 40:60 mixture of (2*S*:3*R*): (2*S*:3*S*).

The diastereomers were separated via normal phase preparative HPLC (Higgins Silica Gel column) using 13% ether/hexane as eluent. The separated diastereomers (20 mg, 0.13 mmol) dissolved in 0.68 mL of methanol, followed by addition of 0.68 mL of a 10% aq. KOH solution. The reaction was stirred for 2 h at ambient temperature. The crude reaction was then acidified with 1 N NH₄Cl to pH = 2.0 and extracted three times with ethyl acetate. The organic layers were combined and then washed with brine and dried over Na₂SO₄. The desired acid (10.0 mg, 60% yield) was used without further purification.



(2*S*,3*S*)-2-hydroxy-3-methylpent-4-enoic acid

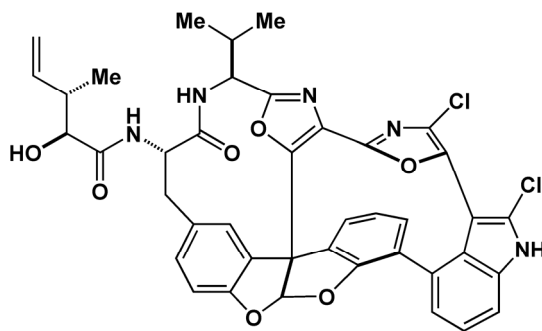
282: ¹HNMR (400 MHz, CD₃OD): δ 5.90 – 5.80 (m, 1H), 5.2-5.0 (m, 2H), 4.06 (d, *J* = 4.3 Hz, 1H), 2.63 (br s, 1H), 1.03 (d, *J* = 6.7 Hz, 3H).



(2S,3R)-2-hydroxy-3-methylpent-4-enoic acid

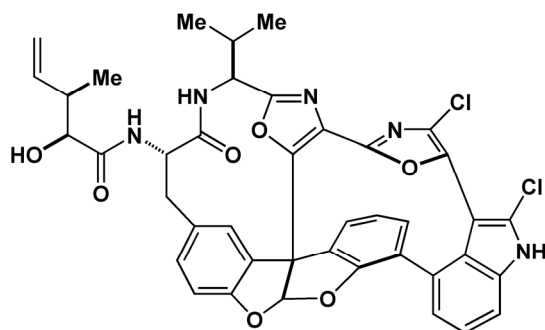
283: $^1\text{H NMR}$ (400 MHz, CD_3OD): δ 5.87 – 5.78 (m, 1H), 5.06 (d, $J = 16.8$ Hz, 1H), 5.01 (d, $J = 10.0$ Hz, 1H), 4.05 (d, $J = 3.6$ Hz, 1H), 2.65 (br s, 1H), 1.12 (d, $J = 6.7$ Hz, 3H).

Compound 284



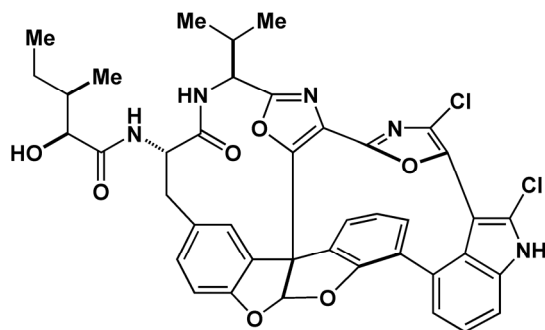
284: $^1\text{H NMR}$ (400MHz, CD_3OD): δ 7.51 – 7.45 (m, 2H), 7.38 – 7.34 (m, 1H), 7.27 (dd, $J = 1.8, 8.5$ Hz, 1H), 7.22 – 7.19 (m, 2H), 7.08 (dd, $J = 1.2, 7.9$ Hz, 1H), 6.96- 6.87 (m, 2H), 6.84 (s, 1H), 5.96 – 5.87 (m, 1H), 5.15 – 5.04 (m, 2H), 4.98 (d, $J = 6.0$ Hz, 1H), 4.60 (dd, $J = 3.6, 11.6$ Hz, 1H), 4.03 (d, $J = 3.6$ Hz, 1H), 3.46 (*app* t, $J = 12.2$ Hz, 1H), 2.81 (dd, $J = 3.6, 12.8$ Hz, 1H), 2.70 – 2.63 (m, 1H), 2.33 – 2.26 (m, 1H), 1.09 (d, $J = 6.8$ Hz, 3H), 1.04 (d, $J = 6.8$ Hz, 3H), 0.97 (d, $J = 6.8$ Hz, 3H).

Compounds 285



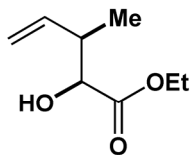
285: ^1H NMR (400MHz, CD_3OD): δ 7.50 – 7.45 (m, 2H), 7.38 – 7.34 (m, 1H), 7.24 (dd, J = 1.8, 8.5 Hz, 1H), 7.23 – 7.18 (m, 2H), 7.07 (dd, J = 1.2, 7.9 Hz, 1H), 6.95 -6.87 (m, 2H), 6.84 (s, 1H), 5.90 – 5.80 (m, 1H), 5.12 – 5.05 (m, 2H), 4.98 (d, J = 6.0 Hz, 1H), 4.58 (dd, J = 3.6, 11.6 Hz, 1H), 3.98 (d, J = 3.6 Hz, 1H), 3.42 (*app t*, J = 12.2 Hz, 1H), 2.77 (dd, J = 3.6, 12.8 Hz, 1H), 2.72 – 2.63 (m, 1H), 2.34 – 2.24 (m, 1H), 1.15 (d, J = 6.8 Hz, 3H), 1.09 (d, J = 6.8 Hz, 3H), 0.96 (d, J = 6.8 Hz, 3H).

Compound 286



286: ^1H NMR (400MHz, CD_3OD): δ 7.51 – 7.46 (m, 2H), 7.38 – 7.34 (m, 1H), 7.24 (dd, J = 1.8, 8.5 Hz, 1H), 7.23 – 7.18 (m, 2H), 7.07 (dd, J = 1.2, 7.9 Hz, 1H), 6.96 – 6.87 (m, 2H), 6.84 (s, 1H), 4.97 (d, J = 6.0 Hz, 1H), 4.60 (dd, J = 3.6, 11.6 Hz, 1H), 3.93 (d, J = 3.6 Hz, 1H), 3.47 (*app t*, J = 12.2 Hz, 1H), 2.80 (dd, J = 3.6, 12.8 Hz, 1H), 2.34 – 2.26 (m, 1H), 1.89 – 1.83 (m, 1H), 1.57 – 1.45 (m, 1H), 1.32 – 1.20 (m, 1H), 1.09 (d, J = 6.8 Hz, 3H), 1.00 (d, J = 6.8 Hz, 3H), 0.96 (d, J = 6.8 Hz, 3H), 0.94 (t, J = 7.3 Hz, 3H).

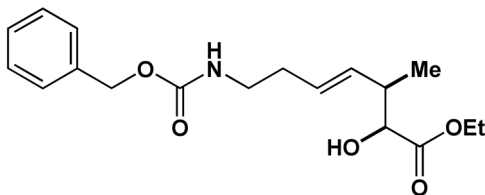
Compound 288



(2S,3R)-ethyl 2-hydroxy-3-methylpent-4-enoate

288: ^1H NMR (400MHz, CDCl_3): 5.90 – 5.81 (m, 1H), 5.16 – 5.08 (m, 2H), 4.32 – 4.15 (m, 2H), 2.77 (d, $J = 6.1$ Hz, 1H), 2.66 - 2.62 (m, 1H), 1.31 (t, $J = 7.0$ Hz, 3H), 1.01 (d, $J = 7.0$ Hz, 3H).

Cbz-Protected Extended Side Chain Ester 289

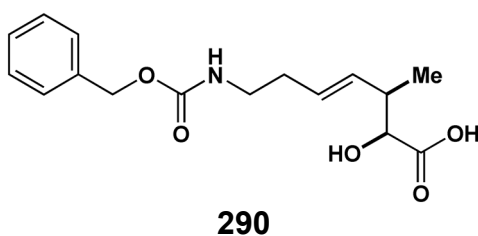


289

Hydroxy ester **288** (29.4 mg, 0.186 mmol) and Cbz protected butenyl amine (48.5 mg, 0.236 mmol) were charged to a dry reaction flask. Under a nitrogen atmosphere, Grubb's Catalyst 2nd Generation (Aldrich) ruthenium catalyst was charged to the reaction flask. The reaction was dissolved in dichloromethane (1.0 mL, 0.19 M). The reaction flask sealed and heated to 40°C protected from light. After 30 min., the initially rose colored solution became light orange. After 3.5 hours, the reaction was cooled and diluted with 20% EtOAc/hexane to precipitate the Cbz butenyl amine homodimer byproduct. The precipitate was filtered off and washed with 10% EtOAc/hexane. The filtrate was condensed *in vacuo* and flash chromatographed with EtOAc/hexanes (20-50% EtOAc) to yield 31 mg of the cross metathesis product **20** as a clear oil (50%).

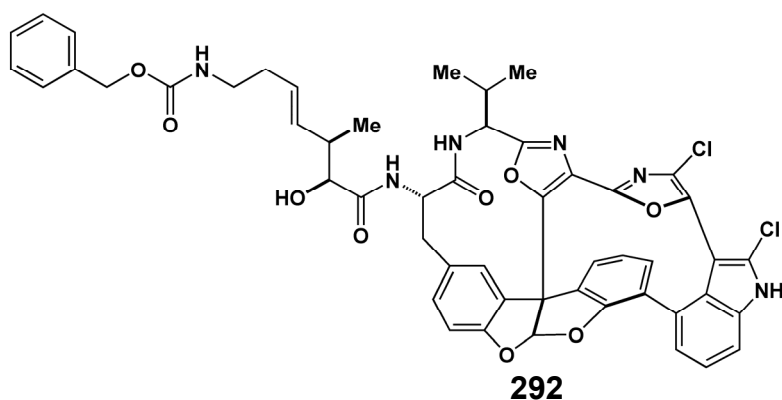
289: Rf=0.57 in 40% EtOAc/hexanes. ^1H NMR (400 MHz, CDCl_3): δ 7.37 – 7.29 (m, 5H), 5.41 – 5.38 (m, 2H), 5.10 (s, 2H), 4.89 (br s, 1H), 4.2 (m, 2H), 4.07 (q, $J = 3.2$ Hz, 1H), 3.30 – 3.24 (m, 1H), 3.17 – 3.09 (m, 1H), 2.73 (d, $J = 6.4$ Hz, 1H), 2.61 (ddd, $J = 3.2$, 1H), 2.20 – 2.16 (m, 2H), 1.26 (t, $J = 7.2$ Hz, 3H), 1.14 (d, $J = 6.8$ Hz, 3H). ^{13}C NMR (300 MHz, CDCl_3): δ 174.67, 156.61, 136.89, 132.64, 128.80, 128.69, 128.25, 74.86, 66.78, 61.85, 41.17, 40.51, 33.10, 17.01, 14.50.

Cbz-Protected Extended Side Chain Acid **290**



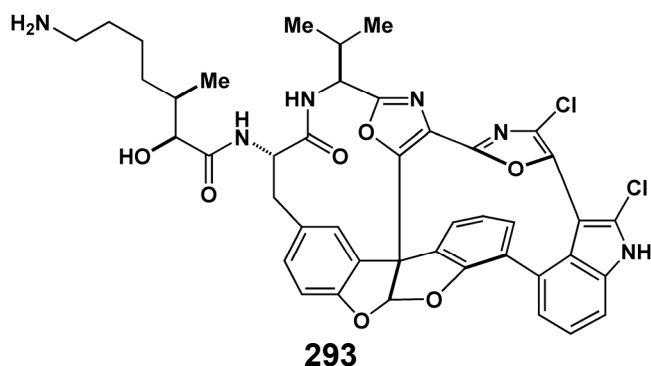
Cross metathesis product **289** (28 mg, 0.084 mmol) was dissolved in methanol (0.7 mL). 0.5 mL of a 10% aqueous KOH solution was added. After 40 min., the reaction was acidified with 1N HCl and partitioned with EtOAc. The organic layer was washed twice with water, dried over Na_2SO_4 , and condensed *in vacuo* to give a yellow oil. The crude mixture was flash chromatographed on silica gel with 20% methanol/ CH_2Cl_2 solvent. 20 mg of product (**290**) was obtained as a slightly yellow oil (76%). **290**: ^1H NMR (400 MHz, CDOD_3): δ 7.33 – 7.26 (m, 5H), 5.50 – 5.48 (m, 2H), 5.07 (s, 2H), 3.95 (br s, 1H), 3.20 – 3.07 (m, 2H) 2.60 (br s, 1H), 2.17 (q, $J = 6.4$ Hz, 2H), 1.98 (s, 1H), 1.09 (d, $J = 6.4$ Hz, 3H). ^{13}C NMR (300 MHz, CDOD_3): δ 177.22, 159.00, 138.60, 133.90, 129.58, 129.50, 129.05, 128.89, 76.14, 67.46, 42.30, 41.78, 34.30, 17.61.

Cbz-Protected Extended Side Chain Syndistatin **292**



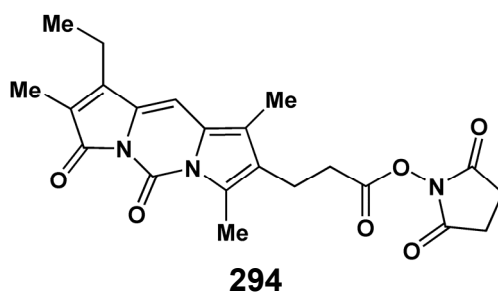
Syndistatin core amine **291** (12.2 mg, 0.018 mmol) was dissolved in THF (0.15 mL) to form a slightly green solution. 0.185 mL of a 0.12 M solution of **290** (6.8 mg, 0.02 mmol) was added via syringe. The reaction was cooled to 0°C. 4-methylmorpholine (NMM) (2.0 mg, 0.02 mmol) was added to the reaction, followed by diethylcyanophosphonate (DEPC) (4.5 mg, 0.027 mmol). After 5 min, the ice bath was removed, and the reaction was allowed to warm to ambient temperature stirring for 3 hours. The reaction was diluted in 10 mL EtOAc, and washed with NaHCO₃, H₂O, brine, and dried over Na₂SO₄. The reaction mixture was purified via flash chromatography with 60% EtOAc/hexane. To remove a trace impurity, the product was re-chromatographed. 10 mg of the desired coupled product was obtained as a white foam (55% yield). **292**: R_f = 0.55 in 70% EtOAc/hexanes. ¹HNMR (400 MHz, CDOD₃): δ 7.48-7.45 (m, 2H), 7.36-7.14 (13 unsym. Lines, m, 8H), 7.05 (*app* dd, *J* = 7.2, 1.2 Hz, 1H), 6.90 (t, *J* = 6.8 Hz, 1H), 6.83 (d, *J* = 8 Hz, 1H), 6.80 (s, 1H), 5.53-5.50 (m, 2H), 5.05 (s, 2H), 4.97 (d, *J* = 6 Hz, 1H), 4.54 (dd, *J* = 12, 3.6 Hz, 2H), 3.96 (d, *J* = 3.6, 1H), 3.41 (t, *J* = 12 Hz, 1H), 3.20 (t, *J* = 7.2 Hz, 1H), 2.76 (dd, *J* = 12.8, 3.2, 1H), 2.65 (m, 1H), 2.32-2.21 (m, 3H), 1.12 (d, *J* = 6.8 Hz, 3H), 1.08 (d, *J* = 6.8 Hz, 3H), 0.96 (d, *J* = 6.8 Hz, 3H).

Extended Side Chain Amine Syndistatin **293**



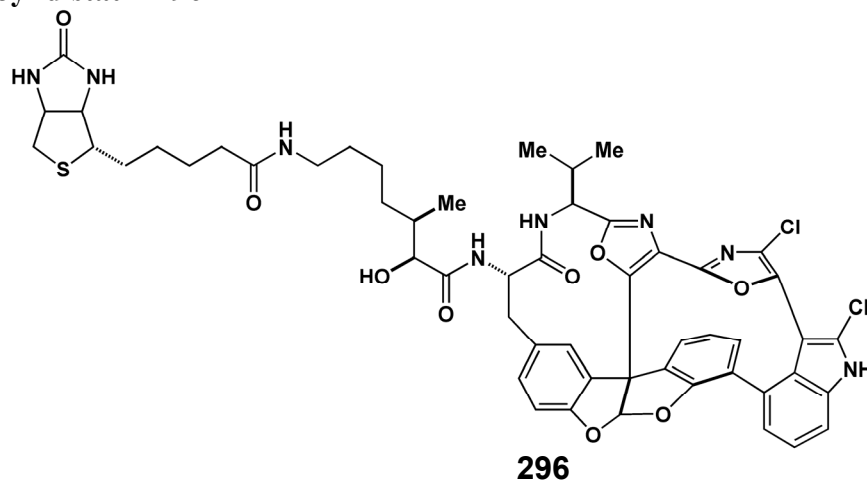
292 (10 mg, 0.01 mmol) was dissolved in 0.8 mL dry methanol pre-saturated with H₂ gas. 5.0 mg 10% Pd/C was added to the reaction (0.004 mmol Pd, 47 mol %), and the reaction was placed under a H₂ balloon at room temperature. After 45 min, the reaction was filtered through a plug of Celite with methanol washing. The crude material was used without purification. 8 mg (~100 % yield) of a white foam was obtained. **293**: ¹H NMR (400 MHz, CDOD₃): δ 7.50 (d, *J* = 1.6 Hz, 1H), 7.46 (d, *J* = 8 Hz, 1H), 7.32 (t, *J* = 7.2 Hz, 1H), 7.26 (app dt, *J* = 8, 2 Hz, 1H), 7.07 (dd, *J* = 7.6, 1.2 Hz, 1H), 6.93 (t, *J* = 7.6 Hz, 1H), 6.88 (d, *J* = 8 Hz, 1H), 4.97 (d, *J* = 6 Hz, 1H), 4.61 (s, 1H), 3.96 (d, *J* = 8 Hz, 1H), 3.46 (t, *J* = 12 Hz, 1H), 2.82 (dd, *J* = 12, 2.8 Hz, 1H), 2.67 (t, *J* = 6 Hz, 1H), 2.30 (app m, *J* = 6.4 Hz, 1H), 1.97 (br s, 1H), 1.09 (d, *J* = 6.8 Hz, 3H), 1.01 (d, *J* = 6.8 Hz, 3H), 0.96 (d, *J* = 6.8 Hz, 3H). ES-MS: calculated. for C₄₃H₄₀Cl₂N₆O₇[M+H]⁺ 823.23, found: 823.30; calculated. for C₄₃H₄₀Cl₂N₆O₇[M-H]⁻ 821.23, found: 821.25.

Xanthoglow Acid 294



The dipyrinone fluorophore termed Xanthoglow was prepared according to the literature procedure (Browner and Lightner *JOC*, **2002**, *67*: 2713-2716). Xanthoglow acid (40 mg, 0.12 mmol) and N-hydroxysuccinimide (46 mmol, 0.38 mmol) were charged to a reaction flask under a nitrogen atmosphere, and dissolved in dioxane (1.8 mL, 0.07M). EDC (25 mg, 0.13 mmol) was added to the reaction, and the green/black solution was stirred at ambient temperature protected from light for 19 hours. The reaction was diluted in EtOAc and washed five times with H₂O and twice with brine. The organic layer was dried over Na₂SO₄. The crude reaction mixture was subjected to flash chromatography (50% EtOAc/benzene). **294** was obtained as a green solid product (19 mg, 37%). **294**: ¹HNMR (400 MHz, CDCl₃): δ 6.39 (s, 1H), 2.85 – 2.83 (m, 6h), 2.75 – 2.73 (m, 2H), 2.66 (s, 3H), 2.54 (q, *J* = 8 Hz, 2H), 2.14 (s, 3H), 1.96 (s, 3H), 1.22 (t, *J* = 8 Hz, 3H).

Biotinylated Syndistatin **296**

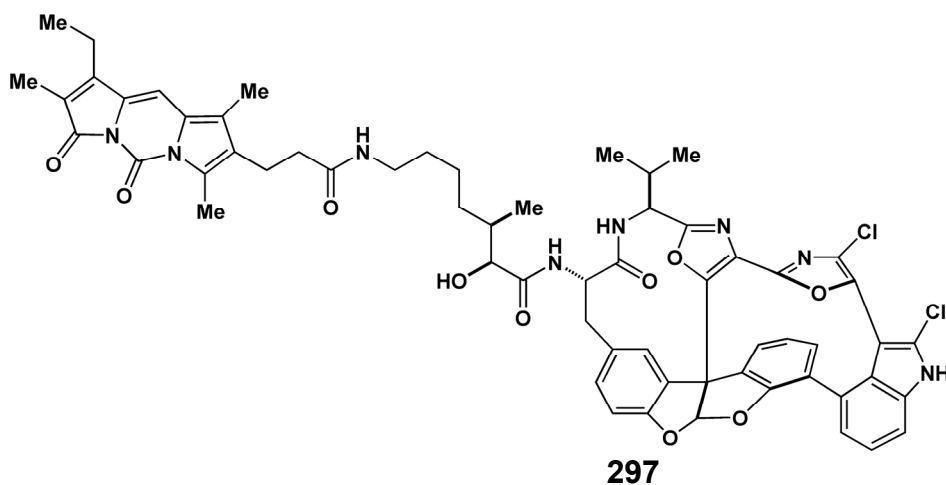


293 (1.8 mg, 0.002 mmol) was dissolved in DMF (0.2 mL, 0.01M). NHS-activated biotin (Fluka) (1.7 mg, 0.005 mmol) was added as a solid to the reaction. The reaction was stopped after stirring for 5 h at ambient temperature. The reaction was dissolved in 10 mL ethyl acetate, and washed three times with a 1:1 solution of H₂O/brine, and dried over Na₂SO₄. The preparative thin

layer chromatography with 10% MeOH/CH₂Cl₂ provided the of the desired biotinylated compound as a white foam (2.0 mg, 87%).

296: R_f = 0.30 in 10% methanol/CH₂Cl₂. ¹HNMR (400 MHz, CDOD₃): δ 7.51 (d, *J* = 1.6 Hz, 1H), 7.47 (dd, *J* = 8.4, 0.8 Hz, 1H), 7.36 (t, *J* = 7.2, 1H), 7.28 (dd, *J* = 8, 2 Hz, 1H), 7.20 (*app* d, *J* = 7.2 Hz, 2H), 7.08 (dd, *J* = 7.6, 1.2, 1H), 6.94 (t, *J* = 7.6 Hz, 1H), 6.89 (d, *J* = 8 Hz, 1H), 6.84 (s, 1H), 4.97 (d, *J* = 6 Hz, 1H), 4.61 (dd, *J* = 11.6, 3.2, 1H), 4.45 (q, *J* = 4 Hz, 1H), 4.25 (dd, *J* = 8, 4.8 Hz, 1H), 3.94 (d, *J* = 3.6 Hz, 1H), 3.46 (*app* t, *J* = 8.4, 1H), 3.27-3.13 (m, 3H), 2.89 (dd, *J* = 9.2, 4.8 Hz, 1H), 2.82 (dd, 12.8, 3.2 Hz, 1H), 2.68 (d, *J* = 12.8 Hz, 1H), 2.30 (*app* m, 1H), 2.20 (t, *J* = 7.2 Hz, 2H), 1.96 (m, 1H), 1.72-1.40 (m, 9H), 1.30 (m, 3H), 1.1 (d, *J* = 6.8 Hz, 3H), 1.10 (d, *J* = 6.8 Hz, 3H), 0.97 (d, *J* = 6.8 Hz, 3H). HRMS(FAB) calculated. for C₅₃H₅₄Cl₂N₈O₉S [M-H]⁻ 1049.3112, found: 1049.3199.

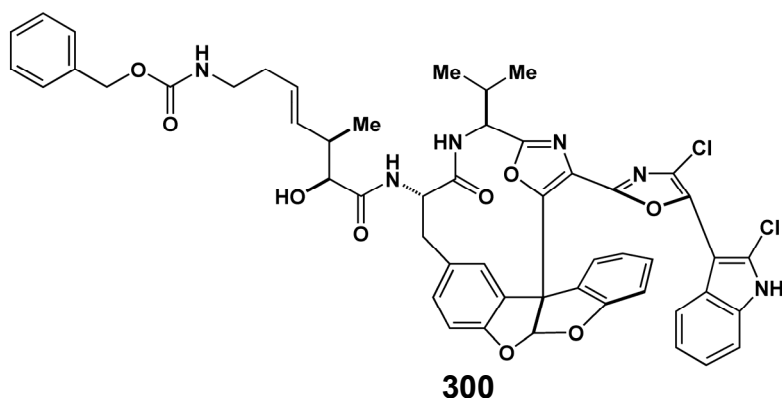
Fluorescent Syndistatin Analog 297



293 (2.1 mg, 0.002 mmol) was dissolved in DMF (0.2 mL, 0.01M). NHS-activated xanthoglow (**294**) (1.6 mg, 0.003 mmol) was added as a solid to the reaction. The reaction after 1 hour stirring at ambient temperature, the reaction was diluted in EtOAc. The organic layer was washed with water and brine and then dried over Na₂SO₄. The crude reaction mixture was

subjected to preparative TLC with 10% methanol/CH₂Cl₂. 2.3 mg of **4** was isolated as a yellow solid (88%). **297**: ¹HNMR (400 MHz, CDOD₃): δ 7.48 (*app* dd, *J* = 2.4 Hz, 1.2, 2H), 7.46 (d, *J* = 1.2, 1H), 7.36 (t, *J* = 8 Hz, 1H), 7.25 – 7.18 (m, 3H), 7.07 (dd, *J* = 7.6, 1.2, 1H), 6.93 (t, *J* = 7.6 Hz, 1H), 6.84 (*app* d, *J* = 8 Hz, 1H), 6.82 (*app* d, *J* = 4.2 Hz, 1H), 4.96 (d, *J* = 6 Hz, 1H), 4.58 (m, 1H), 3.90 (d, *J* = 3.6 Hz, 1H), 3.45 (t, *J* = 12.4, 1H), 3.17 – 3.10 (m, 2H), 2.86 – 2.74 (m, 3H), 2.62 – 2.56 (m, 3H), 2.16 (m, 3H), 1.46 – 1.29 (m, 5H), 1.09 (d, *J* = 6.8 Hz, 3H), 0.96 (d, 6.4 Hz, 6H).

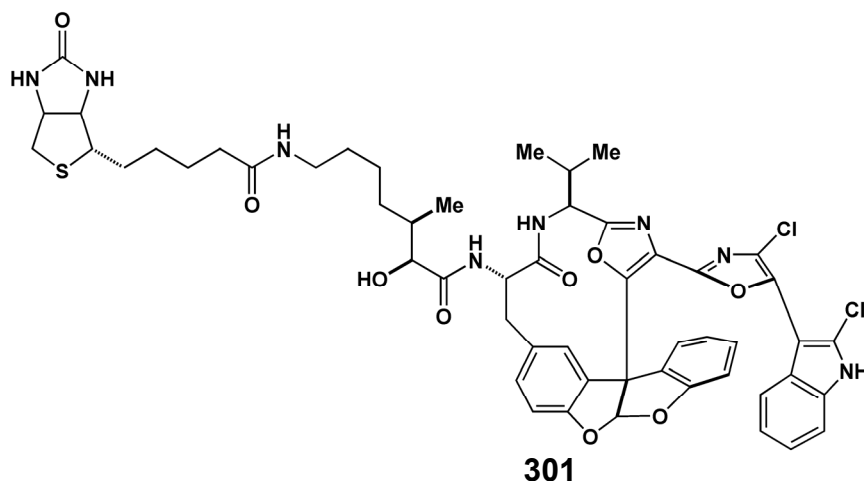
Cbz-Protected Extended Side Chain seco Analog **300**



Noncyclized syndistatin core amine **299** (7 mg, 0.010 mmol) was dissolved in THF (0.15 mL). 0.1 mL of a 0.11 M solution of **290** (3.5 mg, 0.011 mmol) was added via syringe. The reaction was cooled to 0°C. 4-methylmorpholine (NMM) (1.2 mg, 0.012 mmol) was added to the reaction, followed by diethylcyanophosphonate (DEPC) (2.7 mg, 0.015 mmol). After 5 min, the ice bath was removed, and the reaction was allowed to warm to ambient temperature stirring for 2.5 hours. The reaction was diluted in 10 mL EtOAc, and washed with NaHCO₃, H₂O, brine, and dried over Na₂SO₄. The reaction mixture was purified via flash chromatography with 55% EtOAc/hexane. 5.8 mg of the desired coupled product was obtained as a white foam (58% yield).

300: $^1\text{H NMR}$ (400 MHz, CDCl_3): δ 8.81 (br s, 1H), 7.39 – 7.07 (m, 15H), 6.92 (d, $J = 7.2$ Hz), 1H), 6.85 (*app* dd, $J = 10.8, 8.4$, 1H), 6.72 (t, $J = 7.2$ Hz, 1H), 6.51 (d, $J = 8$ Hz, 1H), 6.26 (d, $J = 7.6$ Hz, 1H), 5.56 – 5.30 (m, 3H), 5.08 (m, 2H), 4.94 (t, $J = 6$ Hz, 1H), 4.34 (t, $J = 8.4$ Hz, 1H), 3.98 (br s, 1H), 3.39 – 3.16 (m, 4H), 2.66 (d, $J = 8.8$ Hz, 1H), 2.34 – 2.16 (m, 3H), 1.06 (d, $J = 6.8$ Hz, 3H), 1.03 (d, $J = 6.8$ Hz, 3H), 0.94 (d, $J = 6.8$ Hz, 3H). ES-MS: calculated. for $\text{C}_{51}\text{H}_{46}\text{Cl}_2\text{N}_6\text{O}_9$ $[\text{M}+\text{Na}]^+$ 979.27, found: 979.35; calculated. for $\text{C}_{51}\text{H}_{46}\text{Cl}_2\text{N}_6\text{O}_9$ $[\text{M}-\text{H}]^-$ 955.27, found: 956.55.

Biotinylated *seco* Syndistatin Analog **301**

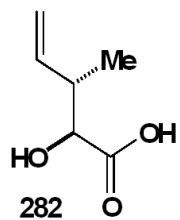


300 (5.8 mg, 0.006 mmol) was dissolved in 0.3 mL dry methanol pre-saturated with H_2 gas. 10% Pd/C (7.2 mg, 0.007 mmol, 94 mol %) was added to the reaction, and the reaction was placed under a H_2 balloon at room temperature. After 1 h, the reaction was filtered through a plug of Celite with methanol washing. The crude material was then dissolved in DMF (0.2 mL) and the NHS-activated biotin was added as a solid. The reaction was stirred for 3 hours, and then diluted in 10 mL EtOAc and washed three times with a 1:1 H_2O /brine solution. The separated organic layer was dried over Na_2SO_4 . Purification using reverse phase HPLC (40 → 100%

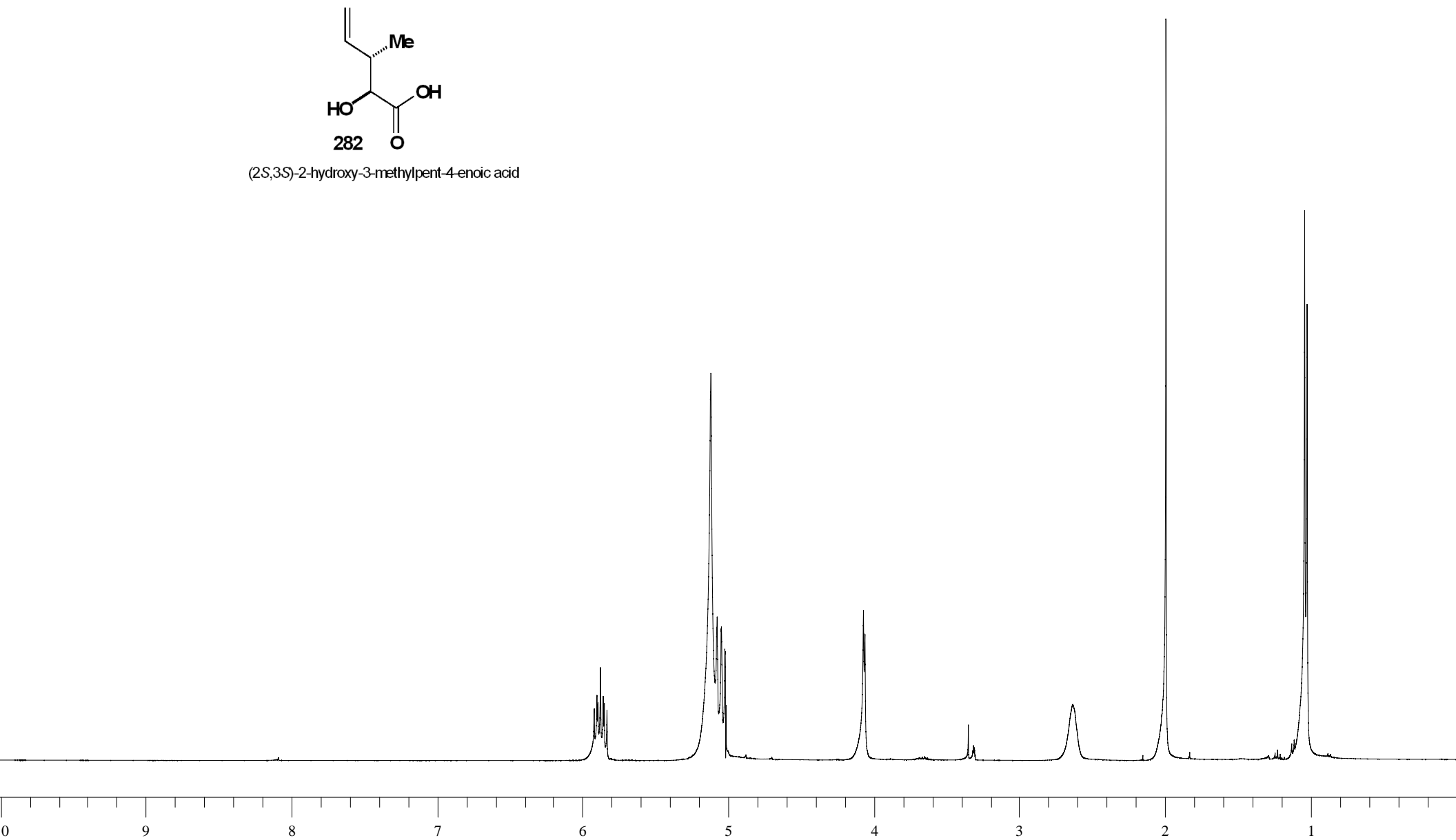
methanol/H₂O gradient, Higgins Inc. C₁₈ column) yielded 3 mg of the desired biotinylated compound **4** (48% over two steps).

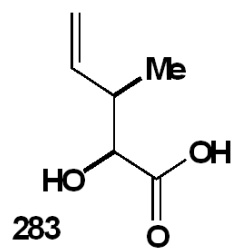
301: ¹HNMR (400 MHz, CD₃OD): δ 7.38 (*app* d, *J* = 8 Hz, 2H), 7.27 – 7.22 (m, 3H), 7.17 – 7.07 (m, 5H), 6.93 (d, *J* = 8 Hz, 1H), 6.82 (*app* dt, *J* = 8, 1.6 Hz, 1H), 6.73 (t, *J* = 7.6 Hz, 1H), 6.43 (d, *J* = 8 Hz, 1H), 4.51 (*app* dd, *J* = 4, 3.6 Hz, 2H), 4.23 (q, *J* = 4 Hz, 1H), 3.93 (d, *J* = 4 Hz, 1H), 3.21 – 3.10 (m, 3H), 2.89 – 2.82 (m, 2H), 2.66 (d, *J* = 12.4, 1H), 2.20 – 2.13 (m, 2H), 1.95 (br s, 1H), 1.73 – 1.22 (m, 12H), 1.04 – 0.99 (m, 9H). HRMS(FAB) calculated for C₅₃H₅₆Cl₂N₈O₉S (M+Li): 1057.3423, found: 1057.3376.

3.8 Chapter 3 Appendix

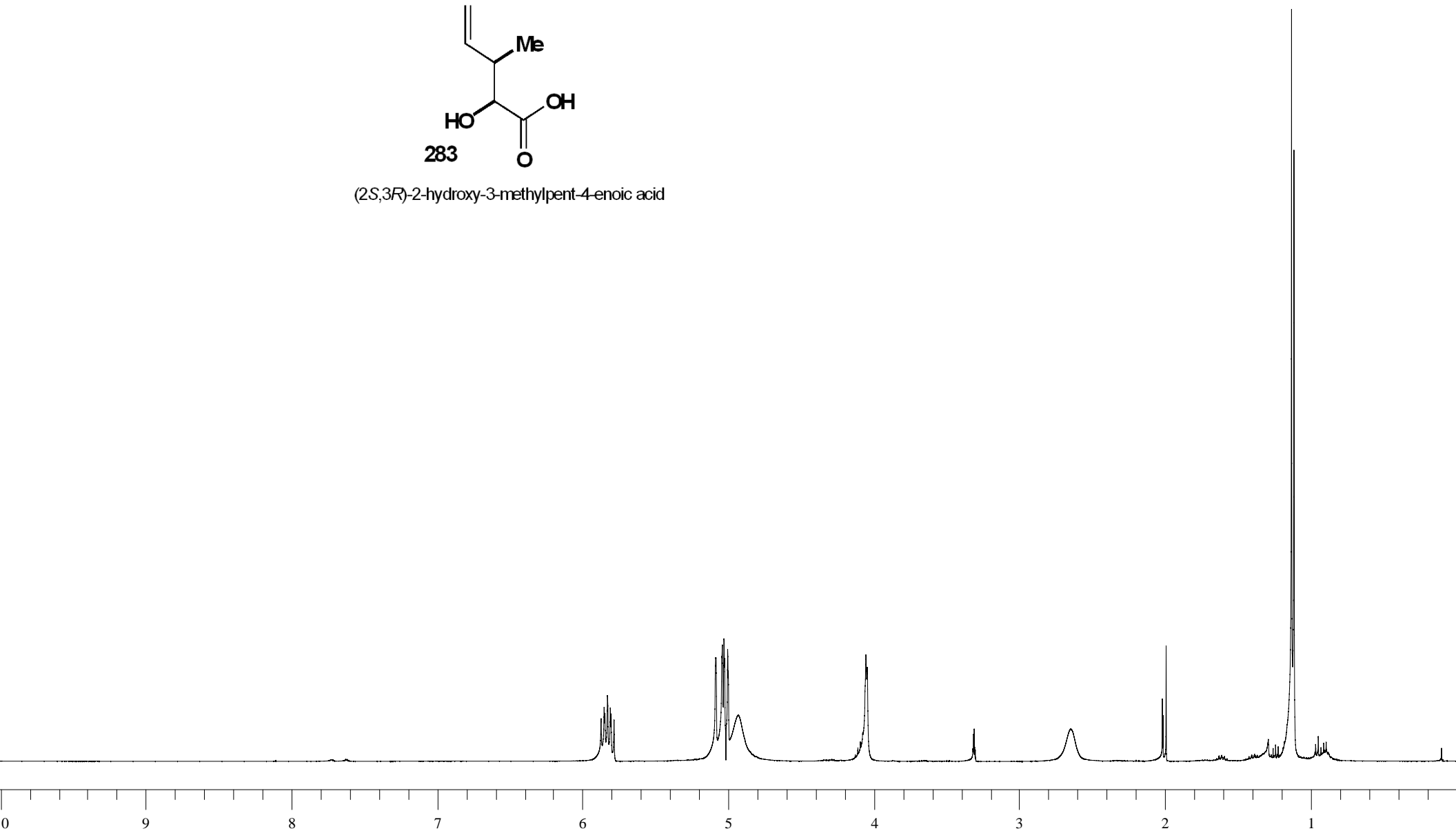


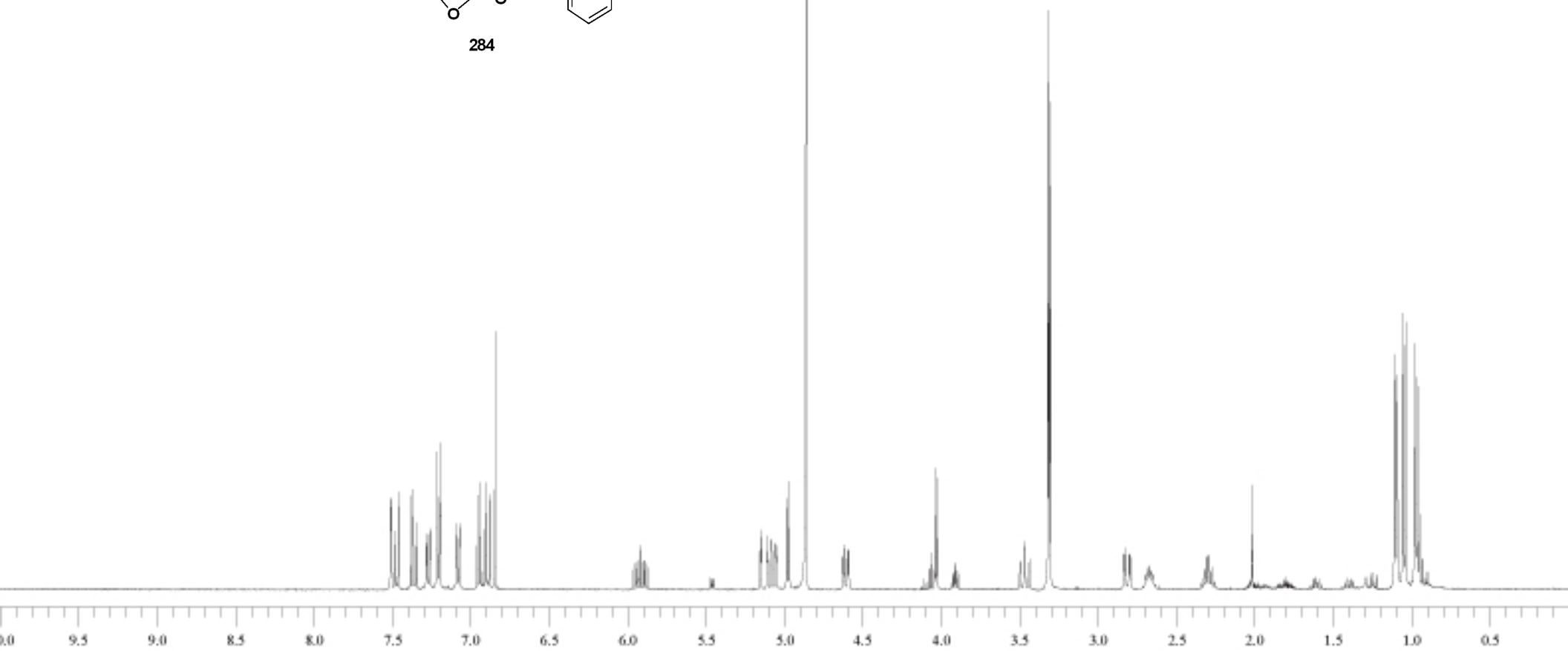
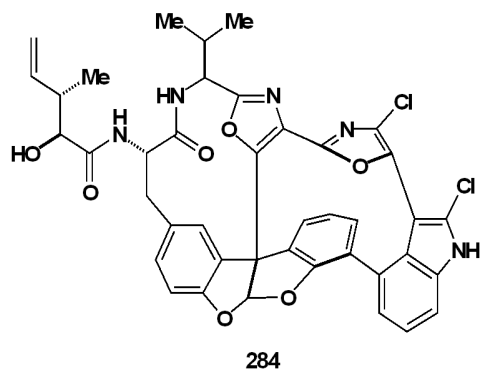
(2S,3S)-2-hydroxy-3-methylpent-4-enoic acid

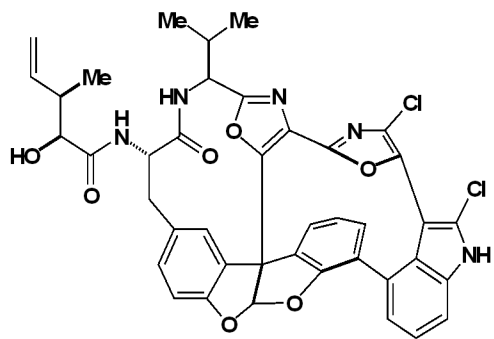




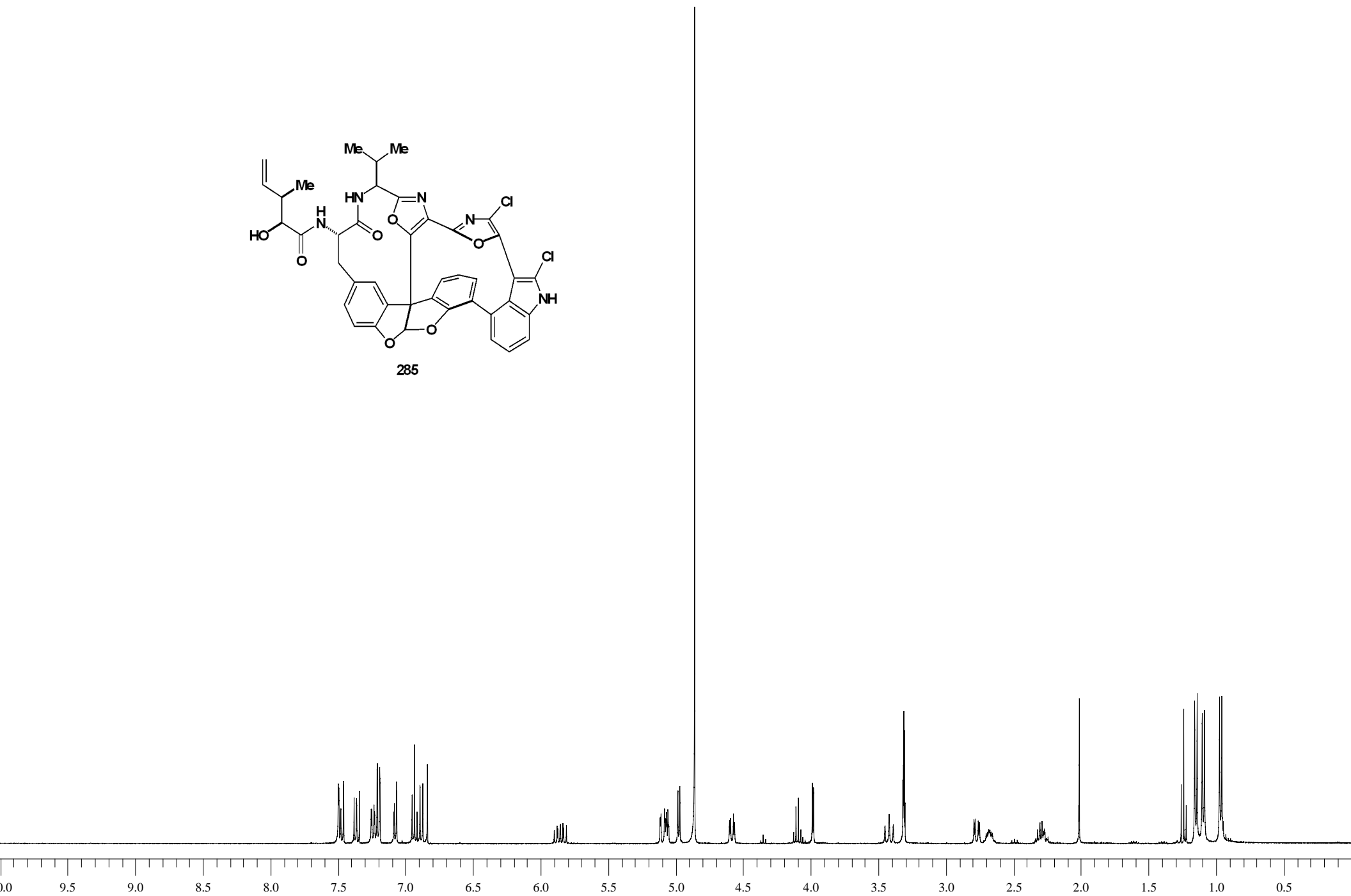
(2*S*,3*R*)-2-hydroxy-3-methylpent-4-enoic acid

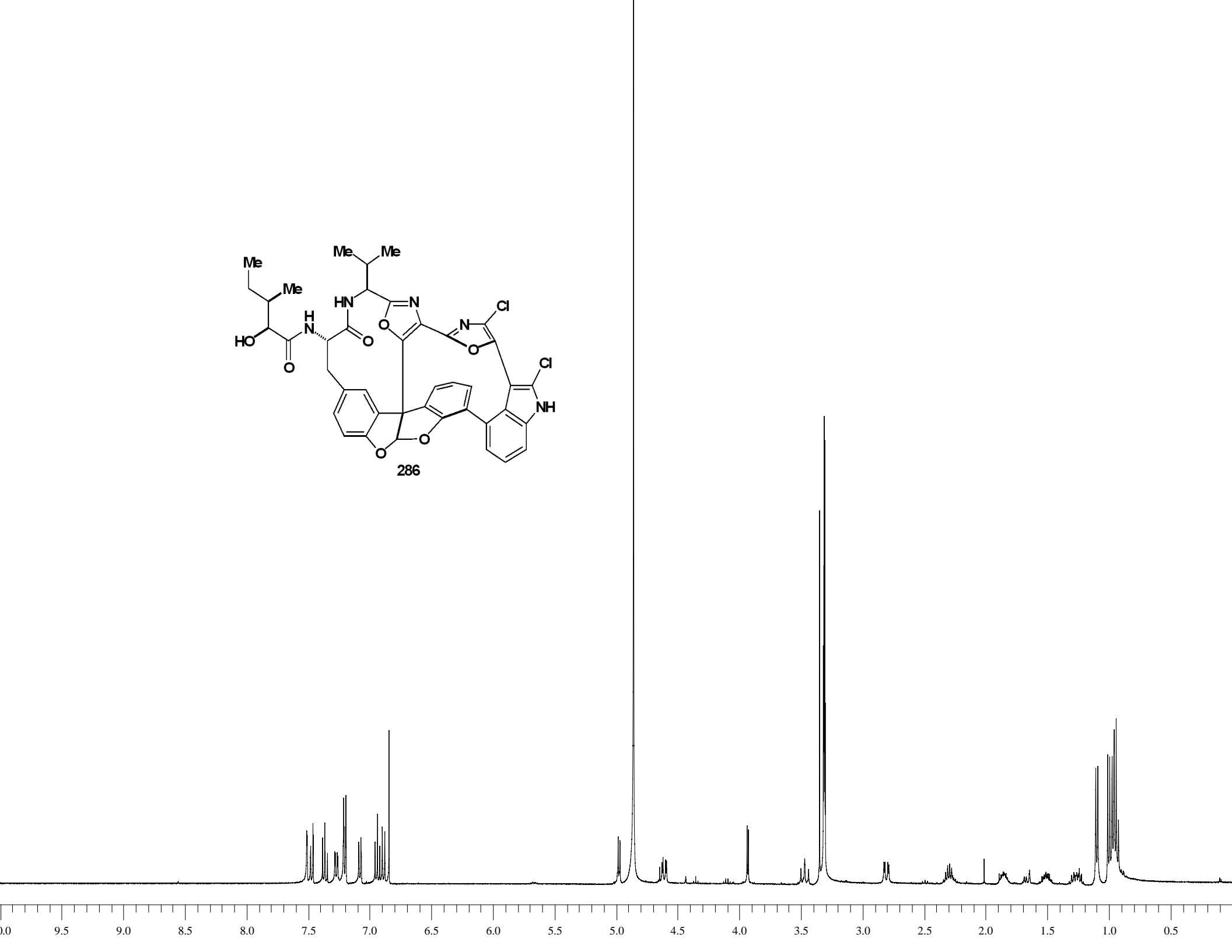
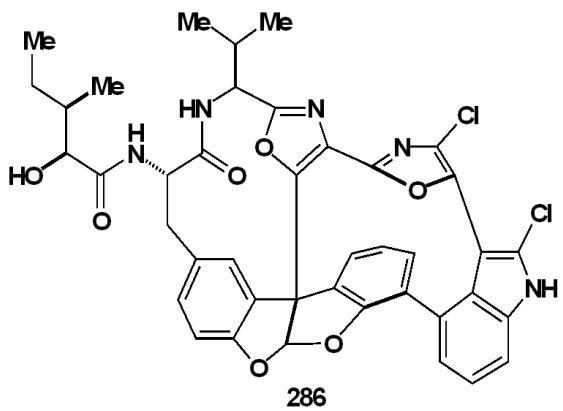


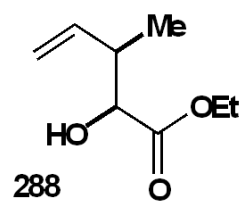




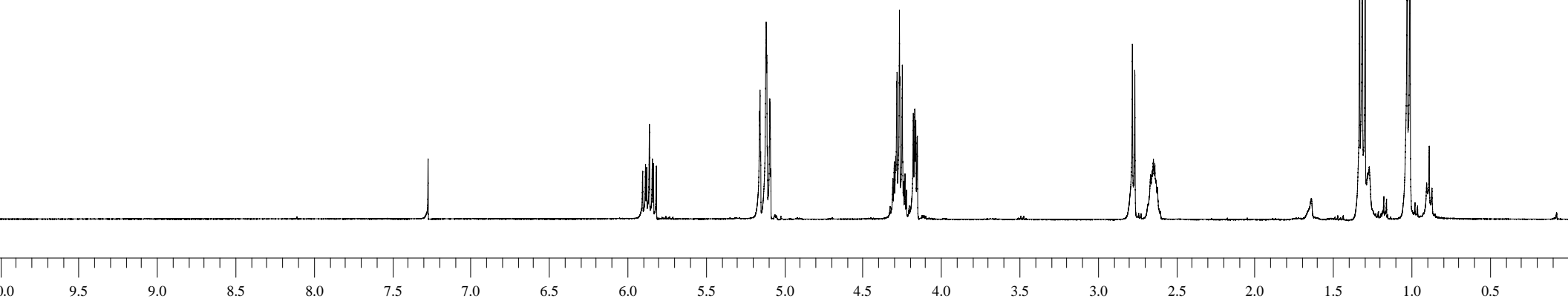
285



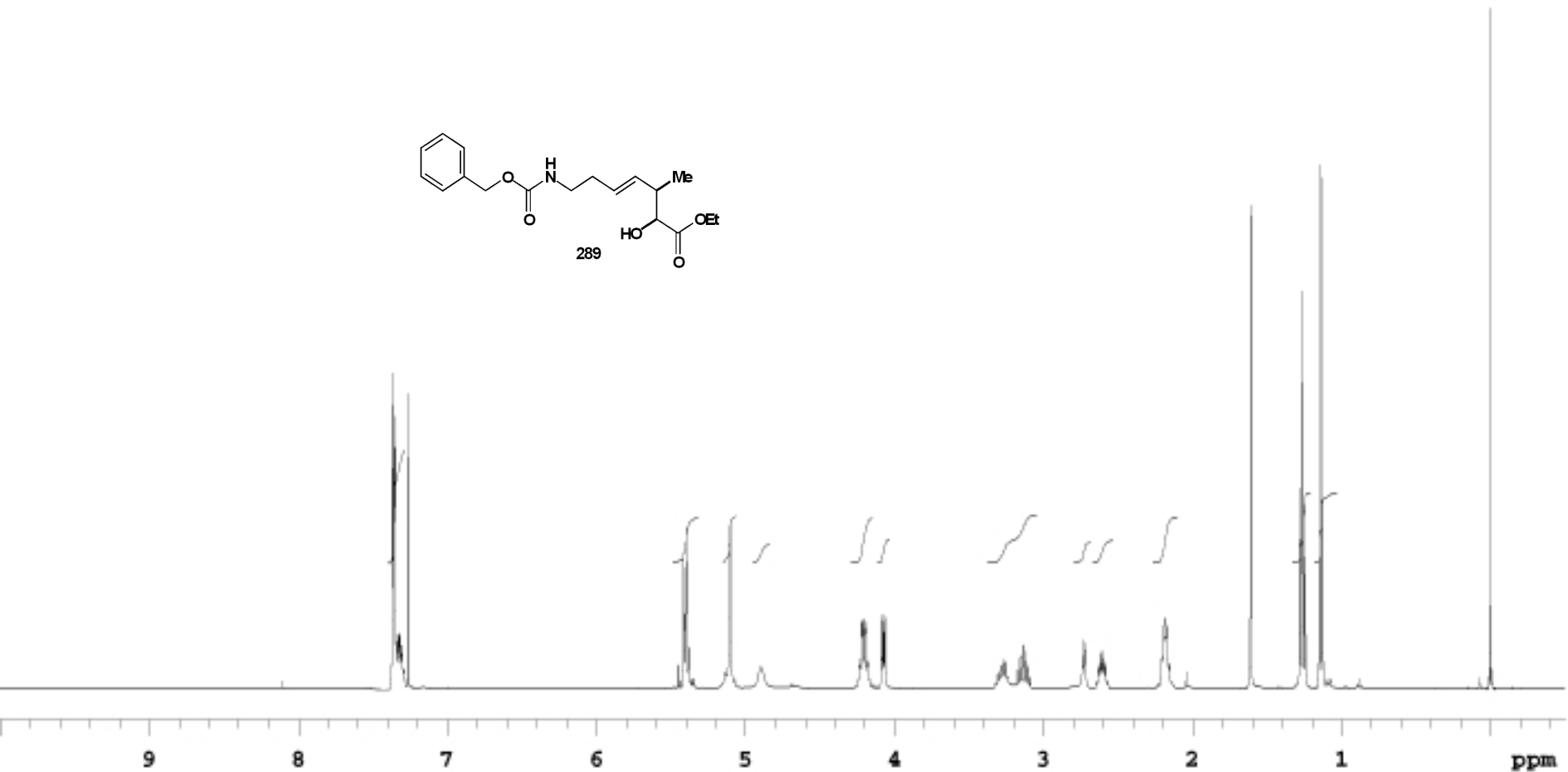
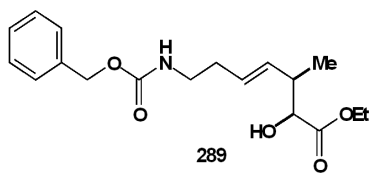




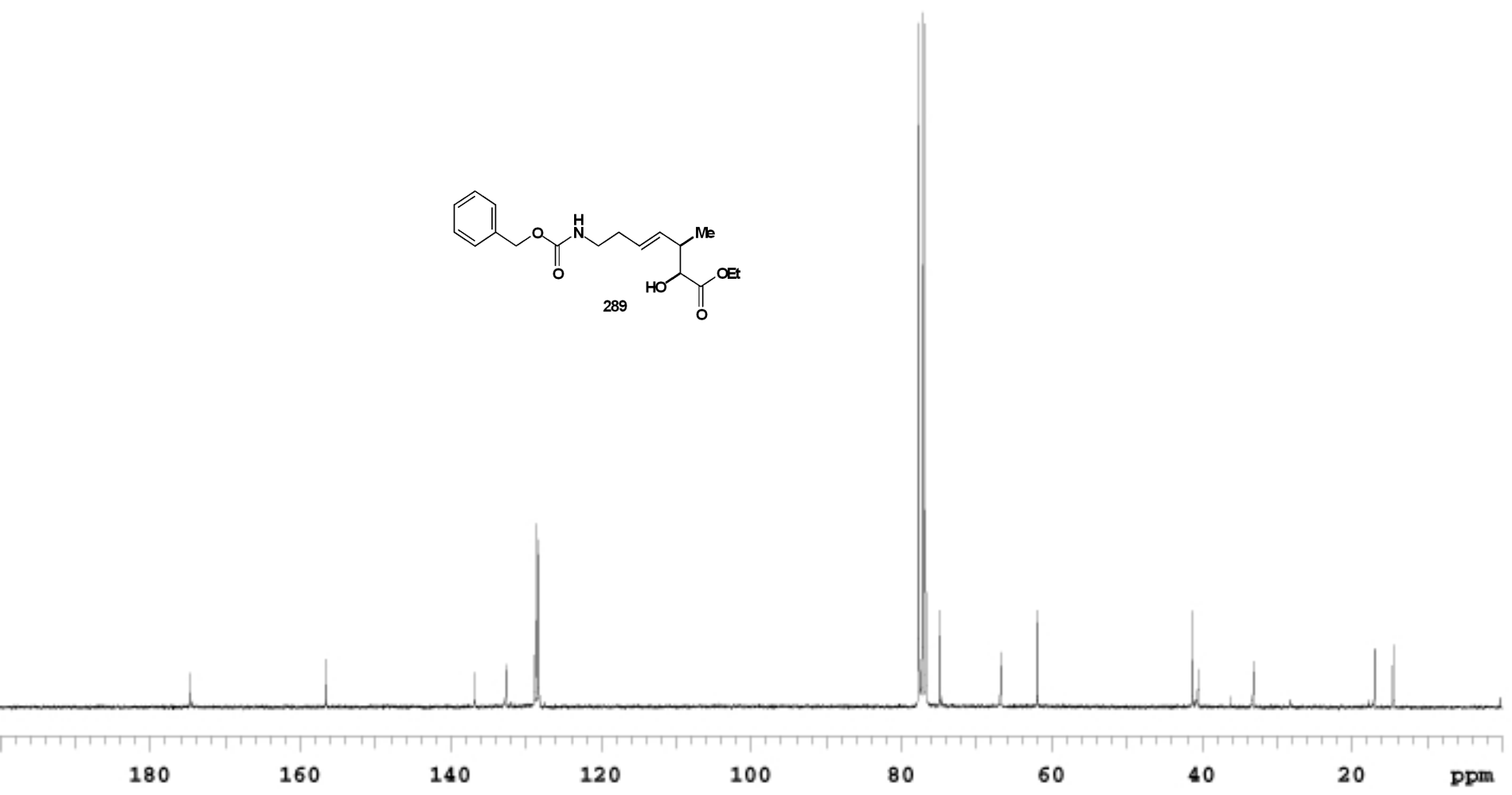
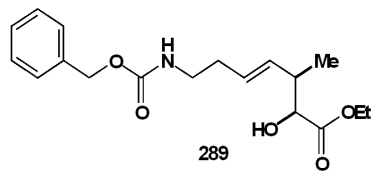
(2S,3R)-ethyl 2-hydroxy-3-methylpent-4-enoate



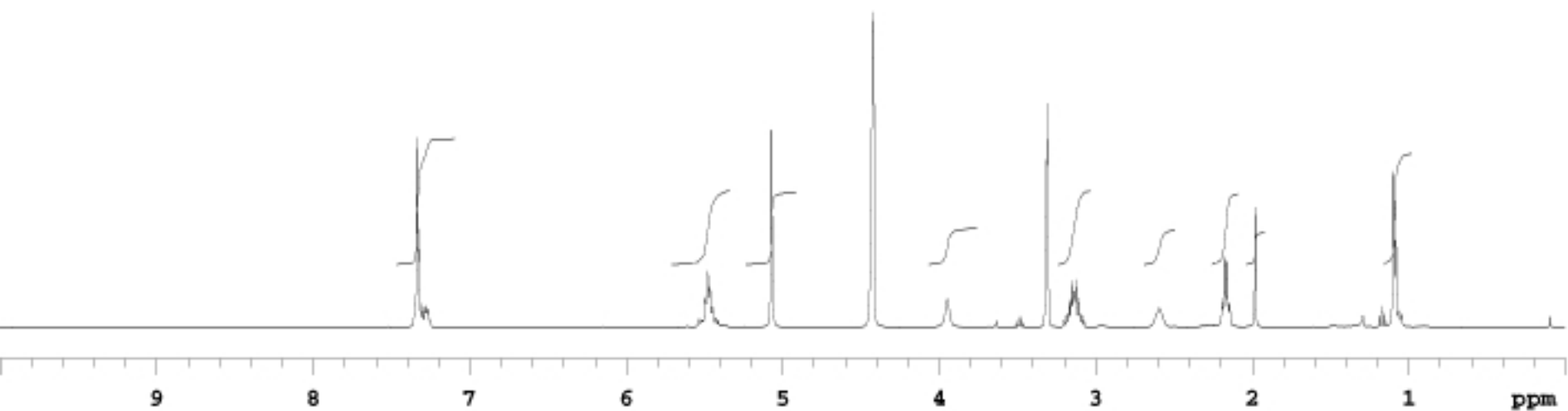
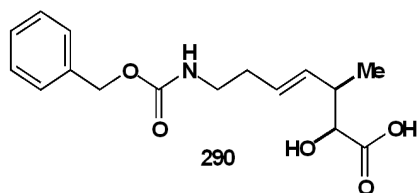
Pulse Sequence: s2pul



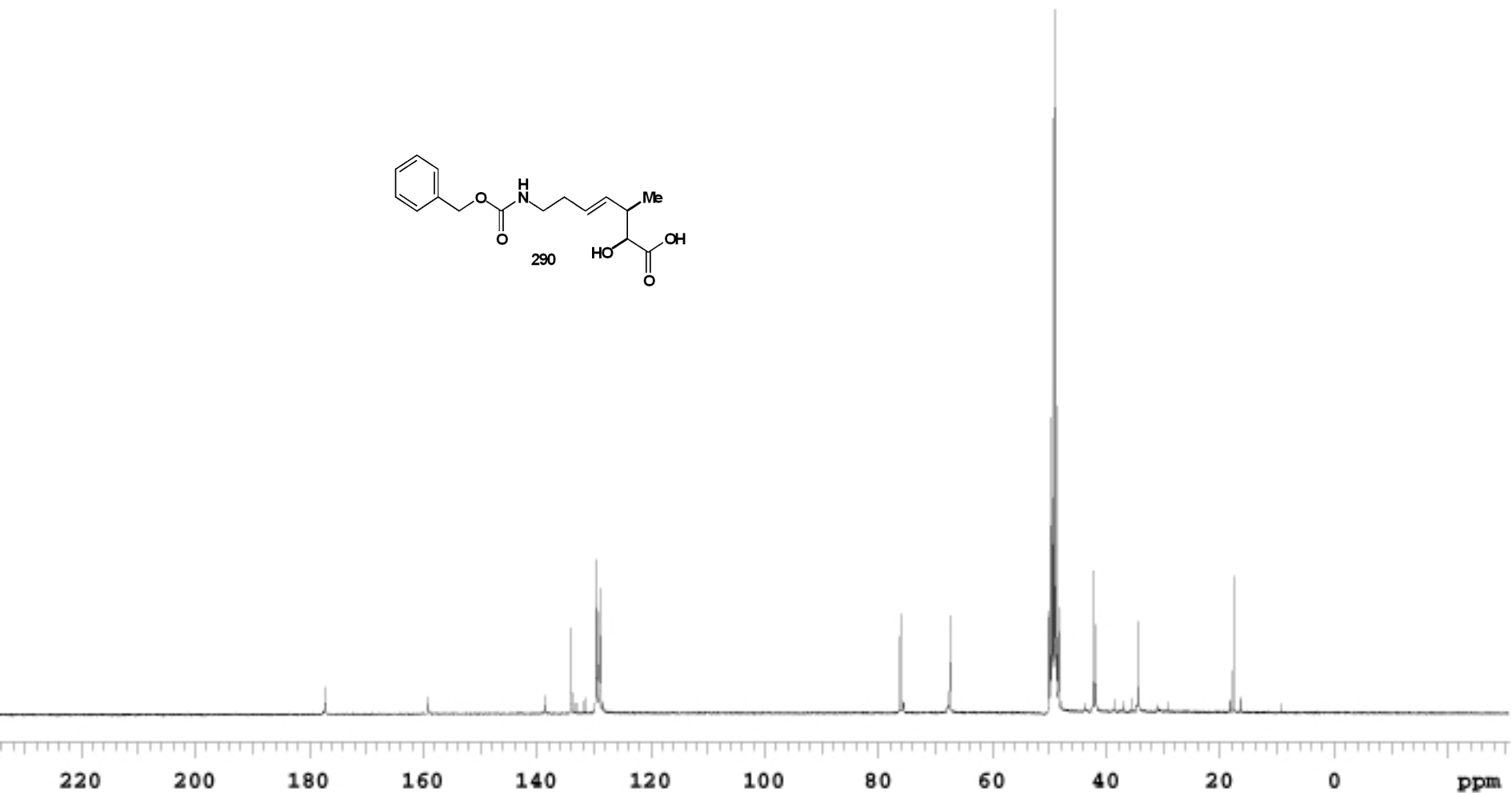
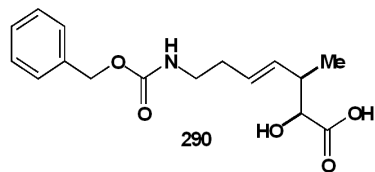
Pulse Sequence: s2pul



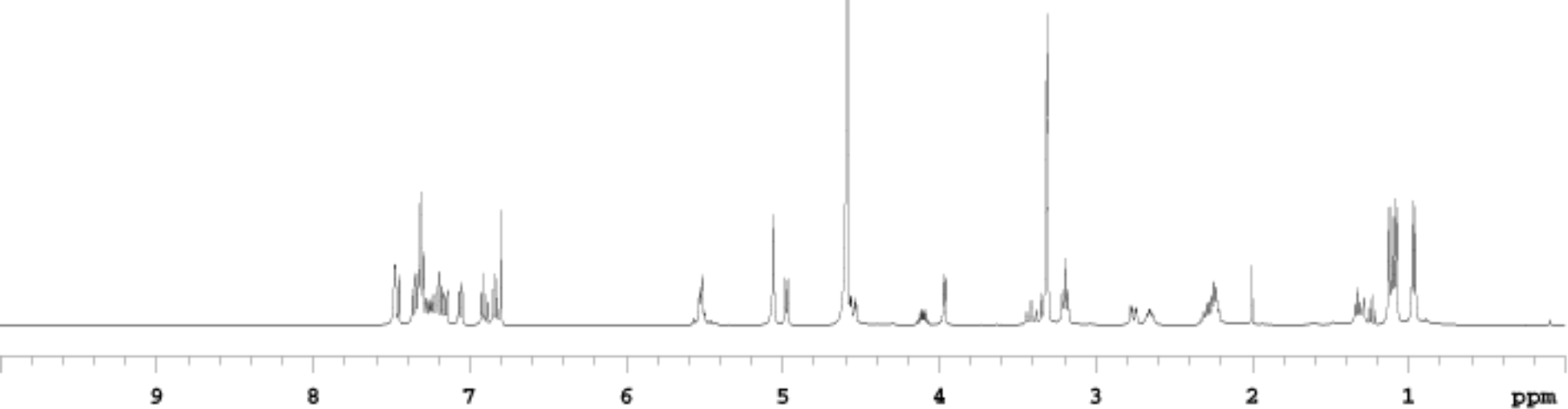
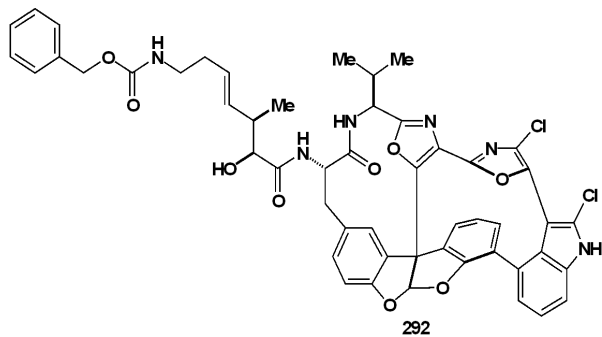
Pulse Sequence: s2pul



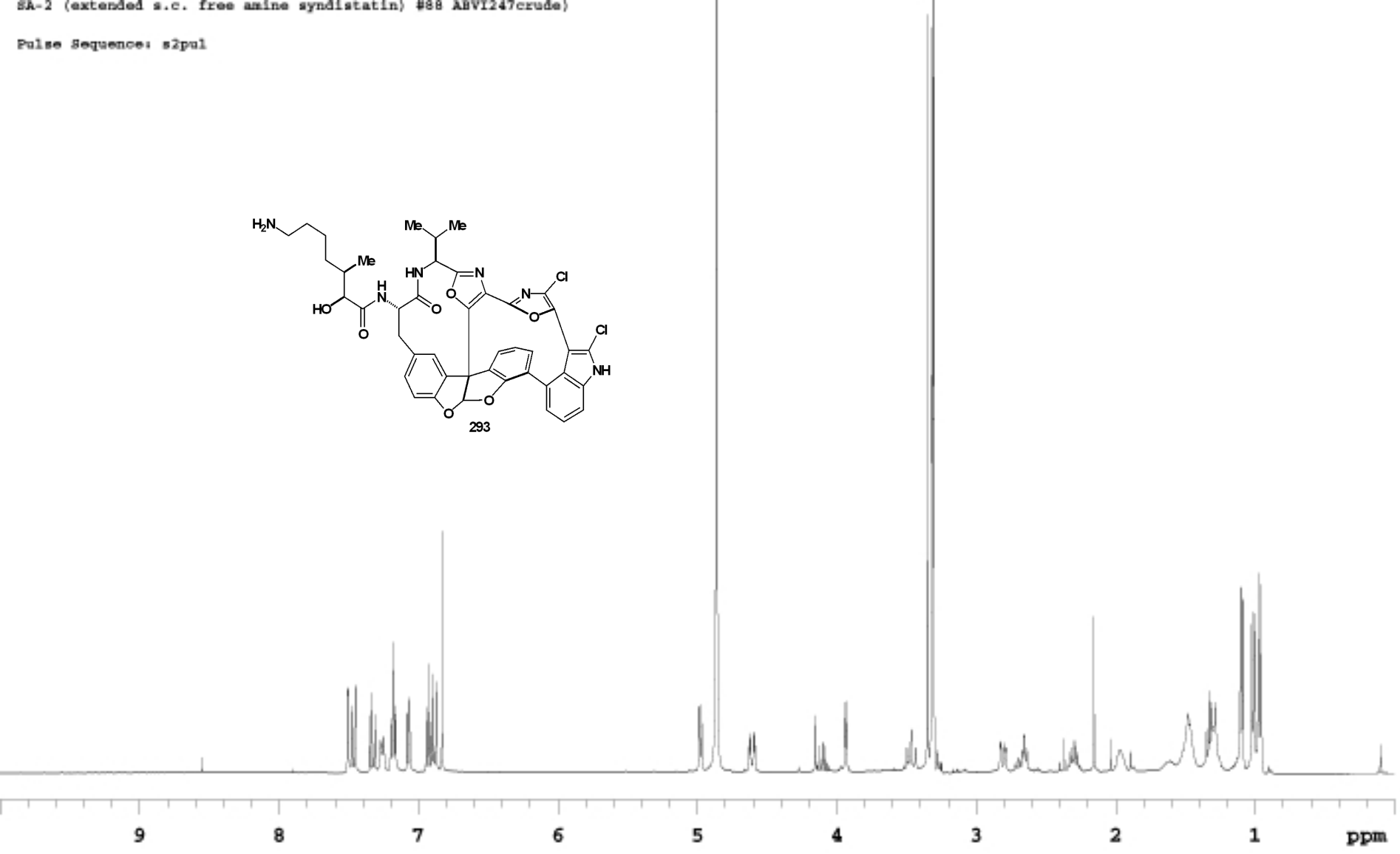
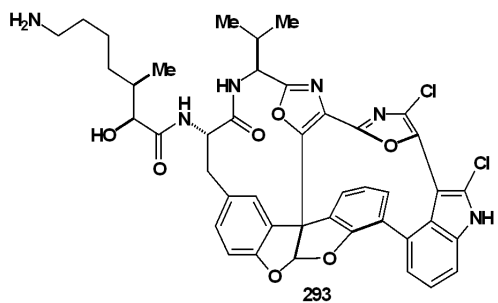
Pulse Sequence: s2pul

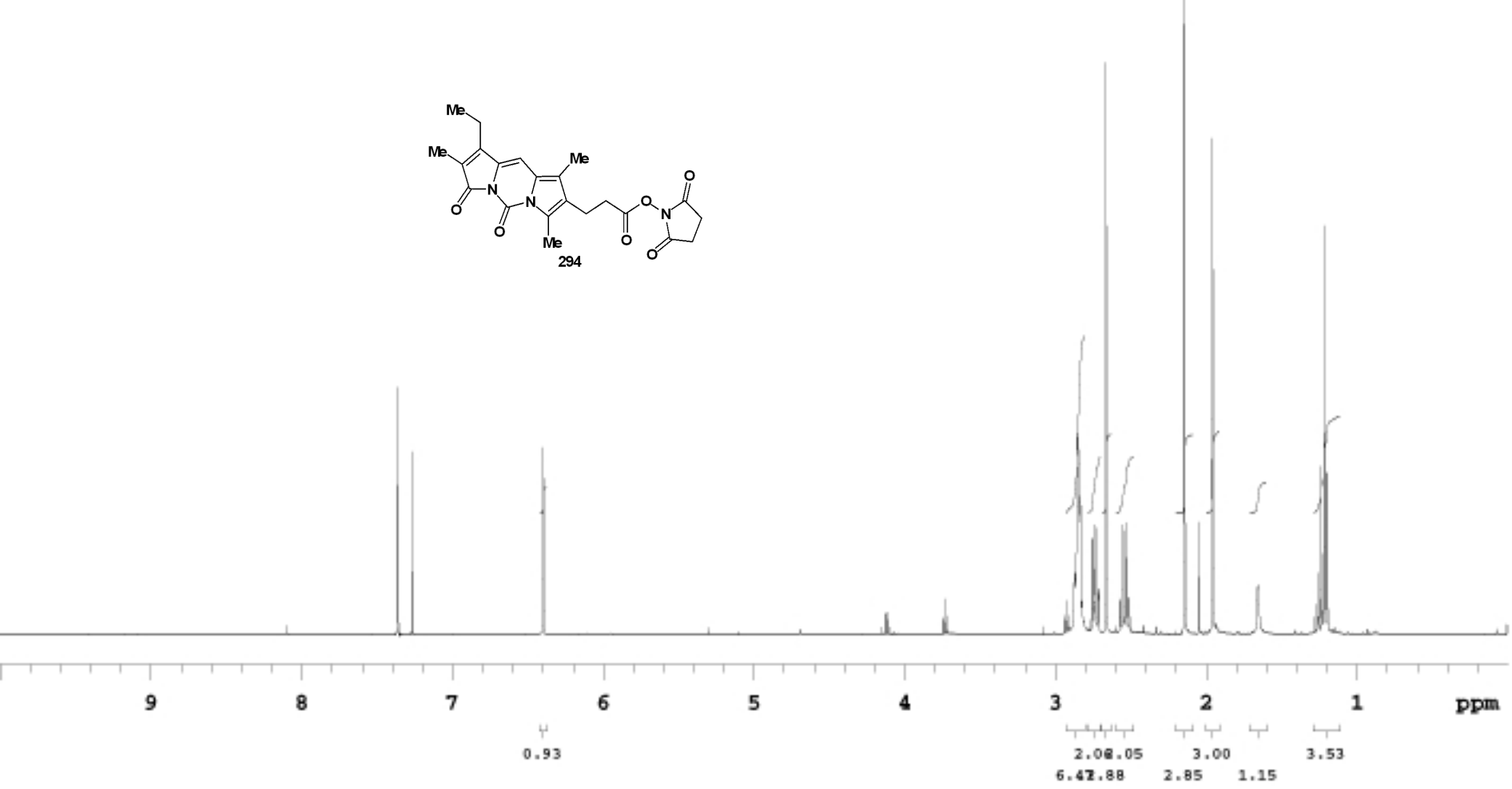
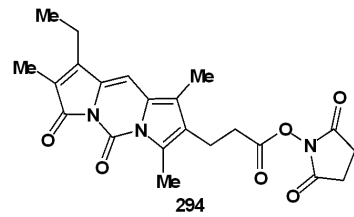


Pulse Sequence: s2pul

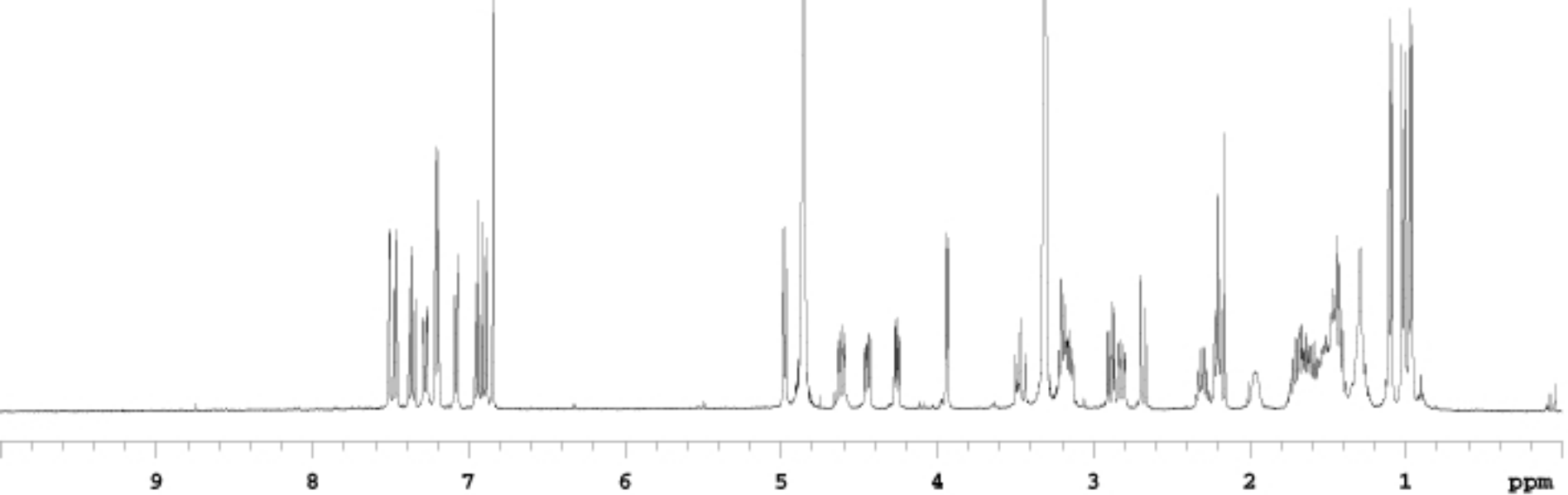
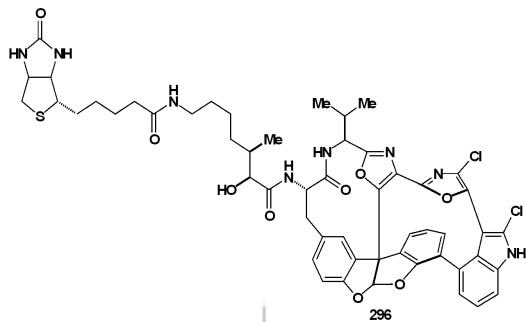


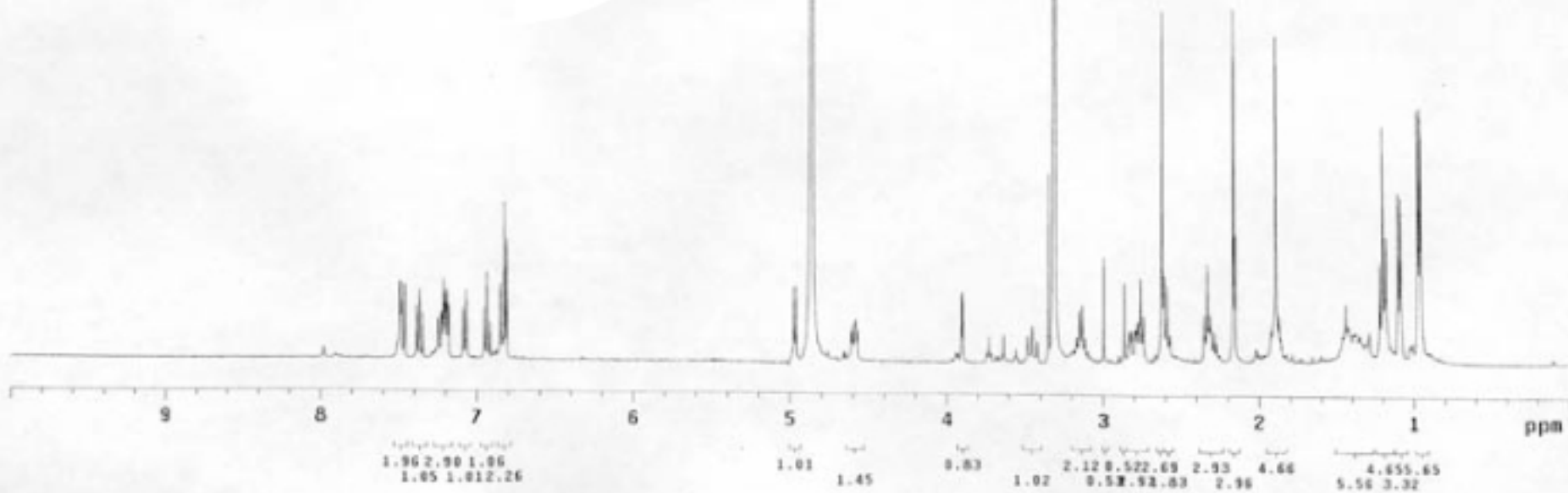
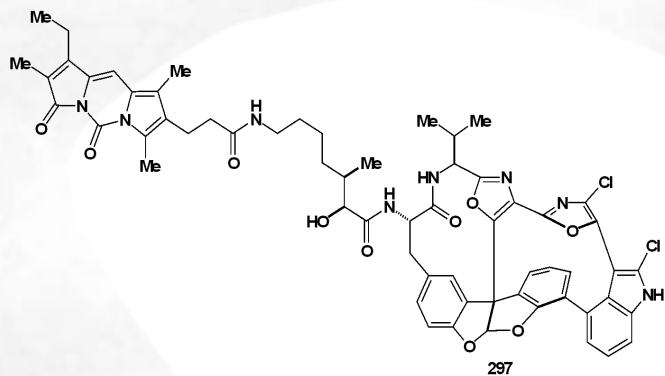
Pulse Sequence: s2pul



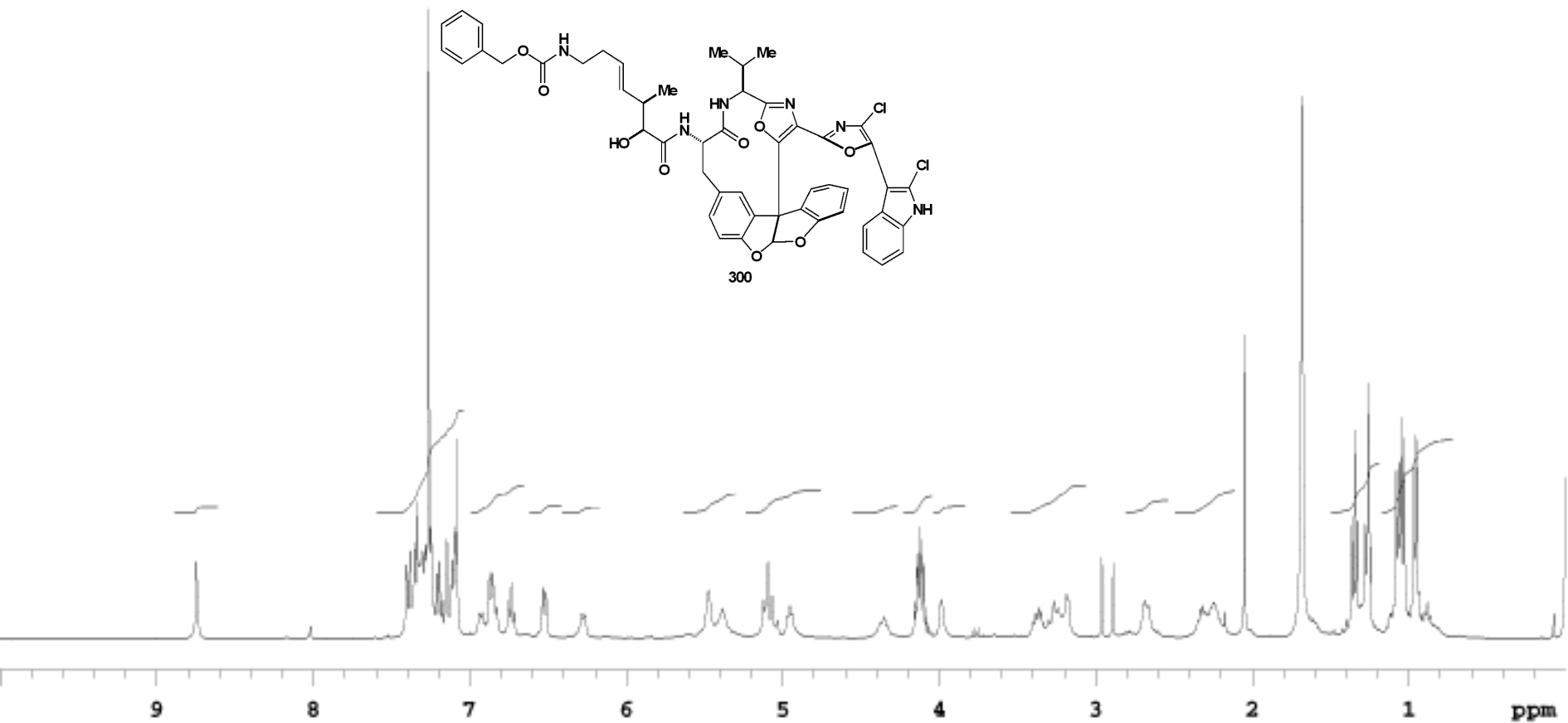


Pulse Sequence: s2pul

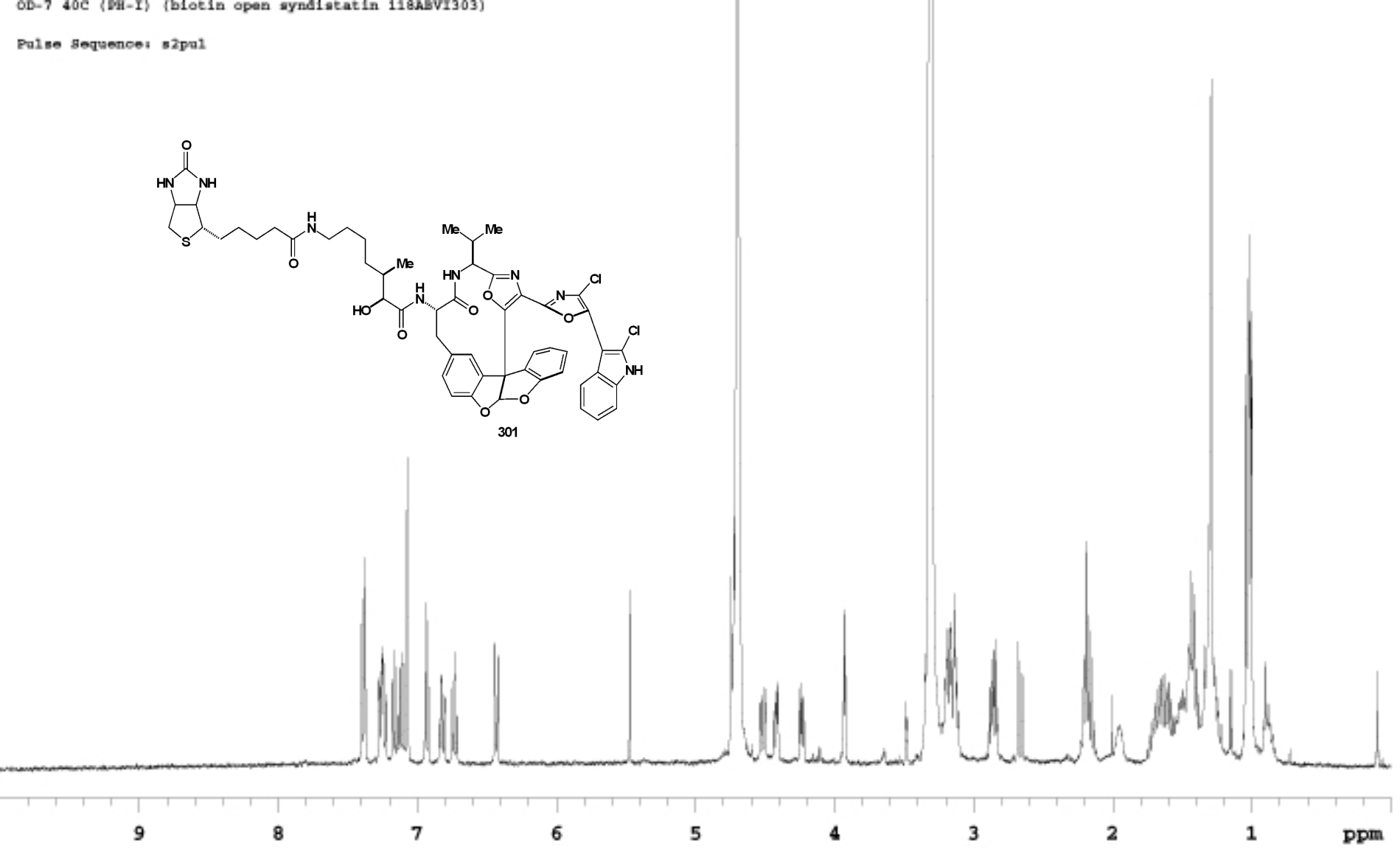
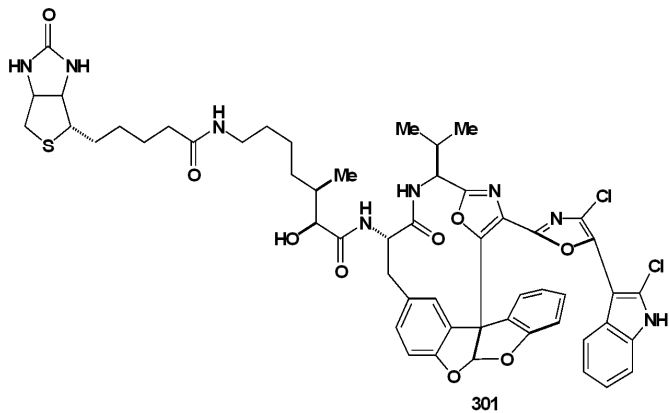




Pulse Sequence: s2pul



Pulse Sequence: s2pul



9

8

7

6

5

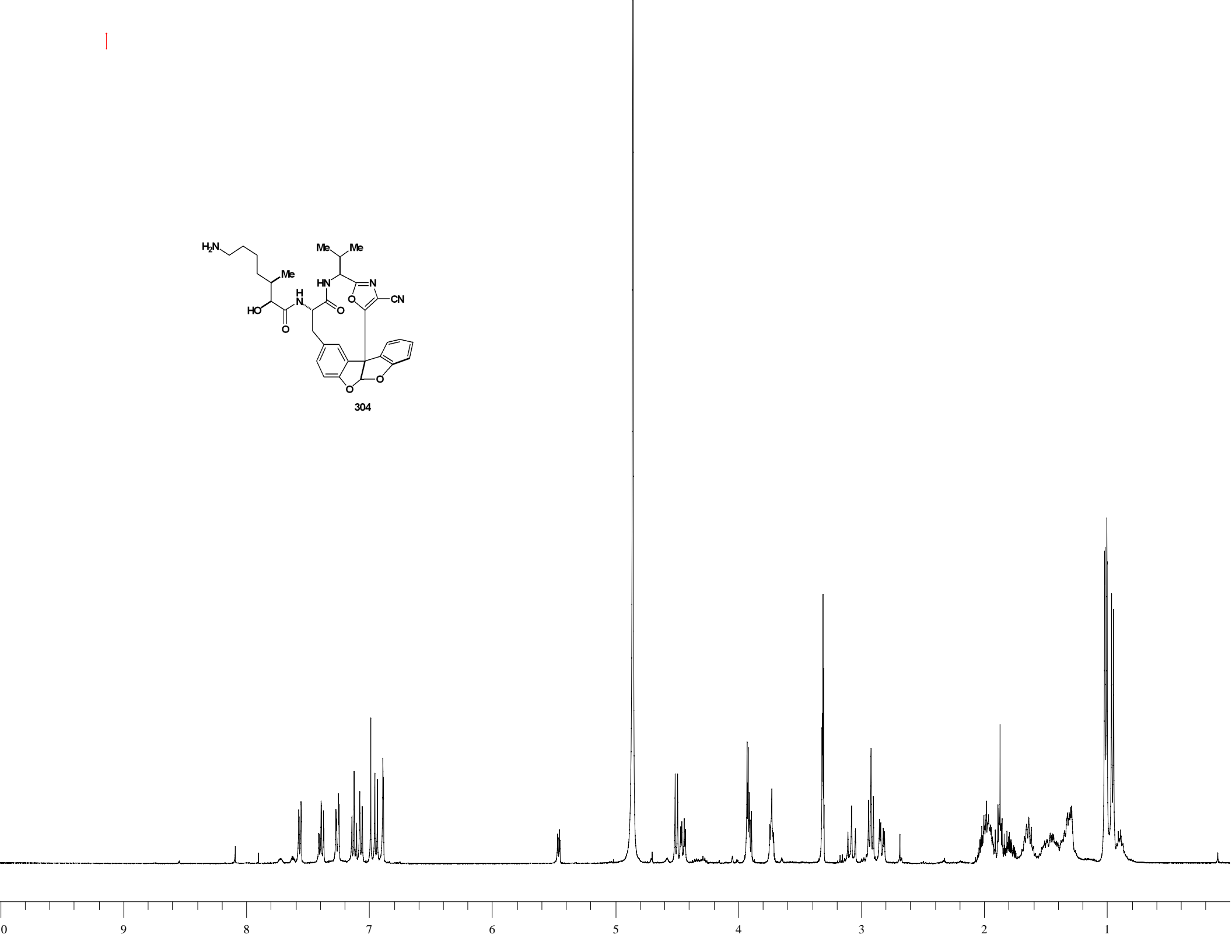
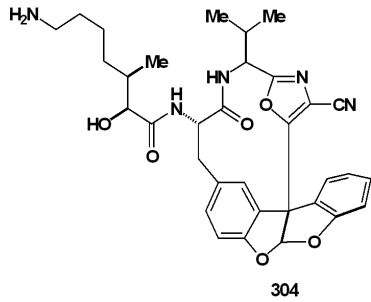
4

3

2

1

ppm

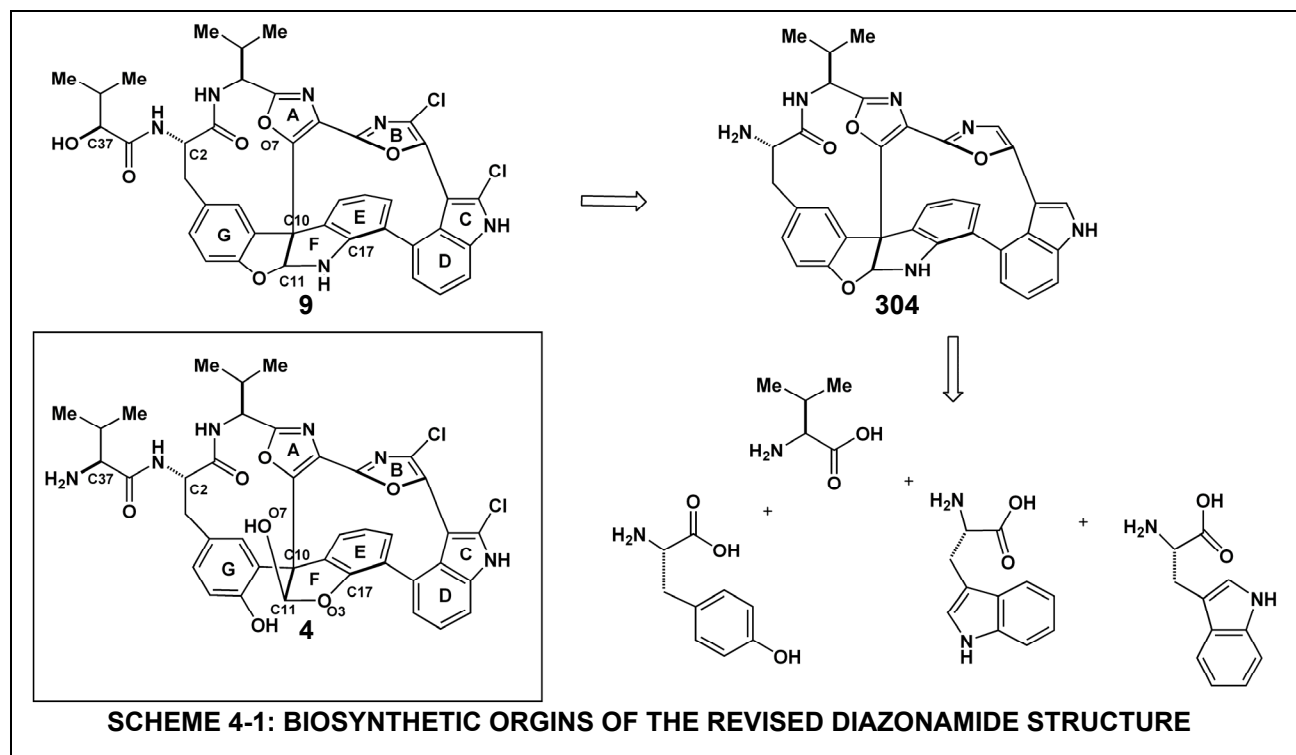


CHAPTER FOUR

Total Synthesis of Diazonamide A

4.1 Introduction

The total synthesis of diazonamide A outline below was both mandated and partially inspired by the structural revision of the molecule. The revelation that diazonamide A had been misassigned obviously presented a new target for total synthesis, but it also revealed a clearer understanding of the biosynthetic origins of the molecule. One of the most interesting aspects of the original Fenical diazonamide A (**4**) structure was its lack of clear biosynthetic origins (Section 1.5).⁷ However, there is no mystery concerning the constituency of the corrected diazonamide A structure. The diazonamide core (**304**) is composed of four oxidatively cross-linked, proteinogenic amino acids.⁴⁹ Other than clarifying the biosynthetic origins of the molecule, the structural revision presented fairly minor changes to the overall structure,



especially to the diazonamide core (**304**). The overall architecture and stereochemistry of the compound was not corrected, as is often the case with natural product misassignments. The oxygen congener for diazonamide A (**9**), syndistatin, was shown to possess identical biological activity as the natural product (**Chapter 2**). In fact, substituting the amine of the valine side chain for the hydroxyl of the (*S*)- α -hydroxy isovaleramide side chain is a simple operation that has no effect on the devised synthetic strategies. However, the re-assignment of the benzofuran oxygen (O3, **4**) with the amine of the revised structure **9** irrevocably changes the identity of the molecule as a synthetic target and radically casts aside the previous synthetic approaches.

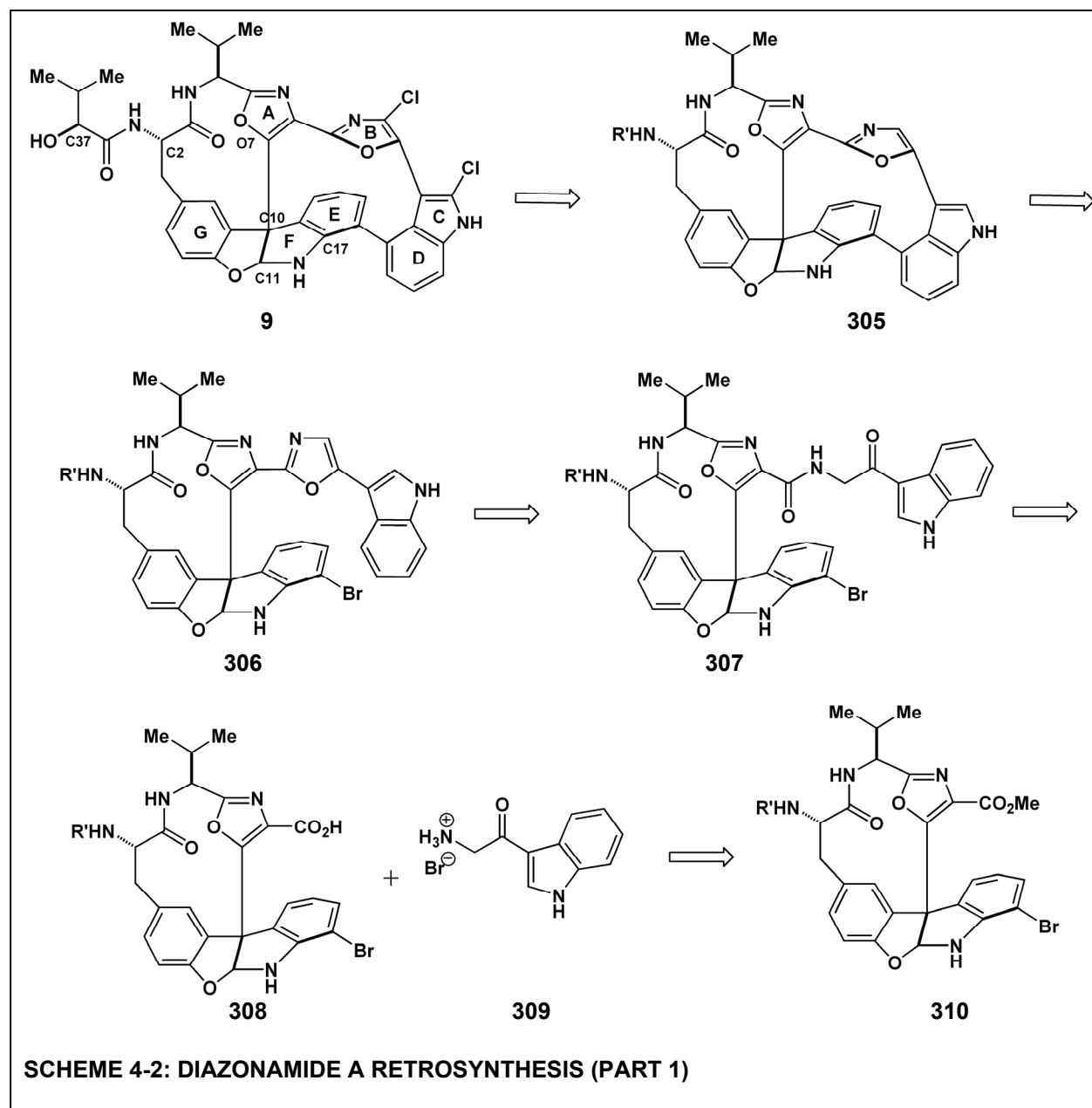
A new design had to be formulated to pursue the total synthesis of the revised diazonamide A structure. Following the perceived biosynthetic origins inherent in the revised diazonamide A structure, it was resolved to attempt construction of the diazonamide core through the oxidative restructuring of a peptide-derived substrate. This successful approach, in combination with the modification and use of previous diazonamide methodologies developed by the Harran group, allowed for the total synthesis of diazonamide A.

4.2 Retrosynthesis

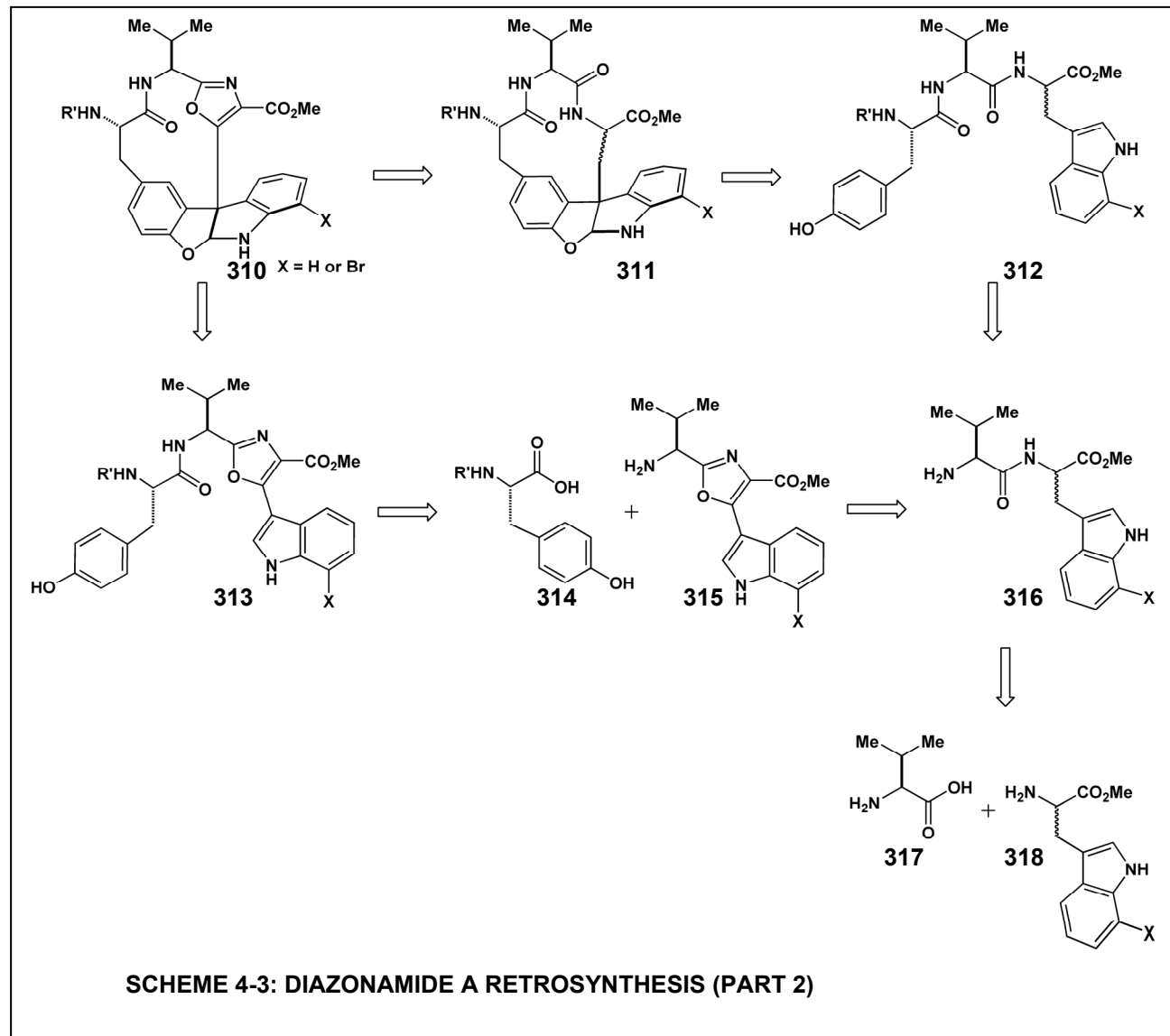
The devised approach was shaped by two overarching themes. The first was to access the diazonamide C10 core through the oxidation of a peptidyl derived structure. This idea arose from the obvious biosynthetic origins of the diazonamide core (**Scheme 4-1, 304**). The second feature that guided the synthetic design was the previous, successful, work undertaken by the Harran group in the total synthesis of Fenical's original diazonamide A structure (**Section 1.2.3.11**). As described, there are two major challenges in the diazonamide A total synthesis (**Section 1.2.2**): the C10 quaternary carbon center and the formation of the C16-C18 biaryl bond. This design seeks to use a biosynthetically inspired approach to the C10 center containing macrocycle. Then,

the formation of the C16-C18 bond would be performed using the successful photochemistry established in the Harran group.

The proposed retrosynthesis begins with removal of the side chain and peripheral chlorines, yielding the diazonamide core **305**. Guided by the Harran group's previous diazonamide A synthesis, the diazonamide core **305** is transformed to acyclic bromoarene variant



306 through scission of the C16-C18 biaryl bond. In a forward direction, this critical bond would be formed using the photochemistry developed previously in a very similar structural context by the Harran group. Excision of the B-C-D-ring component from **306** produces macrocycle **310**. The B-C-D rings would be introduced from coupling of **310** to a ketotryptamine component followed by oxidative oxazole formation. The critical macrocycle **310** is deconstructed directly into oxazole **313** or, in two steps, to tripeptide **312**. Oxazole **313** is broken down to a tyrosine component **314** and amine component **315**. **315** arises, through dipeptide **316**, from valine (**317**) and 7-bromotryptophan **318**.



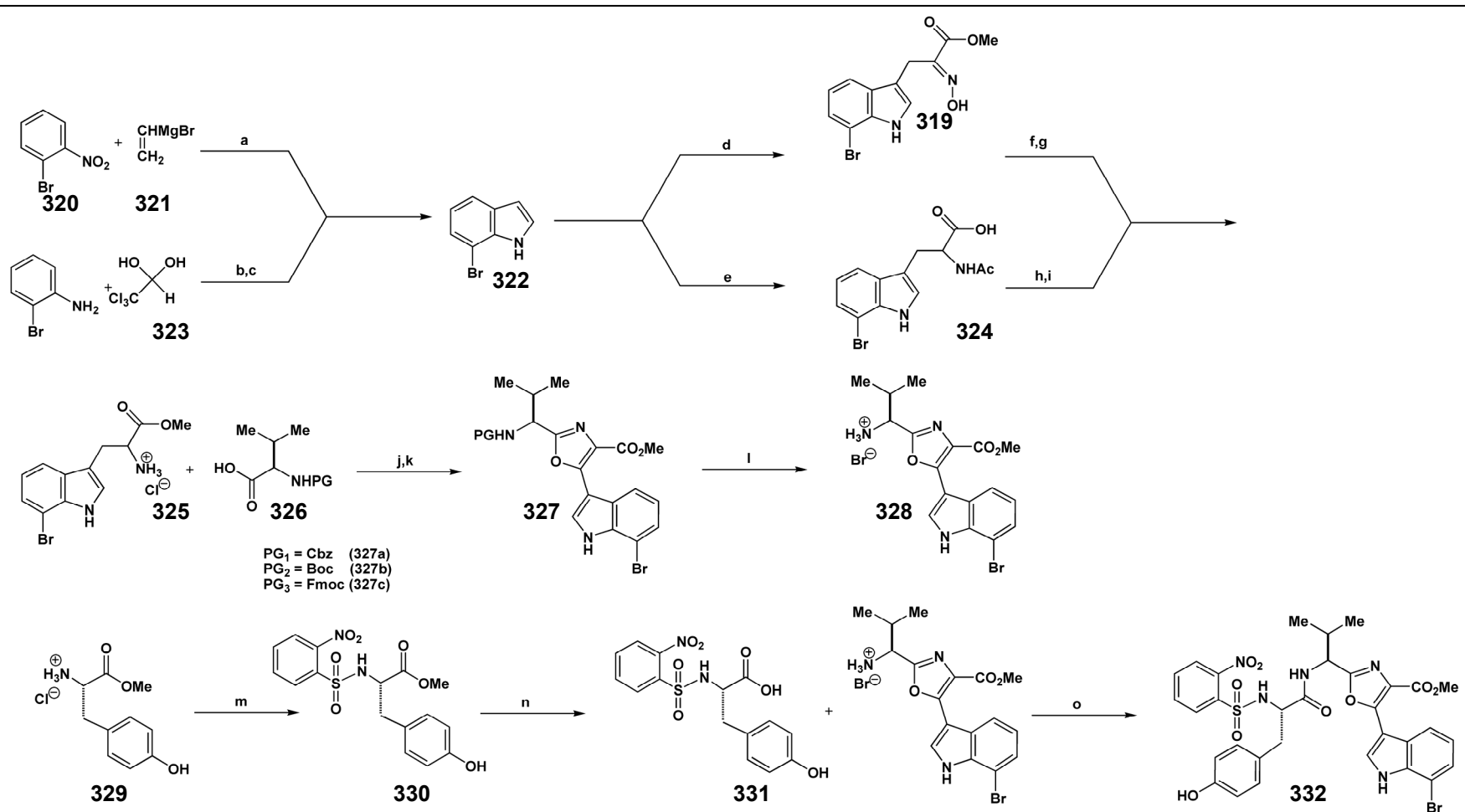
This synthetic design is highly convergent and utilizing simple and accessible building blocks. In a synthetic direction, macrocycle **310** arises from the amino acids tyrosine, valine, and tryptophan. The introduction of the remaining component of the diazonamide core, the BCD portion, from a peptidyl derived source means the entire molecule originates from amino acids.

4.3 Total Synthesis of Diazonamide A

4.3.1 Synthesis of Peptide Derived Oxidation Substrate

The synthesis commences (**Scheme 4-4**) with accessing 7-bromoindole **322** through either of two routes. The early efforts used a Bartoli indole synthesis⁹⁹ reaction with 1-bromo-2-nitrobenzene and vinyl magnesium bromide (**321**). A procedure more amenable to large scale production of **322** was the formation of 7-bromoisatin from chloral hydrate (**323**) and 2-bromoaniline, followed by reduction with LiAlH₄. Incorporation of the 7-bromoindole into 7-bromotryptophan was also accomplished through two methods. Oxime **319** was produced through a reaction with methyl-3-bromopyruvate oxime. Aluminum amalgam reduction and hydrochloride salt formation yielded racemic 7-bromotryptophan methyl ester hydrochloride **325**. **325** was also accessed through the reaction of 7-bromoindole with serine and acetic anhydride to give acetamide **324**. Deacetylation, followed by hydrochloride salt with TMSCl in MeOH produced **325**.

7-bromotryptophan methyl ester hydrochloride (**325**) was coupled with protected valine to give the dipeptide product as a mixture of diastereomers (94%). The dipeptide was subjected to four-electron Yonemitsu oxidation¹⁰⁰ to produce oxazolyl indole product **327** (66%). Cbz-, Fmoc-, and Boc-protected valine were all explored in the development of the synthesis (**327a**, **327b**, **327c**), and Cbz-valine was found to be superior and used in large scale production.



a) aq. NH₄Cl, THF, -40 °C (43%) b) i) NH₂OH(HCl), HCl, Na₂SO₄, H₂O ii) H₂SO₄, 85 °C, 10 min c) LiAlH₄ (66%) d) L-serine, Ac₂O, AcOH 75 °C, 2 h, (65%) e) methyl-3-bromopyruvate oxime, Na₂CO₃, CH₂Cl₂ (54%, 87% borsm) f) Al, 2% aq. HgCl₂, THF/H₂O 4 °C g) HCl, ether (58% two steps) h) aq. HBr, microwave 150 °C, 5 min (90%) i) TMSCl, MeOH, 80 °C, 1.5 h (95%) j) TBTU, DIPEA, DMF, 4 °C, 2 h, (94%) k) DDQ, THF 75 °C, 13 h (66%) l) 33% HBr/AcOH, 30 min, (90%) m) 2-nitrobenzene sulfonyl chloride CH₂Cl₂/phosphate buffer pH 9.0, 4.5 h, (67%) n) KOH, H₂O/EtOH, 2h, (86%) o) TBTU, DIPEA, DMF, 0 °C, 4 h (91%)

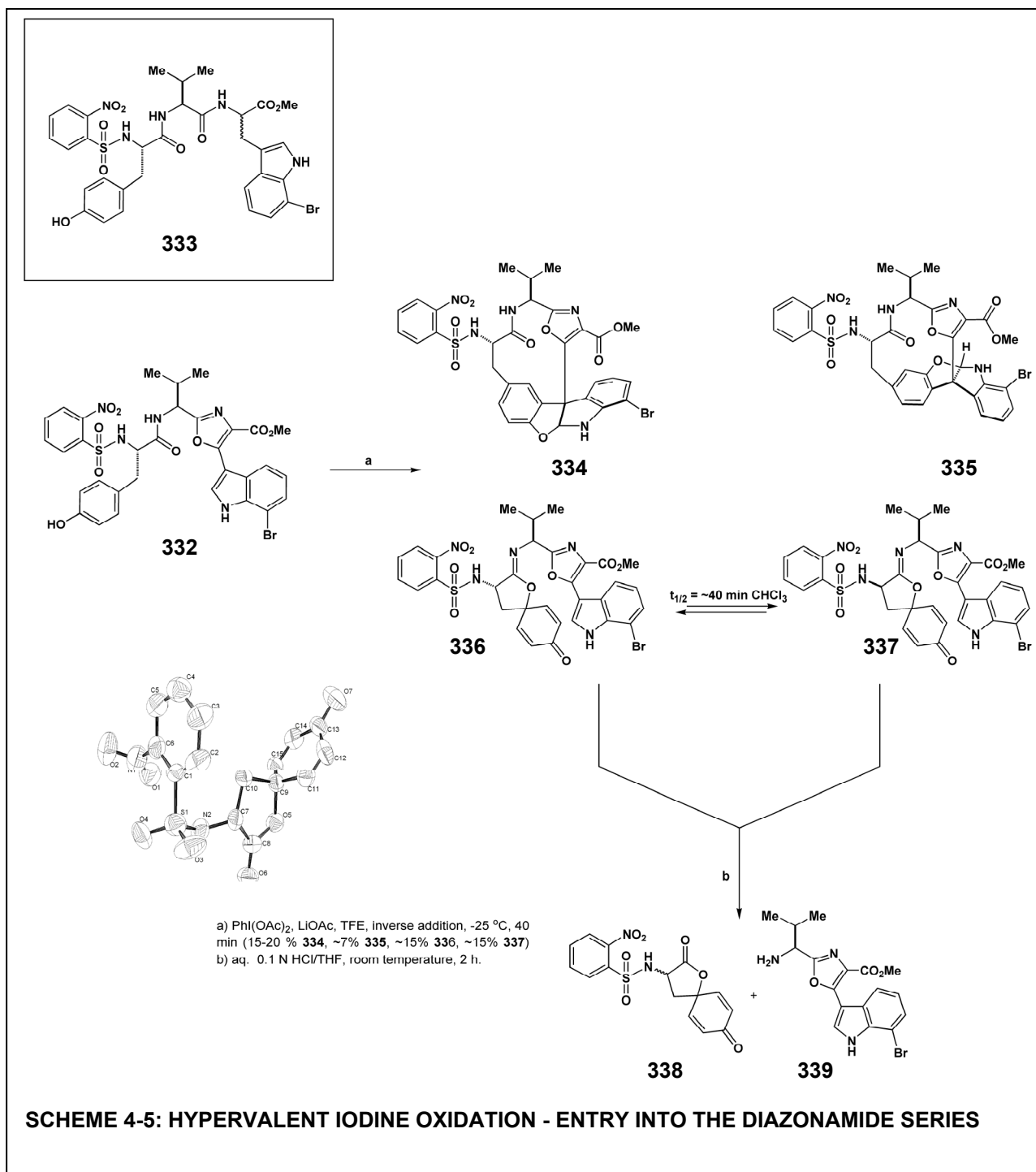
SCHEME 4-4: SYNTHESIS OF TRIPEPTIDE OXIDATION SUBSTRATE

Degradation of the carbamate protecting group with HBr/AcOH produced the dipeptide hydrobromide salt **328** (90%). Fukuyama's *o*-nitrophenylsulfonamide (Nos) protecting group¹⁰¹ was selected as the tyrosine amine protecting group. The oxidation reactions envisioned forming the diazonamide core included phenolic oxidation reactions, and this motivated the selection of the Nos protecting group since literature precedent had shown it did not interfere in such oxidation reactions¹⁰². Nos-protected tyrosine (**331**) was produced in two steps from commercial L-tyrosine methyl ester hydrochloride. The peptide coupling reaction between **331** and **328** to form **332** was explored using various methods, but the TBTU reaction (91%) offered the best combination of yield and cost efficiency.

4.3.2 Formation of the Diazonamide C10 Macrocycle Via a Hypervalent Iodine Oxidation Reaction

The critical transformation in this synthesis is the formation of the diazonamide C10 macrocycle through oxidation of substrate **332**. A mixture of diastereomers of tripeptide **333** (Scheme 4-5) was initially subjected to hypervalent iodine oxidation in 2,2,2-trifluoroethanol (TFE), but this produced an intractable mixture of products with no desired compound evident. However treatment of the oxidized tripeptide **332** with iodobenzene diacetate in TFE with excess lithium acetate at -25 °C produces four major isolated products, including the desired macrocycle **334** in ~15 -20% yield. The undesired diastereomeric C10-(*R*), C11-(*S*) product **335** was also formed in ~8% yield, in addition to equal amounts (~15%) of the epimeric spirodienone imidates **336** and **337** (the epimeric assignment is not a definitive assignment). Innumerable other products were also formed in smaller amounts making a complete mass balance of the reaction impossible (~40% of the mass unaccounted). All of the isolated products (**334** – **337**) are likely

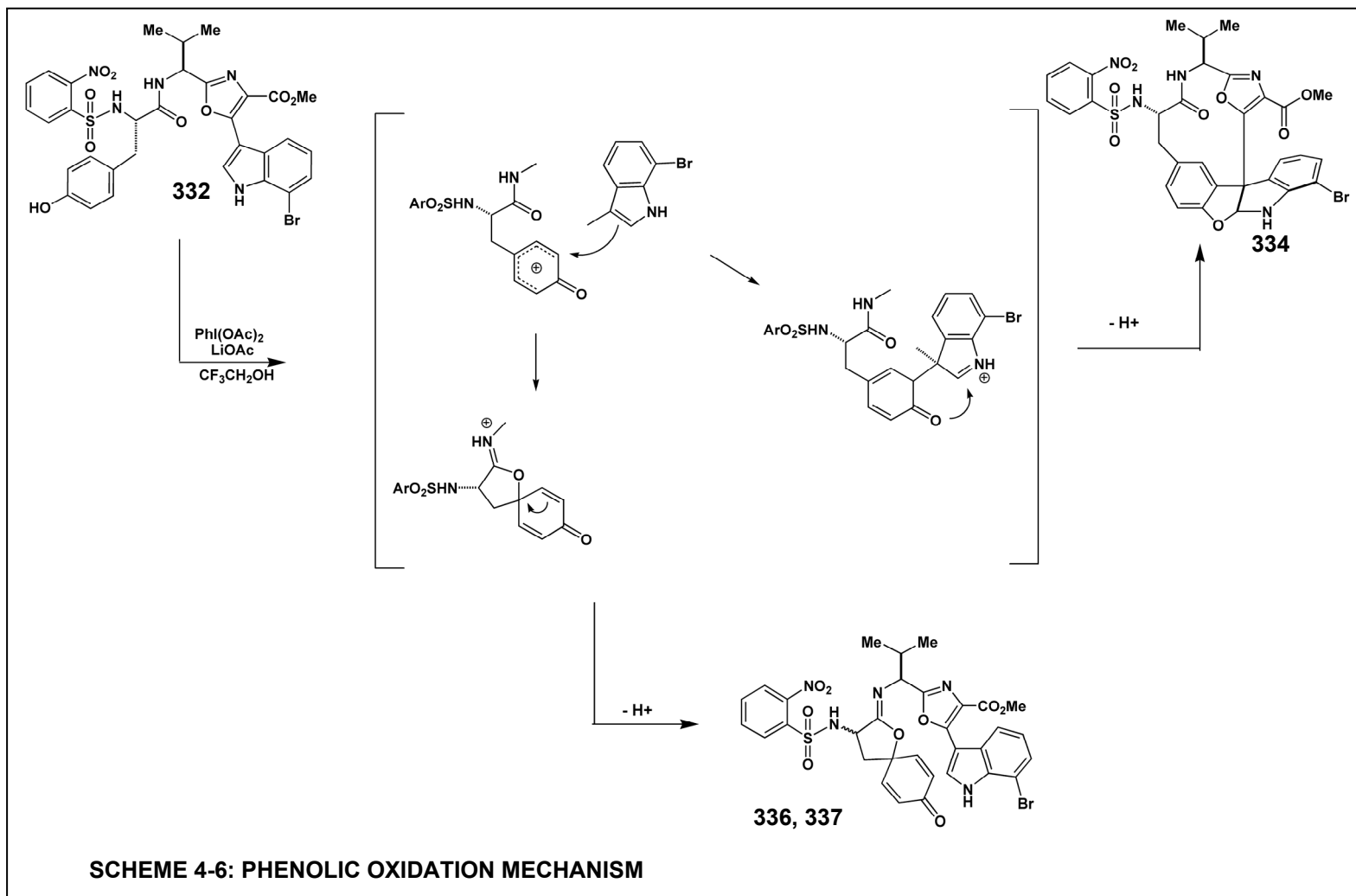
substrates for oxidation under the reaction conditions, and therefore any apparent selectivity observed in the reaction could not be truly representative of the ratio of products formed. The spriodienone imidates **336** and **337** rapidly interconvert with a half-life of ~40 min in

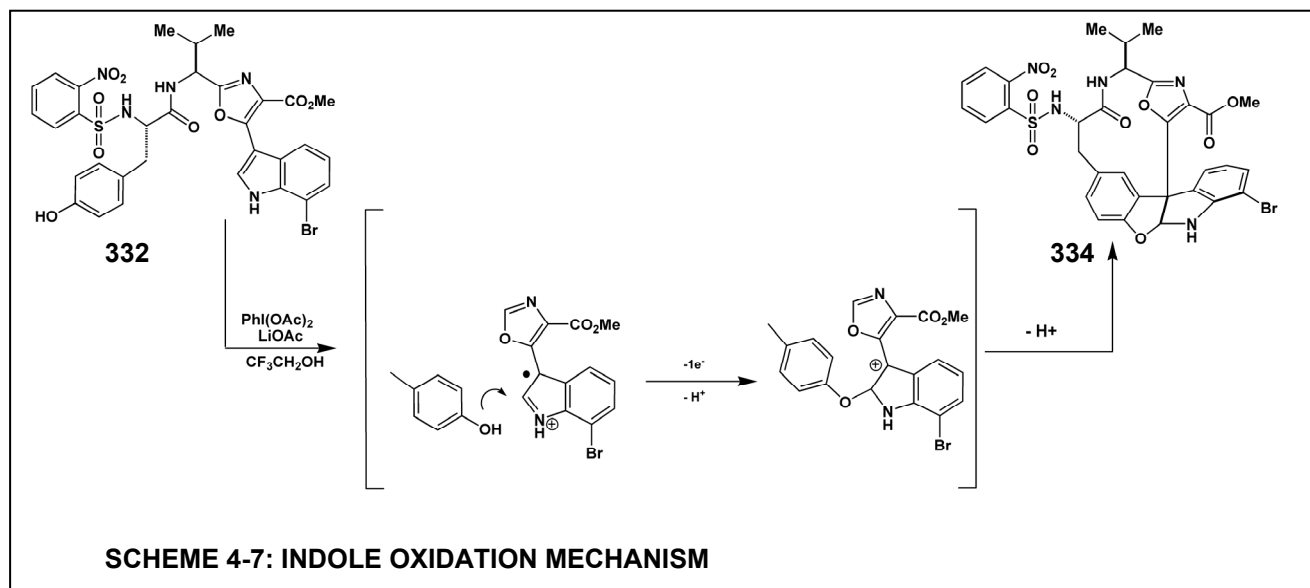


chloroform. The imidates **336** and **337** are also unstable and partially hydrolyze upon chromatography on silica gel to form lactone **338** (**Scheme 4-5**: X-ray structure of **338**) and the dipeptide amine **339**. The instability of the spirodienone imidates is exploited to aid in the purification of the desired compound **334**. The four oxidation products (**334-337**) show similar TLC R_f values in all elution solvent systems examined. Through treatment of the crude oxidation reaction mixture with dilute aqueous HCl, the imidates are hydrolyzed aiding the chromatographic purification of the desired product **334**.

4.3.2.1 Possible Hypervalent Iodine Oxidation Mechanisms

Based on the extensive published accounts concerning phenolic oxidation, the initial thinking in the diazonamide approach focused on such a mechanism (**Scheme 4-6**). The results of treating tripeptide **332** with iodobenzene diacetate are certainly consistent with a phenolic oxidation method. Phenoxenium species (**Scheme 4-6**) is generated in the presence of two pendant nucleophiles. Attack of the indole on the phenoxenium group would be followed by a back-attack of the phenol oxygen and deprotonation would generate the cyclized product **334**. Alternatively, the phenoxenium species could be engaged by the nucleophilic amide functional group, which upon loss of proton would generate the spirodienone imidates **336** and **337**. An alternative mechanism is depicted in **Scheme 4-7**. The oxazoylindole could also be a substrate for oxidation with the hypervalent iodine reagent. In this mechanism, single electron oxidation of the oxazoylindole unit would generate a radical cation. Nucleophilic attack of the phenol at the indole 2-position, followed by a loss of proton and a second single electron oxidation would generate a cation intermediate. A Friedel-Crafts alkylation would then generate the cyclized product **334**. In this scenario, the iodobenzene diacetate is capable of oxidizing both the phenol



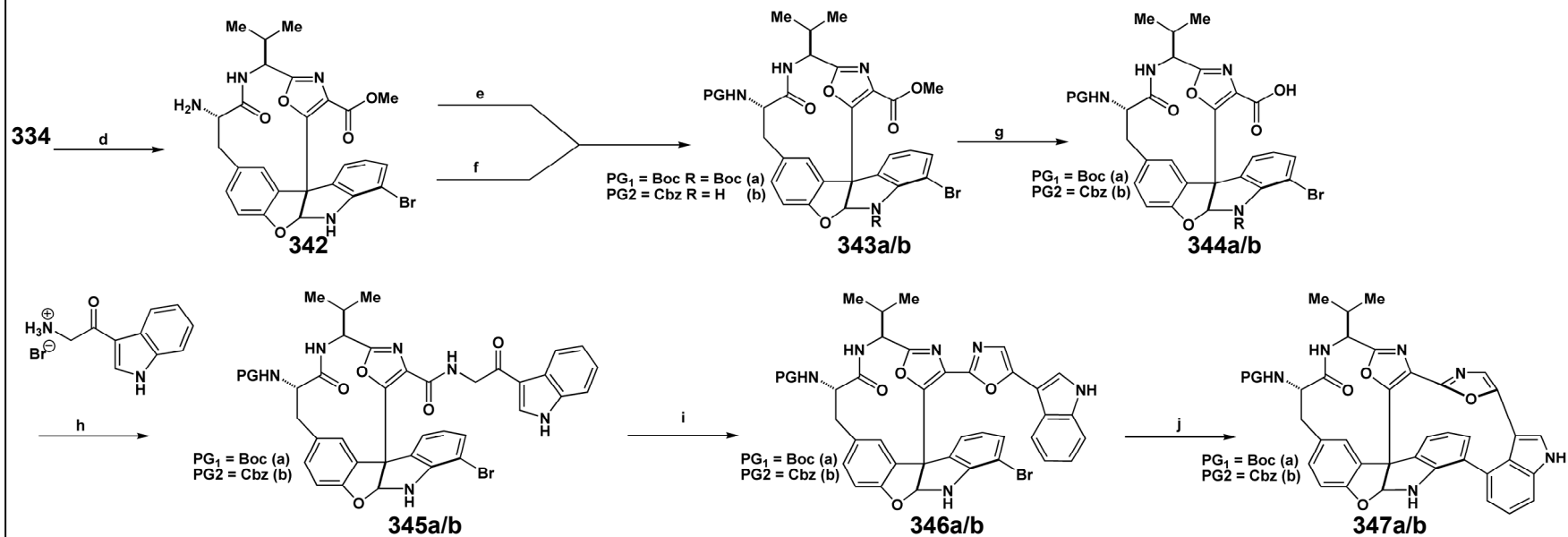
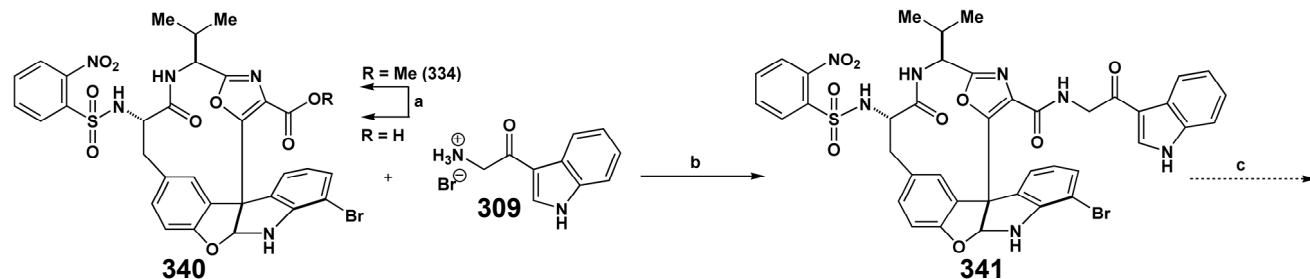


and the oxazoylindole units. Oxidation of the phenol leads to spirodienone imidates whereas oxidation of the indole leads to the cyclized products. Evidence supporting this hypothesis includes the reaction of the acetylated oxazoylindole component (**Scheme 4-7**) to give a mixture of products, including one tentatively assigned as oxidized TFE adduct product.

4.3.3 Synthesis and Photochemistry of Bis-Oxazole 346

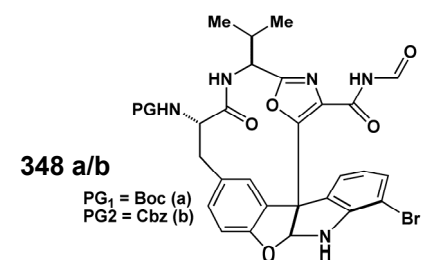
With formation of the desired C10 aminal macrocycle **334**, the right hand portion of the molecule was elaborated following established Harran lab precedent⁴⁶ (**Scheme 4-8**). Initially **334** was saponified to produce acid **340**. TBTU peptide coupling with ketotryptamine **309** yielded **341** (67%), which failed to form the desired bis-oxazole compound upon dehydration. This failure was due to the Nos protecting group, which mandated a protecting group switch. The Nos group was removed with thiophenol to yield amine **342** (73%)¹⁰¹, which was re-protected with either the Boc (**343a**) or Cbz protecting group (**343b**). The re-protected macrocycle was

saponified to produce acid **344a/b**, and then was TBTU coupled with ketotryptamine **309** to produce compound **345a/b**. **345** possesses all of the constituents of the diazonamide core, and upon dehydration to form bis-oxazole **346a/b**, all of the diazonamide aromatic rings are in place. The formation of the C16-C18 biaryl bond using photochemistry had been performed successfully by the Harran group in a molecular context similar to **346** (**Scheme 1-20**).⁴⁶ Their success was subsequently emulated by the Nicolaou group's total synthesis of the revised diazonamide A structure (**Scheme 1-25**) with a substrate closely related to **346**.⁴⁷ Based on these prior precedents, the production of only trace amounts of **347a/b** from **346a/b** was an unexpected failure. The major product of this photochemical reaction proved to be degraded formimide **348a/b**. The reaction conditions were varied, including the use of different solvents and different additives, but the results of the reaction were unchanged. The formation of **348a/b** was even a facile process upon irradiation of **346** with no additives. The unexpected failure of this reaction is likely attributable to the increased electron density of the aniline photochemistry substrate (**346a/b**) relative to the benzofuran containing substrate (**Scheme 1-20**). In the photochemistry step from the Nicolaou synthesis, the aniline nitrogen existed as a cyclic amide (**Scheme 1-25, 255**), likely attenuating the electron density of the E-F-rings.⁴⁷ Based on the proposed mechanism for the C16-C18 bond formation⁴⁶(**Section 1.2.3.11**), an increase in the electron density of the E-ring would prevent the initial electron transfer from the C-D indole component. This would explain a poor conversion to the desired cyclized product **347**.



a) LiOH, 4:1 MeOH:H₂O, 0 °C - r.t., 5 h b) DEPC, NMM, DMF 0 °C - r.t., 3.5 h (67%) c) Cl₆C₂, PPh₃, EtN₃, CH₂Cl₂ d) PhSH, K₂CO₃, DMF, r.t., 2 h (73%) e) Boc₂O, pyr., DMAP, DMF, 0 °C - r.t., 3 h, (84%) f) Cbz-OSu, DMF, 0 °C - r.t., 1.5 h, (76% two steps) g) LiOH, 4:1 MeOH:H₂O, 0 °C - r.t., 5 h (Boc = 84%, Cbz = 98%) h) DEPC, NMM, DMF 0 °C - r.t., 3.5 h (Boc = 65%, Cbz = 86%) i) Cl₆C₂, PPh₃, EtN₃, CH₂Cl₂, 0 °C, 15 min (Boc = 62%, Cbz = 74 %) j) *hν* 300 nm, epichlorohydrin, LiOAc, H₂O, CH₃CN (**347** Boc = ~5%, Cbz = ~5%, **348** Boc = 53% Cbz = 50%).

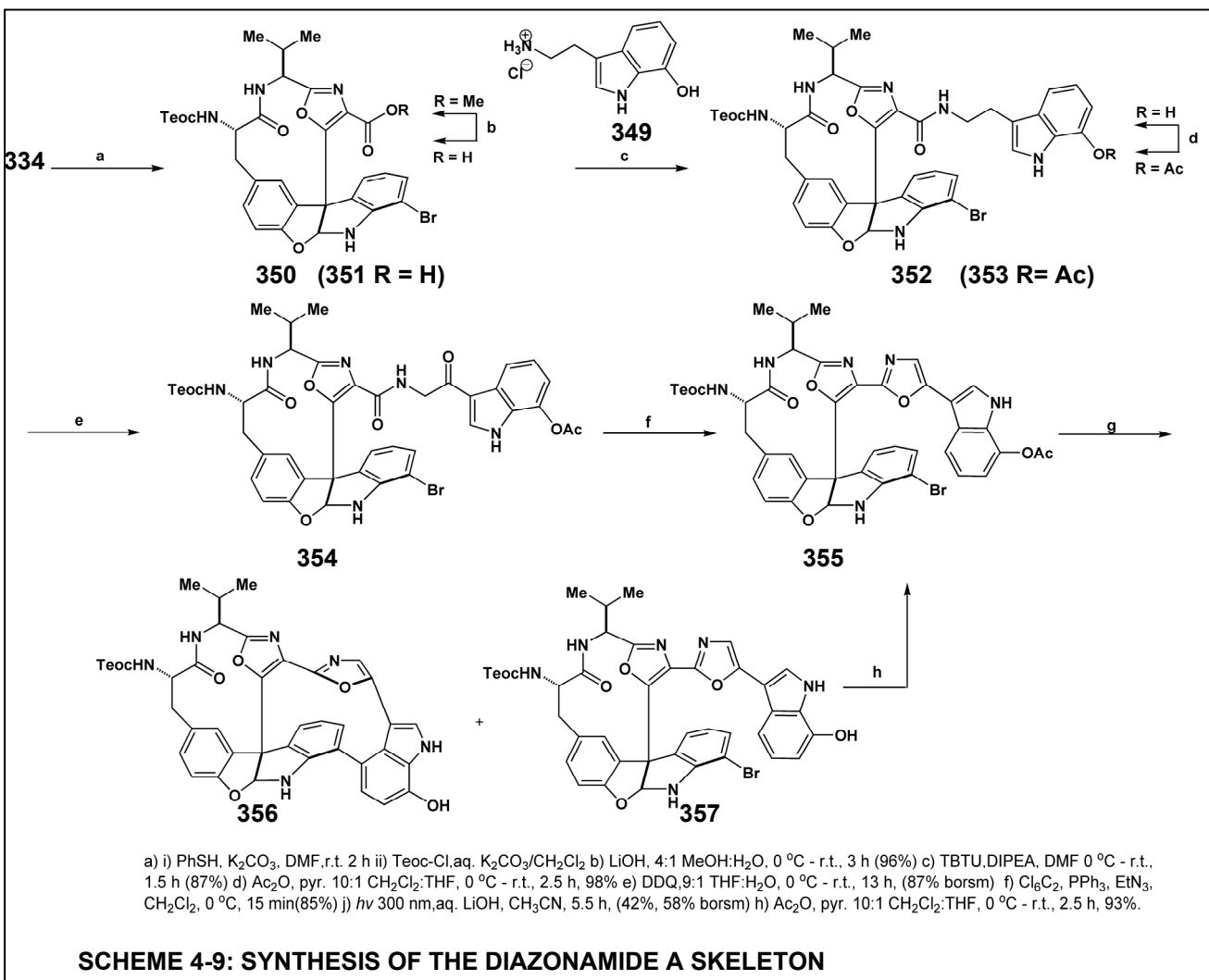
SCHEME 4-8: SYNTHESIS OF PHOTOCHEMISTRY SUBSTRATE



The formation of the major product **348** remains inexplicable, and there are no obvious mechanisms detailing how a cleaved, oxidized product could be generated under the reaction conditions. The excised indole component could not be isolated in a pure form, and the indications were that several closely related indole compounds were produced. Identification of the indole piece could have greatly aided understanding the formation of **348**. The small amount of desired diazonamide core produced (**347**) was subjected to *N*-chlorosuccinimide chlorination following the successful procedure developed by Magnus²⁸ and used by the Harran group.⁴⁵ None of the desired chlorinated compound was formed however. The enhanced electrodensity of the aminal containing macrocycle lead to the electrophilic chlorination of the E-ring, in addition to the expected chlorination of the B- and C-rings. These two unexpected set backs, both due to the enhanced electrodensity of the E-ring, required the development of modified methodologies to complete the total synthesis.

4.3.4 Successful Photochemical Formation of the Diazonamide Core

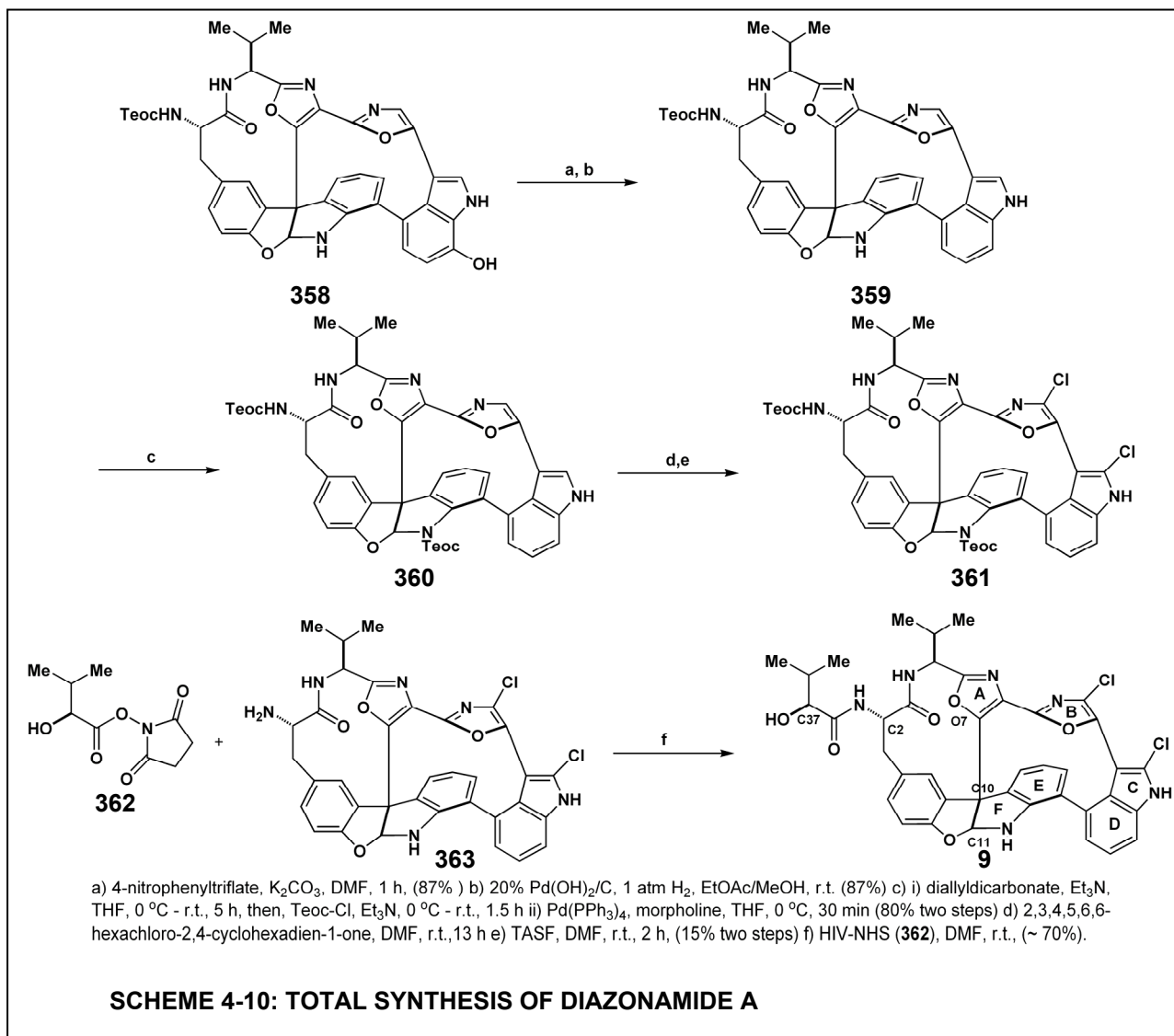
First, the photochemical formation of the C16-C18 bond was solved through the incorporation of the 7-hydroxytryptamine component **349** into the photochemistry substrate (**Scheme 4-9**). The presence of the 7- hydroxyindole was postulated to dramatically increase the electrodensity of the C-D indole, thereby facilitating the initial electron transfer into the E-ring. The Teoc protected macrocycle **350** was prepared from the Nos-protected macrocycle (70% two steps), saponified (**351**) (96%), and coupled with the 7-hydroxytryptamine hydrochloride **349** to form **352** (87%). The compound was immediately acetylated (**353**) to protect the labile hydroxyindole moiety (98%). DDQ oxidation (**354**) (87%) and dehydration (**355**) (85%) were



successful processes, generating bis-oxazole photochemical substrate **355**. Treatment of **355** with aq. LiOH immediately prior to photolysis liberates the 7-hydroxyindole, and the photochemical reaction is successful in producing the desired cyclized product **356** in reasonable yields (42%). The recovered deacetylated bis-oxazole compound **357** can be re-acetylated and resubjected to the photochemistry.

4.3.5 Diazonamide Chlorination and Endgame

This solution to the photochemistry obstacle then required the removal of the 7-hydroxy group (**Scheme 4-10**). This was achieved through initial formation of the aryl triflate (87%) followed by reduction to generate the Teoc-protected diazonamide core **359** (87%). The only synthetic obstacle remaining was the peripheral chlorination. To accomplish this end, the nucleophilicity of the E-ring had to be attenuated, and an obvious way to achieve this was through substitution on the aminal secondary amine. Due to the severe steric constraints of the diazonamide structure however, the aminal nitrogen was not the most reactive nucleophile present. The exposure of **360** to electrophilic species led to the acylation of the C-ring indole nitrogen instead. To overcome this unwanted nucleophilic primacy, the indole nitrogen was first protected as the Alloc, then, the aminal nitrogen was acylated with the Teoc carbamate. Alloc removal produced chlorination substrate bis-Teoc compound **361** (80% two steps). Chlorination with 2,3,4,5,6,6-hexachloro-2,4-cyclohexadien-1-one was achieved, although in a low yield (~20%). Removal of the Teoc groups with TASF (**363**), followed by introduction of the side chain with the NHS activated ester of the α -hydroxy-isovaleric acid (**362**) produced diazonamide **A 9**).



4.4 Discussion

The described total synthesis of diazonamide A details a very concise route to the complex natural product starting from amino acid precursors. The synthesis converges five components in a total of 19 steps to produce diazonamide A. The biosynthetically-inspired oxidation of the peptidyl substrate **332** was the defining and critical reaction of the synthesis. This remarkable transformation, in one step, converts a simple modified tripeptide into a diazonamide related compounds, complete with all of the requisite stereochemistry. Upon the

successful synthesis of the diazamide macrocycle **334**, introducing the the right side of the molecule seemed to only require the utilization of the previously develop methods. However, the effects of substituting the benzofuran oxygen for the indoline amine was not anticipated and proved to have major implications. The difference in the electron density of the E-ring was especially important due the chemistry involved in completing the synthesis. Both the photochemistry and the chlorination were vulnerable to the effects of the nitrogen resonance contribution. These failures were overcome through amending the developed methodologies, but at the cost of lengthening synthesis by several more steps.

The total synthesis possesses three major limiting steps. The first is the hypervalent iodine oxidation. Obviously, due to the low yield of the product, the ability to supply material through this step is limited, but relative to the amount of synthetic complexity produced from a accessible, simple substrate, a low yield could be acceptable. However, the tripeptide oxidation substrate **332** is far from optimal. It requires the use of the non-typical, non-commercially accessible Nos protecting group. In addition to having to make the Nos-protected tyrosine in two steps, this protecting group is not suitable for entire synthesis and must be switched, which adds two more operations to the synthesis.

The photochemical bond formation has a modest yield, and unlike the previous Harran work, the synthesis of the photochemistry precursor requires the incorporation 7-hydroxytryptamine instead of tryptamine. The use of this more limiting component mandates the introduction of three more synthetic operations, but is the only known method capable of forming the C16-C18 bond in this synthetic context. However, perhaps the biggest choke point in the described total synthesis is the chlorination reaction. In the previously published work, the chlorination of the oxazolyl-indole rings with NCS is a facile and controlled process.^{28, 45, 46} For

the diazonamide core however, a method had to be introduced to inactivate the unwanted chlorination of the E-ring, requiring more synthetic operations. And even with aminal nitrogen deactivated through substitution, the chlorination is a poor yielding reaction.

4.5 Conclusions

The total synthesis of diazonamide A has been accomplished through the discovery of a novel oxidation reaction that forms the aminal macrocycle **334**. Two possible mechanisms for the hypervalent iodine oxidation have been postulated and both fit the observed experimental results. Cbz-tripeptide **343b** undergoes a successful oxidation reaction to form the cyclized macrocycle. This result eliminates the need for the Nos-protecting group and cuts four steps off the diazonamide synthetic route.

This achievement, in combination with the modification of methodologies previously employed by the Harran group, produced the natural product in 19-steps from amino acid precursors. With a synthetic route to diazonamide A, the SAR and biological characteristics of the molecule may be further explored.

4.6 Experimental Section

4.6.1 General Methods

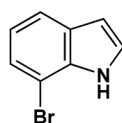
All operations involving moisture and / or oxygen sensitive materials were conducted under an atmosphere of nitrogen in flame-dried glassware. Unless noted otherwise, materials were obtained from commercially available sources and used without further purification. Tetrahydrofuran (THF) was distilled from sodium benzophenone ketyl under a nitrogen atmosphere. Dichloromethane (CH_2Cl_2) and triethylamine (Et_3N) were distilled from calcium hydride under a nitrogen atmosphere. Flash chromatography was performed on E. Merck silica gel 60 (240-400 mesh) using the protocol of Still, Kahn, and Mitra (*J. Org. Chem.* **1978**, *43*,

2923). Thin layer chromatography was performed using precoated plates purchased from E. Merck (silica gel 60 PF254, 0.25mm) and spots were visualized with long-wave ultraviolet light followed by an appropriate staining reagent. Nuclear magnetic resonance (NMR) spectra were recorded on either a Varian Inova-400 or Mercury-300 magnetic resonance spectrometer. ^1H NMR chemical shifts are given in parts-per-million (δ) downfield from tetramethylsilane using the residual solvent signal ($\text{CHCl}_3 = \delta 7.27$, acetone = $\delta 2.05$, methanol = $\delta 4.87$, tetrahydrofuran = $\delta 1.73$) as internal standard. ^1H NMR information is tabulated in the following format: multiplicity (s, singlet; d, doublet; t, triplet; q, quartet; m, multiplet, td, triplet of doublet; dt, doublet of triplet), coupling constant(s) (J) in hertz, number of protons. The prefix *app* is occasionally applied in cases where the true signal multiplicity was unresolved and *br* indicates a broad signal. Proton decoupled ^{13}C NMR spectra are reported in ppm (δ) relative to residual CHCl_3 ($\delta 77.23$) or methanol ($\delta 49.15$). Infrared spectra were recorded on a Perkin-Elmer FT-IR Spectrum 1000 using samples prepared as thin films between salt plates. Electrospray ionization mass spectra (ES-MS) were recorded at the Howard Hughes Medical Institute Biopolymers Facility, Department of Biochemistry, UT Southwestern Medical Center at Dallas. Also, ES-MS were also recorded on a Shimadzu LC-MS. High resolution mass spectra (HRMS) and Fast Atom Bombardment (FAB) mass spectra were recorded at the NIH mass spectrometry facility at the University of Washington, MO. Fluorescence spectra were recorded on a Perkin Elmer luminescence spectrometer LS50B. UV-visible spectra were recorded on a Shimadzu UV-visible spectrophotometer UV-1601. Optical rotations were measured at 25°C on a Perkin-Elmer 241 MC polarimeter and reported as: $[\alpha]_{\lambda}^T$ ($c = \text{g}/100 \text{ mL}$, solvent).

The data presented and tabulated in the appendix was produced by A. Burgett. But the overall synthetic work was the product of several researchers. The final procedure for the LiAlH_4

reduction of 7-bromoindole was developed by Dr. Yan Gao. The procedure for the Nos-protection of tyrosine was first developed by Dr. Qi Wei and subsequently improved upon by A. Burgett. The incorporating the 7-hydroxyindole component to allow for successful photochemistry was first achieved by Prof. Patrick Harran, as was the first successful chlorination of the final structure.

4.6.2 Compound Data

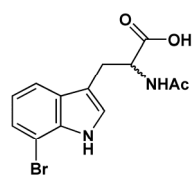


7-bromo-1H-indole
322

Method A: 800 mL of a 1.0 M vinyl magnesium bromide solution (Aldrich) (0.80 mol) was cannulated to a dry reaction flask under nitrogen and cooled to $-40\text{ }^{\circ}\text{C}$. 1-bromo-2-nitrobenzene (50.3 g, 0.25 mol) was dissolved in 100 mL THF. The light yellow solution was cannulated into a dry addition funnel and brought up to a final volume of 250 mL THF. The 1-bromo-2-nitrobenzene solution was added over 5 min to the rapidly stirring vinyl magnesium bromide solution. **Caution:** The rapid mixing evolved formed considerable gas and increased the reaction temperature. The reaction flask was well vented and the temperature was maintained at $-40\text{ }^{\circ}\text{C}$. The reaction was stirred at 1 hr at $-40\text{ }^{\circ}\text{C}$. 300 mL of a saturated NH_4Cl was added slowly to the reaction and the reaction was stirred for 20 min at $-40\text{ }^{\circ}\text{C}$. The cooling bath was then removed and the reaction was stirred warming to ambient temperature for an additional 20 min. The reaction mixture was then filtered through Celite to remove solid byproduct. $\sim 80\%$ of the THF was removed *in vacuo*, and the reaction mixture was then dissolved in ~ 500 mL ethyl ether. The filtered white solid was extracted with ethyl ether until free of desired by TLC. The ethyl

ether fractions were combined and washed with H₂O (400 mL), and brine (300 mL). The organic phase was dried over Na₂SO₄. The crude reaction mixture was condensed *in vacuo* and chromatographed with hexanes to obtain the desired compound (21 g, 43%) as a faintly yellow solid.

Method B: 7-bromoisatin was prepared according to the published procedure.¹⁰³ LiAlH₄ pellets (41.7 g, 1.1 mol) (Aldrich) were slowly added to 900 mL anhydrous Et₂O at 0 °C under nitrogen. The solution was warmed to ambient temperature and stirred for 4 h. The solution was re-cooled to 0 °C. 7-bromoisatin (25 g, 110 mmol) was dissolved in 200 mL THF. The 7-bromoisatin solution was added dropwise to the LiAlH solution over 90 min. The solution was then allowed to warm to ambient temperature and stirred for 12 h. The solution was then re-cooled to 0 °C and very carefully quenched with a 15% H₂O/THF solution (~400 mL). The solution was filtered through a pad of Celite and washed with Et₂O. The solvent was removed *in vacuo*, extracted twice with Et₂O, and the organic phase was dried over Na₂SO₄. Column chromatography (hexanes) yielded 7-bromo-1*H*-indole (14.3 g, 66%). **322**: R_f = 0.8 (40% EtOAc/hexanes). ¹HNMR (400 MHz, CDCl₃): δ 8.33 (br s, 1H), 7.58 (d, *J* = 8.0 Hz, 1H), 7.34 (d, *J* = 2.7 Hz, 1H), 7.26 (t, *J* = 2.7 Hz, 1H), 7.00 (t, *J* = 7.8 Hz, 1H), 6.63 (dd, *J* = 0.9, 2.1 Hz, 1H).



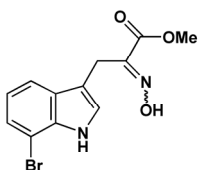
2-acetamido-3-(7-bromo-1*H*-indol-3-yl)propanoic acid

324

This procedure was modified from the published Konda-Yamada et al protocol.¹⁰⁴ 7-bromo-1*H*-indole (**322**) (5.2 g, 26.5 mmol) was dissolved in acetic acid (62.4 mL, 220 mmol). Acetic anhydride (20.8 mL) was then added to the reaction, followed by L-serine (5.6 g, 53.0 mmol). The reaction was heated to 75 °C and stirred for 2 h, producing a clear orange solution. The

reaction was cooled, 500 mL of Et₂O was added, and the reaction was basified with a 30% w/v aq. NaOH solution until the aqueous pH = 11. The organic layer was separated, and the aqueous layer was extracted twice more with 500 mL Et₂O. The organic layers were combined and extracted with 300 mL 1 N NaOH. The cloudy dark brown aqueous layers were combined. ~ 1g of Na₂S₂O₄ was added and well mixed. The solution was cooled in an ice bath for 40 min to produce a clear dark red solution. The solution was neutralized with conc. HCl. ~ One-half of the volume was removed *in vacuo*, and the solution was further acidified to pH ~3. Upon cooling at 4 °C, some product crystals precipitated and were collected. Most of the material did not crystallize out. The aqueous solution was extracted with ethyl acetate and condensed *in vacuo*. The product was purified with column chromatography on silica gel (10% isopropanol/ethyl acetate 1% acetic acid). Product was obtained pure as a light yellow foam (4.3 g, 65%).

324: ¹HNMR (400 MHz, (CD₃)₂CO): δ 10.24 (br s, 1H), 7.62 (d, *J* = 7.0 Hz, 1H), 7.32 – 7.30 (m, 2H), 7.25 (br d, *J* = 7.6 Hz, 1H), 6.98 (t, *J* = 7.6 Hz, 1H), 4.81 – 4.76 (6 line m, 1H), 3.32 (dd, *J* = 5.5, 14.6 Hz, 1H), 3.19 (dd, *J* = 7.3, 15.0 Hz, 1H), 1.89 (s, 3H).

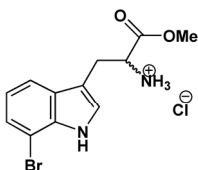


methyl 3-(7-bromo-1H-indol-3-yl)-2-(hydroxyimino)propanoate

319

Adapted from Jamison procedure.²² 7-bromo-1H-indole (**322**) (11.1 g, 56.6 mmol) was dissolved in 166 mL of CH₂Cl₂. Oven-dried sodium carbonate (7.8 g, 73.6 mol) was added as a solid and did not fully dissolve. Methyl-3-bromopyruvate oxime (11.9 g, 60.7 mmol) was added as a solution in dichloromethane (125 mL) via slow addition from addition funnel (~ 2 mL/min). The reaction was stirred at ambient temperature under nitrogen for a total of 26 h. TLC showed

majority of substrate was converted to product with a small amount of lower R.f. byproduct being formed. Most of the CH_2Cl_2 was removed *in vacuo* and the reaction mixture was resuspended in 400 mL EtOAc, washed with water (200 mL) and brine (200 mL), and dried over Na_2SO_4 . The organic phase was condensed to a yellow oil and flash chromatographed using EtOAc/hexanes (20%EtOAc - 40% EtOAc). 3.8 g of pure starting material was recovered (34%). The product was very slightly impure and crystallized from EtOAc/hexane to yield 9.5 g solid product (54%, borsm 87%). **319**: $R_f = 0.34$ (40% EtOAc/hexanes). $^1\text{HNMR}$ (400 MHz, CDCl_3): δ 8.21 (br s, 1H), 7.72 (d, $J = .7$ Hz, 1H), 7.35 (d, $J = 7.7$ Hz, 1H), 7.21 (d, $J = 1.8$ Hz, 1H), 7.02 (t, $J = 7.7$ Hz, 1H), 4.09 – 4.11 (m, 2H), 3.83 (s, 3H).



7-bromotryptophan methyl ester hydrochloride

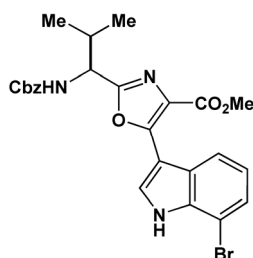
325

Method A: Oxime **319** (3.2 g, 10.4 mmol) was dissolved in 100 mL THF and cooled to 0 °C. Aluminum foil was weighed and cut into small pieces (~0.5 in²). ~1.25 g of aluminum was added to the reaction, followed by 10 mL H_2O . 3.4 mL of a 2% aq. HgCl_2 was added slowly to the reaction. ~1.25 g more of aluminum foil was added gradually in several portions. The reaction was allowed to warm to ambient temperature and stirred approximately 14 h. 90 mL of sat. aq. NaHCO_3 was added to the reaction. The black solution was filtered through a pad of Celite with EtOAc washing. The organic layer was separated, and the aqueous layer was extracted twice with EtOAc. The combined organic layers were washed with H_2O , brine, and dried over Na_2SO_4 . The crude product was dissolved in 40 mL Et_2O (0.25 M) and cooled in an ice-water bath. 11 mL of a 1.0 M $\text{HCl}/\text{Et}_2\text{O}$ was added over 10 min. The reaction was stirred for 30 min. Then 40 mL

hexane was added to promote precipitation. The solid was filtered off and triturated with Et₂O to yield the product as a white solid (1.8 g, 58%).

Method B: 2-acetamido-3-(7-bromo-1H-indol-3-yl)propanoic acid (**324**) (3.97 g, 12.3 mmol) was charged in 250 mg portions (0.77 mmol) into 16-2 mL Smith Process VialsTM. Each tube was sealed, and 1.83 mL of H₂O was added to each tube via syringe to give a suspension. 0.45 mL of a 48% aqueous HBr solution (2.7 mmol) was then added per tube. Each tube was then irradiated with microwave heating for 5 min at a temperature of 150 °C in a Personal Chemistry 300W Smith Creator microwave reactor. The homogenous light orange solution was pooled from all 16 tubes, and cooled in an ice bath. The crude reaction was carefully basified with 20% NaOH to pH 5.0 with a precipitate forming at > pH 5.0. The suspension transferred to two 50 mL polypropylene tubes and cooled on ice for 10 min. The tubes were then centrifuged for 5 min at 3,000 rpm at 4 °C in a Sorvall table top centrifuge. The solution was decanted, the solid was resuspended in 10 mL ice cold H₂O, and placed on ice again for 10 min. The centrifugation and decantation were repeated. The product was dried to give a light brown colored solid (3.3 g, 95%). The deacetylated product (2-amino-3-(7-bromo-1H-indol-3-yl)propanoic acid) (3.30 g, 11.7 mmol) was partially dissolved in 33 mL of anhydrous MeOH (0.35 M). TMSCl (6.36 g, 58.5 mmol) was slowly added to produce a homogeneous, dark brown solution. The reaction was refluxed for 90 min, at which time NMR analysis of an aliquot indicated the reaction was complete. The reaction was cooled, and the methanol was removed *in vacuo* to yield a gray flaky solid (3.3 g, 90%). **325**: ¹HNMR (400 MHz, (CD₃)₂SO): δ 11.09 (br s, 1H), 7.50 (d, *J* = 7.7 Hz, 1H), 7.28 (d, *J* = 7.3 Hz, 1H), 7.19 (d, *J* = 2.6 Hz, 1H), 6.93 (t, *J* = 7.7 Hz, 1H), 3.62 (app t, *J* = 6.6 Hz, 1H), 3.54 (s, 3H), 3.00 (dd, *J* = 6.2, 14.3 Hz, 1H), 2.92 – 3.33 (dd, *J* = 6.6, 14.3 Hz,

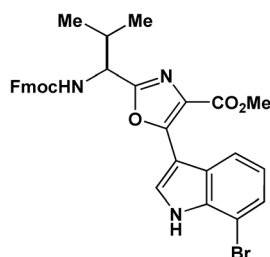
1H). ¹³C NMR (75 MHz, CD₃OD): 170.7, 136.7, 129.9, 127.0, 125.6, 121.7, 118.6, 109.1, 106.0, 54.7, 53.9, 27.6.



327a

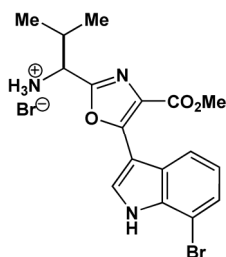
7-bromotryptophan methyl ester hydrochloride (**325**) (15 g, 50 mmol) and Cbz-valine (13.8 g, 55 mmol) were charged to a dry round bottom and purged with nitrogen. TBTU (19.3 g, 60 mmol) was charged to dry vials under nitrogen and added as a solid. The reaction was dissolved in DMF (180 mL, 0.28 M) and cooled to 0 °C. DIPEA (8.7 mL, 50 mmol) was charged to a dry addition funnel under nitrogen, and added slowly to the cooled reaction solution. The reaction was stirred at 0 °C for 10 min post DIPEA addition, and then allowed to warm to ambient temperature. The yellow solution was stirred at ambient temperature for 90 min. The reaction was then diluted in 750 mL of EtOAc and washed with water (2 x 500 mL) and brine (1 x 500 mL), and dried over Na₂SO₄. The crude reaction mixture was flash chromatographed on silica gel. Due to the poor solubility of the reaction products, the column is loaded in a large volume of CH₂Cl₂ (~150 mL), and 8% EtOAc/CH₂Cl₂ is used to elute the column. The white solid product was obtained as a mixture of diastereomers, which were carried forward without separation (25.7 g, 96 %). The product diastereomers (25.7g, 48 mmol) were charged to a 3L three-neck round bottom with an attached water condenser, and dissolved in 1.1 L THF (0.04 M). DDQ (24.2 g, 106 mmol) was charged to a dry flask in the atmosphere and added as a solid to the starting material. The solution became dark purple/black upon DDQ addition. The reaction is heated to 70-75 °C for 15

154.1, 134.6, 130.1, 126.3, 125.6, 123.5, 122.5, 120.4, 105.2, 104.9, 80.3, 54.5, 32.9, 28.4, 19.1, 18.3.



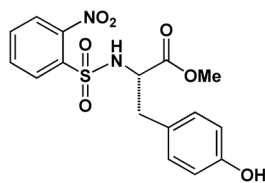
327c

See attached appendix: Compound **327c** ¹H NMR Spectra.



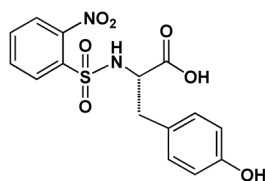
328

DDQ product (**327a**) (27 g, 53 mmol) was dissolved in 90 mL of a 33% HBr/AcOH solution (0.59 M) to initially give a paste. The reaction was stirred and manually mixed with a spatula for 20 min until an even light pink paste was obtained. The reaction was then diluted with 500 mL of ethyl ether and stirred to fully precipitate the product, which is removed by filtration. The precipitate was triturated several times with ethyl ether until the filtrate is colorless. 24 g (50 mmol, 96%) of product was obtained as a light pink solid. **328**: ¹H NMR (400 MHz, CD₃OD): δ 8.79 (s, 1H), 8.12 (d, *J* = 7.9 Hz, 1H), 7.45 (d, *J* = 7.9 Hz, 1H), 7.16 (app t, *J* = 7.9 Hz, 1H), 4.59 (d, *J* = 6.7 Hz, 1H), 3.95 (s, 3H), 2.53 – 2.45 (m, 1H), 1.21 (d, *J* = 6.7 Hz, 1H), 1.09 (d, *J* = 6.7 Hz, 1H). ¹³C NMR (75 MHz, CD₃OD): 164.1, 157.0, 156.7, 136.5, 132.6, 127.9, 126.8, 124.6, 123.7, 121.3, 106.4, 104.8, 55.4, 52.6, 32.8, 19.1, 18.4.



330

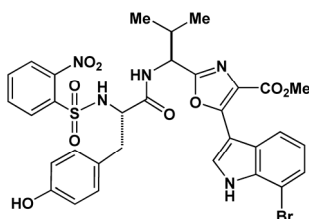
L-tyrosine methyl ester hydrochloride (Adv. Chem. Tech) (36.4 g, 167 mmol) was dissolved in 475 mL potassium phosphate buffer pH 9.0. 2-nitrobenzene sulfonyl chloride (Aldrich) (38.3 g, 173 mmol) was dissolved in 475 mL of DCM and added to the reaction. The biphasic solution was rapidly stirred to ensure mixing for 4.5 h. The yellow organic layer was separated, washed with brine, and dried over Na₂SO₄. The crude reaction mixture was chromatographed with 2% EtOAc/DCM, and the product was obtained as a bright yellow solid (40.0 g, 67%). **330**: ¹H NMR (400 MHz, (CD₃)₂SO): δ 9.20 (s, 1H), 8.74 (br s, 1H), 7.86 (d, *J* = 8.4 Hz, 1H), 7.80 – 7.75 (m, 1H), 7.66 – 7.64 (m, 2H), 6.94 (d, *J* = 8.4 Hz, 2H), 6.54 (d, *J* = 8.4 Hz, 2H), 4.04 (m, 1H), 3.46 (s, 3H), 2.90 (dd, *J* = 5.5, 13.6 Hz, 1H), 2.74 (dd, *J* = 9.5, 13.9 Hz, 1H).



331

Nos-tyrosine methyl ester (**330**) (55.63 g 146.3 mmol) was dissolved in 640 mL EtOH. KOH (50.87 g, 908 mmol) was dissolved in 360 mL of EtOH and 91 mL H₂O. The KOH solution was added slowly, and the reaction was then stirred for 3 h. The EtOH was removed *in vacuo*, and the residue was diluted with H₂O and extracted three times with EtOAc. The combined organic layers were washed with brine and dried over Na₂SO₄. *In vacuo* concentration provided an orange oil. The product was purified through crystallization from boiling H₂O/MeOH (1.7 L H₂O and 10 mL MeOH) to yield the product as a yellow solid (50.47 g, 94%). **331**: IR (film): 3338,

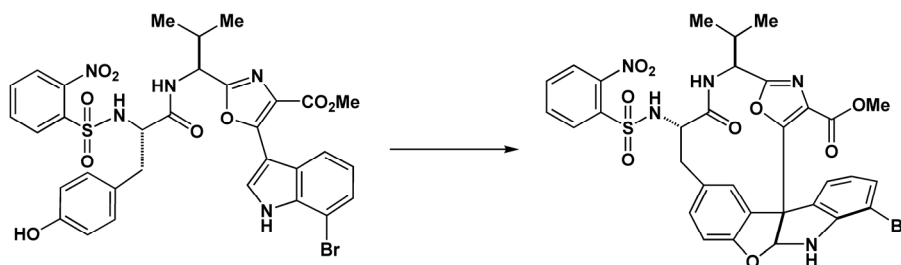
2484, 2216, 2071, 1944, 1719, 1612, 1542, 1515, 1364, 1265, 1123, 976, 827, 741 cm^{-1} . ^1H NMR (400 MHz, $(\text{CD}_3)_2\text{SO}$): δ 9.17 (s, 1H), 8.49 (d, $J = 8.8$ Hz, 1H), 7.84 (d, $J = 8.4$ Hz, 1H), 7.77 – 7.72 (5 line m, 1H), 7.62 – 7.60 (m, 2H), 6.95 (d, $J = 8.4$ Hz, 2H), 6.53 (d, $J = 8.4$ Hz, 2H), 3.96 (m, 1H), 2.92 (dd, $J = 4.7, 13.6$ Hz, 1H), 2.72 (dd, $J = 9.5, 13.9$ Hz, 1H). ^{13}C NMR (75 MHz, CD_3OD) 174.4, 157.3, 135.2, 134.6, 133.8, 131.6, 131.5, 131.3, 128.4, 126.0, 116.2, 59.9, 38.7.



332

Valine oxazyl-7-bromoindole methyl ester hydrobromide (**328**) (19.7 g, 0.0416 mol) and *o*-nitrosulfonylated tyrosine (16.1 g, 44.0 mmol) were charged to a dry flask and dissolved in anhydrous DMF (190 mL, 0.2 M). Not all of the material was soluble. The reaction flask was cooled to 0 °C. TBTU (14.3 g, 44.4 mmol) was charged to dry vials under a nitrogen atmosphere and added as a solid in portions to the reaction. DIPEA (14.9 mL, 85.6 mol) was added to the reaction over 7 min (fast drop-wise addition). The solution became homogeneous after addition of DIPEA. After 30 min at 0 °C, the ice bath was removed and the reaction was allowed to warm to ambient temperature and stir for 4 h. The reaction was diluted with 600 mL EtOAc and washed three times with 300 mL H_2O . The aqueous layers were combined and back extracted twice with 100 mL EtOAc. The combined organics were washed three times with 300 mL sat. NaHCO_3 , once with 300 mL brine, and dried over Na_2SO_4 . The yellow oil was flash chromatographed with EtOAc/hexane (50% - 70% EtOAc/hexane). 27.9 g (91%) of the tripeptide product was obtained as a bright yellow solid. **332**: $[\alpha]_D^{25} = 14.04$ ($c = 1.0$, CHCl_3), ^1H NMR (400

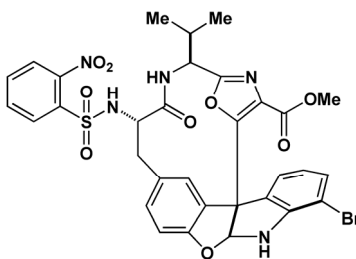
mHz, (CD₃CN): δ 10.04 (s, 1H), 8.70 (d, $J = 2.9$ Hz, 1H), 8.10 (d, $J = 8.0$ Hz, 1H), 7.87 (dd, $J = 1.5, 7.7$ Hz, 1H), 7.80 – 7.64 (m, 3H), 7.46 (d, $J = 7.7$ Hz, 1H), 7.20 – 7.10 (m, 2H), 6.87 (d, $J = 8.4$ Hz, 2H), 6.61 (br s, 1H), 6.39 (d, $J = 8.4$ Hz, 2H), 4.84 – 4.79 (m, 1H), 4.24 – 4.19 (m, 1H), 3.89 (s, 3H), 2.96 (dd, $J = 5.1, 13.9$ Hz, 1H), 2.78 (dd, $J = 8.8, 13.9$ Hz, 1H), 2.28 – 2.20 (m, 1H), 0.91 (d, $J = 7.0$ Hz, 3H), 0.85 (d, $J = 7.0$ Hz, 3H). ¹³C NMR (75 MHz, CD₃CN): 171.1, 163.9, 160.3, 156.7, 154.6, 148.3, 135.6, 135.0, 134.2, 134.0, 131.4, 131.3, 131.2, 127.8, 127.4, 126.5, 126.3, 124.5, 123.5, 121.7, 115.9, 105.7, 105.5, 60.1, 54.1, 52.4, 39.1, 32.5, 19.4, 18.9. ES-MS: calcd. for C₃₂H₃₀BrN₅O₉S [M+H]⁺: 740.09, found: 740.19, 742.18; calcd. for C₃₂H₃₀BrN₅O₉S [M-H]⁻: 738.08, found: 738.15, 740.13.



Tripeptide (**332**) (12 g, 160 mmol) was charged to a dry 500 mL flask under nitrogen. Lithium acetate (3.2 g, 480 mmol) added to the reaction flask, and the starting were dissolved in 70 mL 2,2,2-trifluoroethanol (TFE). A small amount of LiOAc failed to dissolve. Iodobenzene diacetate (PIDA) (5.0 g, 160.0 mol) was charged to a dry 2 L flask under N₂, dissolved in 1 L TFE, and cooled to -25 °C. The tripeptide(**332**)/LiOAc solution was transferred to an addition funnel under nitrogen in a total volume of 100 mL TFE. The tripeptide/LiOAc solution was rapidly added to a vigorously stirring PIDA solution over 2.5 min (addition as a fast stream from addition funnel (0.02M final concentration)). The reaction temperature maintained at -25 °C during the slightly exothermic reaction. The reaction solution was initially yellow, but became light green within the first minute of addition, and then turned slightly darker green over time.

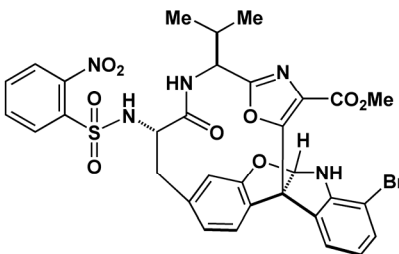
The reaction was stirred at -25°C for 40 min. Solid NaHCO_3 (3.4 g, 400 mmol) was then added, and the solution was stirred for an additional 30 minutes at -25°C . The reaction color became a light tan. The reaction was filtered cold to remove the solid NaHCO_3 , and the TFE was recovered *in vacuo* to yield a dark brown foam/solid crude mixture.

The dilute reaction conditions limited the size of the reaction to 12 g of tripeptide starting material. Following the procedure described, 18 g more tripeptide was reacted in one 12 g batch and one 6 g batch. (30 g total tripeptide). Four major products are produced in this reaction: the desired cyclized compound (**334**), the undesired cyclized diastereomer (**335**), and two spirodienone imidate diastereomers (**336**, **337**). To simplify the purification of the desired compound, the two spirodienone imidates were hydrolyzed using the following procedure before chromatography. The crude mixture was dissolved in 300 mL THF, and then 300 mL of a 0.1 N aq. HCl solution was added. The reaction was stirred at room temperature for 30 min. The reaction was diluted with 500 mL EtOAc, and washed twice with 200 mL of pH 5.0 buffer. The combined aqueous phase was back extracted once with EtOAc, and the combined organics were washed once with 200 mL brine and dried over Na_2SO_4 . This hydrolysis produces lactone **338** as a mixture of epimers. The crude mixture was then condensed, and flash chromatographed multiple times using EtOAc/ CH_2Cl_2 as solvent to obtain 4.3 g (15 %) of the pure desired cyclized compound as a yellow solid.



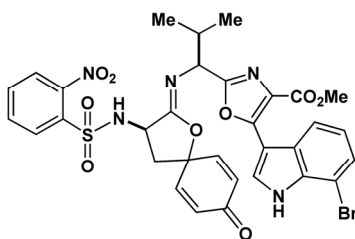
334

334: $[\alpha]_D^{25} = -56.10$ ($c = 1.0$, CHCl_3), IR (film): 2963, 1732, 1681, 1613, 1588, 1540, 1494, 1472, 1440, 1362, 1223, 1169, 1114, 1086, 1060, 942, 769, 588 cm^{-1} . ^1H NMR (400 MHz, CDCl_3): δ 8.16 – 8.13 (m, 1H), 7.90 – 7.86 (m, 1H), 7.80 – 7.75 (m, 2H), 7.26 (dd, $J = 0.9, 8.3$ Hz, 1H), 7.21 (d, $J = 1.9$ Hz, 1H), 7.07 – 7.04 (m, 2H), 6.81 (d, $J = 8.3$ Hz, 1H), 6.75 (d, $J = 3.4$ Hz, 1H), 6.66 – 6.61 (m, 1H), 6.25 (d, $J = 9.8$ Hz, 1H), 5.74 ($J = 8.3$ Hz, 1H), 5.45 (d, $J = 3.4$ Hz, 1H), 4.90 – 4.86 (m, 1H), 3.97 - 3.90 (m, 1H), 3.57 (s, 3H), 3.31 (t, $J = 12.2$ Hz, 1H), 2.86 (dd, $J = 3.4, 12.7$ Hz, 1H), 2.40 – 2.30 (m, 1H), 0.89 (d, $J = 6.8$ Hz, 3H), 0.84 (d, $J = 6.8$ Hz, 3H). ^1H COSY NMR: see attached appendix. ^{15}N -HSQC: see attached appendix. ^{13}C NMR (75 MHz, CDCl_3): 171.1, 160.4, 157.7, 147.2, 135.0, 134.1, 133.1, 131.8, 130.6, 130.4, 129.4, 128.2, 127.9, 125.5, 121.5, 121.4, 111.3, 102.7, 102.4, 61.0, 54.2, 52.4, 39.3, 29.5, 19.2, 17.8. ES-MS: calcd. for $\text{C}_{32}\text{H}_{28}\text{BrN}_5\text{O}_9\text{S}$ $[\text{M}+\text{H}]^+$: 738.09, found: 738.21, 740.19; calcd. for $\text{C}_{32}\text{H}_{30}\text{BrN}_5\text{O}_9\text{S}$ $[\text{M}-\text{H}]^-$: 736.07, found: 736.10, 738.09.



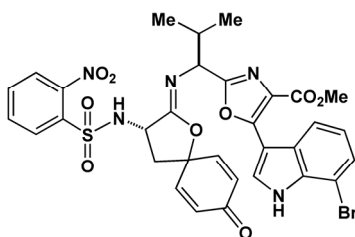
335

335: ^1H NMR (400 MHz, CDCl_3): δ 8.20 – 8.17 (m, 1H), 8.00 – 7.96 (m, 1H), 7.88 – 7.82 (m, 2H), 7.45 (d, $J = 1.5$ Hz, 1H), 7.27 (dd, $J = 1.1, 8.1$ Hz, 1H), 7.16 (br s, 1H), 7.10 (d, $J = 7.0$ Hz, 1H), 7.01 (dd, $J = 1.8, 8.1$ Hz, 1H), 6.85 (d, $J = 7.0$ Hz, 1H), 6.76 (d, $J = 3.7$ Hz, 1H), 6.67 -6.63 (m, 1H), 5.69 (br s, 1H), 5.44 (d, $J = 3.7$ Hz, 1H), 4.33 (br s, 1H), 3.88 – 3.80 (m, 1H), 3.63 (dd, $J = 3.3, 13.5$ Hz, 1H), 3.57 (s, 3H), 3.08 – 2.98 (m, 1H), 2.41 – 2.31 (m, 1H), 1.29 (d, $J = 6.6$ Hz, 3H), 1.03 (d, $J = 6.6$ Hz, 1H). Crystal structure: crystallized from acetonitrile.



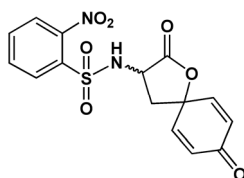
336

336: IR (film): 3435, 1636, 1540, 1431, 1369, 1283, 1209, 1172, 1126, 1086, 556 cm^{-1} . ^1H NMR (400 MHz, CDCl_3): δ 8.83 (d, $J = 3.1$ Hz, 1H), 8.76 (br s, 1H), 8.09 (dd, $J = 1.2, 7.9$ Hz, 1H), 8.01 (d, $J = 7.9$ Hz, 1H), 7.69 (dd, $J = 1.2, 7.9$ Hz, 1H), 7.66 – 7.61 (m, 1H), 7.57 – 7.52 (m, 1H), 7.49 (d, $J = 7.9$ Hz, 1H), 7.20 – 7.15 (m, 1H), 6.75 (dd, $J = 3.1, 9.8$ Hz, 1H), 6.67 (dd, $J = 3.1, 9.8$ Hz, 1H), 6.32 (dd, $J = 1.8, 9.8$ Hz, 1H), 6.17 (dd, $J = 1.8, 9.8$ Hz, 1H), 4.73 (d, $J = 7.9$ Hz, 1H), 4.40 (dd, $J = 8.5, 10.4$ Hz, 1H), 3.91 (s, 3H), 2.83 (dd, $J = 7.9, 13.4$ Hz, 1H), 2.50 (dd, $J = 10.4, 13.4$ Hz, 1H), 2.39 – 2.29 (m, 1H), 0.98 (d, $J = 6.7$ Hz, 3H), 0.93 (d, $J = 6.7$ Hz, 3H). ^1H COSY NMR: see attached appendix. ^{13}C NMR (75 MHz, CD_3CN): δ 185.2, 164.0, 161.2, 160.9, 154.2, 147.7, 146.0, 135.6, 135.2, 134.2, 134.1, 131.8, 131.0, 130.3, 129.0, 127.5, 126.5, 126.3, 124.4, 123.5, 121.5, 105.8, 79.5, 61.4, 54.4, 52.4, 41.0, 33.5, 19.6, 19.2. ES-MS: calcd. for $\text{C}_{32}\text{H}_{28}\text{BrN}_5\text{O}_9\text{S}$ $[\text{M}+\text{H}]^+$: 738.09, found: 737.70, 739.70. calcd. for $\text{C}_{32}\text{H}_{28}\text{BrN}_5\text{O}_9\text{S}$ $[\text{M}+\text{Na}]^+$: 761.08, found: 759.65, 761.65; calcd. for $\text{C}_{32}\text{H}_{30}\text{BrN}_5\text{O}_9\text{S}$ $[\text{M}+\text{H}]^-$: 736.07, found: 735.85, 737.85.



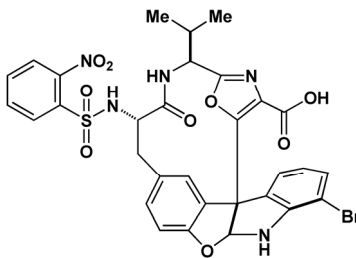
337

337: $[\alpha]_D^{25} = -30.80$ ($c = 0.5$, CHCl_3) $^1\text{H NMR}$ (400 MHz, CDCl_3): δ 8.85 (d, $J = 3.1$ Hz, 1H), 8.79 (br s, 1H), 8.19 (dd, $J = 1.8, 7.3$ Hz, 1H), 8.06 (d, $J = 7.9$ Hz, 1H), 7.86 (dd, $J = 1.8, 7.3$ Hz, 1H), 7.79 – 7.70 (m, 3H), 7.49 (d, $J = 7.9$ Hz, 1H), 7.23 (app t, $J = 7.9$ Hz, 1H), 6.75 (dd, $J = 3.1, 10.4$ Hz, 1H), 6.53 (dd, $J = 3.1, 10.4$ Hz, 1H), 6.23 (dd, $J = 1.8, 10.4$ Hz, 1H), 6.17 (dd, $J = 1.8, 9.8$ Hz, 1H), 4.67 (d, $J = 6.7$ Hz, 1H), 4.53 (dd, $J = 8.5, 11.0$ Hz, 1H), 3.97 (s, 3H), 2.75 (dd, $J = 8.5, 13.4$ Hz, 1H), 2.39 (dd, $J = 11.0, 13.4$ Hz, 1H), 2.19 - 2.10 (m, 1H), 0.84 (d, $J = 6.7$ Hz, 3H), 0.82 (d, $J = 6.7$ Hz, 3H). ES-MS: calcd. for $\text{C}_{32}\text{H}_{28}\text{BrN}_5\text{O}_9\text{S}$ $[\text{M}+\text{H}]^+$: 738.09, found: 737.60, 739.60. calcd. for $\text{C}_{32}\text{H}_{28}\text{BrN}_5\text{O}_9\text{S}$ $[\text{M}+\text{Na}]^+$: 761.08, found: 759.80, 761.80; calcd. for $\text{C}_{32}\text{H}_{30}\text{BrN}_5\text{O}_9\text{S}$ $[\text{M}-\text{H}]^-$: 736.07, found: 735.90, 737.90.



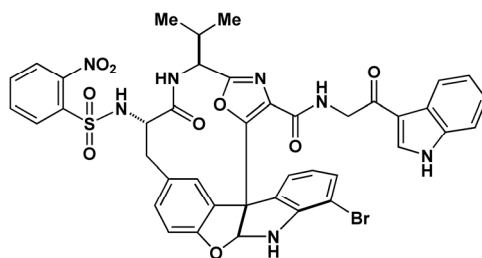
338

338: $^1\text{H NMR}$ (400 MHz, CDCl_3): δ 8.18 – 8.15 (m, 1H), 8.01 – 7.99 (m, 1H), 7.82 – 7.80 (m, 2H), 6.83 – 6.79 (m, 2H), 6.37 – 6.30 (m, 3H), 4.60 (d, $J_{\text{AB}} = 9.2$ Hz, 1H), 4.57 (d, $J_{\text{AB}} = 9.2$ Hz, 1H), 2.86 (dd, $J = 8.8, 13.6$ Hz, 1H), 2.60 – 2.54 (m, 1H). $^{13}\text{C NMR}$ (75 MHz, CDCl_3): δ 184.1, 172.7, 147.6, 147.5, 145.7, 143.7, 134.3, 134.2, 133.6, 130.8, 130.3, 129.5, 52.9, 39.2. ES-MS: calcd. for $\text{C}_{32}\text{H}_{30}\text{BrN}_5\text{O}_9\text{S}$ $[\text{M}-\text{H}]^-$: 363.03, found: 363.00. X-ray crystal data: see attached appendix.



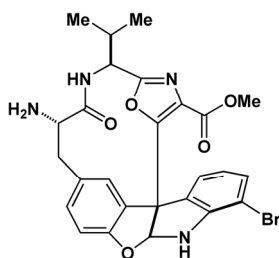
340

Saponification adapted from the Wang procedure.¹⁰⁵ Cyclized core (**334**) (64 mg, 0.09 mmol) was dissolved in a 4:1 MeOH/H₂O (0.5 mL) and cooled to 0 °C. Lithium hydroxide monohydrate (7 mg, 0.16 mmol) was added as a solid to the reaction, and the reaction was then warmed to ambient temperature and stirred for 5 h. The reaction was cooled to 0 °C and slowly neutralized with 1N HCl, which caused a white precipitate to form. The reaction was diluted in EA, washed with H₂O, brine, and dried over Na₂SO₄. The product was used without further purification. **340**: ¹H NMR: see attached appendix.



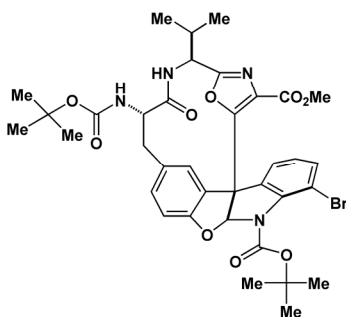
341

Acid **340** (62 mg, 0.09 mmol), and ketotryptamine hydrobromide (27 mg, 0.10 mmol) were dissolved in 0.35 mL of DMF (0.25 M). The reaction was cooled to 0 °C. 4-methylmorpholine was added (20 μL, 0.18 mmol), followed by diethyl cyanophosphonate (DEPC) (17 μL, 0.10 mmol). The reaction was allowed to warm to ambient temperature, and stirred for 3.5 h. The reaction was diluted in ~ 10 mL EtOAc, washed with H₂O and brine, and dried over Na₂SO₄. The solvent was removed *in vacuo*, and flash chromatography with 70% EtOAc/hexane yielded the desired coupled product (53 mg, 67%). **341**: ¹H NMR: see attached appendix.



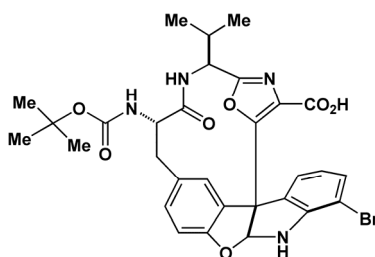
342

Product **334** (1.14 g, 1.54 mmol) was charged to a reaction flask and dissolved in anhydrous DMF (10.2 mL, 0.15 M) under nitrogen to give a yellow solution. Oven dried solid K_2CO_3 (654 mg, 4.73 mmol) was added to the reaction and did not fully dissolve. Thiophenol (0.41 mL, 4.05 mmol) was syringed into the reaction drop-wise. After 2 h the reaction was complete. The homogenous reaction had turned from light yellow to brown. The reaction was diluted with 50 mL EtOAc and washed three times with ~15 mL of a 1:1 mixture of water:brine. The combined colorless aqueous phase was back extracted with EtOAc. The combined bright yellow organic layers were dried over Na_2SO_4 , condensed, and immediately subjected to flash chromatography. The column was initially eluted with dichloromethane to remove the excess thiophenol and non-polar byproducts. The column was then flushed with 10% methanol/dichloromethane to elute the desired compound (73%). **342**: 1H NMR (400 MHz, $CDCl_3$): δ 7.30 - 7.25 (m, 2H), 7.11 - 7.06 (m, 2H), 6.82 (d, J = 8.6 Hz, 1H), 6.75 (d, J = 4.3 Hz, 1H), 6.68 - 6.63 (m, 1H), 5.42 (d, J = 3.7 Hz, 1H), 5.38 (d, J = 9.2 Hz, 1H), 5.12 (dd, J = 4.9, 9.2 Hz, 1H), 3.61 (s, 3H), 3.25 - 3.07 (m, 2H), 2.81 (dd, J = 3.1, 12.2 Hz, 1H), 2.57 - 2.46 (m, 1H), 1.06 (d, J = 6.7 Hz, 3H), 0.90 (d, J = 6.7 Hz, 3H). ES-MS: calcd. for $C_{26}H_{25}BrN_4O_5$ $[M+H]^+$: 553.11, found: 552.90, 554.90; calcd. for $C_{32}H_{30}BrN_5O_9S$ $[M-H]^-$: 551.09, found: 551.00, 553.00.



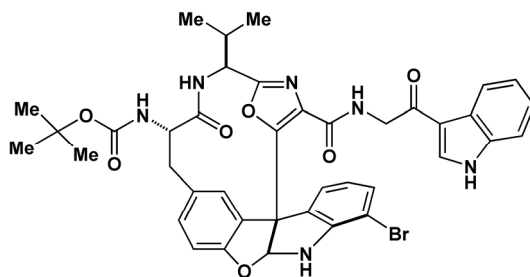
343a

Amine **342** (169 mg, 0.31 mmol) was dissolved in 1.0 mL DMF under nitrogen. Di-*tert*-butyl dicarbonate was added via syringe (0.2 mL, 0.87 mmol). The reaction was cooled to 0 °C. Pyridine was added via syringe (54 μ L, 0.67 mmol), followed by solid DMAP (3.4 mg, 0.03 mmol). The reaction was allowed to warm to ambient temperature and stirred for 3 h. The reaction was diluted in 20 mL EtOAc, washed with water and brine, and dried over Na₂SO₄. Purification with flash chromatography (20%-25% EtOAc/CH₂Cl) provided the bis-Boc protected product (192 mg, 84%). **343a**: ¹HNMR (400 MHz, (CDCl₃): δ 8.38 (s, 1H), 7.55 (d, J = 7.9 Hz, 1H), 7.29 – 7.26 (m, 1H), 7.21 (d, J = 7.3 Hz, 1H), 7.13 – 7.10 (m, 1H), 6.99 (d, J = 8.6 Hz, 1H), 6.74 (br s, 1H), 6.11 (d, J = 6.1 Hz, 1H), 5.22 (d, J = 9.2 Hz, 1H), 4.76 – 4.70 (m, 1H), 3.36 (s, 3H), 3.27 – 3.19 (m, 1H), 2.81 (dd, J = 2.4, 12.8 Hz, 1H), 2.19 – 2.08 (m, 1H), 1.46 (s, 9H), 1.47 (s, 9H), 1.06 – 0.97 (m, 6H). ES-MS: calcd. for C₃₆H₄₁BrN₄O₉ [M+H]⁺: 753.21, found: 753.10, 755.10; calcd. for C₃₆H₄₁BrN₄O₉ [M+Na]⁺: 775.19, found: 775.15, 777.15 calcd. for C₃₆H₄₁BrN₄O₉ [M-H]⁻: 751.20, found: 751.20, 753.20.



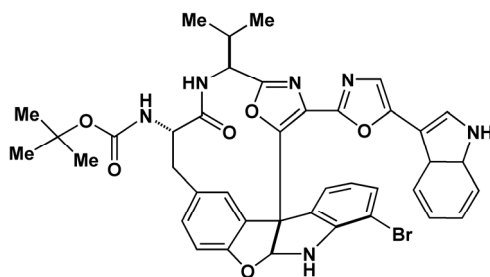
344a

Procedure: see saponification for compound **334**. **344a**: ^1H NMR (300 MHz, CD_3OD): δ 7.39 (br s, 1H), 7.20 (d, $J = 7.3$ Hz, 2H), 7.14 (dd, $J = 1.8, 7.9$ Hz, 1H), 7.06 (br s, 1H), 6.77 (d, $J = 7.9$ Hz, 1H), 6.65 – 6.60 (m, 1H), 4.95 (d, $J = 7.9$ Hz, 1H), 4.07 – 4.00 (m, 1H), 3.19 (t, $J = 12.2$ Hz, 1H), 2.77 (dd, $J = 3.1, 12.8$ Hz, 1H), 2.40 – 2.28 (m, 1H), 1.00 (d, $J = 6.7$ Hz, 3H), 0.95 (d, $J = 6.7$ Hz, 3H).



345a

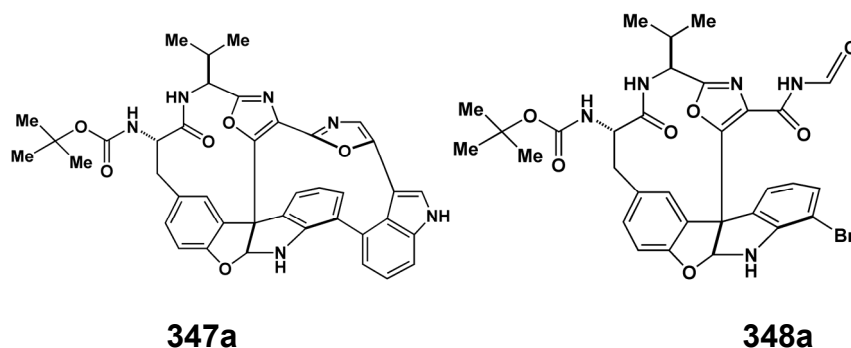
Procedure: see coupling reaction of **338** (65%). **345a**: ^1H NMR: see attached appendix: ES-MS: calcd. for $\text{C}_{40}\text{H}_{39}\text{BrN}_6\text{O}_7$ $[\text{M}-\text{H}]^-$: 793.19, found: 793.05, 795.05.



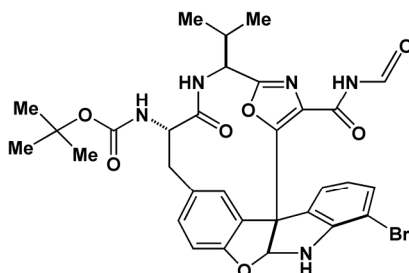
346a

Procedure: see dehydration procedure for compound **355** (62%). **346a**: ^1H NMR (400 MHz, CDCl_3): δ 8.75 (s, 1H), 7.71 (d, $J = 7.3$ Hz, 1H), 7.45 (dd, $J = 1.8, 7.3$ Hz, 1H), 7.30 – 7.20 (m, 2H), 7.14 – 7.06 (m, 2H), 6.85 (d, $J = 3.1$ Hz, 1H), 6.79 (d, $J = 7.9$ Hz, 1H), 6.49 (app t, $J = 7.9$ Hz, 1H), 6.00 (d, $J = 7.9$ Hz, 1H), 5.65 (d, $J = 3.1$ Hz, 1H), 5.29 (d, $J = 9.8$ Hz, 1H), 5.01 (dd, $J = 5.5, 7.9$ Hz, 1H), 4.03 – 3.94 (m, 1H), 3.24 (app t, $J = 12.2$ Hz, 1H), 2.84 (dd, $J = 3.1, 12.2$ Hz, 1H), 2.44 – 2.31 (m, 1H), 1.44 (s, 9H), 1.05 (d, $J = 6.7$ Hz, 3H), 0.94 (d, $J = 6.7$ Hz, 3H). ES-

MS: calcd. for $C_{40}H_{39}BrN_6O_6$ $[M+H]^+$: 779.21, found: 779.05, 781.05; calcd. for $C_{40}H_{39}BrN_6O_6$ $[M-H]^-$: 777.20, found: 775.05, 777.05.

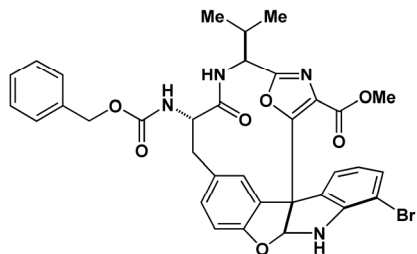


In a quartz photoreactor tube, bisoxazole (**346a**) (11 mg, 0.014 mmol) was dissolved ~ 0.1 THF, followed by dilution in 2.5 mL CH_3CN . 0.8 mL of a 0.06 M aq. lithium acetate (0.04 mmol). The tube was septum sealed and subjected to three rounds of freeze/pump/thaw deoxygenation. The reaction was then placed under nitrogen, and epichlorohydrin (7 μ L, 0.09 mmol) was added via syringe. The tubes were then photolyzed with 300 nm light in a Rayonet photoreactor for 3 h. The faint yellow reaction mixture was then poured into a 1:1 EtOAc/ H_2O partition (15 mL). The organic phase was separated, and the aqueous phase was back extracted once with EtOAc. The combined organic layer were dried over Na_2SO_4 . Preparative TLC (75% EtOAc/hexane) yielded starting material (4 mg, 36%), the undesired byproduct (5 mg, 50%), and only a trace amount of the desired cyclized product (~5%).



348a: 1H NMR (400 MHz, $CDCl_3$): δ 9.17 (d, $J = 9.9$ Hz, 1H), 9.10 (d, $J = 10.6$ Hz, 1H), 7.49 – 7.4m, 1H), 7.31 – 7.28 (m, 1H), 7.15 – 7.10 (m, 2H), 6.95 (d, $J = 4.0$ Hz, 1H), 6.82 (d, $J =$

8.1 Hz, 1H), 6.67 (app t, $J = 7.7$ Hz, 1H), 5.77 (d, $J = 8.4$ Hz, 1H), 5.44 (d, $J = 4.0$ Hz, 1H), 5.15 (d, $J = 8.8$ Hz, 1H), 5.10 (dd, $J = 5.5, 8.8$ Hz, 1H), 3.90 – 3.84 (m, 1H), 3.31 (app t, $J = 12.1$ Hz, 1H), 2.80 (dd, $J = 2.6, 12.1$ Hz, 1H), 2.40 -2.32 (m, 1H), 1.45 (s, 9H), 1.11 (d, $J = 6.6$ Hz, 1H), 0.94 (d, $J = 6.6$ Hz, 1H). ES-MS: $C_{31}H_{32}BrN_5O_7$ [M-H]⁻: 664.14, found: 664.05, 666.05.

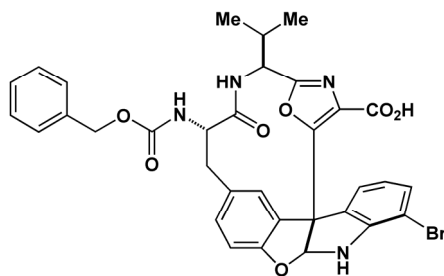


343b

Cyclized product **334** (4.3 g, 5.8 mmol) was charged to a reaction flask and dissolved in anhydrous DMF (29 mL, 0.2 M) under nitrogen to give a yellow solution (it required ~ 5 min for the compound to fully dissolve). Oven dried solid K_2CO_3 (2.47 g, 17.9 mmol) was added to the reaction and did not fully dissolve. Thiophenol (1.54 mL, 1.66 g, 15.0 mmol) was syringed into the reaction over 4 min. After 2 h the reaction was complete. During the reaction, the clear, yellow solution color turned brown and slightly cloudy. The reaction was diluted with 200 mL EtOAc and washed three times with a 100 mL of a 1:1 mixture of water:brine. The combined colorless aqueous phases were back extracted with 100 mL EtOAc. The combined bright yellow organic layers were immediately condensed and subjected to flash chromatography, initially eluting with CH_2Cl_2 to remove nonpolar byproducts and thiophenol. The column was then flushed with 10% methanol/ CH_2Cl_2 to elute the desired compound. The free amine compound was immediately Cbz protected with the following procedure. The crude amine compound was dissolved in anhydrous DMF (29 mL, 0.2M), and the reaction was cooled to 0 °C. N-(benzyloxycarbonyl)-succinimide (1.63 g, 6.4 mmol) was added to the reaction as a solid. 20 min

after addition of Cbz-OSu, the reaction flask was removed for the ice bath and allowed to warm to ambient temperature. The reaction was complete at 90 min. The reaction was diluted with 200 mL EtOAc, and washed with 200 mL water, twice with 100 mL water, three times with 100 mL sat. NaHCO₃ and once with 100 mL brine. The combined aqueous was back extracted once with EtOAc, and the combined organic phases were dried over Na₂SO₄. After condensation, the thick yellow oil was purified via flash chromatography with EtOAc/hexanes (35-50% EtOAc). The desired Cbz protected compound was isolated as an off-white solid (2.96 g, 76% over two steps).

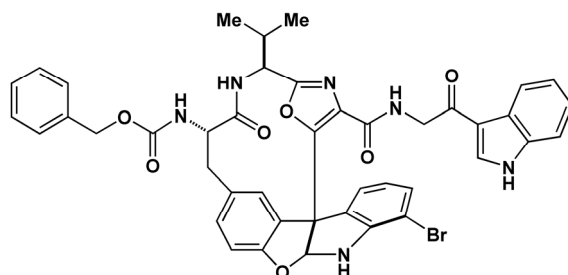
343b: R_f = 0.43 (30% EtOAc/CH₂Cl₂). ¹HNMR (400 MHz, CDCl₃): δ 7.40 – 7.30 (m, 6H), 7.27 – 7.24 (m, 1H), 7.12 (dd, *J* = 1.8, 8.1 Hz, 1H), 7.08 (d, *J* = 7.3 Hz, 1H), 6.82 (d, *J* = 8.4 Hz, 1H), 6.75 (d, *J* = 3.7 Hz, 1H), 6.65 (app t, *J* = 7.7 Hz, 1H), 5.95 (d, *J* = 8.8 Hz, 1H), 5.48 -5.44 (m, 2H), 5.07 – 5.01 (m, 3H), 4.08 – 4.02 (m, 1H), 3.59 (s, 3H), 3.29 (app t *J* = 12.1 Hz, 1H), 2.86 (dd, *J* = 3.7, 12.8 Hz, 1H), 2.51 – 2.43 (m, 1H), 1.02 (d, *J* = 7.0 Hz, 3H), 0.87 (d, *J* = 7.0 Hz, 1H).



344b

Compound **343b** (2.8 g, 4.1 mmol) was dissolved in 60 mL methanol and cooled in an ice bath. A 1.45 M aqueous lithium hydroxide solution was prepared and 14.3 mL was slowly added via addition funnel to the reaction (20.7 g, 21.0 mmol). After addition of the aq. LiOH, precipitate began to form. The reaction was warmed to room temperature, and the minimal amount of methanol (24 mL, final conc. 0.04 M) was added to dissolve the precipitate. After 4.5 h, the

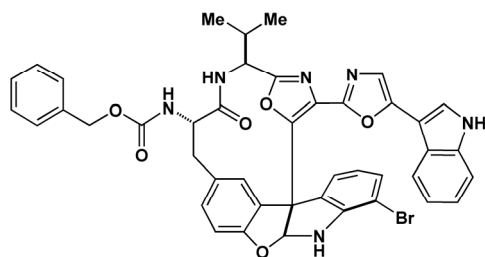
reaction was complete. The reaction was re-cooled in an ice bath and neutralized with a 1.0 N HCl solution. The desired carboxylic acid compound immediately crashed out as a white solid. The reaction was diluted in 400 mL EtOAc and washed once with 100 mL of a 1:1 H₂O:brine solution, once with 100 mL of brine, and finally dried over Na₂SO₄. 2.7 g of the crude carboxylic acid product (98%) was obtained as a white solid and used directly without purification. **344b**: R_f = 0.2 (10% MeOH/CH₂Cl₂). ¹H NMR (400 MHz, CD₃OD, 40 °C): δ 7.38 – 7.27 (m, 6H), 7.23 (dd, J = 0.7, 8.1 Hz, 1H), 7.18 (br s, 1H), 7.15 (dd, J = 0.7, 7.3 Hz, 1H), 6.82 – 6.78 (m, 2H), 6.62 (app t, J = 7.7 Hz, 1H), 5.10 (br s, 2H), 4.92 – 4.88 (m, 1H), 4.20 – 4.14 (m, 1H), 3.24 – 3.16 (m, 1H), 2.84 (dd, J = 3.7, 12.5 Hz, 1H), 2.34 – 2.24 (m, 1H), 1.05 (d, J = 6.6 Hz, 3H), 0.93 (d, J = 6.6 Hz, 3H). ES-MS: calcd. for C₃₃H₂₉BrN₄O₇ [M-H]⁻: 671.11, found: 671.50, 673.20.



345b

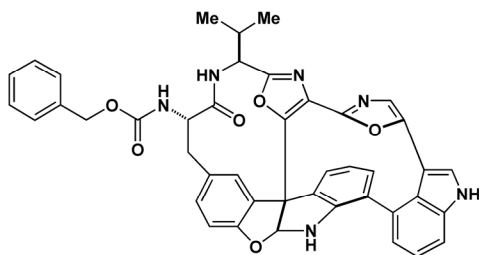
Procedure: see coupling reaction of **338** (86%). **345b**: ¹H NMR (400 MHz, (CDCl₃): δ 9.21 (br s, 1H), 8.27 (d, J = 7.0 Hz, 1H), 7.95 (br s, 1H), 7.76 (d, J = 1.8 Hz, 1H), 7.45 (br s, 1H), 7.36 – 7.30 (m, 5H), 7.26 – 7.24 (m, 1H), 7.16 (d, J = 8.1 Hz, 1H), 7.12 (d, J = 7.3 Hz, 1H), 7.10 (d, J = 4.4 Hz, 1H), 7.05 (d, J = 7.7 Hz, 1H), 8.75 (d, J = 8.1 Hz, 1H), 6.60 – 6.56 (m, 1H), 6.16 (d, J = 8.4 Hz, 1H), 5.74 (br s, 1H), 5.63 (d, J = 8.8 Hz, 1H), 5.12 (dd, J = 5.5, 8.8 Hz, 1H), 4.99 (s, 2H), 4.55 (d, J = 4.8 Hz, 2H), 4.05 – 4.01 (m, 1H), 3.30 (d, J = 12.1 Hz, 1H), 2.80 (dd, J = 2.9, 12.5 Hz, 1H), 2.45 – 2.37 (m, 1H), 1.11 (d, J = 6.6 Hz, 3H), 0.95 (d, J = 6.6 Hz, 3H). ¹³C NMR (75 MHz, CD₃CN): δ 190.2, 173.6, 161.6, 161.4, 157.9, 156.5, 153.0, 148.5, 138.1, 137.5, 134.0,

132.3, 131.9, 131.5, 131.2, 130.4, 129.5, 129.0, 128.9, 128.8, 126.5, 124.5, 123.4, 122.7, 122.5, 121.7, 118.4, 115.3, 113.1, 111.3, 103.0, 102.7, 79.2, 67.1, 62.4, 59.6, 54.0, 46.5, 38.7, 29.8, 19.8, 18.3. ES-MS: $C_{43}H_{37}BrN_6O_7$ $[M+H]^+$: 829.20, found: 829.00, 831.00. calcd. for $C_{43}H_{37}BrN_6O_7$ $[M-H]^-$: 827.17, found: 827.15, 829.15.

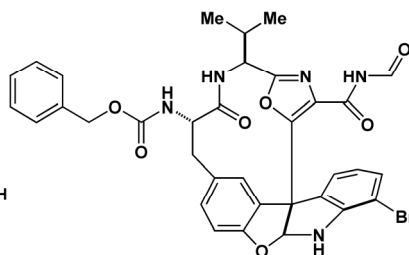


346b

Procedure: see dehydration procedure for compound **355** (74%). **346b**: 1H NMR (400 MHz, CD_3CN): δ 9.81 (br s, 1H), 7.71 (d, $J = 7.3$ Hz, 1H), 7.51 (d, $J = 7.3$ Hz, 1H), 7.40 – 7.31 (m, 6H), 7.27 – 7.16 (m, 4H), 7.06 (br s, 1H), 7.20 (d, $J = 7.9$ Hz, 1H), 6.96 (d, $J = 7.3$ Hz, 1H), 6.91 (d, $J = 3.7$ Hz, 1H), 6.88 (br s, 1H), 6.87 (d, $J = 7.9$ Hz, 1H), 6.40 (d, $J = 7.9$ Hz, 1H), 6.37 (d, $J = 4.3$ Hz, 1H), 6.17 (d, $J = 7.9$ Hz, 1H), 4.80 (t, $J = 7.3$ Hz, 1H), 4.15 – 4.09 (m, 1H), 3.09 (t, $J = 12.2$ Hz, 1H), 2.86 (dd, $J = 3.7, 12.2$ Hz, 1H), 2.19 – 2.15 (m, 1H), 0.98 (d, $J = 6.7$ Hz, 3H), 0.95 (d, $J = 6.7$ Hz, 3H).

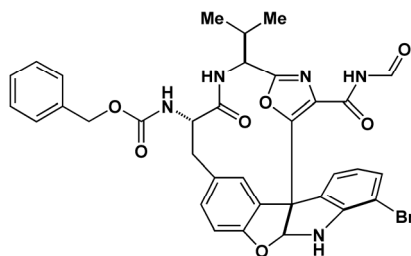


347b

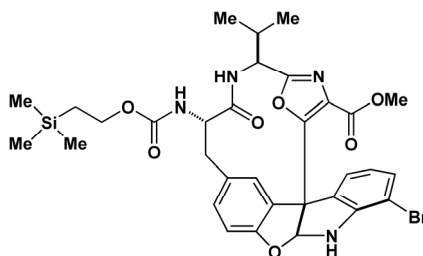


348b

Procedure: see photoreaction of (**347a** and **348a**).



348b: ^1H NMR (400 MHz, CD_3CN): δ 9.42 (d, $J = 9.9$ Hz, 1H), 9.01 (d, $J = 9.9$ Hz, 1H), 7.94 – 7.30 (m, 6H), 7.28 (dd, $J = 1.1, 8.1$ Hz, 1H), 7.19 9.42 (d, $J = 8.1$ Hz, 1H), 7.14 9.42 (d, $J = 7.3$ Hz, 1H), 6.88 (d, $J = 4.0$ Hz, 1H), 6.84 (d, $J = 8.1$ Hz, 1H), 6.70 (d, $J = 8.8$ Hz, 1H), 6.65 (d, $J = 7.3$ Hz, 1H), 6.64 (d, $J = 7.3$ Hz, 1H), 6.21 (d, $J = 4.0$ Hz, 1H), 6.16 (d, $J = 8.1, 1\text{H}$), 4.98 (dd, $J = 5.9, 8.8$ Hz, 1H), 4.04 – 3.99 (m, 1H), 3.17 (app t, $J = 12.1$ Hz, 1H), 2.84 (dd, $J = 3.3, 12.5$ Hz, 1H), 2.30 – 2.22 (m, 1H), 1.03 (d, $J = 6.6$ Hz, 3H), 0.91 (d, $J = 6.6$ Hz, 3H). ^{13}C NMR (75 MHz, CDCl_3): δ 173.5, 162.6, 161.6, 158.1, 156.6, 148.6, 132.6, 132.1, 131.2, 130.9, 130.6, 129.5, 129.0, 128.8, 128.5, 122.8, 121.8, 111.4, 102.7, 102.6, 67.2, 62.7, 59.6, 54.3, 30.0, 19.6, 18.3. ES-MS: calcd. for $\text{C}_{34}\text{H}_{30}\text{BrN}_5\text{O}_7$ $[\text{M}+\text{H}]^+$: 700.14, found: 700.05, 702.05; ES-MS: calcd. for $\text{C}_{34}\text{H}_{30}\text{BrN}_5\text{O}_7$ $[\text{M}+\text{Na}]^+$: 722.12, found: 722.00, 724.00. calcd. for $\text{C}_{34}\text{H}_{30}\text{BrN}_5\text{O}_7$ $[\text{M}-\text{H}]^-$: 698.13, found: 698.00, 700.00.



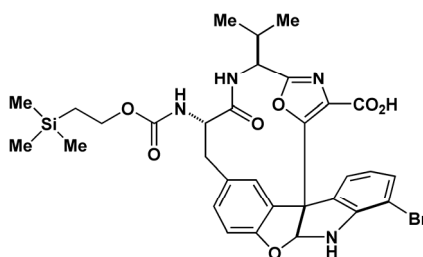
350

Cyclized product **334** (1.14 g, 1.54 mmol) was charged to a reaction flask and dissolved in anhydrous DMF (10.2 mL, 0.15 M) under nitrogen to give a yellow solution (it required ~ 5 min for the compound to fully dissolve). Oven dried solid K_2CO_3 (654 mg, 4.73 mmol) was added to the reaction and did not fully dissolve. Thiophenol (0.41 mL, 442mg, 4.05 mmol) was syringed

into the reaction drop-wise. After 2 h, the reaction was complete. During the reaction, the clear, yellow solution color turned brown and slightly cloudy. The reaction was diluted with 50 mL EtOAc and washed three times with ~15 mL of a 1:1 mixture of water:brine. The combined colorless aqueous was back extracted with EtOAc. The combined bright yellow organic layers were dried over Na₂SO₄, condensed and immediately subjected to flash chromatography, initially eluting with dichloromethane to remove excess thiophenol and nonpolar byproducts. The column was then flushed with 10% methanol/dichloromethane to elute the desired compound.

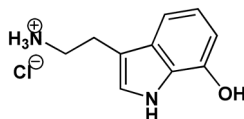
The crude amine compound (assume 851 mg, 1.54 mmol) was dissolved in 9 mL of CH₂Cl₂. K₂CO₃ (285 mg, 2.06 mmol) was dissolved in 9 mL H₂O, and this solution was added to the starting material solution to form biphasic mixture. Stirring vigorously to ensure mixing, 2-(trimethylsilyl)carbon chloridate (Teoc-Cl) (0.43 mL, 2.5 mmol) was added via syringe (fast drop-wise addition). Reaction was complete after 15 min. The reaction was diluted with 50 mL EtOAc and washed with H₂O, brine, and dried over Na₂SO₄. The crude mixture was purified via FC with 35% EtOAc/hex to yield the desired product as an off-white foam (752 mg, 70% two steps). **350**: ¹H NMR (400 MHz, CDCl₃): δ 7.30 (d, *J* = 1.8 Hz, 1H), 7.28 (d, *J* = 0.7 Hz, 1H), 7.27 – 7.25 (m, 1H), 7.12 (dd, *J* = 1.8, 8.1 Hz, 1H), 7.08 (d, *J* = 7.3 Hz, 1H), 6.84 (d, *J* = 8.1 Hz, 1H), 6.76 (d, *J* = 3.7 Hz, 1H), 6.67 – 6.63 (m, 1H), 5.76 (d, *J* = 8.4 Hz, 1H), 5.41 (d, *J* = 3.7 Hz, 1H), 5.26 (d, *J* = 9.2 Hz, 1H), 5.04 (dd, *J* = 4.8, 8.4 Hz, 1H), 4.19 – 4.14 (m, 2H), 4.01 – 3.94 (m, 1H), 3.60 (s, 3H), 3.28 (app t, *J* = 12.1 Hz, 1H), 2.85 (dd, *J* = 3.3, 12.5 Hz, 1H), 2.52 – 2.45 (m, 1H), 1.04 (d, *J* = 7.0 Hz, 3H), 0.99 (d, *J*_{AB} = 7.3 Hz, 1H), 0.98 (d, *J*_{AB} = 7.0 Hz, 1H), 0.89 (d, *J* = 7.0 Hz, 3H). 0.46 (s, 9H). ¹³C NMR (75 MHz, CDCl₃): δ 172.8, 161.3, 160.8, 157.3, 156.1, 156.0, 147.2, 131.6, 130.5, 130.2, 129.6, 128.9, 127.7, 121.5, 121.2, 110.9, 102.5, 102.4, 63.7, 62.3, 58.7, 54.0, 52.2, 38.3, 29.3, 19.3, 17.7, 17.6, -1.74. ES-MS: calcd. for C₃₂H₃₇BrN₄O₇Si [M+H]⁺:

700.14, found: 700.05, 702.05; calcd. for $C_{32}H_{37}BrN_4O_7Si$ $[M+Na]^+$: 722.12, found: 722.00, 724.00. calcd. for $C_{32}H_{37}BrN_4O_7Si$ $[M-H]^-$: 698.13, found: 698.00, 700.00.



351

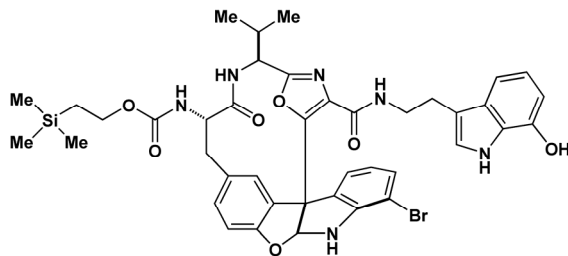
Teoc-protected cyclized core **350** (905 mg, 1.30 mmol) was dissolved in 19 mL MeOH and cooled to 0 °C. An aqueous 1.4 M LiOH solution (4.6 mL, 6.5 mmol, 5 eq) was added dropwise, over 15 min at 0°C. White precipitation began to form upon addition. The reaction was warmed to room temperature, and 4.8 mL methanol added to dissolved precipitate. The reaction was stirred at room temperature for 3 h, then cooled in an ice bath, and slowly neutralized with 6.46 mL of a aq.1 N HCl. A white solid crashed out, which is the desired compound. The reaction was partitioned with 200 mL EtOAc, and the organic layer was washed once with brine and dried over Na_2SO_4 . The reaction was condensed *in vacuo*, producing a white/yellow foam 840 mg (96%), which was carried forward without any purification (**351**).



349

7- Benzyloxytryptamine (Biosynth AG) (399 mg, 1.50 mmol) was charged to a reaction flask under nitrogen and dissolved with 12.7 mL EtOH (0.12 M). 1.53 mL of a 1.0 M HCl in ether solution was added slowly to the suspension over ~10 min. The faintly yellow solution became homogenous and was stirred for 5 min. 20% palladium (II) hydroxide on carbon was added, and the reaction was placed under a H_2 atmosphere. The reaction was stirred for 165 min, and then

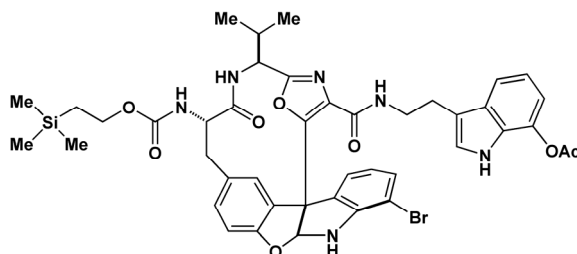
filtered through Celite. The solvent was removed *in vacuo*, and then azeotroped with benzene to remove the EtOH. The light brown foam product (348 mg, ~100%) was dissolved in DMF to give a faint pink solution, protected from light, and used immediately in the subsequent coupling reaction. **349**: $^1\text{H NMR}$ (400 MHz, CD_3OD): δ 7.12 (s, 1H), 7.06 (dd, $J = 0.7, 8.1$ Hz, 1H), 6.89 – 6.85 (m, 1H), 6.54 (dd, $J = 0.7, 7.7$ Hz, 1H), 3.24 – 3.19 (m, 2H), 3.10 – 3.07 (m, 2H).



352

Acid **351** (840 mg, 1.23 mmol) and TBTU (450 mg, 1.4 mmol) were charged to a reaction flask and then dissolved with a 0.1 M solution of 7-hydroxytryptamine hydrochloride in DMF (14.1 mL, 1.41 mmol). The faintly yellow colored solution was cooled in an ice bath, and DIPEA (0.47 mL, 350 mg, 2.7 mmol) was added slowly drop-wise over 5 min. The reaction color turned light green. After 5 min post DIPEA addition, the ice bath was removed and the reaction was allowed to warm to ambient temperature and stir for 1.5 h. The reaction became light orange in color. The reaction was diluted in 100 mL EtOAc and washed once with 80 mL sat. NH_4Cl , twice with 50 mL water. The aqueous layer was back extracted once with 50 mL EtOAc, and the combined organic layers were washed once with 50 mL brine and dried over Na_2SO_4 . FC with 30% EtOAc/benzene yielded a white foam (903 mg, 87%), which was immediately carried forward to the acetylation step to prevent decomposition. **352**: $^1\text{H NMR}$ (400 MHz, CDCl_3): δ 8.21 (br s, 1H), 7.45 (d, $J = 1.5$ Hz, 1H), 7.28 – 7.27 (m, 1H), 7.23 (dd, $J = 0.7, 8.1$ Hz, 1H), 7.14 (d, $J = 7.3$ Hz, 1H), 7.12 (d, $J = 7.7$ Hz, 1H), 7.07 (dd, $J = 1.8, 8.1$ Hz, 1H), 6.99 (app t, $J = 5.9$ Hz, 1H),

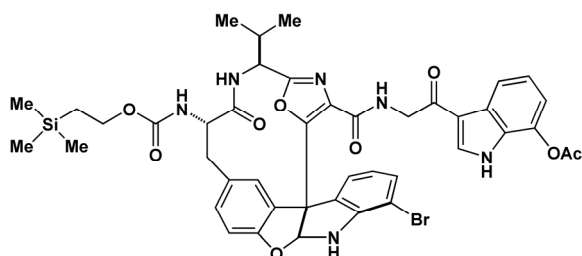
6.90 (d, $J = 2.2$ Hz, 1H), 6.83 (app t, $J = 7.7$ Hz, 1H), 6.79 (d, $J = 8.1$ Hz, 1H), 6.63 (app t, $J = 7.7$ Hz, 1H), 6.56 (d, $J = 7.3$ Hz, 1H), 5.77 (s, 1H), 5.62 (d, $J = 9.5$ Hz, 1H), 5.42 (d, $J = 4.4$ Hz, 1H), 5.29 (d, $J = 9.2$ Hz, 1H), 5.05 (dd, $J = 5.9, 9.2$ Hz, 1H), 4.17 (dd, $J = 7.3, 9.5$ Hz, 2H), 4.00 – 3.85 (m, 1H), 3.65 – 3.55 (m, 2H), 3.33 – 3.27 (m, 1H), 2.97 – 2.93 (m, 2H), 2.80 (dd, $J = 2.9, 12.8$ Hz, 1H), 2.29 – 2.17 (m, 1H), 1.05 (d, $J = 6.6$ Hz, 3H), 1.01 (d, $J_{AB} = 7.3$ Hz, 1H), 0.98 (d, $J_{AB} = 7.0$ Hz, 1H), 0.90 (d, $J = 6.6$ Hz, 3H), 0.48 (s, 9H).



353

Coupled product **352** (903 mg, 1.10 mmol) was dissolved in a 10:1 mixture of CH_2Cl_2 (43 mL):THF (4.3 mL) (0.02 M) to give a colorless solution. The solution was cooled to 0°C . Acetic anhydride (0.50 mL, 540 mg, 5.4 mmol) was syringed in with a slow dropwise addition. Pyridine (0.43 mL, 420 mg, 5.4 mmol) was added in an identical fashion. Following addition, the ice bath was removed, and the reaction was allowed to warm to ambient temperature and stirred for 2.5 h. The reaction was diluted with 200 mL EtOAc and washed 9x with 50 mL sat. NH_4Cl to remove all excess pyridine. The organic layer was then washed twice with 50 mL of brine and dried over Na_2SO_4 . The solvent was removed *in vacuo*, and azeotroped twice from benzene and 3X with CHCl_3 to remove any trace amounts of EtOAc or pyridine. 933 mg (98%) of slightly off-white solid was obtained without the need for further purification. **353**: ^1H NMR (400 MHz, CDCl_3): δ 8.06 (br s, 1H), 7.47 (d, $J = 1.8$ Hz, 1H), 7.43 (d, $J = 7.7$ Hz, 1H), 7.26 – 7.25 (m, 1H), 7.23 – 7.21 (m, 2H), 7.16 (d, $J = 7.3$ Hz, 1H), 7.08 – 7.03 (m, 2H), 6.99 – 6.95 (m, 3H), 6.78 (d, $J = 8.1$ Hz, 1H), 6.67 – 6.62 (m, 1H), 5.78 (d, $J = 9.2$ Hz, 1H), 5.47 (d, $J = 4.4$ Hz, 1H), 5.30 (d, $J = 9.2$

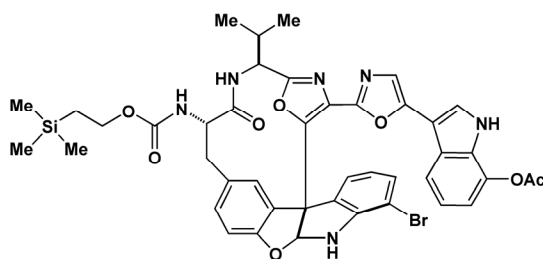
Hz, 1H), 5.08 (d, $J = 7.7$ Hz, 1H), 5.08 (dd, $J = 5.9, 9.2$ Hz, 1H), 4.16 (d, $J_{AB} = 7.7$ Hz, 1H), 4.14 (d, $J_{AB} = 7.3$ Hz, 1H), 3.97 – 3.90 (m, 1H), 3.63 – 3.58 (m, 2H), 3.29 (app t, $J = 12.2$, 1H), 2.98 – 2.94 (m, 2H), 2.81 (dd, $J = 3.3, 12.5$ Hz, 1H), 2.40 (s, 3H), 2.33 – 2.26 (m, 1H), 1.06 (d, $J = 6.6$ Hz, 3H), 1.01 (d, $J_{AB} = 7.3$ Hz, 1H), 0.97 (d, $J_{AB} = 7.0$ Hz, 1H), 0.91 (d, $J = 6.6$ Hz, 3H), 0.43 (s, 9H). ^{13}C NMR (75 MHz, CDCl_3): δ 172.8, 169.4, 160.5, 159.8, 157.0, 156.1, 152.5, 147.5, 136.3, 131.6, 131.5, 130.4, 129.9, 128.6, 128.5, 128.0, 122.8, 121.4, 121.0, 119.5, 116.6, 114.1, 113.4, 110.8, 103.3, 102.3, 63.7, 61.7, 58.6, 53.2, 39.5, 38.3, 28.7, 25.4, 22.3, 21.2, 19.5, 17.8, -1.3.



354

Aceylated product **353** (924 mg, 1.05 mmol) was dissolved in 9:1 THF:H₂O (22.7 mL:2.5 mL) and cooled to 0 °C. DDQ (586 mg, 2.5 mmol) was charged to a dry vial in the open atmosphere and added in one dose as a solid to the reaction. The solution color turned dark brown/black upon DDQ addition. After 15 min stirring at 0 °C, the ice bath was removed and the reaction flask was wrapped in foil. After 13 h stirring at ambient temperature, the reaction color had turned red. The reaction was diluted in 100 mL EtOAc, and washed twice with 50 mL NaHCO₃ and once with 50 mL H₂O. The aqueous layer was back extracted once, and the combined organic layers were washed twice with brine and dried over Na₂SO₄. The lightly red organic layer was condensed, and the crude mixture was purified with FC using EtOAc/dichloromethane as a solvent system. 767 mg of desired oxidized product was obtained as a faint yellow foam in addition to 44 mg of

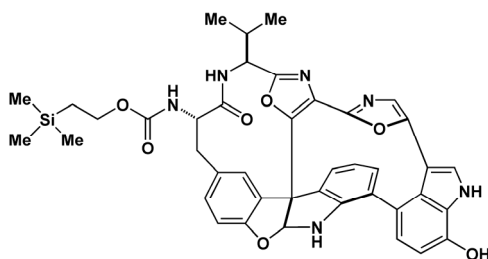
recovered starting material (87% borsm). **354**: ^1H NMR (400 MHz, CDCl_3): δ 9.10 (br s, 1H), 7.94 – 7.91 (m, 1H), 7.80 (br s, 1H), 7.47 (d, $J = 1.8$ Hz, 1H), 7.26 (d, $J = 7.7$ Hz, 1H), 7.24 – 7.13 (m, 4H), 7.08 – 7.06 (m, 2H), 6.78 (d, $J = 8.1$ Hz, 1H), 6.62 (app t, $J = 7.7$ Hz, 1H), 5.86 (d, $J = 8.8$ Hz, 1H), 5.56 (d, $J = 4.0$ Hz, 1H), 5.37 (d, $J = 9.2$ Hz, 1H), 5.13 (dd, $J = 5.1, 9.2$ Hz, 1H), 4.63 – 4.61 (m, 2H), 4.19 – 4.14 (m, 2H), 3.99 – 3.92 (m, 1H), 3.34 – 3.27 (m, 1H), 2.81 (dd, $J = 3.3, 12.5$ Hz, 1H), 2.47 – 2.40 (m, 1H), 2.37 (s, 3H), 1.13 (d, $J = 7.0$ Hz, 1H), 1.02 – 0.96 (m, 5H), 0.05 (s, 9H). ^{13}C NMR (75 mHz, CDCl_3): δ 188.8, 172.8, 171.4, 169.5, 161.0, 160.1, 157.2, 156.2, 153.3, 147.5, 136.4, 132.6, 131.5, 131.4, 130.4, 130.0, 128.8, 128.7, 128.0, 127.9, 123.2, 121.5, 121.0, 119.8, 116.0, 115.3, 103.2, 102.5, 63.8, 61.8, 60.6, 58.9, 53.5, 45.9, 21.2, 19.5, 17.8, 14.4, -1.3.



355

Hexachloroethane (105 mg, 0.44 mmol) and triphenylphosphine (114 mg, 0.43 mmol) were charged to a reaction flask and dissolved in 4.5 mL CH_2Cl_2 . The clear solution was cooled to 0 °C. Triethylamine (86 μL , 62 mg, 0.61 mmol) was added slowly over 2 min. The solution was stirred for 8 min at 0 °C and turned faint yellow. The DDQ product **354** (39 mg, 0.044 mmol) was dissolved in 1.2 mL CH_2Cl_2 and added slowly drop-wise over 7 min. The reaction solution became bright yellow initially, but turned to orange after 10 min of stirring. TLC indicates reaction is complete at 10 min. At 15 min, 250 μL of H_2O was added to the reaction. The reaction was condensed *in vacuo* at low temperature (water bath temperature < 10 °C) to remove

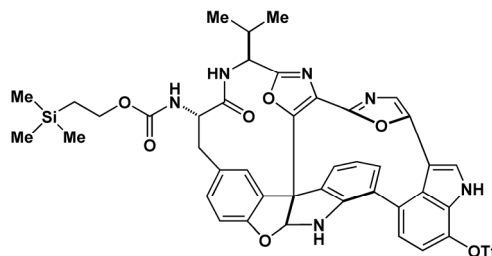
dichloromethane. 10 mL EtOAc was added and the mixture triturated well. A precipitate formed and was filtered off. The reaction was re-condensed, and immediately FC with 60% EtOAc/benzene. A second column was required to remove trace amount of triphenylphosphine oxide. 32 mg of bis-oxazole product (85%) was obtained as a light yellow foam. **355**: ^1H NMR (400 MHz, CD_3CN): δ 9.90 (br s, 1H), 7.61 (d, $J = 8.1$ Hz, 1H), 7.38 (d, $J = 2.7$ Hz, 1H), 7.25 (s, 1H), 7.21 – 7.16 (m, 2H), 7.05 – 6.99 (m, 4H), 6.90 (d, $J = 3.7$ Hz, 1H), 6.87 (d, $J = 8.4$ Hz, 1H), 6.82 – 6.75 (br m, 1H), 6.45 – 6.41 (m, 1H), 6.34 (br s, 1H), 5.88 (br s, 1H), 4.77 (t, $J = 7.3$ Hz, 1H), 4.15 – 4.03 (m, 3H), 3.06 (d, $J = 12.1$ Hz, 1H), 2.83 (dd, $J = 3.7, 12.5$ Hz, 1H), 2.39 (br s, 2H), 2.17 – 2.13 (m, 1H), 0.99 (d, $J = 6.6$ Hz, 3H), 0.96 (d, $J = 6.6$ Hz, 3H). ^{13}C NMR (75 mHz, CDCl_3): δ 172.7, 169.3, 162.4, 157.3, 156.3, 152.0, 149.7, 148.5, 147.2, 136.7, 131.8, 130.3, 129.9, 129.3, 128.9, 128.7, 128.5, 126.6, 123.8, 122.1, 121.5, 117.4, 115.2, 111.0, 105.4, 102.6, 102.2, 63.9, 62.4, 58.7, 54.9, 38.2, 29.9, 19.2, 18.5, 17.8, -1.3.



356

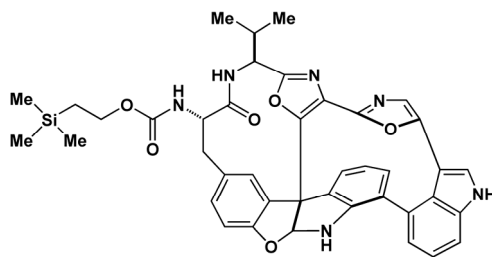
Bis-oxazole **355** (297 mg, 0.34 mmol) was dissolved in 88.5 mL (CH_3CN) in a photochemical reaction apparatus. A 0.035 M solution of aq. LiOH was prepared and 19.5 mL was added to the reaction (0.68 mmol, 2 eq). The solution color turned from very faint yellow to yellow upon addition of the aq. LiOH solution. The reaction was sparged with argon extensively for 20 min, and then photolyzed at 300 nm while sparging gently. The reaction color became light green after 3 h, and the reaction was stopped after 5.5 h. The reaction was diluted in 400 mL EtOAc,

washed twice with 100 mL H₂O, and once with 100 mL brine. The aqueous was back extracted once, and the lightly purple colored combined organic layer was dried over Na₂SO₄. FC with 60% EtOAc/hexanes. Yielded 108 mg (42%) of the desired photocyclized product with 88 mg of recovered deacetylated starting material (58% borsm). **356**: ¹H NMR: See attached appendix. ES-MS: calcd. for C₄₁H₄₀N₆O₇Si [M+H]⁺: 757.27, found: 757.30.



358

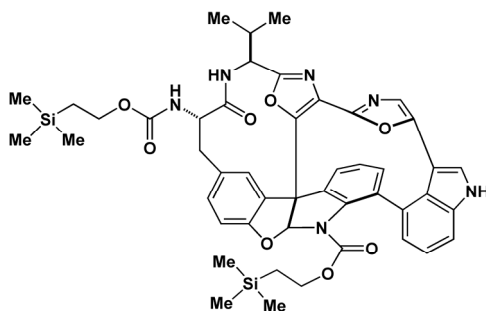
Photochemistry product **356** (110 mg, 0.145 mmol), over dried K₂CO₃ (62 mg, 0.45 mmol), and 4-nitrophenyltrifluoromethanesulfonate (60 mg, 0.221 mmol) were charged to a reaction flask under nitrogen. 2.4 mL of DMF (0.06 M) was added via syringe and the reaction was stirred at ambient temperature. The reaction solution was initially light brown in color with a small amount of K₂CO₃ failing to dissolve. The reaction was stopped after 1 h, and it had turned bright yellow in color. The reaction was diluted in ~15 mL of EtOAc, washed twice with 10 mL water, once with brine, and dried over Na₂SO₄. The condensed yellow/brown oil was purified via FC using EtOAc/hexanes (45-80% EtOAc) solvent. The triflate product (112, 87%) was isolated as a yellow foam. **358**: R_f = 0.35 (60% EtOAc/hexanes). ¹H NMR: see attached appendix ¹³C NMR (75 MHz, CDCl₃): δ 173.2, 161.0, 158.2, 156.3, 154.6, 152.1, 149.3, 146.2, 135.3, 131.9, 130.3, 130.1, 129.9, 129.2, 128.9, 128.8, 128.7, 128.6, 127.5, 126.6, 125.6, 123.2, 122.0, 121.1, 120.9, 120.8, 116.8, 115.1, 110.7, 104.9, 104.4, 63.9, 61.3, 58.9, 55.0, 37.8, 30.4, 19.1, 18.2, 17.8, -1.3.



359

The triflate product **358** (71 mg, 0.080 mmol) was dissolved in 1.2 mL of dry methanol and 0.4 mL EtOAc. Triethylamine (55 μ L, 40 mg, 0.40 mmol) was added drop-wise to the solution at ambient temperature. 20% palladium hydroxide on carbon (7 mg, 0.01 mmol, 13 mol. %) was added and the reaction was placed under a H₂ balloon. Due to low conversion, after 1 h 11 mg more Pd(OH)₂/C (0.017 mmol, 21 mol %) was added, and the reaction was placed under the H₂ balloon again. In the course of the reaction, Pd(OH)₂/C was added three times again: after 2 h, 6 mg (0.01 mmol, 12 mol %), after 3 h, 16 mg (0.025 mmol, 32 mol %), and after 4 h, 6 mg more was added (0.01 mmol, 12 mol %) (total Pd(OH)₂/C used 47 mg, 0.07 mmol, 88 mol %). After 5 h, the reaction was stopped, and filtered through a plug of Celite and washed extensively with EtOAc. Solvent was removed *in vacuo*, and the crude mixture was dissolved in EtOAc. The product was washed twice with water, then brine, and dried over Na₂SO₄. The product was purified via FC using EtOAc/hex. 51 mg (87%) of desired product was obtained. **359**: R_f = 0.13 (60% EtOAc/hexanes). $[\alpha]_D^{25} = -192.8^\circ$ (c = 1.0, CHCl₃), IR (film): 3305, 2946, 1667, 1493, 1250, 1116, 1073, 837, 752 cm⁻¹. ¹H NMR (400 MHz, CD₃OD): δ 7.52 (dd, *J* = 1.1, 8.4 Hz, 1H), 7.45 (s, 1H), 7.38 (d, *J* = 1.5 Hz, 1H), 7.34 (d, *J* = 8.4 Hz, 1H), 7.32 (d, *J* = 8.1 Hz, 1H), 7.19 – 7.15 (m, 2H), 7.52 (dd, *J* = 1.1, 7.3 Hz, 1H), 6.88 (s, 1H), 6.81 (dd, *J* = 1.1, 7.7 Hz, 1H), 6.76 (d, *J* = 8.1 Hz, 1H), 6.61 – 6.57 (m, 1H), 6.33 (s, 1H), 4.90 (m, 1H), 4.25 (dd, *J* = 3.3, 11.7 Hz, 1H), 4.20 – 4.14 (m, 2H), 3.37 (t, *J* = 12.5 Hz, 1H), 2.79 (dd, *J* = 3.3, 12.8, 1H), 2.30 – 2.20 (m, 1H), 1.09 (d, *J* = 6.6 Hz, 3H), 1.05 – 0.97 (m, 5H), 0.07 (s, 9H). ¹³C NMR (75 mHz, CDCl₃):

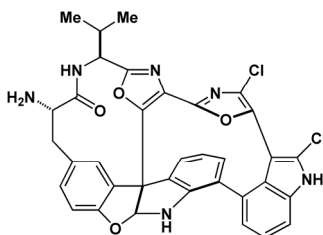
δ 173.1, 160.6, 158.3, 156.3, 154.4, 152.0, 149.3, 147.8, 137.1, 131.3, 130.5, 130.3, 129.8, 128.9, 128.4, 127.7, 127.3, 126.4, 125.0, 124.8, 123.6, 123.0, 122.8, 122.1, 120.8, 111.9, 110.7, 104.7, 63.9, 61.5, 59.0, 54.9, 38.0, 30.3, 19.2, 18.1, 17.9, -1.3. ES-MS: calcd. for $C_{41}H_{40}N_6O_6Si$ $[M+H]^+$: 741.29, found: 741.15. calcd. for $C_{41}H_{40}N_6O_6Si$ $[M+Na]^+$: 763.27, found: 763.20. calcd. for $C_{41}H_{40}N_6O_6Si$ $[M-H]^-$: 739.27, found: 739.20.



360

Teoc diazonamide core **359** (38 mg, 0.05 mmol) was dissolved in 0.5 mL THF and cooled to 0 °C. Freshly distilled triethylamine (TEA) (20 mg, 0.21 mmol) was added via syringe, followed by diallyl pyrocarbonate (12 mg, 0.07 mmol). The reaction was allowed to warm to ambient temperature and monitored by TLC over 5 h, during which more equivalents of diallyl pyrocarbonate were added (total amount 0.33 mmol). The reaction was then re-cooled to 0 °C and TEA was added via syringe (152 mg, 1.5 mmol), followed by Teoc-Cl (137 mg, 0.76 mmol). The reaction was stirred for 90 min. The reaction was then diluted in 15 mL EtOAc and washed three times with sat. aq. NH_4Cl , then H_2O , brine, and dried over Na_2SO_4 . The solvent was removed *in vacuo*. The crude reaction mixture was immediately subject to Alloc deprotection with the following procedure. The product was dissolved in 0.6 mL THF and cooled to 0 °C. Morpholine (22 mg, 0.25 mmol) was added via syringe. 0.1 mL of a 0.02 M $Pd(PPh_3)_4$ stock solution in THF added to the reaction (0.002 mmol). The reaction was stirred at 0 °C for 30 min. Then, the reaction was diluted in EtOAc, washed three times with aq. sat. NH_4Cl , the H_2O and

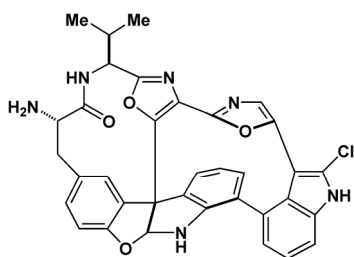
brine, and dried over Na₂SO₄. The reaction mixture was FC, elution with a mixture of 10% CH₃CN/ 5% EtOAc/ 3% MeOH/ 82% CHCl₃ (35 mg, 80%). **360**: $[\alpha]_D^{25} = -221.3$ (c = 1.0, 70% CHCl₃/ 30% CH₃OH), IR (film): 2360, 1757, 1666, 1514, 1250, 1204, 919, 838, 768 cm⁻¹. ¹H NMR (400 MHz, 70% CDCl₃/30% CD₃OD): δ 8.38 (s, 1H), 7.48 (dd, *J* = 1.1, 8.1 Hz, 1H), 7.46 (s, 1H), 7.33 – 7.28 (m, 2H), 7.23 (dd, *J* = 1.5, 7.3 Hz, 1H), 7.20 – 7.16 (m, 2H), 7.10 – 7.03 (m, 3H), 6.78 (s, 1H), 4.51 (d, *J* = 7.7 Hz, 1H), 4.27 (dd, *J* = 3.3, 12.1, 1H), 4.20 – 4.08 (m, 4H), 3.28 (t, *J* = 12.5 Hz, 1H), 2.83 (dd, *J* = 3.3, 12.5 Hz, 1H), 2.03 – 1.97 (m, 1H), 1.03 (d, *J* = 6.6 Hz, 3H), 1.01 – 0.91 (m, 7H), 0.04 (s, 9H), 0.01 (s, 9H). ¹³C NMR (75 MHz, CDCl₃): δ 172.8, 167.3, 163.0, 156.6, 155.1, 153.3, 152.9, 148.6, 146.2, 136.6, 135.5, 134.6, 134.2, 133.8, 131.6, 131.3, 130.0, 129.7, 127.5, 126.7, 126.6, 125.6, 122.8, 122.1, 122.0, 119.9, 111.6, 102.6, 68.1, 63.6, 63.2, 56.3, 56.2, 37.9, 30.1, 29.5, 19.3, 18.6, 17.5, 17.0, -1.8, -1.9. ES-MS: calcd. for C₄₇H₅₀Cl₂N₆O₈Si₂ [M+Na]⁺: 975.25, found: 975.25. calcd. for C₄₇H₅₀Cl₂N₆O₈Si₂ [M-H]⁻: 951.25, found: 951.20.



363

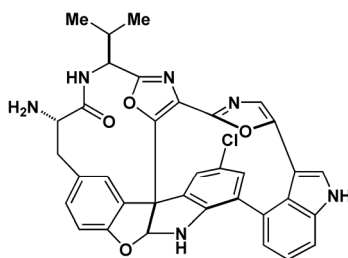
Bis-Teoc compound 360 (8 mg, 0.009 mmol) was dissolved in anhydrous, degassed DMF (0.20 mL) and cooled to 0 °C. A 0.25 M 2,3,4,5,6,6' hexachloro-2,4-cyclohexa-2,4-dienone solution in DMF was prepared under a nitrogen atmosphere. 35 μL (0.009 mmol) of the reagent solution was added to the starting material. The reaction was protected from light and warmed to ambient temperature and stirred for 12 h. Then, the reaction was re-cooled to 0 °C and a fresh reagent solution was prepared. (17 μL, 0.005 mmol) was added to the reaction, and the reaction

was stirred for a further 13 h at ambient temperature. Then the reaction was re-cooled to 0 °C and 10 mg of a DIPEA resin was added to the reaction to remove reagent byproduct. The reaction stirred for 4 h at ambient temperature. The resin was filtered off, and washed with EtOAc. The reaction was diluted in EtOAc, washed with sat. NaHCO₃, H₂O, and brine, and dried over Na₂SO₄. The solvent was removed *in vacuo*, and the crude mixture was purified with preparative TLC (40% EtOAc/benzene). The desired bis-chlorinated product (361) was obtained as an impure mixture. The product was deprotected with the following procedure. The impure product (~1 mg, 0.001 mmol) was dissolved in 0.1 mL DMF. A 0.2 M TASF solution was prepared under nitrogen and added via syringe (0.1 mL, 0.02 mmol). The reaction was stirred for 2 h, diluted in EtOAc, washed three times with NaHCO₃, then brine, and dried over Na₂SO₄. The desired product was purified with preparative TLC (15% MeOH/CH₂Cl₂) to yield the desired compound as a white film (1 mg, 15% two steps). **363**: ¹H NMR: See attached appendix. ES-MS: calcd. for C₃₅H₂₆Cl₂N₆O₄ [M+H]⁺: 665.15, found: 665.15. calcd. for C₃₅H₂₆Cl₂N₆O₄ [M+Na]⁺: 687.13, found: 687.00. calcd. for C₃₅H₂₆Cl₂N₆O₄ [M-H]⁻: 663.13, found: 663.15.



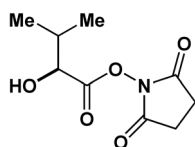
363a

363a: ¹H NMR: See attached appendix. ES-MS: calcd. for C₃₅H₂₇ClN₆O₄ [M-H]⁻: 629.17, found: 629.20.



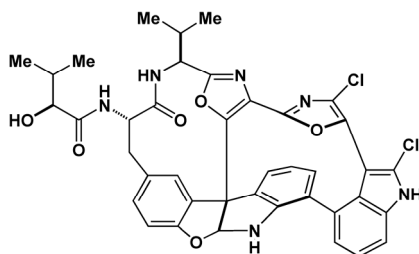
363b

363b: ^1H NMR: See attached appendix. Compound 267 ^1H NMR Spectra. ES-MS: calcd. for $\text{C}_{35}\text{H}_{27}\text{ClN}_6\text{O}_4$ $[\text{M}-\text{H}]^-$: 629.17, found: 629.20.



362

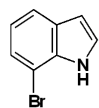
362: ^1H NMR (400 MHz, CDOD_3): δ 4.30 (d, $J = 4.8$ Hz, 1H), 2.84 (s, 4H), 2.20 – 2.10 (m, 1H), 1.08 (d, $J = 6.6$ Hz, 3H), 1.04 (d, $J = 6.6$ Hz, 3H).



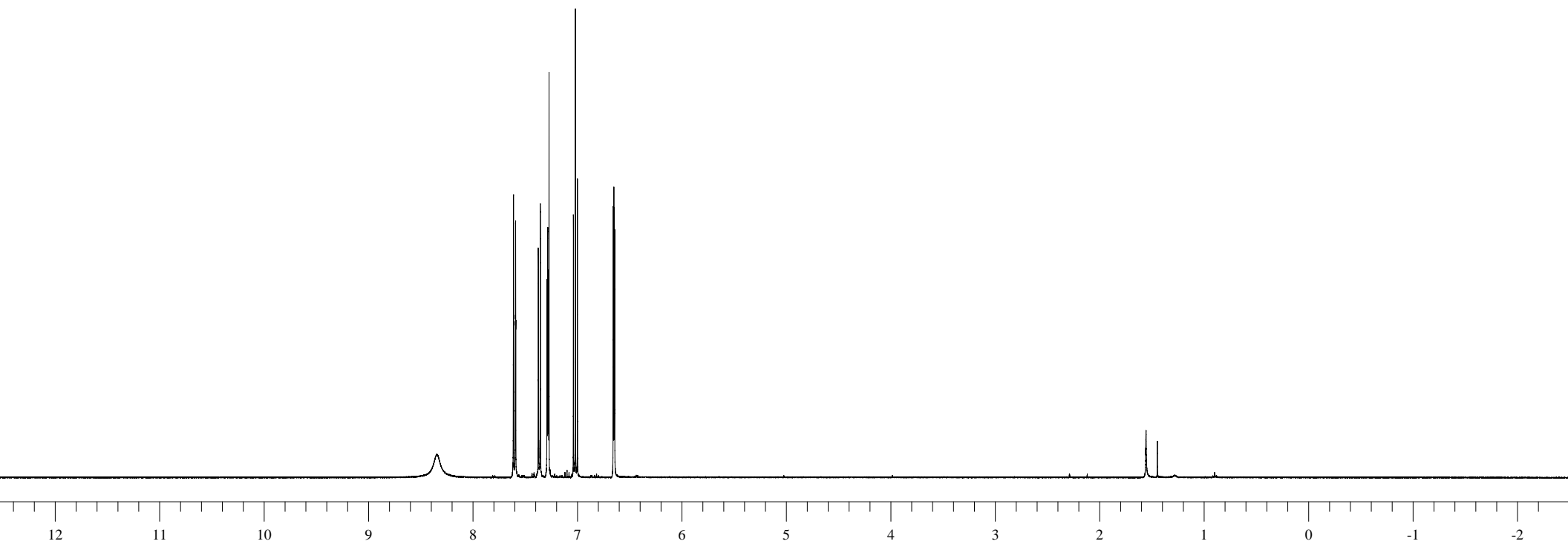
9

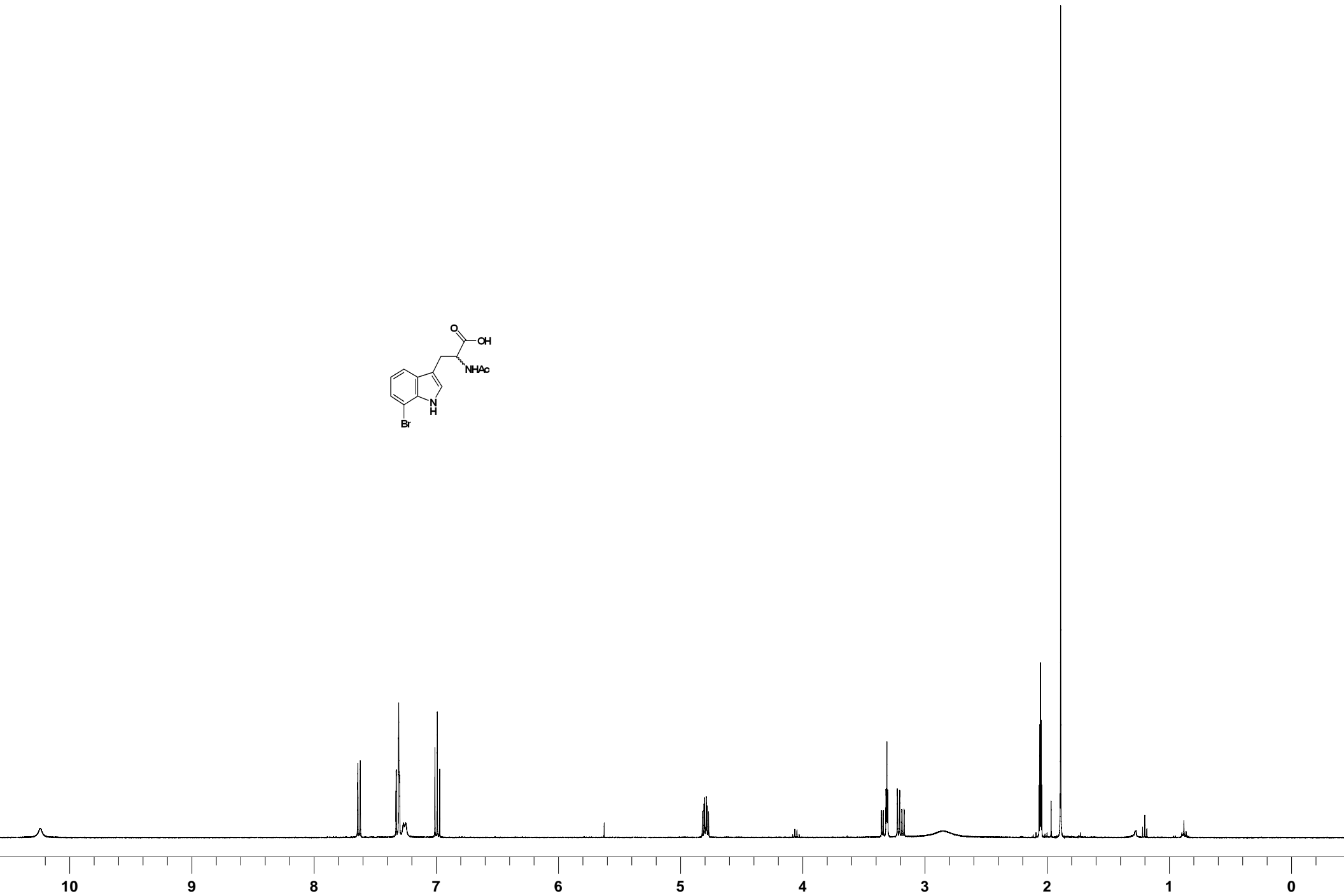
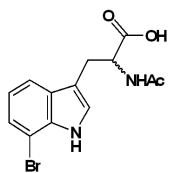
Amine (**363**) (1 mg, 0.001 mmol) was dissolved in 0.1 mL DMF. A small amount of HIV-NHS was added as a solid. The reaction was stirred at room temperature for 2 h, then diluted in EtOAc, washed with NaHCO_3 multiple times, H_2O , and brine, and dried over Na_2SO_4 . The product was purified via preparative TLC ($\text{MeOH}/\text{CH}_2\text{Cl}_2$) to give the desired diazonamide A product (~ 1 mg) as a white film. **9:** ^1H NMR: see attached appendix. ES-MS: calcd. for $\text{C}_{35}\text{H}_{27}\text{ClN}_6\text{O}_4$ $[\text{M}-\text{H}]^-$: 629.17, found: 629.20.

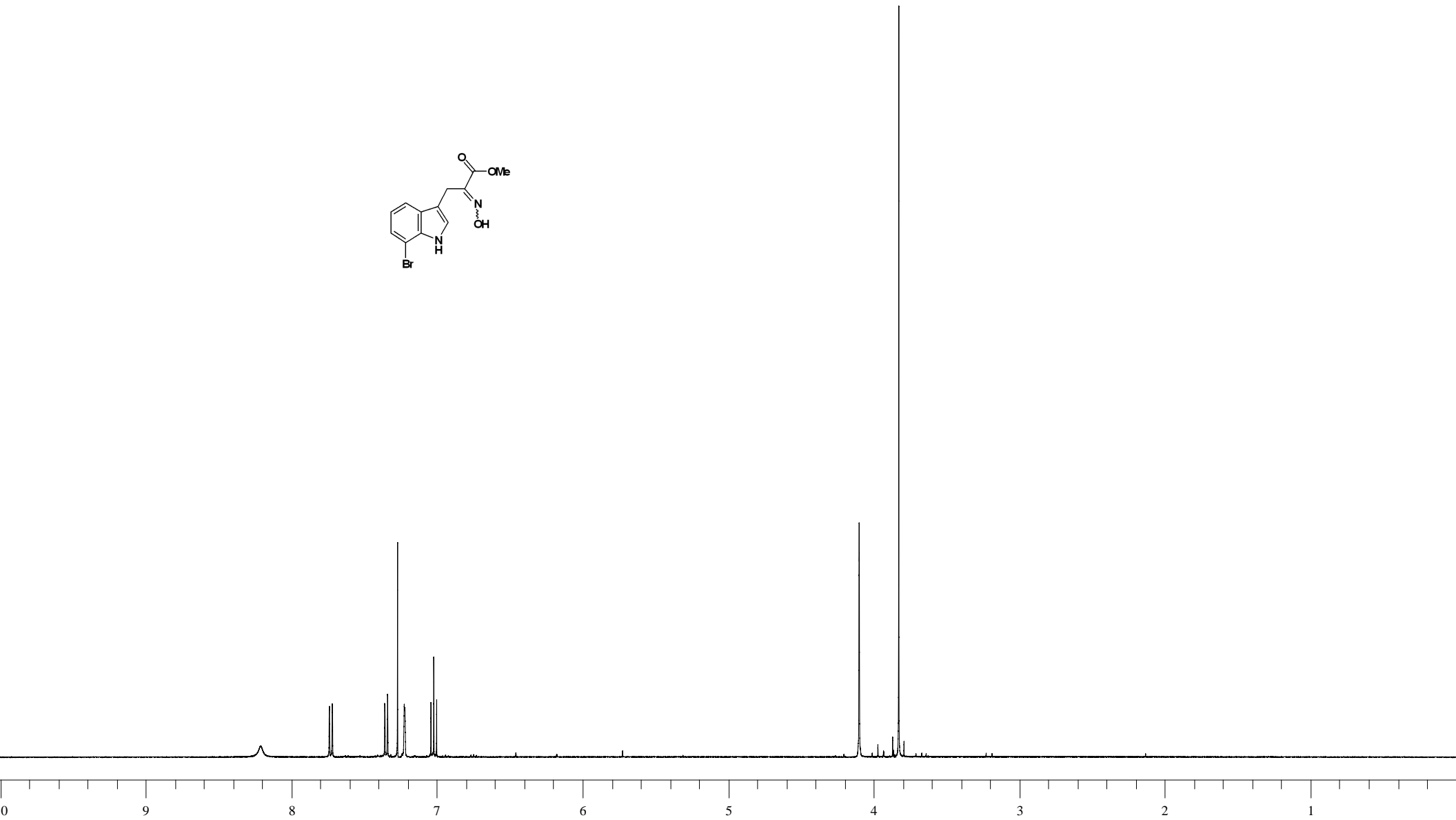
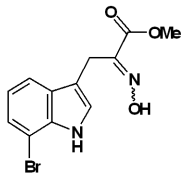
4.7 Chapter 4 Appendix

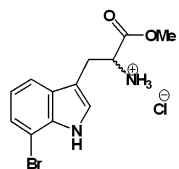


7-bromo-1Hindole

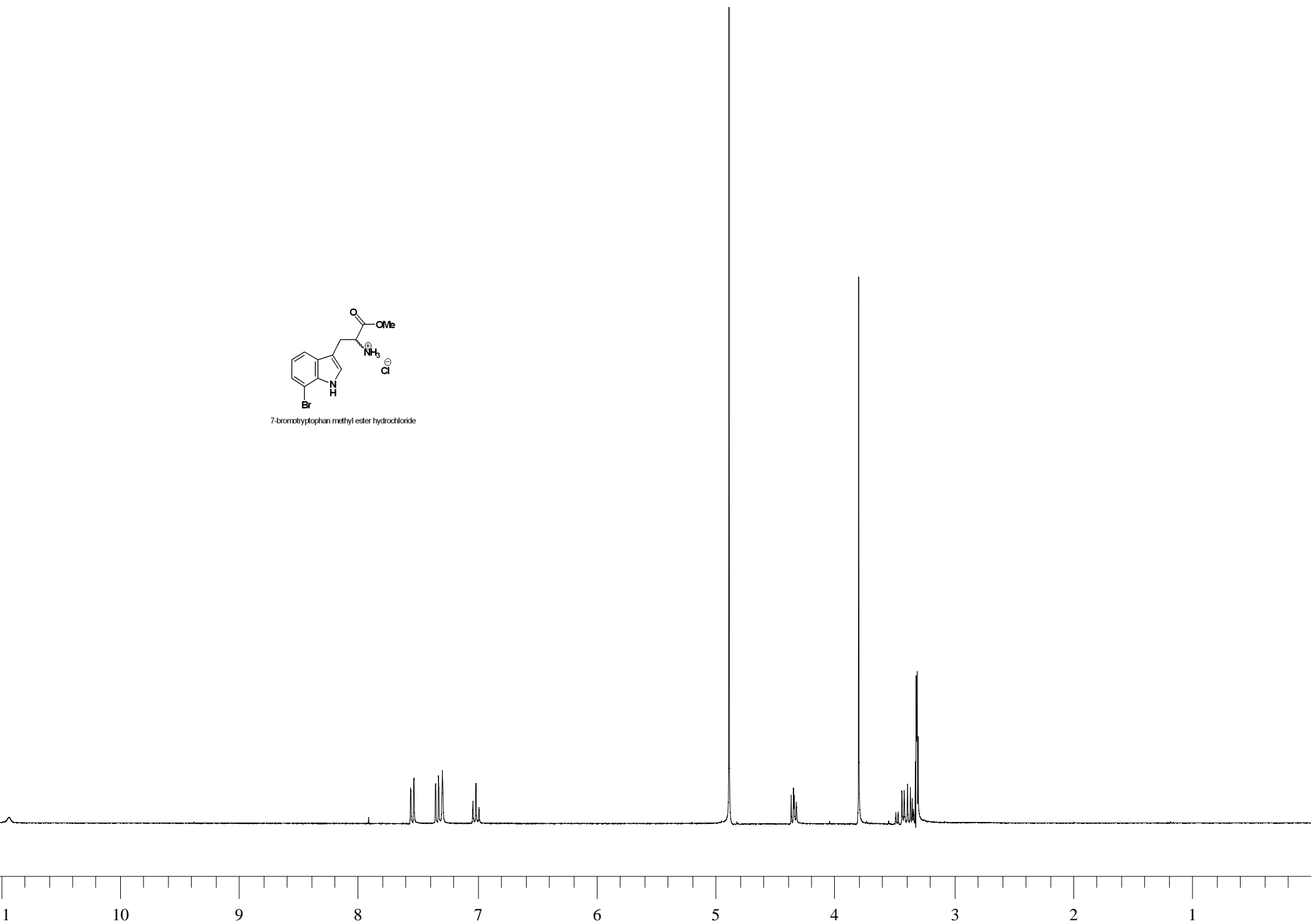








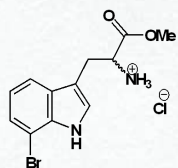
7-bromotryptophan methyl ester hydrochloride



I-AbromotrprOMEH^{Br}

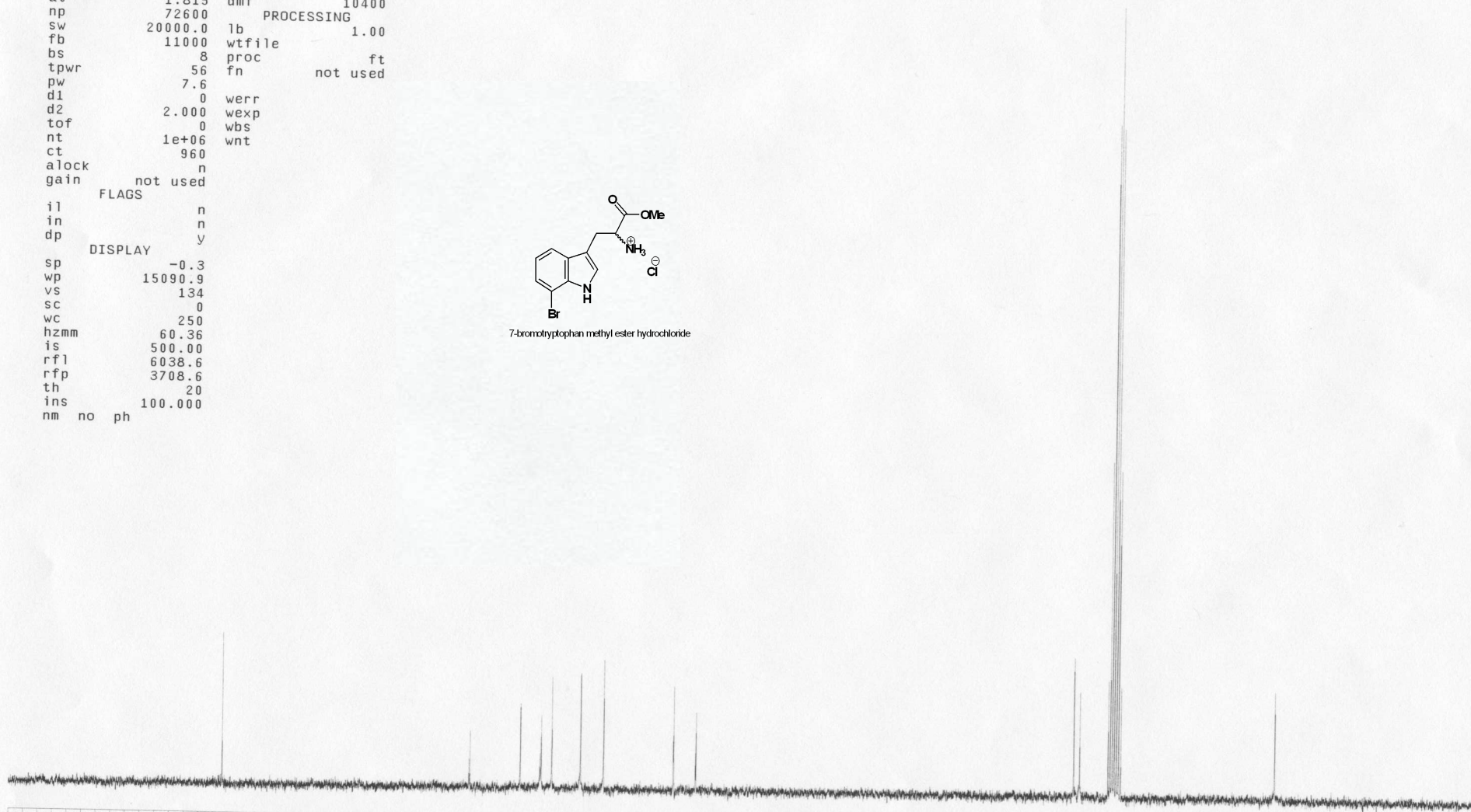
exp1 std13c

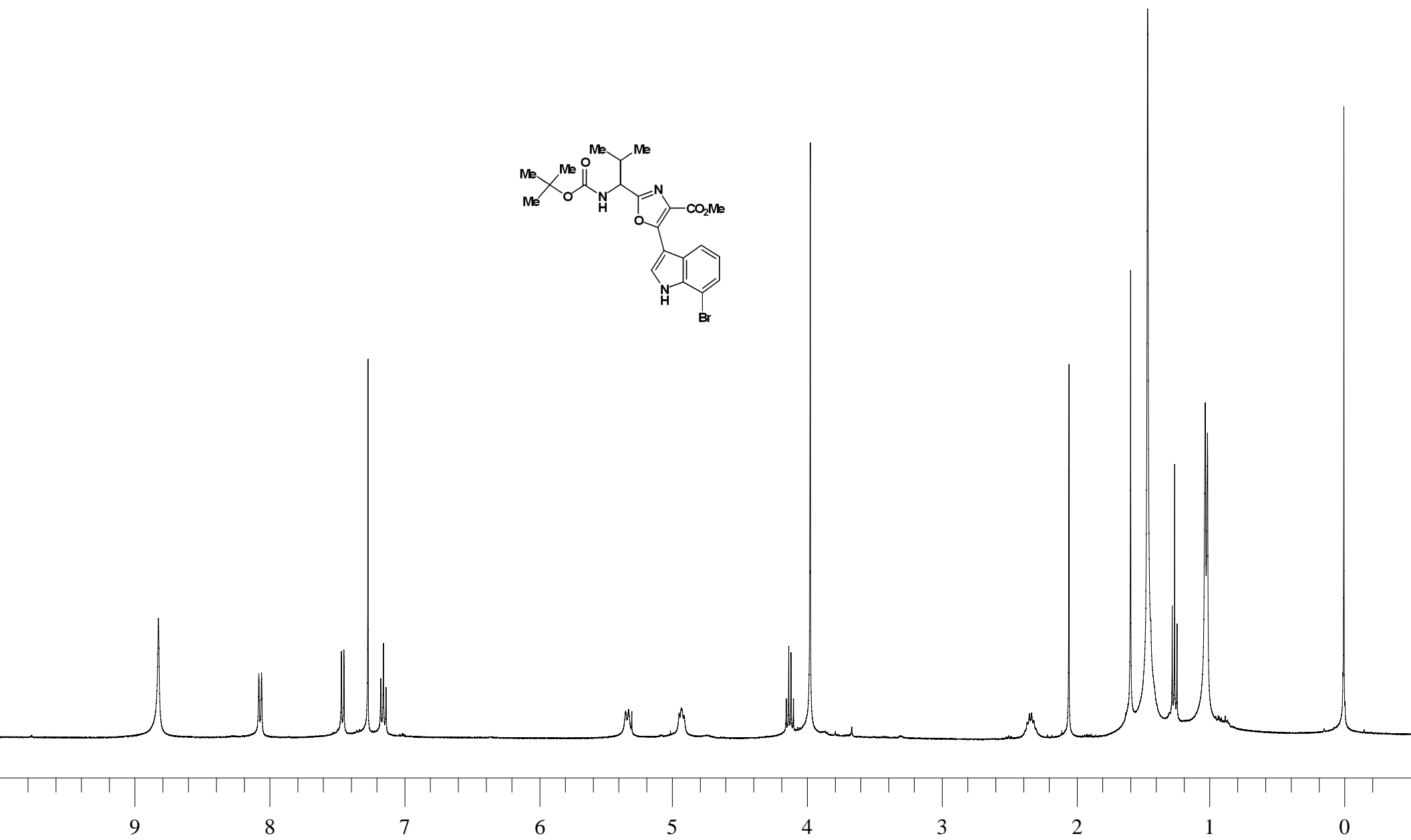
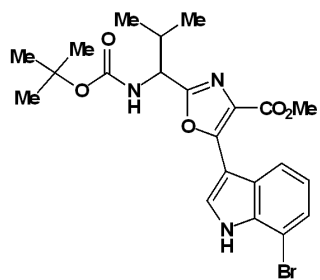
SAMPLE		DEC. & VT	
date	May 12 2003	dfrq	300.079
solvent	CD3OD	dn	H1
file	exp	dpwr	37
ACQUISITION		PROCESSING	
sfrq	75.462	dof	0
tn	C13	dm	nyy
at	1.815	dmm	w
np	72600	dmf	10400
sw	20000.0	lb	1.00
fb	11000	wtfile	
bs	8	proc	ft
tpwr	56	fn	not used
pw	7.6		
d1	0	werr	
d2	2.000	wexp	
tof	0	wbs	
nt	1e+06	wnt	
ct	960		
alock	n		
gain	not used		
FLAGS			
il	n		
in	n		
dp	y		
DISPLAY			
sp	-0.3		
wp	15090.9		
vs	134		
sc	0		
wc	250		
hzmm	60.36		
is	500.00		
rfl	6038.6		
rfp	3708.6		
th	20		
ins	100.000		
nm	no ph		

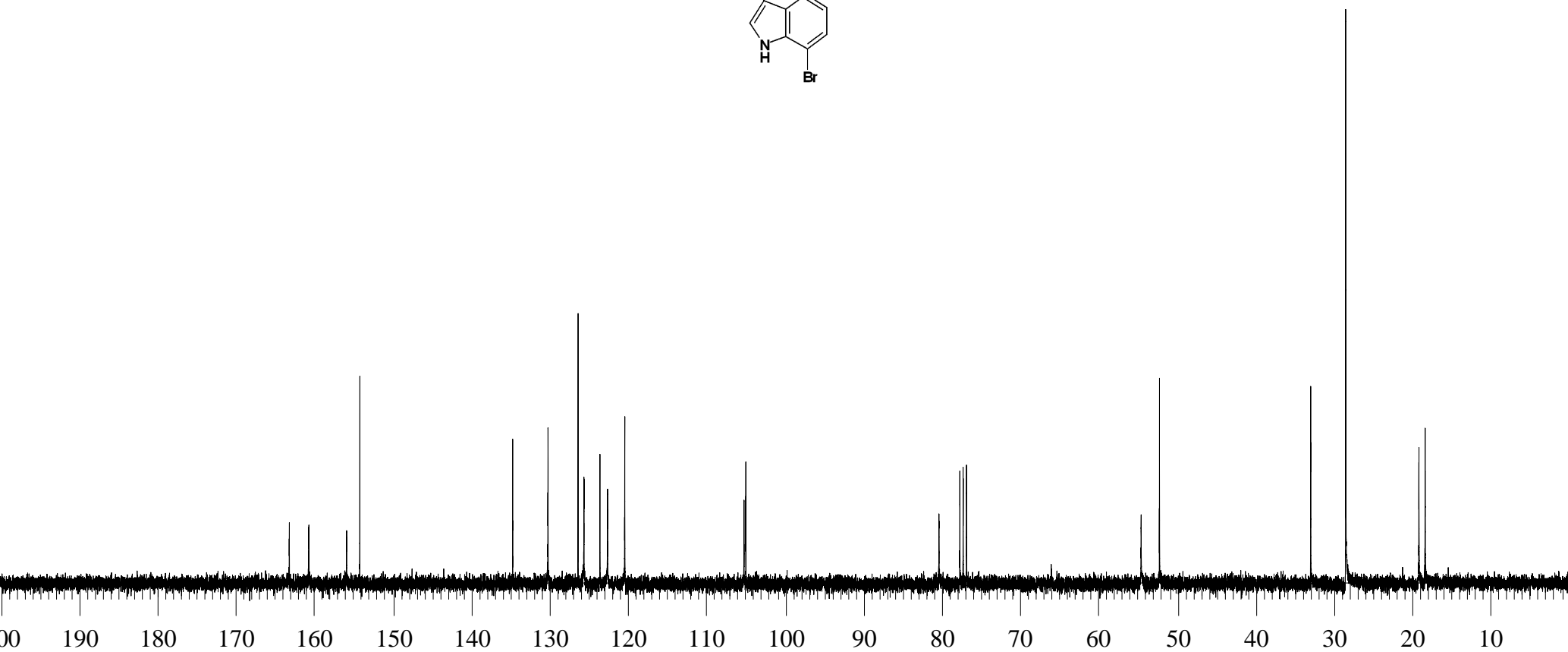
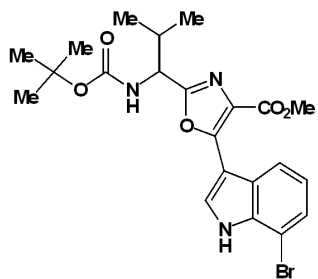


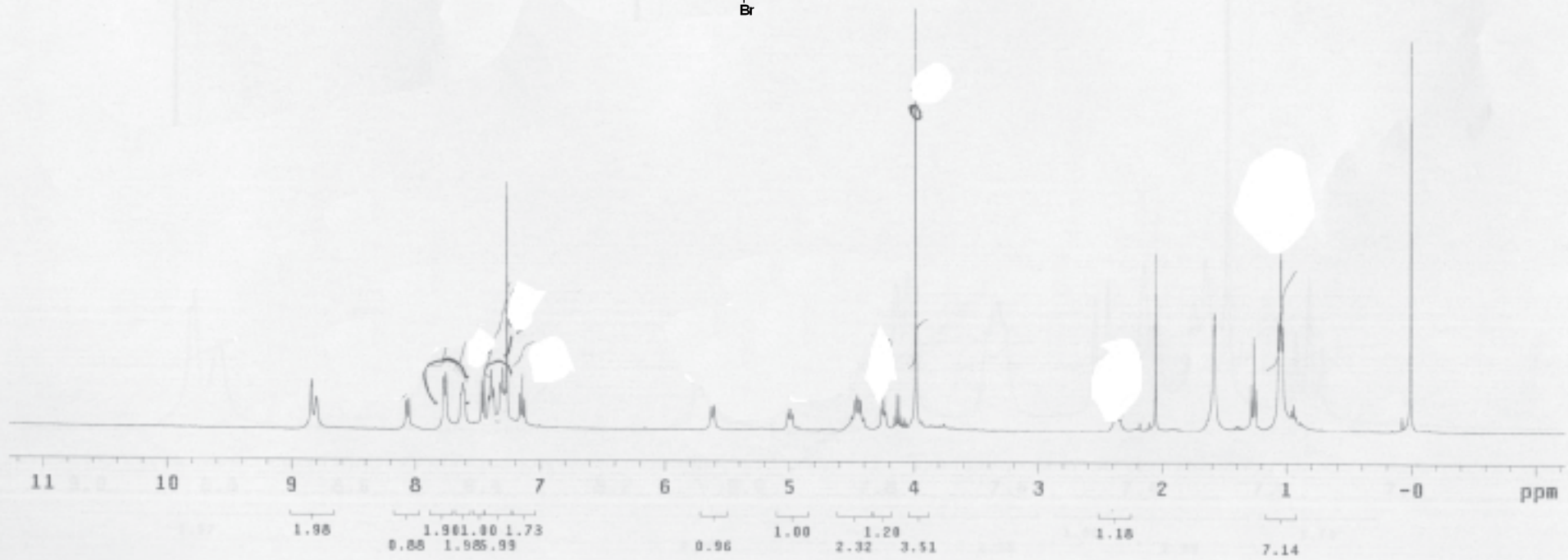
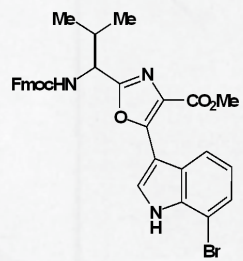
7-bromotryptophan methyl ester hydrochloride

180 160 140 120 100 80 60 40 20 ppm

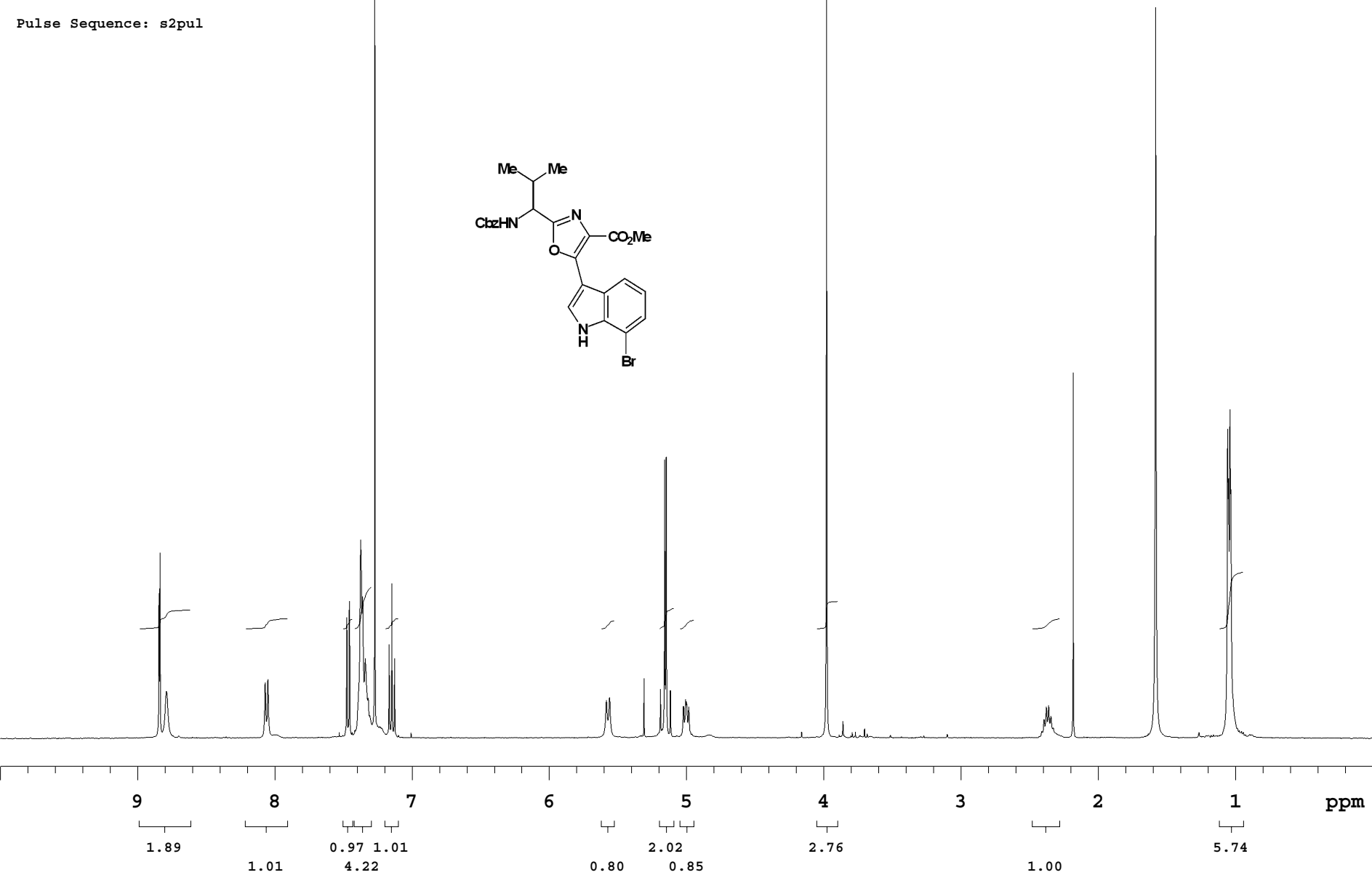
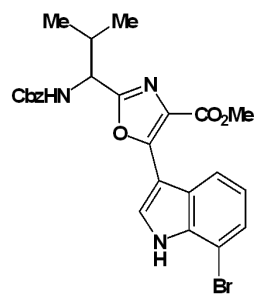


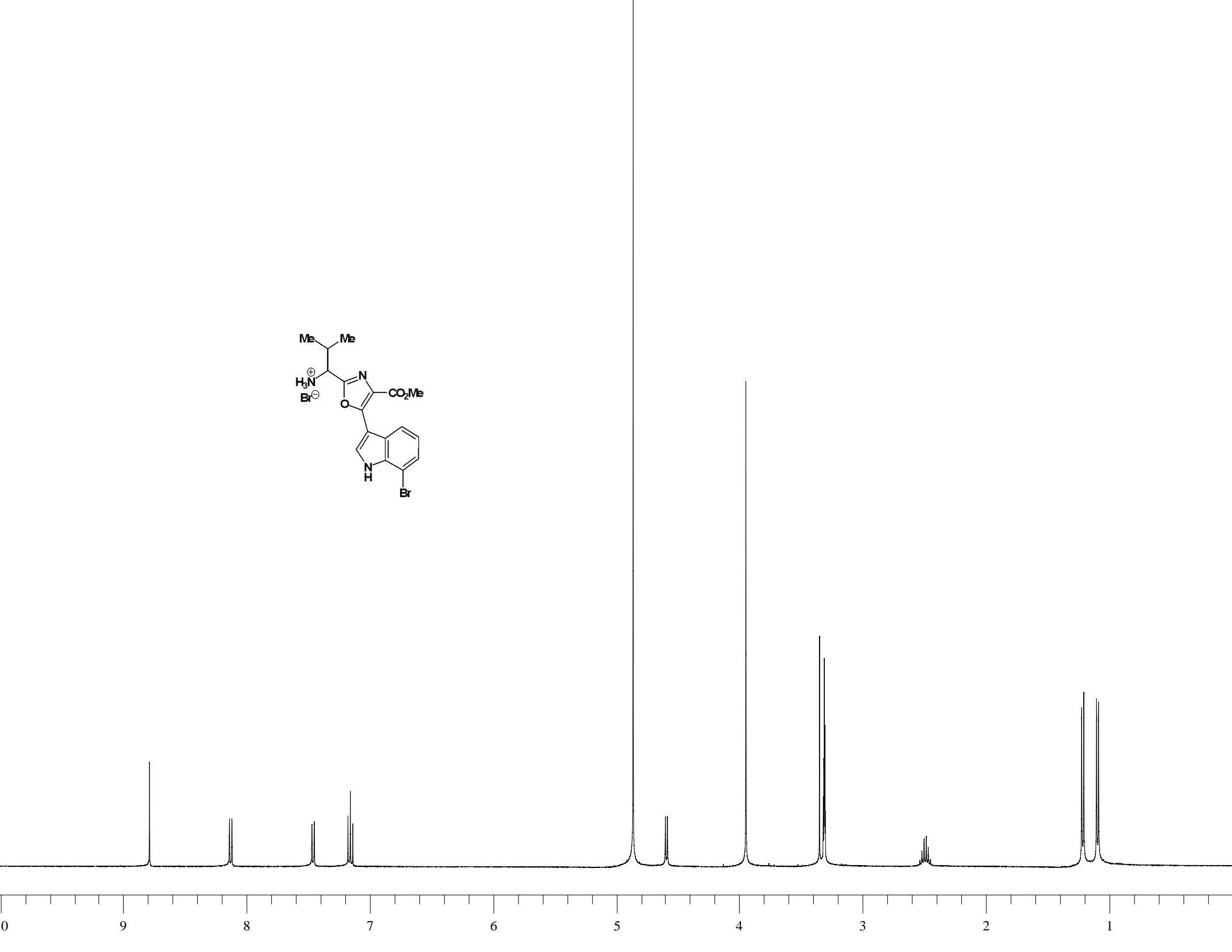
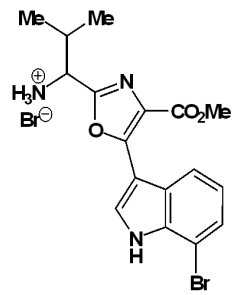


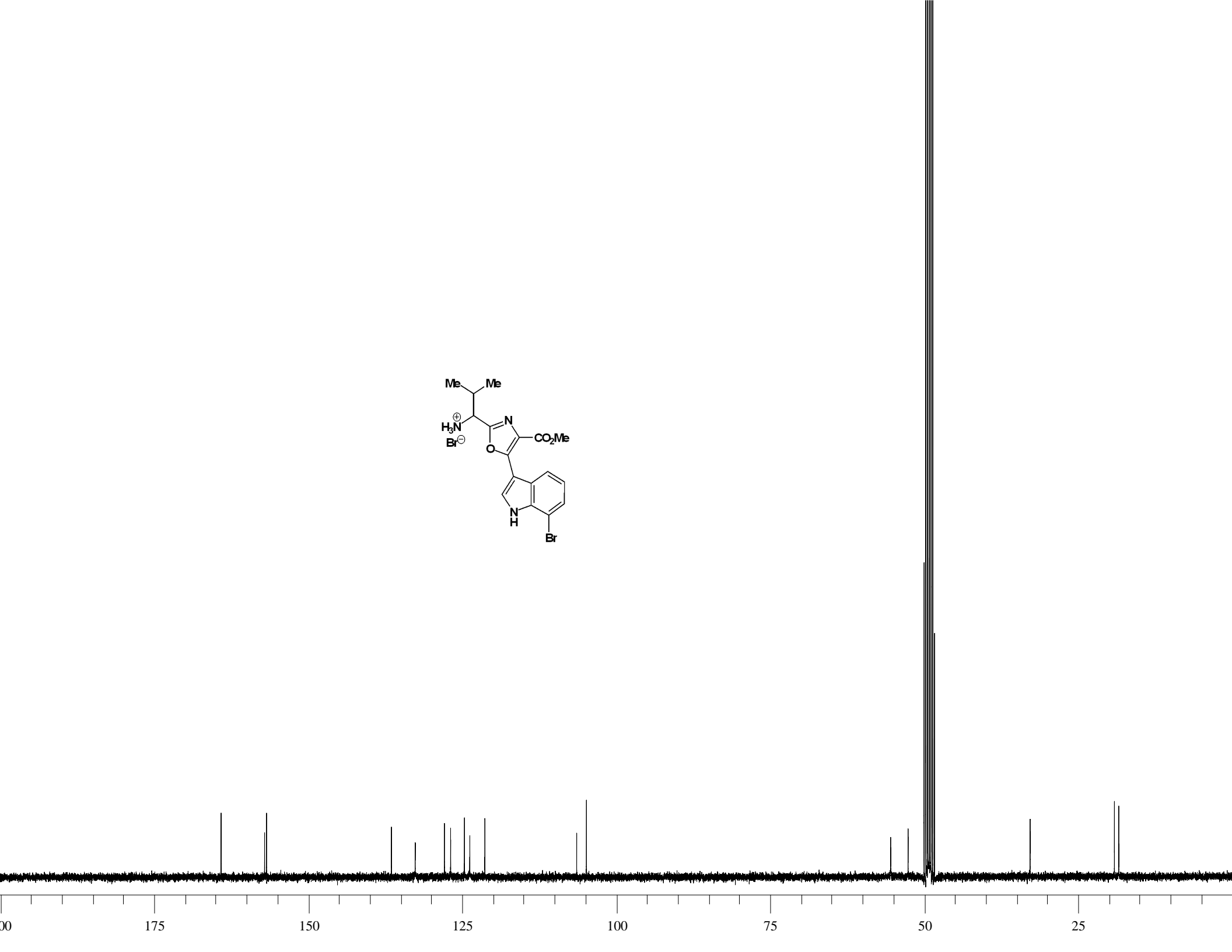
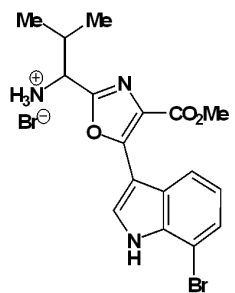


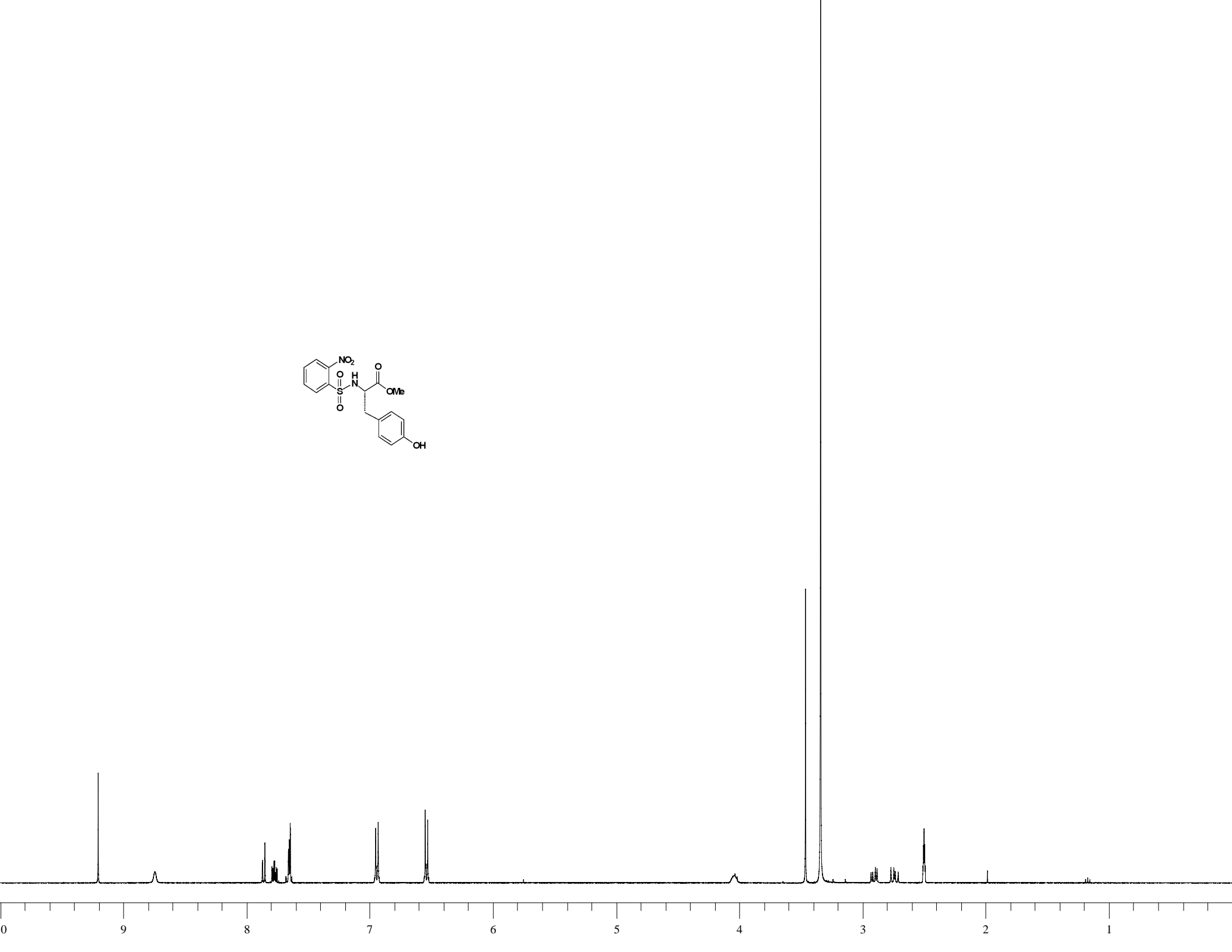
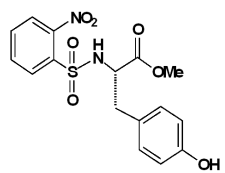


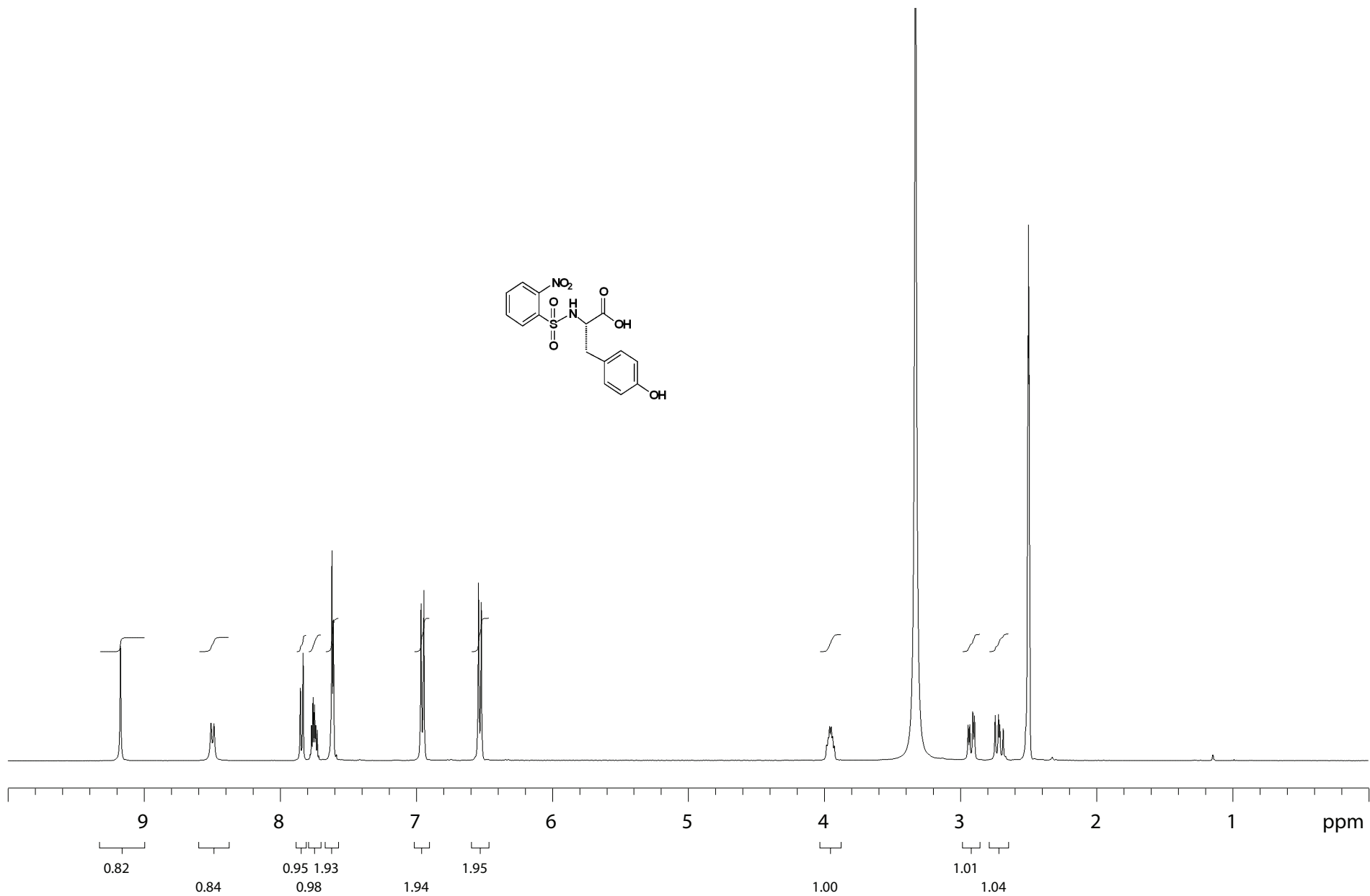
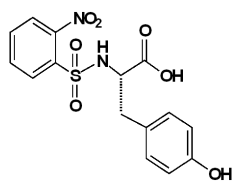
Pulse Sequence: s2pul

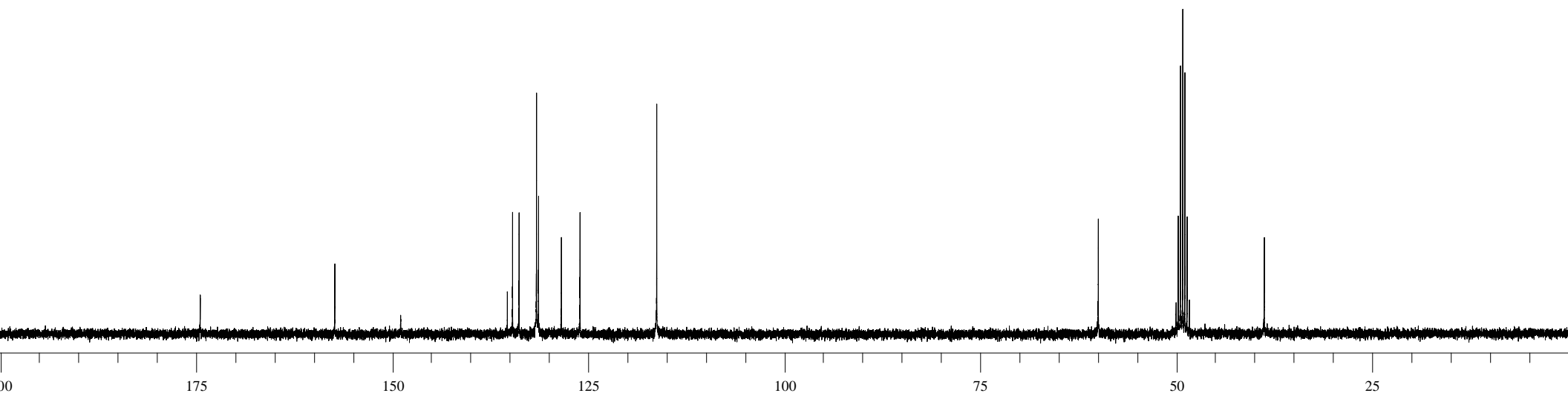
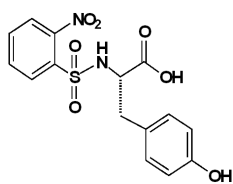






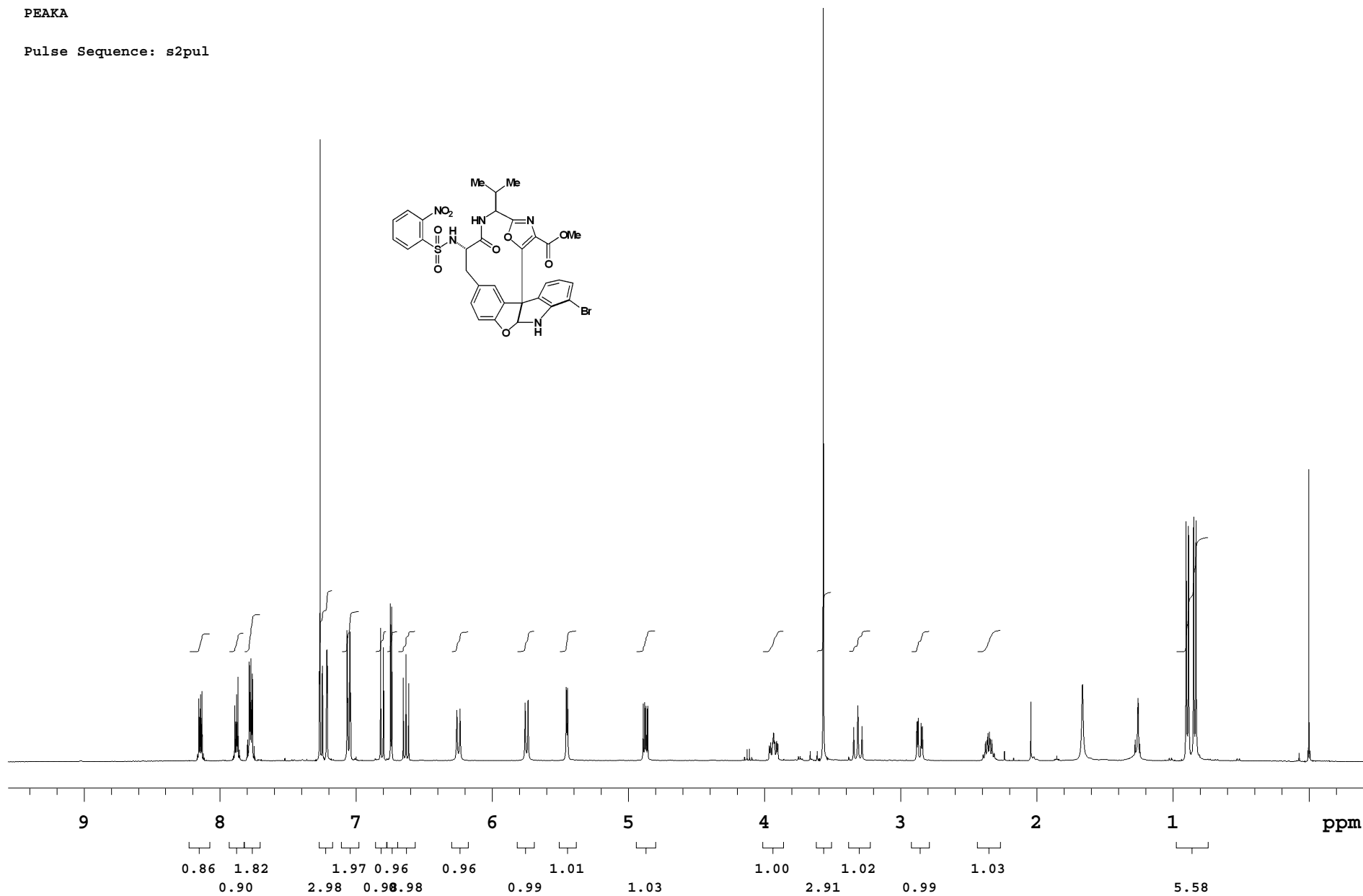
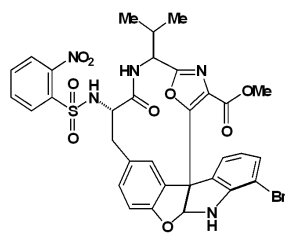






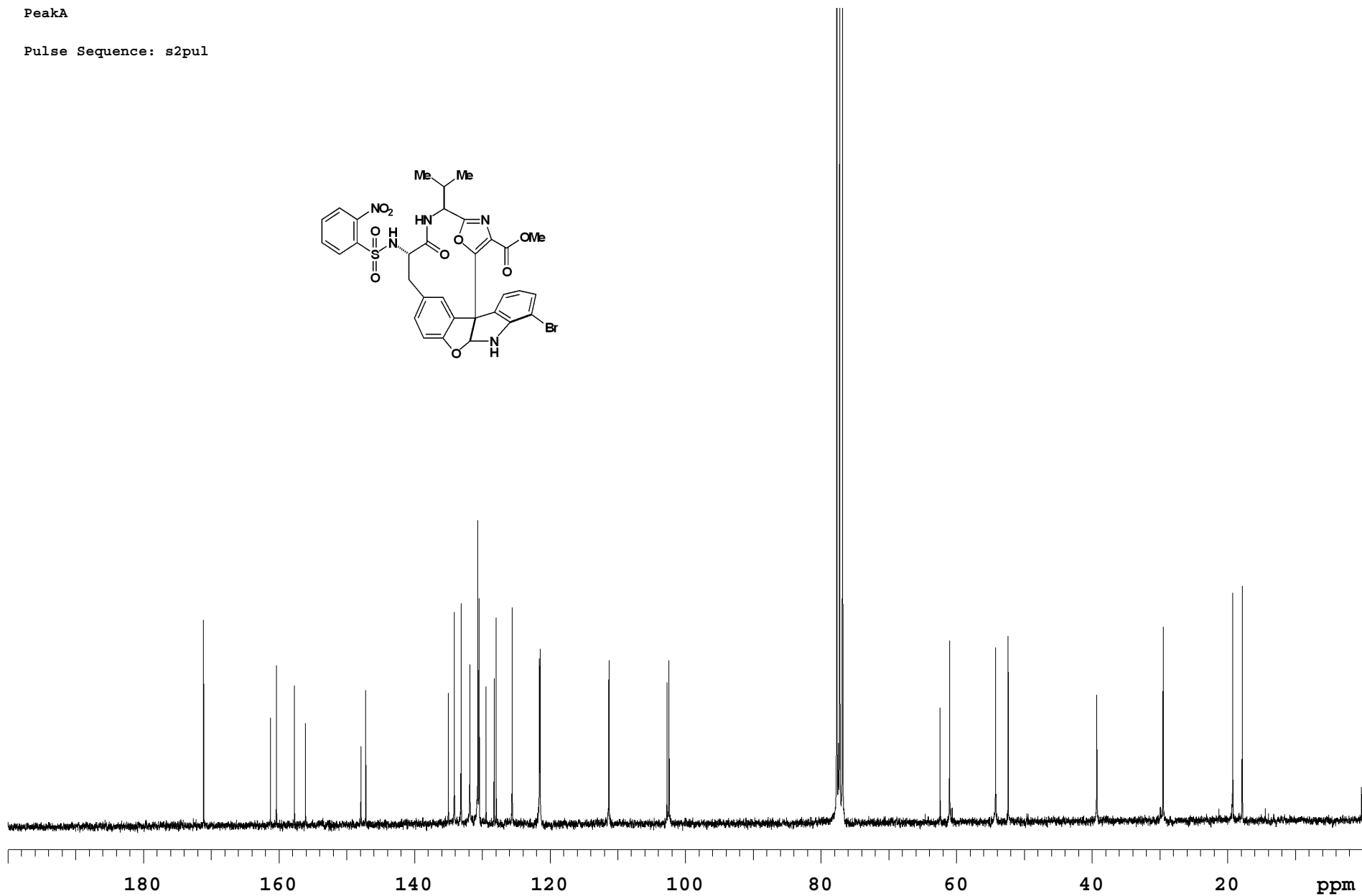
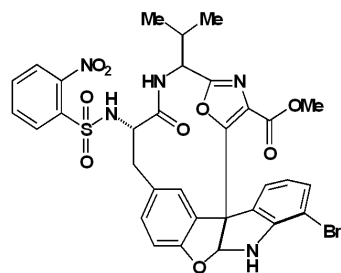
PEAKA

Pulse Sequence: s2pul



PeakA

Pulse Sequence: s2pul

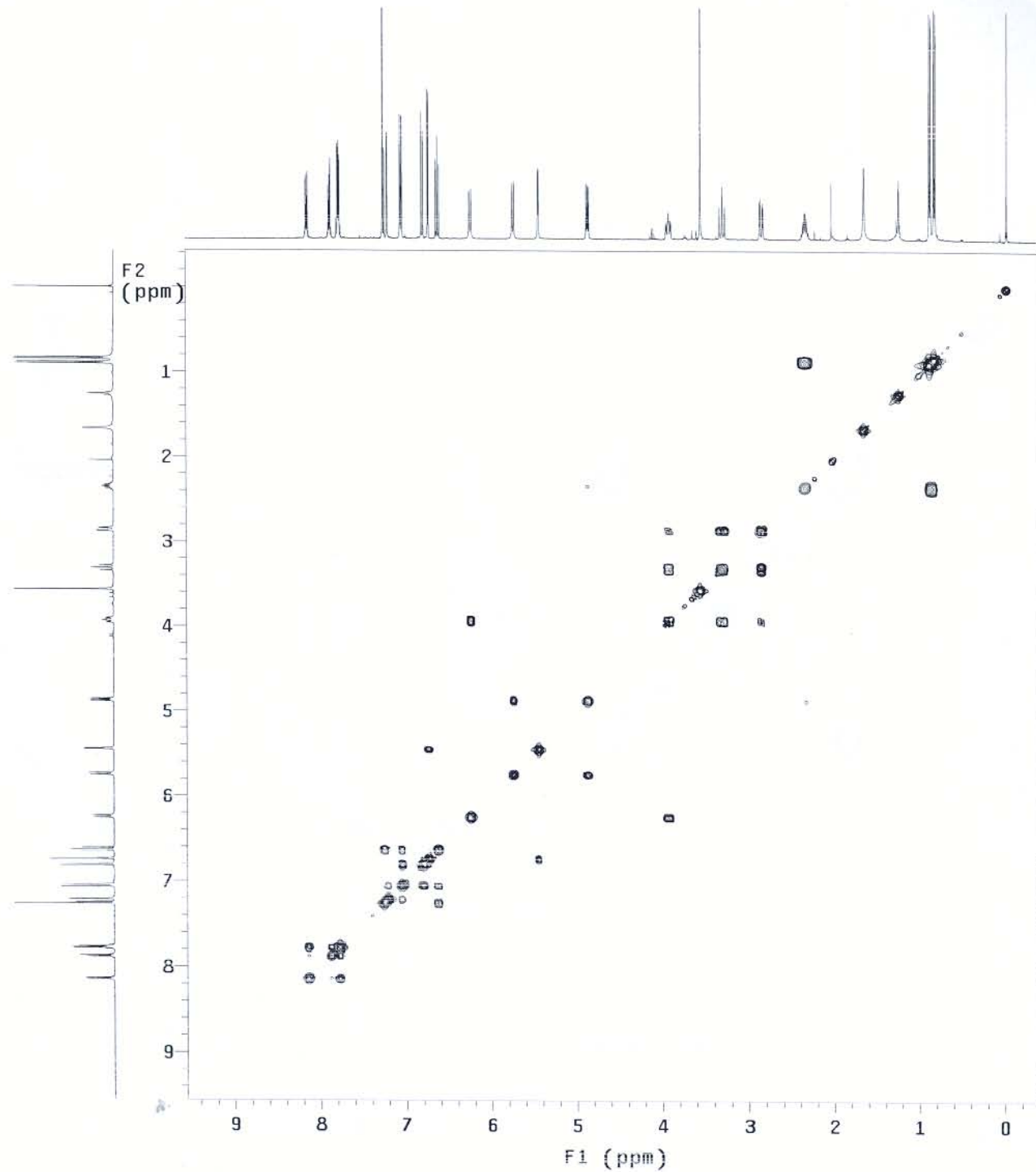
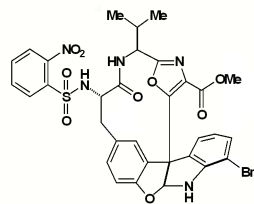


PEAKA

Pulse Sequence: relayh

Solvent: CDC13
Ambient temperature
File: PEAKACOSY
INOVA-400 "peie400"

Relax. delay 1.000 sec
COSY 90-90
Acq. time 0.128 sec
Width 4000.0 Hz
2D Width 4000.0 Hz
8 repetitions
256 increments
OBSERVE H1, 399.7792995 MHz
DATA PROCESSING
Sine bell 0.064 sec
F1 DATA PROCESSING
Sine bell 0.032 sec
FT size 1024 x 1024
Total time 39 min, 57 sec



N15 Gradient HSQC

Pulse Sequence: gNhsqc

Solvent: CDCl3

Temp. 25.0 C / 298.1 K

INOVA-500 "saturn500"

Relax. delay 1.000 sec

Acq. time 0.064 sec

Width 1906.8 Hz

2D Width 2200.0 Hz

2048 repetitions

2 x 48 increments

OBSERVE H1, 499.6953661 MHz

DATA PROCESSING

Line broadening 10.0 Hz

Gauss apodization 0.100 sec

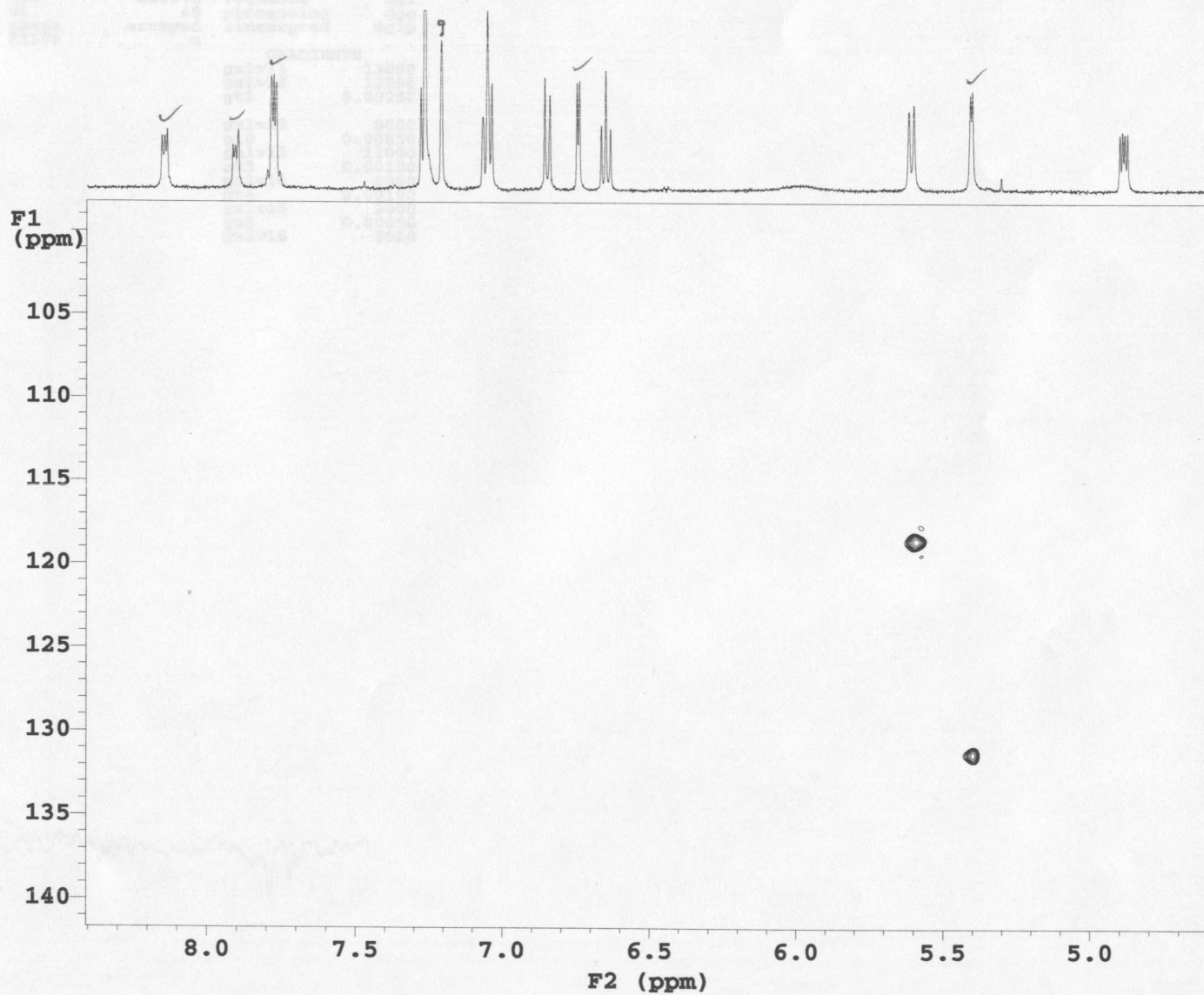
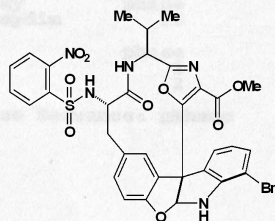
F1 DATA PROCESSING

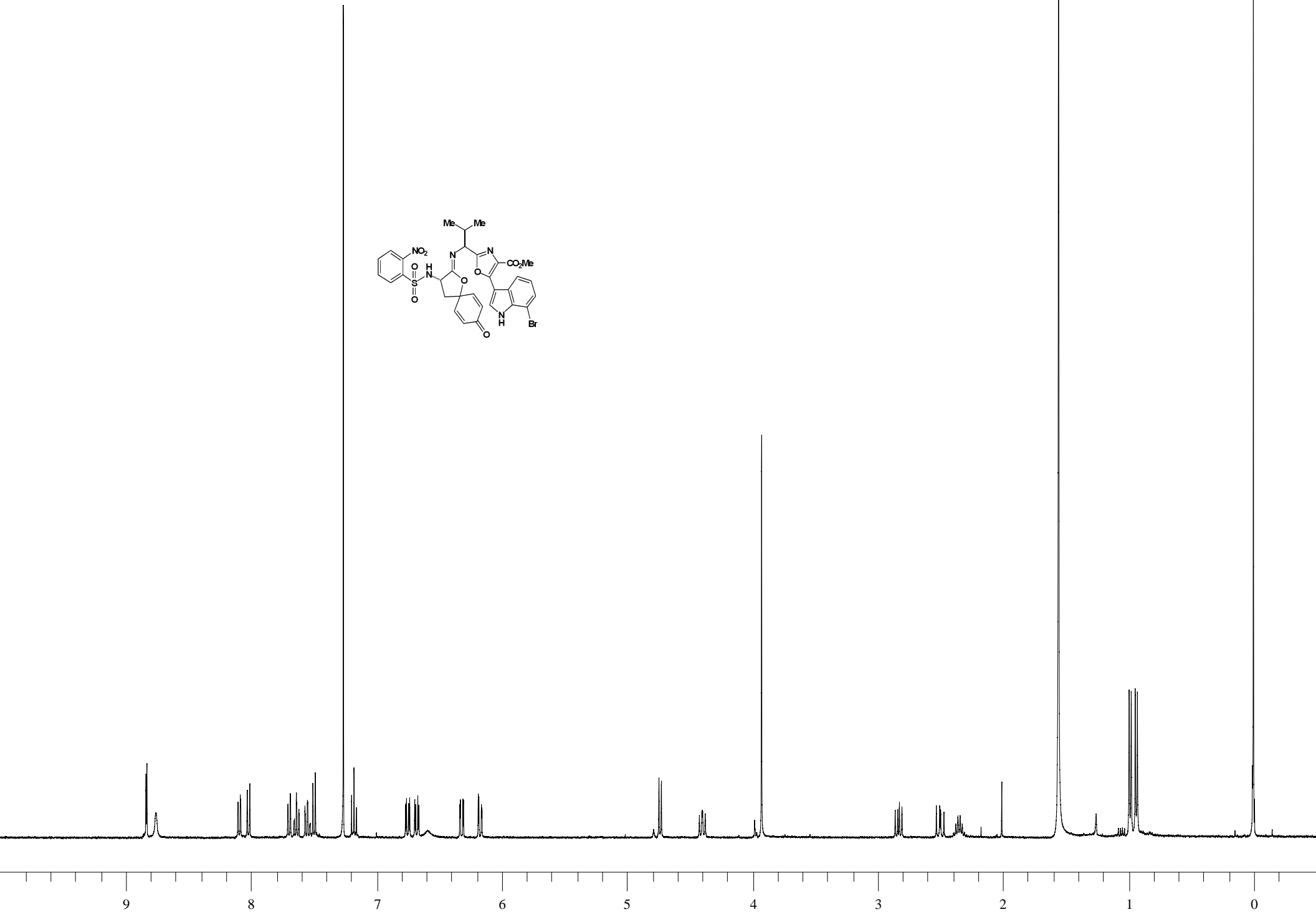
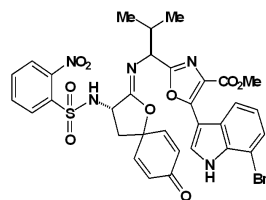
Sq. sine bell 0.121 sec

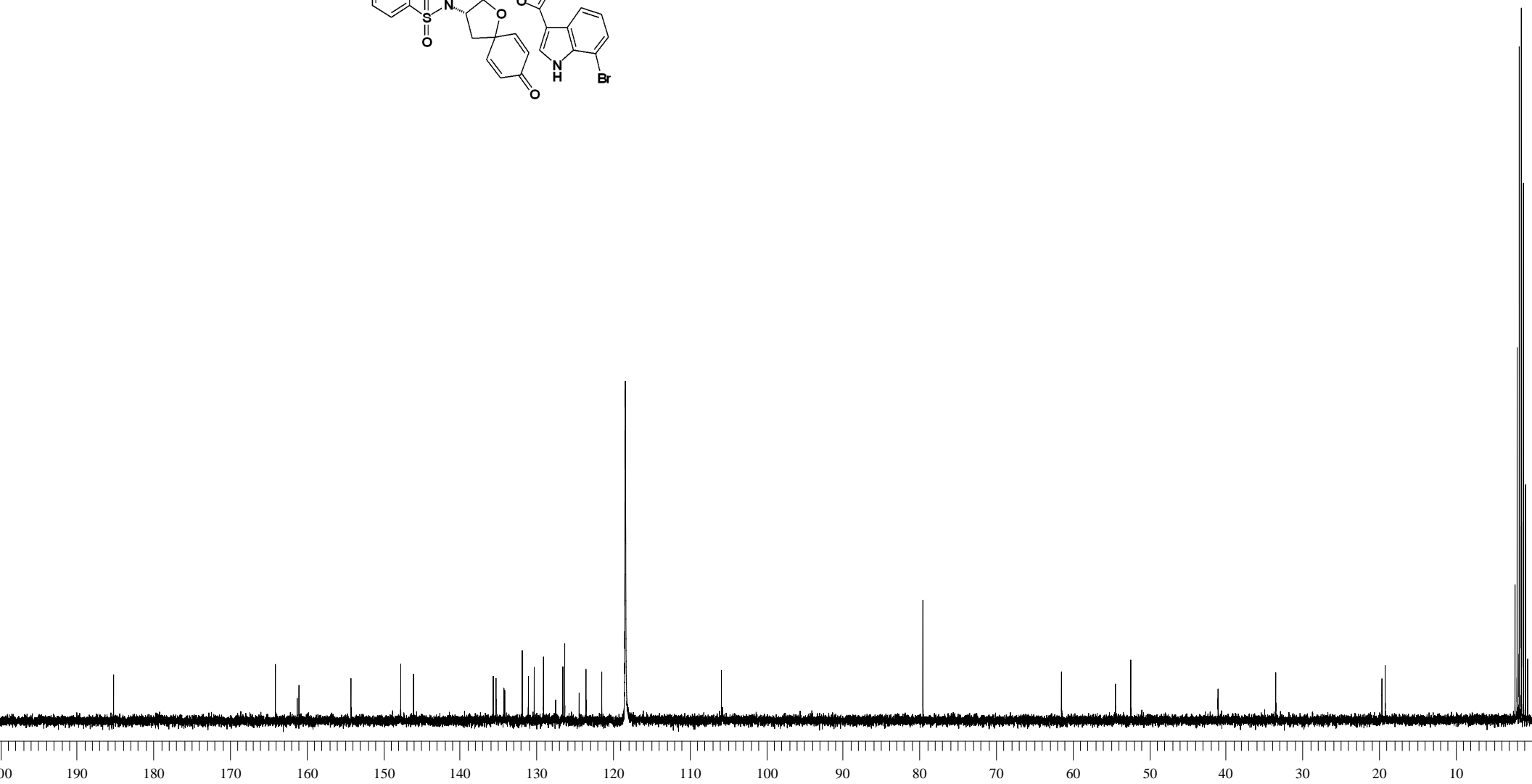
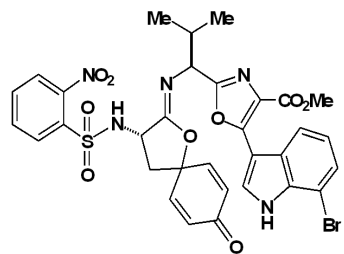
Shifted by -0.121 sec

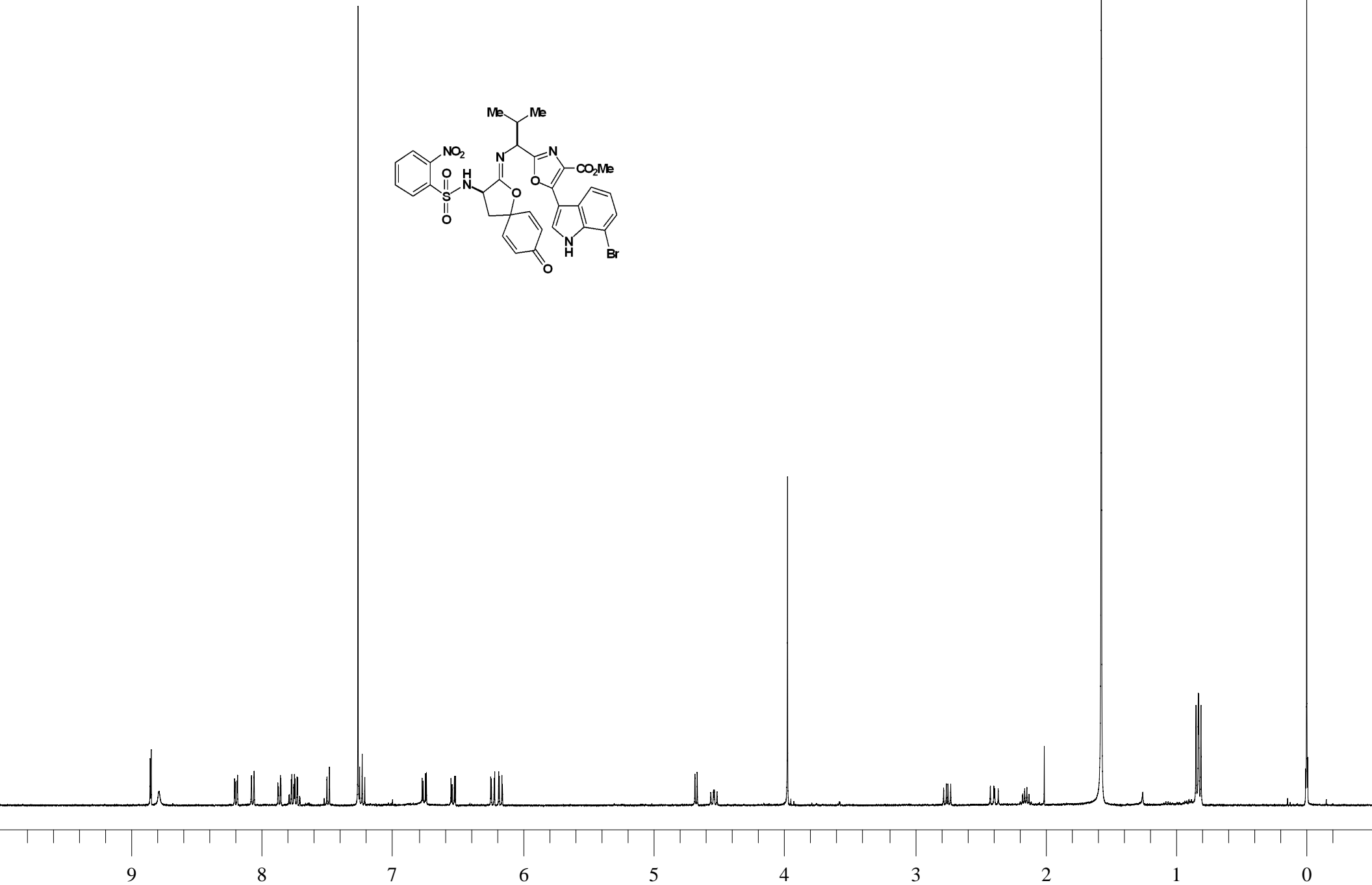
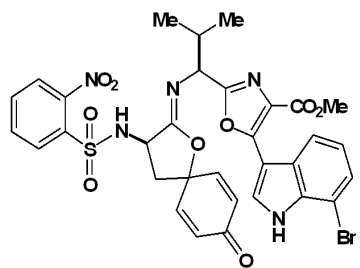
FT size 2048 x 2048

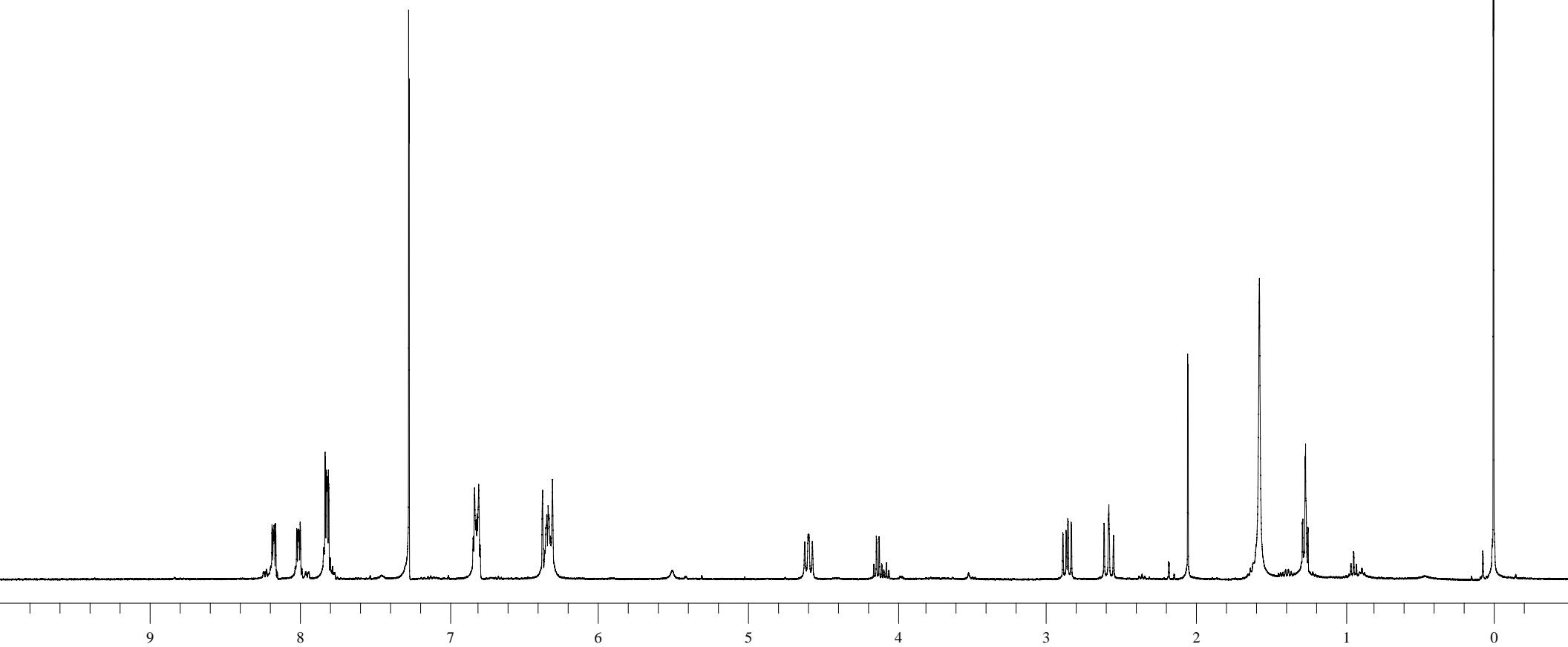
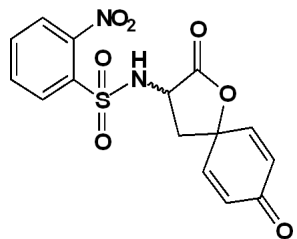
Total time 60 hr, 57 min, 17 sec

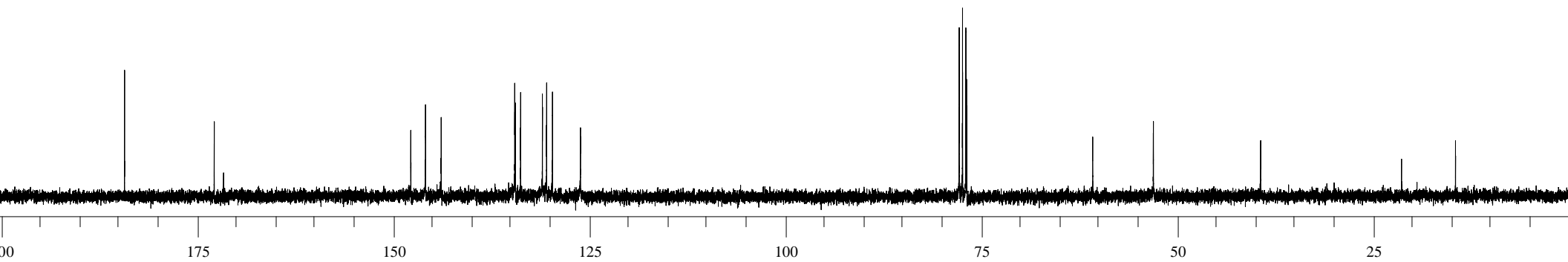
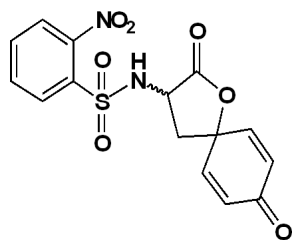








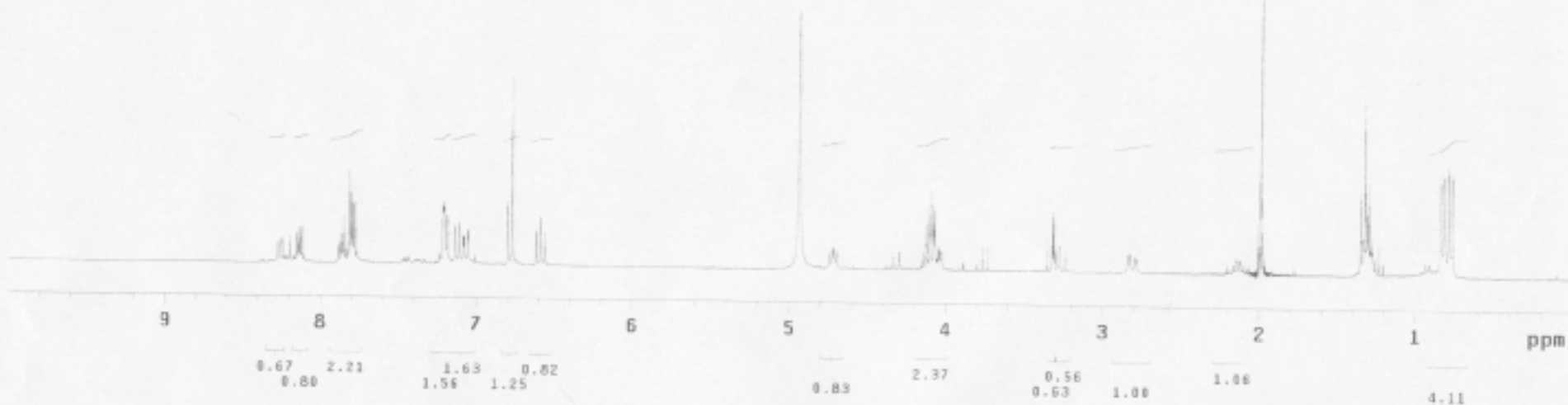
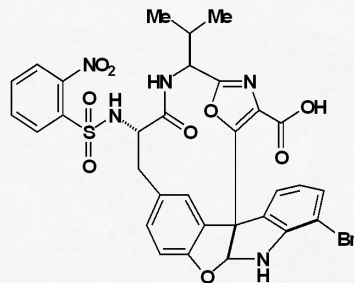


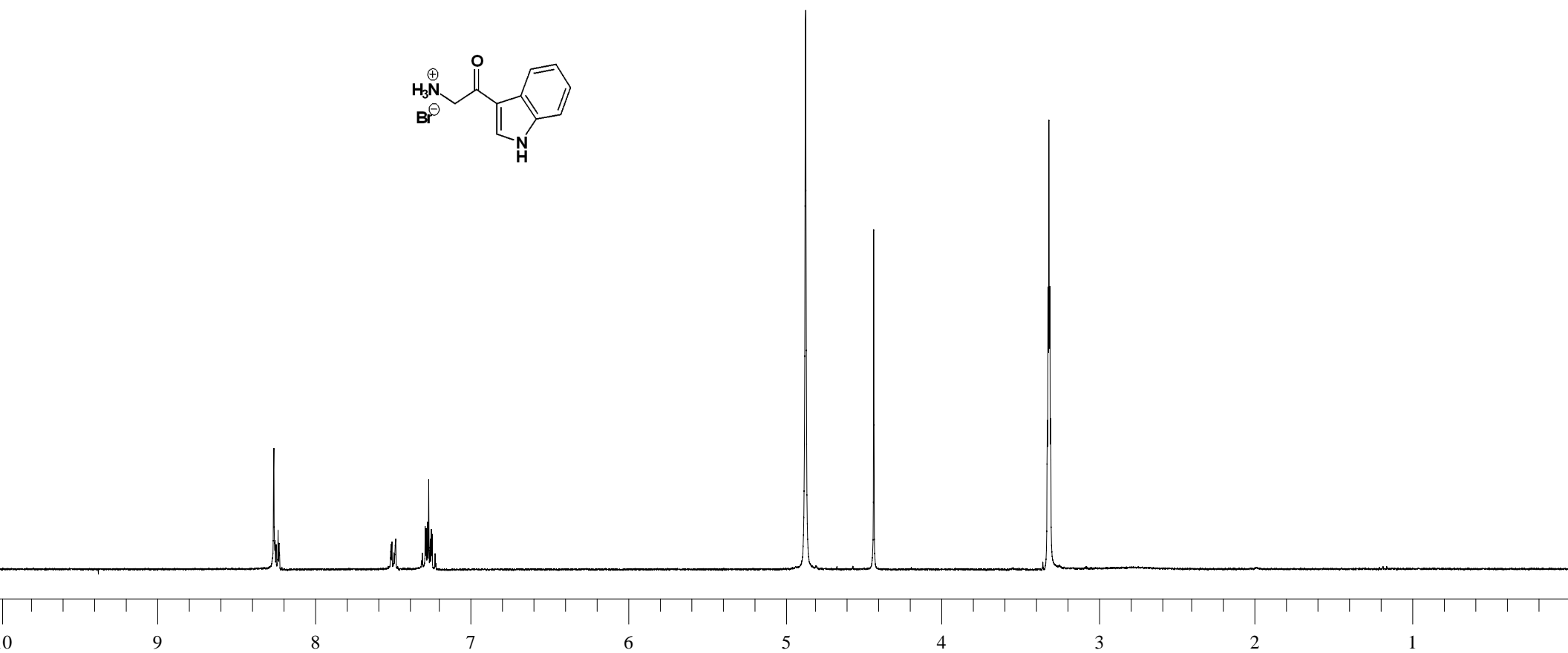
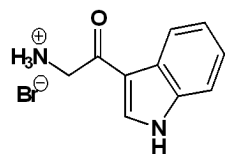


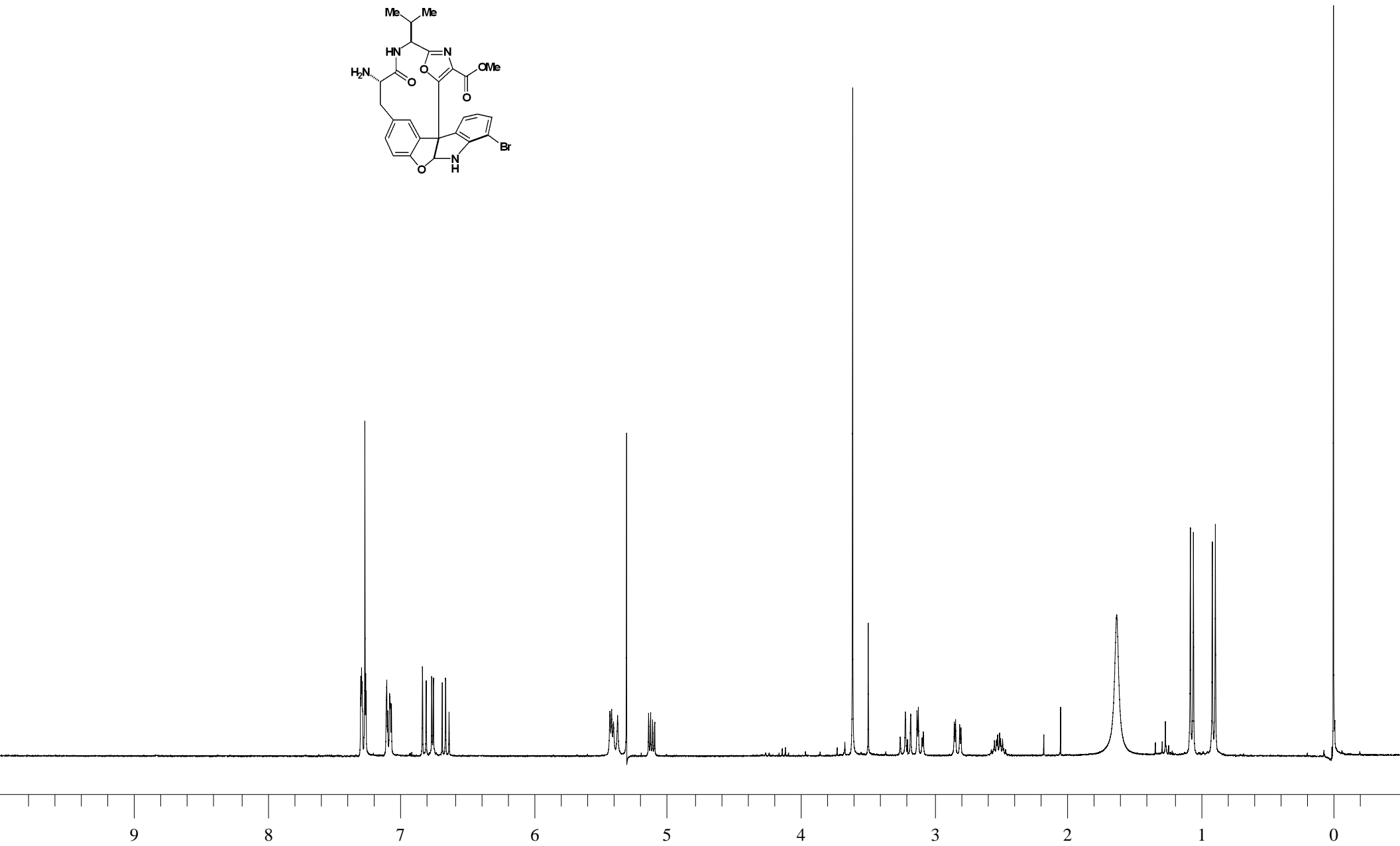
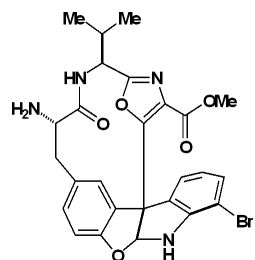
#25 (ABVI129recoveredsm)

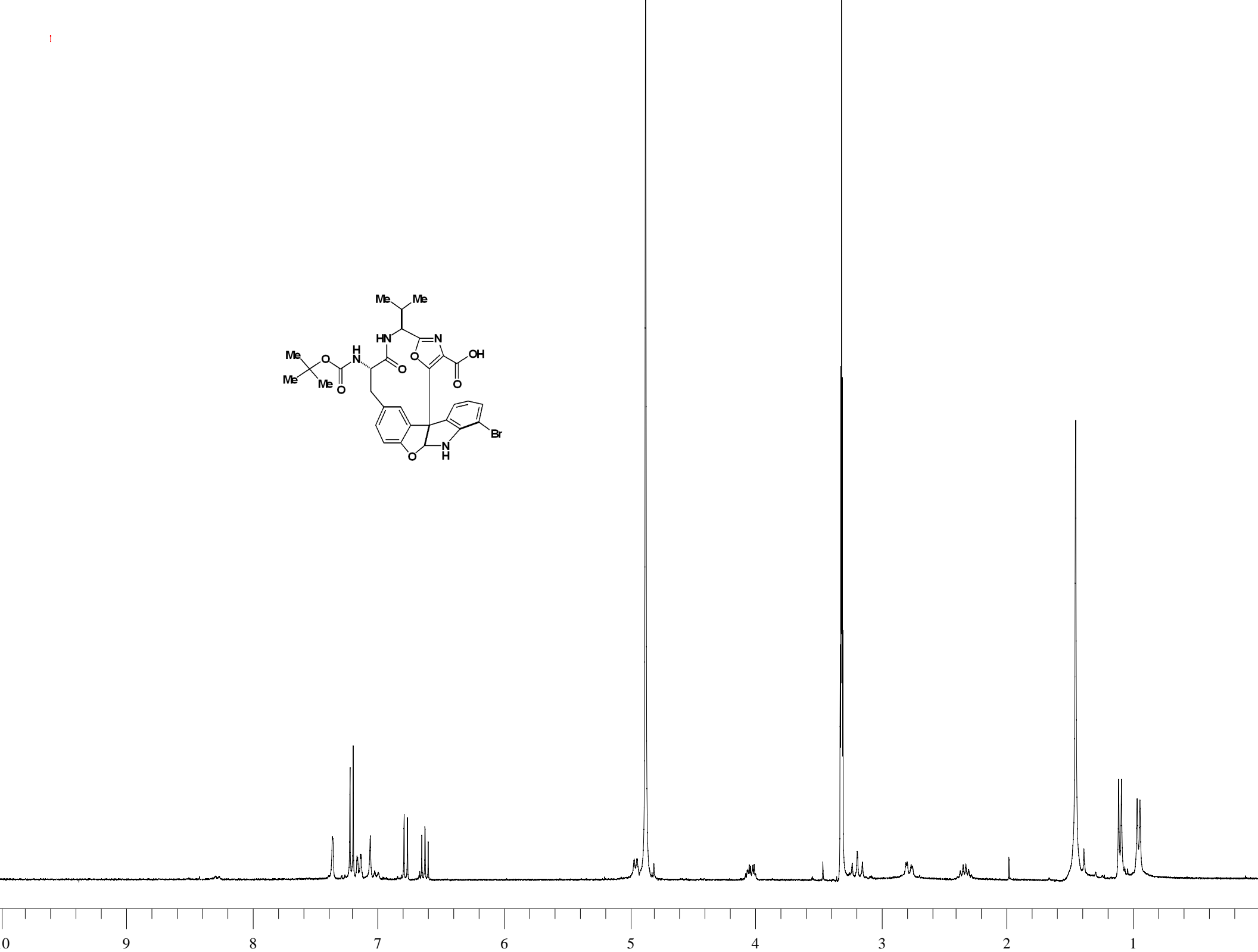
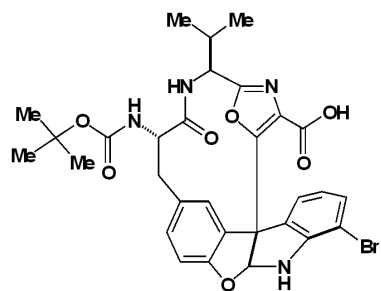
exp1 std1h

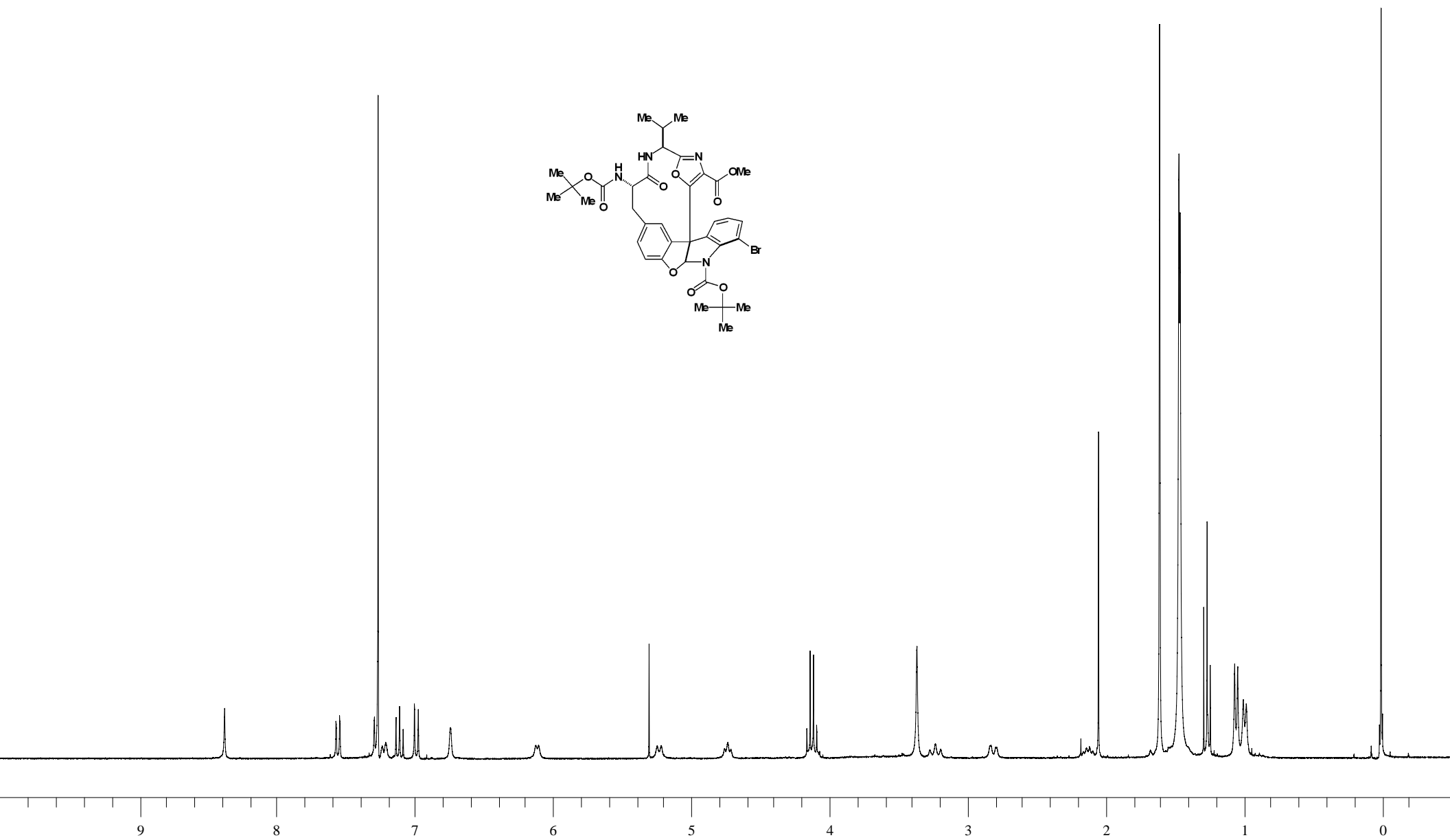
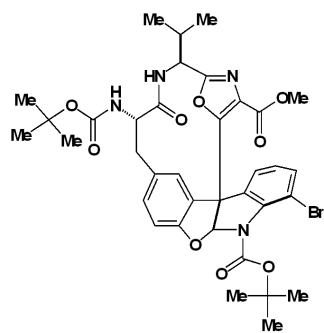
SAMPLE		DEC. & VT	
date	Mar 25 2003	dfrq	300.879
solvent	CD30d	dn	H1
file	exp	dpwr	30
ACQUISITION		PROCESSING	
sfrq	300.879	dof	0
tn	H1	de	nnn
at	1.998	dem	C
mp	20000	def	200
sw	5005.0	wtfile	
fb	not used	proc	ft
bs	8	fn	not used
tpwr	58		
pw	7.2	werr	
dl	2.000	wexp	
tof	0	wbs	
nt	64	wnt	
ct	64		
clock	n		
gain	not used		
FLAGS			
ll	n		
in	n		
dp	y		
DISPLAY			
sp	-0.2		
wp	3000.6		
vs	291		
sc	0		
vc	250		
hzem	12.00		
ls	219.34		
rfl	1936.9		
rffp	993.3		
th	20		
ins	1.000		
nm	cdc	ph	

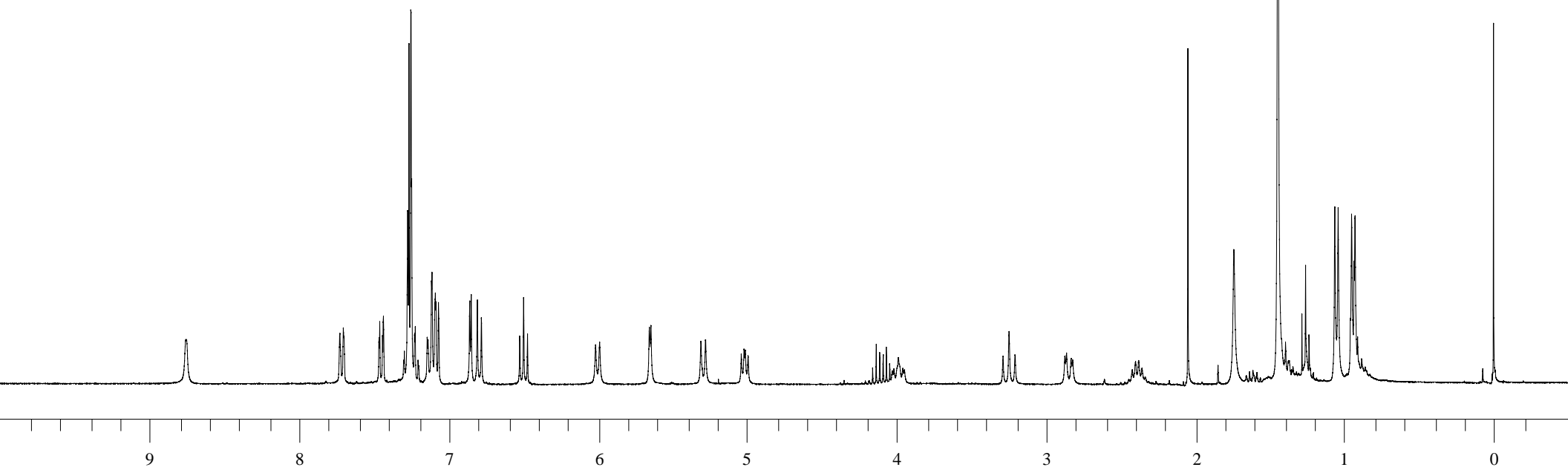
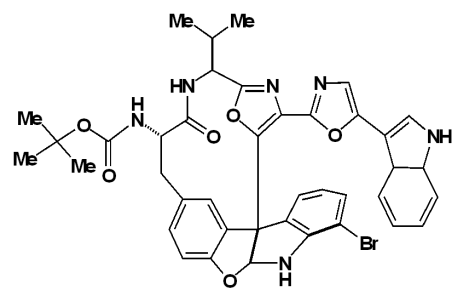


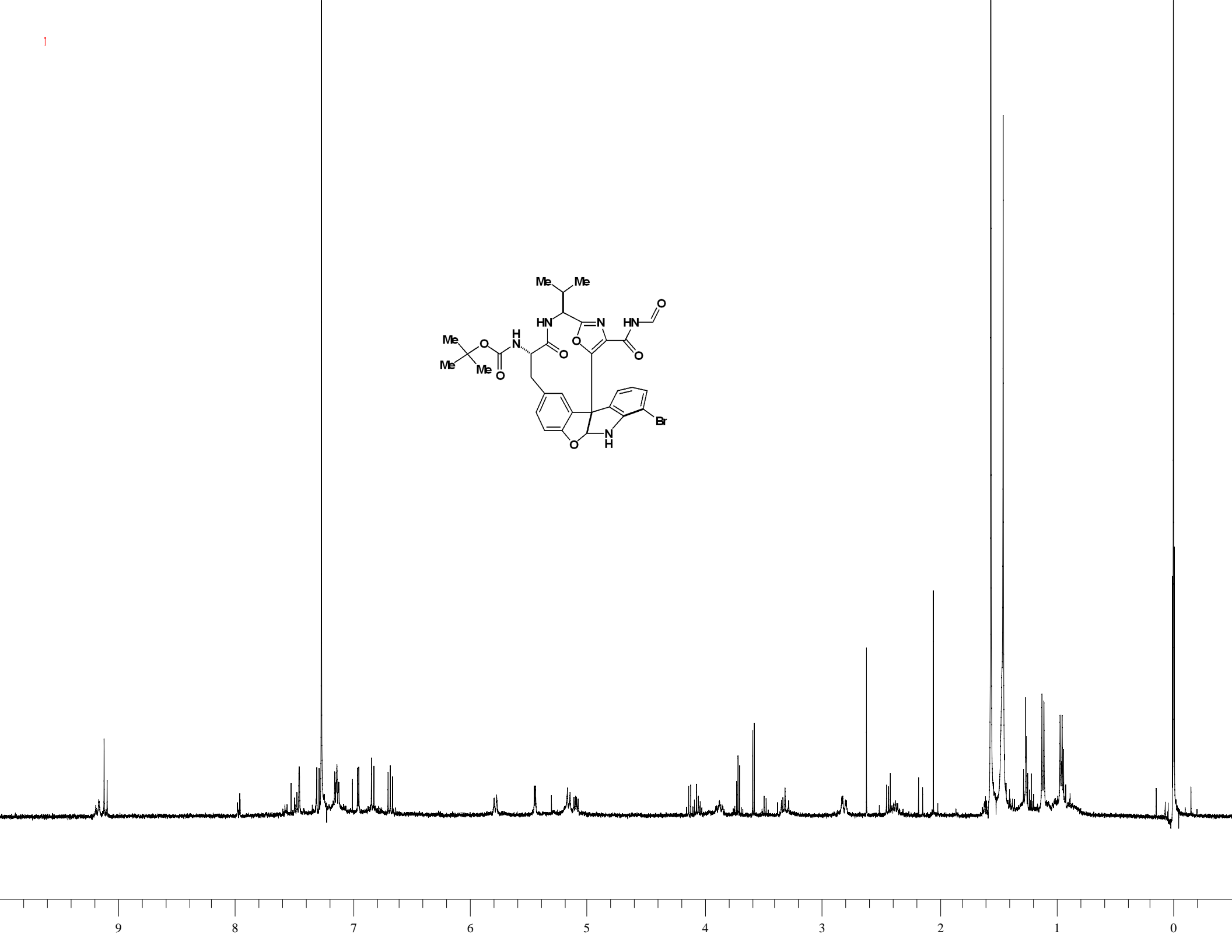
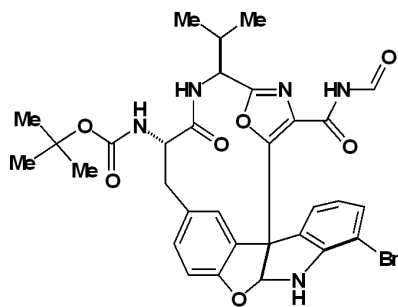


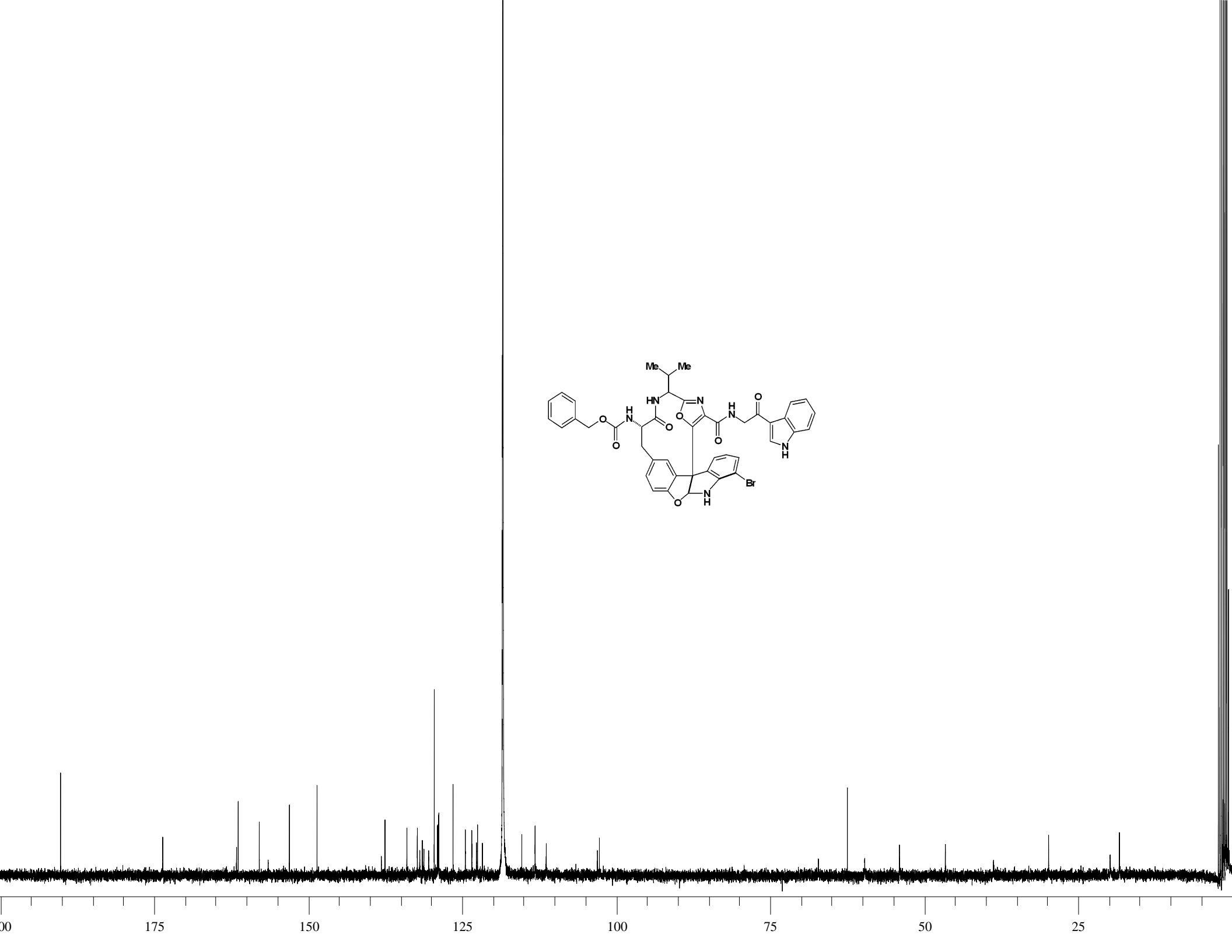


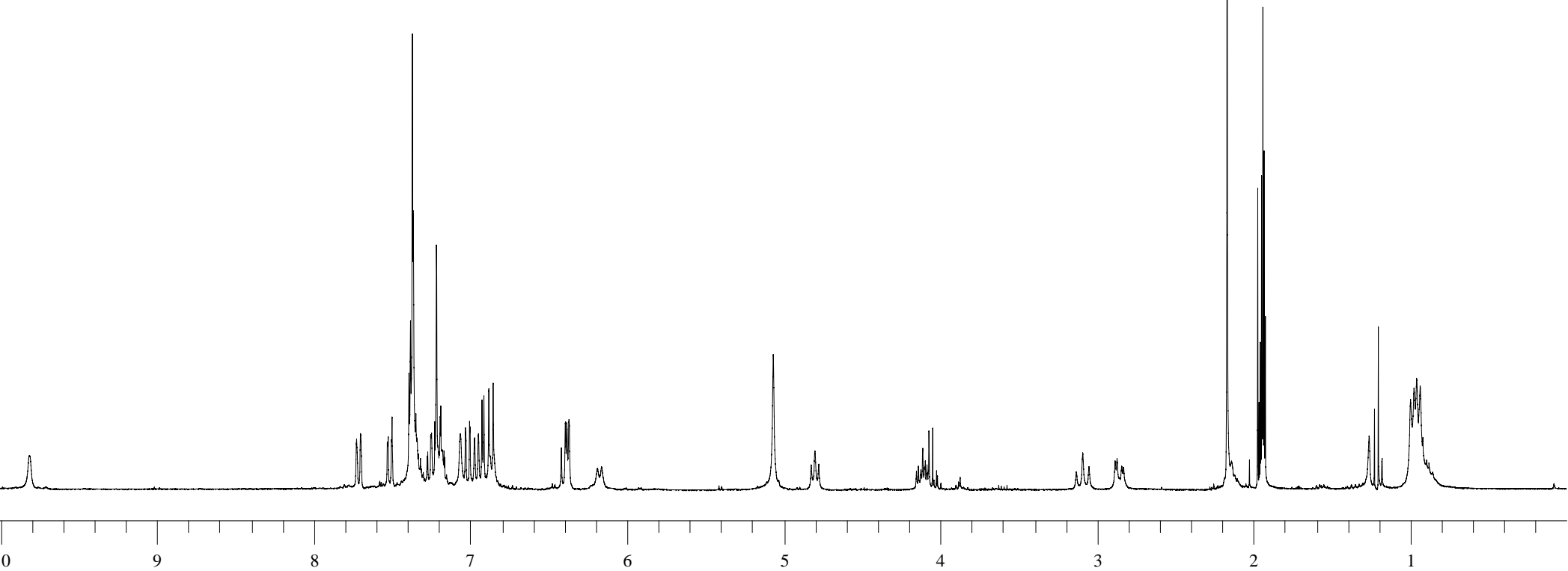
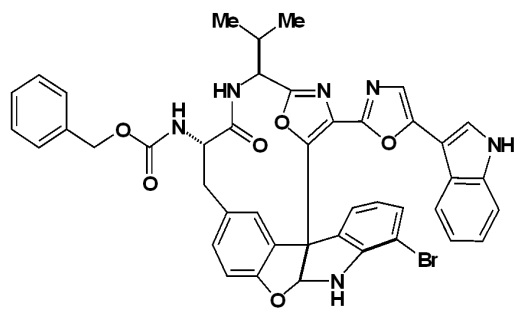


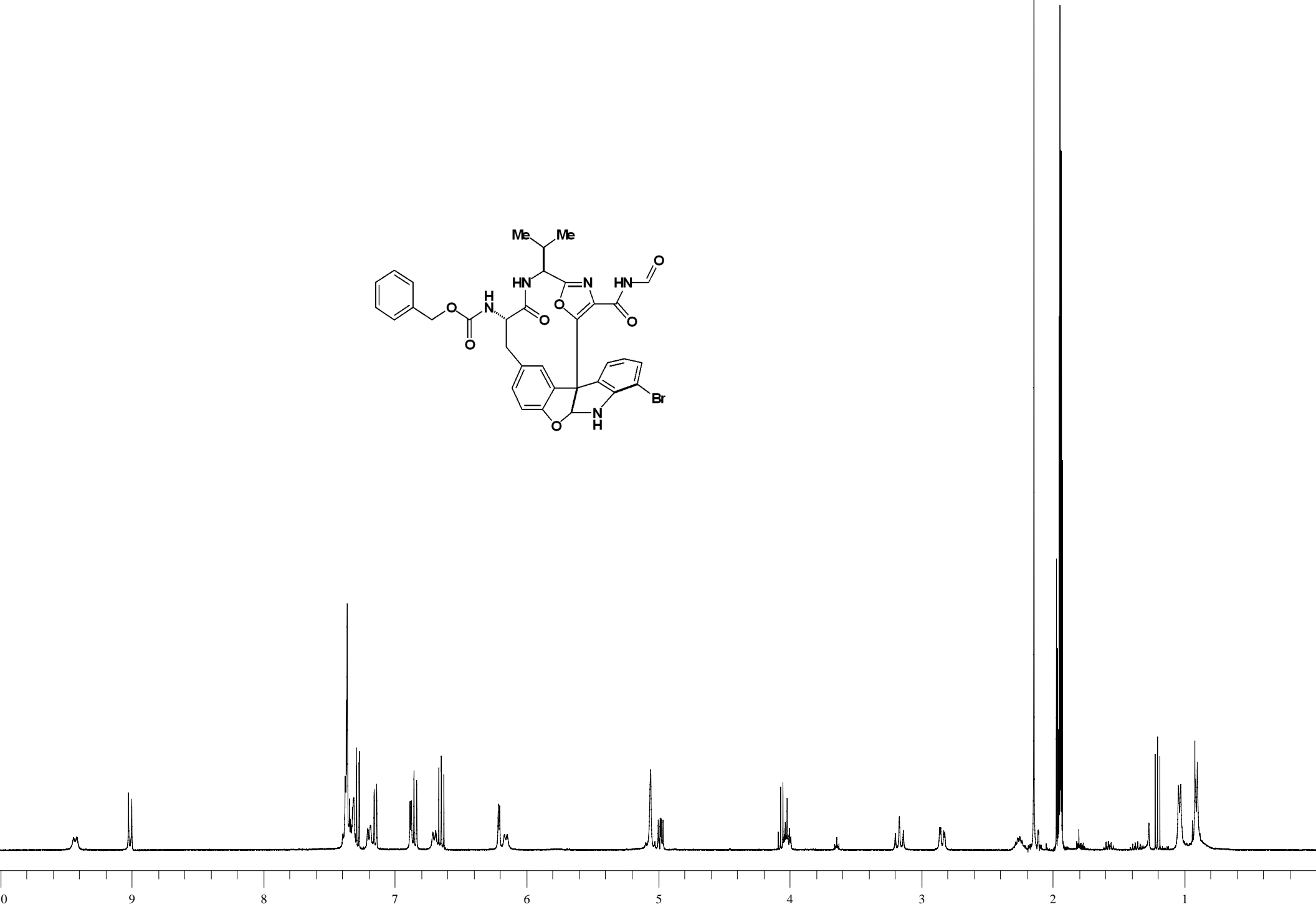
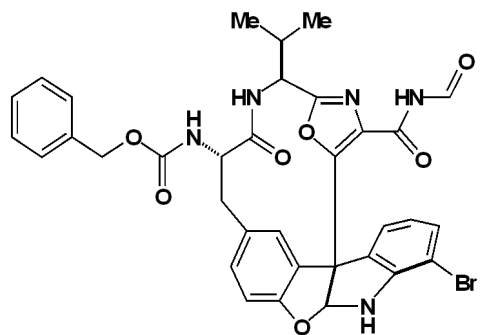


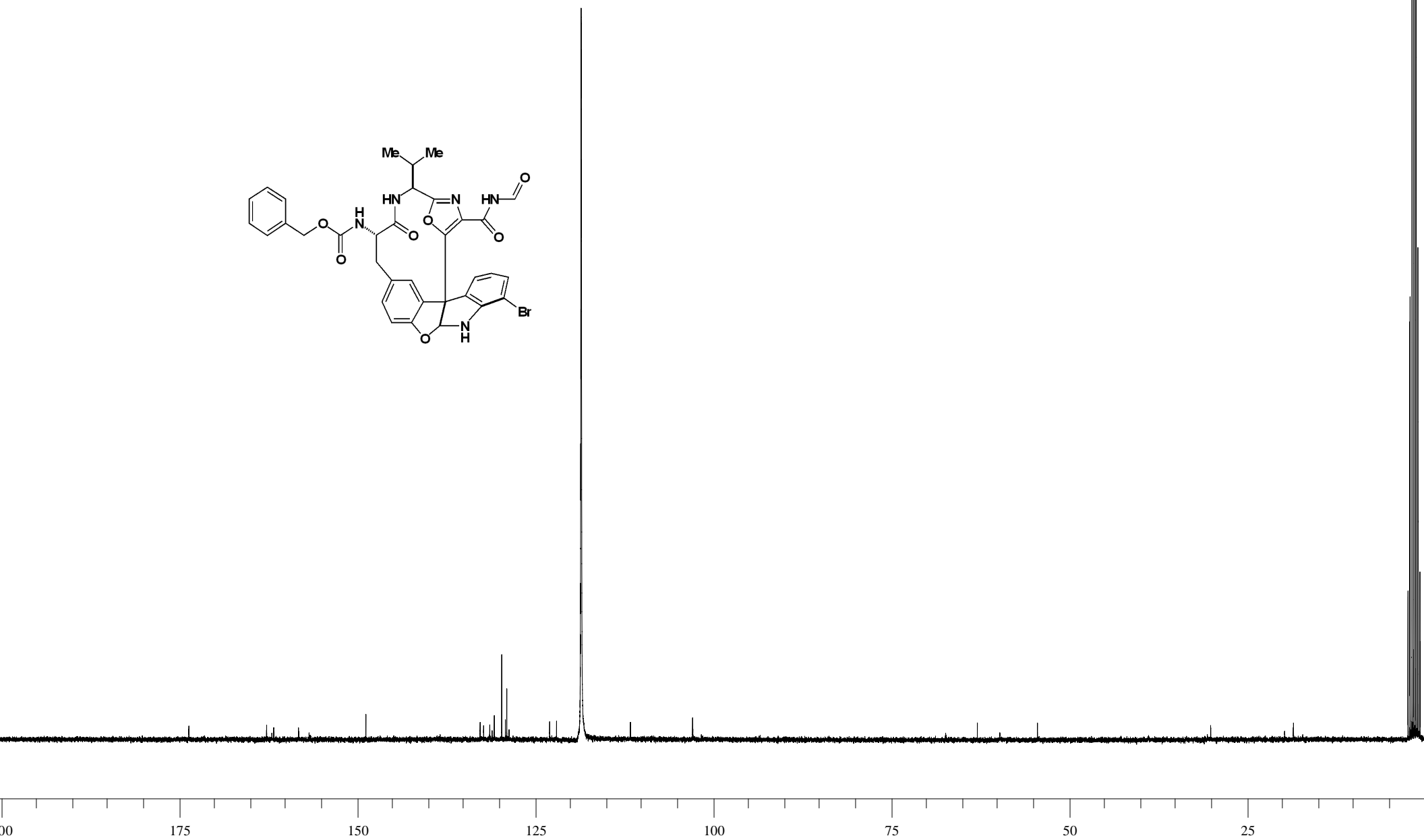
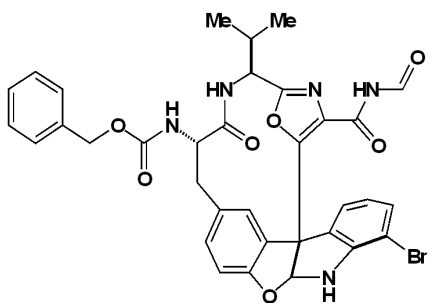


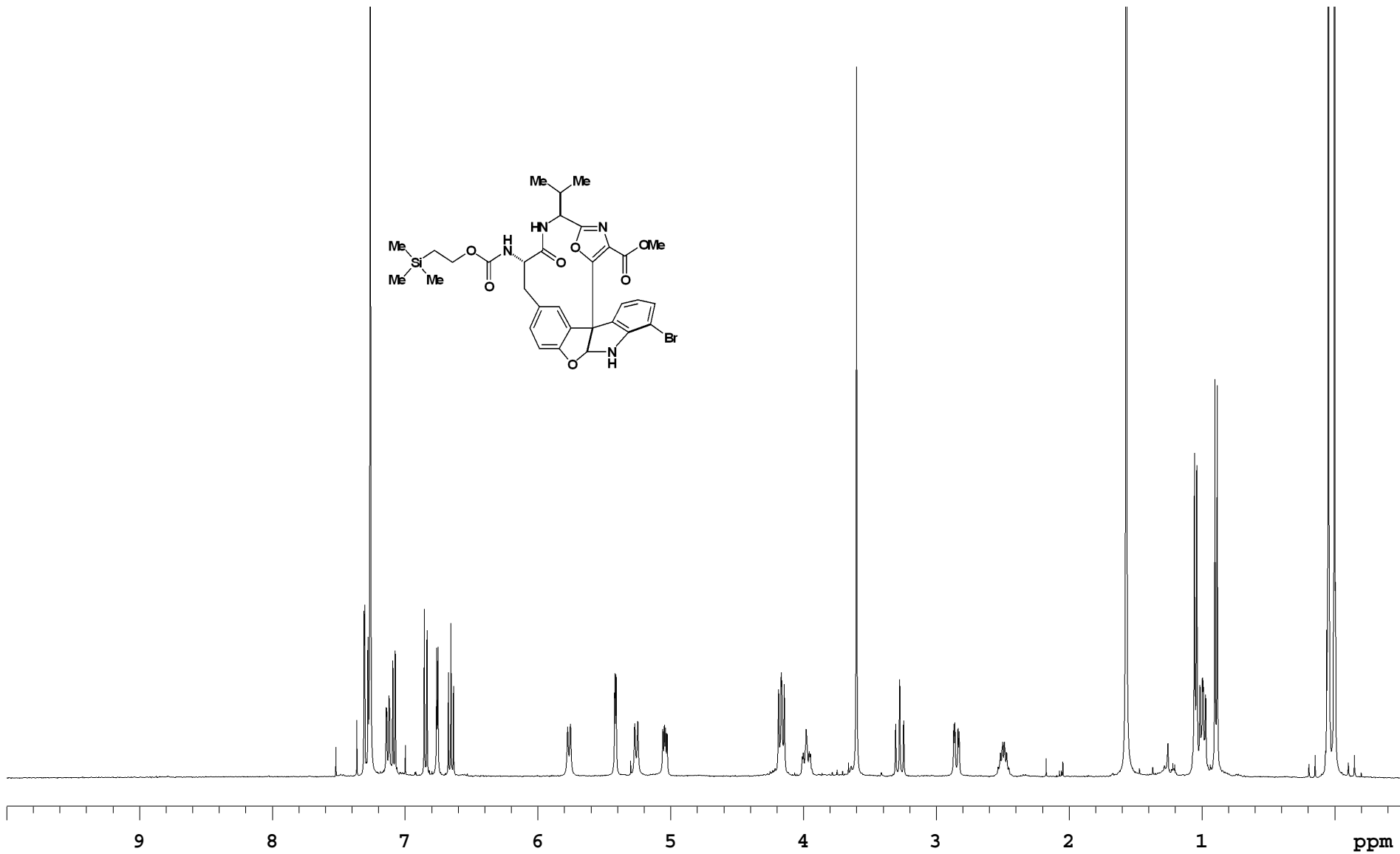
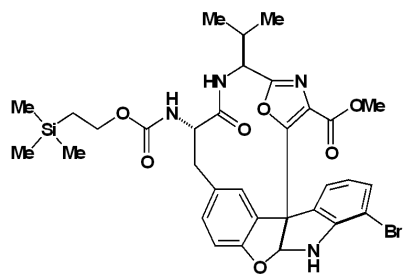


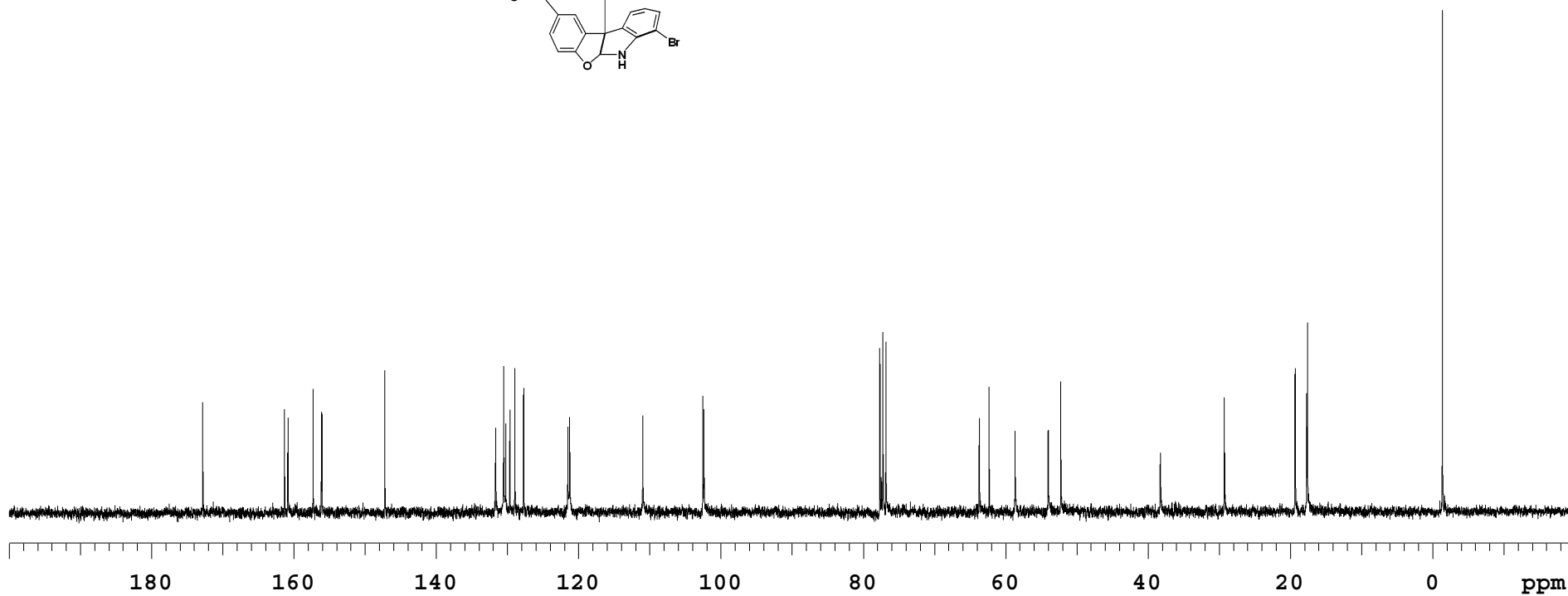
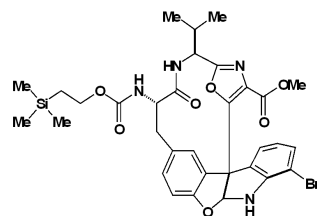


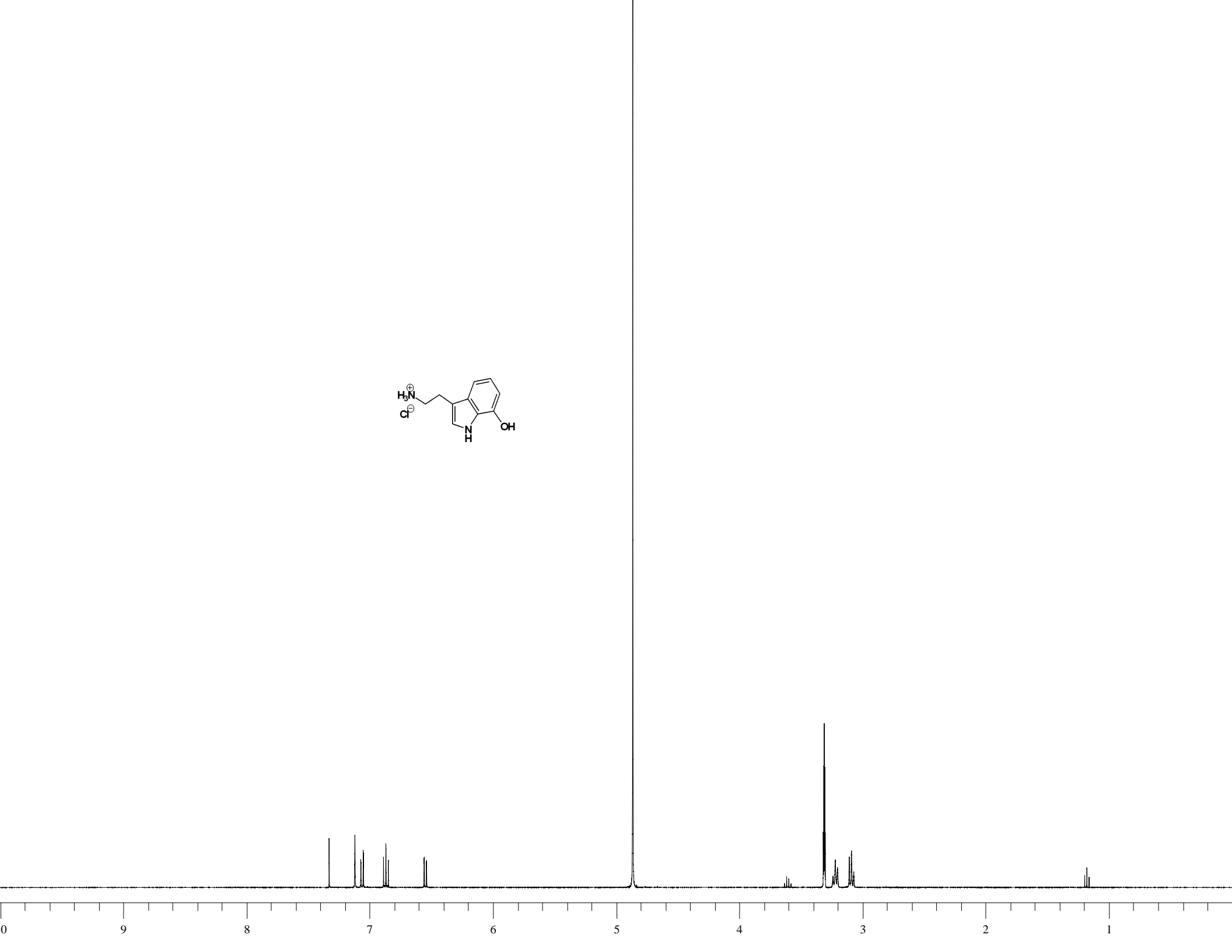
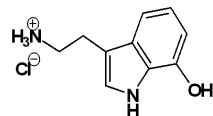


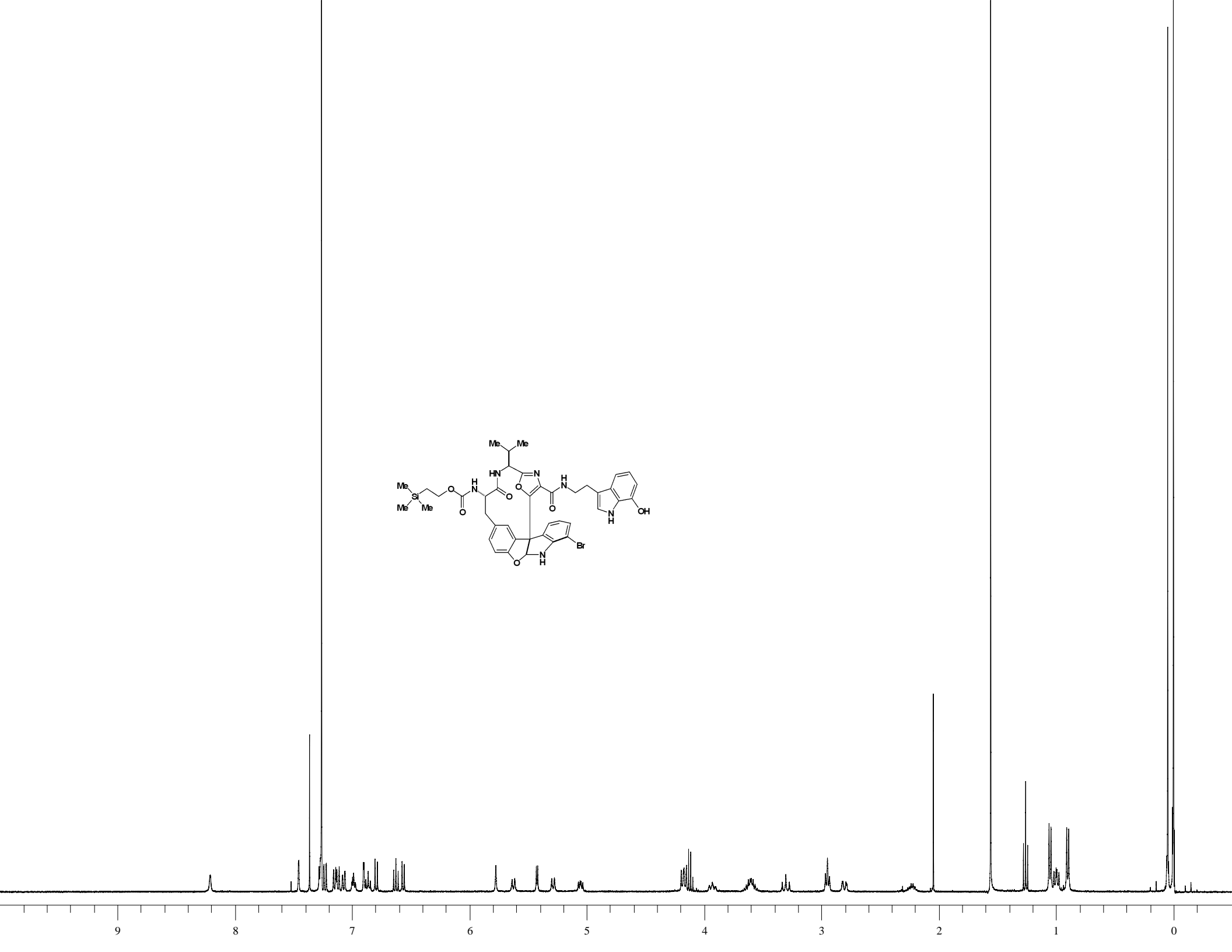
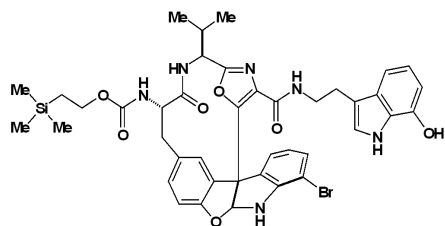


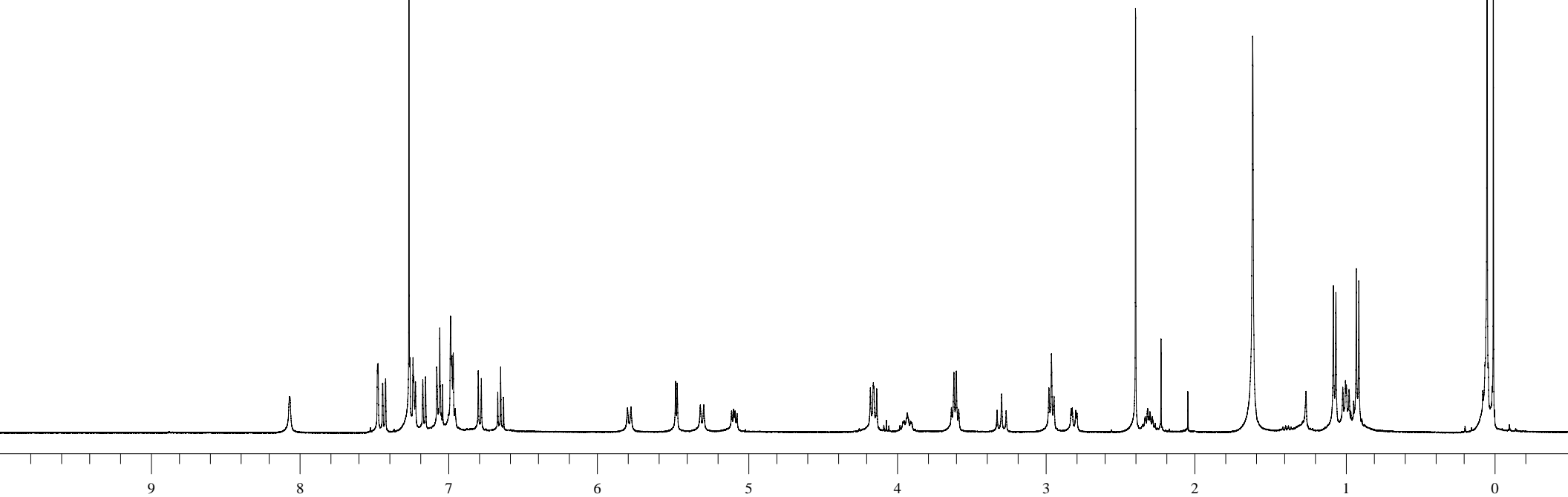
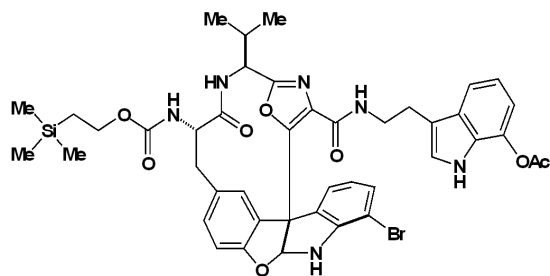


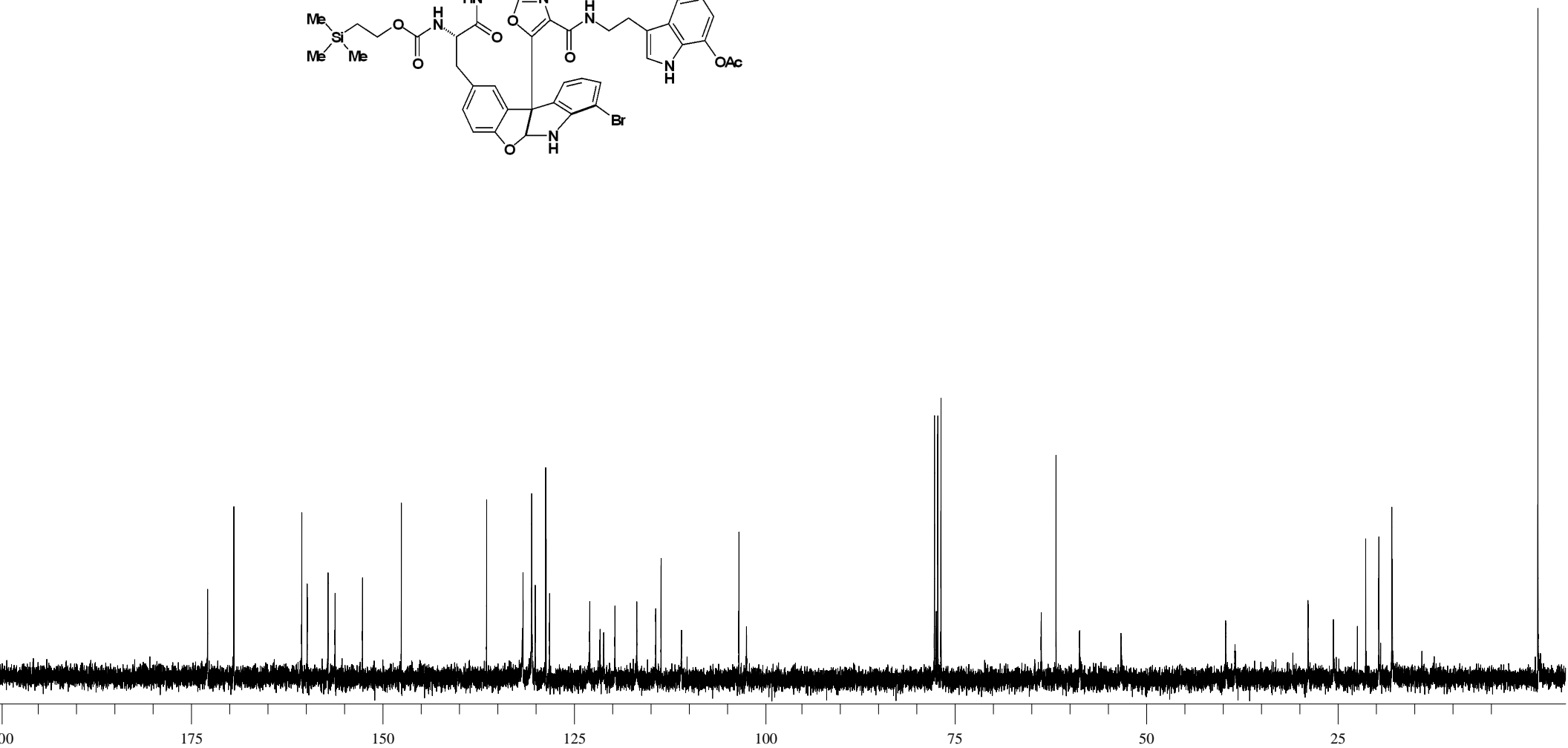
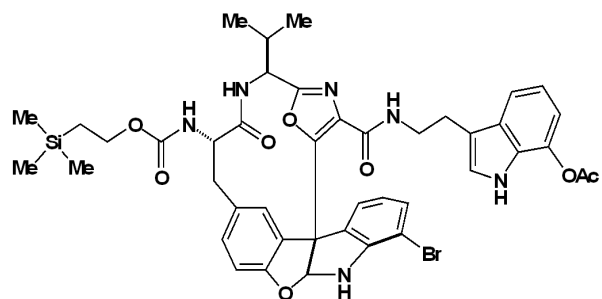


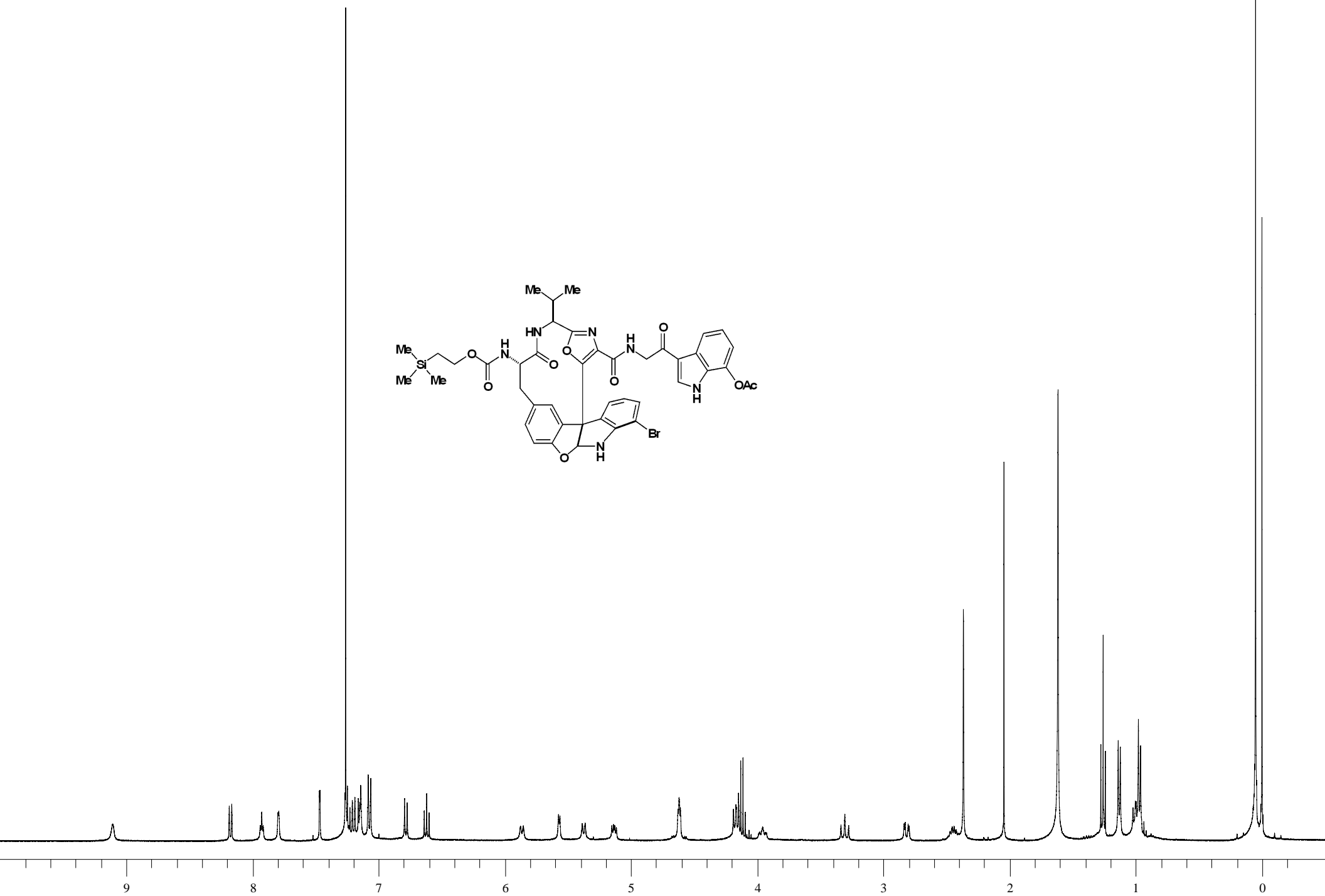
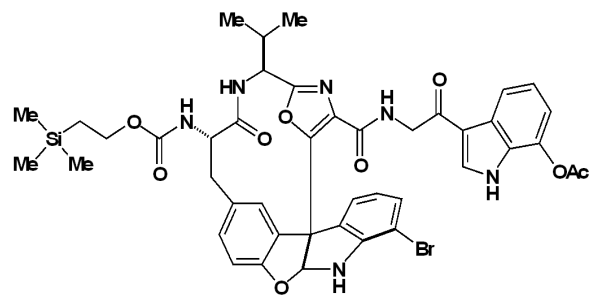






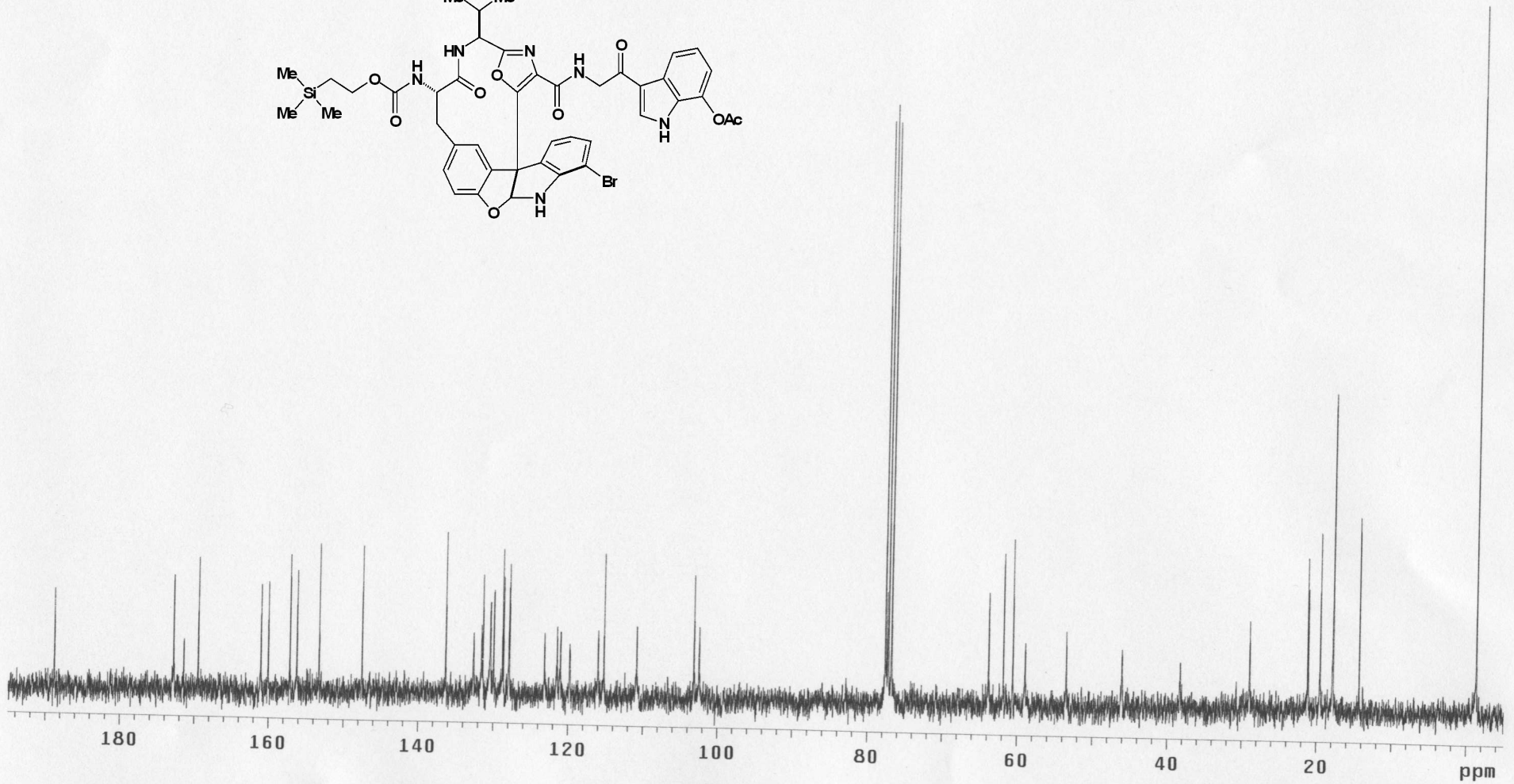
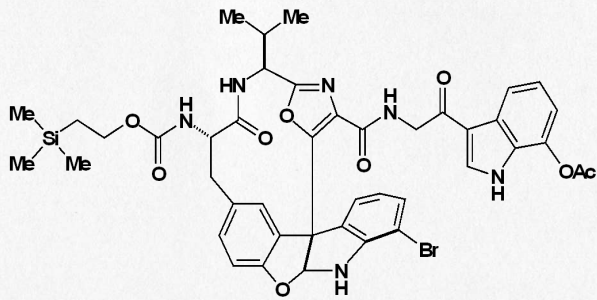


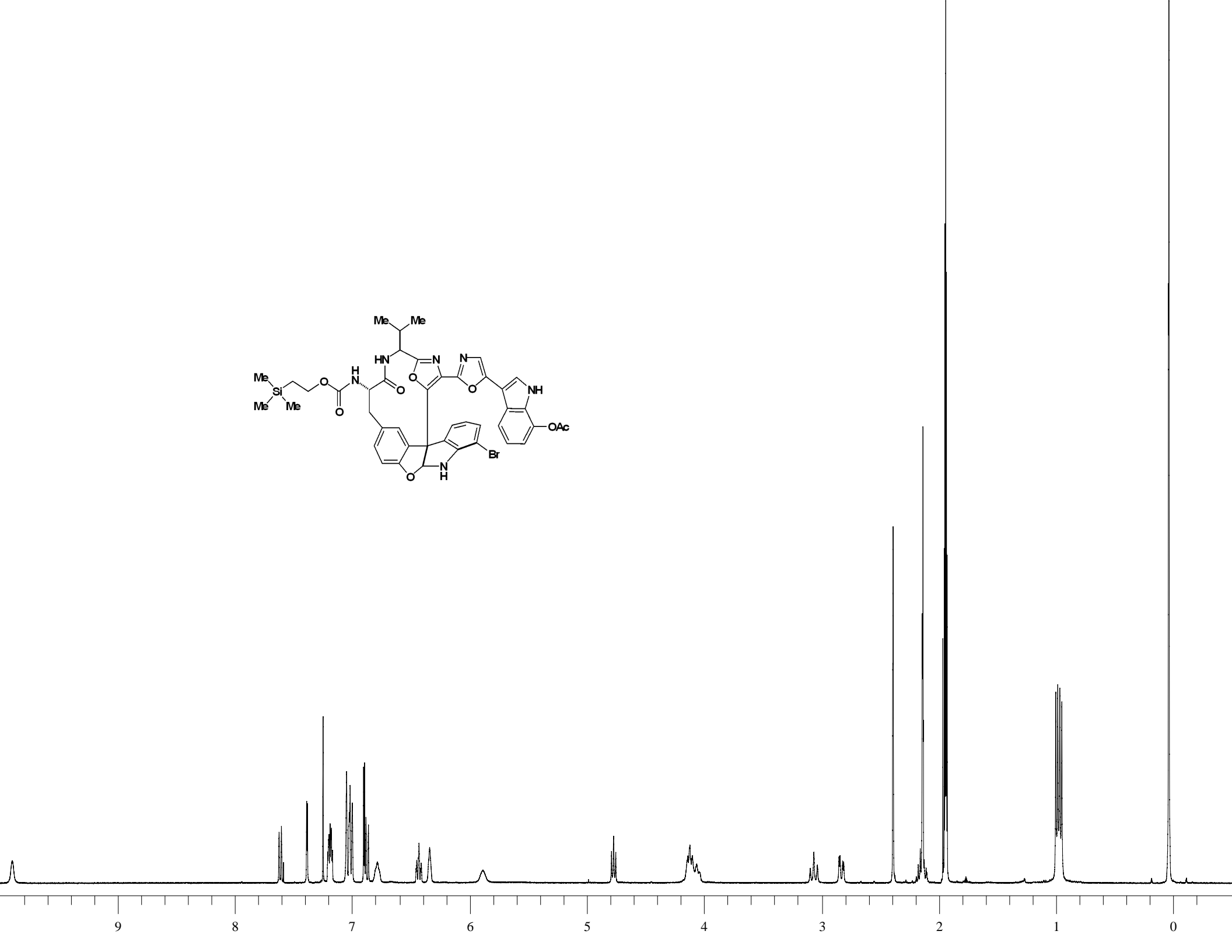
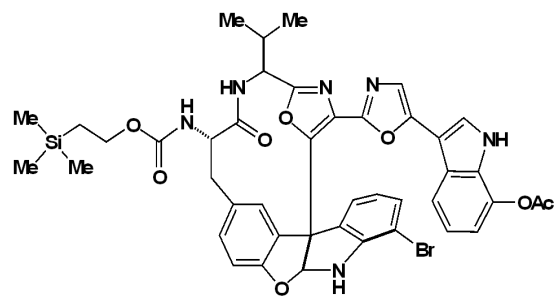


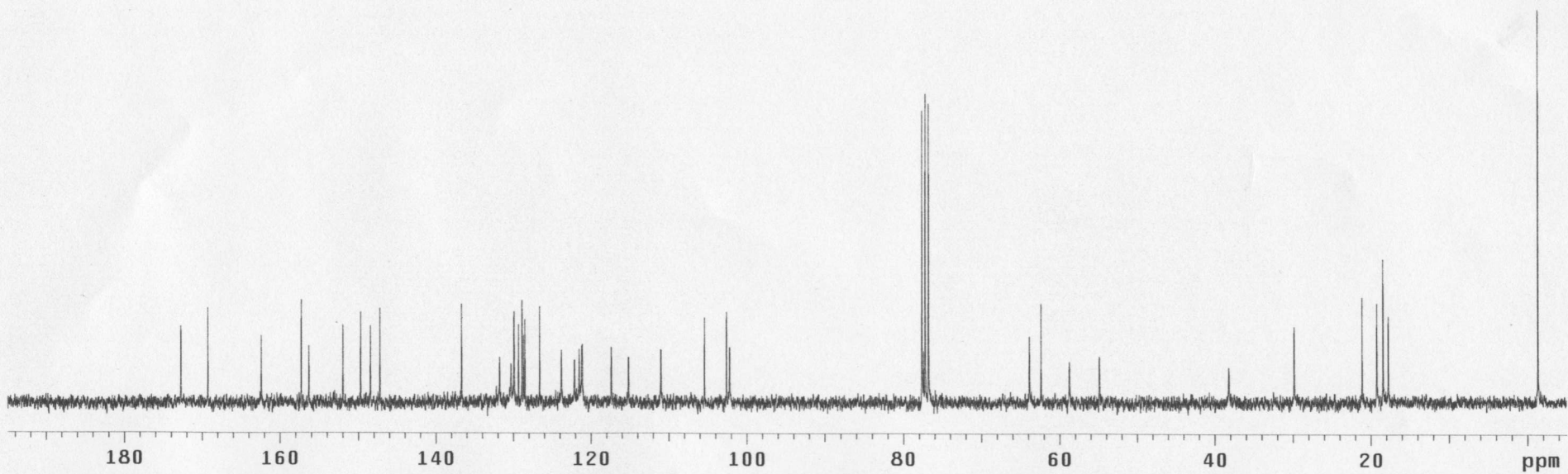
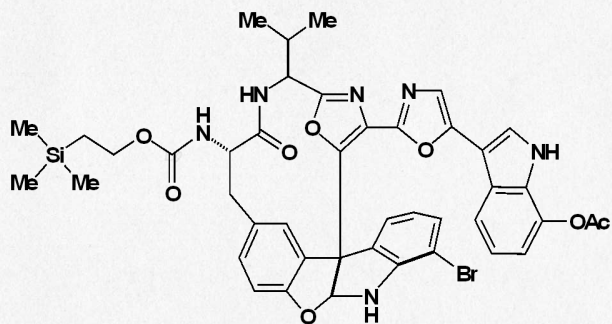


#191(ABVII113DDQproddes)

Pulse Sequence: s2pu1



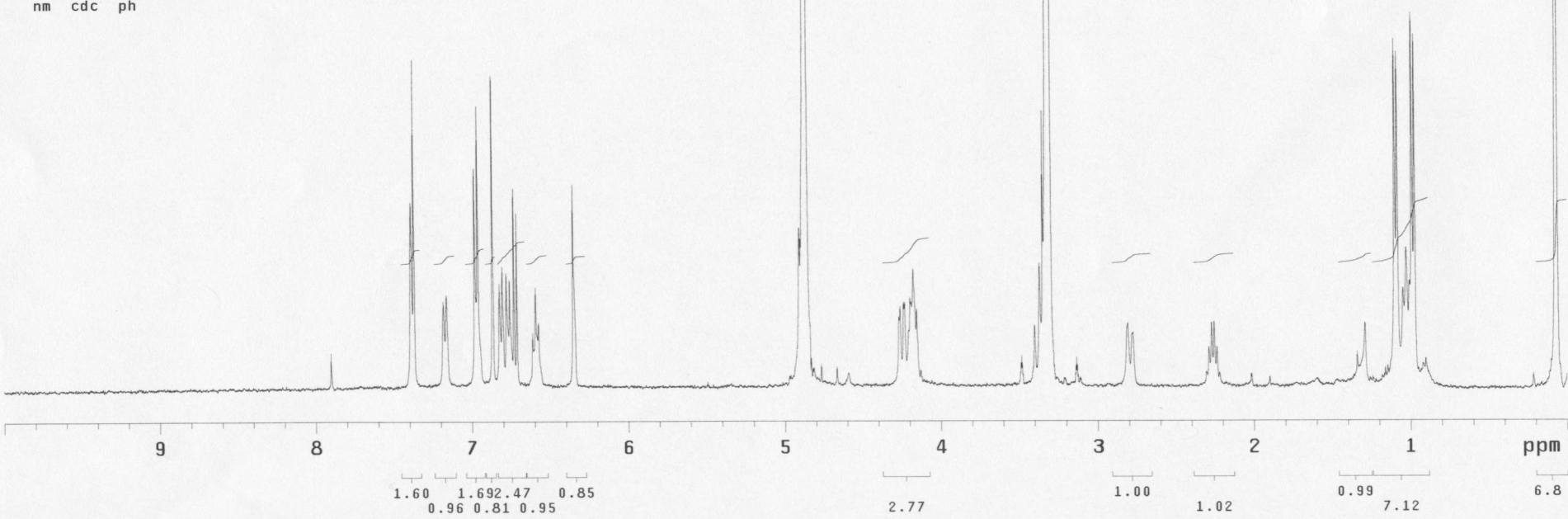
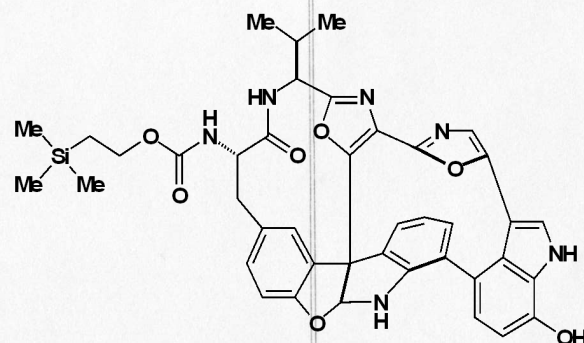




#204B (ABVII121recoveredSM)

exp1 std1h

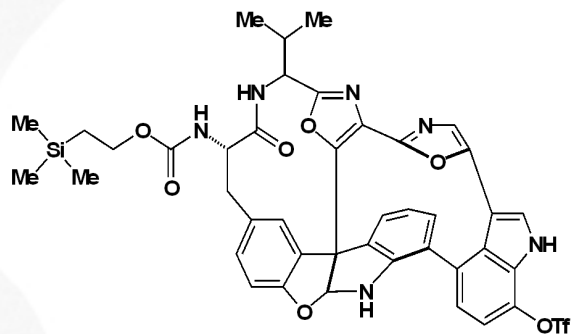
SAMPLE		DEC. & VT	
date	Sep 13 2003	dfrq	399.783
solvent	CD300	dn	H1
file	exp	dpwr	30
ACQUISITION			
sfrq	399.783	dm	nnn
tn	H1	dmm	c
at	3.744	dmf	200
np	44932	dseq	
sw	6000.6	dres	1.0
fb	3000	homo	n
bs	8	DEC2	
tpwr	54	dfrq2	0
pw	5.1	dn2	
d1	2.000	dpwr2	1
tof	0	dof2	0
nt	64	dm2	n
ct	24	dmm2	c
alock	n	dmf2	200
gain	not used	dseq2	
FLAGS			
il	n	dres2	1.0
in	n	homo2	n
dp	y	PROCESSING	
hs	nn	lb	0.50
DISPLAY			
sp	-0.2	wtfile	
wp	3997.8	proc	ft
vs	2749	fn	not used
sc	0	math	f
wc	250	werr	
hzmm	15.99	wexp	
is	453.60	wbs	
rfl	2318.7	wnt	
rfp	1323.3		
th	20		
ins	1.000		
nm	cdc	ph	



#204 (ABVII1210Tfpure)

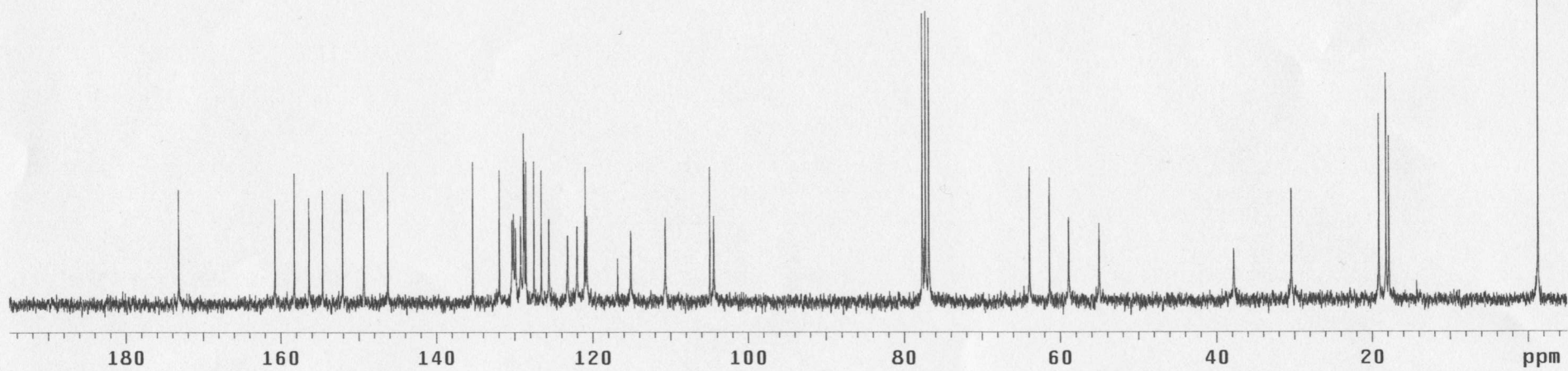
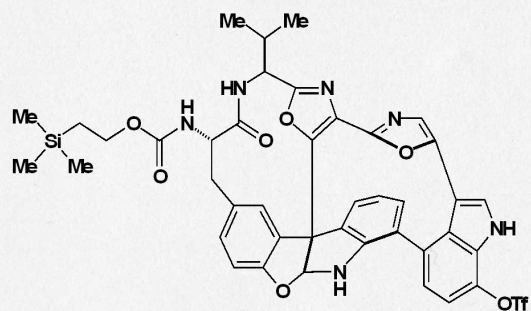
expl stdih

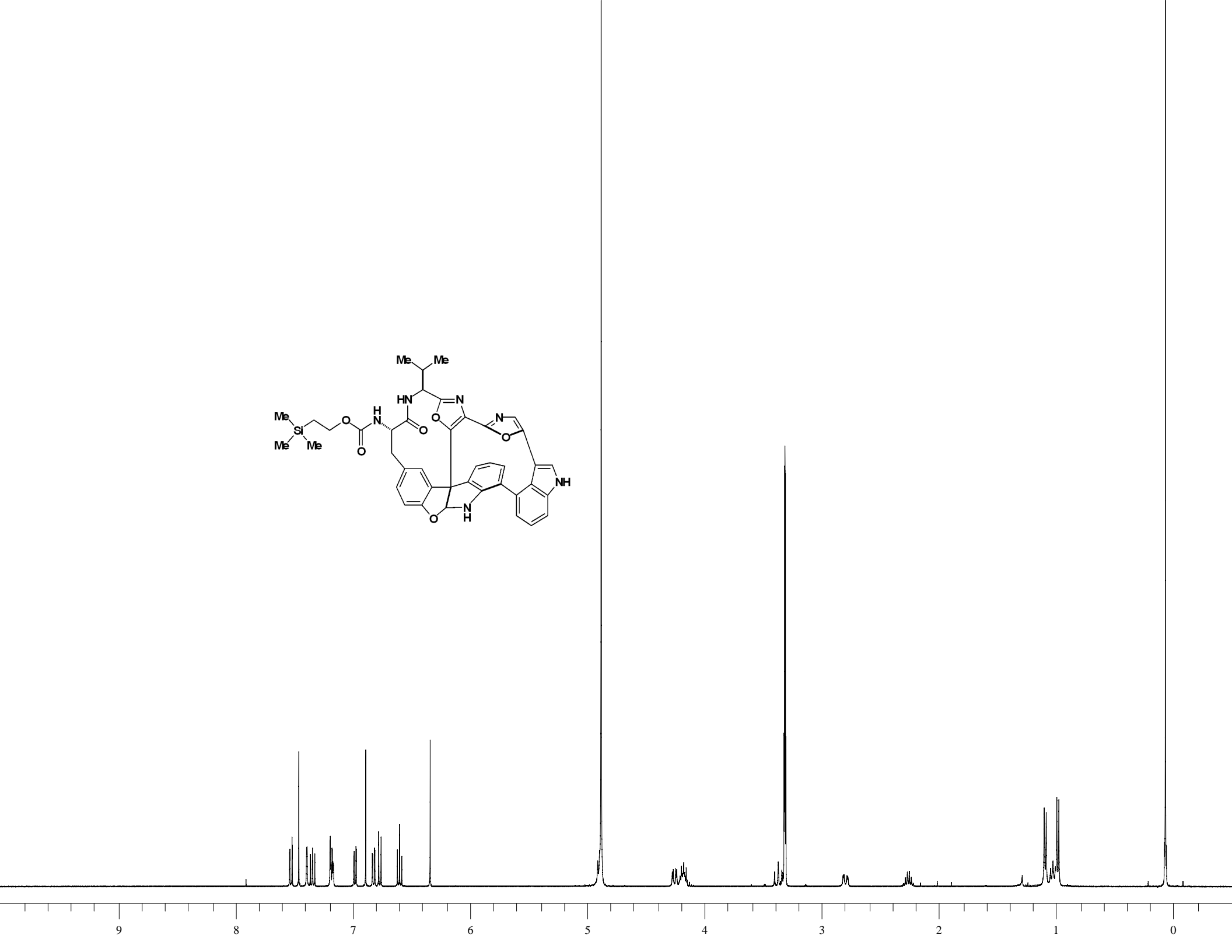
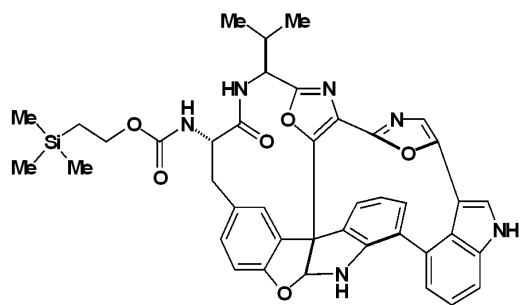
SAMPLE		DEC. & VT	
date	Sep 12 2003	dfrq	399.781
solvent	CDCl3	dn	H1
file	exp	dpwr	38
ACQUISITION		dof	8
sfrq	399.781	dm	nmn
tn	H1	dsm	c
at	3.744	dof	200
np	44932	dseq	
sw	6000.6	dres	1.0
fb	3000	homo	n
bs	8	DEC2	
tpwr	54	dfrq2	8
pw	5.1	dn2	
d1	2.000	dpwr2	1
tof	0	dof2	8
nt	64	dm2	n
ct	32	dsm2	c
alock	n	dof2	200
gain	not used	dseq2	
FLAGS		dres2	1.0
il	n	homo2	n
in	n	PROCESSING	
dp	y	lb	0.50
hs	nn	wtfile	
DISPLAY		proc	ft
sp	0.0	fn	not used
wp	3997.8	math	f
vs	508		
sc	0	werr	
wc	250	wexp	
hzm	15.89	wbs	
fs	2900.83	wmt	
rfl	896.4		
rff	0		
th	20		
ins	1.000		
nm	cdc ph		



#200 (ABVII1210TfC13)

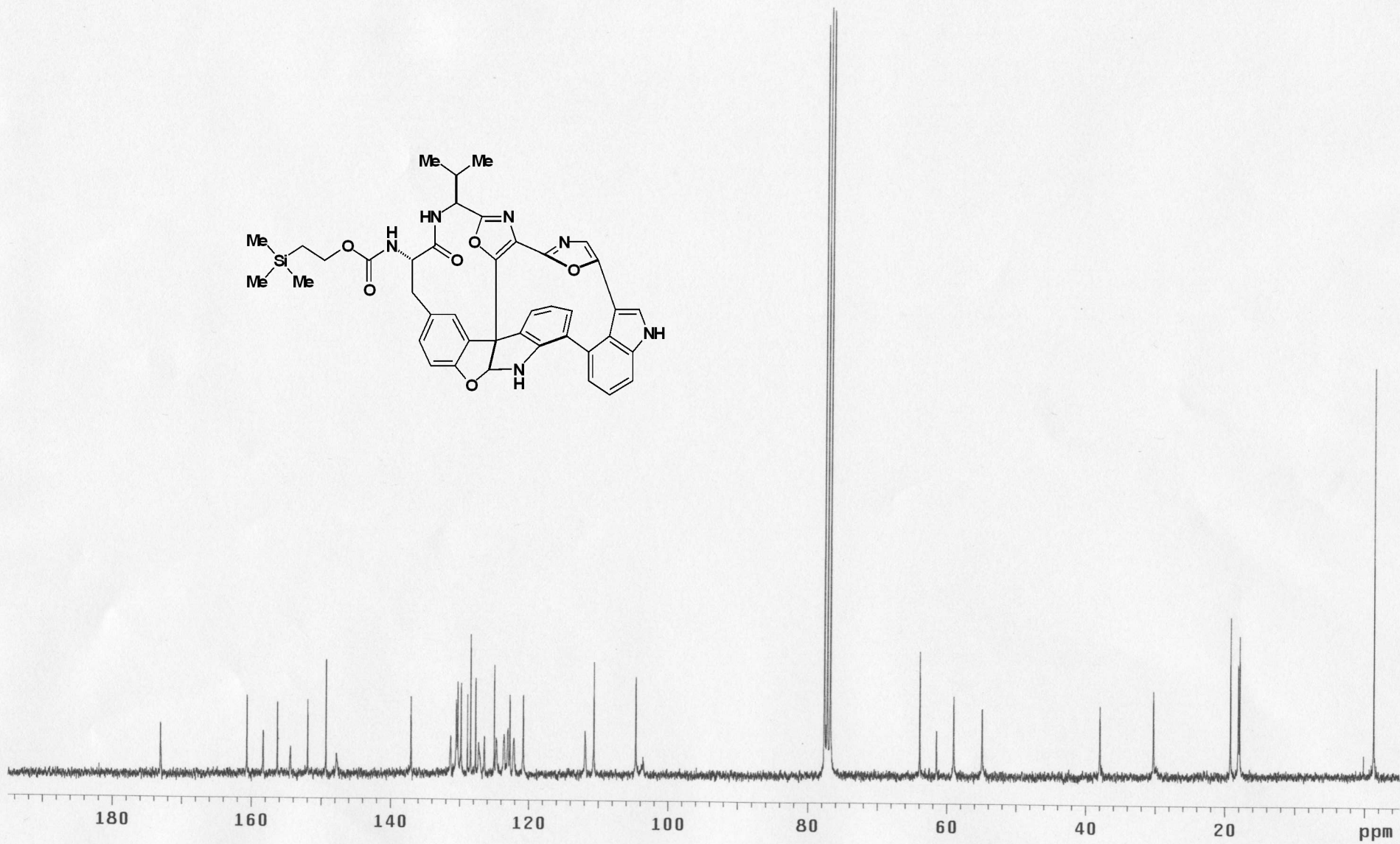
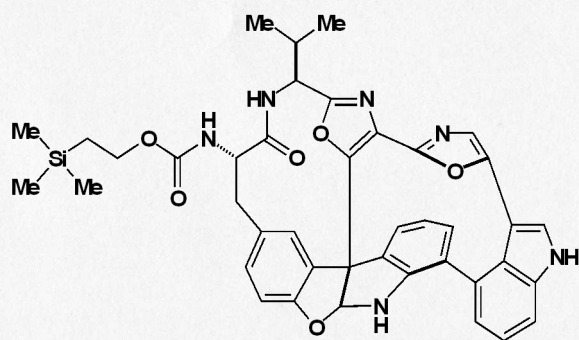
Pulse Sequence: s2pu1

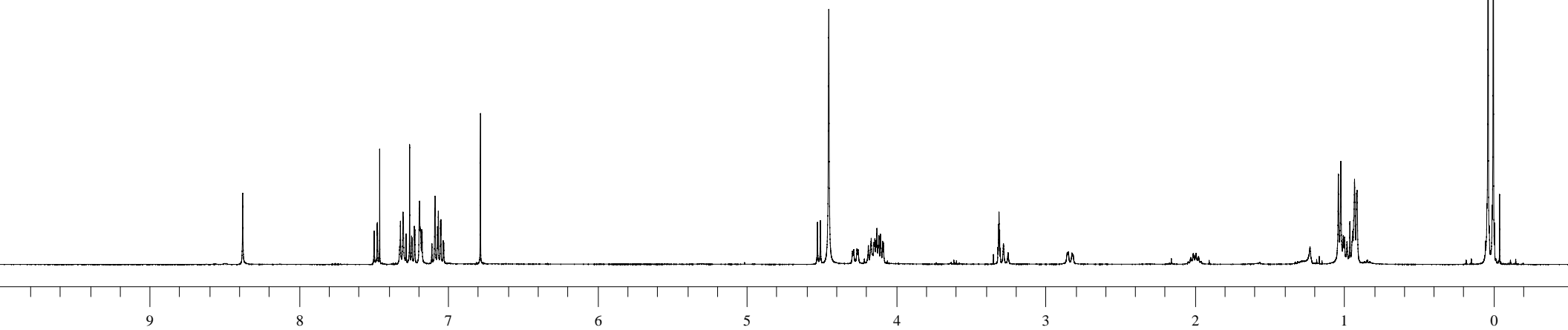
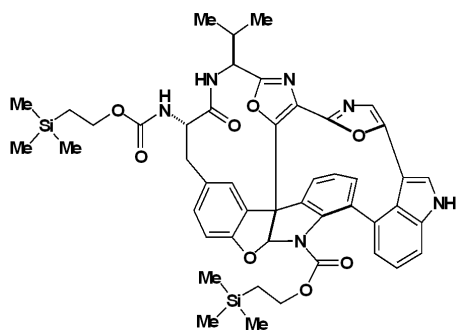




¹³C OBSERVE

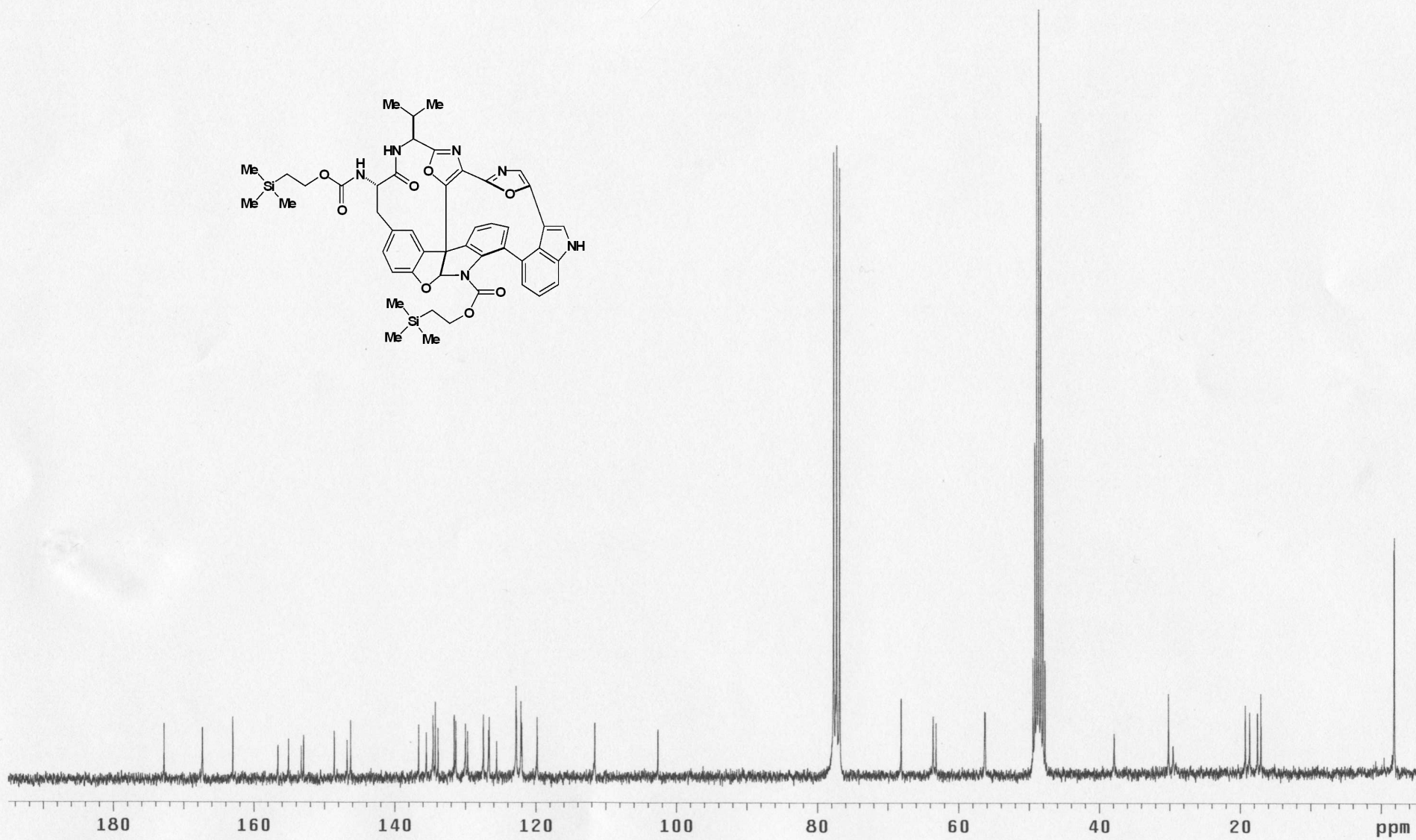
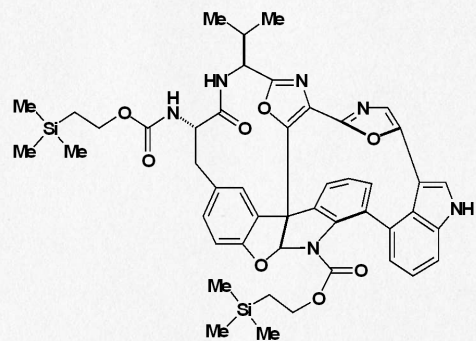
Pulse Sequence: s2pu1





#304A (ABVII286Bis-Teoc)

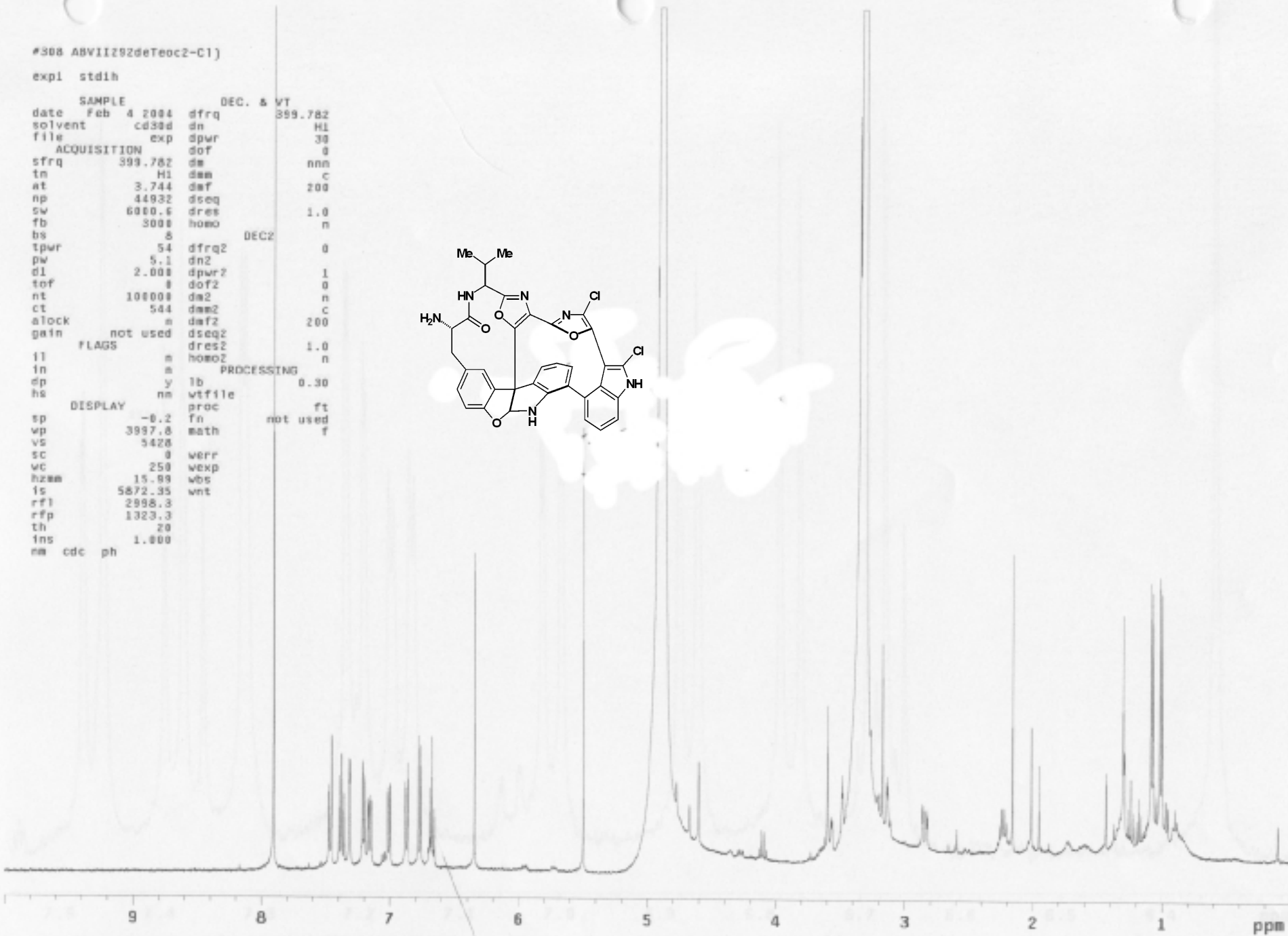
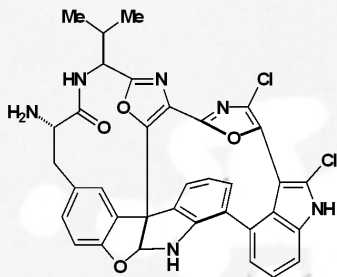
Pulse Sequence: s2pu1



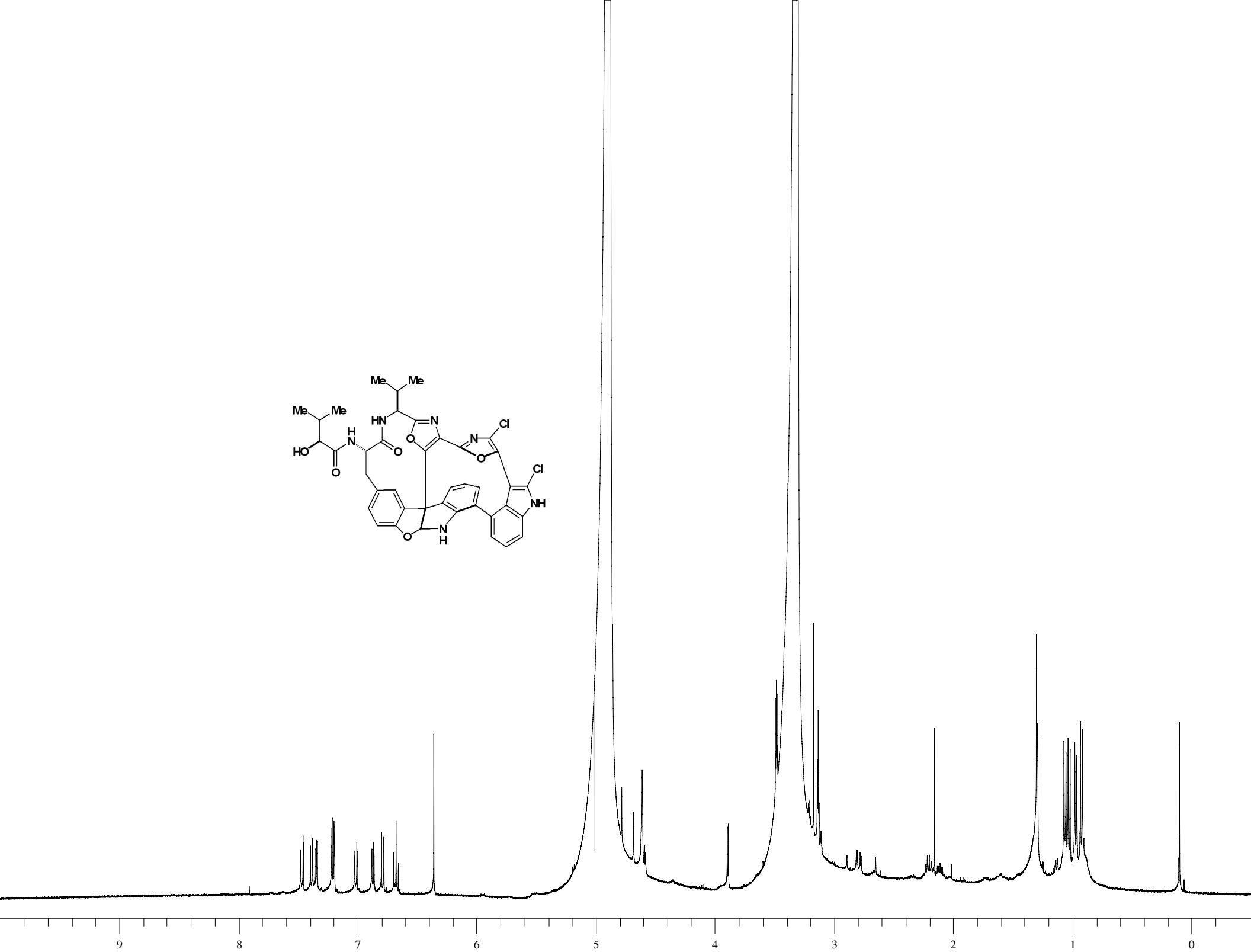
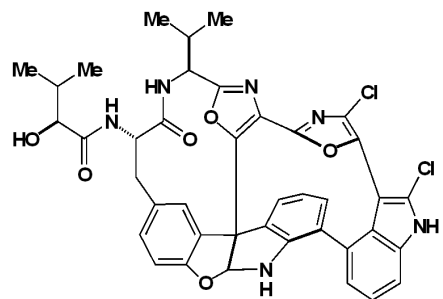
#308 ABVII292deTeoc2-C1)

expl stdih

SAMPLE		DEC. & VT	
date	Feb 4 2004	dfrq	399.782
solvent	cd3sd	dn	HL
file	exp	dpwr	38
ACQUISITION		dof	0
sfrq	399.782	ds	nnn
tn	H1	dsm	c
at	3.744	daf	200
np	44932	dseq	
sw	6000.6	dres	1.0
fb	3000	homo	n
bs	8	DEC2	
tpwr	54	dfrq2	0
pw	5.1	dn2	
d1	2.000	dpwr2	1
tof	0	dof2	0
nt	100000	dm2	n
ct	544	dsm2	c
atock	m	daf2	200
gain	not used	dseq2	
FLAGS		dres2	1.0
fl	m	homo2	n
in	m	PROCESSING	
dp	y	lb	0.30
hs	nm	wtfile	
DISPLAY		proc	ft
sp	-0.2	fn	not used
wp	3997.8	math	f
vs	5428		
sc	0	werr	
vc	250	wexp	
hzam	15.88	wbs	
is	5872.35	wnt	
rfl	2998.3		
rfp	1323.3		
th	20		
ins	1.800		
nm	cdc ph		



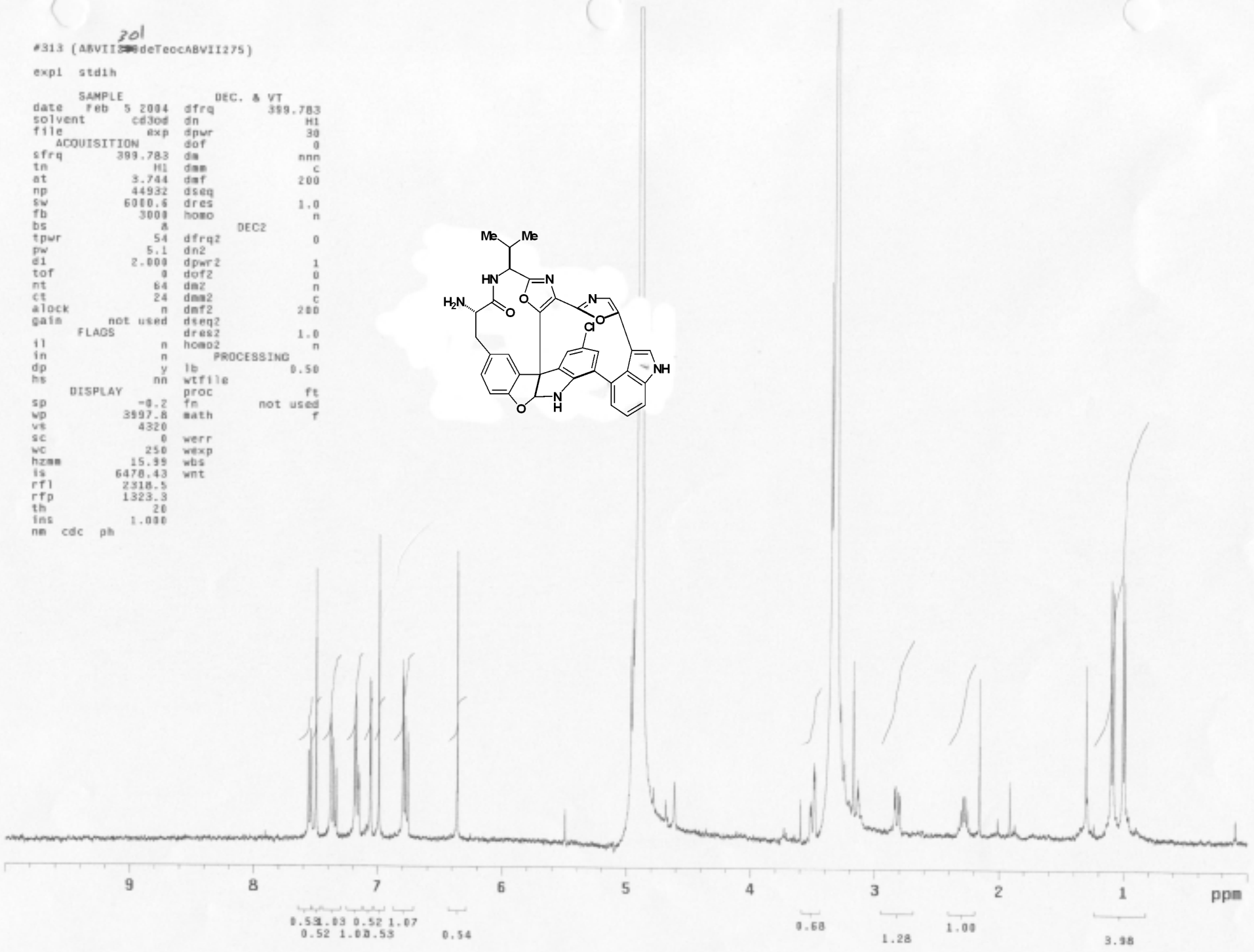
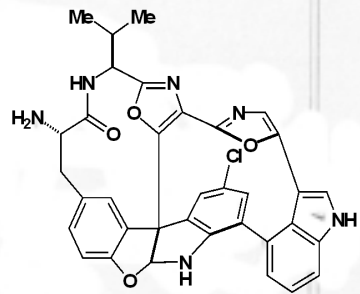
1.38.04 1.141.29 1.04
1.38.49 1.22.28



201
#313 (ABVII200deTeocABVII275)

expl stdih

SAMPLE		DEC. & VT	
date	Feb 5 2004	dfrq	399.783
solvent	cd3od	dn	H1
file	exp	dpwr	30
ACQUISITION		dof	0
sfrq	399.783	dm	nnn
tn	H1	dsm	c
at	3.744	daf	200
np	44932	dseq	
sw	6000.6	dres	1.0
fb	3000	homo	n
bs	8	DEC2	
tpwr	54	dfrq2	0
pw	5.1	dn2	
d1	2.000	dpwr2	1
tof	0	dof2	0
nt	84	dm2	n
ct	24	dsm2	c
alock	n	daf2	200
gain	not used	dseq2	
FLAGS		dres2	1.0
il	n	homo2	n
in	n	PROCESSING	
dp	y	lb	0.50
hs	nn	wtfile	
DISPLAY		proc	ft
sp	-0.2	fn	not used
wp	3997.8	math	f
vs	4320		
sc	0	werr	
wc	250	wexp	
hzmm	15.99	wbs	
is	6478.43	wnt	
rfl	2318.5		
rfp	1323.3		
th	20		
lms	1.000		
nm	cdc	ph	



A colorless plate crystal having approximate dimensions of 0.7 x 0.4 x 0.2 mm was mounted on a glass fiber. X-ray measurement on the selected crystal was performed on an Enraf-Nonius KappaCCD diffractometer at 293 K using MoK α radiation ($\lambda = 0.71069\text{\AA}$) and a graphite monochromator.

Unit Cell dimensions were obtained by a least squares fit to the optimized setting angles of all measured reflections in the full θ range. Intensity data were collected using COLLECT software (nonius, Netherlands) in ϕ and ω range with κ offsets. Data reduction was done using DENZO (Otwinowski, Z and Minor, W. *Methods Enzymol.* 1996, 276). The data were collected at 20°C using ω -2 θ scan to a maximum 2 θ of 41°. Of the 2239 reflections collected 2220 were unique (Rint=0.06). Intensity of equivalent reflections was averaged. Based on systematic absences of: h00: $h = 2n+1$, 0k0: $k = 2n+1$, and 00l: $l=2n+1$, the space group was unambiguously determined to be P2₁2₁2₁. The data were corrected for Lorentz and Polarization effects.

The structure was solved by direct methods using SHELXS-97 (Sheldrick, G. M. SHELXS97: A Program for Crystal Structure Refinement; University of Gottingen, Gottingen, Germany, 1997) and refined by full-matrix least squares refinement using SHELXL-97 (Sheldrick, G. M. SHELXL97: A Program for Crystal Structure Refinement; University of Gottingen, Gottingen, Germany, 1997). The function minimized was $\sum w(|F_o|^2 - |F_c|^2)^2$ and the weight w defined as $w = 1 / [\sigma^2(F_o^2) + (0.1009 * P)^2]$ where $P = (F_o^2 + 2F_c^2) /$

3. All the non-hydrogen atoms were refined anisotropically. The hydrogen atoms were fixed by geometrical considerations.

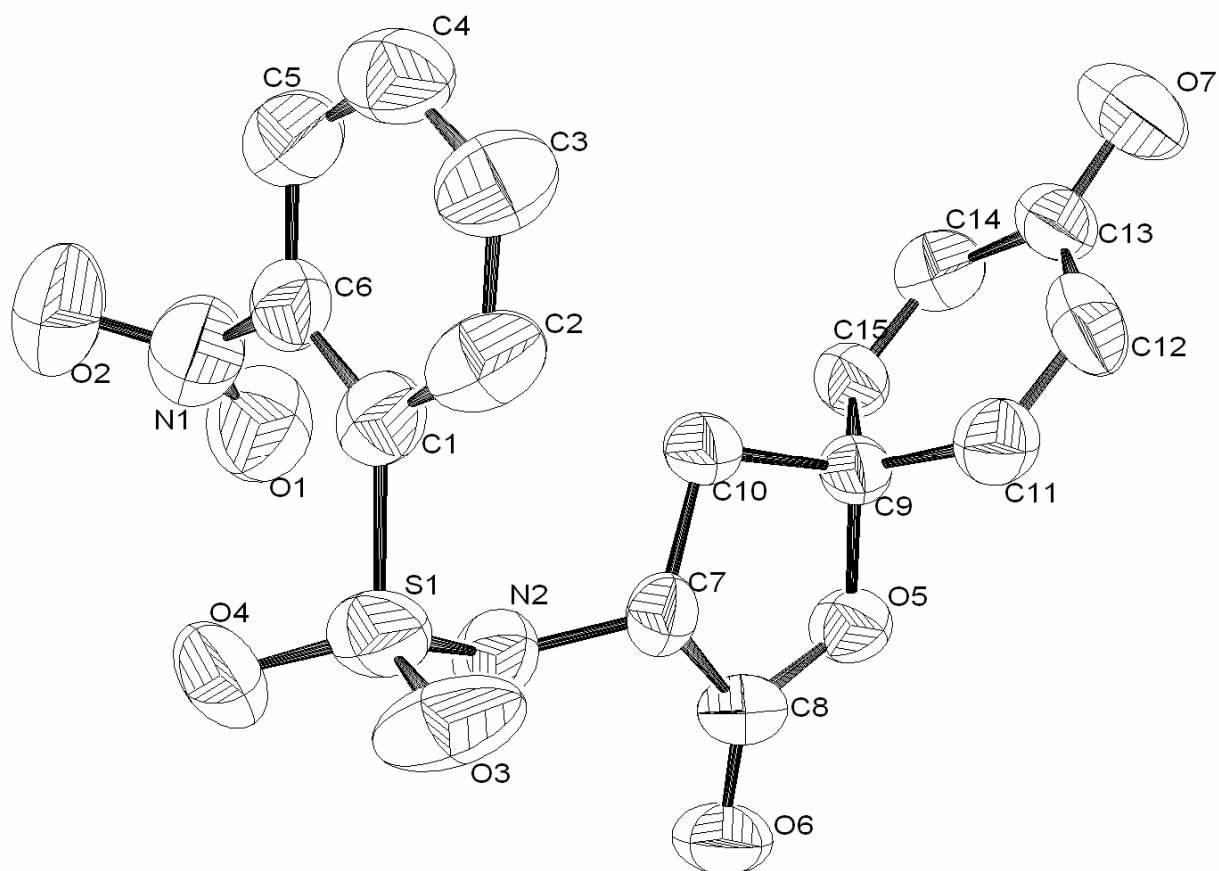


Table 1. Crystal data and structure refinement for **338**

A. Crystal Data

Empirical formula	C ₁₅ H ₁₂ N ₂ O ₇ S ₁
Formula weight	354.61
Wavelength	0.71073 Å
Crystal system, space group	Orthorhombic, Pbc _a
Unit cell dimensions	a = 12.6120(5) Å b = 13.2490(5) Å c = 18.6910(9) Å
Volume	3123.2(2) Å ³

Calculated density	1.550 Mg/m ³
Absorption coefficient	0.251 mm ⁻¹

B. Intensity Measurements

Diffractometer	Enraf-Nonius
Detector	Kappa CCD
Radiation	RMoKa (λ=0.71069Å)
Temperature	293(2) K
Scan-Type	ω-2θ
Theta range for data collection	2.71 to 20.81 deg.
Reflections collected / unique	1563 / 1563 [R(int) = 0.0000]
Correction	Lorentz-Polarization

C. Structure Solution and Refinement

Refinement method	Full-matrix least-squares on F ²
Data / restraints / parameters	1563 / 0 / 274
Goodness-of-fit on F ²	0.749
R indices (all data)	R1 = 0.0816, wR2 = 0.0583
Largest diff. peak and hole	0.109 and -0.108 e.Å ⁻³

Table 2. Atomic coordinates ($\times 10^4$) and equivalent isotropic displacement parameters ($\text{Å}^2 \times 10^3$)
 For 338. U(eq) is defined as one third of the trace of the orthogonalized Uij tensor.

	x	y	z	U (eq)
C (1)	-352 (3)	7580 (4)	3046 (2)	58 (1)
C (2)	-299 (4)	8570 (4)	3284 (2)	72 (1)
C (3)	-1086 (4)	8967 (5)	3722 (2)	77 (2)
C (4)	-1883 (4)	8376 (5)	3944 (2)	74 (1)
C (5)	-1941 (3)	7394 (5)	3737 (2)	68 (1)
C (6)	-1189 (3)	7006 (4)	3275 (2)	58 (1)
N (1)	-1335 (3)	5984 (4)	3037 (2)	84 (1)
O (1)	-1345 (3)	5807 (3)	2392 (2)	99 (1)
O (2)	-1467 (3)	5329 (3)	3481 (2)	117 (1)
S (1)	692 (1)	7150 (1)	2487 (1)	71 (1)
O (3)	1533 (2)	7843 (3)	2562 (1)	97 (1)
O (4)	854 (2)	6092 (2)	2619 (2)	100 (1)
N (2)	255 (3)	7189 (3)	1661 (2)	62 (1)
C (7)	-64 (3)	8152 (3)	1355 (2)	47 (1)
C (8)	80 (3)	8107 (3)	553 (2)	53 (1)
O (5)	-702 (2)	8641 (2)	233 (1)	55 (1)
C (9)	-1481 (3)	9027 (3)	742 (2)	45 (1)
C (10)	-1222 (3)	8450 (4)	1446 (2)	54 (1)
O (6)	778 (2)	7730 (2)	223 (1)	68 (1)
C (11)	-1346 (4)	10133 (3)	825 (2)	59 (1)
C (12)	-2133 (4)	10763 (3)	816 (2)	70 (1)
C (13)	-3223 (4)	10435 (3)	675 (2)	60 (1)
O (7)	-3968 (3)	11015 (3)	708 (2)	96 (1)
C (14)	-3331 (4)	9391 (4)	452 (2)	60 (1)
C (15)	-2543 (3)	8745 (3)	471 (2)	52 (1)

Table 3. Bond lengths [Å] for 338.

C (1) -C (6)	1.369 (5)	C (7) -C (8)	1.512 (5)
C (1) -C (2)	1.387 (6)	C (7) -C (10)	1.523 (5)
C (1) -S (1)	1.775 (4)	C (8) -O (6)	1.185 (4)
C (2) -C (3)	1.392 (6)	C (8) -O (5)	1.352 (4)
C (3) -C (4)	1.339 (7)	O (5) -C (9)	1.459 (4)
C (4) -C (5)	1.359 (7)	C (9) -C (15)	1.479 (5)
C (5) -C (6)	1.382 (6)	C (9) -C (11)	1.484 (5)
C (6) -N (1)	1.437 (5)	C (9) -C (10)	1.557 (5)
N (1) -O (2)	1.212 (4)	C (11) -C (12)	1.296 (5)
N (1) -O (1)	1.228 (5)	C (12) -C (13)	1.466 (6)
S (1) -O (3)	1.409 (3)	C (13) -O (7)	1.216 (5)
S (1) -O (4)	1.437 (3)	C (13) -C (14)	1.450 (5)
S (1) -N (2)	1.641 (3)	C (14) -C (15)	1.312 (6)
N (2) -C (7)	1.454 (5)		

Table 4. Bond angles [°] for 338

C (6) -C (1) -C (2)	117.5 (4)	N (2) -C (7) -C (10)	116.7 (3)
C (6) -C (1) -S (1)	125.3 (4)	C (8) -C (7) -C (10)	103.6 (3)
C (2) -C (1) -S (1)	117.1 (3)	O (6) -C (8) -O (5)	122.2 (3)
C (1) -C (2) -C (3)	120.8 (5)	O (6) -C (8) -C (7)	128.4 (3)
C (4) -C (3) -C (2)	119.7 (5)	O (5) -C (8) -C (7)	109.2 (3)
C (3) -C (4) -C (5)	120.9 (5)	C (8) -O (5) -C (9)	112.8 (2)
C (4) -C (5) -C (6)	119.7 (5)	O (5) -C (9) -C (15)	107.4 (3)
C (1) -C (6) -C (5)	121.2 (5)	O (5) -C (9) -C (11)	109.7 (3)
C (1) -C (6) -N (1)	121.7 (4)	C (15) -C (9) -C (11)	112.9 (4)
C (5) -C (6) -N (1)	117.1 (5)	O (5) -C (9) -C (10)	103.7 (3)
O (2) -N (1) -O (1)	122.2 (5)	C (15) -C (9) -C (10)	110.8 (3)
O (2) -N (1) -C (6)	118.8 (4)	C (11) -C (9) -C (10)	111.9 (3)
O (1) -N (1) -C (6)	119.0 (4)	C (7) -C (10) -C (9)	103.6 (3)
O (3) -S (1) -O (4)	120.8 (2)	C (12) -C (11) -C (9)	123.1 (4)
O (3) -S (1) -N (2)	109.0 (2)	C (11) -C (12) -C (13)	121.9 (4)
O (4) -S (1) -N (2)	103.9 (2)	O (7) -C (13) -C (14)	123.0 (5)
O (3) -S (1) -C (1)	106.9 (2)	O (7) -C (13) -C (12)	121.9 (4)
O (4) -S (1) -C (1)	108.5 (2)	C (14) -C (13) -C (12)	115.0 (4)
N (2) -S (1) -C (1)	107.1 (2)	C (15) -C (14) -C (13)	122.9 (4)
C (7) -N (2) -S (1)	119.4 (3)	C (14) -C (15) -C (9)	122.0 (4)
N (2) -C (7) -C (8)	108.8 (3)		

Table 5. Anisotropic displacement parameters ($\text{\AA}^2 \times 10^3$) for 338.

	U11	U22	U33	U23	U13	U12
C (1)	52 (3)	72 (3)	48 (2)	10 (2)	-8 (2)	-3 (2)
C (2)	55 (3)	107 (4)	54 (3)	-1 (3)	-3 (2)	-15 (3)
C (3)	77 (4)	89 (4)	64 (3)	-11 (3)	7 (3)	-12 (3)
C (4)	69 (4)	98 (4)	55 (3)	-8 (3)	0 (3)	14 (4)
C (5)	44 (3)	101 (5)	60 (3)	14 (3)	-7 (2)	-2 (3)
C (6)	56 (3)	64 (3)	55 (2)	13 (2)	-5 (2)	3 (3)
N (1)	80 (3)	89 (4)	84 (3)	18 (3)	-6 (2)	-9 (2)
O (1)	120 (3)	79 (2)	99 (3)	-2 (2)	2 (2)	-4 (2)
O (2)	146 (3)	87 (3)	117 (3)	42 (2)	14 (2)	-3 (2)
S (1)	47 (1)	111 (1)	56 (1)	13 (1)	-5 (1)	14 (1)
O (3)	43 (2)	179 (3)	70 (2)	-4 (2)	1 (2)	-26 (2)
O (4)	99 (2)	112 (2)	89 (2)	31 (2)	5 (2)	56 (2)
N (2)	63 (2)	75 (3)	49 (2)	11 (2)	-2 (2)	0 (2)
C (7)	49 (3)	48 (3)	45 (2)	8 (2)	-4 (2)	-4 (2)
C (8)	44 (2)	62 (3)	52 (2)	-8 (2)	6 (2)	0 (2)
O (5)	54 (2)	69 (2)	42 (1)	4 (1)	5 (1)	7 (2)
C (9)	53 (3)	44 (2)	38 (2)	-1 (2)	5 (2)	7 (2)
C (10)	59 (3)	57 (3)	47 (2)	4 (2)	12 (2)	14 (2)
O (6)	53 (2)	89 (2)	64 (2)	-2 (2)	14 (1)	15 (2)
C (11)	59 (3)	54 (3)	64 (3)	-2 (2)	1 (2)	-6 (3)
C (12)	93 (4)	45 (3)	72 (3)	-2 (2)	-7 (2)	17 (3)
C (13)	70 (3)	62 (3)	47 (2)	2 (2)	5 (2)	23 (3)
O (7)	106 (3)	95 (2)	87 (2)	-10 (2)	-2 (2)	48 (2)
C (14)	50 (3)	78 (4)	52 (2)	-2 (2)	-7 (2)	-3 (3)
C (15)	46 (3)	50 (3)	61 (2)	2 (2)	-1 (2)	4 (2)

Table 6. Hydrogen coordinates ($\times 10^4$) and isotropic displacement parameters ($\text{\AA}^2 \times 10^3$) for anthony2.

	x	y	z	U (eq)
H (2)	270 (30)	8880 (30)	3148 (17)	45 (11)
H (3)	-1010 (40)	9730 (40)	3910 (30)	126 (19)
H (4)	-2420 (40)	8680 (30)	4211 (18)	82 (14)
H (5)	-2490 (30)	6890 (30)	3786 (19)	72 (14)
HN2	-330 (40)	6640 (40)	1610 (30)	150 (20)
H (7)	450 (30)	8620 (20)	1543 (15)	51 (11)
H (101)	-1630 (30)	7700 (30)	1525 (18)	91 (13)
H (102)	-1330 (30)	8800 (30)	1813 (17)	57 (13)
H (11)	-640 (30)	10280 (20)	878 (16)	46 (11)
H (12)	-1920 (40)	11630 (40)	840 (20)	145 (19)
H (14)	-3930 (30)	9190 (30)	323 (18)	44 (12)
H (15)	-2570 (30)	8030 (30)	343 (17)	63 (11)

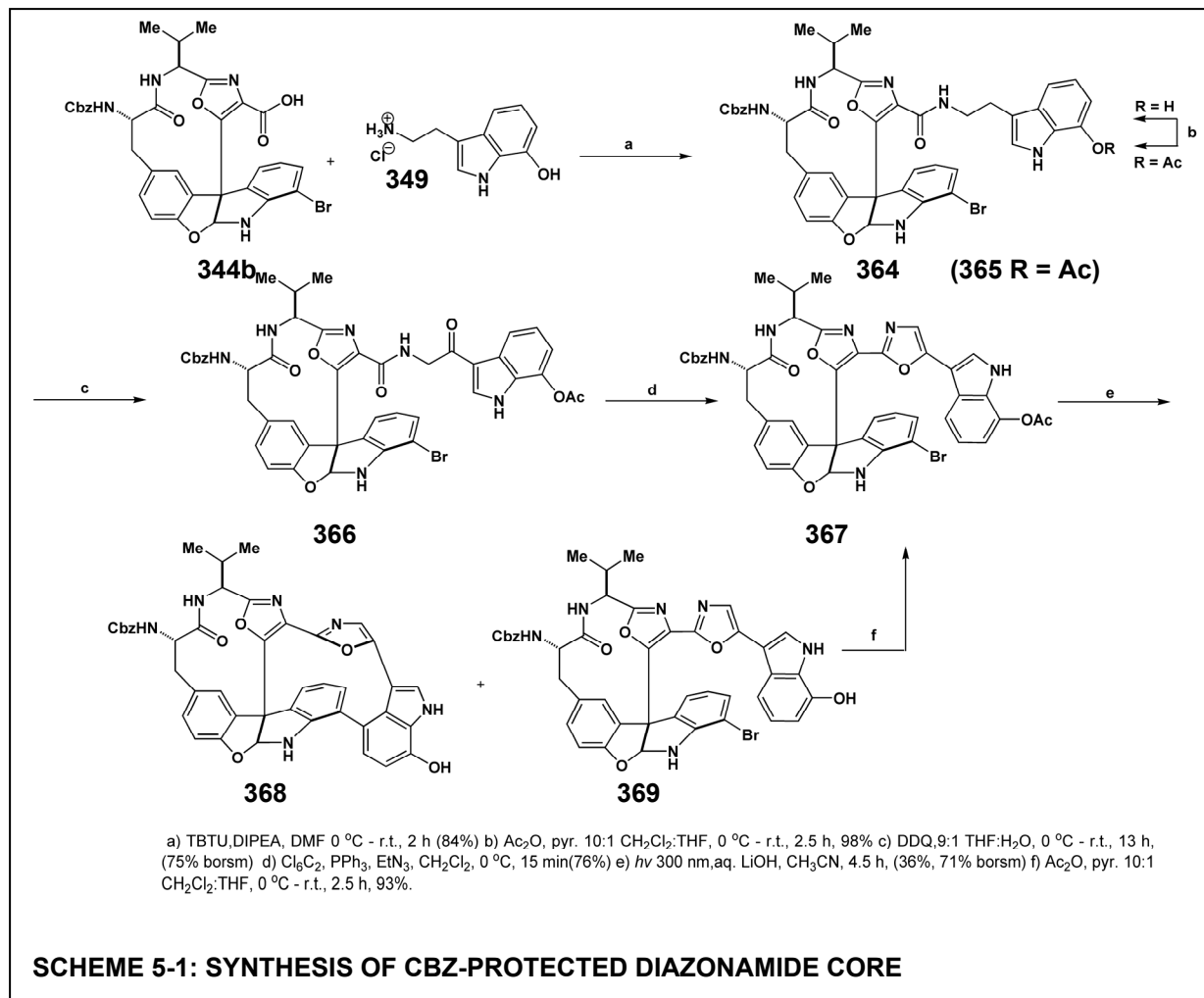
CHAPTER FIVE

Synthesis and Evaluation of Diazonamide A Analogs

5.1 Introduction

The successful total synthesis of diazonamide A granted access to further explore the biological activity and SAR of the natural product. In many respects these studies were a continuation of the prior work described in the syndistatin series (**Chapter 3** and **4**). Dissimilar to most cases, the biological activity of diazonamide A was already characterized prior to its total synthesis, and through the syndistatin compound, the initial SAR indications were determined and probe analogs were synthesized. The major practical difference compared to syndistatin, however, is the concise and scalable nature of the diazonamide A total synthesis. Unprecedented amounts of material and late stage diazonamide analogs could be synthesized, evaluated for biological function, and used to further explore the cellular mode of action and possible pharmacological utility of the diazonamides. As with any SAR undertaking, a major goal was the identification of simplified, more-synthetically accessible diazonamide analogs that retained full biological activity. In the case of diazonamide A, there was also a need to make a full range of probe analogs to complement the syndistatin probes described previously (**Chapter 3**).

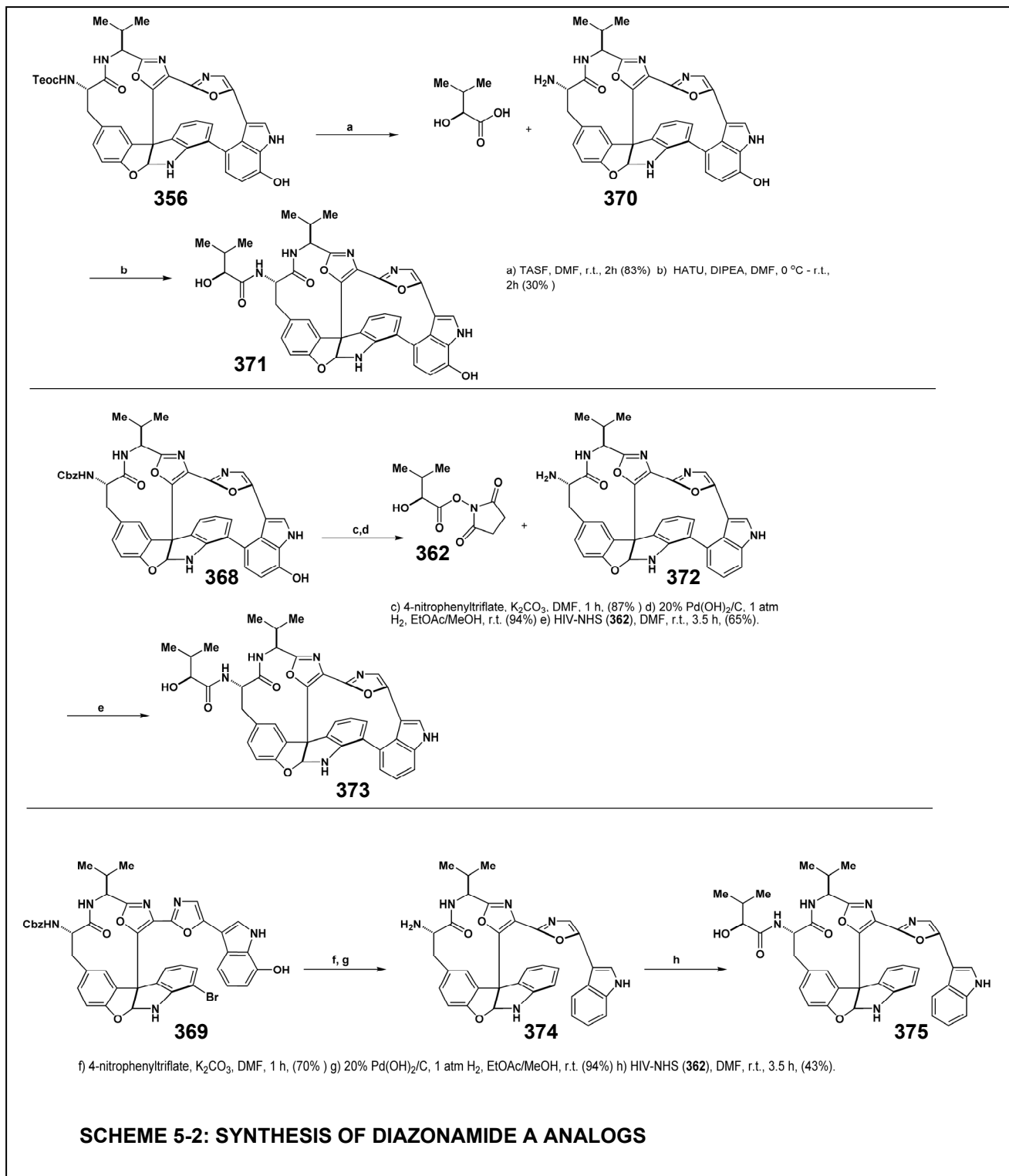
The developed route to diazonamide A could also be explored as a modular synthesis. A modular synthesis would allow for the incorporation of different amino acid building block in the total synthesis. This possibility is feasible due to the convergent nature of the synthesis and the concise number of steps. If successful, the modular approach could be a power method in further probing the SAR of the molecule and generating new and complex natural-product-like



compounds. The amino acid component whose replacement would most likely be tolerated is valine. Substitution of valine, especially with another aliphatic amino acid, would not be anticipated to interfere with the developed total synthesis.

5.2 Synthesis and Evaluation of Simplified Diazonamide Analogs

The initial SAR studies focused on compounds related to synthetic intermediates. To pursue this, the Cbz-protected C10 macrocyclic core **344b** was elaborated into the diazonamide core (**Scheme 5-1**) **368** using the chemistry described for the total synthesis (**Section 4.3.4**).



Based on the syndistatin SAR data, the complete diazonamide structure was required for biological activity, but there was no indication of whether additional substituents on the

diazonamide skeleton were tolerated. Therefore, the first synthetic intermediate to be evaluated was phenol **356** (Scheme 5-2). This compound, accessible in 14 steps, was converted into diazonamide A analog **371**. The next analog in this series to be created was the non-chlorinated diazonamide core **368**. This compound is produced via triflate formation and reduction of the phenol **356**. For the Cbz-protected compound, the triflate reduction is accompanied by hydrogenolysis of the Cbz group to produce amine **372**. Introduction of the HIV side chain completes analog **373** in 16 overall steps. Both of these analogs were evaluated for cytotoxicity against a panel of cell lines. In this assay, the averaged IC_{50} value for diazonamide A was 3 nM.

Analog **371** had an average $IC_{50} = 17$ nM and **373** possessed an $IC_{50} = 3$ nM, or, equipotent to diazonamide A. This finding was a major achievement in searching for a simplified SAR analog. The chlorination of the diazonamide core requires four steps additional steps and is very poor yielding. Non-chlorinated diazonamide **373** could be produced in hundreds of milligrams, and for the first time, a diazonamide related compound could be evaluated in *in vivo* mouse tumor xenograft models. These studies were conducted by Dr. Noelle Williams, and a manuscript reporting the results has been submitted for publication. To provide an inactive control version of **373**, non-cyclized analog **375** was prepared from bis-oxazole **369** through reduction to amine **374**. The non-cyclized negative control analog is similar to the syndistatin negative control compound **273**.

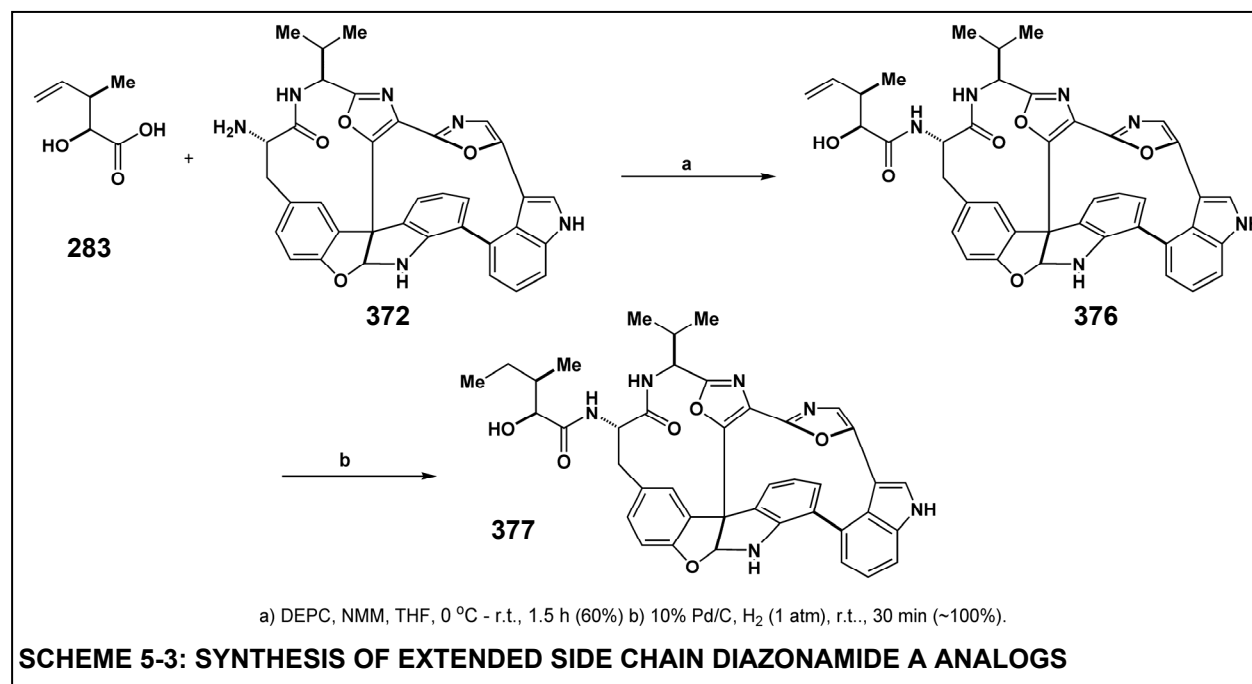
5.3 Synthesis of Extended Side Chain Diazonamide A Analogs

The pharmacological experiments involving tissue distributions of analog **373** necessitated the development of a control analog for mass spectrometry. The ideal for such a control is a compound very similar structurally but possessing a slight different mass. To this

end, analog **377** was synthesized through hydrogenation of coupled product **376**. An analogous syndistatin compound (**285**) had been previously made.

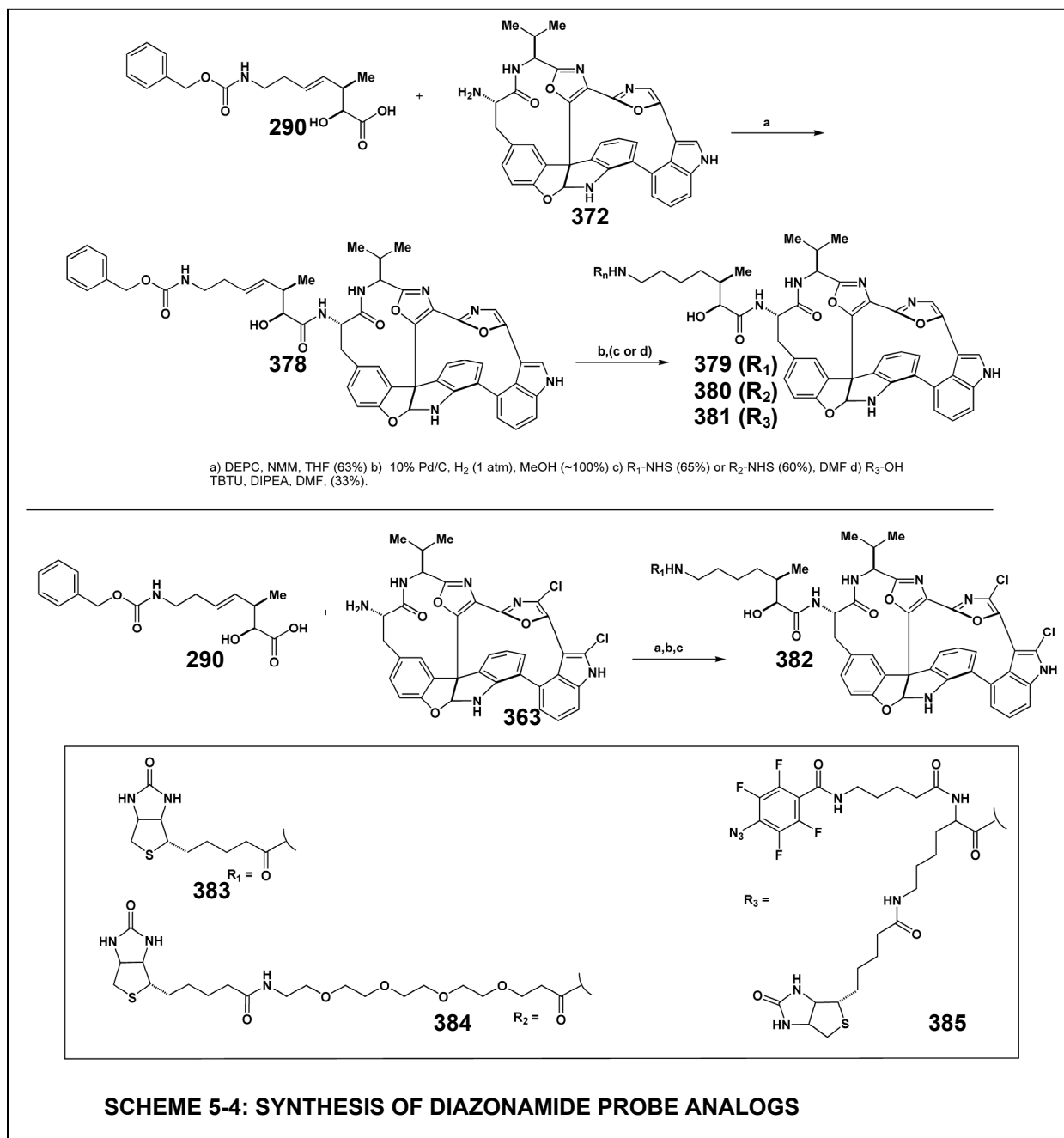
5.4 Synthesis of Diazonamide A Probe Analogs

With the developed synthesis of diazonamide A, it was possible to generate probes analogs similar to the syndistatin probe analogs (**Chapter 3**). Using the developed approach with the extended side chain **290**, biotinylated forms of both **373** (**379**) and diazonamide A (**9**) (**382**) were prepared (**Scheme 5-4**). These compounds were analogous to the syndistatin biotinylated



compound **296**. In addition, the biotinylated analog **380** was also prepared. This compound incorporated a PEG linker between biotin and the diazonamide core. The PEG linker increases the space and should maintain an extended conformation in aqueous media. Both of these

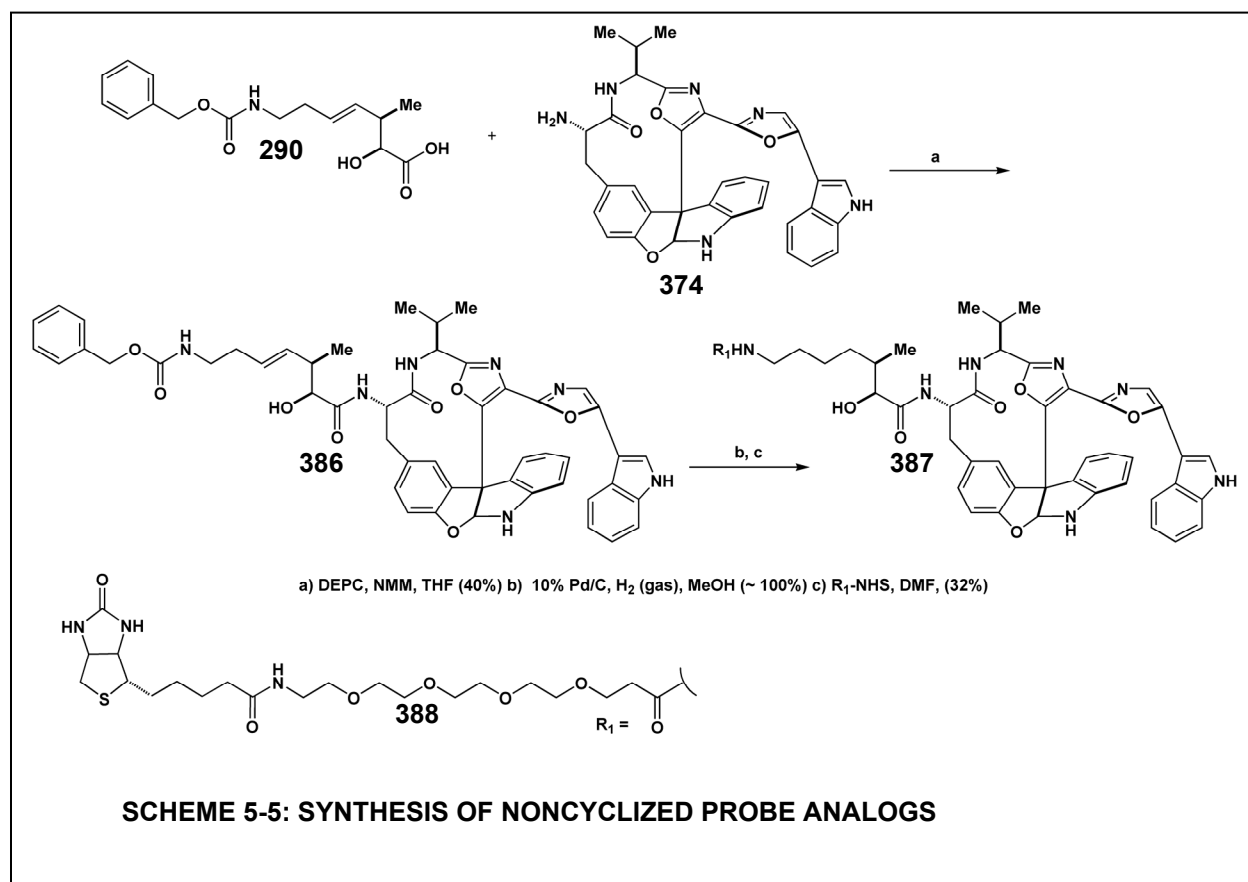
attributes should make it a superior affinity chromatography reagent compared to **379**. To compliment the experimental used of **380**, negative control compound **387** (Scheme 5-5) was



also prepared. An addition tool for exploring the molecular pharmacology of the diazonamides was the synthesis of the photocrosslinking, biotinylated compound **381**. The incorporation of the aryl azide containing group **385** produced a diazonamide compound capable of covalently

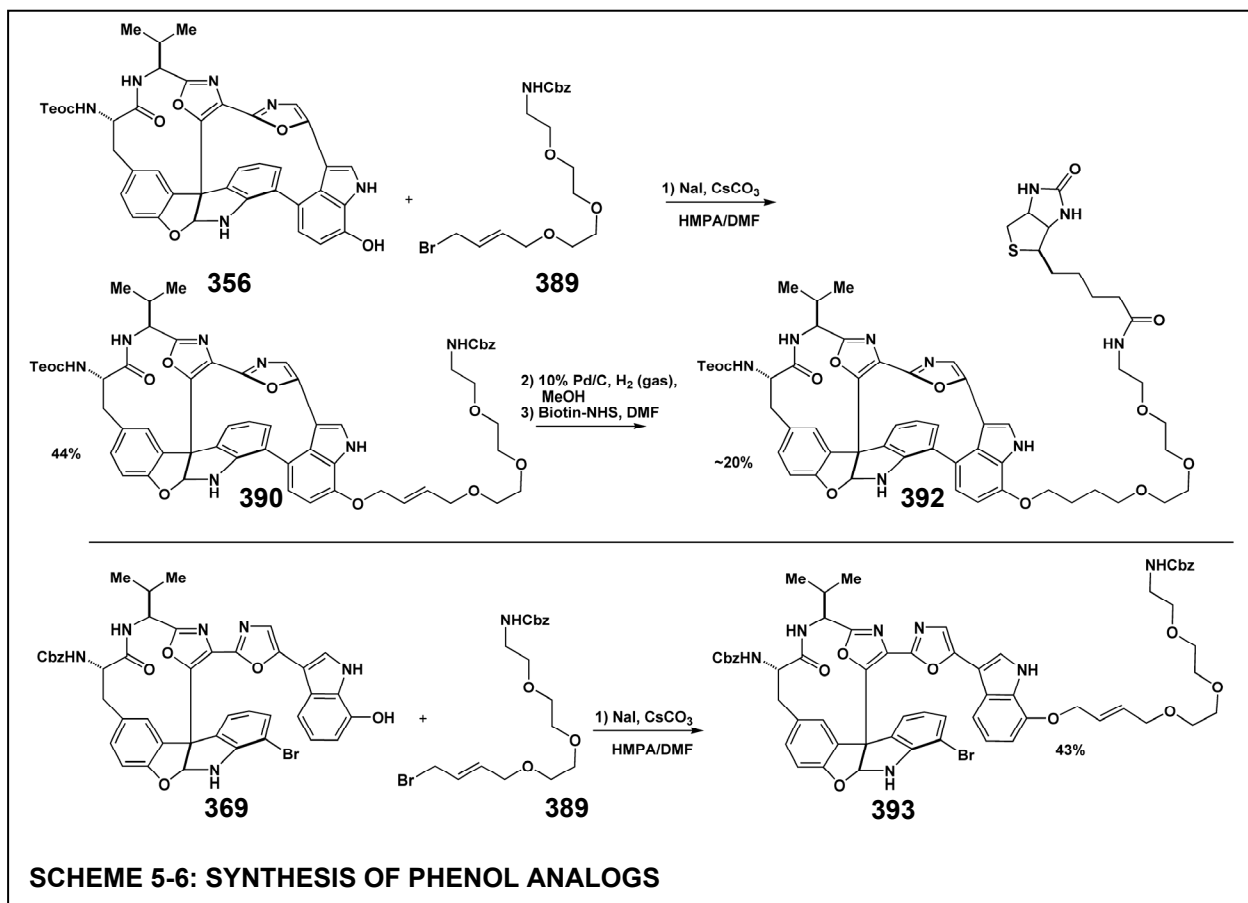
binding the cellular target up photoactivation. The presence of biotin in **385** would then allow for the bound protein/diazonamide complex to be affinity purified with avidin. The photoactivation of **381** was successfully tested in aqueous buffer.

The synthesis of the phenol containing diazonamide synthetic intermediates, such as **356** (Scheme 5-6), introduced a point of functionalization on the right side of the molecule. Linker **389** was successfully appended on the phenol through a direct nucleophilic displacement reaction. Palladium mediated hydrogenolysis of the Cbz group allowed



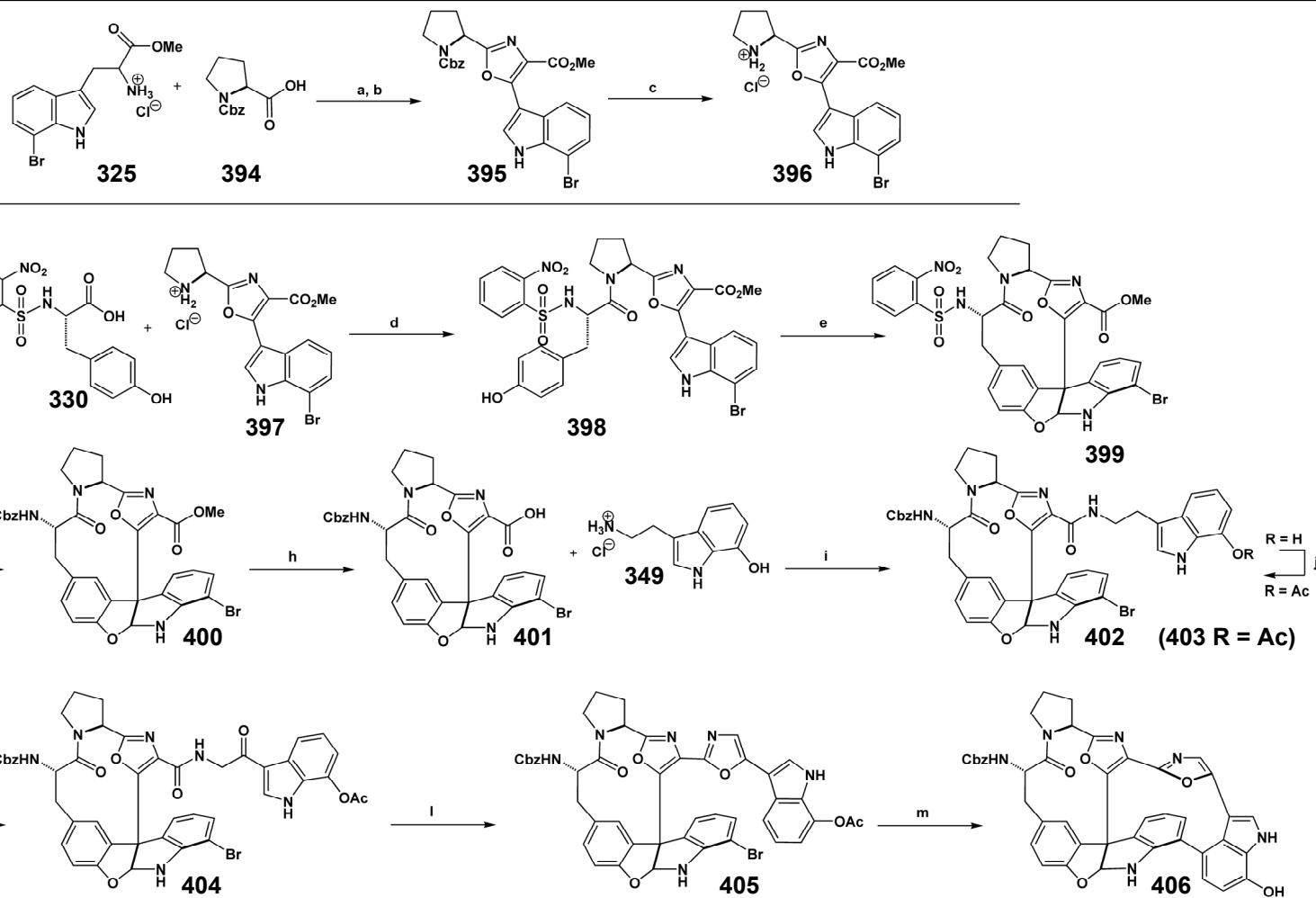
for biotinylation of the resultant amine to be achieved. The ability to functionalize this position in the noncyclized compound (**369**) was also successful with this method. Due to material restrictions, the phenol based analogs **392** and **393** were not transformed into the complete

diazonamide analogs. Therefore, the effect of functionalizing the phenolic position on the biological activity could not be evaluated. The ability, however, to modify the right side of the structure could be important in fully exploring the molecular pharmacology of the molecule.



5.5 Synthesis of Proline Containing Diazonamide Core

To explore the possible modular nature of the diazonamide A synthesis, a proline residue was substituted for valine. In designing this approach, it was postulated that most of the steps in



a) TBTU, DIPEA, DMF, 4 °C, 2 h, (95 %) b) DDQ, THF, 75 °C, 13 h (67%) c) 33% HBr/AcOH, 30 min, (95%) d) TBTU, DIPEA, DMF, 0 °C, 4 h (85%) e) PhI(OAc)₂, LiOAc, TFE, -25 °C, 40 min, (17%) f) PhSH, K₂CO₃, DMF, r.t, 2 h g) Cbz-OSu, DMF, 0 °C - r.t., 1.5 h, (90% two steps) h) LiOH, 4:1 MeOH:H₂O, 0 °C - r.t, 5 h (95%) i) TBTU, DIPEA, DMF 0 °C - r.t., 2 h (84%) j) Ac₂O, pyr. 10:1 CH₂Cl₂:THF, 0 °C - r.t., 2.5 h, (98%) k) DDQ, 9:1 THF:H₂O, 0 °C - r.t., 13 h, (74% borsm) l) Cl₆C₂, PPh₃, EtN₃, CH₂Cl₂, 0 °C, 15 min (69%) m) *hν* 300 nm, aq. LiOH, CH₃CN, 4.5 h, (~25%).

SCHEME 5-7: SYNTHESIS OF PROLINE ANALOG DIAZONAMIDE CORE

the synthesis would not be affected by the presence of the proline containing substrate. The real question was whether the hypervalent iodine oxidation would generate the desired C10 macrocycle in the proline series. The proline synthesis began with the TBTU coupling of proline with 7-bromotryptophan followed by DDQ oxidation (**395**) (**Scheme 5-7**). Deprotection of the Cbz group (**396**, 95%) and TBTU coupling with the Nos-protected tyrosine (**398**, 85%) proceeded uneventfully to produce oxidation substrate **398**. Subjecting this compound to the hypervalent iodine oxidation conditions formed the desired C10 macrocycle **399** in yields similar to the valine case.

The macrocycle **399** was then elaborated using the developed methodology to the fully cyclized photochemistry product **406**. A lack of material supply prevented the completion of the synthesis in the proline series of compounds, but this synthesis strongly indicates diazonamide proline analog could be achieved and evaluated. Therefore, other amino acids could also very likely be incorporated in place of valine.

5.6 Discussion

The most important SAR finding for diazonamide A was the discovery that the non-chlorinated analog retained the full potency of the natural product. As discussed (**Section 4-4**), the low yielding chlorination was a major choke point in the diazonamide A total synthesis. It should be noted that the non-chlorinated syndistatin analog (**277**) exhibited a substantial loss of potency ($IC_{50} = 240$ nM SK-MEL-5 cells). There is no apparent explanation of the discrepancy in potency between non-chlorinated diazonamide A **373** and **277**. It is possible that the compounds are metabolized differently by cells, and that the lack of the peripheral chlorines in **277** make it more susceptible to cellular clearance. Phenol analog **371** was less cytotoxic against the screened

cell line panel, but it still retained substantial potency (IC_{50}). This is the first finding concerning the SAR of the right hand portion of the molecule, other than the peripheral chlorines. The synthesis of analogs **391** and **393** through substitution off the phenol opens up the right side of the molecule for further SAR exploration. The synthesis of the diazonamide probe analogs **379**, **380**, **381**, and **387** provide a suite of tools for affinity chromatography that compliment the syndistatin biotinylated analogs. Bi-functional analog **381** is potentially an important compound since it could be used to isolate all of the cellular binding partners of diazonamide, regardless of binding affinity.

Finally, the incorporation of the proline residue in place of valine allows for an intrinsic exploration of the SAR of the molecule. Various diazonamide analogs containing different residues at this position may be synthesized and evaluated. Evaluating the proline-containing analog especially would give an indication of the importance valine side chain in diazonamide's SAR. Also, replacing the secondary amide of valine with the tertiary amide of proline could alter the compound's solubility in aqueous media and the pharmacokinetics.

5.7 Conclusions

The non-chlorinated diazonamide A analog **373** retains the full potency of the natural product. Non-chlorinated diazonamide A is a much more synthetically accessible target, and several hundred milligrams of the compound were prepared for tumor efficacy studies. In addition, several diazonamide A probe analogs were synthesized, including a bi-functional photocrosslinking/biotinylated analog. These analogs may be used to further explore the molecular pharmacology of the molecule. Further, a method was developed to functionalize the right-hand side of the molecule. Finally, a diazonamide core containing proline in place of valine

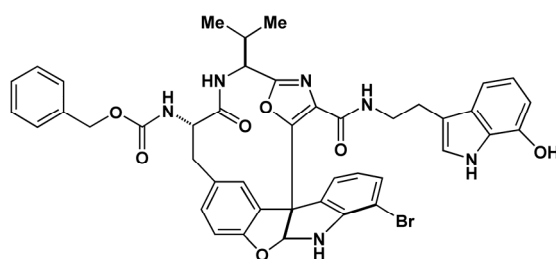
was prepared, suggesting developed route to diazonamide A could be used as a modular synthesis.

5.8 Experimental Section

5.8.1 General Notes

Bi-functional probe component **385** was prepared chiefly by Dr. Kendra Carter. Dr. Noelle Williams characterized the biological activity of the diazonamide analogs and also undertook the tumor animal studies. A forthcoming publication will detail Dr. Williams research with non-chlorinated analog **373**. The probe analogs were given to Dr. Gelin Wang, who took over the exploration of the diazonamide molecular pharmacology.

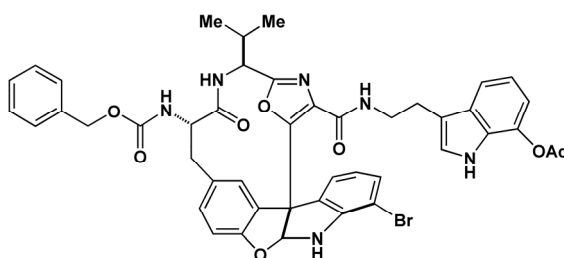
5.8.2 Compound Data



364

Acid **344b** (2.68 g, 4.0 mmol) and TBTU (1.53 g, 5.0 mmol) were charged to a reaction flask and then dissolved with a 0.1 M solution of 7-hydroxytryptamine hydrochloride (**349**) in DMF (47 mL, 5.0 mmol). The light brown colored solution was cooled in an ice bath, and DIPEA (1.40 mL, 1.03 g, 8.0 mmol) was added slowly drop-wise. The reaction color turned olive green. After 5 min post DIPEA addition, the ice bath was removed and the reaction was allowed to warm to ambient temperature and stir for 2 h. The reaction became tan in color. The reaction was diluted in 350 mL EtOAc and washed once with 100 mL sat. ammonium chloride, three times with 100

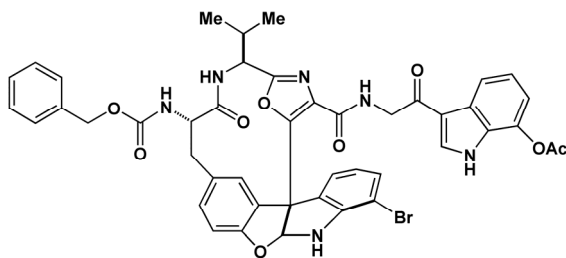
mL water, and once with 100 mL brine. The aqueous was back extracted three times with 75 mL EtOAc. The combined, tan colored organic layers were combined and dried over Na₂SO₄. FC with EtOAc/benzene (25% to 40% EtOAc) yielded a pinkish hued white solid (2.8 g, 84%), which was immediately carried forward to the acetylation step to prevent decomposition. **364**: R_f = 0.55 (40 % EtOAc/benzene). ¹HNMR (400 mHz, (CDCl₃): δ 8.34 (br s, 1H), 7.45 (s, 1H), 7.39 – 7.33 (m, 5H), 7.23 – 7.21 (m, 1H), 7.14 (d, *J* = 7.7 Hz, 1H), 7.10 (d, *J* = 7.7 Hz, 1H), 7.06 (d, *J* = 8.4 Hz, 1H), 7.02 – 6.90 (m, 1H), 6.87 – 6.83 (m, 2H), 6.78 (d, *J* = 8.1 Hz, 1H), 6.62 (app t, *J* = 7.7 Hz, 1H), 6.57 (d, *J* = 7.7 Hz, 1H), 6.39 (br s, 1H), 5.84 (d, *J* = 8.8 Hz, 1H), 5.50 (d, *J* = 9.2 Hz, 1H), 5.46 (d, *J* = 4.4 Hz, 1H), 5.10 (s, 2H), 5.04 (dd, *J* = 5.9, 9.2 Hz, 1H), 4.01 – 3.90 (m, 1H), 3.62 – 3.58 (m, 2H), 3.31 (t, *J* = 12.1 Hz, 1H), 2.96 – 2.92 (m, 2H), 2.82 (dd, *J* = 3.3, 12.5 Hz, 1H), 2.25 – 2.17 (m, 1H), 1.04 (d, *J* = 6.6 Hz, 3H), 0.89 (d, *J* = 6.6 Hz, 3H). ES-MS: calcd. for C₄₃H₃₉BrN₆O₇ [M+H]⁺: 831.21, found: 831.25, 833.25; calcd. for C₄₅H₄₁BrN₆O₈ [M+Na]⁺: 853.20, found: 853.25, 855.25; calcd. for C₄₅H₄₁BrN₆O₈ [M-H]⁻: 829.20, found: 829.25, 831.25.



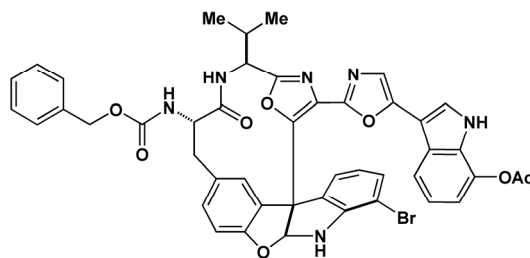
365

Coupled product **364** (2.8 g, 3.4 mmol) was dissolved in a 10:1 mixture of CH₂Cl₂ (100 mL):THF (10 mL) (0.03 M) to give a slight pink solution. The solution was cooled to 0°C. Acetic anhydride (1.58 mL, 1.71 g, 17.0 mmol) was added via syringe (fast drop-wise addition). Pyridine (1.36 mL, 1.33 g, 17.0 mmol) was added in an identical fashion. Following addition, the

reaction was allowed to warm to ambient temperature and stirred for 2.5 h. The reaction was diluted with 500 mL EtOAc and washed 10X with 100 mL sat.NH₄Cl to remove all excess pyridine. The organic layer was then washed twice with 100 mL of brine and dried over Na₂SO₄. The solvent was removed *in vacuo*, and azeotroped several times with CHCl₃ and benzene to remove any trace amounts of EtOAc or pyridine. 2.9 g (98%) of slightly off-white solid was obtained without the need for further purification. **365**: R_f = 0.44 (25 % EtOAc/CH₂Cl₂). ¹H NMR (400 mHz, (CDCl₃): δ 8.04 (br s, 1H), 7.48 (d, *J* = 1.5 Hz, 1H), 7.43 (d, *J* = 7.7 Hz, 1H), 7.38 – 7.34 (m, 5H), 7.26 (m, 1H), 7.26 – 7.24 (m, 2H), 7.17 (d, *J* = 7.3 Hz, 1H), 7.09-7.04 (m, 2H), 7.00 – 6.95 (m, 3H), 6.80 (d, *J* = 8.1 Hz, 1H), 6.68 – 6.63 (m, 1H), 5.78 (d, *J* = 9.2 Hz, 1H), 5.43 (d, *J* = 9.2 Hz, 1H), 5.11 – 5.07 (m, 3H), 3.98 – 3.92 (m, 1H), 3.61 (dd, *J* = 7.0, 13.1 Hz, 2H), 3.31 (t, *J* = 12.1 Hz, 1H), 2.97 (d, *J* = 7.0 Hz, 2H), 2.83 (dd, *J* = 3.3, 12.5 Hz, 1H), 2.40 (s, 3H), 2.33 – 2.28 (m, 1H), 1.06 (d, *J* = 6.6 Hz, 3H), 0.91 (d, *J* = 6.6 Hz, 3H). ¹³C NMR (75 mHz, CDCl₃): δ 172.6, 169.3, 160.4, 159.9, 157.0, 155.7, 152.5, 147.4, 136.3, 135.9, 131.7, 131.3, 130.5, 130.4, 130.3, 129.8, 128.7, 128.6, 128.5, 128.4, 128.1, 128.0, 122.8, 121.5, 121.0, 119.5, 116.6, 114.2, 113.5, 110.8, 103.3, 102.1, 68.1, 67.0, 61.8, 58.7, 53.1, 39.5, 38.3, 28.6, 25.7, 25.4, 21.2, 19.6, 17.8. ES-MS: calcd. for C₄₅H₄₁BrN₆O₈ [M+H]⁺: 873.22, found: 873, 875; calcd. for C₄₅H₄₁BrN₆O₈[M+Na]⁺: 895.2, found: 895, 897. calcd. for C₄₅H₄₁BrN₆O₈ [M-H]⁻: 897.21, found: 871, 873.

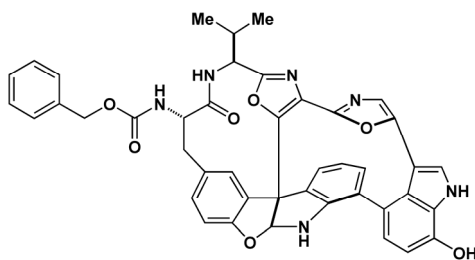


Acetylated product **365** (2.9 g, 3.0 mmol) was dissolved in 71 mL THF and 8 mL H₂O (0.04 M). The reaction was cooled to 0°C. DDQ (1.87 g, 8.1 mmol) was charged to a dry vial in the atmosphere and added directly to the reaction to give a dark brown/black solution. The reaction was allowed to warm to ambient temperature and stirred, covered in foil, for 15 h. The reaction was then diluted in 400 mL EtOAc and washed twice with 100 mL sat. NaHCO₃. The aqueous phase was back extracted once, and the combined organic layers were washed twice with brine and dried over Na₂SO₄. The purple/black solution was condensed, and purified using FC with 25% EtOAc/CH₂Cl₂. 2 g of product was obtained (69%) as pinkish/white solid and 240 mg of starting material was also recovered (75% borsm). **366**: ¹H NMR (400 MHz, (CDCl₃): δ 8.59 (br s, 1H), 7.56 (d, *J* = 8.1 Hz, 1H), 7.35 – 7.33 (m, 5H), 7.26 (d, *J* = 2.9 Hz, 1H), 7.22 – 7.19 (m, 3H), 7.13 – 7.06 (m, 3H), 6.84 – 6.82 (m, 2H), 6.50 (app t, *J* = 7.7 Hz, 1H), 5.87 (br s, 1H), 5.56 (br s, 1H), 5.50 (br s, 1H), 5.13 – 5.05 (m, 2H), 5.01 – 4.97 (m, 1H), 4.06 – 3.99 (m, 1H), 3.29 – 3.21 (m, 1H), 2.86 (dd, *J* = 3.7, 12.5 Hz, 1H), 2.42 – 2.35 (m, 4H), 1.04 (d, *J* = 6.6 Hz, 3H), 0.94 (d, *J* = 6.6 Hz, 3H). ¹³C NMR (75 MHz, CDCl₃): δ 188.8, 172.8, 169.6, 161.0, 160.2, 157.2, 155.9, 153.3, 147.6, 136.5, 136.0, 132.7, 131.8, 131.3, 130.6, 130.5, 130.4, 129.9, 128.9, 128.8, 128.7, 128.5, 128.2, 128.0, 123.3, 121.5, 121.1, 119.9, 116.1, 115.4, 110.9, 103.3, 102.5, 77.5, 67.3, 61.9, 58.9, 53.4, 46.1, 28.9, 21.2, 19.7, 17.9.



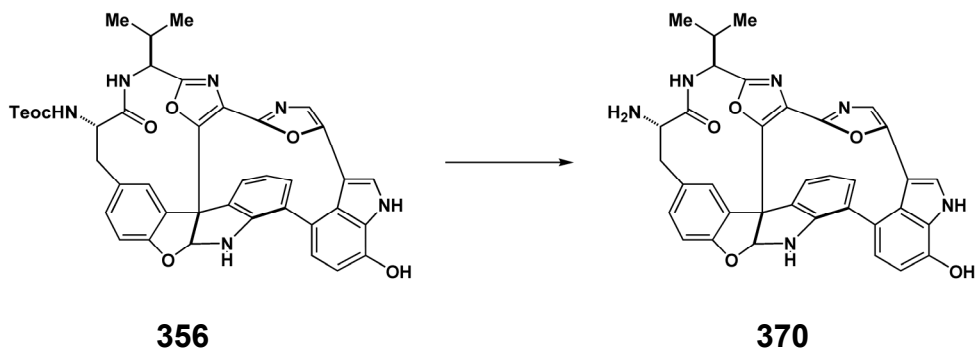
367

Hexachloroethane (2.68 g, 11.0 mmol) and triphenylphosphine (3.0 g 11.0 mol) were charged to a reaction flask and dissolved in 110 mL CH₂Cl₂. The clear solution was cooled to 0 °C and stirred for 10 min. Triethylamine (1.59 g, 16.0 mol) was added slowly drop-wise over 7 min. In a separated flask, very dry (azeotroped several times from benzene) DDQ product **366** (1.0 g, 0.0011 mol) required several minutes and gentle heating to dissolve in 60 mL CH₂Cl₂. The solution became yellow in color. The starting material was added via syringe as a fast stream over 15 min. The starting material had a tendency to form a gel upon addition to the cold reaction atmosphere, and constant regulation of the rate of addition had to be maintained. The solution became bright yellow initially, but turned to an orange/red after 5 min of stirring. TLC indicates reaction is complete at 10 min. At 15 min, 300 μL of H₂O was added to the reaction. The reaction was condensed *in vacuo* to remove the CH₂Cl₂. The crude reaction mixture was re-dissolved in EtOAc to give a red/orange colored solution. A triphenylphosphine oxide precipitate formed and was filtered off. The reaction was re-condensed, and immediately FC with 50% EtOAc/benzene. A second column was required to remove trace amount of triphenylphosphine oxide. 0.740 g of bis-oxazole product (76%) was obtained as a light yellow foam. **367**: R_f = 0.42 (60 % EtOAc/benzene). ¹HNMR (400 MHz, (CDCl₃): δ 8.54 (br s, 1H), 7.58 (d, *J* = 8.1 Hz, 1H), 7.38 – 7.34 (m, 5H), 7.28 (m, 1H), 7.25 – 7.19 (m, 3H), 7.16 – 7.08 (m, 5H), 6.88 – 6.85 (m, 2H), 6.52 (app t, *J* = 7.7 Hz, 1H), 5.85 (d, *J* = 8.4 Hz, 1H), 5.52 (d, *J* = 3.3 Hz, 1H), 5.48 (d, *J* = 9.2 Hz, 1H), 5.13 (s, 2H), 5.02 (dd, *J* = 5.5, 8.1 Hz, 1H), 4.08 – 4.00 (m, 1H), 3.26 (t, *J* = 12.1 Hz, 1H), 2.88 (dd, *J* = 3.3, 12.5 Hz, 1H), 2.45 – 2.39 (m, 4H), 1.06 (d, *J* = 6.9 Hz, 1H), 0.97 (d, *J* = 6.9 Hz, 1H).

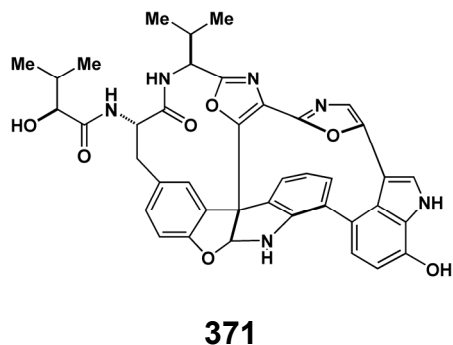


368

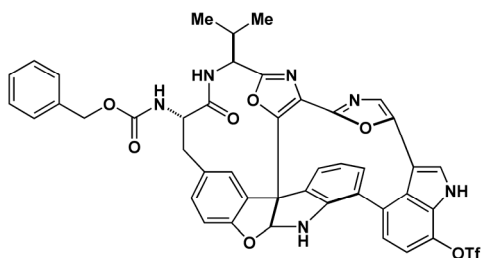
Bis-oxazole **367** (300 mg, 0.35 mmol) was dissolved in 81 mL (CH₃CN) in a photochemical reaction apparatus. 27 mL of a 0.03 M solution of aq. LiOH (0.08 mmol) was added to the reaction. The solution color turned from very faint yellow to yellow upon addition of the aq. LiOH solution. The reaction was sparged with argon extensively for 25 min, and then photolyzed at 300 nm while sparging gently. The reaction color became yellow/tan after 3 h, and the reaction was stopped at 4.5 h. The reaction was diluted in 250 mL EtOAc, washed once with 100 mL H₂O, once with 100 mL sat. ammonium chloride, once again with 100 mL H₂O and once with 100 mL brine. The organic layer was dried over Na₂SO₄. FC with 30% EtOAc/CH₂Cl₂. Yielded 93 mg (36%) of the desired photocyclized product as a faint pink solid and 118 mg (41%) of deacetylated recovered starting material (77% borsm). **368**: R_f = 0.31 (60 % EtOAc/CH₂Cl₂). ¹HNMR (400 MHz, (CDCl₃): δ 9.23 (br s, 1H), 7.44 (s, 1H), 7.38 – 7.32 (m, 5H), 7.23 (m, 1H), 7.11 (d, *J* = 8.1 Hz, 1H), 7.07 (d, *J* = 7.3 Hz, 1H), 6.88 – 6.84 (m, 3H), 6.82 – 6.77 (m, 2H), 6.55 (d, *J* = 7.3 Hz, 1H), 6.55 (t, *J* = 7.3 Hz, 1H), 6.34 (br s, 1H), 6.10 (br s, 1H), 5.51 (d, *J* = 10.3 Hz, 1H), 5.14 (s, 2H), 5.07 (dd, *J* = 4.8, 8.4 Hz, 1H), 4.15 – 4.07 (m, 1H), 3.50 (t, *J* = 12.1 Hz, 1H), 2.83 (dd, *J* = 3.3, 12.5 Hz, 1H), 2.47 – 2.43 (m, 1H), 1.05 (d, *J* = 7.0 Hz, 1H), 0.93 (d, *J* = 7.0 Hz, 1H). ES-MS: calcd. for C₄₃H₃₄N₆O₇ [M+H]⁺: 747.26, found: 747.25; calcd. for C₄₃H₃₄N₆O₇ [M+Na]⁺: 769.24, found: 769.15. calcd. for C₄₃H₃₄N₆O₇ [M-H]⁻: 745.24, found: 745.15. X-ray data: see attached appendix.



Procedure: Compound **356** subjected to the TASF deprotection protocol described for compound **363**. Amine **370** used without purification (83%). **370**: ^1H NMR: see attached appendix.

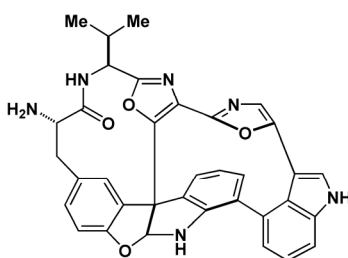


Amine **370** (3 mg, 0.005 mmol), (*S*)-Hydroxyisovaleric acid (1 mg, 0.010 mmol), and HATU (4 mg, 0.010 mmol) were charged to a dry reaction flask in a nitrogen atmosphere and then dissolved in 0.2 mL DMF. The reaction was cooled to 0 °C and DIPEA (1 μL , 0.006 mmol) was added. The reaction was allowed to warm to ambient temperature and stirred for 2 h. The reaction was dissolved in 10 mL EtOAc, washed with sat. NaHCO_3 , H_2O , and brine. Dried over Na_2SO_4 . Desired product was purified via reverse phase HPLC (C_{18} Higgins MeOH/ H_2O gradient). (~1 mg, 30%). **371**: ^1H NMR: see attached appendix. ES-MS: calcd. for $\text{C}_{40}\text{H}_{36}\text{N}_6\text{O}_7$ $[\text{M}+\text{H}]^+$: 713.27, found: 713.30; calcd. for $\text{C}_{40}\text{H}_{36}\text{N}_6\text{O}_7$ $[\text{M}+\text{Na}]^+$: 735.25; found: 735.25; calcd. for $\text{C}_{43}\text{H}_{40}\text{Cl}_2\text{N}_6\text{O}_7$ $[\text{M}-\text{H}]^-$ 711.25, found: 711.25.



368a

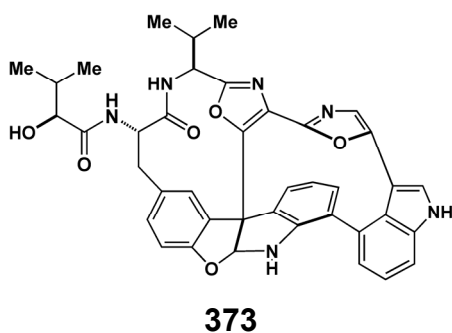
Photochemistry product **368** (83 mg, 0.110 mmol), oven-dried K_2CO_3 (47 mg, 0.34 mmol), and 4-nitrophenyltrifluoromethanesulfonate (46 mg, 0.170 mmol) charged to reaction flask in nitrogen glove bag. 2.7 mL of (0.04 M) was added via syringe and the reaction was stirred at ambient temperature. The reaction solution was initially light brown in color with a small amount of K_2CO_3 failing to dissolve. The reaction was complete after 3.5 h, and it had turned bright yellow in color. The reaction was diluted in ~10mL of EtOAc, washed twice with water, once with brine, and dried over Na_2SO_4 . The condensed yellow/brown oil was purified via FC using 65% EtOAc/hexanes solvent. 85 mg (87%) of product was isolated as a yellow-white foam. **368a**: $R_f = 0.66$ (80 % EtOAc/hexanes). 1H NMR: see attached appendix. ^{13}C NMR: see attached appendix.



372

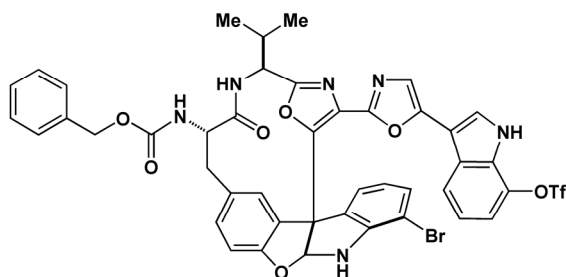
Triflate product **368a** (390 mg, 0.44 mmol) was dissolved in 6.2 mL of dry methanol and 2 mL EtOAc (8.2 mL). Triethylamine (206 μ L, 150 mg, 1.48 mmol) was added drop-wise to the solution at ambient temperature. 20% palladium hydroxide on carbon (691 mg, 1.3 mmol, 300 mol%) was added and the reaction was placed under a H_2 balloon. The large excess of

Pd(OH)₂/C was used to ensure a rapid, clean conversion, and was based on experience with the certain batch of Pd(OH)₂/C that might have lost some activity. After 85 min, the reaction was stopped, and filtered through a plug of Celite and washed extensively with EtOAc. Solvent was removed *in vacuo*, and the crude mixture was dissolved in EtOAc. The solution was washed twice with H₂O, once with brine, and dried over Na₂SO₄. The crude product (247 mg, 94%) did not require any subsequent purification. **372**: ¹H NMR: see attached appendix. ES-MS: calcd. for C₃₅H₂₈N₆O₄ [M+H]⁺: 597.22, found: 597.25; calcd. for C₃₅H₂₈N₆O₄ [M+Na]⁺: 619.21; found: 619.25; calcd. for C₃₅H₂₈N₆O₄ [M-H]⁻: 595.21, found: 595.25.



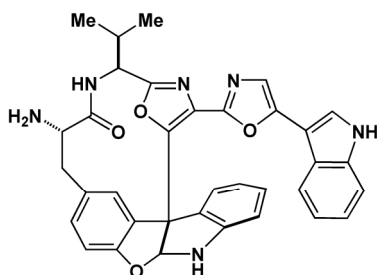
Non-chlorinated diazonamide core **372** (37 mg, 0.062 mmol) was dissolved in 0.3 mL DMF and cooled in an ice bath. A 0.23 M stock solution of (*S*)-hydroxyisovaleric acid NHS activated ester (**362**) was prepared, and 0.4 mL (0.092 mmol, 1.5 eq) was added to the starting material. After 3.5 h, the reaction was complete. The reaction was diluted in EtOAc, washed 3X with sat. NaHCO₃, then H₂O and brine and dried over Na₂SO₄. The product is poorly soluble in EtOAc, and great care must be made not to lose material during the extraction. The product is poorly soluble in most organic solvents. It is highly soluble in 10-50% methanol/dichloromethane, DMF, and DMSO. Due to problems with solubility, FC methods are not suitable for purification. Reverse phase HPLC with a 40%-100% methanol/H₂O gradient was used to purify the compound. Isolated 27 mg of desired from HPLC (65%). **373**: R_f = 0.27 (90 % EtOAc/hexane).

$[\alpha]_D^{25} = -230.9^\circ$ ($c = 0.01$, 30% $\text{CH}_3\text{OH}/\text{CHCl}_3$). IR (film): 3396, 2360, 1651, 1493, 668 cm^{-1} . ^1H NMR (400 MHz, 90% $\text{CDOD}_3/\text{CHCl}_3$): δ 7.52 (dd, $J = 8.4, 0.8$ Hz, 1H), 7.46 (s, 1H), 7.40 (d, $J = 1.6$ Hz, 1H), 7.34 (m, 1H), 7.21 – 7.17 (m, 2H), 7.00 (dd, $J = 7.6, 1.2$ Hz, 1H), 6.89 (s, 1H), 6.82 (dd, $J = 7.6, 0.8$, 1H), 6.78 (d, $J = 8.4$ Hz, 1H), 6.61 (t, $J = 7.6$ Hz, 1H), 6.36 (s, 1H), 4.60 (dd, $J = 11.6, 3.6$ Hz, 1H), 3.89 (d, $J = 3.6$, 1H), 3.43 – 3.34 (m, 1H), 2.80 (dd, $J = 11.6, 3.2$ Hz, 1H), 2.27 – 2.22 (m, 1H), 2.14 – 2.00 (m, 1H), 1.07 (d, $J = 6.8$ Hz, 3H), 1.03 (d, $J = 6.8$ Hz, 3H), 0.96 (d, $J = 6.8$ Hz, 3H), 0.92 (d, $J = 6.8$ Hz, 3H); ^{13}C NMR (300 MHz, 30% $\text{CDOD}_3/\text{CHCl}_3$) δ 174.3, 173.0, 160.7, 158.0, 154.1, 151.9, 149.2, 148.2, 137.1, 130.8, 130.2, 130.1, 129.7, 128.3, 128.1, 127.6, 127.5, 126.3, 124.8, 123.7, 122.9, 122.8, 122.6, 121.3, 120.4, 111.8, 110.3, 104.5, 102.4, 75.6, 61.3, 55.8, 54.9, 37.9, 31.7, 30.1, 18.9, 18.6, 17.6, 15.4. ES-MS: calculated. for $\text{C}_{40}\text{H}_{36}\text{N}_6\text{O}_6$ $[\text{M}+\text{H}]^+$ 697.27, found: 697.20; calculated. for $\text{C}_{43}\text{H}_{40}\text{Cl}_2\text{N}_6\text{O}_7$ $[\text{M}+\text{H}]^+$ 695.28, found: 695.25.



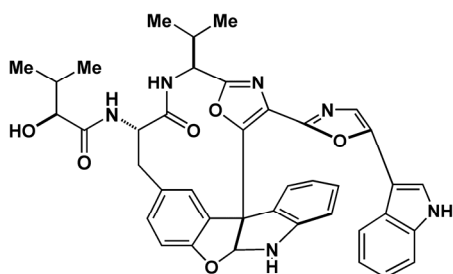
369a

Procedure: Compound **369** subjected to the triflate formation procedure described for compound **373**. FC 25% with $\text{EtOAc}/\text{CH}_2\text{Cl}_2$ (70 %). **369a**: ^1H NMR: see attached appendix. ES-MS: calcd. for $\text{C}_{44}\text{H}_{34}\text{BrF}_3\text{N}_6\text{O}_9\text{S}$ $[\text{M}+\text{Na}]^+$: 981.11, found: 981.15, 983.15. calcd. for $\text{C}_{44}\text{H}_{34}\text{BrF}_3\text{N}_6\text{O}_9\text{S}$ $[\text{M}-\text{H}]^-$: 959.25, found: 957.12, 959.12.



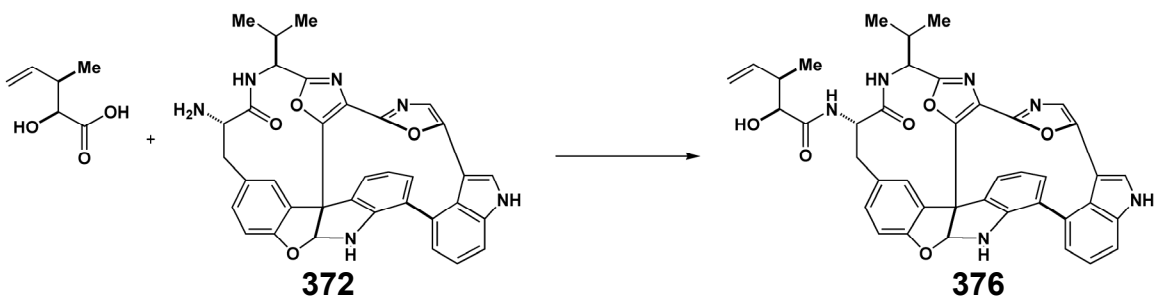
374

Procedure: see reduction procedure for compound **372**. Use crude amine for subsequent coupling with no purification. **374**: ^1H NMR: see attached appendix. ES-MS: calcd. for $\text{C}_{35}\text{H}_{30}\text{N}_6\text{O}_4$ $[\text{M}+\text{H}]^+$: 599.24, found: 599.25. calcd. for $\text{C}_{35}\text{H}_{30}\text{N}_6\text{O}_4$ $[\text{M}+\text{Na}]^+$: 621.22, found: 621.25. calcd. for $\text{C}_{35}\text{H}_{30}\text{N}_6\text{O}_4$ $[\text{M}-\text{H}]^-$: 597.23, found: 597.30.

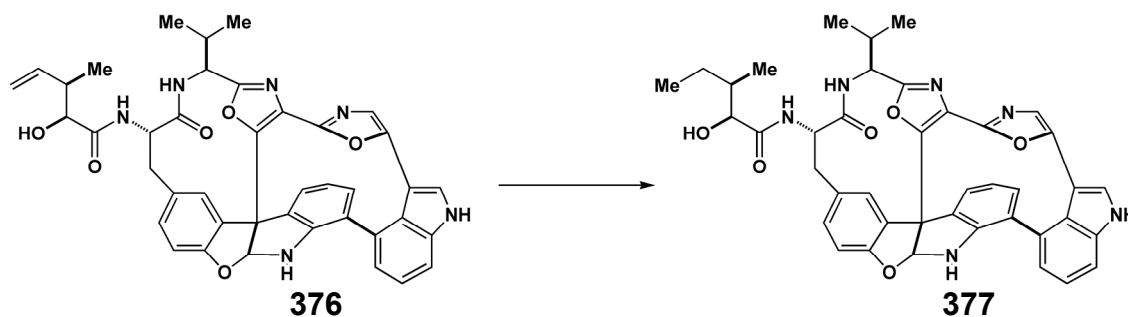


375

Procedure: see coupling of HIV-NHS for compound **373** (43%). **375**: ^1H NMR: see attached appendix. ES-MS: calcd. for $\text{C}_{40}\text{H}_{38}\text{N}_6\text{O}_6$ $[\text{M}+\text{H}]^+$: 699.29, found: 699.30. calcd. for $\text{C}_{40}\text{H}_{38}\text{N}_6\text{O}_6$ $[\text{M}+\text{Na}]^+$: 721.27, found: 721.30. calcd. for $\text{C}_{40}\text{H}_{38}\text{N}_6\text{O}_6$ $[\text{M}-\text{H}]^-$: 697.28, found: 697.40.

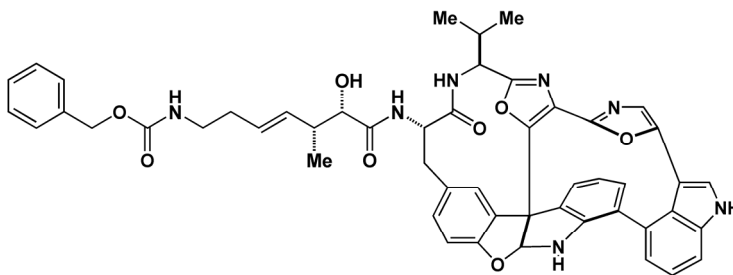


Amine **372** (3.0 mg, 0.005 mmol) was dissolved in 0.2 mL THF and cooled to 0 °C. Acid **2** was added as a stock solution (0.08 M in THF, 0.09 mL, 0.007 mmol). DEPC (4.3 mg, 0.026 mmol) was then added, followed by 4-methylmorpholine (3.7 mg, 0.026 mmol). The solution was warmed to ambient temperature and stirred for 1.5 h. The reaction was diluted in 10 mL ethyl acetate and washed with NaHCO₃, water, NH₄Cl, water, and brine, and finally dried over Na₂SO₄. The product was purified with preparative TLC (10% methanol/dichloromethane). Acylated product **376** (2 mg, 60% yield) was obtained as a white film. **376**: $R_f = 0.72$ (10% MeOH/CH₂Cl₂). ¹HNMR (400 MHz, CDOD₃): δ7.52 (dd, $J = 8.4, 1.2$ Hz, 1H), 7.46 (s, 1H), 7.39 (d, $J = 1.6$ Hz, 1H), 7.34 (m, 1H), 7.19 - 7.16 (m, 2H), 7.00 (dd, $J = 7.6, 1.2$ Hz, 1H), 6.89 (s, 1H), 6.83 (dd, $J = 7.2, 1.2$ Hz, 1H), 6.78 (d, $J = 8.4$, 1H), 6.62 (t, $J = 7.2$ Hz, 1H), 6.35(s, 1H), 5.89 – 5.80 (m, 1H), 5.11 – 5.05 (m, 2H), 4.57 (dd, $J = 12.0, 3.2$ Hz, 1H), 3.98 (d, $J = 3.6$ Hz, 1H), 3.35 (app t, $J = 12.0$ Hz, 1H), 2.76 (dd, $J = 12.8, 3.2$ Hz, 1H), 2.68 (m, 1H), 2.24 (m, 1H), 1.15 (d, $J = 10.8$ Hz, 3H), 1.06 (d, $J = 10.8$ Hz, 3H), 0.96 (d, $J = 6.8$ Hz).



Acylated product **376** (2.0 mg, 0.003 mmol) was combined with 10% palladium on carbon (~ 1 mg, 0.001 mmol) and dissolved in 0.3 mL dry methanol. The reaction was stirred under a hydrogen atmosphere for 30 min. The reaction was filtered through Celite, and the desired product was purified via reverse phase HPLC (Higgins C18 column, 60% → 100 % MeOH in

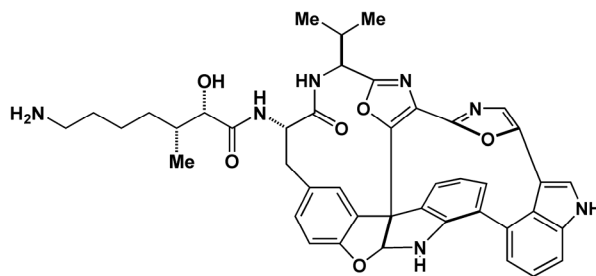
H₂O gradient). The desired product **5** (2.0 mg, ~ 100%) was obtained as a white film. **377**: $R_f = 0.65$ (10% MeOH/CH₂Cl₂). ¹HNMR (400 MHz, CDOD₃): δ 7.52 (dd, $J = 8.4, 0.8$ Hz, 1H), 7.45 (s, 1H), 7.40 (d, $J = 1.6$ Hz, 1H), 7.34 (m, 1H), 7.21 – 7.17 (m, 2H), 7.00 (dd, $J = 7.2, 1.2$ Hz, 1H), 6.89 (s, 1H), 6.83(d, $J = 7.2$ Hz, 1H), 6.78 (d, $J = 8.0$ Hz, 1H), 6.62 (t, $J = 7.2$ Hz, 1H), 6.36 (s, 1H), 4.59 (dd, $J = 12.0, 3.2$ Hz, 1H), 3.93 (d, $J = 4.4$ Hz, 1H), 3.43- 3.34 (m, 1H), 2.79 (dd, $J = 12.8, 3.6$ Hz, 1H), 2.30 – 2.21 (m, 1H), 1.88 – 1.84 (m, 1H), 1.54 – 1.48 (m, 1H), 1.07 (d, $J = 6.8$ Hz, 3H), 1.00 (d, $J = 6.8$ Hz, 3H), 0.96 (d, $J = 6.8$ Hz, 3H), 0.943 (t, $J = 7.6$ Hz, 3H). ES-MS: calculated. for C₄₁H₃₈N₆O₆ [M+H]⁺ 711.28, found:711.25; calculated. for C₄₃H₄₀Cl₂N₆O₇ [M-H]⁻ 709.28, found:709.35.



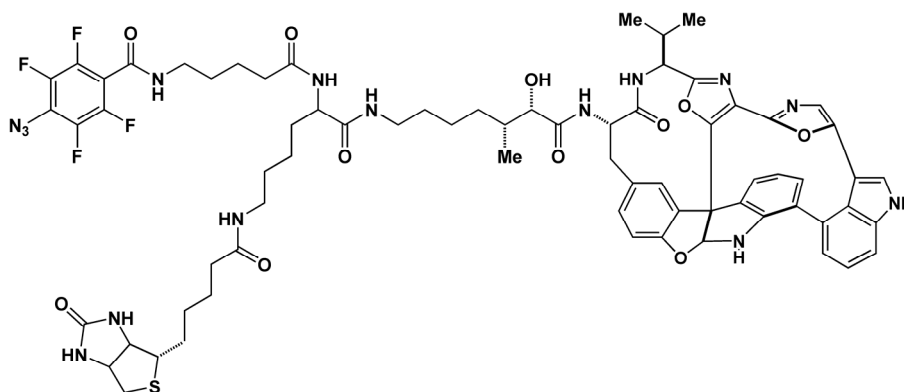
378

Procedure: Amine **372** and acid **290** subjected to DEPC coupling procedure described for compound **292** (63%). FC with 4% MeOH/CH₂Cl₂ (63%). **378**: $R_f = 0.57$ (10% MeOH/CH₂Cl₂).

¹H NMR: see attached appendix. ES-MS: C₅₁H₄₇N₇O₈ [M+Na]⁺: 908.34, found: 908.30.

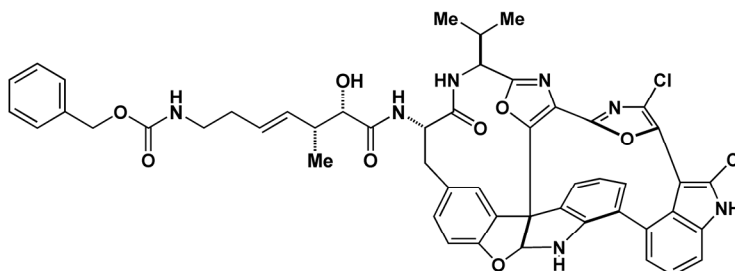


378a



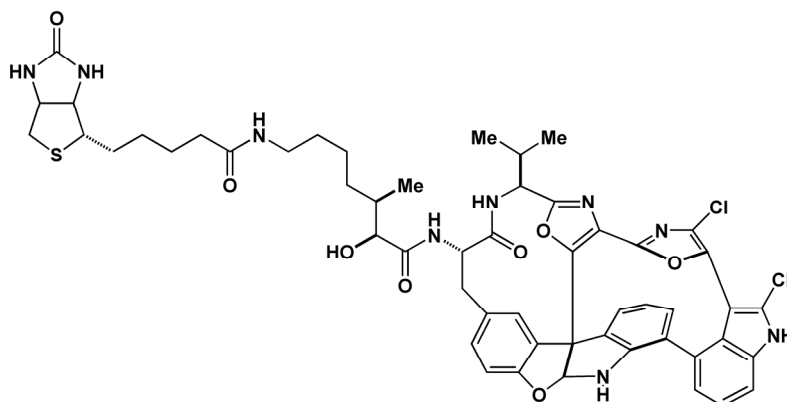
381

Amine **378a** (4.5 mg, 0.006 mmol) and acid **385** (4 mg, 0.006 mmol) were dissolved in 0.2 mL DMF and cooled to 0 °C. 0.1 mL of a 0.14 M TBTU in DMF stock solution was added, followed by DIPEA (1.5 μ L, 0.008 mmol). The reaction was stirred for 2 h, then diluted in EtOAc, washed with sat. aq. NaHCO₃, H₂O, and brine, and dried over Na₂SO₄. The desired compound (3 mg, 33%) was purified via reverse phase HPLC (C₁₈ Higgins column, 40% → 100% MeOH in H₂O gradient). **381**: ¹H NMR: see attached appendix. ES-MS: calcd. for C₇₁H₇₇F₄N₁₅O₁₁S [M+Na]⁺: 1446.55, found: 1446.60. calcd. for C₇₁H₇₇F₄N₁₅O₁₁S [M-H]⁻: 1422.55, found: 1422.65.



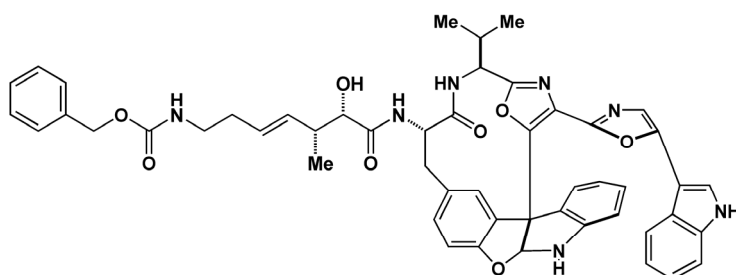
363a

Procedure: Amine **363** and acid **290** subjected to DEPC coupling procedure described for compound **292**. **363a**: ¹H NMR: see attached appendix.



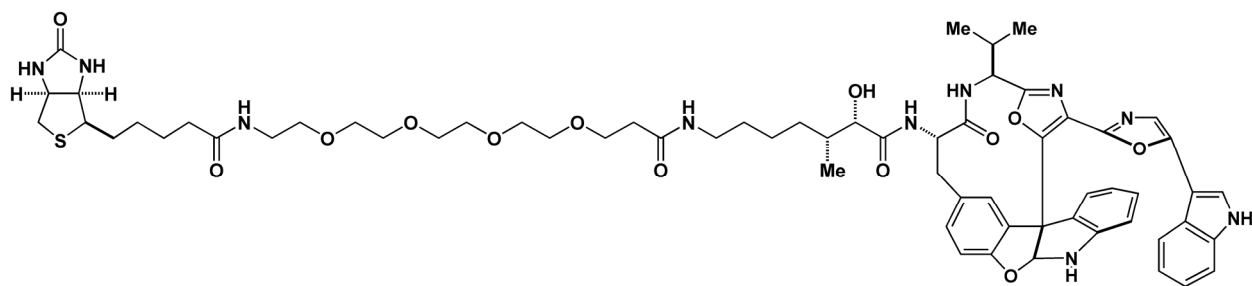
382

Procedure: Compound **363a** subject to the procedure reduction/biotinylation as described for compound **296**. **382**: ^1H NMR: see attached appendix. ES-MS: calculated. for $\text{C}_{53}\text{H}_{55}\text{Cl}_2\text{N}_9\text{O}_8\text{S}$ $[\text{M}+\text{Na}]^+$ 1070.32, found: 1070.25; calculated. for $\text{C}_{53}\text{H}_{55}\text{Cl}_2\text{N}_9\text{O}_8\text{S}$ $[\text{M}-\text{H}]^-$ 1046.32, found: 1046.40.



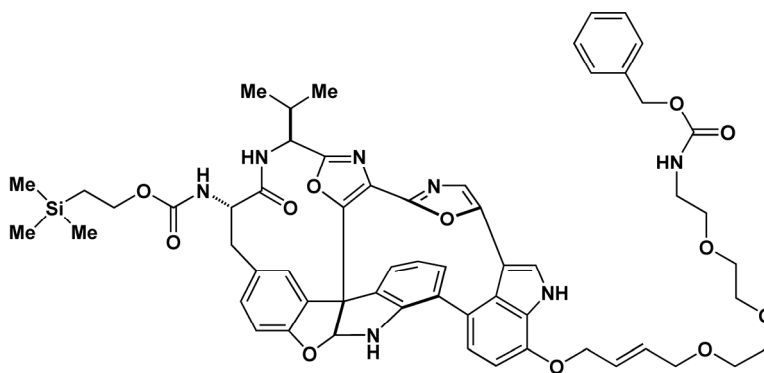
386

Procedure: Amine **374** and acid **290** subjected to DEPC coupling procedure described for compound **292**. pTLC (10% MeOH/ CH_2Cl_2) (35%). **386**: ^1H NMR: see attached appendix. ES-MS: calcd. for $\text{C}_{51}\text{H}_{49}\text{N}_7\text{O}_8$ $[\text{M}+\text{H}]^+$: 888.37, found: 888.55. calcd. for $\text{C}_{51}\text{H}_{49}\text{N}_7\text{O}_8$ $[\text{M}+\text{Na}]^+$: 911.36, found: 911.35. calcd. for $\text{C}_{51}\text{H}_{49}\text{N}_7\text{O}_8$ $[\text{M}-\text{H}]^-$: 886.36, found: 886.45.



387

Procedure: Compound **386** was subjected to the reduction/biotinylation procedure described for compound **296**. Purified via reverse phase HPLC (C₁₈ Higgins column, 60% → 100% MeOH in H₂O gradient) (32%). **387**: ¹H NMR: see attached appendix. ES-MS: calcd. for C₆₄H₈₀N₁₀O₁₃S [M+Na]⁺: 1252.56, found: 1252.60.

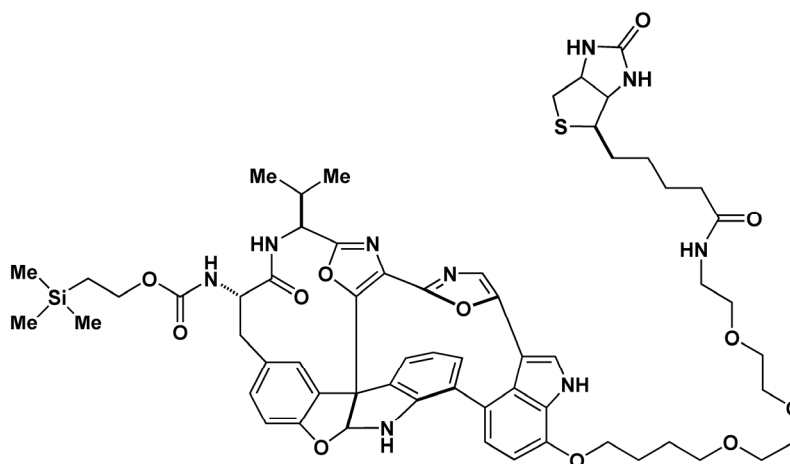


390

Teoc-photochemistry product **356** (11 mg, 0.014 mmol), oven dried sodium iodide (9 mg, 0.06 mmol), and cesium carbonate (10 mg, 0.03 mmol) were charged to a dry reaction flask in a nitrogen atmosphere. The flask was placed at 0 °C, and the starting material and reagents were dissolved in DMF (0.18 mL) and HMPA (0.2 mL). 35 μL of a 0.65 M (0.023 mmol) solution of the linker element **389** in THF was added to the reaction. The reaction was stirred at 0 °C for 45 min, at which point it was allowed to warm to ambient temperature. After a further 8 h stirring, the reaction was diluted in EtOAc, washed with H₂O twice, followed by brine, and dried over

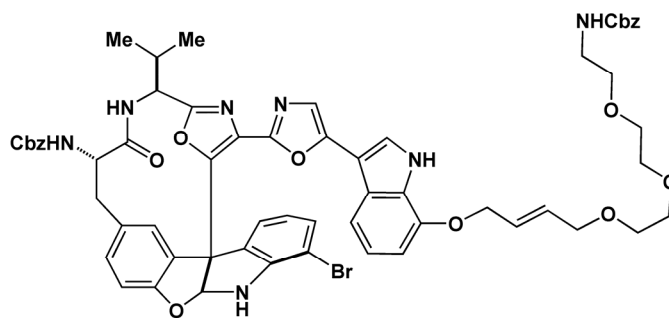
Na₂SO₄. The desired product (7 mg, 44%) was purified via pTLC (90% EtOAc/hexanes). **390**:

¹H NMR: see attached appendix.



392

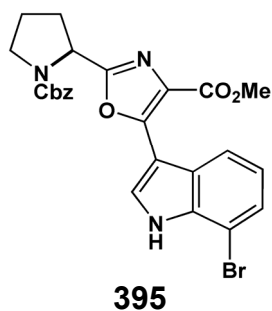
Procedure: Compound **390** subject to the reduction/biotinylation procedure described for compound **296**. (~20%). **392**: ¹H NMR: see attached appendix. ES-MS: calcd. for C₆₁H₇₅N₉O₁₂SSi [M+H]⁺: 1186.51, found: 1186.60.



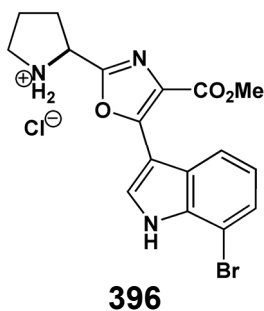
393

Procedure: Compound **369** was subject to the acylation procedure described for compound **391**.

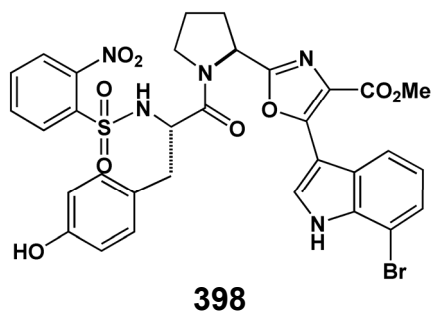
pTLC (70% EtOAc/hexanes) (43%). **391**: ¹H NMR: see attached appendix.



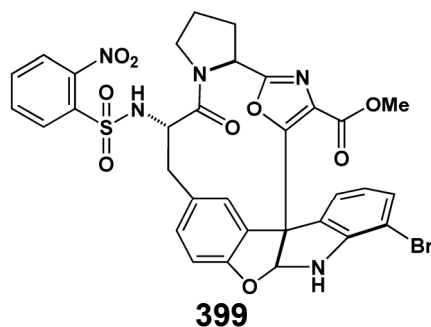
Procedure: Peptide coupling and DDQ oxidation were performed following the procedure described for compound **327a**. FC with 25% CH₃CN/CHCl₃ (95% coupling reaction, 67% DDQ reaction). **395**: $R_f = 0.29$ (60% EtOAc/hexanes). ¹H NMR spectra: see attached appendix.



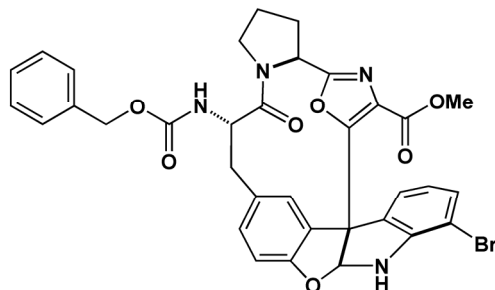
Procedure: Deprotection of **395** was performed as described for compound **327a** (95%). **396**: ¹HNMR (400 MHz, CDOD₃): δ 11.81 (br s, 1H), 8.78 (s, 1H), 8.14 (d, $J = 8.1$ Hz, 1H), 8.14 (d, $J = 8.1$ Hz, 1H), 7.17 – 7.14 (m, 1H), 5.12 – 5.08 (m, 1H), 3.94 (s, 3H), 3.57 – 3.50 (m, 2H), 2.70 – 2.61 (m, 1H), 2.59 – 2.52 (m, 1H), 2.36 – 2.21 (m, 2H).



Procedure: TBTU coupling with compound **396** and tyrosine **330** performed as described for compound **332**. FC with 25% CH₃CN/CHCl₃. (85%). **398**: R_f = 0.33(25% CH₃CN/CHCl₃). ¹H NMR: see attached appendix.

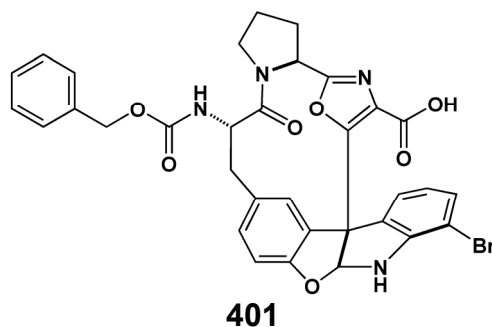


Procedure: Tripeptide **396** subjected PIDA oxidation as described for compound **334**. FC with 20% CH₃CN/CHCl₃. (17%). **399**: R_f = 0.75 (25% EtOAc/CH₂Cl₂). ¹H NMR (400 MHz, CDCl₃): δ 8.05 – 8.02 (m, 1H), 7.80 – 7.78 (m, 1H), 7.71 – 7.60 (m, 2H), 7.29 – 7.27 (m, 1H), 7.19 (dd, *J* = 1.8, 8.4 Hz, 1H), 7.15 – 7.14 (m, 1H), 7.06 (d, *J* = 3.7 Hz, 1H), 6.99 (d, *J* = 7.0 Hz, 1H), 6.81 (d, *J* = 8.1 Hz, 1H), 6.65 – 6.61 (m, 1H), 5.42 (d, *J* = 3.7 Hz, 1H), 4.78 (dd, *J* = 4.4, 7.7 Hz, 1H), 4.74 (m, 1H), 3.94 – 3.89 (m, 1H), 3.84 – 3.78 (m, 1H), 3.68 (s, 3H), 3.34 – 3.23 (m, 2H), 2.43 – 2.37 (m, 1H), 2.29 – 2.10 (m, 4H). ¹³C NMR (75 MHz, CDCl₃): 167.4, 161.5, 161.2, 157.7, 155.6, 147.8, 147.1, 134.1, 133.9, 132.7, 131.8, 130.6, 130.0, 129.3, 129.1, 128.1, 127.3, 125.4, 121.1, 120.9, 110.8, 102.9, 101.0, 62.1, 57.1, 56.0, 52.3, 46.3, 39.5, 29.5, 25.7. ES-MS: calcd. for C₃₂H₂₆BrN₅O₉S [M+H]⁺: 736.07, found: 736.00, 738.00; C₃₂H₂₆BrN₅O₉S [M+Na]⁺: 758.05, found: 757.95, 759.95; calcd. for C₃₂H₂₆BrN₅O₉S [M-H]⁻: 734.06, found: 734.05, 736.05.

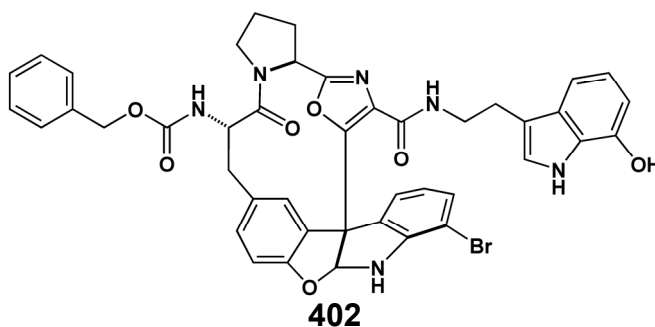


400

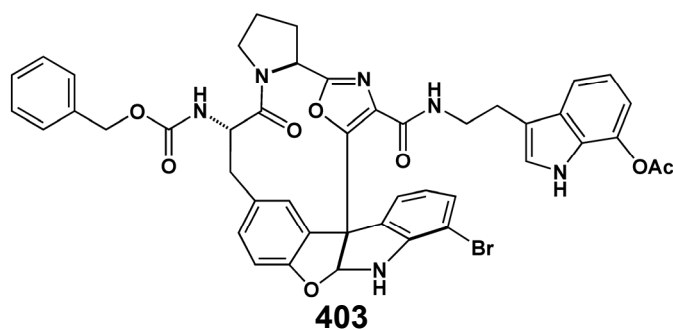
Procedure: Cyclized compound **399** subjected to the deprotection/Cbz reprotection procedure described for compound **343b**. (90%). **400**: $R_f = 0.24$ (90% EtOAc/hexanes). ^{13}C NMR (75 MHz, CDCl_3): 168.7, 161.6, 157.5, 155.8, 155.3, 147.2, 136.4, 131.8, 130.4, 129.9, 129.4, 129.1, 128.6, 128.3, 128.2, 128.1, 121.0, 120.8, 110.6, 102.9, 100.9, 67.0, 56.0, 54.6, 52.3, 46.3, 37.9, 29.5, 25.7.



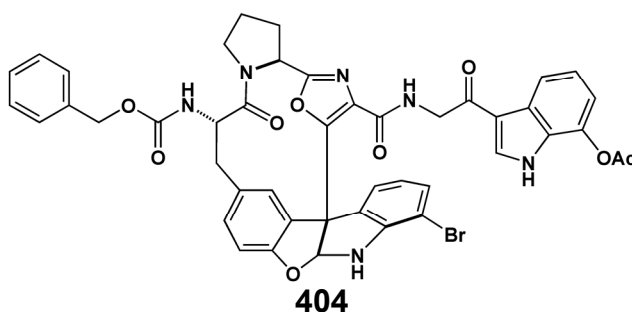
Procedure: Compound **400** saponified as described for compound **344b** (95%). **401**: $R_f = 0.43$ (10% MeOH/ CH_2Cl_2). ^1H NMR: see attached appendix. ^{13}C NMR (75 MHz, 80% $\text{CD}_3\text{OD}/20\%$ CDCl_3): 170.1, 163.6, 162.7, 158.4, 156.9, 156.5, 148.9, 137.7, 132.6, 131.7, 131.1, 130.9, 130.4, 129.5, 129.4, 129.1, 129.0, 128.8, 122.3, 121.3, 111.0, 103.2, 102.7, 67.8, 62.9, 57.0, 55.5, 47.3, 38.1, 30.5, 26.3.



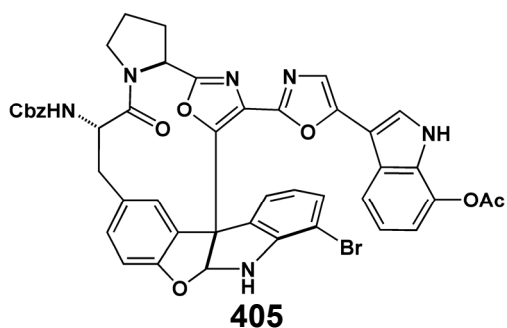
Procedure: Acid **401** and amine **349** subject to the TBTU coupling procedure described for compound **352**. **402**: ^1H NMR: see attached appendix.



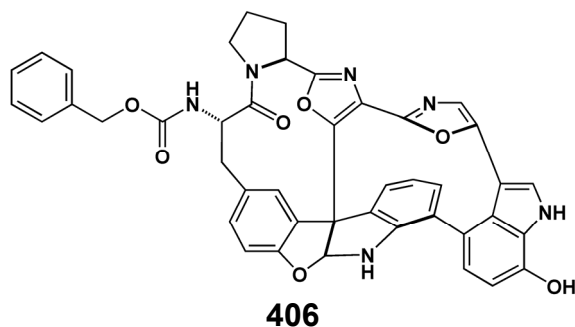
Procedure: Coupled product **402** acetylated using the procedure detailed for compound **353**. **403**: $R_f = 0.56$ (40% EtOAc/CH₂Cl₂). ¹H NMR: see attached appendix. ¹³C NMR (75 MHz, CDCl₃): 169.4, 168.6, 161.4, 160.6, 157.1, 155.4, 151.9, 147.3, 136.5, 136.2, 131.8, 130.8, 130.3, 130.2, 129.7, 129.4, 129.0, 128.6, 128.6, 128.2, 128.0, 127.9, 122.8, 121.1, 120.6, 119.3, 116.6, 114.1, 113.2, 110.4, 103.5, 100.5, 66.9, 61.8, 56.4, 54.6, 46.5, 39.4, 37.5, 30.3, 25.9, 25.5, 21.1.



Procedure: Compound **403** subjected to the DDQ oxidation procedure described for compound **354**. FC 35% EtOAc/CH₂Cl₂ (74%). **404**: $R_f = 0.35$ (40% EtOAc/CH₂Cl₂). ¹H NMR: see attached appendix. ¹³C NMR (75 MHz, CDCl₃): 188.9, 169.4, 168.8, 161.2, 161.0, 157.2, 155.5, 152.3, 147.4, 136.5, 136.4, 132.5, 131.9, 130.8, 130.5, 129.9, 129.5, 128.9, 128.8, 128.5, 128.3, 128.1, 128.0, 127.9, 123.1, 121.1, 120.8, 119.8, 116.0, 115.4, 110.6, 103.5, 101.0, 67.1, 61.9, 56.4, 54.7, 46.7, 46.2, 37.9, 30.3, 29.9, 26.0, 21.1. ES-MS: calcd. for C₄₅H₃₇BrN₆O₉ [M+H]⁺: 885.19, found: 885.00, 887.00; C₄₅H₃₇BrN₆O₉ [M+Na]⁺: 907.17, found: 907.20, 909.20; calcd. for C₄₅H₃₇BrN₆O₉ [M-H]⁻: 883.17, found: 883.17, 885.17.

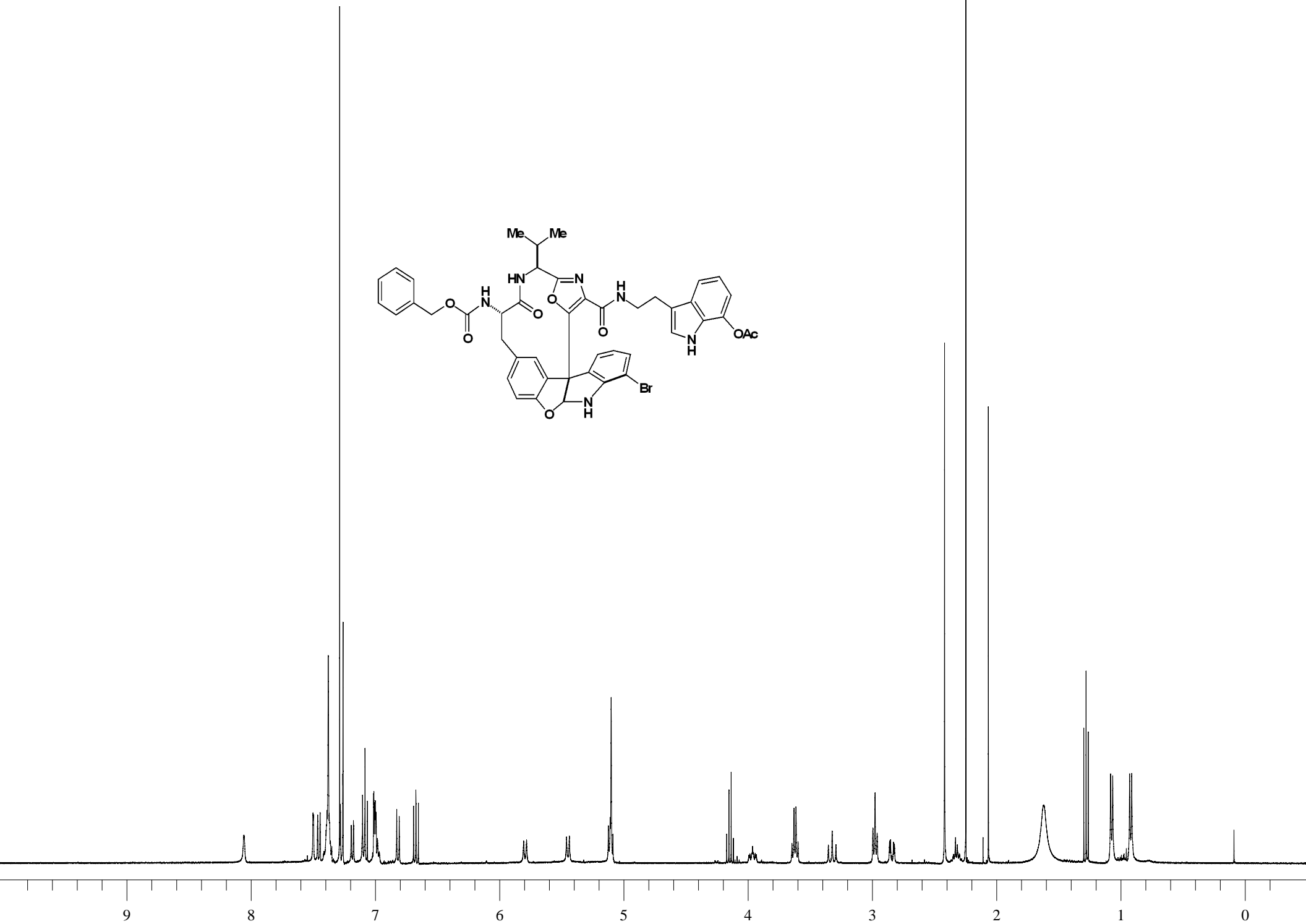
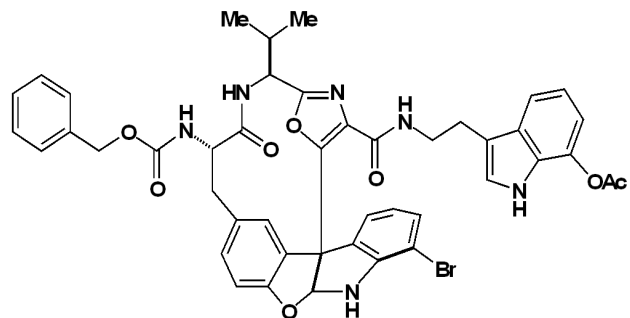


Procedure: DDQ product **354** subjected to the dehydration procedure for compound **354**. PTLC 80% EtOAc/benzene. (69%). **405**: $R_f = 0.10$ (80% EtOAc/hexanes). $^1\text{H NMR}$: see attached appendix.



Procedure: Bis-oxazole **355** subjected to the photochemistry procedure described for compound **356**. pTLC (50% $\text{CH}_3\text{CN}/\text{CHCl}_3$). Slightly impure compound obtained consistent the desired cyclized product, but not conclusive. Mass matches the desired mass. **406**: $^1\text{H NMR}$: see attached appendix –ES-MS: calcd. for $\text{C}_{43}\text{H}_{32}\text{N}_6\text{O}_7$ $[\text{M}+\text{H}]^+$: 746.24, found: 746.30; $\text{C}_{43}\text{H}_{32}\text{N}_6\text{O}_7$ $[\text{M}+\text{Na}]^+$: 768.23, found: 768.20; calcd. for $\text{C}_{45}\text{H}_{37}\text{BrN}_6\text{O}_9$ $[\text{M}-\text{H}]^-$: 744.23, found: 744.40.

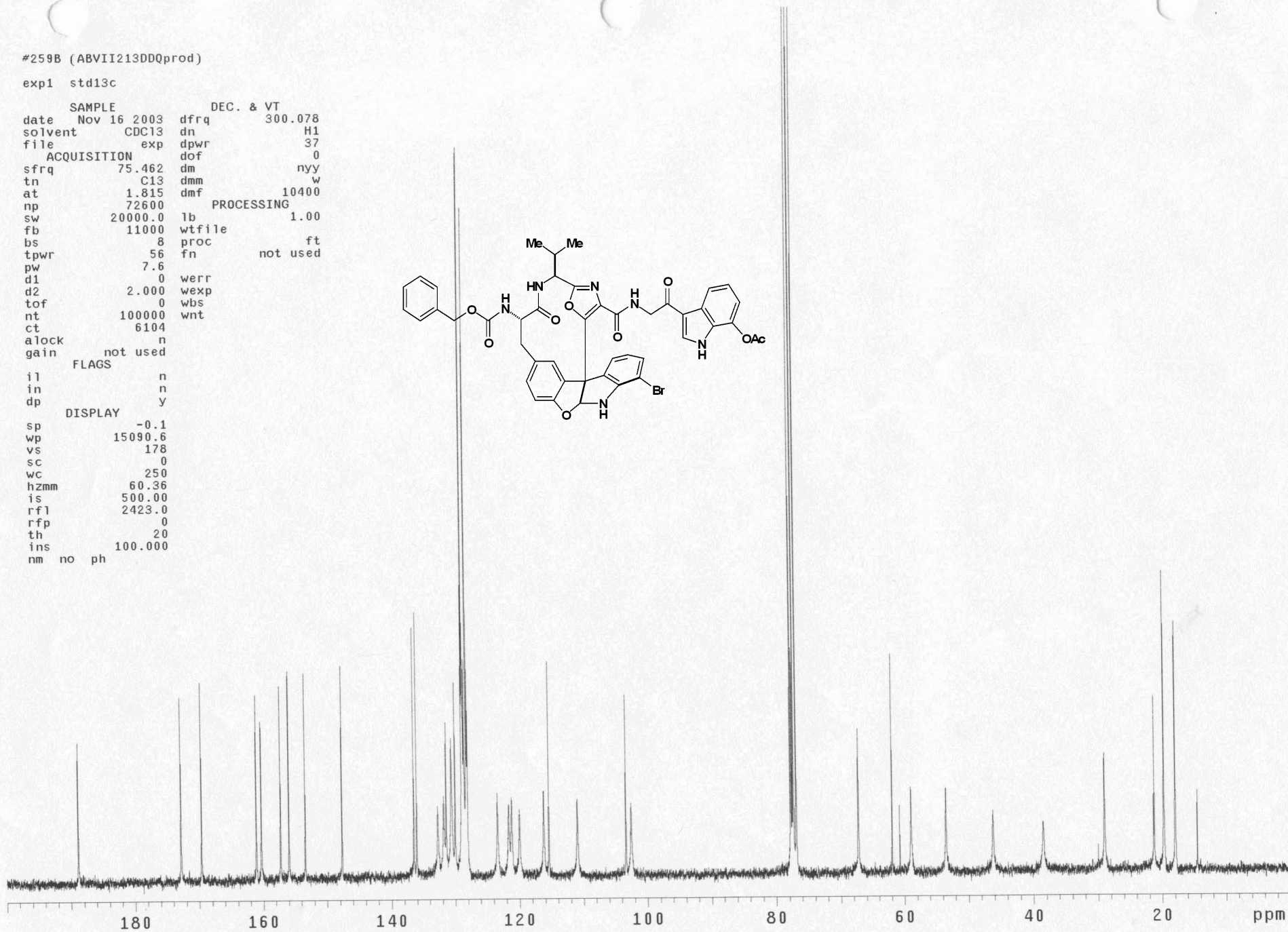
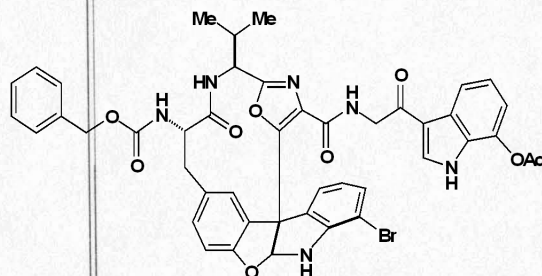
5.9 Chapter 5 Appendix

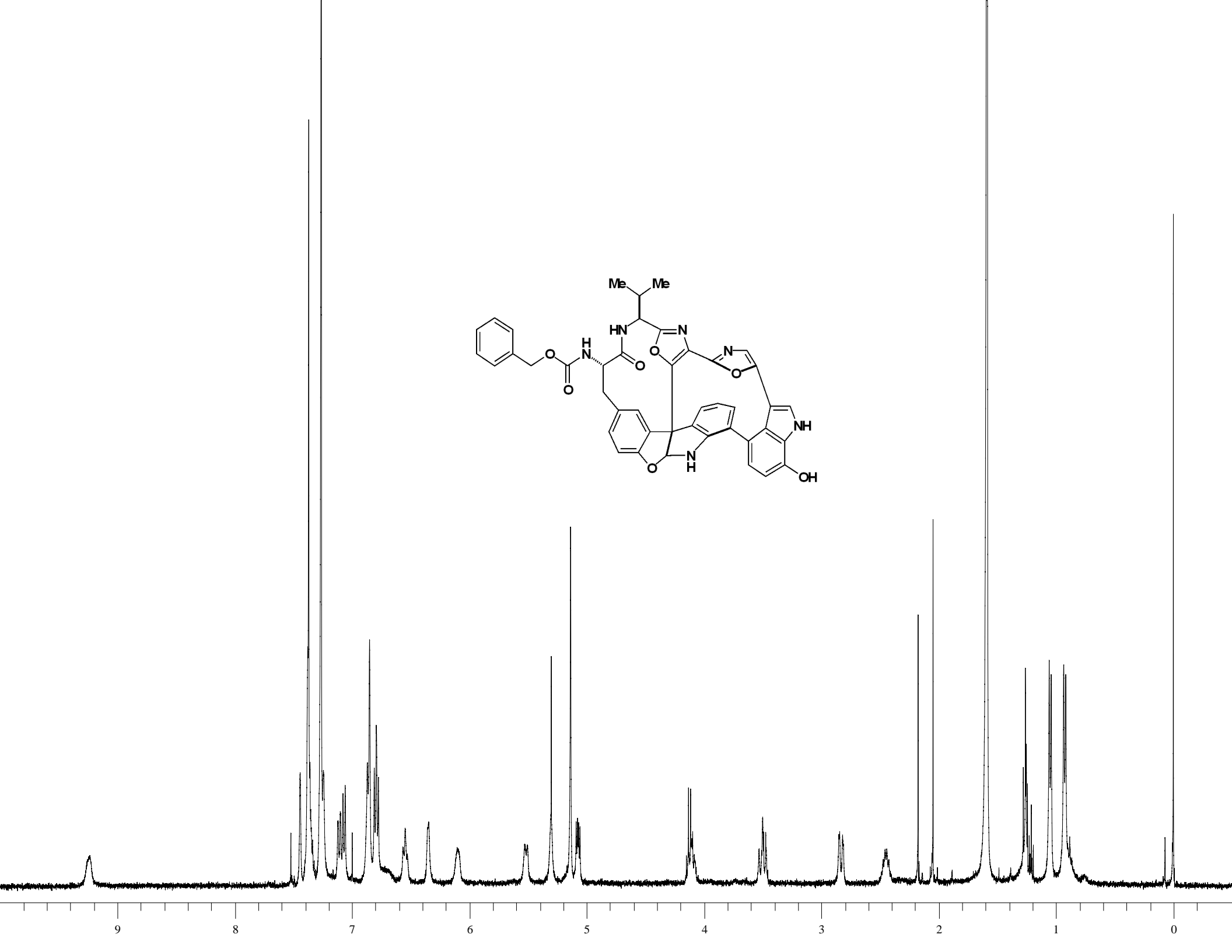
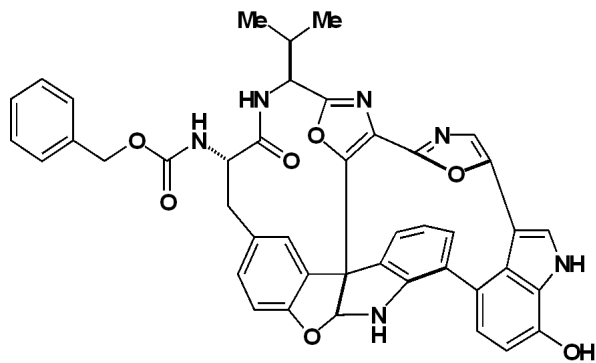


#259B (ABVII213DDQprod)

exp1 std13c

SAMPLE		DEC. & VT	
date	Nov 16 2003	dfrq	300.078
solvent	CDC13	dn	H1
file	exp	dpwr	37
ACQUISITION			
sfrq	75.462	dof	0
tn	C13	dm	nyy
at	1.815	dmm	w
np	72600	dmf	10400
sw	20000.0	PROCESSING	
fb	11000	lb	1.00
bs	8	wtfile	ft
tpwr	56	proc	not used
pw	7.6	fn	
d1	0	werr	
d2	2.000	wexp	
tof	0	wbs	
nt	100000	wnt	
ct	6104		
alock	n		
gain	not used		
FLAGS			
il	n		
in	n		
dp	y		
DISPLAY			
sp	-0.1		
wp	15090.6		
vs	178		
sc	0		
wc	250		
hzmm	60.36		
is	500.00		
rfl	2423.0		
rfp	0		
th	20		
ins	100.000		
nm	no	ph	

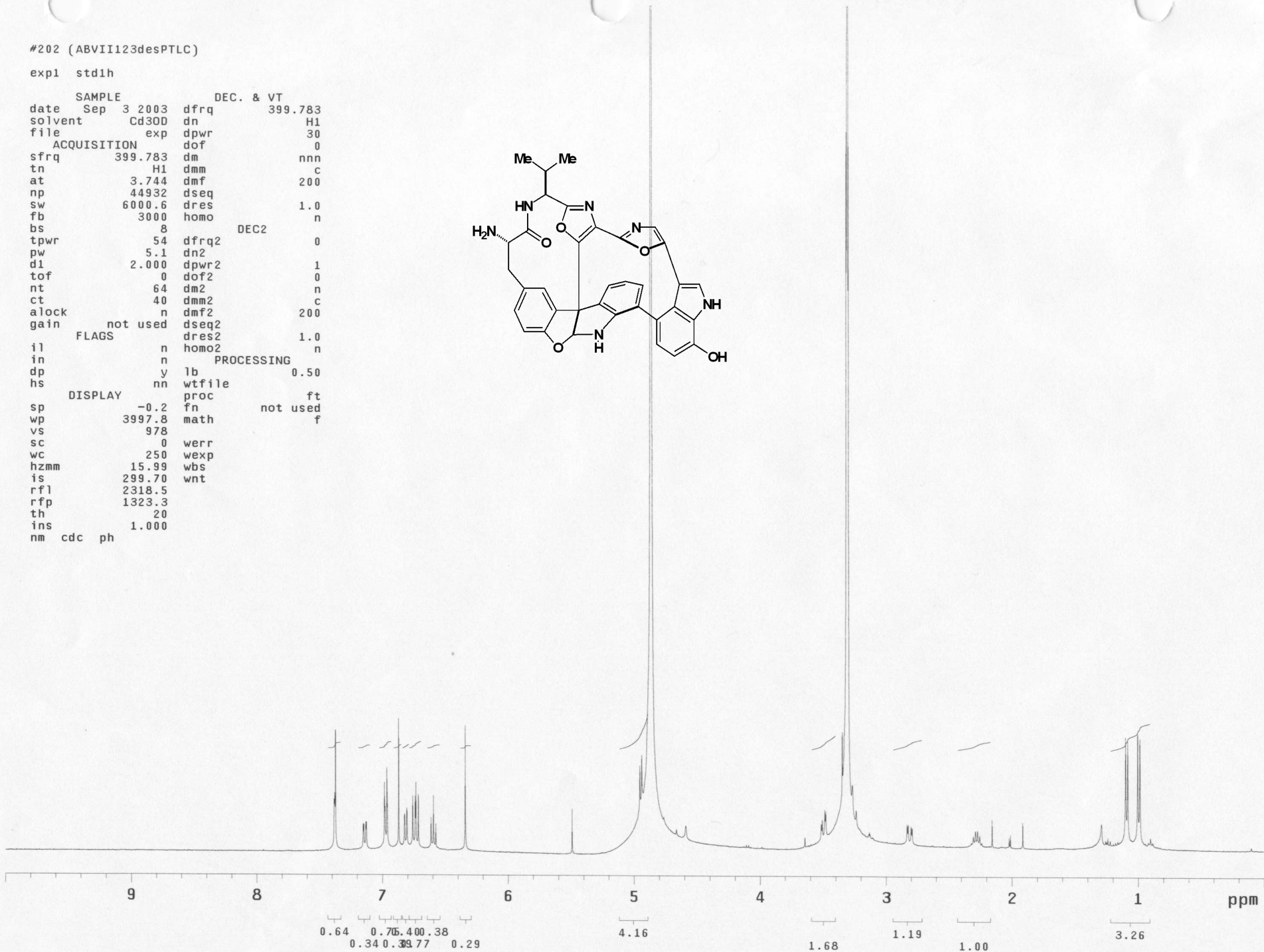
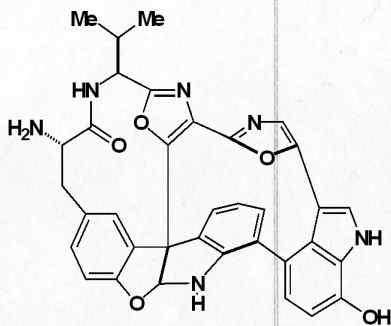




#202 (ABVII123desPTLC)

expl std1h

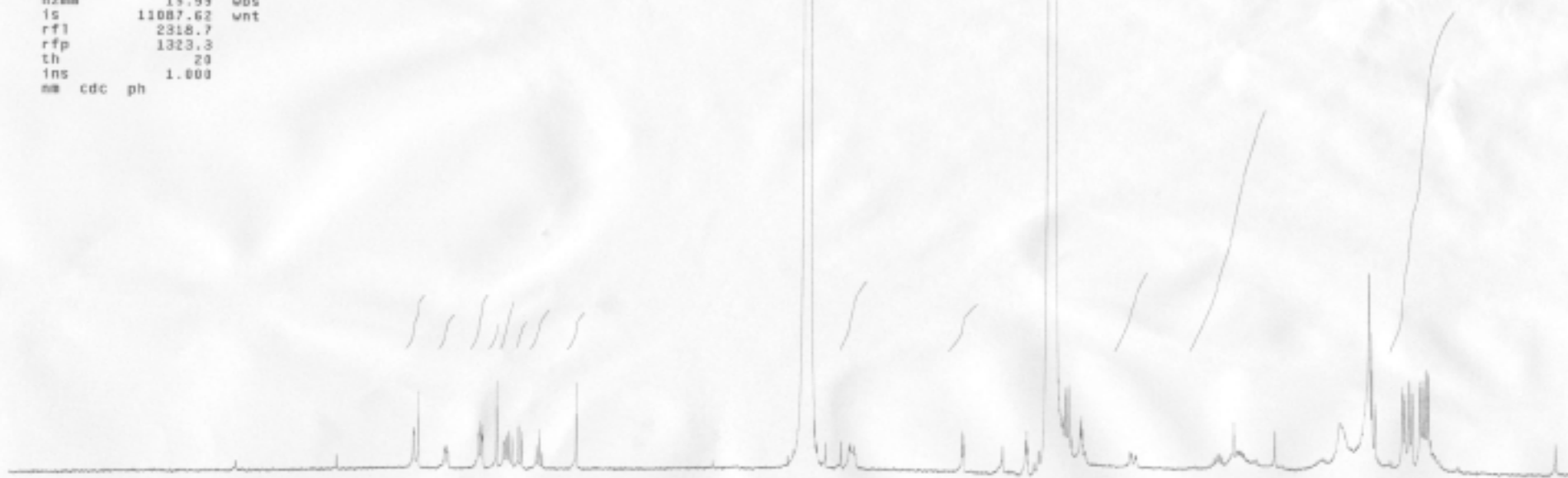
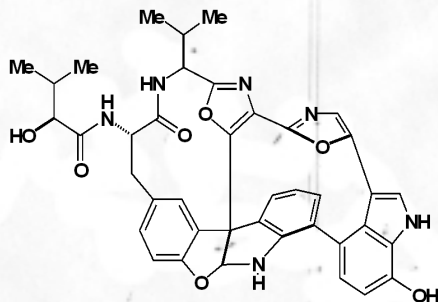
SAMPLE		DEC. & VT	
date	Sep 3 2003	dfrq	399.783
solvent	Cd300	dn	H1
file	exp	dpwr	30
ACQUISITION		dof	0
sfrq	399.783	dm	nnn
tn	H1	dmm	c
at	3.744	dmf	200
np	44932	dseq	
sw	6000.6	dres	1.0
fb	3000	homo	n
bs	8	DEC2	
tpwr	54	dfrq2	0
pw	5.1	dn2	
d1	2.000	dpwr2	1
tof	0	dof2	0
nt	64	dm2	n
ct	40	dmm2	c
alock	n	dmf2	200
gain	not used	dseq2	
FLAGS		dres2	1.0
il	n	homo2	n
in	n	PROCESSING	
dp	y	lb	0.50
hs	nn	wtfile	
DISPLAY		proc	ft
sp	-0.2	fn	not used
wp	3997.8	math	f
vs	978		
sc	0	werr	
wc	250	wexp	
hzmm	15.99	wbs	
is	299.70	wnt	
rfl	2318.5		
rfp	1323.3		
th	20		
ins	1.000		
nm	cdc ph		



#205 (ABVII125HPLC)

expl stdih

date	Sep 15 2003	dfrq	399.783
solvent	CD300	dn	H1
file	exp	dpwr	30
ACQUISITION			
sfrq	399.783	ds	mnn
tn	H1	dsm	c
at	3.744	daf	260
np	44932	dseq	
sw	6000.6	dres	1.0
fb	3008	homo	n
bs	8	DEC2	
tpwr	54	dfrq2	0
gw	5.1	dn2	
d1	2.800	dpwr2	1
tof	0	dof2	0
nt	64	dm2	n
ct	56	dsm2	c
alock	n	daf2	200
gain	not used	dseq2	
FLAGS			
il	n	dres2	1.0
in	n	homo2	n
dp	y	PROCESSING	
hs	nn	lb	0.50
DISPLAY			
sp	-0.2	wtfile	
wp	3997.8	proc	ft
vs	4111	fn	not used
sc	0	math	f
wc	250	werr	
hzmm	15.99	wexp	
is	11087.62	wbs	
rf1	2318.7	wnt	
rfp	1323.3		
th	20		
ins	1.000		
nm	cdc ph		



9

8

7

6

5

4

3

2

1

ppm

1.10 1.10 0.83
0.72 0.50 0.57 0.77

1.45

0.98

1.66

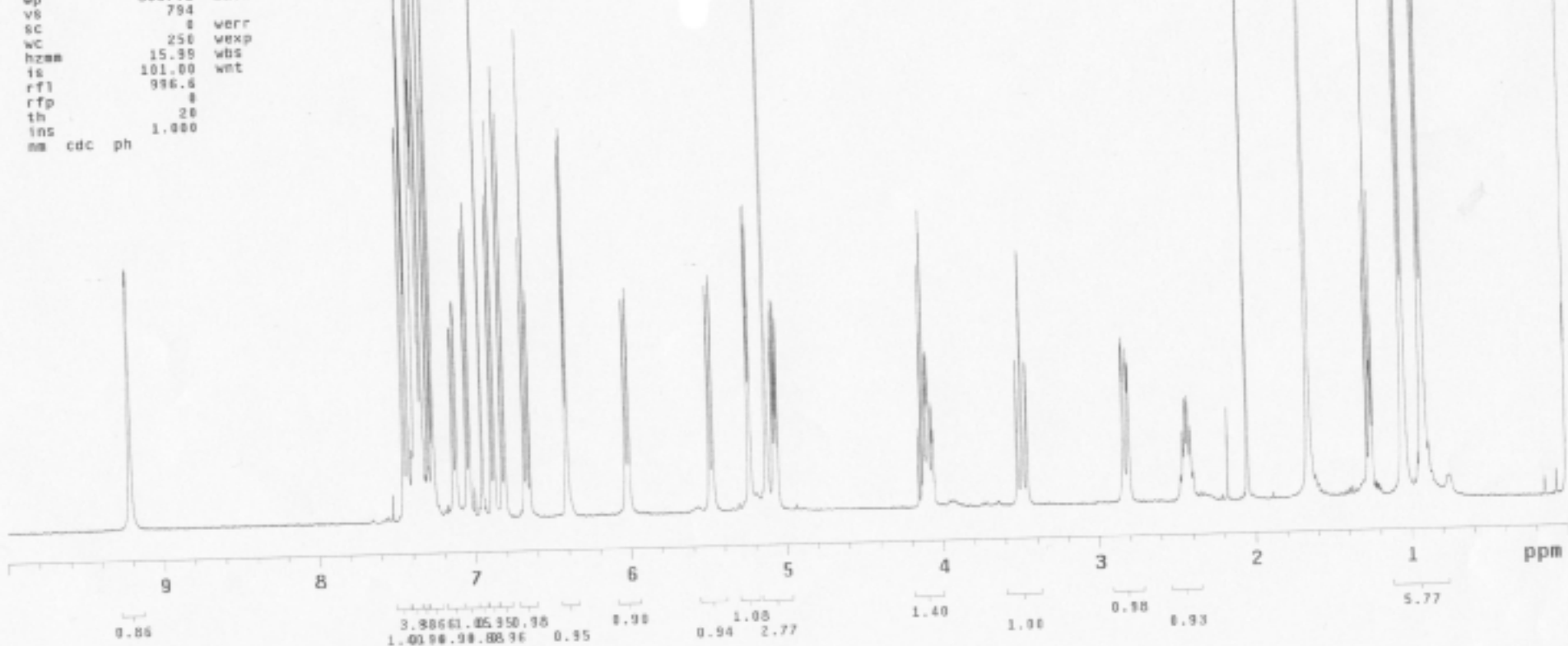
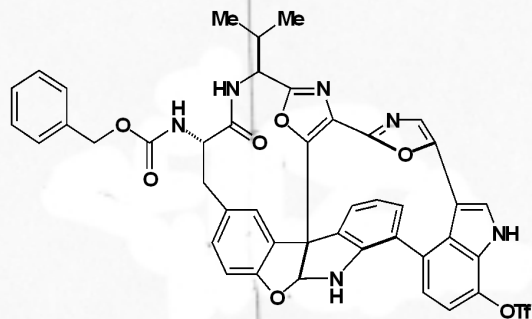
5.83

7.11

#271 (ABVII2330TF)

expl stdih

SAMPLE		DEC. & VT	
date	Nov 24 2003	dfrq	399.781
solvent	CDCl3	dn	H1
file	exp	dpwr	30
ACQUISITION			
sfrq	399.781	dm	nmn
in	H1	dsm	c
at	3.744	daf	200
ap	44932	dseq	
sw	6080.6	dres	1.8
fb	3000	homo	n
bs	8	DEC2	
tpwr	54	dfrq2	0
pw	5.1	dn2	
d1	2.000	dpwr2	1
tof	8	dof2	0
nt	64	dm2	n
ct	8	dsm2	c
alock	n	daf2	200
gain	not used	dseq2	
FLAGS		dres2	1.0
il	n	homo2	n
in	n	PROCESSING	
dp	y	fb	0.50
hs	nn	vtfile	
DISPLAY		proc	ft
sp	-0.0	fn	not used
wp	3997.8	math	r
vs	794		
sc	8	werr	
wc	250	wexp	
hzem	15.99	wbs	
is	101.00	wnt	
rfl	996.6		
rtp	8		
th	20		
ins	1.000		
nm	cdc ph		

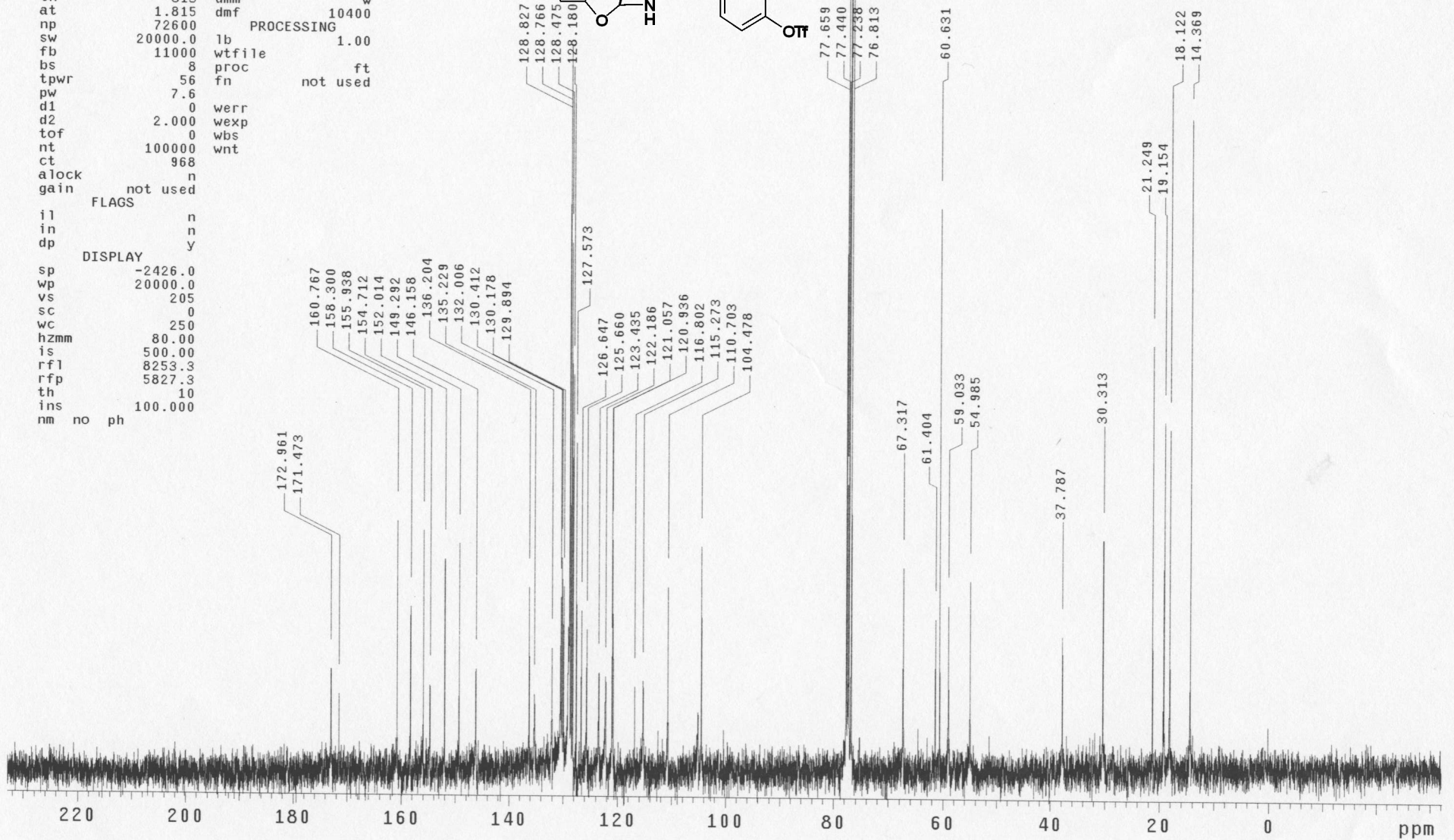
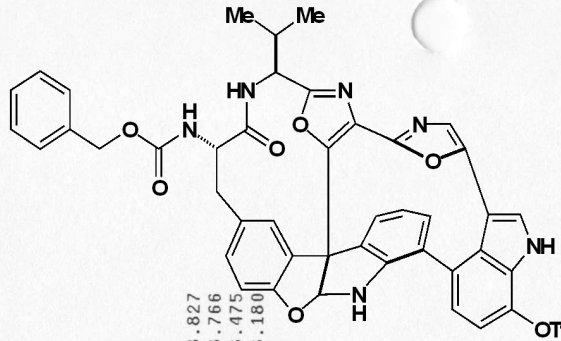


13C OBSERVE

AMU 2330 T6

exp1 std13c

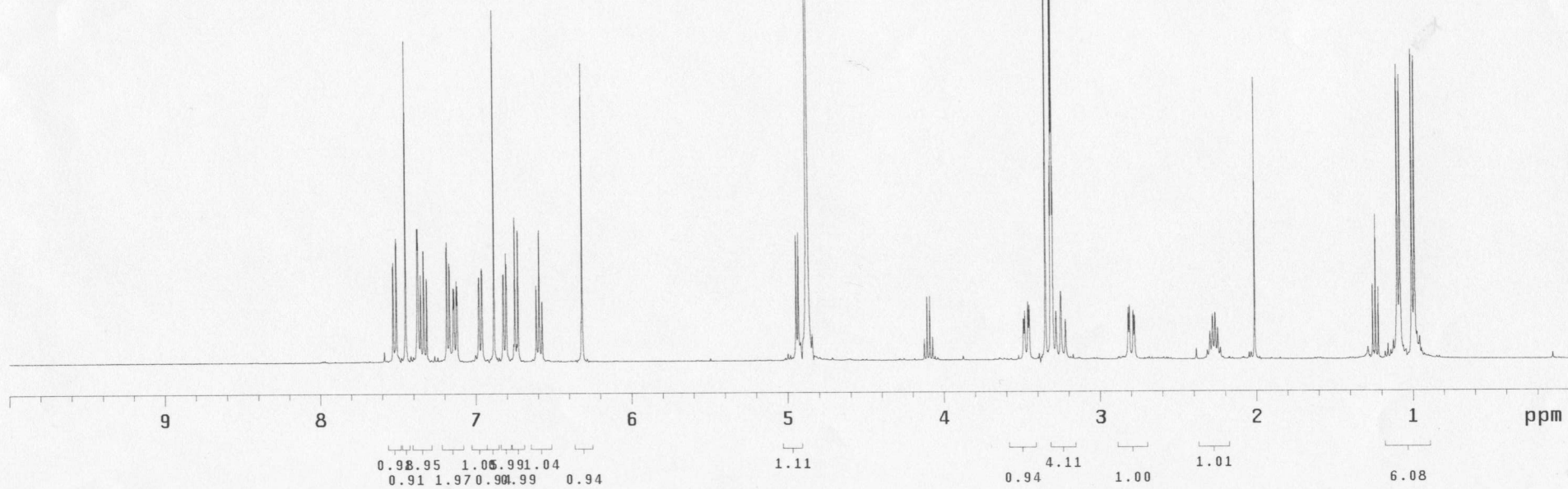
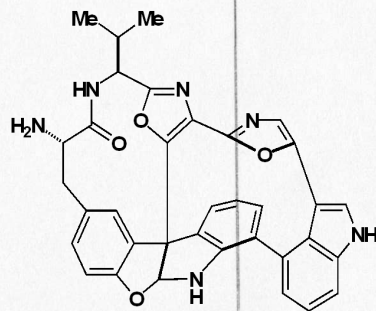
SAMPLE DEC. & VT
date Nov 24 2003 dfrq 300.078
solvent CDC13 dn H1
file exp dpwr 37
ACQUISITION dof 0
sfrq 75.462 dm nyy
tn C13 dmm w
at 1.815 dmf 10400
np 72600
sw 20000.0 lb 1.00
fb 11000 wtfile
bs 8 proc ft
tpwr 56 fn not used
pw 7.6
d1 0 werr
d2 2.000 wexp
tof 0 wbs
nt 100000 wnt
ct 968
alock n
gain not used
FLAGS
il n
in n
dp y
DISPLAY
sp -2426.0
wp 20000.0
vs 205
sc 0
wc 250
hzmm 80.00
is 500.00
rfl 8253.3
rfp 5827.3
th 10
ins 100.000
nm no ph

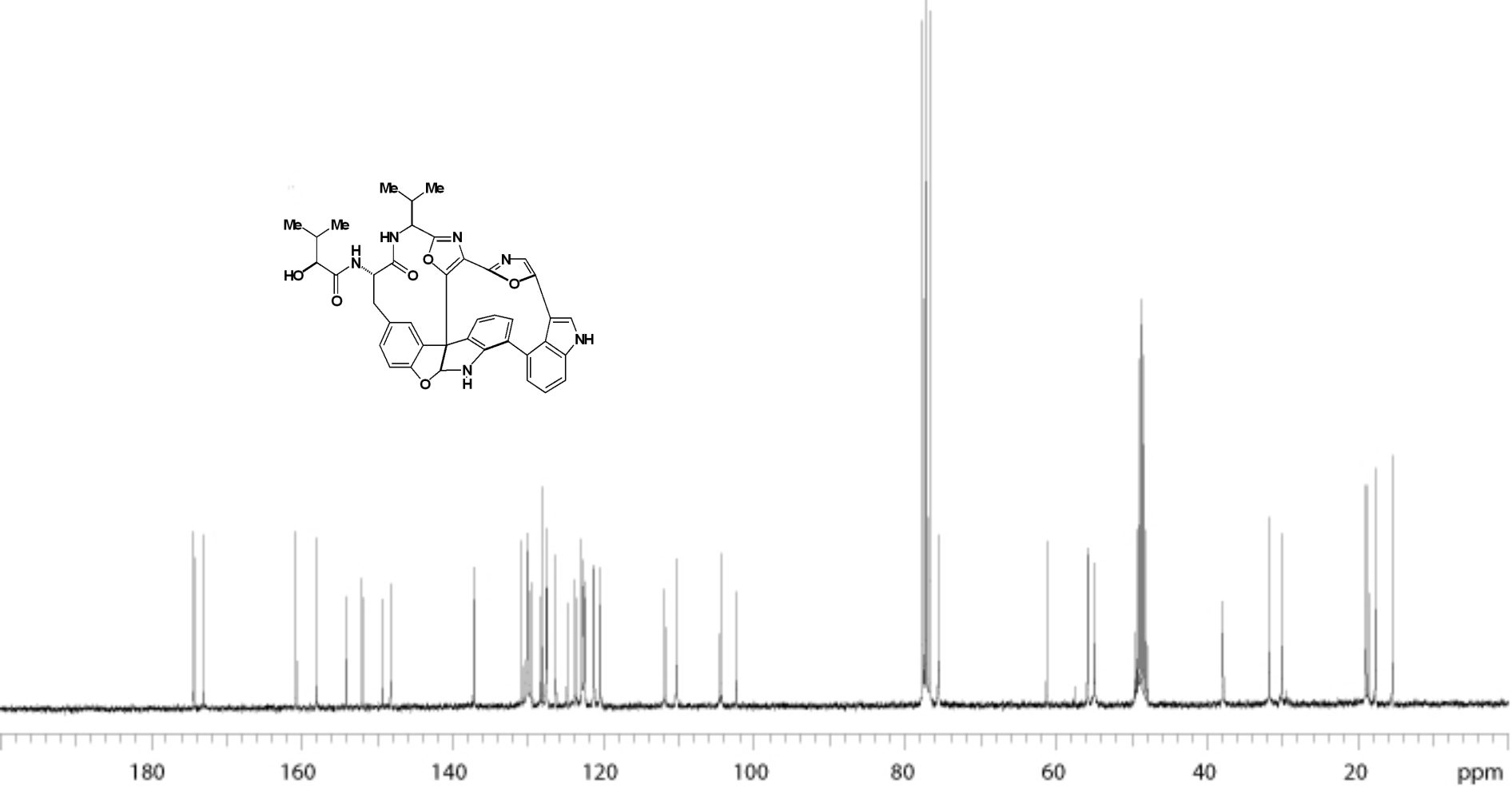
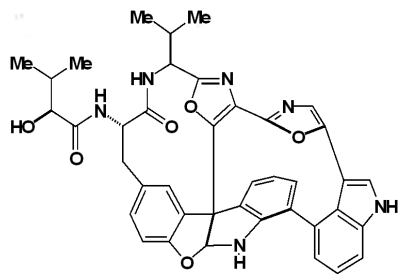


#272 (aBVII235NH2corecrude)

exp8 std1h

SAMPLE		DEC. & VT	
date	Nov 24 2003	dfrq	399.783
solvent	cd3od	dn	H1
file	exp	dpwr	30
ACQUISITION		dof	0
sfrq	399.783	dm	nnn
tn	H1	dmm	c
at	3.744	dmf	200
np	44932	dseq	
sw	6000.6	dres	1.0
fb	3000	homo	n
bs	8	DEC2	
tpwr	54	dfrq2	0
pw	5.1	dn2	
d1	2.000	dpwr2	1
tof	0	dof2	0
nt	64	dm2	n
ct	16	dmm2	c
alock	n	dmf2	200
gain	not used	dseq2	
FLAGS		dres2	1.0
il	n	homo2	n
in	n	PROCESSING	
dp	y	lb	0.50
hs	nn	wtfile	
DISPLAY		proc	ft
sp	-0.2	fn	not used
wp	3997.8	math	f
vs	319		
sc	0	werr	
wc	250	wexp	
hzmm	15.99	wbs	
is	1219.93	wnt	
rfl	2318.7		
rfp	1323.3		
th	.20		
ins	1.000		
nm	cdc	ph	

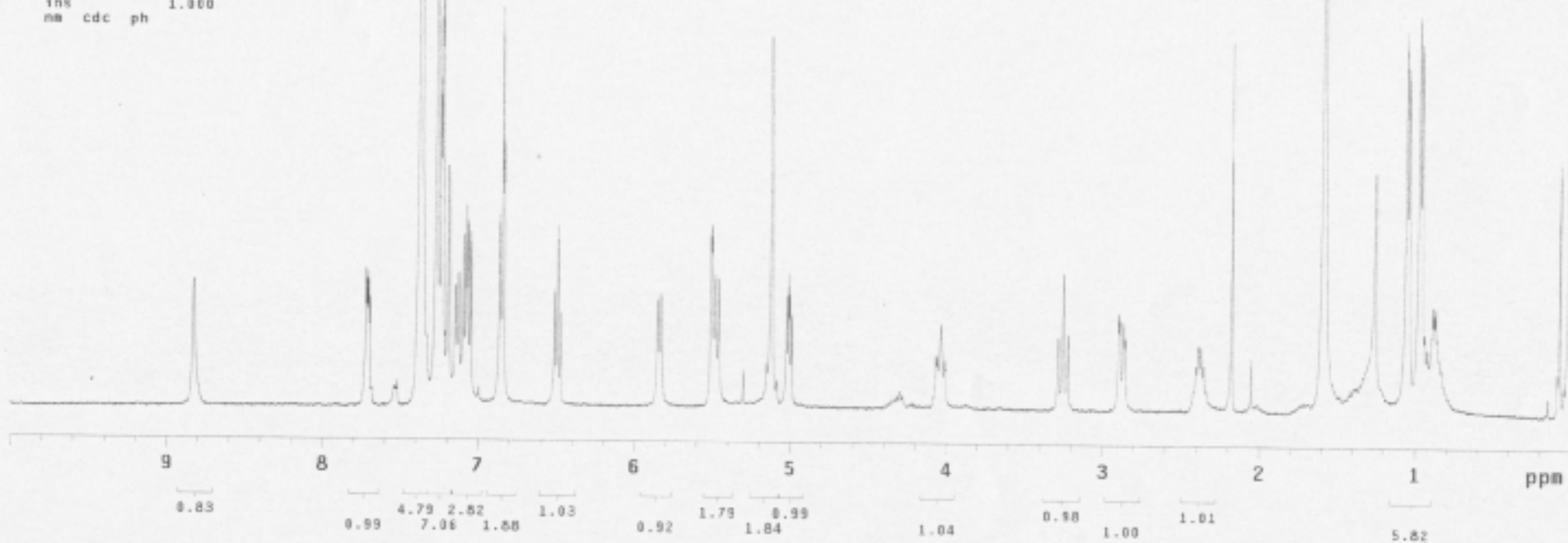
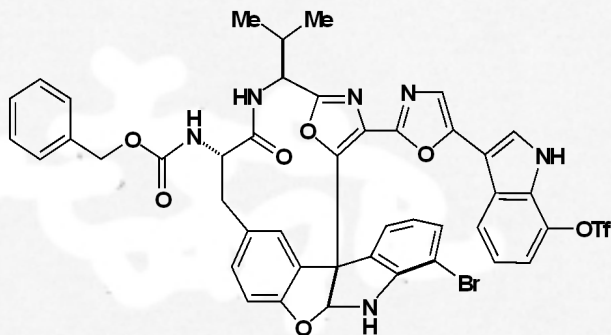




#578 (ABVIII281 00-1 opencomOTF)

expl stdlh

SAMPLE		DEC. & VT	
date	Nov 30 2004	dfrq	399.781
solvent	CDC13	dn	H1
file	exp	dpwr	30
ACQUISITION			
cfreq	399.781	dm	nmn
tn	H1	dms	c
at	3.744	daf	200
np	44932	dseq	
sw	6000.6	dres	1.0
fb	3800	homo	n
bs	4	DEC2	
tpwr	54	dfrq2	0
pw	5.1	dm2	
d1	2.060	dpwr2	1
tof	0	dof2	0
nt	64	dm2	n
ct	16	dsm2	c
alock	n	daf2	200
gain	not used	dseq2	
flags		dres2	1.0
fl	n	homo2	n
fn	n	PROCESSING	
dp	y	lb	0.50
hs	nn	vtfile	
DISPLAY			
sp	-0.8	proc	ft
wp	3997.8	fn	not used
vs	678	math	f
sc	0	werr	
wc	250	wexp	
hzmm	15.99	wbs	
fs	320.47	wnt	
rfl	995.7		
rff	0		
th	20		
ins	1.060		
nm	cdc	ph	



VIII283 00-2 openDzcompoundcrude

n)

DEC. & VT

2004 dfrq 399.783

lod dn H1

exp dpwr 30

399.783 dot 0

H1 dm nnn

3.744 def 200

44932 dseq

6800.6 dres 1.0

3080 homo n

4 DEC2

54 dfrq2 0

5.1 dn2

2.000 dpwr2 1

0 dof2 0

64 dm2 n

32 dmm2 c

n dmf2 200

not used dseq2

FLAGS dres2 1.0

m homo? n

n PROCESSING

y lb 0.50

nn wtfile

ft

sp -0.2

wp 3997.8

vs 1220

sc 0 werr

wc 250 wexp

hzmm 15.99

is 2073.12

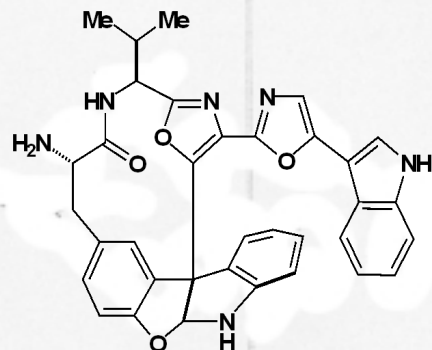
rfl 2318.7

rfp 1323.3

th 20

ins 1.800

am cdc ph



1.07 3.52 2.50 0.84
1.66 1.58 0.81

0.92

0.90

0.68

0.95 0.92

0.96

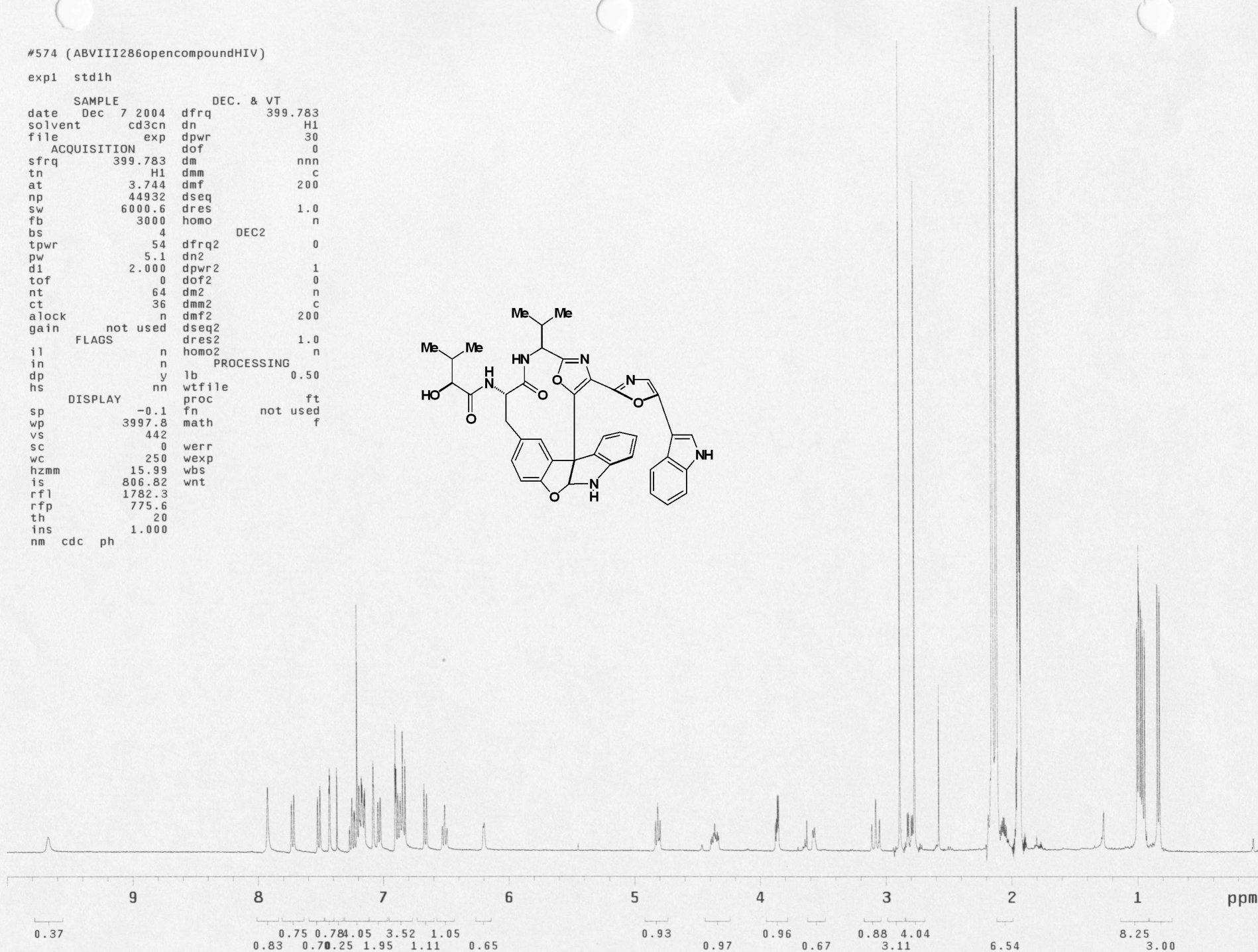
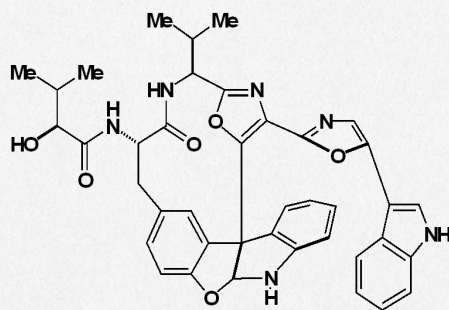
5.14

ppm

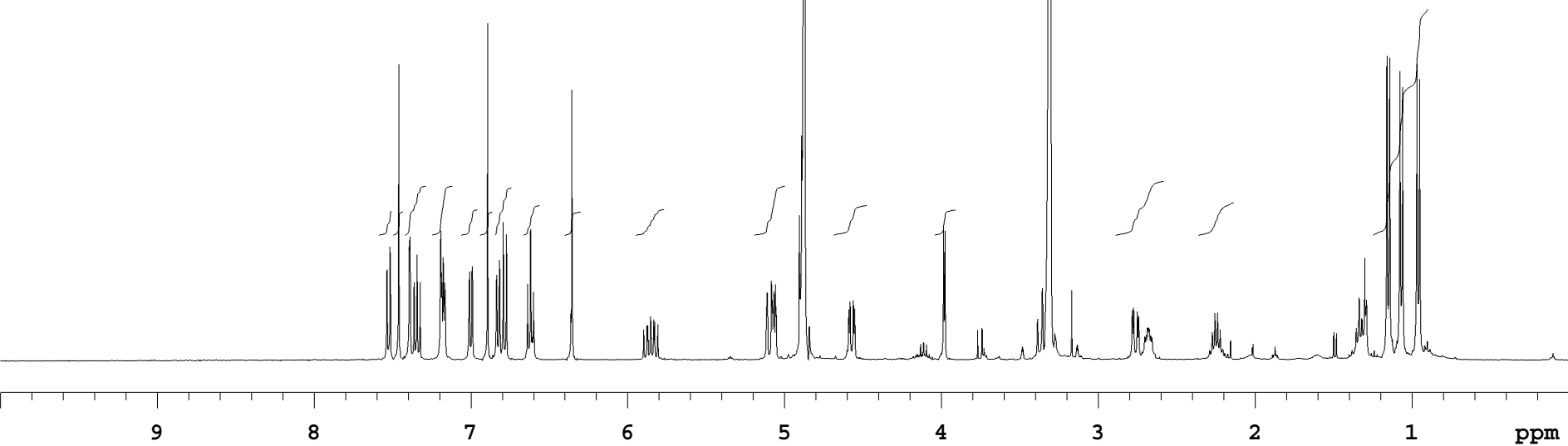
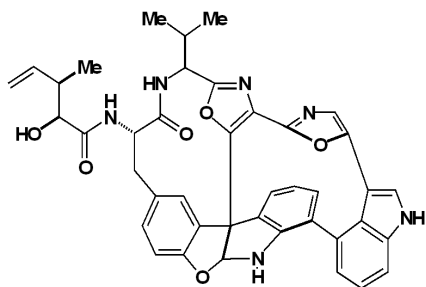
#574 (ABVIII286opencompoundHIV)

exp1 std1h

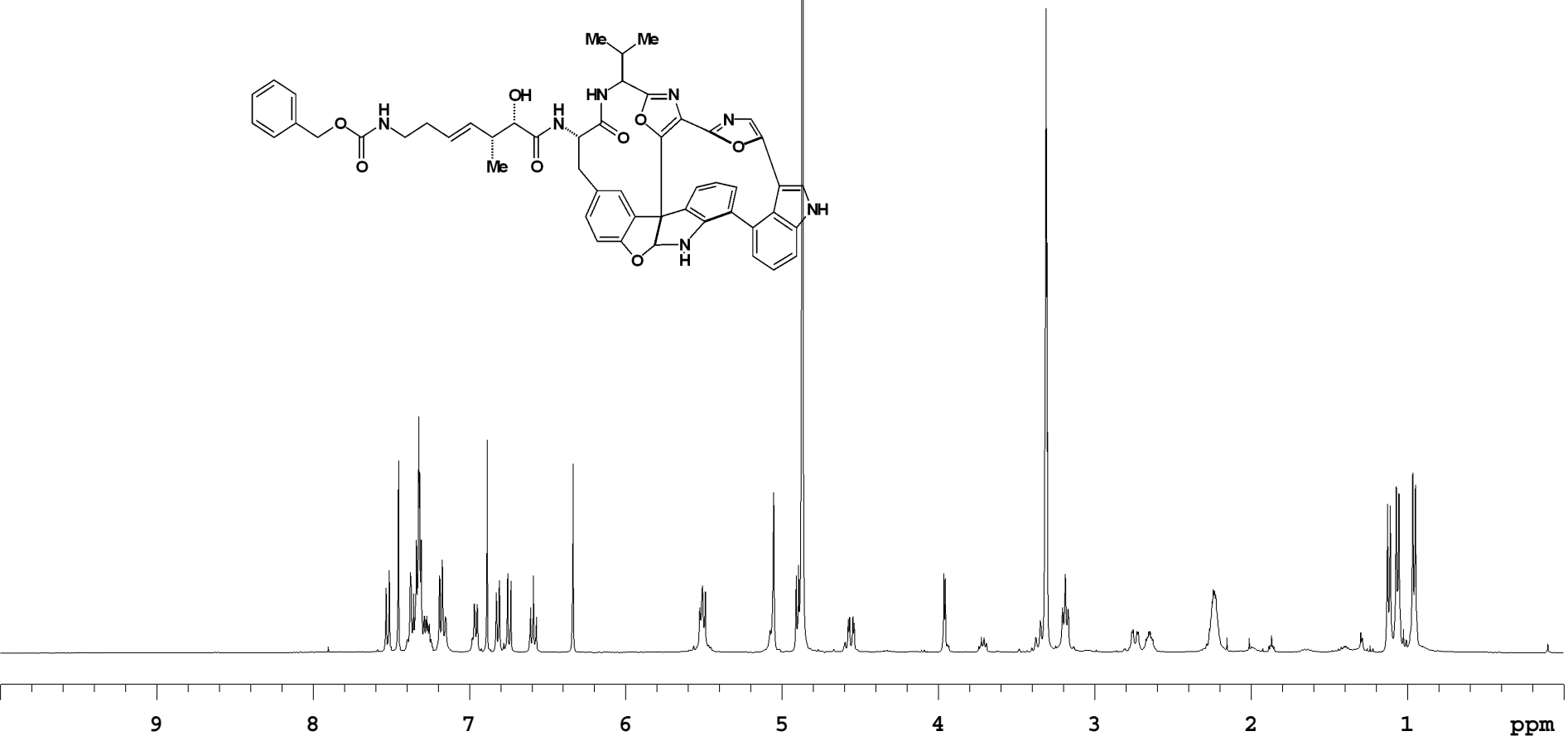
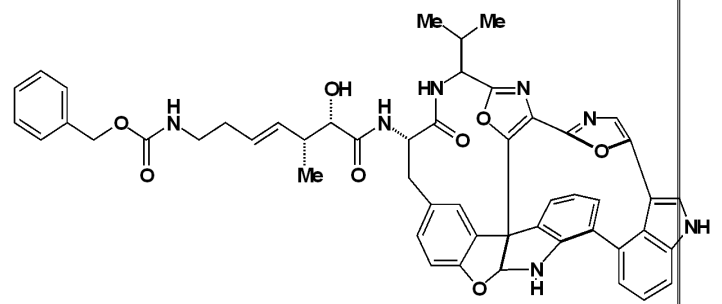
SAMPLE		DEC. & VT	
date	Dec 7 2004	dfrq	399.783
solvent	cd3cn	dn	H1
file	exp	dpwr	30
ACQUISITION		dof	0
sfrq	399.783	dm	nnn
tn	H1	dmm	c
at	3.744	dmf	200
np	44932	dseq	
sw	6000.6	dres	1.0
fb	3000	homo	n
bs	4	DEC2	
tpwr	54	dfrq2	0
pw	5.1	dn2	
d1	2.000	dpwr2	1
tof	0	dof2	0
nt	64	dm2	n
ct	36	dmm2	c
alock	n	dmf2	200
gain	not used	dseq2	
FLAGS		dres2	1.0
il	n	homo2	n
in	y	PROCESSING	0.50
dp	n	lb	
hs	nn	wtfiler	
DISPLAY		proc	ft
sp	-0.1	fn	not used
wp	3997.8	math	f
vs	442		
sc	0	werr	
wc	250	wexp	
hzmm	15.99	wbs	
is	806.82	wnt	
rfl	1782.3		
rfp	775.6		
th	20		
ins	1.000		
nm	cdc ph		



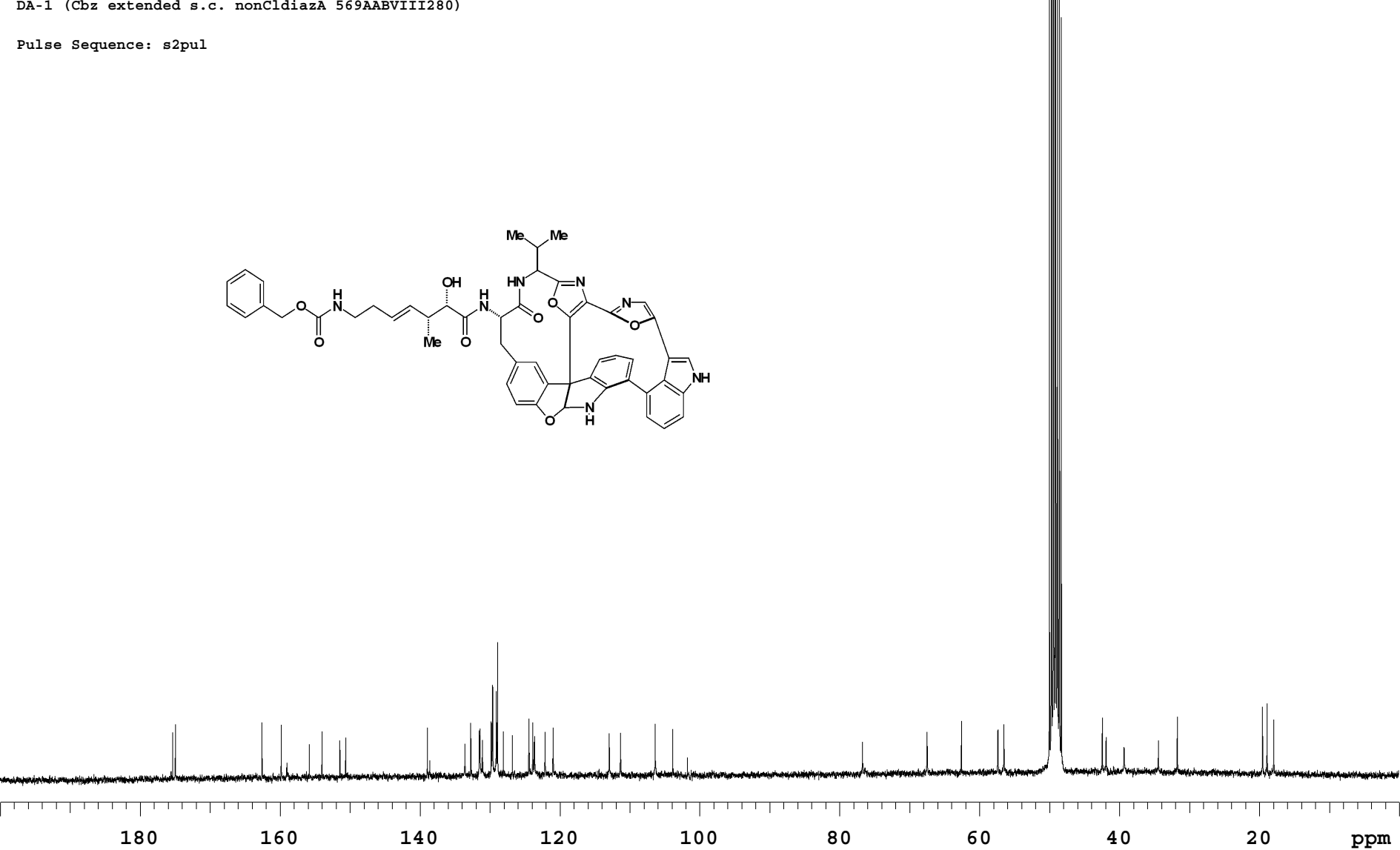
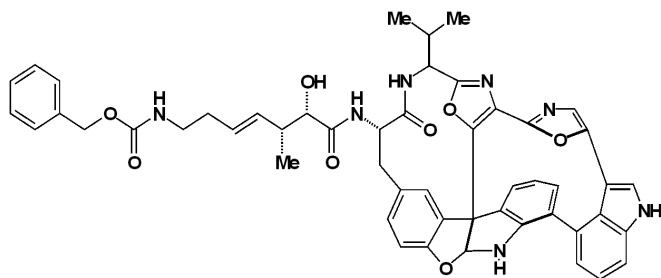
Pulse Sequence: s2pul



Pulse Sequence: s2pul



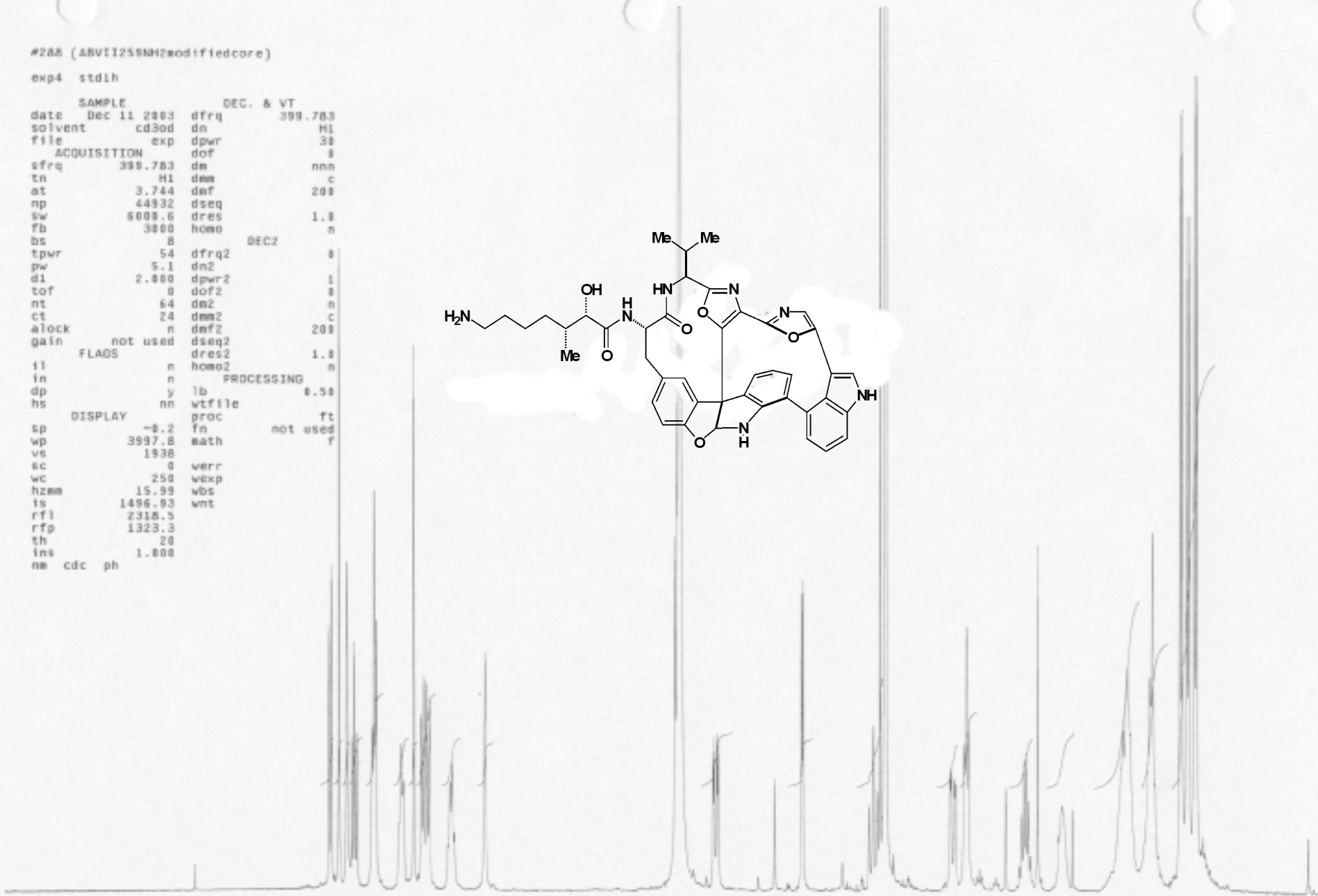
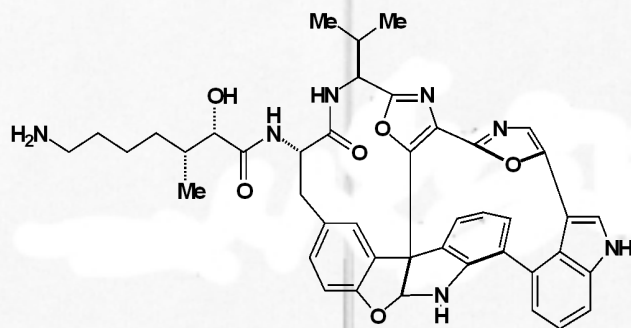
Pulse Sequence: s2pul



#288 (ABVII259NH2modifiedcore)

exp4 stdih

SAMPLE		DEC. & VT	
date	Dec 11 2003	dfrq	399.783
solvent	cd3od	dn	H1
file	exp	dpwr	30
ACQUISITION		dof	
sfrq	399.783	dm	nnn
tn	H1	dwm	c
at	3.744	daf	200
np	44932	dseq	
sw	6008.6	dres	1.0
fb	3800	homo	n
bs	8	DEC2	
tpwr	54	dfrq2	0
pw	5.1	dm2	
d1	2.000	dpwr2	1
tof	0	dof2	0
nt	64	dm2	n
ct	24	dwm2	c
alock	n	daf2	200
gain	not used	dseq2	
FLAGS		dres2	1.0
il	n	homo2	n
in	n	PROCESSING	
dp	y	lb	0.50
hs	nn	wtfile	
DISPLAY		groc	ft
sp	-0.2	fn	not used
wp	3997.8	math	f
vs	1938		
sc	0	werr	
wc	250	wexp	
hzem	15.99	wbs	
ts	1496.93	wnt	
rfl	2318.5		
rfp	1323.3		
th	20		
ins	1.000		
nm	cdc ph		



9 8 7 6 5 4 3 2 1 ppm

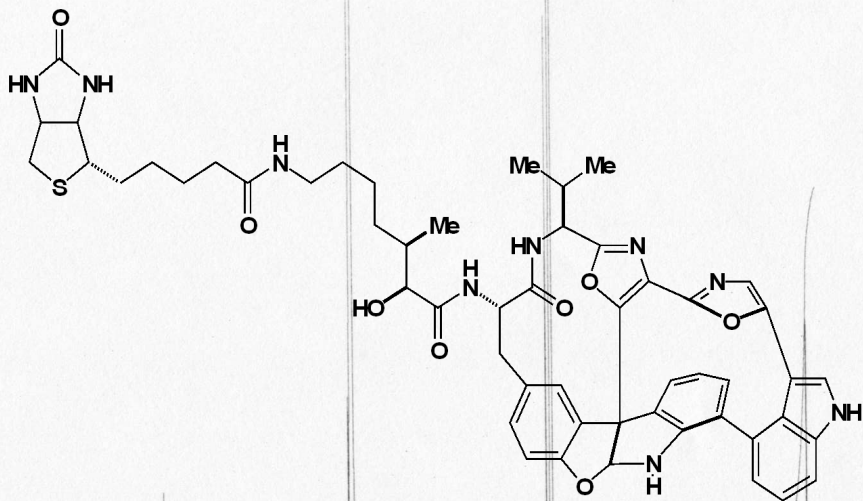
0.38 90.90 0.90 0.98
0.9599 0.99.90 0.89

1.11 1.00 2.29 1.50 1.42 1.15 3.90 3.02 8.85

#279B (ABVII247biotindzrepurified)

exp2 std1h

SAMPLE		DEC. & VT	
date	Dec 6 2003	dfrq	399.783
solvent	cd3od	dn	H1
file	exp	dpwr	30
ACQUISITION		dof	0
sfrq	399.783	dm	nnn
tn	H1	dmm	c
at	3.744	dmf	200
np	44932	dseq	
sw	6000.6	dres	1.0
fb	3000	homo	n
bs	8	DEC2	
tpwr	54	dfrq2	0
pw	5.1	dn2	
d1	2.000	dpwr2	1
tof	0	dof2	0
nt	64	dm2	n
ct	56	dmm2	c
alock	n	dmf2	200
gain	not used	dseq2	
FLAGS		dres2	1.0
il	n	homo2	n
in	n	PROCESSING	
dp	n	lb	0.50
hs	nn	wtfile	
DISPLAY		proc	ft
sp	-995.1	fn	not used
wp	6000.4	math	f
vs	2432		
sc	0	werr	
wc	250	wexp	
hzmm	24.00	wbs	
is	1997.04	wnt	
rfl	2318.5		
rfp	1323.3		
th	20		
ins	1.000		
nm	cdc ph		



12 11 10 9 8 7 6 5 4 3 2 1 -0 -1 ppm

0.08 0.23 7.80 9.90 9.94
0.08 0.10 0.95 8.0 0.86

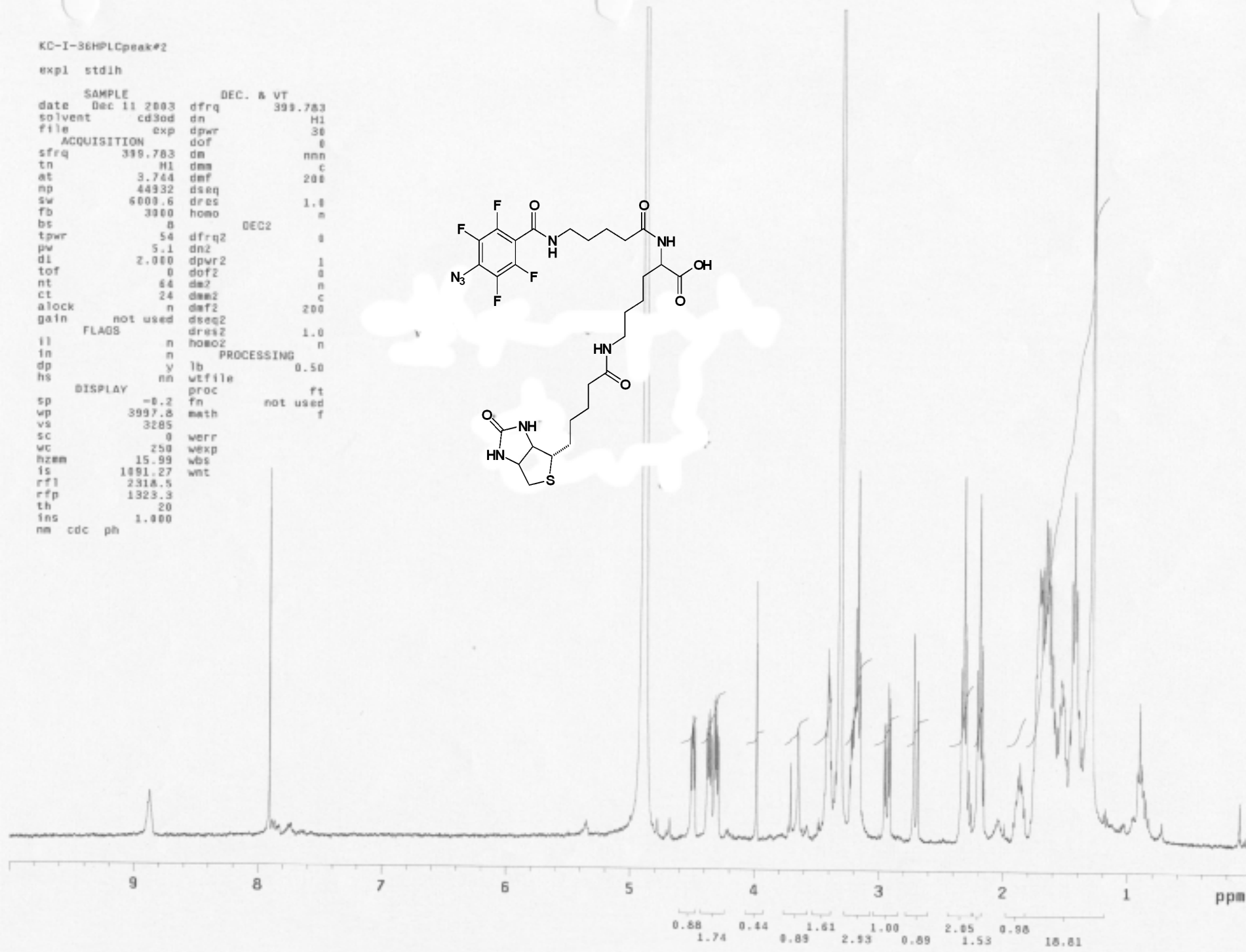
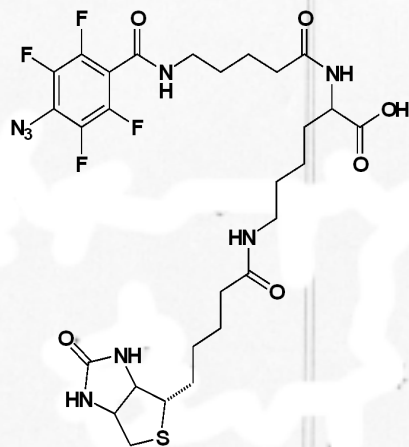
1.370 9.9
1.18 1.00

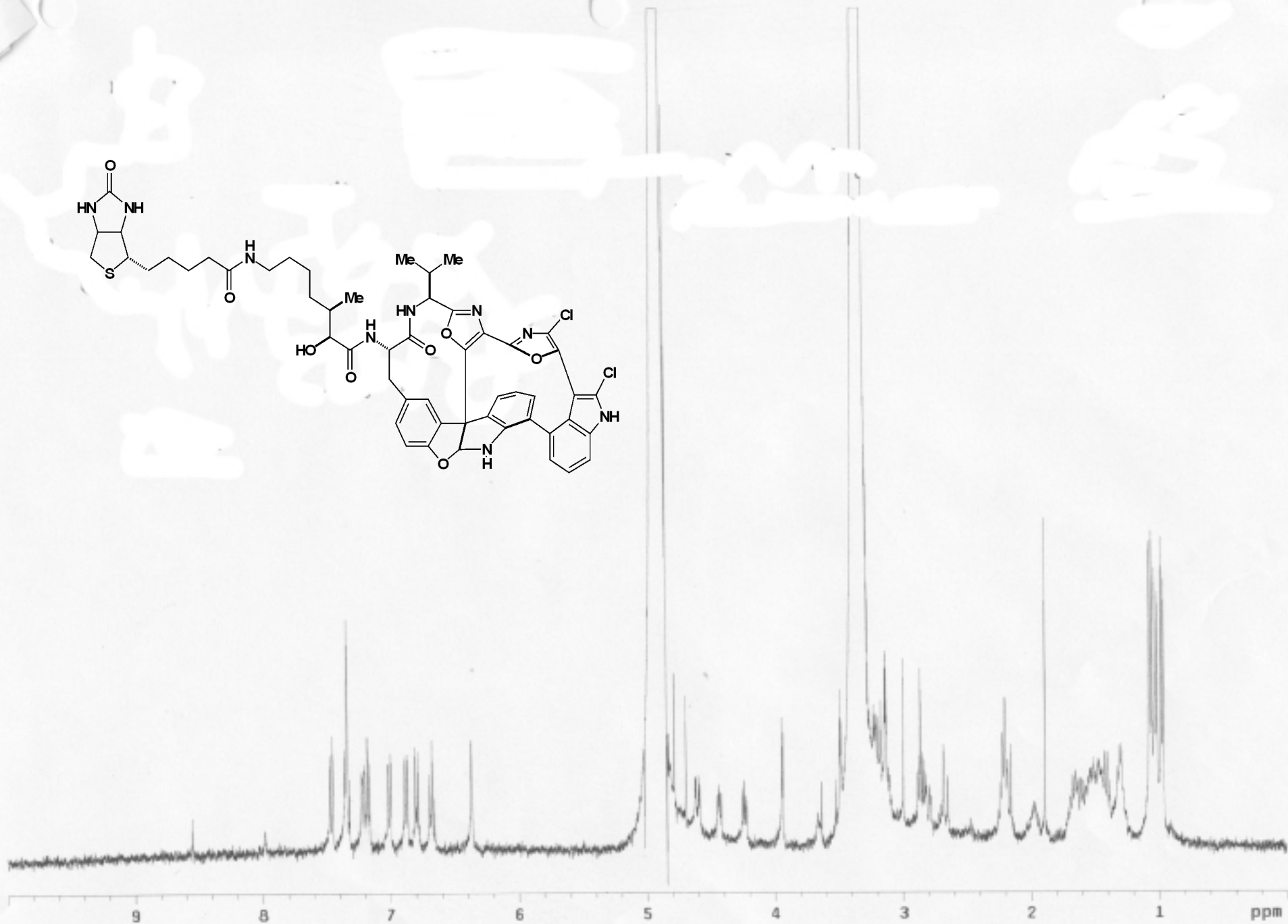
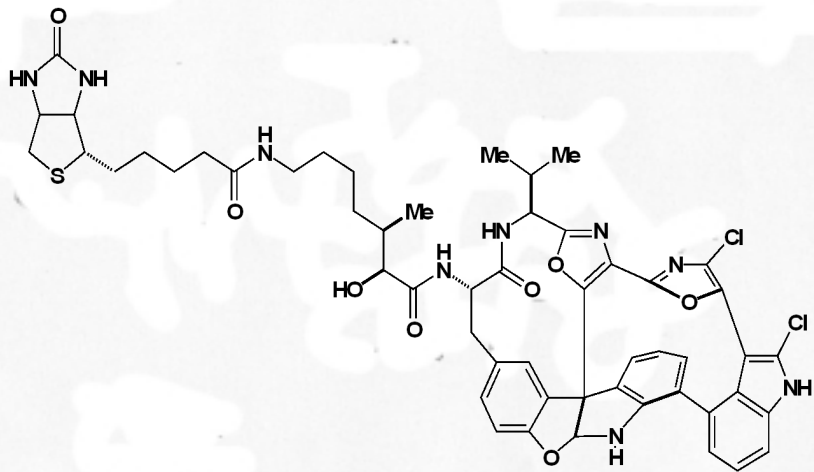
3.56 1.21 1.91 9.92
2.24 3.55 18.09

KC-I-36HPLCpeak#2

expl stdih

SAMPLE		DEC. & VT	
date	Dec 11 2003	dfrq	399.763
solvent	cd3od	dn	H1
file	exp	dpwr	30
ACQUISITION			
sfrq	399.763	dm	nm
tn	H1	dsm	c
at	3.744	daf	200
np	44332	dseq	
sw	6000.6	dres	1.0
fb	3900	homo	m
bs	0	DEC2	
tpwr	54	dfrq2	0
pw	5.1	dn2	
dl	2.000	dpwr2	1
tof	0	dof2	0
nt	64	ds2	n
ct	24	dsm2	c
alock	n	daf2	200
gain	not used	dseq2	
FLAOS		dres2	1.0
ll	n	homo2	n
in	n	PROCESSING	
dp	y	lb	0.50
hs	nn	wtfile	
DISPLAY		proc	ft
sp	-0.2	fn	not used
wp	3997.8	math	f
vs	3285		
sc	0	werr	
wc	250	wexp	
hzem	15.99	wbs	
is	1091.27	wnt	
rfl	2318.5		
rfp	1323.3		
th	20		
ins	1.000		
nm	cdc	ph	

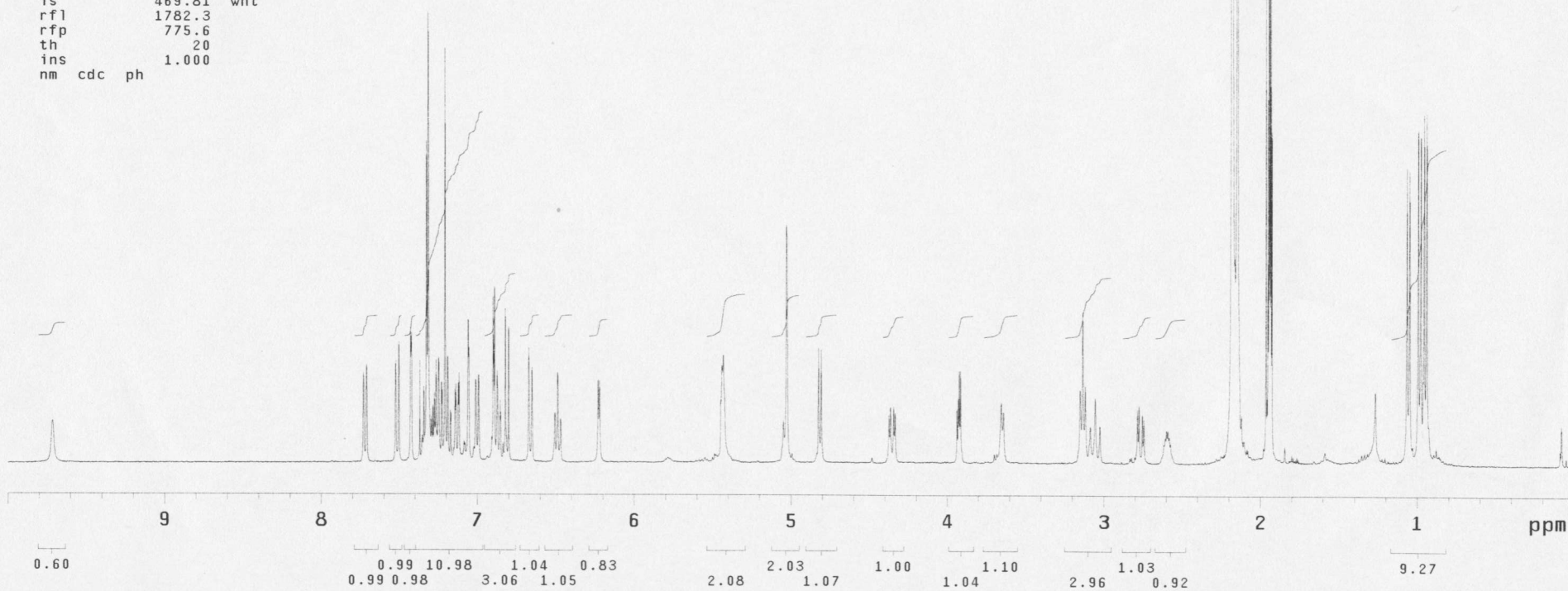
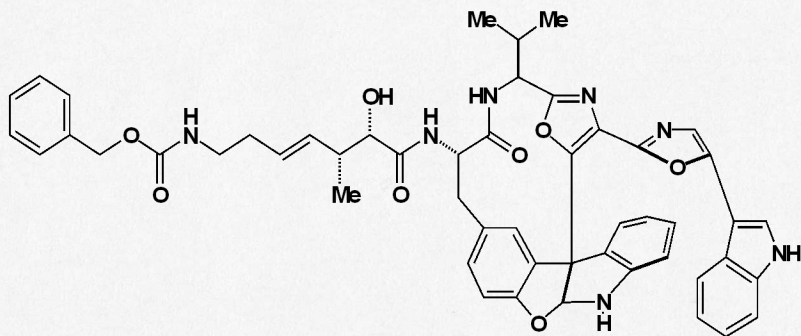




#572 (ABVIII2830D-3 openorendoifieds.c.)

exp1 std1h

SAMPLE		DEC. & VT	
date	Dec 5 2004	dfrq	399.783
solvent	cd3cn	dn	H1
file	exp	dpwr	30
ACQUISITION			
sfrq	399.783	dm	nnn
tn	H1	dmm	c
at	3.744	dmf	200
np	44932	dseq	
sw	6000.6	dres	1.0
fb	3000	homo	n
bs	4	DEC2	
tpwr	54	dfrq2	0
pw	5.1	dn2	
d1	2.000	dpwr2	1
tof	0	dof2	0
nt	64	dm2	n
ct	20	dmm2	c
alock	n	dmf2	200
gain	not used	dseq2	
FLAGS		dres2	1.0
il	n	homo2	n
in	n	PROCESSING	
dp	y	lb	0.50
hs	nn	wtfile	
DISPLAY			
sp	-0.1	proc	ft
wp	3997.8	fn	not used
vs	1216	math	f
sc	0	werr	
wc	250	wexp	
hzmm	15.99	wbs	
is	469.81	wnt	
rfl	1782.3		
rfp	775.6		
th	20		
ins	1.000		
nm	cdc ph		

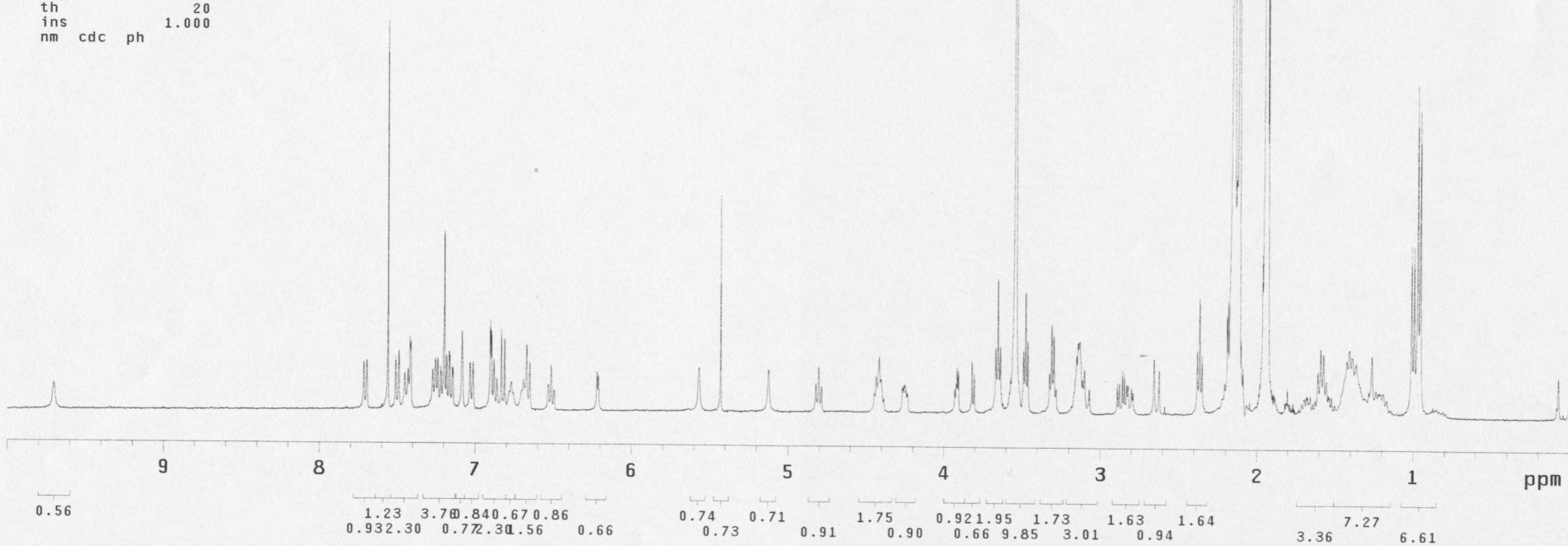
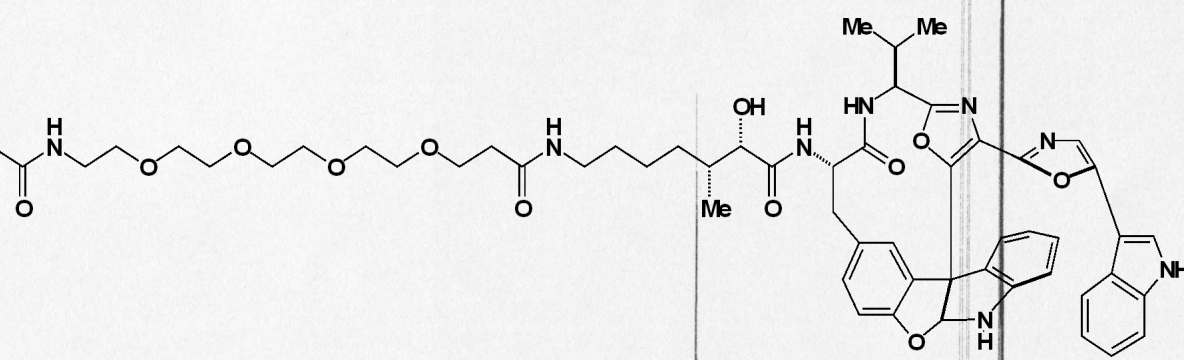
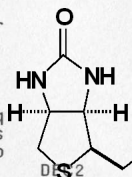


573

#583 (ABVIII284 openbiotincompound70%CH3
CN/CHC13)

exp1 std1h

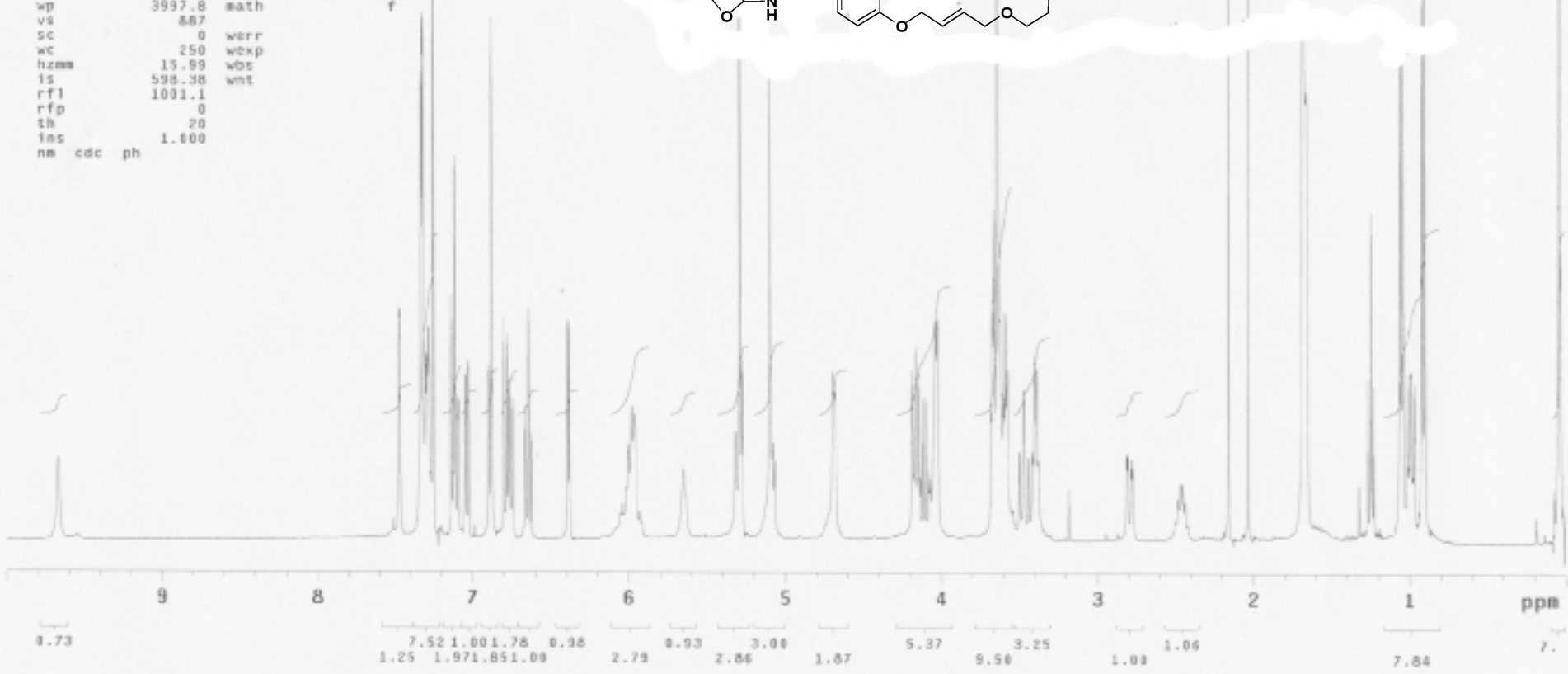
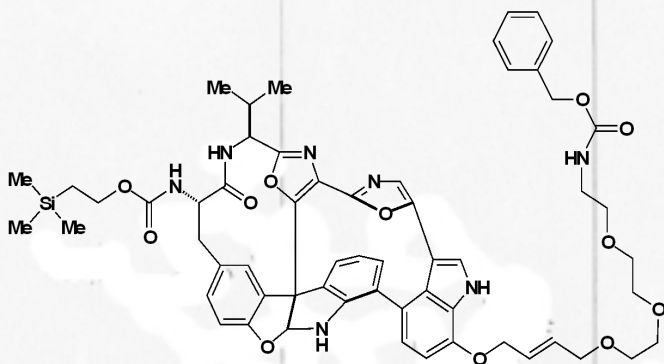
SAMPLE		DEC. & VT	
date	Dec 7 2004	dfrq	399.783
solvent	cd3cn	dn	H1
file	exp	dpwr	30
ACQUISITION			
sfrq	399.783	dm	nnn
tn	H1	dmm	c
at	3.744	dmf	200
np	44932	dseq	1.0
sw	6000.6	dres	1.0
fb	3000	homo	1.0
bs	4	dfrq2	0
tpwr	54	dn2	1
pw	5.1	dpwr2	0
d1	2.000	dof2	0
tof	0	dm2	n
nt	64	dmm2	c
ct	32	dmf2	200
alock	n	dseq2	1.0
gain	not used	dres2	1.0
PROCESSING			
il	n	homo2	n
in	n	lb	0.50
dp	y	wtfile	
hs	nn	proc	ft
DISPLAY			
sp	-0.1	fn	not used
wp	3997.8	math	f
vs	1609		
sc	0	werr	
wc	250	wexp	
hzmm	15.99	wbs	
is	806.82	wnt	
rfl	1782.5		
rfp	775.6		
th	20		
ins	1.000		
nm	cdc ph		



#3586 (ABVIII89PTLCband#2des)

exp1 stdih

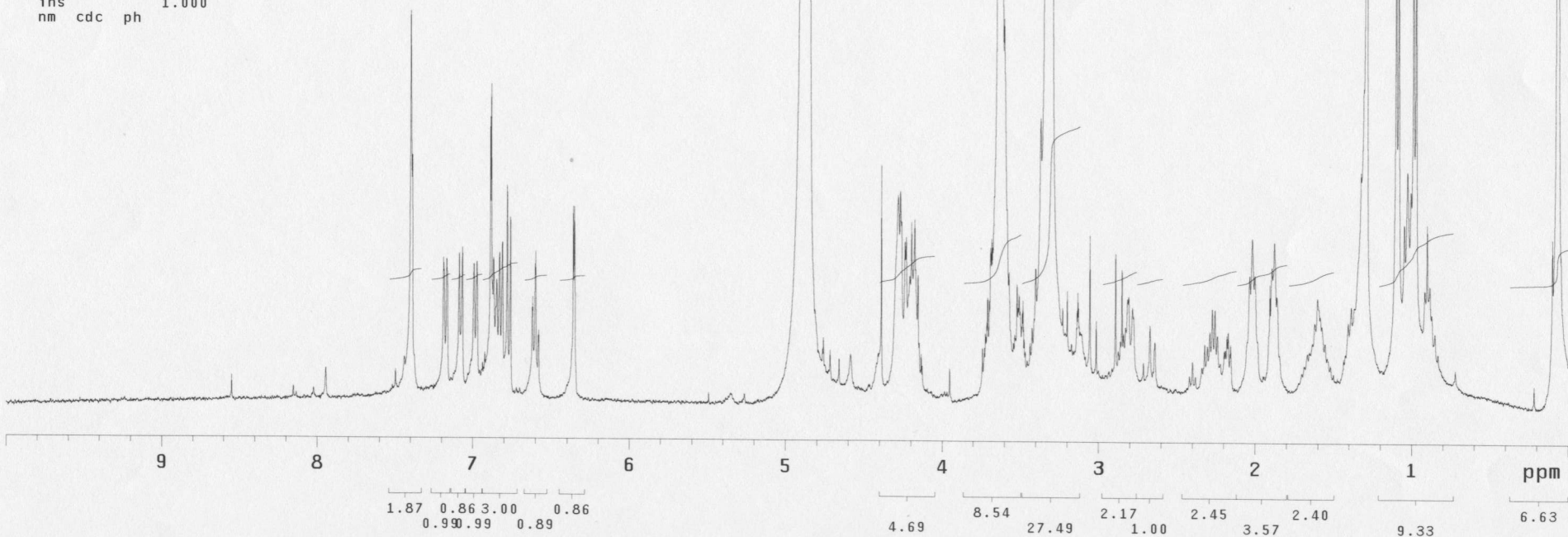
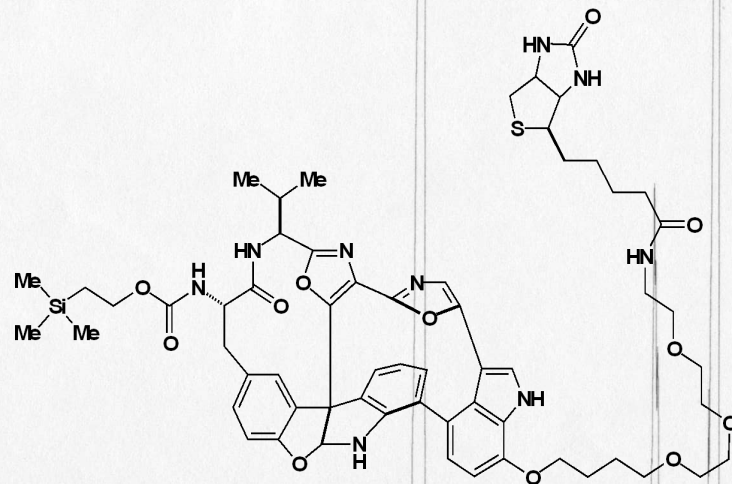
SAMPLE		DEC. & VT	
date	Mar 28 2004	dfrq	399.781
solvent	CDC13	dn	H1
file	exp	dpwr	30
ACQUISITION			
sfrq	399.781	dm	ann
tn	H1	dsm	c
at	3.744	daf	200
np	44932	dseq	
sw	6000.6	dres	1.0
fb	3880	homo	n
bs	8	DEC2	
tpwr	54	dfrq2	0
pw	5.1	dn2	
d1	2.480	dpwr2	1
tof	0	dof2	0
nt	64	ds2	n
ct	16	dsm2	c
alock	n	daf2	200
gain	not used	dseq2	
il	n	dres2	1.0
in	n	homo2	n
dp	y	PROCESSING	8.50
hs	nn	lb	
DISPLAY			
sp	-1.1	wtfile	ft
wp	3997.8	proc	not used
vs	887	math	f
sc	0	werr	
wc	250	wexp	
hzmm	15.99	wbs	
is	598.38	wnt	
rfl	1001.1		
rfp	0		
th	20		
ies	1.600		
nm	cdc	ph	



#363 (ABVIII90biotinylationrxnHPLC)

exp1 std1h

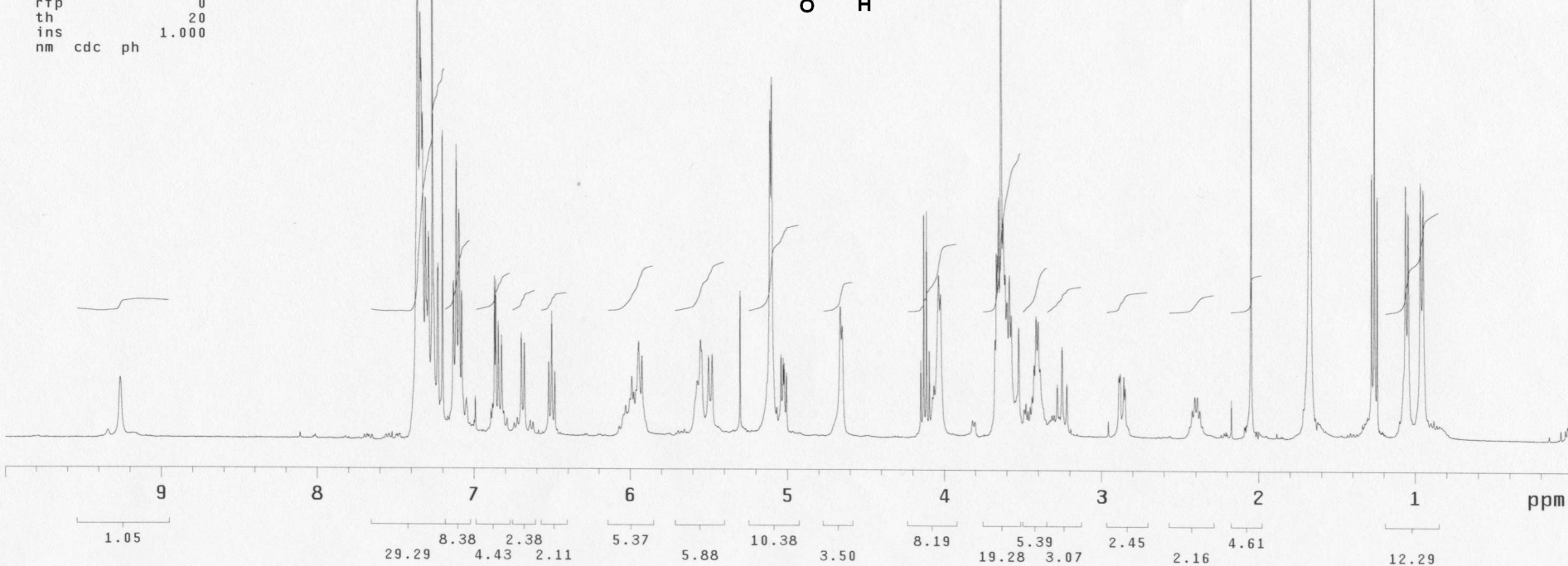
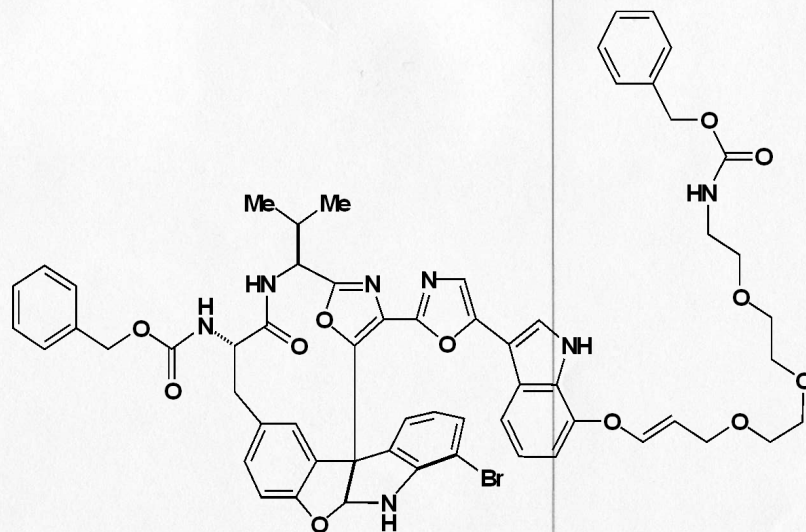
SAMPLE		DEC. & VT	
date	Mar 25 2004	dfrq	399.783
solvent	cd3od	dn	H1
file	exp	dpwr	30
ACQUISITION			
sfrq	399.783	dm	nnn
tn	H1	dmm	c
at	3.744	dmf	200
np	44932	dseq	
sw	6000.6	dres	1.0
fb	3000	homo	n
bs	8		
		DEC2	
tpwr	54	dfrq2	0
pw	5.1	dn2	
d1	2.000	dpwr2	1
tof	0	dof2	0
nt	64	dm2	n
ct	32	dmm2	c
alock	n	dmf2	200
gain	not used	dseq2	
FLAGS			
il	n	dres2	1.0
in	n	homo2	n
dp	y	PROCESSING	
hs	nn	lb	0.50
DISPLAY			
sp	-0.2	wtfile	
wp	3997.8	proc	ft
vs	4913	fn	not used
sc	0	math	f
wc	250	werr	
hzmm	15.99	wexp	
is	260.78	wbs	
rfl	2318.5	wnt	
rfp	1323.3		
th	20		
ins	1.000		
nm	cdc ph		



#359B (ABVIII91PTLC#2des)

exp1 std1h

SAMPLE		DEC. & VT	
date	Mar 20 2004	dfrq	399.781
solvent	CDC13	dn	H1
file	exp	dpwr	30
ACQUISITION			
sfrq	399.781	dm	nnn
tn	H1	dmm	c
at	3.744	dmf	200
np	44932	dseq	
sw	6000.6	dres	1.0
fb	3000	homo	n
bs	8	DEC2	
tpwr	54	dfrq2	0
pw	5.1	dn2	
d1	2.000	dpwr2	1
tof	0	dof2	0
nt	64	dm2	n
ct	24	dmm2	c
alock	n	dmf2	200
gain	not used	dseq2	
FLAGS			
il	n	homo2	1.0
in	n	PROCESSING	
dp	y	lb	0.50
hs	nn	wtfile	
DISPLAY			
sp	-0.0	fn	not used
wp	3997.8	math	f
vs	248		
sc	0	werr	
wc	250	wexp	
hzmm	15.99	wbs	
is	351.87	wnt	
rfl	996.2		
rfp	0		
th	20		
ins	1.000		
nm	cdc ph		

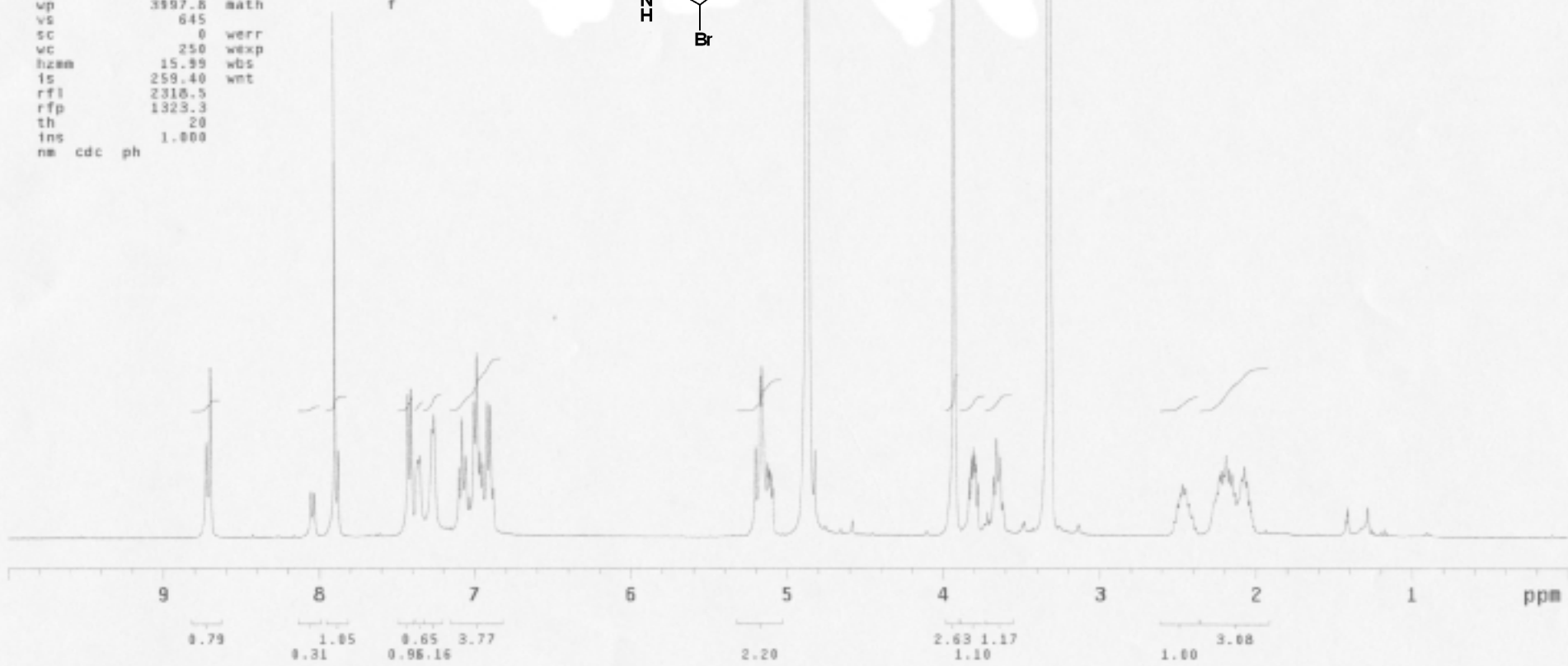
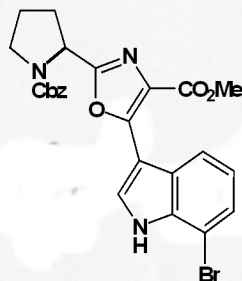


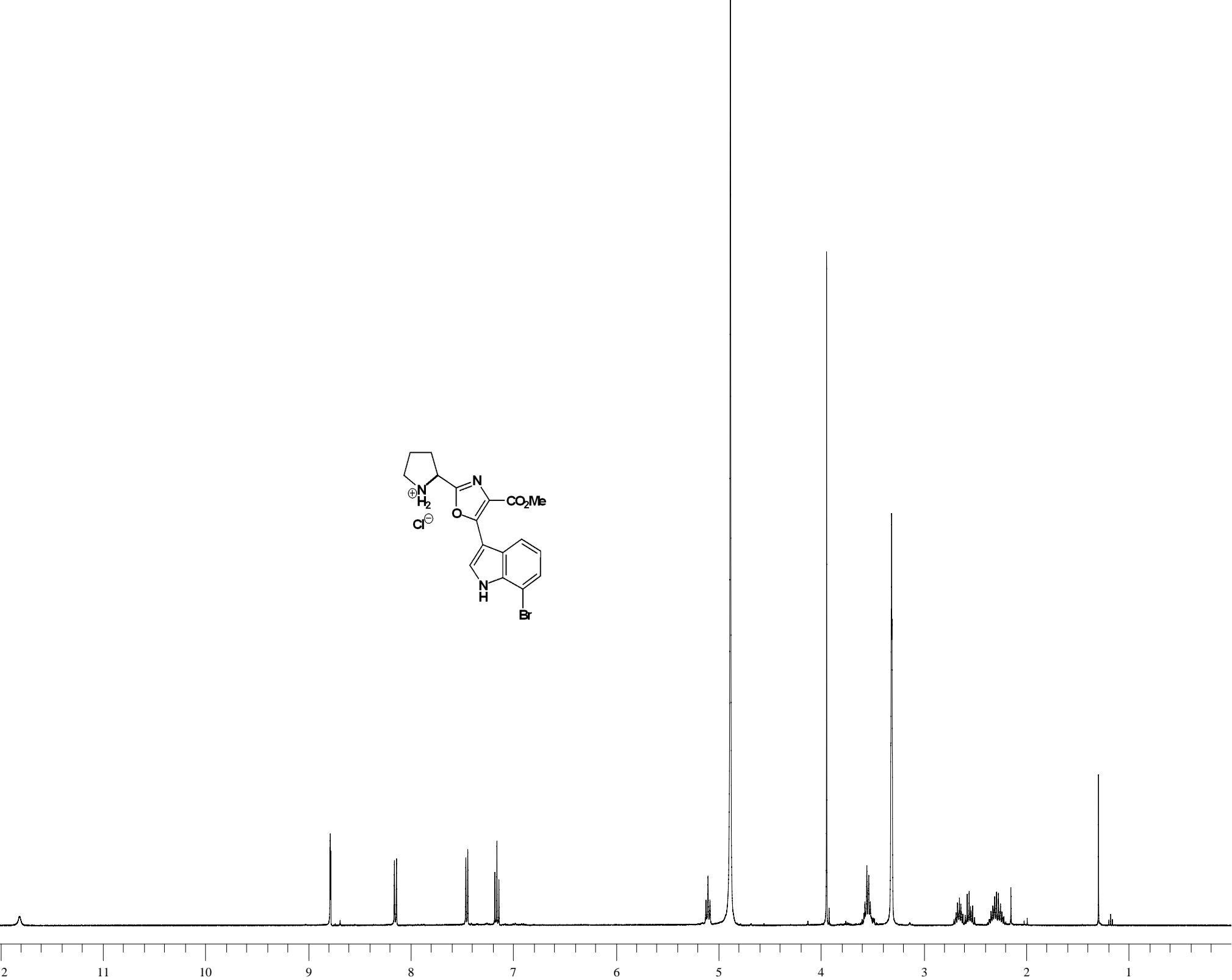
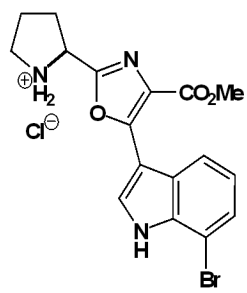
414D

#414 (ABVIII125purified)

expl stdlh

SAMPLE		DEC. & VT	
date	Apr 19 2004	dfrq	399.783
solvent	cd3od	dn	H1
file	exp	dpwr	38
ACQUISITION			
sfrq	399.783	dm	nnn
tn	H1	dsm	c
at	3.744	dmf	200
np	44932	dseq	
sw	6088.6	dres	1.0
fb	3000	homo	n
bs	8	DEC2	
tpwr	54	dfrq2	0
pw	5.1	dn2	
d1	2.000	dpwr2	1
tof	0	dof2	0
nt	64	dm2	n
ct	64	dsm2	c
alock	n	dmf2	200
gain	not used	dseq2	
FLAGS			
il	n	homo2	n
in	n	PROCESSING	
dp	y	lb	0.50
hs	nn	wtfile	
DISPLAY			
sp	-0.2	proc	ft
up	3997.8	fn	not used
vs	645	math	f
sc	0	werr	
wc	250	wexp	
hzam	15.99	wbs	
is	259.40	wmt	
rfl	2318.5		
rfp	1323.3		
th	20		
ins	1.000		
nm	cdc	ph	

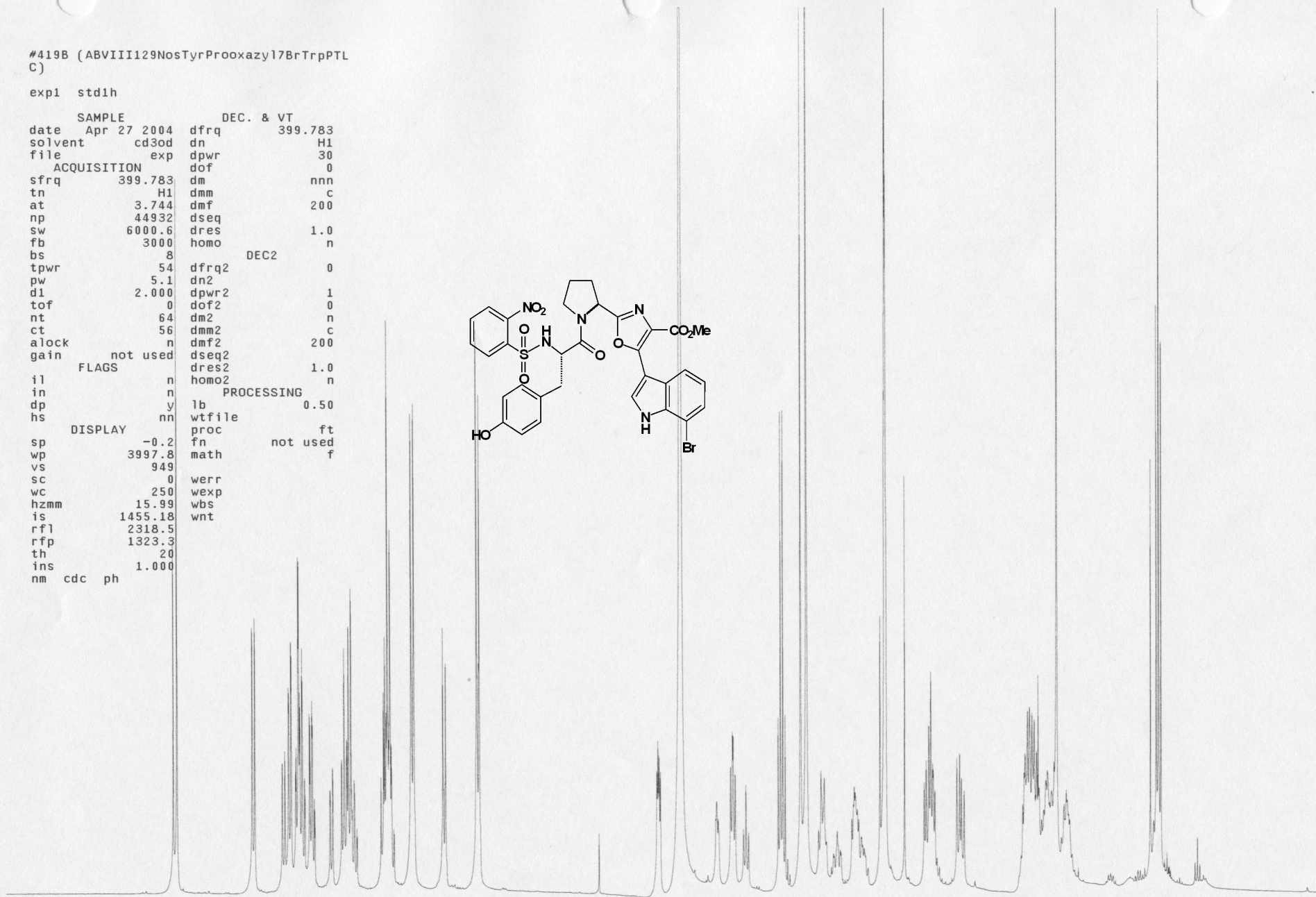
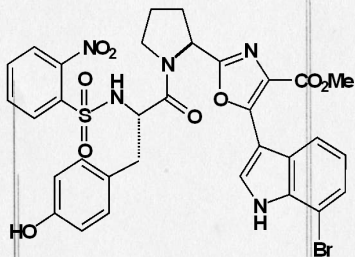




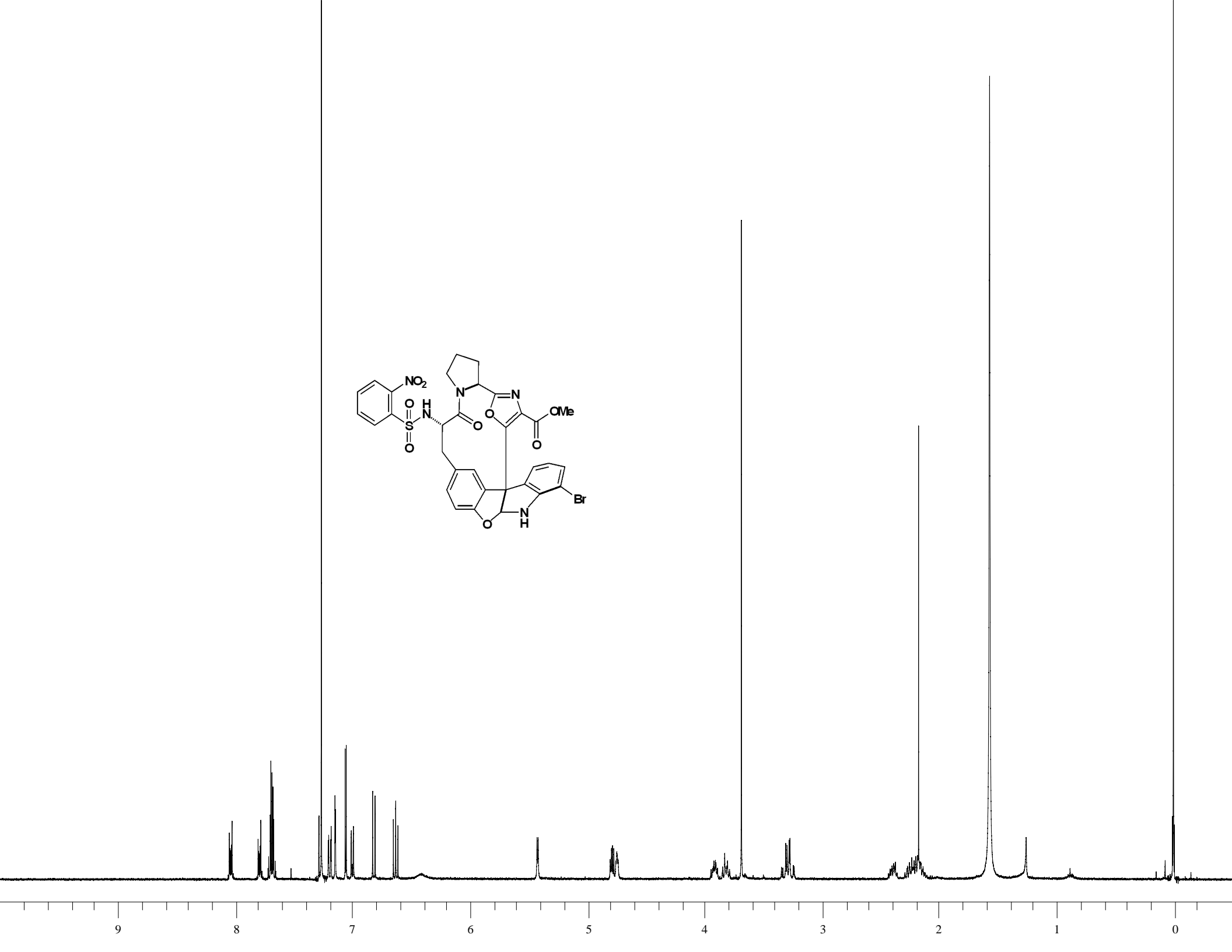
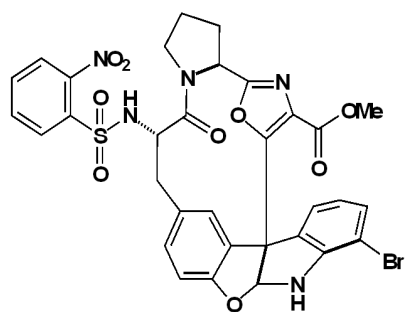
#419B (ABVIII129NosTyrProoxazyl7BrTrpPTL
C)

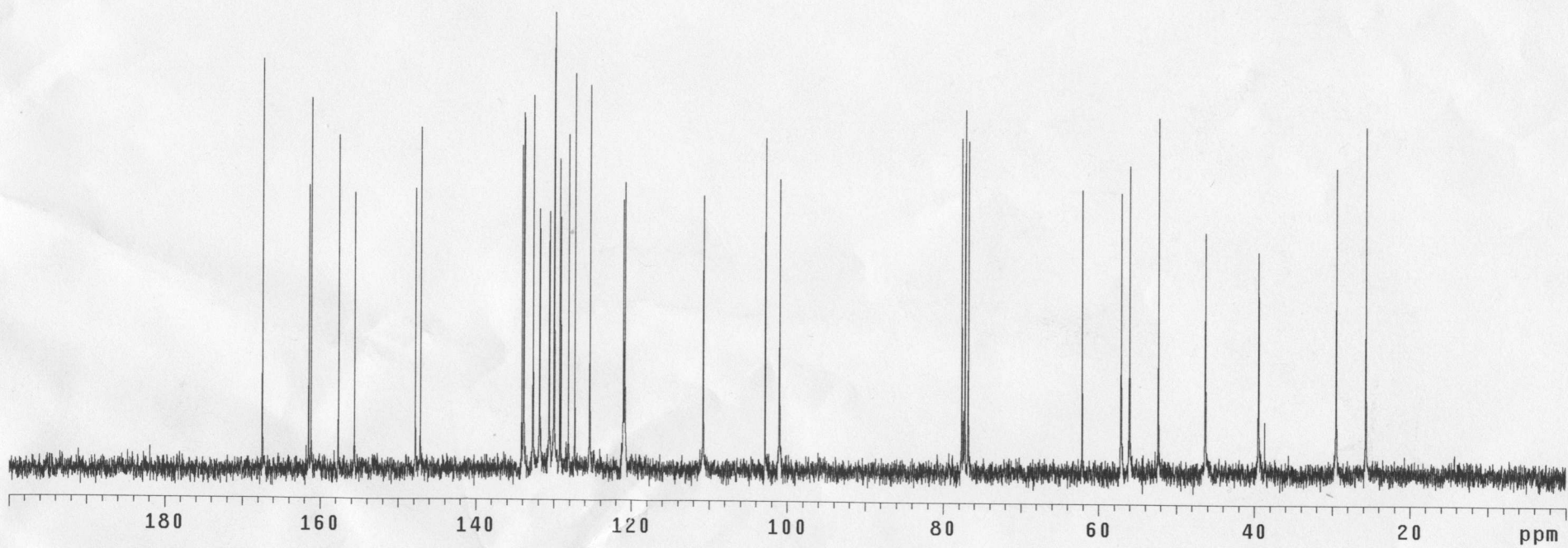
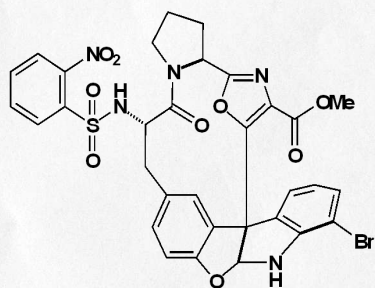
expl std1h

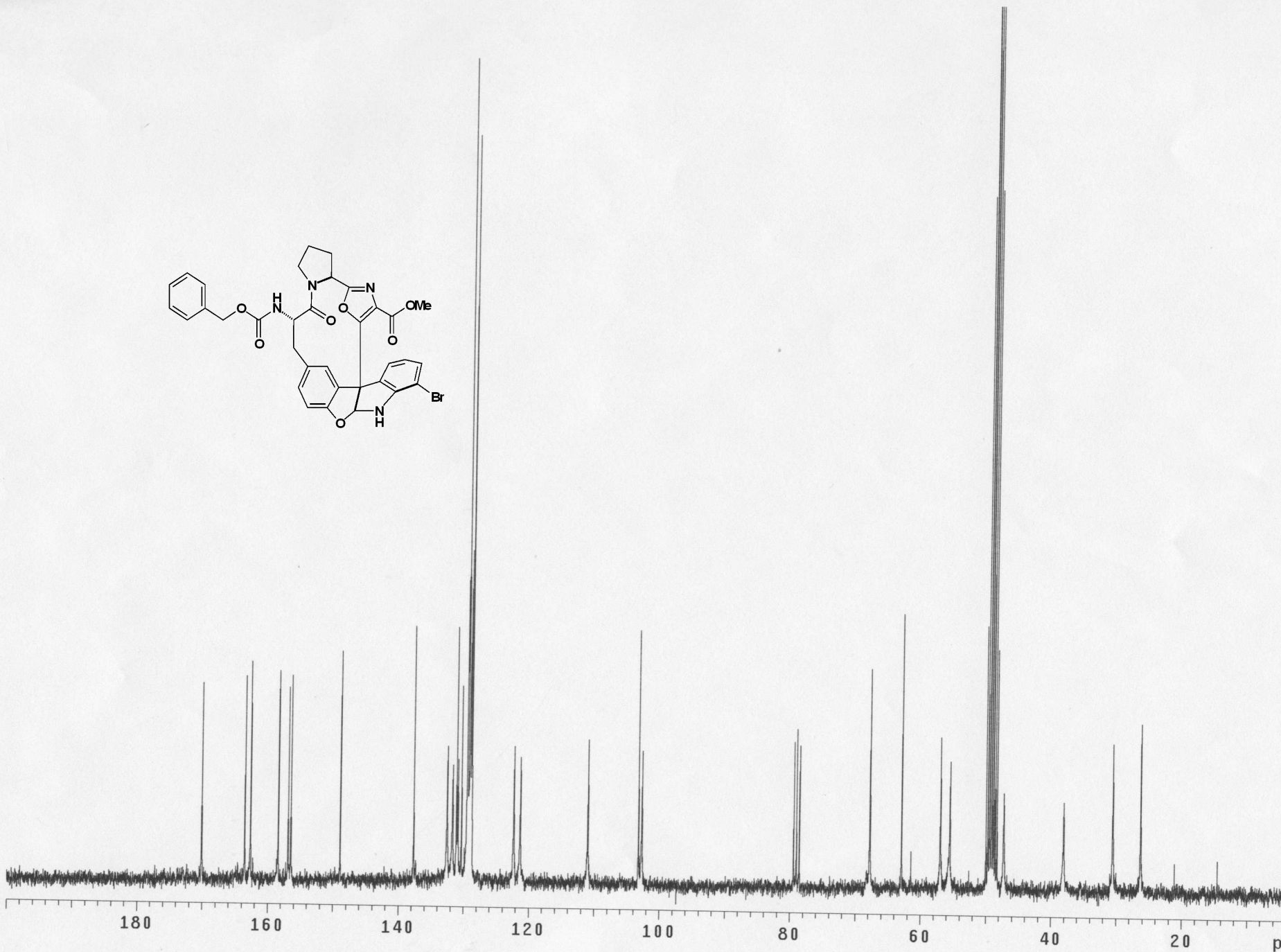
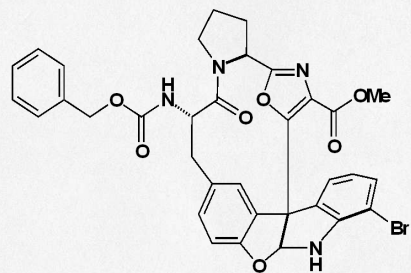
SAMPLE		DEC. & VT	
date	Apr 27 2004	dfrq	399.783
solvent	cd3od	dn	H1
file	exp	dpwr	30
ACQUISITION			
sfrq	399.783	dm	nnn
tn	H1	dmm	c
at	3.744	dmf	200
np	44932	dseq	
sw	6000.6	dres	1.0
fb	3000	homo	n
bs	8		
tpwr	54	DEC2	
pw	5.1	dfrq2	0
d1	2.000	dn2	
tof	0	dpwr2	1
nt	64	do2	0
ct	56	dm2	n
alock	n	dmm2	c
gain	n	dmf2	200
FLAGS	not used	dseq2	
il	n	dres2	1.0
in	n	homo2	n
dp	y		
hs	nn	PROCESSING	
		lb	0.50
DISPLAY			
sp	-0.2	wtfile	
wp	3997.8	proc	ft
vs	949	fn	not used
sc	0	math	f
wc	250	werr	
hzmm	15.99	wexp	
is	1455.18	wbs	
rfl	2318.5	wnt	
rfp	1323.3		
th	20		
ins	1.000		
nm	cdc ph		



9	8	7	6	5	4	3	2	1	ppm				
1.10	0.80	3.97	2.14	1.86	1.81	0.67	0.66	0.48	2.56	0.59	1.91	1.06	8.17
		0.43	2.63	0.88			1.22	1.12	1.49				



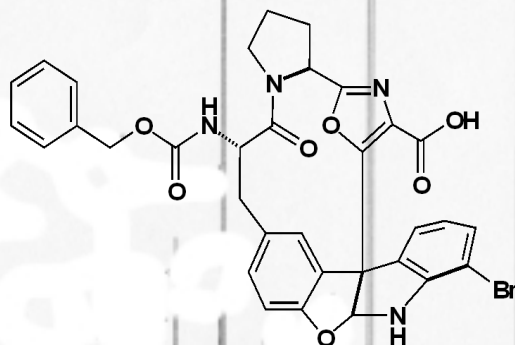




#467 (ABVIII199Proc00Hcrude)

exp1 std1h

SAMPLE		DEC. & VT	
date	Jun 25 2004	dfrq	300.078
solvent	CDC13	dn	H1
file	exp	dpwr	30
ACQUISITION			
sfrq	300.078	dof	0
tn	H1	dm	inn
at	1.938	dsm	c
np	20000	def	200
PROCESSING			
sw	5005.0	wtfile	
fb	not used	proc	ft
bs	16	fn	not used
tpwr	58		
pw	7.2	werr	
d1	2.000	wexp	
tof	0	wbs	
nt	16	wnt	
ct	16		
alock	n		
gain	not used		
FLAGS			
l1	n		
in	n		
dp	y		
DISPLAY			
sp	-121.8		
wp	3000.6		
vs	844		
sc	0		
wc	250		
h2nm	12.00		
lc	4796.75		
rf1	3115.5		
rfp	893.3		
th	20		
ins	1.000		
nm	cdc ph		



3.00 1.39 1.26
1.45 0.77

0.80
1.58

1.00
2.81

2.35 1.93

1.65 1.79

9

8

7

6

5

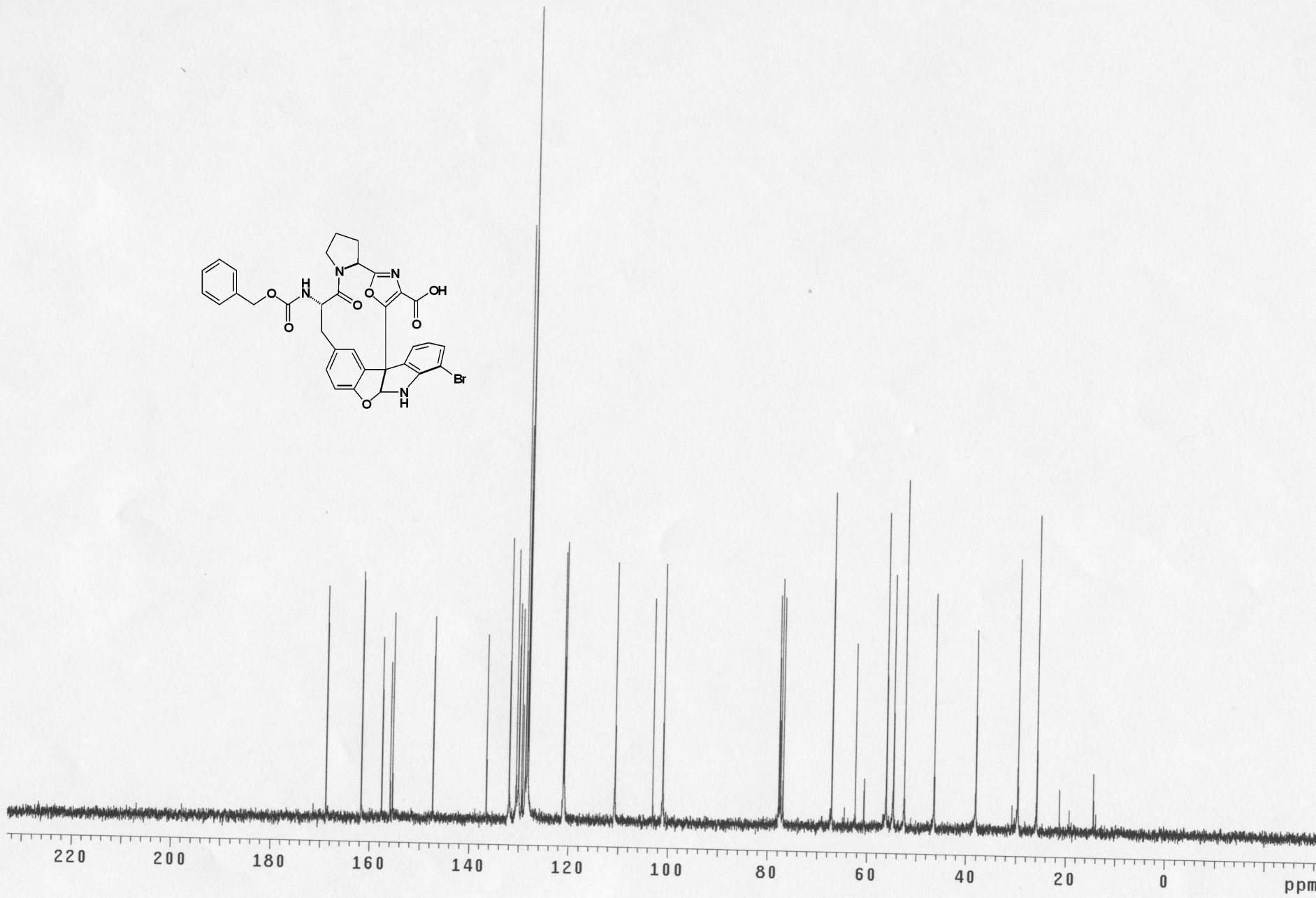
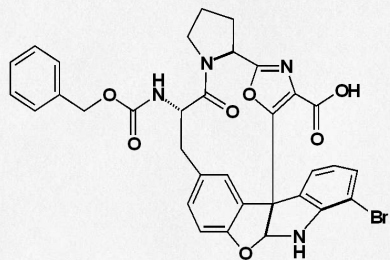
4

3

2

1

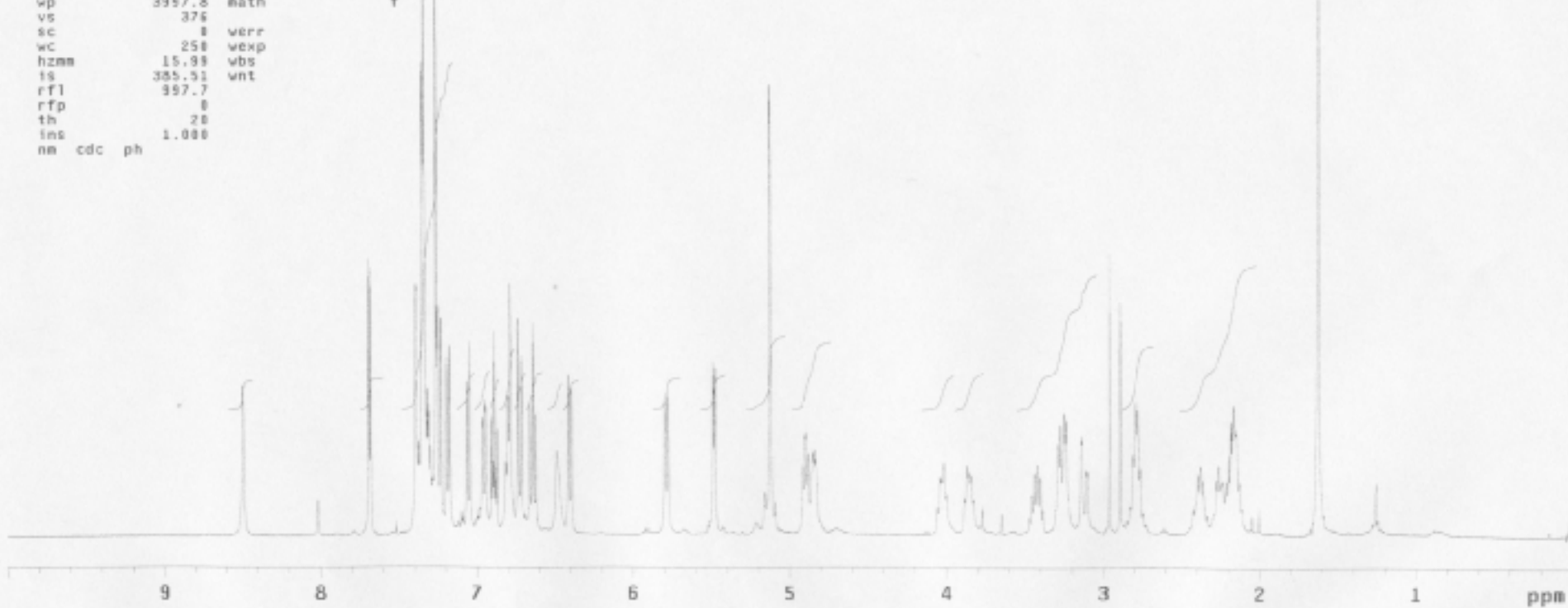
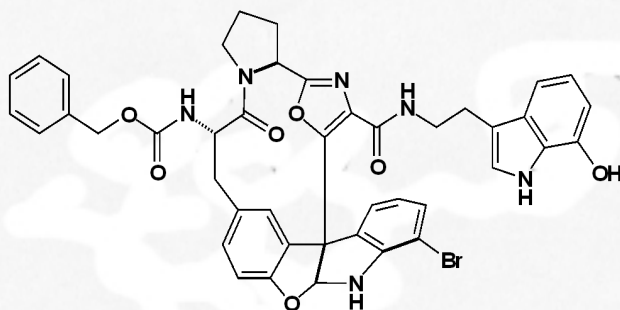
ppm



#470 (ABVIII2#3desspot)

expl stdlh

SAMPLE		DEC. & YT	
date	Jun 26 2004	dfrq	399.781
solvent	CDCl3	dn	H1
file	exp	dpwr	30
ACQUISITION			
sfrq	399.781	dm	nmn
tn	H1	dmm	c
at	3.744	dof	200
np	44932	dseq	
sw	6000.6	dres	1.0
fb	3800	homo	n
bs	4	DEC2	
tpwr	54	dfrq2	0
pw	5.1	dn2	
d1	2.000	dpwr2	1
tof	0	dof2	0
nt	16	dm2	n
ct	16	dmm2	c
alock	n	dof2	200
gain	not used	dseq2	
FLAOS		dres2	1.0
l1	n	homo2	n
in	m	PROCESSING	
dp	y	lb	0.50
hs	nm	wtfile	
DISPLAY		proc	ft
sp	-0.1	fn	not used
wp	3957.8	math	f
vs	376		
sc	0	werr	
wc	250	wexp	
hzmm	15.99	wbs	
ts	385.91	wnt	
rf1	997.7		
rfp	0		
th	20		
ins	1.000		
nm	cdc ph		



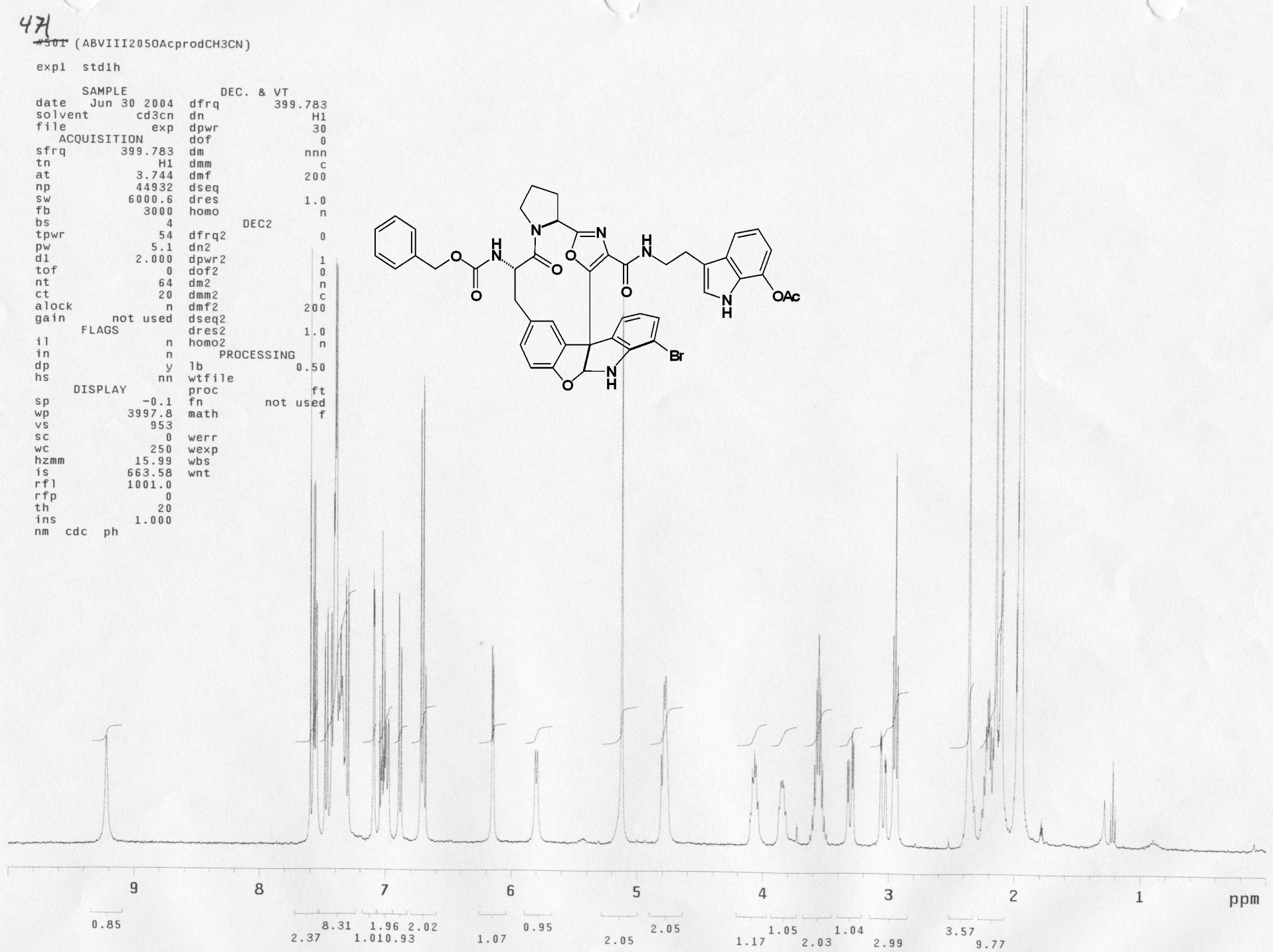
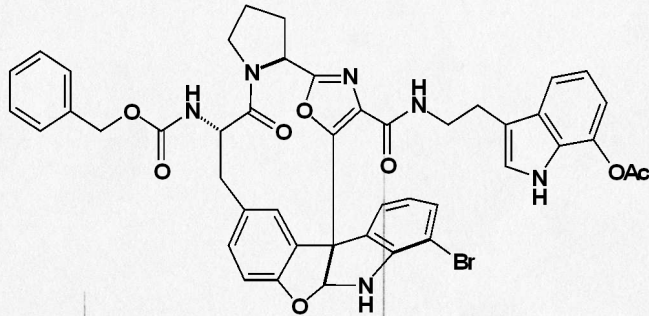
0.83 10.16 1.13 77.090.84 0.90 1.00.00.970.77 0.94 1.92 2.14 1.98 1.10 1.00 3.96 1.88 4.25

47

4501 (ABVII12050AcprodCH3CN)

expl std1h

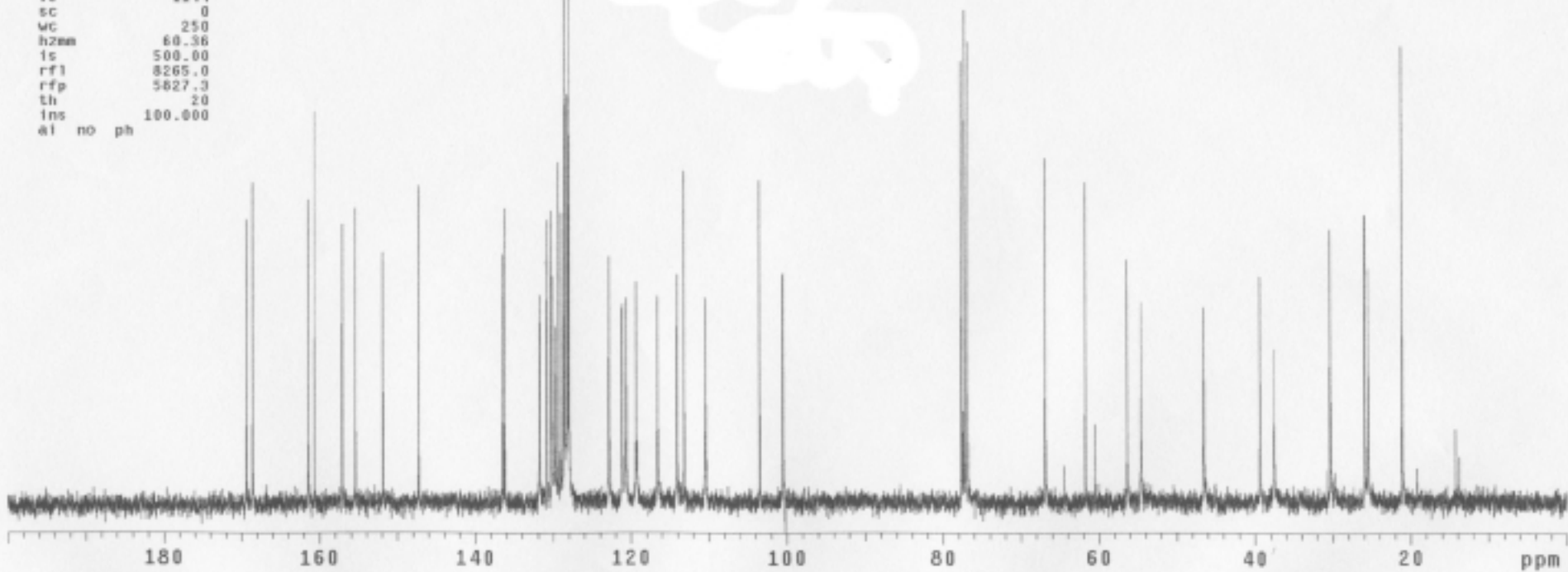
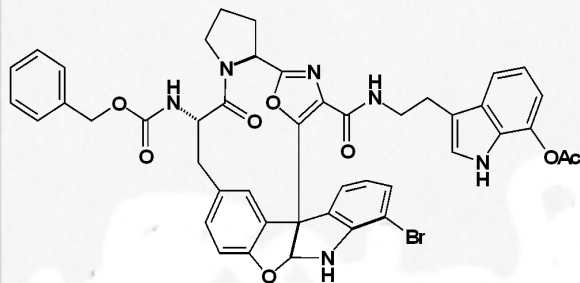
SAMPLE		DEC. & VT	
date	Jun 30 2004	dfrq	399.783
solvent	cd3cn	dn	H1
file	exp	dpwr	30
ACQUISITION			
sfrq	399.783	dm	nnn
tn	H1	dmm	c
at	3.744	dmf	200
np	44932	dseq	
sw	6000.6	dres	1.0
fb	3000	homo	n
bs	4	DEC2	
tpwr	54	dfrq2	0
pw	5.1	dn2	
d1	2.000	dpwr2	1
tof	0	dof2	0
nt	64	dm2	n
ct	20	dmm2	c
alock	n	dmf2	200
gain	not used	dseq2	
FLAGS			
il	n	dres2	1.0
in	n	homo2	n
dp	y	PROCESSING	
hs	nn	lb	0.50
DISPLAY			
sp	-0.1	wtfile	
wp	3997.8	proc	ft
vs	953	fn	not used
sc	0	math	f
wc	250	werr	
hzmm	15.99	wexp	
is	663.58	wbs	
rfl	1001.0	wnt	
rfp	0		
th	20		
ins	1.000		
nm	cdc ph		

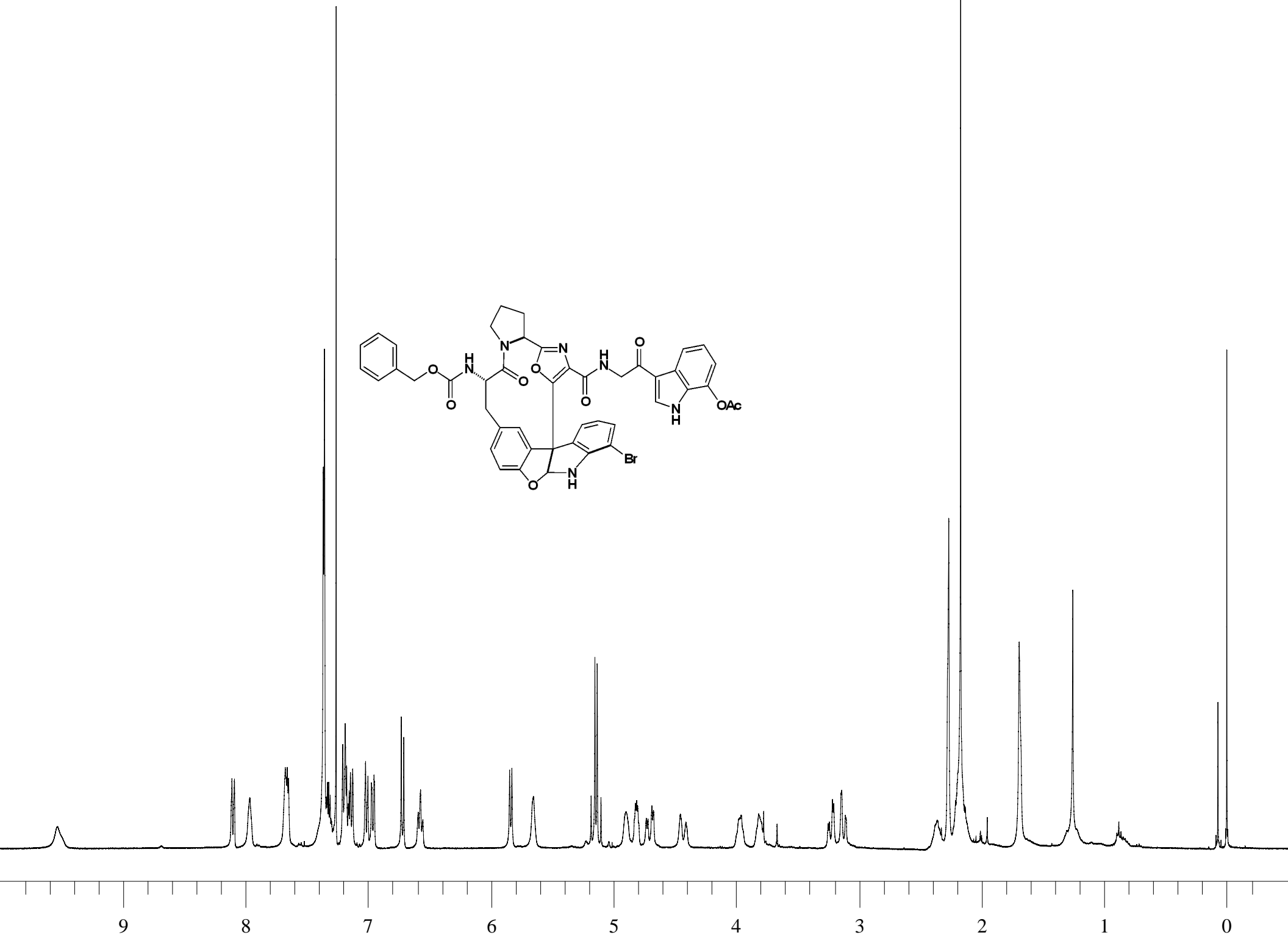
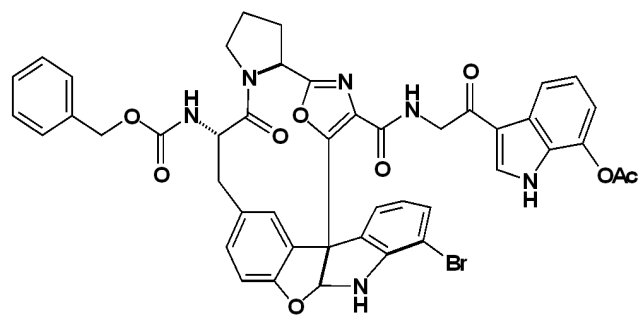


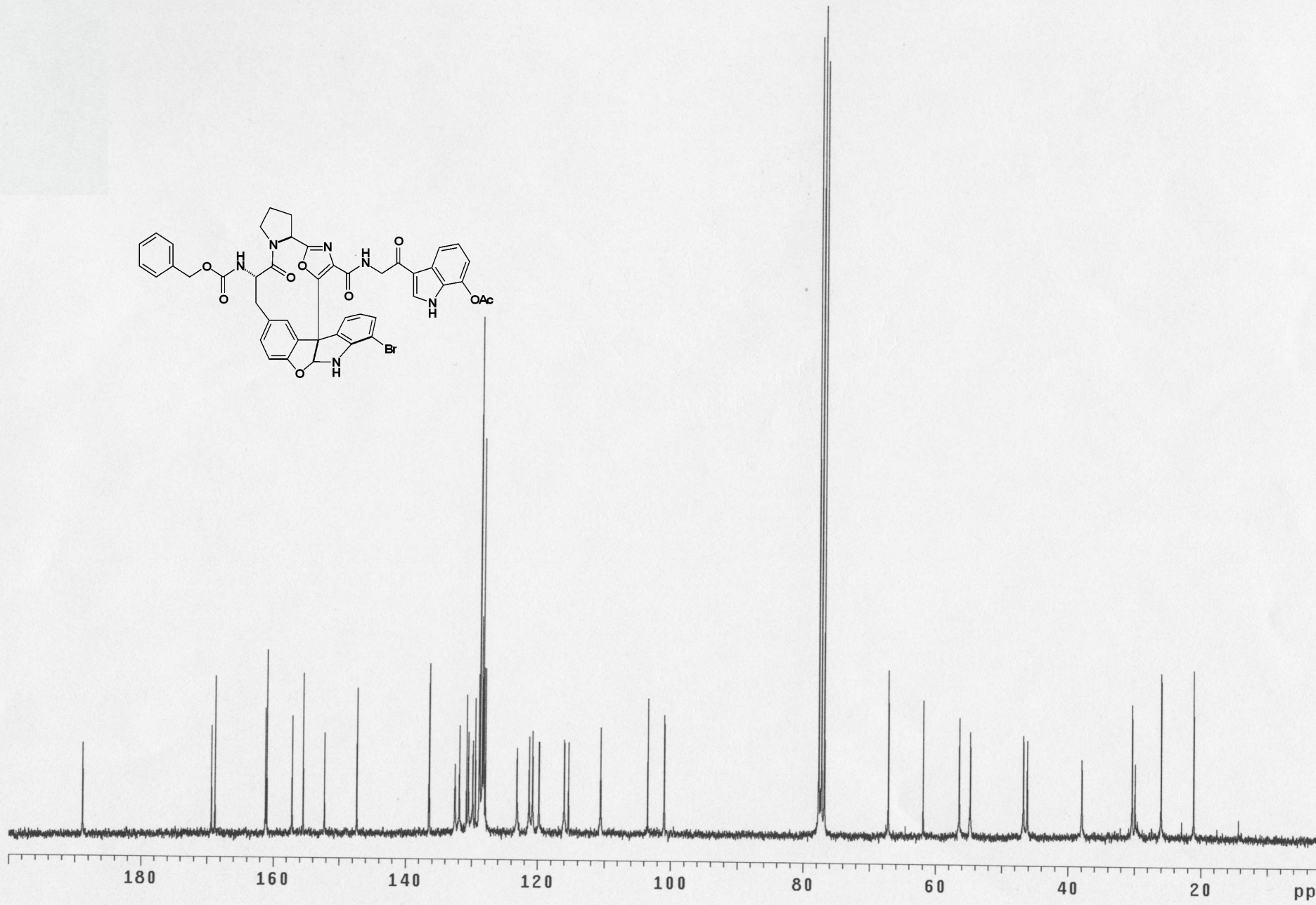
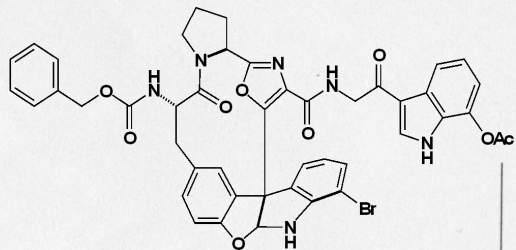
140-05587E

expl std13c

SAMPLE		DEC. & VT	
date	Jun 28 2004	dfreq	300.078
solvent	CDC13	dn	H1
file	exp	dpwr	37
ACQUISITION		dof	0
sfrq	75.462	ds	myy
tn	C13	dsm	w
at	1.000	dmf	10400
np	40000	PROCESSING	
sw	20000.0	lb	1.00
fb	not used	wfile	
bs	8	proc	ft
tpwr	58	fn	not used
pw	6.0		
d1	0	werr	
d2	1.000	wexp	
tof	0	wbs	
nt	10000	wnt	
ct	424		
elock	n		
gain	30		
FLAGS			
il	n		
in	n		
dp	y		
DISPLAY			
sp	-0.5		
wp	15090.8		
vs	1144		
sc	0		
wc	250		
hzmm	60.36		
lc	500.00		
rf1	8265.0		
rfp	5827.3		
th	20		
ins	100.000		
al	no	ph	



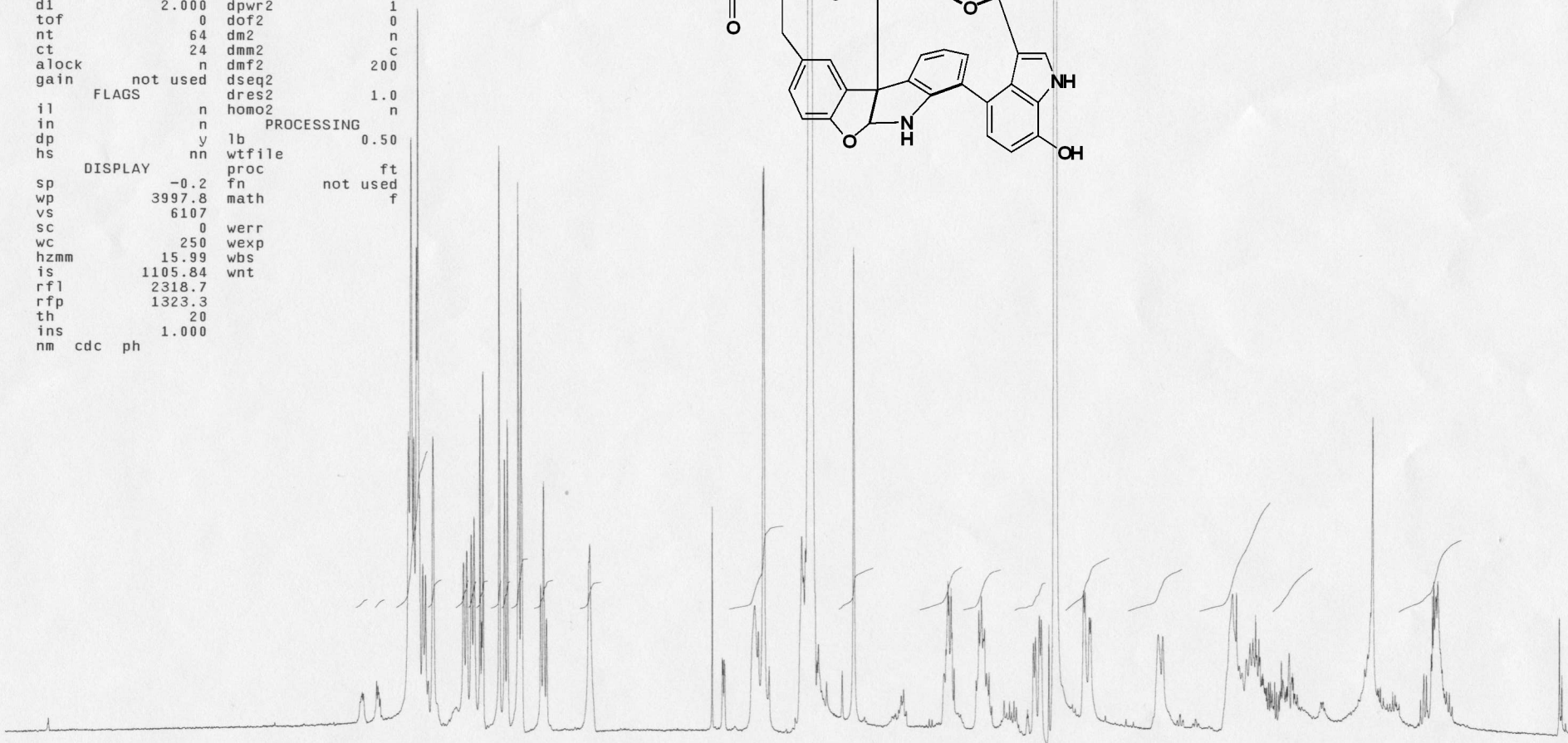
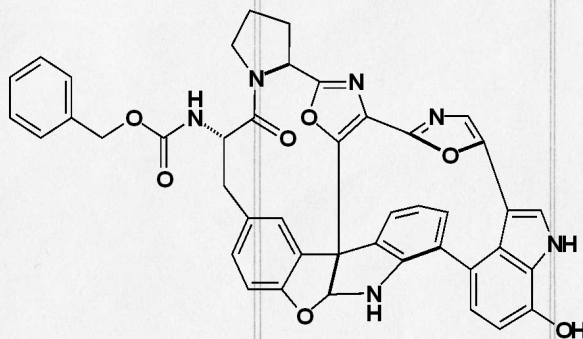




#496C (ABVII237photochemdes?PTLC)

exp1 std1h

SAMPLE		DEC. & VT	
date	Aug 6 2004	dfrq	399.783
solvent	cd3od	dn	H1
file	exp	dpwr	30
ACQUISITION		dof	0
sfrq	399.783	dm	nnn
tn	H1	dmm	c
at	3.744	dmf	200
np	44932	dseq	
sw	6000.6	dres	1.0
fb	3000	homo	n
bs	8	DEC2	
tpwr	54	dfrq2	0
pw	5.1	dn2	
d1	2.000	dpwr2	1
tof	0	dof2	0
nt	64	dm2	n
ct	24	dmm2	c
alock	n	dmf2	200
gain	not used	dseq2	
FLAGS		dres2	1.0
il	n	homo2	n
in	n	PROCESSING	
dp	y	lb	0.50
hs	nn	wtfile	
DISPLAY		proc	ft
sp	-0.2	fn	not used
wp	3997.8	math	f
vs	6107		
sc	0	werr	
wc	250	wexp	
hzmm	15.99	wbs	
is	1105.84	wnt	
rfl	2318.7		
rfp	1323.3		
th	20		
ins	1.000		
nm	cdc ph		



9 8 7 6 5 4 3 2 1 ppm

0.31 5.65 1.01 9.96 1.01
0.30 1.010 9.96 9.8 78 0.95

2.99 1.49 1.55 1.46 0.98 1.90 1.51 3.93 1.58 2.61

A colorless plate crystal having approximate dimensions of 0.7 x 0.4 x 0.2 mm was mounted on a glass fiber. X-ray measurement on the selected crystal was performed on an Enraf-Nonius KappaCCD diffractometer at 293 K using MoK α radiation ($\lambda = 0.71069\text{\AA}$) and a graphite monochromator.

Unit Cell dimensions were obtained by a least squares fit to the optimized setting angles of all measured reflections in the full θ range. Intensity data were collected using COLLECT software (nonius, Netherlands) in ϕ and ω range with κ offsets. Data reduction was done using DENZO (Otwinowski, Z and Minor, W. *Methods Enzymol.* 1996, 276). The data were collected at 20°C using ω -2 θ scan to a maximum 2 θ of 41°. Of the 2239 reflections collected 2220 were unique (Rint=0.06). Intensity of equivalent reflections was averaged. Based on systematic absences of: h00: $h = 2n+1$, 0k0: $k = 2n+1$, and 00l: $l=2n+1$, the space group was unambiguously determined to be P2₁2₁2₁. The data were corrected for Lorentz and Polarization effects.

The structure was solved by direct methods using SHELXS-97 (Sheldrick, G. M. SHELXS97: A Program for Crystal Structure Refinement; University of Gottingen, Gottingen, Germany, 1997) and refined by full-matrix least squares refinement using SHELXL-97 (Sheldrick, G. M. SHELXL97: A Program for Crystal Structure Refinement; University of Gottingen, Gottingen, Germany, 1997). The function minimized was $\sum w(|F_o|^2 - |F_c|^2)^2$ and the weight w defined as $w = 1 / [\sigma^2(F_o^2) + (0.1009 * P)^2]$ where $P = (F_o^2 + 2F_c^2) / 3$. All the non-hydrogen atoms were refined anisotropically. The hydrogen atoms were fixed by geometrical considerations.

The final R and RW are 0.0089 and 0.146 respectively, for 2220 reflections. The maximum and minimum peaks on the final Fourier map corresponded to 0.34 and $-0.23 \text{ e}/\text{\AA}^3$.

Atomic scattering factors were taken from International Tables for Crystallography; (Kluwer Academic:Dordrecht, The Netherlands, 1992; Vol. C, Tables 4.2.6.8 and 6.1.1.4.)

ORTEP-3 (Johnson, C. K. ORTEPII; Report ORNL-5138; Oak Ridge

National Laboratory, Oak Ridge, TN, 1976) was used to generate the crystallographic drawings(Fig.1).

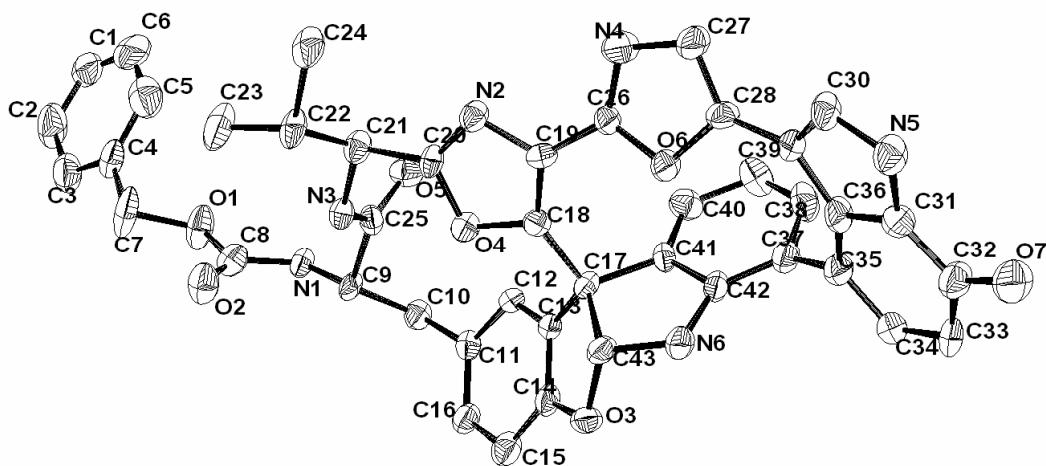


Fig. 1

Tables 1-6 below show the data collection parameters, the atomic coordinates of non-hydrogen atoms and, bond lengths and bond angles, anisotropic thermal parameters of non-hydrogen atoms and atomic coordinates of hydrogen atoms

Table 1. Crystal data and structure refinement for 368.

A. Crystal Data

Empirical formula	C ₅₀ H ₃₅ N ₆ O ₇
Crystal system	Orthorhombic
Formula weight	831.84
Wavelength	0.71069 Å
Unit cell dimensions	a = 9.0850(3) Å b = 17.5720(5) Å c = 25.2410(5) Å
Volume	4029.51(19) Å ³
Space Group	P2 ₁ 2 ₁ 2 ₁
Calculated density	1.371 g/cm ³
Absorption coefficient	0.094 mm ⁻¹

B. Intensity Measurements

Diffractometer	Enraf-Nonius
Detector	Kappa CCD
Radiation	MoK α (λ =0.71069Å)
Temperature	293(2) K
Scan-Type	ω -2 θ
θ range for data collection	2.32° to 20.66°.
Reflections collected / unique	2340 / 2220 [R(int) = 0.0900]
Correction	Lorentz-Polarization

C. Structure Solution and Refinement

Structure Solution	Direct Methods
Refinement method	Full-matrix least-squares on F ²
Data / restraints / parameters	2220 / 0 / 544
Goodness-of-fit on F ²	1.025
R indices (all data)	R1 = 0.0894, wR2 = 0.1468
Largest diff. peak and hole	0.343 and -0.229 e.Å ⁻³

Table 2. Atomic coordinates (x 104) and equivalent isotropic displacement parameters (Å² x 103) for 368. U(eq) is defined as one third of the trace of the orthogonalized Uij tensor.

	x	y	z	U (eq)
C (1)	7213 (15)	8555 (12)	7570 (6)	97 (5)
C (2)	7720 (17)	8777 (8)	8047 (7)	113 (5)
C (3)	7900 (17)	8233 (8)	8454 (5)	94 (4)
C (4)	7715 (14)	7488 (7)	8366 (5)	75 (3)
C (5)	7261 (16)	7271 (8)	7875 (8)	99 (4)
C (6)	7029 (17)	7794 (14)	7474 (6)	112 (6)
C (7)	7886 (15)	6931 (8)	8797 (6)	103 (5)
O (1)	6486 (8)	6562 (4)	8878 (3)	82 (2)
C (8)	6477 (15)	5898 (6)	9142 (4)	64 (3)
O (2)	7532 (10)	5629 (4)	9373 (3)	76 (2)
N (1)	5082 (10)	5609 (4)	9123 (3)	49 (2)
C (9)	4869 (11)	4826 (4)	9301 (3)	45 (2)
C (10)	3237 (11)	4711 (4)	9466 (4)	48 (3)
C (11)	3023 (11)	3933 (5)	9702 (4)	47 (3)
C (12)	2945 (11)	3295 (5)	9371 (3)	43 (2)
C (13)	3089 (10)	2569 (4)	9577 (3)	38 (2)
C (14)	3184 (12)	2470 (5)	10111 (4)	48 (3)
C (15)	3196 (12)	3066 (5)	10462 (4)	60 (3)
C (16)	3134 (12)	3810 (5)	10248 (4)	52 (3)
O (3)	3395 (8)	1714 (3)	10255 (2)	54 (2)
C (17)	3384 (11)	1843 (5)	9297 (3)	44 (3)
C (18)	4622 (11)	1932 (5)	8889 (3)	43 (2)
C (19)	5162 (12)	1593 (5)	8448 (3)	47 (2)
N (2)	6166 (9)	2072 (4)	8198 (3)	48 (2)
C (20)	6233 (10)	2675 (5)	8497 (4)	44 (2)
O (4)	5331 (7)	2627 (3)	8930 (2)	45 (2)
C (21)	6966 (11)	3434 (5)	8401 (4)	49 (3)
C (22)	8625 (11)	3393 (5)	8332 (4)	57 (3)
C (23)	9324 (16)	4195 (7)	8330 (6)	98 (4)
C (24)	8999 (13)	2977 (7)	7815 (4)	77 (3)
N (3)	6528 (9)	3936 (4)	8846 (3)	43 (2)
C (25)	5246 (12)	4294 (5)	8831 (4)	46 (3)
O (5)	4429 (8)	4277 (4)	8439 (3)	57 (2)
C (26)	4741 (11)	886 (5)	8210 (4)	46 (3)
N (4)	4841 (12)	692 (4)	7716 (3)	68 (3)
C (27)	4290 (15)	-36 (5)	7707 (4)	70 (3)
C (28)	3839 (12)	-267 (5)	8184 (4)	50 (3)
O (6)	4168 (8)	319 (3)	8520 (2)	50 (2)
C (29)	3331 (11)	-978 (5)	8400 (3)	49 (3)
C (30)	3814 (12)	-1668 (5)	8228 (4)	57 (3)
N (5)	3269 (10)	-2255 (4)	8513 (3)	64 (2)
C (31)	2332 (13)	-1937 (5)	8889 (4)	58 (3)
C (32)	1565 (14)	-2332 (5)	9265 (4)	67 (3)
O (7)	1702 (10)	-3090 (4)	9293 (3)	85 (3)
C (33)	688 (16)	-1900 (6)	9601 (4)	81 (4)
C (34)	603 (14)	-1093 (6)	9534 (4)	67 (3)
C (35)	1369 (13)	-697 (5)	9151 (4)	57 (3)

C (36)	2325 (13)	-1136 (5)	8822 (4)	54 (3)
C (37)	1206 (12)	124 (5)	9039 (4)	53 (3)
C (38)	343 (13)	352 (6)	8602 (4)	66 (3)
C (39)	321 (14)	1075 (6)	8402 (4)	70 (3)
C (40)	1243 (13)	1599 (6)	8628 (4)	58 (3)
C (41)	2113 (10)	1412 (4)	9054 (3)	40 (2)
C (42)	2007 (11)	682 (5)	9272 (4)	45 (2)
N (6)	2990 (11)	618 (4)	9704 (3)	57 (2)
C (43)	3833 (12)	1289 (5)	9776 (4)	50 (3)

Table 3. Bond lengths [Å] for 368. Estimated standard deviations in the least significant figures are given in parentheses.

C (1) -C (2)	1.347 (18)	C (20) -C (21)	1.510 (12)
C (1) -C (6)	1.37 (2)	C (21) -N (3)	1.482 (12)
C (2) -C (3)	1.414 (17)	C (21) -C (22)	1.519 (14)
C (3) -C (4)	1.338 (16)	C (22) -C (24)	1.534 (14)
C (4) -C (5)	1.361 (18)	C (22) -C (23)	1.545 (15)
C (4) -C (7)	1.471 (16)	N (3) -C (25)	1.324 (12)
C (5) -C (6)	1.38 (2)	C (25) -O (5)	1.237 (10)
C (7) -O (1)	1.443 (14)	C (26) -N (4)	1.296 (11)
O (1) -C (8)	1.344 (12)	C (26) -O (6)	1.372 (10)
C (8) -O (2)	1.216 (13)	N (4) -C (27)	1.375 (12)
C (8) -N (1)	1.366 (15)	C (27) -C (28)	1.334 (12)
N (1) -C (9)	1.459 (11)	C (28) -O (6)	1.368 (10)
C (9) -C (25)	1.549 (13)	C (28) -C (29)	1.438 (13)
C (9) -C (10)	1.554 (14)	C (29) -C (30)	1.360 (12)
C (10) -C (11)	1.503 (12)	C (29) -C (36)	1.431 (13)
C (11) -C (12)	1.400 (12)	C (30) -N (5)	1.351 (12)
C (11) -C (16)	1.398 (12)	N (5) -C (31)	1.392 (12)
C (12) -C (13)	1.384 (12)	C (31) -C (32)	1.366 (14)
C (13) -C (14)	1.362 (12)	C (31) -C (36)	1.417 (12)
C (13) -C (17)	1.484 (12)	C (32) -O (7)	1.338 (12)
C (14) -C (15)	1.372 (13)	C (32) -C (33)	1.391 (16)
C (14) -O (3)	1.389 (11)	C (33) -C (34)	1.429 (16)
C (15) -C (16)	1.416 (13)	C (34) -C (35)	1.380 (14)
O (3) -C (43)	1.475 (11)	C (35) -C (36)	1.428 (14)
C (17) -C (41)	1.512 (13)	C (35) -C (37)	1.478 (13)
C (17) -C (18)	1.534 (13)	C (37) -C (42)	1.354 (13)
C (17) -C (43)	1.605 (13)	C (37) -C (38)	1.412 (14)
C (18) -C (19)	1.354 (12)	C (38) -C (39)	1.366 (15)
C (18) -O (4)	1.384 (10)	C (39) -C (40)	1.370 (14)
C (19) -N (2)	1.392 (11)	C (40) -C (41)	1.374 (13)
C (19) -C (26)	1.431 (13)	C (41) -C (42)	1.399 (12)
N (2) -C (20)	1.303 (11)	C (42) -N (6)	1.414 (12)
C (20) -O (4)	1.369 (10)	N (6) -C (43)	1.418 (12)

Table 4. Bond Angles [°] for 368. Estimated standard deviations in the least significant figures are given in parentheses.

C(2)-C(1)-C(6)	118.9(14)	C(21)-C(22)-C(24)	109.9(9)
C(1)-C(2)-C(3)	119.6(13)	C(21)-C(22)-C(23)	111.4(9)
C(4)-C(3)-C(2)	121.8(13)	C(24)-C(22)-C(23)	109.9(9)
C(3)-C(4)-C(5)	117.6(12)	C(25)-N(3)-C(21)	119.8(8)
C(3)-C(4)-C(7)	121.0(13)	O(5)-C(25)-N(3)	122.6(9)
C(5)-C(4)-C(7)	121.3(13)	O(5)-C(25)-C(9)	119.7(9)
C(4)-C(5)-C(6)	121.7(14)	N(3)-C(25)-C(9)	117.3(8)
C(1)-C(6)-C(5)	120.1(14)	N(4)-C(26)-O(6)	112.7(7)
O(1)-C(7)-C(4)	108.1(10)	N(4)-C(26)-C(19)	127.9(8)
C(8)-O(1)-C(7)	117.8(9)	O(6)-C(26)-C(19)	119.4(8)
O(2)-C(8)-O(1)	124.7(11)	C(26)-N(4)-C(27)	103.6(8)
O(2)-C(8)-N(1)	127.1(9)	C(28)-C(27)-N(4)	112.4(8)
O(1)-C(8)-N(1)	108.1(11)	C(27)-C(28)-O(6)	105.3(8)
C(8)-N(1)-C(9)	117.6(9)	C(27)-C(28)-C(29)	134.8(8)
N(1)-C(9)-C(25)	107.7(7)	O(6)-C(28)-C(29)	119.2(8)
N(1)-C(9)-C(10)	109.4(8)	C(28)-O(6)-C(26)	106.0(6)
C(25)-C(9)-C(10)	109.7(7)	C(30)-C(29)-C(36)	105.7(8)
C(11)-C(10)-C(9)	110.4(8)	C(30)-C(29)-C(28)	123.3(9)
C(12)-C(11)-C(16)	117.9(8)	C(36)-C(29)-C(28)	131.0(8)
C(12)-C(11)-C(10)	119.8(8)	N(5)-C(30)-C(29)	113.1(8)
C(16)-C(11)-C(10)	121.4(8)	C(30)-N(5)-C(31)	106.3(7)
C(13)-C(12)-C(11)	120.6(8)	C(32)-C(31)-N(5)	125.5(8)
C(14)-C(13)-C(12)	119.8(7)	C(32)-C(31)-C(36)	125.9(10)
C(14)-C(13)-C(17)	110.4(7)	N(5)-C(31)-C(36)	108.6(9)
C(12)-C(13)-C(17)	129.1(8)	O(7)-C(32)-C(31)	119.7(10)
C(13)-C(14)-C(15)	122.7(8)	O(7)-C(32)-C(33)	124.4(10)
C(13)-C(14)-O(3)	113.0(7)	C(31)-C(32)-C(33)	116.0(9)
C(15)-C(14)-O(3)	124.1(9)	C(32)-C(33)-C(34)	120.0(10)
C(14)-C(15)-C(16)	117.3(9)	C(35)-C(34)-C(33)	123.8(11)
C(11)-C(16)-C(15)	121.4(9)	C(34)-C(35)-C(36)	116.2(9)
C(14)-O(3)-C(43)	107.9(7)	C(34)-C(35)-C(37)	125.1(10)
C(13)-C(17)-C(41)	119.1(8)	C(36)-C(35)-C(37)	118.5(9)
C(13)-C(17)-C(18)	111.4(7)	C(31)-C(36)-C(35)	118.0(9)
C(41)-C(17)-C(18)	109.8(7)	C(31)-C(36)-C(29)	106.2(8)
C(13)-C(17)-C(43)	102.0(7)	C(35)-C(36)-C(29)	135.8(8)
C(41)-C(17)-C(43)	101.3(7)	C(42)-C(37)-C(38)	115.6(8)
C(18)-C(17)-C(43)	112.5(8)	C(42)-C(37)-C(35)	124.8(10)
C(19)-C(18)-O(4)	106.4(8)	C(38)-C(37)-C(35)	118.8(9)
C(19)-C(18)-C(17)	140.6(9)	C(39)-C(38)-C(37)	124.1(9)
O(4)-C(18)-C(17)	112.4(7)	C(38)-C(39)-C(40)	117.6(10)
C(18)-C(19)-N(2)	110.0(8)	C(39)-C(40)-C(41)	121.1(9)
C(18)-C(19)-C(26)	129.1(9)	C(40)-C(41)-C(42)	119.2(8)
N(2)-C(19)-C(26)	120.6(8)	C(40)-C(41)-C(17)	129.6(8)
C(20)-N(2)-C(19)	105.1(7)	C(42)-C(41)-C(17)	110.6(8)
N(2)-C(20)-O(4)	112.6(8)	C(37)-C(42)-C(41)	122.0(9)
N(2)-C(20)-C(21)	130.3(8)	C(37)-C(42)-N(6)	128.0(9)
O(4)-C(20)-C(21)	116.5(7)	C(41)-C(42)-N(6)	109.4(8)
C(20)-O(4)-C(18)	105.8(7)	C(42)-N(6)-C(43)	112.0(7)
N(3)-C(21)-C(20)	106.6(7)	N(6)-C(43)-O(3)	112.4(8)
N(3)-C(21)-C(22)	112.4(8)	N(6)-C(43)-C(17)	105.6(8)
C(20)-C(21)-C(22)	114.5(8)	O(3)-C(43)-C(17)	104.0(7)

**Table 5. Anisotropic displacement parameters ($\text{\AA}^2 \times 10^3$) for 368.
The anisotropic displacement factor exponent takes the form:
 $-2 \pi^2 [h^2 a^{*2} U_{11} + \dots + 2 h k a^* b^* U_{12}]$**

	U11	U22	U33	U23	U13	U12
C (1)	43 (9)	171 (17)	77 (10)	37 (10)	-19 (7)	-13 (10)
C (2)	98 (12)	82 (9)	161 (15)	52 (10)	-39 (11)	-41 (9)
C (3)	96 (10)	97 (10)	90 (9)	9 (8)	-28 (8)	-37 (9)
C (4)	58 (8)	69 (8)	97 (10)	19 (7)	4 (7)	-19 (7)
C (5)	80 (11)	94 (10)	124 (13)	-27 (11)	3 (10)	6 (9)
C (6)	61 (10)	197 (18)	77 (11)	-46 (13)	20 (8)	-17 (14)
C (7)	49 (9)	84 (9)	176 (13)	47 (9)	-5 (9)	-23 (8)
O (1)	57 (6)	56 (4)	134 (7)	30 (5)	-7 (5)	-18 (4)
C (8)	65 (10)	53 (7)	72 (8)	17 (6)	8 (7)	-8 (7)
O (2)	62 (6)	67 (5)	98 (6)	21 (4)	-12 (5)	-11 (4)
N (1)	47 (7)	39 (4)	60 (5)	2 (3)	6 (4)	-7 (4)
C (9)	59 (8)	31 (5)	44 (5)	5 (4)	1 (5)	-13 (5)
C (10)	52 (8)	32 (5)	61 (6)	-11 (4)	8 (5)	-3 (5)
C (11)	39 (7)	44 (5)	57 (7)	-3 (5)	8 (5)	-7 (5)
C (12)	51 (7)	47 (6)	33 (5)	-1 (4)	5 (4)	-9 (5)
C (13)	39 (6)	33 (5)	41 (6)	-1 (4)	4 (4)	-9 (4)
C (14)	45 (8)	42 (6)	57 (7)	2 (5)	2 (5)	-11 (5)
C (15)	65 (8)	62 (7)	54 (6)	4 (6)	13 (6)	-6 (6)
C (16)	56 (8)	45 (6)	54 (7)	-5 (5)	9 (5)	-14 (5)
O (3)	72 (6)	50 (4)	39 (4)	4 (3)	3 (3)	-6 (4)
C (17)	45 (7)	43 (5)	45 (6)	5 (4)	11 (5)	-3 (5)
C (18)	55 (7)	34 (5)	39 (6)	12 (4)	-5 (5)	-5 (5)
C (19)	57 (7)	48 (6)	36 (5)	-9 (5)	14 (5)	-6 (6)
N (2)	44 (5)	44 (4)	57 (5)	-2 (4)	13 (4)	-1 (4)
C (20)	29 (6)	43 (5)	59 (6)	-3 (5)	8 (5)	-2 (5)
O (4)	46 (4)	38 (3)	51 (4)	0 (3)	9 (3)	0 (3)
C (21)	39 (7)	37 (5)	70 (7)	-3 (5)	8 (5)	0 (5)
C (22)	35 (8)	55 (6)	80 (8)	3 (5)	14 (5)	3 (5)
C (23)	66 (10)	87 (9)	139 (11)	-14 (8)	41 (8)	-20 (8)
C (24)	41 (8)	84 (8)	106 (9)	-9 (7)	20 (6)	2 (6)
N (3)	34 (6)	38 (4)	57 (5)	5 (4)	5 (4)	1 (4)
C (25)	45 (8)	44 (5)	48 (6)	4 (5)	-16 (6)	-11 (6)
O (5)	51 (5)	64 (4)	54 (4)	-4 (4)	2 (4)	12 (4)
C (26)	53 (7)	34 (5)	50 (6)	-6 (5)	5 (5)	-5 (5)
N (4)	103 (9)	44 (5)	55 (6)	0 (4)	15 (5)	-6 (5)
C (27)	101 (10)	44 (6)	65 (8)	-11 (5)	18 (7)	-8 (6)
C (28)	66 (8)	42 (5)	42 (6)	-12 (5)	18 (5)	4 (6)
O (6)	58 (5)	38 (4)	53 (4)	-2 (3)	12 (3)	-3 (3)
C (29)	52 (7)	47 (6)	49 (6)	-2 (5)	9 (5)	-11 (5)
C (30)	47 (7)	47 (6)	78 (7)	-14 (6)	15 (5)	-7 (6)
N (5)	73 (7)	38 (4)	80 (6)	3 (4)	15 (5)	-9 (5)
C (31)	68 (8)	45 (6)	60 (7)	-7 (5)	15 (6)	-8 (6)
C (32)	92 (10)	43 (6)	67 (7)	-7 (5)	24 (7)	-7 (6)
O (7)	124 (8)	44 (4)	88 (5)	5 (3)	14 (5)	-11 (5)
C (33)	105 (11)	64 (7)	75 (8)	7 (6)	11 (7)	-49 (8)
C (34)	85 (10)	65 (7)	52 (7)	-16 (5)	12 (6)	-23 (7)
C (35)	67 (8)	46 (6)	58 (6)	-7 (5)	14 (6)	-11 (6)

C (36)	65 (8)	32 (5)	66 (7)	-11 (5)	8 (6)	-9 (5)
C (37)	55 (7)	43 (6)	62 (7)	-5 (5)	16 (6)	-15 (6)
C (38)	61 (8)	53 (7)	83 (8)	-18 (6)	-9 (7)	-13 (6)
C (39)	71 (9)	57 (7)	82 (8)	-13 (6)	-14 (7)	4 (7)
C (40)	72 (8)	48 (6)	54 (7)	3 (5)	1 (6)	9 (6)
C (41)	35 (6)	34 (5)	52 (6)	-5 (4)	1 (5)	-6 (5)
C (42)	41 (6)	44 (6)	50 (6)	-8 (5)	9 (5)	-9 (5)
N (6)	71 (7)	41 (4)	59 (5)	2 (4)	8 (5)	-15 (5)
C (43)	66 (8)	43 (5)	42 (6)	1 (4)	8 (5)	-9 (6)

Table 6. Hydrogen coordinates ($\times 10^4$) and isotropic displacement parameters ($\text{\AA}^2 \times 10^3$) for 368.

	x	y	z	U (eq)
H (1)	6991	8912	7310	117
H (2)	7950	9285	8108	136
H (3)	8154	8397	8792	113
H (5)	7102	6757	7807	119
H (6)	6749	7629	7139	134
H (7A)	8629	6558	8704	124
H (7B)	8194	7186	9120	124
H (9)	5519	4718	9602	54
H (10A)	2960	5095	9723	58
H (10B)	2607	4768	9158	58
H (12)	2796	3360	9009	52
H (15)	3243	2985	10826	72
H (16)	3168	4227	10475	62
H (22)	9039	3104	8628	68
H (23A)	9004	4467	8021	146
H (23B)	10377	4149	8325	146
H (23C)	9025	4466	8642	146
H (24A)	8619	2468	7829	115
H (24B)	10049	2960	7771	115
H (24C)	8565	3242	7521	115
H (27A)	3470	-59	7462	84
H (27B)	5046	-380	7580	84
H (30A)	3535	-1732	7860	69
H (30B)	4880	-1679	8247	69
H (33)	156	-2135	9870	97
H (34)	-4	-820	9762	81
H (38)	-247	-12	8440	79
H (40)	1281	2090	8491	69

References

1. Pettit, G. R., Marine animals and terrestrial plant anticancer constituents. *Pure and Applied Chem.* **1994**, *66*, (10/11), 2271-2281.
2. Rinehart, K. L., Antitumor compounds from tunicates. *Medicinal Research Reviews* **2000**, *20*, (1), 1-27.
3. Calvert, A. H., Fishing for New Drugs. *J Clin Oncol* **2005**, *23*, (31), 7780-7782.
4. Waller, G., *SeaLife: A Complete Guide to the Marine Environment* Smithsonian Institution Press: Washington D.C., 1996.
5. Davidson, B. S., Ascidiaceae: Producers of Amino Acid Derived Metabolites. *Chemical Reviews* **1993**, *93*, (5), 1771-1791
6. Lindquist, N. L. Secondary Metabolite Production and Chemical Adaptations in the Class Ascidiacea Scripps Institution of Oceanography, University of California, San Diego San Diego 1989.
7. Lindquist, N.; Fenical, W., Isolation and Structure Determination of Diazonamides A and B, Unusual Cytotoxic Metabolites from the Marine Ascidian *Diazona chinensis*. *JACS* **1991**, *113*, 2303-2304.
8. Ritter, T.; Carreira, E. M., The Diazonamides: The Plot Thickens. *Angewandte Chemie International Edition* **2002**, *41*, (14), 2489-2495.
9. Moody, C. J.; Doyle, K. J.; Elliott, M. C.; Mowlem, T. J., Synthesis of heterocyclic natural products: model studies towards diazonamide A. *Pure and Applied Chemistry* **1994**, *66*, ((10/11)), 2107-10.
10. Moody, C. J.; Doyle, K. J.; Elliott, M. C.; Mowlem, T. J., Studies towards the synthesis of diazonamide A. Unexpected formation of a 3,4-bridged indole *Journal of the Chemical Society, Perkin Transactions 1* **1997**, 2413 - 2420.
11. Lach, F.; Moody, C. J., Studies towards the synthesis of diazonamide A. Synthesis of a tyrosine-derived benzofuranone. *Tetrahedron Letters* **2000**, *41*, (35), 6893-6896.
12. Bagley, M. C.; Moody, C. J.; Pepper, A. G., Studies towards the synthesis of diazonamide A. Synthesis of the 4-(oxazol-5-ylmethyl) aryltryptamine fragment. *Tetrahedron Letters* **2000**, *41*, (35), 6901-6904.
13. Bagley, M. C.; Hind, S. L.; Moody, C. J., Studies towards the synthesis of diazonamide A. Synthesis of the indole bis-oxazole fragment. *Tetrahedron Letters* **2000**, *41*, (35), 6897-6900.
14. Palmer, F. N.; Lach, F.; Poriel, C.; Pepper, A. G.; Bagley, M. C.; Slawinb, A. M. Z.; Moody, C. J., The diazo route to diazonamide A: studies on the tyrosine-derived fragment. *Organic and Biomolecular Chemistry* **2005**, *3* 3805 - 3811.
15. Davies, J. R.; Kane, P. D.; Moody, C. J., The Diazo Route to Diazonamide A. Studies on the Indole Bis-oxazole Fragment. *J. Org. Chem.* **2005**, *70*, (18), 7305-7316.
16. Vedejs, E.; Wang, J., A Tyrosine-Derived Benzofuranone Related to Diazonamide A *Organic Letters* **2000**, *2*, (8), 1031-1032.
17. Bagley, M. C.; Hind, S. L.; Moody, C. J., Corrigendum to "Studies towards the synthesis of diazonamide A. Synthesis of the indole bis-oxazole fragment": [Tetrahedron Lett. *41* (2000) 6897]. *Tetrahedron Letters* **2005**, *46*, (49), 8621-8621.

18. Konopelski, J. P.; Hottenroth, J. M.; Oltra, H. M.; Veliz, E. A.; Yang, Z.-C., Synthetic Studies on Diazonamide A. Benzofuranone-Tyrosine and Indole-Oxazole Fragment Support Studies *Synthesis Letters* **1996**, (609-611).
19. Boto, A.; Ling, M.; Meek, G.; Pattenden, G., A synthetic approach towards the aromatic macrocyclic core of diazonamide A based on sp²-sp² coupling protocols. *Tetrahedron Letters* **1998**, 39, (44), 8167-8170.
20. Schley, D.; Radspieler, A.; Christoph, G.; Liebscher, J., α -Arylation of 2-Arylacetates and Benzofuran-2-one with Tricarbonyl(fluoroarene)chromium Complexes. *European Journal of Organic Chemistry* **2002**, 2002, (2), 369-374.
21. Radspieler, A.; Liebscher, J., Synthesis of Chlorooxazoles Related to Natural Products. *Synthesis* **2001**, 5, 745-750.
22. Jamison, T. F. I. Consecutive Use of Two Reactions of Alkyne-Co₂(CO)₆ Complexes in the Total Synthesis of (+)-Epoxydictymene II. Studies Directed Toward the Synthesis of the Diazonamide Marine Natural Products Using Benzofuran Epoxidation-Rearrangements Harvard University Cambridge, 1997.
23. Wipf, P.; Yokokawa, F., Synthetic studies toward diazonamide A. Preparation of the benzofuranone-indolyloxazole fragment. *Tetrahedron Letters* **1998**, 39, (16), 2223-2226.
24. Wipf, P.; Methot, J. L., Synthetic Studies toward Diazonamide A. A Novel Approach for Polyoxazole Synthesis. *Org. Lett.* **2001**, 3, (9), 1261-1264.
25. Vedejs, E., Progress toward Synthesis of Diazonamide A. Preparation of a 3-(Oxazolyl-5-yl)-4-trifluoromethylsulfonyloxyindole and Its Use on Biaryl Coupling Reactions. *Organic Letters* **2000**, 2, (8), 1033-1035.
26. Vedejs, E.; Zajac, M. A., Synthesis of the Diazonamide A Macrocyclic Core via a Dieckmann-Type Cyclization. *Org. Lett.* **2001**, 3, (16), 2451-2454.
27. Zajac, M. A.; Vedejs, E., A Synthesis of the Diazonamide Heteroaromatic Biaryl Macrocyclic/Hemiaminal Core. *Org. Lett.* **2004**, 6, (2), 237-240.
28. Magnus, P.; McIver, E. G., Synthesis of the dichlorobisoxazole-indole portion of the antitumor agent diazonamide by a putative biogenetic strategy. *tetrahedron Letters* **2000**, 41, 831-834.
29. Kreisberg, J. D.; Magnus, P.; McIver, E. G., Vilsmeier methodology for the synthesis of 3-(2-N-phthaloylacyl)indole derivatives, and its application to the synthesis of the GCDEF rings of diazonamide *Tetrahedron Letters* **2001**, 42, (4), 627-629
30. Magnus, P.; Lescop, C., Photo-Fries Rearrangement of the synthesis of the diazonamide macrocycle *tetrahedron Letters* **2001**, 42, (41), 7193-7196.
31. Magnus, P.; Venable (nee Kreisberg), J. D.; Shen, L.; Lynch, V., Some reactions of persistent benzofuranone radicals related to the 'old' diazonamide structure *Tetrahedron Letters* **2005**, 46, 707-710
32. Feldman, K. S.; Eastman, K. J.; Lessene, G., Diazonamide Synthesis Studies: Use of Negishi Coupling to Fashion Diazonamide-Related Biaryls with Defined Axial Chirality. *Org. Lett.* **2002**, 4, (20), 3525-3528.
33. Sawada, T.; Fuerst, D. E.; Wood, J. L., Rhodium-catalyzed synthesis of a C(3) disubstituted oxindole: an approach to diazonamide A. *Tetrahedron Letters* **2003**, 44, (26), 4919-4921.
34. Fuerst, D. E.; Stoltz, B. M.; Wood, J. L., Synthesis of C(3) Benzofuran-Derived Bisaryl Quaternary Centers: Approaches to Diazonamide A. *Organic Letters* **2000**, 2, (22), 3521-3523. .

35. Fuerst, D. E. Progress Toward the Total Synthesis of Diazonamide A. Yale University, New Haven 2003.
36. Nicolaou, K. C.; Snyder, Scott A.; Simonsen, Klaus B.; Koumbis, Alexandros E., Model Studies towards Diazonamide A: Synthesis of the Heterocyclic Core. *Angewandte Chemie* **2000**, *39*, (19), 3473-3478.
37. Nicolaou, K. C.; Huang, X.; Giuseppone, N.; Rao, P. B.; Bella, M.; Reddy, M. V.; Snyder, S. A., Construction of the Complete Aromatic Core of Diazonamide A by a Novel Hetero Pinacol Macrocyclization Cascade Reaction. *Angewandte Chemie International Edition* **2001**, *40*, (24), 4705-4709.
38. Nicolaou, K. C.; Snyder, S. A.; Giuseppone, N.; Huang, X.; Bella, M.; Reddy, M. V.; Rao, P. B.; Koumbis, A. E.; Giannakakou, P.; O'Brate, A., Studies toward Diazonamide A: Development of a Hetero-Pinacol Macrocyclization Cascade for the Construction of the Bis-Macrocyclic Framework of the Originally Proposed Structure. *J. Am. Chem. Soc.* **2004**, *126*, (32), 10174-10182.
39. Nicolaou, K. C.; Snyder, S. A.; Huang, X.; Simonsen, K. B.; Koumbis, A. E.; Bigot, A., Studies toward Diazonamide A: Initial Synthetic Forays Directed toward the Originally Proposed Structure. *J. Am. Chem. Soc.* **2004**, *126*, (32), 10162-10173.
40. Nicolaou, K. C.; Snyder, S. A., *Classics in Total Synthesis II*. Wiley-VCH: 2003; p 639.
41. Nicolaou, K. C.; Rao, P. B.; Hao, J.; Reddy, M. V.; Rassias, G.; Huang, X.; Chen, D. Y. K.; Snyder, S. A., The Second Total Synthesis of Diazonamide A. *Angewandte Chemie International Edition* **2003**, *42*, (15), 1753-1758.
42. Nicolaou, K. C.; Hao, J.; Reddy, M. V.; Rao, P. B.; Rassias, G.; Snyder, S. A.; Huang, X.; Chen, D. Y. K.; Brenzovich, W. E.; Giuseppone, N.; Giannakakou, P.; O'Brate, A., Chemistry and Biology of Diazonamide A: Second Total Synthesis and Biological Investigations. *J. Am. Chem. Soc.* **2004**, *126*, (40), 12897-12906.
43. Jeong, S.; Chen, X.; Harran, P. G., Macrocyclic Triarylethylenes via Heck Endocyclization: A System Relevant to Diazonamide Synthesis. *J. Org. Chem.* **1998**, *63*, (24), 8640-8641.
44. Chen, X.; Esser, L.; Harran, P. G., Stereocontrol in Pinacol Ring-Contraction of Cyclopeptidyl Glycols: The Diazonamide C10 Problem. *Angewandte Chemie International Edition* **2000**, *39*, (5), 937-940.
45. Li, J.; Chen, X.; Burgett, A. W. G.; Harran, P. G., Synthetic seco Forms of (-)-Diazonamide A. *Angewandte Chemie International Edition* **2001**, *40*, (14), 2682-2685.
46. Li, J.; Jeong, S.; Esser, L.; Harran, P. G., Total Synthesis of Nominal Diazonamides - Part 1: Convergent Preparation of the Structure Proposed for (-)-Diazonamide A. *Angewandte Chemie International Edition* **2001**, *40*, (24), 4765-4769.
47. Nicolaou, K. C.; Bella, M.; Chen, D. Y. K.; Huang, X.; Ling, T.; Snyder, S. A., Total Synthesis of Diazonamide A. *Angewandte Chemie* **2002**, *114*, (18), 3645-3649.
48. Nicolaou, K. C.; Chen, D. Y. K.; Huang, X.; Ling, T.; Bella, M.; Snyder, S. A., Chemistry and Biology of Diazonamide A: First Total Synthesis and Confirmation of the True Structure. *J. Am. Chem. Soc.* **2004**, *126*, (40), 12888-12896.
49. Li, J.; Burgett, A. W. G.; Esser, L.; Amezcua, C.; Harran, P. G., Total Synthesis of Nominal Diazonamides - Part 2: On the True Structure and Origin of Natural Isolates. *Angewandte Chemie* **2001**, *113*, (24), 4906-4909.
50. Burgett, A. W. G.; Li, Q.; Wei, Q.; Harran, P. G., A Concise and Flexible Total Synthesis of (-)-Diazonamide A. *Angewandte Chemie International Edition* **2003**, *42*, (40), 4961-4966.

51. Nicolaou, K. C.; Snyder, S. A., Chasing Molecules That Were Never There: Misassigned Natural Products and the Role of Chemical Synthesis in Modern Structure Elucidation. *Angewandte Chemie International Edition* **2005**, 44, (7), 1012-1044.
52. Hills, I. D.; Fu, G. C., Catalytic Enantioselective Synthesis of Oxindoles and Benzofurans that Bear a Quaternary Stereocenter. *Angewandte Chemie International Edition* **2003**, 42, 4082-4085.
53. Vidulova, D. B. Studies Toward the Synthesis of EFGH Ring System of Diazonamide A Pummerer Chemistry Applied Toward the Synthesis of 3,3-Spirocyclic Oxindoles. The Pennsylvania State University, 2005.
54. Monks, A.; Scudiero, D.; Skehan, P.; Shoemaker, R.; Paull, K.; Vistica, D.; Hose, C.; Langley, J.; Cronise, P.; Vaigro-Wolff, A.; Gray-Goodrich, M.; Campbell, H.; Mayo, J.; Boyd, M., Feasibility of a High-Flux Anticancer Drug Screen Using a Diverse Panel of Cultured Human Tumor Cell Lines. *J Natl Cancer Inst* **1991**, 83, (11), 757-766.
55. Developmental Therapeutics Program, N. C. I. w. *DTP Human Tumor Cell Line Screen* <http://dtp.nci.nih.gov/branches/btb/ivclsp.html>.
56. Paull, K. D.; Shoemaker, R. H.; Hodes, L.; Monks, A.; Scudiero, D. A.; Rubinstein, L.; Plowman, J.; Boyd, M. R., Display and Analysis of Patterns of Differential Activity of Drugs Against Human Tumor Cell Lines: Development of Mean Graph and COMPARE Algorithm. *J Natl Cancer Inst* **1989**, 81, (14), 1088-1092.
57. Developmental Therapeutics Program, N. C. I. w. *NSC # 700089 (diazonamide A) NCI Cancer Screen Current Data* <http://dtp.nci.nih.gov/dtpstandard/servlet/MeanGraphSummary?testshortname=NCI+Cancer+Screen+Current+Data&searchtype=NSC&searchlist=700089>.
58. Vervoort, H. C. Novel anticancer agents from Ascidiacea. UNIVERSITY OF CALIFORNIA, SAN DIEGO San Diego, 1999.
59. Cragg, G. M.; Newman, D. J., Antineoplastic agents from natural sources: achievements and future directions. *Expert Opinion on Investigational Drugs* **2000**, 9, (12), 2783-2797.
60. Chabner, B. A.; Roberts, T. G., Chemotherapy and the War on Cancer. *Nature Reviews Cancer* **2005**, 5, (1), 65-72.
61. Suggitt, M.; Bibby, M. C., 50 Years of Preclinical Anticancer Drug Screening: Empirical to Target-Driven Approaches. *Clin Cancer Res* **2005**, 11, (3), 971-981.
62. Nagle, A.; Wooyoung, H.; Gray, N. S., Antimitotic Agents of Natural Origin *Current Drug Targets* **2006**, 7, (3), 305-326.
63. Jordan, M. A.; Wilson, L., Microtubules as a Target for Anticancer Drugs. *Nature Reviews Cancer* **2004**, 4, (4), 253-265.
64. Lowe, J.; Li, H.; Downing, K. H.; Nogales, E., Refined Structure of $\alpha\beta$ -Tubulin at 3.5 Å Resolution *J. Mol. Biol.* **2001**, 313, 1045-1057.
65. McKean, P. G.; Vaughan, S.; Gull, K., The Extended Tubulin Superfamily *Journal of Cell Science* **2001**, 114, 2723-2733.
66. Desai, A.; Mitchison, T. J., Microtubule Polymerization Dynamics. *Annual Review of Cell and Developmental Biology* **1997**, 13, (1), 83-117.
67. Wilson, L.; Jordan, M. A., Microtubule dynamics: taking aim at a moving target. *Chemistry & Biology* **1995**, 2, (9), 569-573.
68. Kline-Smith, S. L.; Walczak, C. E., The Microtubule-destabilizing Kinesin XKCM1 Regulates Microtubule Dynamic Instability in Cells. *Molecular Biology of the Cell* **2002**, 13, 2718-2731.

69. Belmont, L. D.; Mitchison, T. J., Identification of a Protein That Interacts with Tubulin Dimers and Increases the Catastrophe Rate of Microtubules. *Cell* **1996**, 84, (4), 623-631.
70. Cassimeris, L.; Gard, D.; Tran, P. T.; Erickson, H. P., XMAP215 is a long thin molecule that does not increase microtubule stiffness. *Journal of Cell Science* **2001**, 2001, 3025-3033.
71. Jordan, M. A.; Toso, R. J.; Thrower, D.; Wilson, L., Mechanism of mitotic block and inhibition of cell proliferation by taxol at low concentrations *PNAS* **1993**, 90, 9952-9956.
72. Rudner, A. D.; Murray, A. W., The spindle assembly checkpoint. *Current Opinion in Cell Biology* **1996**, 8, (6), 773-780.
73. Clarke, D. J.; Giménez-Abián, J. F., Checkpoints controlling mitosis. *BioEssays* **2000**, 22, (4), 351-363.
74. Timasheff, S. N.; Andreu, J. M.; Na, G. C., Physical and Spectroscopic Methods for the Evaluation of the Interactions of Antimitotic Agents with Tubulin *Pharmacology & Therapeutics*. **1991**, 52, 191-210.
75. Bai, R.; Taylor, G. F.; Cichacz, Z. A.; Herald, C. L.; Kepler, J. A.; Petit, G. R.; Hamel, E., The Spongistatins, Potently Cytotoxic Inhibitors of Tubulin Polymerization, Bind in a Distinct Region of the Vinca Domain. *Biochemistry* **1995**, 34, 9714-9721.
76. Takahashi, M.; Iwasaki, S.; Kobayashi, H.; Okuda, S.; Murai, T.; Sato, Y., Rhizoxin binding to tubulin at the maytansine-binding site. *Biochimica et Biophysica Acta* **1987**, 926, 215-223.
77. Wells, W. A., The Discovery of Tubulin. *J. Cell Biol.* **2005**, 169, (4), 552.
78. Gordaliza, M.; Miguel del Corral, J. M.; Castro, M. A.; Garcia-Garcia, P. A.; San Feliciano, A., Cytotoxic cyclolignans related to podophyllotoxin. *Il Farmaco* **2001**, 56, 297-304.
79. Verdier_Pinard, P.; Sitachitta, N.; Rossi, J. V.; Sackett, D. L.; Gerwick, W. H.; Hamel, E., Biosynthesis of Radiolabeled Curacin A and Its Rapid and Apparently Irreversible Binding to the Colchicine Site of Tubulin *Archives of Biochemistry and Biophysics* **1999**, 370, (1), 51-58.
80. Zhou, J.; Giannakakou, P., Targeting Microtubules for Cancer Chemotherapy. *Curr. Med. Chem.-Anti-Cancer Agents* **2005**, 5, (1), 65-71.
81. Schiff, P. B.; Horwitz, S. B., Taxol stabilizes microtubules in mouse fibroblast cells. *PNAS* **1980**, 77, (3), 1561-1565.
82. Kumar, N., Taxol-induced Polymerization of Purified Tubulin *The Journal of Biological Chemistry* **1981**, 256, (20), 10435-10441.
83. Hamel, E.; Sackett, D. L.; Vourloumis, D.; Nicolaou, K. C., The Coral-Derived Natural Products Eleutherorbin and Sarcodictyins A and B: Effects on the Assembly of Purified Tubulin with and without Microtubule-Associated Proteins and Binding at the Polymer Taxoid Site. *Biochemistry* **1999**, 38, 5490-5498.
84. Hood, K. A.; West, L. M.; Rouwe, B.; Northcote, P. T.; Berridge, M. V.; Wakefield, S. J.; Miller, J. H., Peloruside A, a Novel Antimitotic Agent with Paclitaxel-like Microtubule-stabilizing Activity. In 2002; Vol. 62, pp 3356-3360.
85. Gaitanos, T. N.; Buey, R. M.; Diaz, J. F.; Northcote, P. T.; Teesdale-Spittle, P.; Andreu, J. M.; Miller, J. H., Peloruside A Does Not Bind to the Taxoid Site on {beta}-Tubulin and Retains Its Activity in Multidrug-Resistant Cell Lines. In 2004; Vol. 64, pp 5063-5067.
86. Horwitz, S. B., How to make taxol from scratch *Nature* **1994**, 367, 593-594.
87. Nicolaou, K. C.; Dai, W.-M.; Guy, R. K., Chemistry and Biology of Taxol *Angewandte Chemie* **1994**, 33, 15-44.
88. Mitchison Group, H. M. S., Large Scale Tubulin Preparation

89. Cruz-Monserrate, Z.; Vervoort, H. C.; Bai, R.; Newman, D. J.; Howell, S. B.; Los, G.; Mullaney, J. T.; Williams, M. D.; Pettit, G. R.; Fenical, W.; Hamel, E., Diazonamide A and a Synthetic Structural Analog: Disruptive Effects on Mitosis and Cellular Microtubules and Analysis of Their Interactions with Tubulin. *Mol Pharmacol* **2003**, 63, (6), 1273-1280.
90. Klausner, R. D.; Donaldson, J. G.; Lippincott-Schwartz, J., Brefeldin A: Insights into the Control of Membrane Traffic and Organelle Structure. *JCB* **1992**, 116, 1071-1080.
91. Thomas, G. H., M.N., TOR signalling and control of cell growth. *Curr. Opin. in Cell Biol.* **1997**, 9, 782-787.
92. Butler, M. S., The Role of Natural Product Chemistry in Drug Discovery *J. Nat. Prod.* **2004**, 67, 2141-2153
93. Taunton, J.; Hassig, C. A.; Schreiber, S. L., A Mammalian Histone Deacetylase Related to the Yeast Transcriptional Regulator Rpd3p. *Science* **1996**, 272, 408-411.
94. Crampton, S. L.; Adams, E. G.; Kuentzel, S. L.; Li, L. H.; Badiner, G.; Bhuyan, B. K., Biochemical and cellular effects of didemnins A and B. In 1984; Vol. 44, pp 1796-1801.
95. Crews, C. M.; Collins, J. L.; Lane, W. S.; Snapper, M. L.; Schreiber, S. L., GTP-dependent Binding of the Antiproliferative Agent Didemnin to Elongation Factor 1 α . *Journal of Biological Chemistry* **1994**, 269, (22), 15411-15414.
96. Crews, C. M.; Lane, W. S.; Schreiber, S. L., Didemnin binds to the protein palmitoyl thioesterase responsible for infantile neuronal ceroid lipofuscinosis. *PNAS* **1996**, 93, (9), 4316-4319.
97. Evans, D. A.; Tregay, S. S.; Burgery, C. S.; Paras, N. A.; Vojkovsky, T., C₂-Symmetric Copper(II) Complexes as Chiral Lewis Acids. Catalytic Enantioselective Carbonyl-Ene Reactions with Glyoxylate and Pyruvate Esters. *JACS* **2000**, 122, 7936-7943.
98. Brower, J. O.; Lightner, D. A., Synthesis and Spectroscopic Properties a New Class of Strongly Fluorescent Dipyrrinones. *JOC* **2002**, 67, 2713-2716.
99. Dalpozzo, R.; Bartoli, G., Bartoli Indole Synthesis. *Current Organic Chemistry* **2005**, 9, (2), 163-178.
100. Oikawa, Y.; T.Yoshioka; Mohri, K.; Yonemitsu, O., *Heterocycles* **1979**, 12, 1457-1462.
101. Fukuyama, T.; Jow, C.-K.; Cheung, M., *Tetrahedron Letters* **1995**, 36, 6373-6374.
102. Canesi, S.; Belmont, P.; Bouchu, D.; Rousset, L.; Ciufolini, M. A., Efficient oxidative spirocyclization of phenolic sulfonamides. *Tetrahedron Letters* **2002**, 43, (29), 5193-5195.
103. Tokunaga, T.; Hume, W. E.; Umezome, T.; Okazaki, K.; Ueki, Y.; Kumagai, K.; Hourai, S.; Nagamine, J.; Seki, H.; Taiji, M.; Noguchi, H.; Nagata, R., Oxindole Derivatives as Orally Active Potent Growth Hormone Secretagogues. *J. Med. Chem.* **2001**, 44, (26), 4641-4649.
104. Konda-Yamada, Y.; Okada, C.; Yoshida, K.; Umeda, Y.; Arima, S.; Sato, N.; Kai, T.; Takayanagi, H.; Harigaya, Y., Convenient synthesis of 7' and 6'-bromo--tryptophan and their derivatives by enzymatic optical resolution using α -aminoacylase. *Tetrahedron* **2002**, 58, (39), 7851-7861.
105. Wang, *JOC* **2003**, 68, (4), 1637.

VITAE

Anthony William George Burgett was born in July of 1977 in Littleton, Colorado, the middle child of Buck and Georgeann Burgett. After the completing the second grade, Anthony and his family relocated to Jenks, Oklahoma, a suburb of Tulsa. After graduating from Jenks High School in 1995, Anthony attended the University of Oklahoma as a National Merit Scholar. After four productive, formation, and highly enjoyable years, he received separate bachelor degrees in biochemistry and microbiology. He undertook a Honors Program research project studying the purine salvage pathway in halophilic archaea in the laboratory of Dr. David Nagle. Upon graduation, he entered graduate school at UT-Southwestern Medical Center at Dallas, pursuing research into the synthesis and biology of the diazonamides under the direction of the Dr. Patrick Harran and Dr. Michael Roth. Anthony is very close with his family including his parents, Buck and Georgeann, his brother, Cpt. Michael Burgett U.S. Army, his sister, Georjeana Wurth, and his niece and nephews.

Permanent Address: 104 Hawthorn St.
Fredrick, CO 80530